City University London

School of Engineering and
Mathematical Sciences

"Floating Production Storage Offloading Unit Structural Fatigue Analysis"

"Dissertation Submitted to the City University
In Fulfilment of the Requirement for the
Degree of Doctor of Philosophy"

APRIL-2003

By

Khaled KATTOUA

- **B.Eng. Marine Engineering Technology**
- **MSc. Scientific Computing and Scientific Information Technology**

Contents

Tables

Figures

Acknowledgements

I would like to thank my supervisor **Dr. Cedric D'Mello** for him introducing me to this new revolutionary field of FPSOs Technology. Thanks are also due to Dr. D'Mello for all the guidance throughout the duration of this work and, in particular, for his assistance in arranging and co-ordinating the experimental programme.

Numerous individuals have assisted through discussion, correspondence and provision of published information including:

Organisation	Contacts	Contribution
American Bureau of Shipping	Mr. David Robinson Dr. Bulent Tinink	SafeHull Software Technical Information
Bureau Veritas Marine	Mr. M Huther	Technical Papers
British Steel	Mr. Simon Slater	Supply Of Shipbuilding Material
Det Norske Veritas	Mr. Nigel Winder	Technical Papers and Nauticus Software
Germanischer Lloyd	Dr. Wolfgang Fricke Mr. Kai Fock	Technical Information Poseidon Software
Amerada HESS	Dr. Harry Van Langen	Arranging Site visit to a newly built FPSO (TRITRON Project).
Lloyds Register of Shipping	Mr. Robert Potthurst Mr. Henry Chung Miss D S Quinn	Technical Papers Technical Information ShipRight FDA Software
MARIN	Mr. Henk V. D. Boom	Technical Papers
WS/Atkins Oil and Gas	Mr. Arher Stoddert Mr. Nawaz Hossain Mr. R. van den Wijngaard	FPSOs Conversion Hydrostatic Analysis Finite Element Analysis

Finally I would like to thank my family, specially my father **Moustafa** for his continued moral support during the course of this work, with lots of appreciation and respect to my wife **Ilham** for her encouragement all the way, your support made this study possible.

At this point it is considered appropriate to send a message to all parties involved with the design, fabrication and operation of FPSOs vessels, aimed at encouraging them to publicise information regarding the structural performance of such marine structures. It is believed that only by studying and coding such information, especially that connected to structural failures, will it be possible to come up with better and more reliable, but not utterly conservative, structural design guidelines.

The author firmly believes that the major challenge facing the industry is likely to be a shortage of its fundamental raw material, skilled manpower. Its major problem will be how to attract young people. Oil & gas is loosing the battle, despite all the facts to the contrary its huge contribution to modern life goes virtually unrecognised.

The author believes that one reason lays in the company's obsession with secrecy, which results in a total failure to communicate to the public, the benefits of its expenditure, its technological achievements and the high employment it creates. As a very small example, the author's biggest problem in carrying out this study is the refusal of most companies to provide information on their FPSOs technical data and many other aspects of their development.

Declaration

ABSTRACT

This thesis examines the fatigue behaviour of FPSO structures. It has been compiled as a result of theoretical, analytical and experimental study. The Finite Element approach has been utilized to analyse the FPSO's structure. It is intended that this particular work will enable further computer simulations for fatigue assessment to be carried out.

The thesis starts with the development of the general arrangement, structure and typical details of the City FPSO. The applied loads are then reviewed and this includes the so called static loads due to cargo loading and still water pressure, and the green loads due to dynamic loads induced by the vessel behaviour on waves at sea.

Response to local loads such as, external sea pressure, internal pressure due to the cargo and ballast, wave slamming loads, etc. is then determined. The effect of the top structural loads on the FPSO is discussed with some practical calculation of typical topside processing palates loads.

SCF evaluation methods are considered together with a discussion of the effect of structural dimensioning of local details, the use of specially performed test results conducted on ship structure. In particular, the structural stress concentration factor at the web-toe associated with the max loading conditions is developed.

Confirmation of validity of the SCFs theory is provided from an extensive appraisal of the literature and from laboratory tests of the structure in question. The experimental technique developed in this thesis is based upon geometrical analogy to the simplified Peterson's Neuber notch theory, applied to the system parametric equations of SCFs and the geometric relations. The experimental results are in general accordance with published results.

This research includes a calibration method for S-N Curves required for typical fatigue sensitive details in FPSOs. It also provides improved information on the important link between S-N data and finite element analysis for fatigue life assessment using a linear cumulative damage formulation.

Notations

Symbol	***Units***	***Definition***
A	m^2	Cross-sectional area
A.P		Aft Perpendicular
B	m	Ship Breadth between side shells
B.M	kN-m	Bending Moment
BOPD		Barrel of Oil Per Day
C_1		Constant relating to the mean S-N curve
D	m	Ship Height from Base Line to Weather Deck
dwt	Tonnes	Ship Dead Weight
E	N/m^2	Young's modulus of the material
F	Hertz	Cyclic frequencies
F.P		Forward Perpendicular
g	9.81 m/s^2	Acceleration due to gravity
I	m^4	second moment of area of cross-section of beam about the neutral axis
K_g		Geometric stress concentration factor
K_t		Theoretical stress concentration factor
K_w		Stress concentration due to the weld
K_x		Axial Loading stress concentration factor
K_y		Bending Loading stress concentr ation factor
L	m	Ship Length
M	kN-m	applied bending moment
M		The inverse slope of the S-N curve
N		Number of cycles to failure
P_i and P_e	kN/m^2	Internal and External Pressure
R,r	m	Radius
S.F	kN	Shear Force
T **ULCC**	mm	Plate Thickness Ultra Large Crude oil Carrier
Ux, Uy, Uz		The three translational degrees of freedom in FEM
V		Poisson's ratio of the material

Symbol	Units	Definition
VLCC		Very Large Crude oil Carrier
X	m	Longitudinal distance from A.P
Y	m	distance of point considered from neutral axis
Z	m^3	sectional modulus
θx, θy, θz		The three rotational degrees of freedom in FEM
δ	mm	Deflection
λ		Factor of Safety
ρ	1025 kg/m^3	Sea Water Density
σ_{cc}	N/mm^2 - MPa	Hencky-von Mises stress or the combined "comparative" stress
σ_u	N/mm^2 - MPa	Ultimate Stress
σ_y	N/mm^2 - MPa	Yielding Stress
τ	N/mm^2 - MPa	Combined shear stress due to torsion and/or bending
ω	Radians/Second	Circular frequencies

1. Introduction

1.1 The Fatigue Problem in Oil Tankers and FPSOs

1.1.1 Overview

Fatigue cracking of welded structural details in Oil Tankers and FPSOs (Floating Production Storage and Offloading) vessels due to cyclic loading has always been one of the potential failure modes. Fatigue cracks in riveted connections were rarely observed in old Tankers. With the predominant use of welding as a construction process a large number of fatigue cracks have been observed, *ABS*, (1992). Several factors contributed to this:

- The effects of the welding process on the fatigue performance were not sufficiently investigated.
- The use of construction methods suitable for riveted connections that result in a low fatigue strength when used in combination with welding i.e. overlapped joints used to connect two plates by riveting have very poor fatigue strength as a welded connection.
- Steel and welding material were not well suited for welded ship details.

These initial problems were soon recognized and by using improved materials and construction techniques fatigue cracking of ship structural details became a minor problem.

The development of specialised ship constructions based on the use of improved analysis techniques (Finite Element Method) and the trend to optimise ship structural weight has resulted in an increase of fatigue failures. Consequently, several classification societies have made a fatigue life analysis a recommended procedure.

Most research conducted in the area of fatigue and fracture mechanics has been related to offshore oil platforms. Many of these platforms are located in areas where the ocean environment is extremely hostile and fatigue damage is very likely to occur.

Significant research has also been conducted in the area of steel bridge girders. The dynamic wind and traffic loads make these structures very susceptible for fatigue damage. Many of the design S-N curves presently used for fatigue life evaluations of ships and offshore structures have originally been developed for the steel bridge girder details.

Many of these research results have been adapted for the use with ship details and the more complicated long-term loadings encountered in ships. In addition, significant efforts have been made to develop S-N curves specifically suited for ship structural details.

The development of Very Large Crude Carriers (VLCC) and the use of high tensile steel (HTS) have caused an increase of fatigue cracks in tankers. Although in general, not the cause for significant structural damage fatigue, cracks can cause pollution and require increased inspection and maintenance efforts. FPSOs operating primarily on the North Sea are particularly prone to fatigue damage.

For some tanker classes where extensive fatigue damage has been observed detailed studies have been performed to identify the factors contributing to cause the fatigue damage. The documentation of these studies shows the amount of analysis necessary to obtain reliable results. This fact makes these sophisticated analysis methods unsuitable for standard design and repair procedures.

In order to document the required procedure for a detailed and realistic fatigue life evaluation two research projects on tankers and one recent on FPSOs are mentioned:

- *Hull Cracking of Very Large Ship Structures*, Nippon Kaiji Kyokai (NK). NK, the Japanese Ship Classification Society has performed a 1-year research project on very large crude carriers (VLCC) built with a considerable amount of high-tensile steel (HTS). The results are summarized in *Yoneya, T.*, (1993).

- *Fatigue Evaluation of Tanker Structures*, BP Shipping. In a paper presented at the 1992 shipbuilders meeting of the Tanker Structure Co-operative Forum

the analysis process for fatigue life evaluation of tanker structures is described in *BP*, (1992).

- *FPSO Integrity JIP*, led by (MARIN), Maritime Research Institute Netherlands Joint Industry Project is now on stream. The objective of the Joint Industry project is to provide insight in the fatigue loading of FPSOs and the accuracy and validity of computational models. The results should contribute to reliable life time prediction and site assessment studies for this relative new concept of production. The background of the JIP is presented in *Lotsberg, I.*, (2000).

1.1.2 Fatigue Strength of Ship Structure

It is the resistance of a material to failure under cyclic loading; and it is generally expressed as the stress range giving a 50% probability of fracture after a given number of load cycles. Based on a comparison of S-N test results presented in *Yoneya, T.*, (1993) it has been concluded that the fatigue strength of high tensile steel (HTS) and mild steel (MS) is comparable. An equivalent wave pressure with regard to fatigue strength was developed to account for the actual non-linear relationship between the ranges of wave pressure to wave height. The comparison of the calculated cumulative fatigue damage using both the non-linear and the equivalent linear relationship shows good agreement. The vertical distribution of the equivalent wave height also corresponds well with the vertical distribution of observed cracks. In addition it was attempted to develop a design S-N curve based on service experience. Survey data on several vessels was used to determine the unknown parameters of S-N curves and fatigue life distributions.

Nowadays sophisticated analysis methods are available for fatigue life predictions of details of ships. However, the reliability of such analysis is significantly depending on the fatigue capacity of the considered details (S-N data) used as input. Therefore it is considered important to reduce the uncertainty associated with the S-N data that are being used for design of typical ship details in order to improve confidence in the analysis procedure used to calculate the fatigue capacity of these details. *Francois, M., Healy B., Fricke W.*, (2000), gives an insight on the aspects involved.

The cyclic stresses in the hull girder caused by wave effects are the primary cause for fatigue damage, where wave effects cause hull bending, local pressure variation

on the ship hull and internal pressure variation. It is however important that a reasonable usage of high tensile steel (HTS) can lead to efficiently light and sufficiently strong hull structures if appropriate measures are taken against the increase of local stress range accompanied with the usage of high tensile steel (HTS).

1.1.3 Analysis Techniques

Hull girder bending can be calculated either based on the rule-based loading as defined by the various classification societies or through a complete spectral analysis that takes into account the travel route or site-specific location and the vessel response characteristics.

The combination of the external and internal pressure loads has to take into account the phase angles of the two components, which significantly complicates the process of obtaining the long-term distribution of the stress ranges. One alternative is the use of simplified load combination schemes.

The calculation of the fatigue damage for the combined stresses from hull girder bending internal and external pressure shows that the effects of the pressure terms are small compared to the hull girder bending term.

The 3D Finite Element Analysis utilising a global model structure can be used to evaluate the local bending stresses of longitudinals due to the global transverse deformation, as calculation is based on the beam theory. The local stress of connections to the transverse structure necessary for the calculation of fatigue strength can be analysed using the FEA. An early illustrations on ship structures is given in *Paulling, J. R.*, (1964), And *(DNV)*, (1963).

A close look at the world's tanker fleet reveals several issues regarding its present state and more important its future development and conversion to FPSOs. Some of these issues have been summarized in *John Ferguson*, (1990) mainly:

- Extending the life of existing tanker hulls
- Structural design trends in today's oil carriers' new buildings
- Classification societies hull renovation scheme

1.2 Regulatory Requirements

Regulatory requirements related to fatigue cracking and corrosion has a strong impact on oil carriers operations. Where classification societies impose required inspection intervals, corrosion limits and other measures to ensure structural integrity.

FPSO installations are being increasingly used, particularly for marginal fields and for deep water locations. Fifteen installations or more of this type are currently in operation on the UK Continental Shelf (UKCS) including West of Shetland (WoS), with several more currently under consideration for future Projects. Most of these installations have been built in the last few years, although some have been converted from tankers more than 20 years old. It is likely that many of these installations will continue to be operated for several years to come.

Much research effort has been expended by the offshore industry in assessing the effects of a wide range of hazards (including structural hazards) on the more conventional types of installations. However, the Industry soon recognised at an early stage of developments that further work was required in assessing the effects of certain hazards for the small but growing number of monohull installations.

The use of monohulls as offshore installations has been mainly supported by the use of existing oil tanker Classification and international ship standards (e.g. IMO) the International Maritime Organisation, for design, construction and in-service inspection. However, there are some significant differences between the operational and environmental conditions for trading ships and FPSOs. The Classification Societies have made considerable efforts to produce more specific guidance and rules for floating offshore installations i.e. *ABS*, (1996). Nevertheless, knowledge is still developing and it is important that marine standards are not too readily adopted by FPSO owners and operators without careful consideration of their applicability of these standards offshore and their verification.

The U.K's HSE OSD, (Helth and Saety Executive, Offshore Division) among others, quickly recognised that improvements could be made in the technical knowledge readily accessible to the industry relating to these monohull structures; also it was considered that for the same estimated performance standards variations in minor criteria could have important operating influence on the designed structure in the

field. To this end, the HSE OSD has followed a strategy of research and development activities that would advance the technical expertise base and by encourageing the development and availability of uniform Industry Codes, Standards and Guidelines. These aspect are described by: *Millar, J. L., and White,R. J.*, (2000).

1.3 Consequences of Fatigue Cracking

1.3.1 Requirements for Fatigue Damage Control

The increased number of fatigue related cracks found in oil tankers and converted FPSOs can be explained as follows:

- The trend of reducing ship scantlings based on detailed stress analyses and the increased use of high tensile steel have resulted in an increase of the general stress level. This increase of the stress level has in general not been balanced by improved detail design to cause a reduction of the SCF value for structural details in order to achieve comparable fatigue endurance.

- FPSOs operating on the North Sea experience the most severe loading with respect to fatigue failure.

- The presence of corrosion (general, pitting and grooving) in ballast tanks results in a reduction of the fatigue life of a structural detail

To avoid these durability related problems in the next generation of oil carriers and yet optimise structural weight, it is desirable to perform realistic fatigue analyses of critical structural details. It is also desirable to be able to perform realistic fatigue analyses of repairs to critical structural details in existing vessels. The accuracy of these analyses depends strongly on the representation of the long-term stress ranges and on the use of realistic S-N (Stress range - Number of cycles to failure) curves. The cyclic variation of the stress levels due to the sea environment and additional cyclic components such as loading - unloading is locally magnified by the geometric stress concentration factor (SCF) at hot spots.

This stress concentration factor is due to local changes in geometry resulting in an increased stiffness and consequently increased stress level. Additional stress increases due to the presence of a weld and weld surface imperfections result in the actual peak stress. For welded components the presence of the weld introduces an additional stress concentration, a change in the material properties and micro defects. In complex ship structural details with several hot spots the first fatigue crack will generally be found at the hot spot that has the highest stress concentration in combination with low fatigue strength.

In order to control fatigue damage a combination of improved detail design, improved load estimation procedures and well defined annual inspection and maintenance plan is necessary for FPSOs. An FPSO can typically produce oil for 2-3 Million US dollars per day, leaving possible production stops as a consequence of repair of fatigue cracks as a highly undesirable event.

1.4 Research Efforts

Due to the severity of the problem Class Societies, Shipyards, Universities and Owner/Operators to develop or improve the different components of the Fatigue problem have undertaken many research efforts. Some of these efforts are described in the following to demonstrate different approaches.

1.4.1 Definition and Validation of a Practical Rationally-Based Method for the Fatigue Analysis and Design of Ship Hulls

The Technical and Research Committee of the Society of Naval Architects and Marine Engineers (SNAME) sponsored a pilot project with the purpose of defining and validating an improved rationally-based method of fatigue analysis and design for ship hulls and to demonstrate its practicality.

The results of this project are summarized in *Owen Hughes and Paul Franklin*, (1993). The report stresses the necessity of a rationally based design process opposed to the traditional rule-based design. The proposed method can be reduced to four steps:

- Specifying a lifetime wave environment
- Generating a hydrodynamic model
- Calculating cyclic stresses
- Computing the resulting fatigue damage

1.4.2 Class Requirements and Design Guidelines

Due to the increase in fatigue failures most classification societies have developed guidelines for the fatigue strength assessment of ships and mobile offshore units and have established actual fatigue life analysis requirements as part of the classification rules. These rules and recommendations vary in the extent of the required analysis and the chosen approach. In the following some of these rules and recommendations are briefly discussed:

1.4.2.1 Lloyd's Register of Shipping (LR)

LR has developed an integrated multi-level Fatigue Design Assessment (FDA) system from three levels of analysis, namely Level 1, 2 and 3 explained in *LR*, (1996). The levels are organised in terms of ascending model complexity. Level 1 is intended as a conservative approach to improving the fatigue performance of structural details, and provides a qualitative measure of the fatigue strength.

Level 1 is applied in conjunction with either the Level 2 or Level 3 FDA procedure to confirm the fatigue performance by a quantitative analysis procedure. Critical areas are defined as locations, which due to stress concentration, alignment/discontinuity and corrosion have a higher probability of failure during the life of the ship than the surrounding structure. Critical locations are defined as the specific locations within the critical area that are prone to fatigue damage.

The procedural steps can be summarised as follows:

- Identification of the critical areas with respect to fatigue demand and construction;
- Identification of the critical locations within the critical areas;

- Comparison of the proposed detail design with the Level 1 recommended detail design Standard, and identification of the degree of detail design improvement required.

The S-N methodology has been selected as the most practical methodology for the purpose of a design oriented procedure. Due to the variety of ship structural details configurations, the hot spot stress approach has been considered to be a more suitable estimator than the nominal stress using a classification of structural details.

Since the local weld geometry may affect significantly the fatigue capability, notch parameters have been introduced to enable a more reliable estimate of the fatigue strength estimates as well as provide quality control criteria for the workmanship standard.

The hot spot stress methodology with normalised notch parameters has been implemented as a unified approach to estimate the fatigue strength characteristic of ship structural details.

1.4.2.2 American Bureau of Shipping (ABS)

ABS has published a set of guidelines for the fatigue strength assessment of tankers *ABS*, (1995). In this guide the fatigue life has to be calculated for a nominal vessel service life of 20 years and a long-term sea environment representative for the North Atlantic Ocean. The recommended procedure uses the Palmgren-Miner linear damage model and is based on the UK Department of Energy S-N curves in *U.K. Department of Energy*, (1990).

In the process of re-defining the ABS hull structure design criteria ABS has been developing fatigue assessment and design criteria. The revised criteria contain recommendations for the calculation of the total stress range based on individual stress components corresponding to primary, secondary, additional secondary and tertiary bending. Most important, ABS has introduced guidelines for the use of hot-spot stresses obtained through finite element analyses and has defined a recommended procedure for the assessment of a fatigue design stress based on one specific S-N curve for the use with these stresses.

1.4.2.3 Det Norske Veritas (DNV)

DNV has introduced fatigue control requirements in the DNV Ship Rules as of July 1991. The Fatigue requirements are summarized in *DNV*, (1998).

Fatigue design can be based on either of two methods:

- Fatigue life derived from S-N curves, including the first two stages of fatigue behaviour, crack initiation and crack propagation
- Fatigue analysis by fracture mechanics, then also including the third stage, final fracture

The DNV fatigue control requirements are based on the calculation of the allowable stress range. The derivation of the allowable stress range is based on the Palmgren-Miner Summation and assumes a long-term distribution of the stress ranges can be approximated by a *Weibull* or *Rayleigh Distribution* (***See Section** 8.9.1*).

The fatigue strength is represented by a single S-N curve derived from the *U.K. Department of Energy curves*, (1990) and requires the calculation of the local hot-spot stress concentration factor (SCF).

DNV has revised these fatigue control requirements. Special attention has been given to the definition of the S-N curve for the use with hot spot stresses.

1.4.2.4 Germanischer Lloyd (GL)

GL has issued completely revised fatigue strength requirements for hull structural elements in the *GL*, (1998) edition of the hull rules. A fatigue strength analysis is required for all structures, which are predominantly subjected to cyclic loads such as side framing and side longitudinals. The fatigue strength analysis may either be carried out on the basis of a permissible peak stress range for standard stress spectra or on the basis of a cumulative damage ratio (Palmgren-Miner).
The fatigue strength is classified using the design S-N curves defined by the International Institute of Welding (IIW). For standard welded connections the stress concentration factor (SCF) and the weld quality are recognized in the required curve

parameter. Details not included in the published catalogue of details can be classified on the basis of local stresses or by reference to published experimental work.

GL has developed a concept for the fatigue strength evaluation of ship structural details using stress concentration factors. A reference design S-N curve for the use with hot-spot stresses has been developed based on a notch stress approach and a catalogue of stress concentration factors for ship structural details has been developed, see *GL Catalogue of Details*, (1998), also *Petershagen, H., Fricke, W., Massel, T.*, (1991).

1.4.2.5 Bureau Veritas (BV)

The fatigue assessment procedure used by Bureau Veritas (BV) is based on the use of S-N curves and the (Palmgren-Miner) cumulative damage rule. It is demonstrated in *Beghin, D.,* (1991), where the fatigue behaviour of a typical structural detail of crude oil tankers made either of mild steel or of higher tensile steel is compared. The comparison is aimed at calibrating the procedure for assessment of fatigue strength set up by Bureau Veritas. The fatigue capacity of the structure is represented through the choice of an S-N curve. For the detail chosen for the comparative analysis the S-N curve is selected from the set of curves issued by the U.K. Department of Energy, (1990).

The selected S-N curve is used in conjunction with hot-spot stresses obtained through finite element analyses of the detail. The stress value is determined based on the extrapolation of the stress values at the centre of the last two elements to the hot spot. The calculation of the fatigue damage is based on the Miner cumulative damage model. Additional details can be found in *BV*, (1995).

1.4.2.6 Summary

Classification Societies have in recent years improved fatigue damage assessment requirements acknowledging that the calculation of the fatigue damage is important for design and repair assessment of structural details. All fatigue damage calculation procedures used are based on the use of S-N curves and the (Palmgren-Miner) cumulative damage model. The main difference between classification societies can be found in the choice of the stress location and the definition of the

procedure for the assessment of the fatigue design stress used for the calculation of the long-term distribution of stress ranges; where the type of stress used is directly linked to the choice of S-N curve.

1.4.3 Recent Specialised Research Activities

The side longitudinals of an FPSO permanently installed in hostile North Sea environmental conditions are subjected to a significant dynamic loading. During the last few years a considerable effort has been made to reduce the possibility for fatigue cracking of the connections between the side longitudinals and the transverse frames by improvement of the local geometry to reduce the stress concentrations. A number of finite element analyses of connections between side longitudinals and transverse frames of an FPSO have been performed by *Lotsberg, I., Nygard, M. and Thomsen, T.*, (1998), to improve the local design and achieve increased fatigue lives.

Further more full scale tests on side longitudinals have been presented in *Lotsberg, I., Askheim, D., Haavie, T.*, (2001), where a useful comparison of measurements and Finite Element Analysis are presented in *Rucho, P., Maherault, T., Chen, W., Berstad, A., Samnøy, G.*, (2001). Stress concentration factors have been derived for connections where stiffeners of the web frames are welded to the flange of the longitudinals. It is shown that symmetrical brackets are preferred when considering improved fatigue lives for these connections when the longitudinals are subjected to a dynamic pressure loading. Based on this a modified geometry for such connections have been proposed.

1.5 Aims of This Research

The principle aim of this research work is to examine the fatigue behaviour of FPSO structures and to develop a suitable method for the design analysis of fatigue lives for critical connections subjected to dynamic pressure loading. The work aims to study SCF evaluation methods, considering the effect of structural dimensioning of local connection details, and furthermore to carry out laboratory tests to validate the method. Based on this research, a fatigue assessment method for such connections is proposed. This research aims to provide a calibration method for S-N Curves required for typical fatigue sensitive details in FPSOs. It also intends to provide

improved information on the important link between S-N data and finite element analysis for fatigue life assessment using a linear cumulative damage formulation.

1.6 Outline of This Thesis

Following the introduction in this chapter, the FPSO philosophy, definition, and total building blocks are introduced in Chapter 2. The structural design of the City FPSO, including critical location areas, is developed using state of the art computational design tools in Chapter 3.

An area of particular interest is that of the FPSO structural analysis. This is introduced in Chapter 4 together with an engineering view of the determination of hull structural loadings and the application of finite element analysis to the hull girder. This chapter contains the global finite element analysis (primary analysis).

Chapter 5 presents the analytical procedures for the local finite element modelling (intermediate) of the FPSO structure and includes the fundamental principle of mesh convergence as the basis for accurate and reliable analytical results.

Chapter 6 describes the FPSOs local detail finite element analysis, introducing linear, non-linear, normal modes and buckling static analysis. This work leads to Chapter 7, SCF evaluation and analysis. In this chapter the stress concentration factor considerations are examined with particular emphases on evaluation using finite element analysis, as well as validation of results using theoretical, analytical and experimental techniques. Other related methods are also considered in detail and compared with the proposed method.

Chapter 8 documents the theoretical background for the causes and recognition of the fatigue phenomenon, together with the development and implementation of FPSO fatigue methods and analysis.

The Conclusions from the research work are presented in Chapter 9, where fatigue design recommendations are made. Suggested areas for future work and future theoretical study, together with ideas for possible future analysis and testing, are also presented in this chapter.

2. FPSO Technology

2.1 Floating and Subsea Production Systems

The exploration for offshore oil and gas resources began in the late 1800's. In 1896, an offshore well was drilled off the coast of California. These were drilled from piers generally 100 to 150 m long, some producing from as deep as 200 m of water. The 1938 discovery of the *Creole* field 2km from the Louisiana coast in the Gulf of Mexico marked the first venture into open, unprotected waters. The discovery well was drilled from a 20 by 90 m drilling platform secured to a foundation of timber piles set in 4 m of water.

In the search for oil and gas in offshore areas, the oil industry has continually extended and improved drilling and production technology. The early schemes utilizing fixed structures tied to the seabed that evolved into the use of large steel jacket reinforced concrete production platforms standing in more than 300m water depth, (e.g. the modern jack-up platform illustrated in ***Figure 2-1***). In the early days the fixed platforms were located above the reservoir and wells drilled directly below the platform from the platform deck.

Figure 2-1 Jack-up Platform *(Courtesy of www.offshore-technology.com)*

The first subsea well was completed by *Shell-Oil* in 1960 in the Gulf of Mexico. It came on stream in early January 1961, marking the successful termination of years of intense

research and development, and the beginning of an identifiable subsea production industry and a new era. Subsea completions are now a commonly used option around the world with the total well on their way to the second thousand in number. Initially such wells, or group of wells, were tied back to the existing host platforms, but are increasingly now part of the production scenario for producing to floating production systems.

Stokes A. & Llewelyn D., (1996) point out that the driving necessities of cost reduction and the need to develop fields at ever increasing water depths has led to concepts other than fixed platforms including:

- Tension Leg Platforms (TLP) without Storage
- Floating Production Vessels (FPV) without Storage
- Floating Storage Units (FSU)
- Floating Production Storage and Offloading Vessels (FPSO).
- SPAR buoys. For Storage or for Production and Storage
- Deep Draft Semi-submersibles with Storage and Offloading. (DDSS)

It was an FPS, a converted semi-submersible drilling rig that was used by *Hamilton Brothers* to produce the UK sector's first oil from the *Argyll* field in June 1975. *Petrobras* then adopted the FPS concept in the Brazilian sector and in 1985 an FPSO was used off Africa. But it was not until 1993 that the concept of floating production really took hold as illustrated in ***Figure 2-2***.

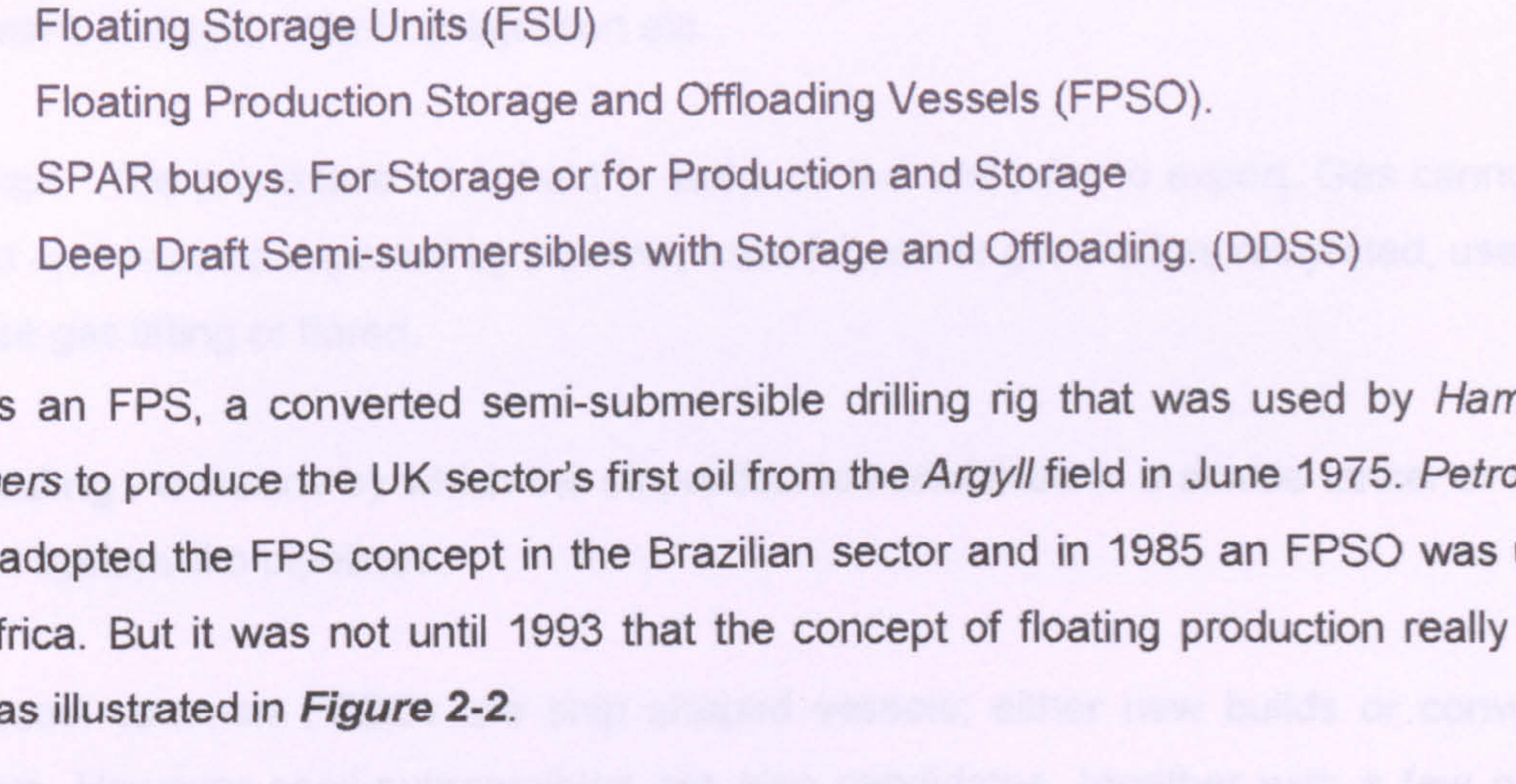

Figure 2-2 Floating Production Systems - by Type 1980-2003 *(Infield Database)*

2.2 FPSO Definition

FPSO - is an acronym for Floating Production Storage and Offloading.
Wennesland J. M., (1995) explained these functions as:

Floating - The body is in equilibrium when floating. This could include Semi-subs, Monohulls, deep draft semi-subs and spars, but does not include TLPs. Note that the motion characteristics of the deep-draft semi-sub and the spar permit the use of deck mounted "dry trees" whereas the first two types, have normally to deploy subsea completed "wet trees".

Production - The unit supports processing equipment to fully treat live well fluids, with separation gas compression, water injection, cooling and heating systems, water treatment, fuel gas, chemical injection etc.

Storage - The processed oil is held in tanks on the unit prior to export. Gas cannot be stored and must be exported by pipeline, used for power generation, reinjected, used for subsea gas lifting or flared.

Offloading - a means by which the oil product is transferred to a shuttle tanker or other export system like pipelines.

The most common FPSOs are ship shaped vessels; either new builds or converted tankers. However semi-submersibles are also candidates, together with a few others less known concepts as illustrated in ***Figure 2-3***.

***Figure 2-3 Terra Nova FPSOs** (Courtesy of Newfound-Land Offshore)*

2.3 Monohulls General Description

Monohull and ship shaped vessels (Monohulls for short) are characterized by a single hull or box shape structure, which may be a new build or the result of a ship conversion. These vessels form the mass of the FPSOs in operation to date. The earlier versions were converted crude oil tankers (e.g. converted tanker for the *Castellon* Field in 1976) and the design characteristics of the new build have inherited and evolved from the basic tanker design characteristics. ***Figure 2-4*** illustrates an in operation FPSO and a conventional shuttle tanker.

***Figure 2-4 Monohull FPSO** (Courtesy of www.offshore-technology.com)*

The major variables in Monohull FPSO design are:

- Size or storage capacity of the vessel
- Mooring system
- Hull material
- New build or conversion

The required storage capacity and sea keeping performance generally dictate the physical size of a Monohull FPSO. The dimensional constraints result from the allowable ratios between the principal dimensions considering basic unit strength and sea keeping characteristics. Within sea keeping are included motion behaviours, hydrostatic and hydrodynamic stabilities.

2.4 FPSO Total System Building Blocks

A topical example of the FPSO's total systems is illustrated in ***Figure 2-5*** with respect to a Monohull vessel. However, these are the main building blocks on the vessel: vessel hull including *Storage*, *Turret* and S*wivel deck*, based P*rocessing plant*, O*ffloading system* to shuttle tankers or export line and other units such as *Accommodation*, *Flaring*, etc.

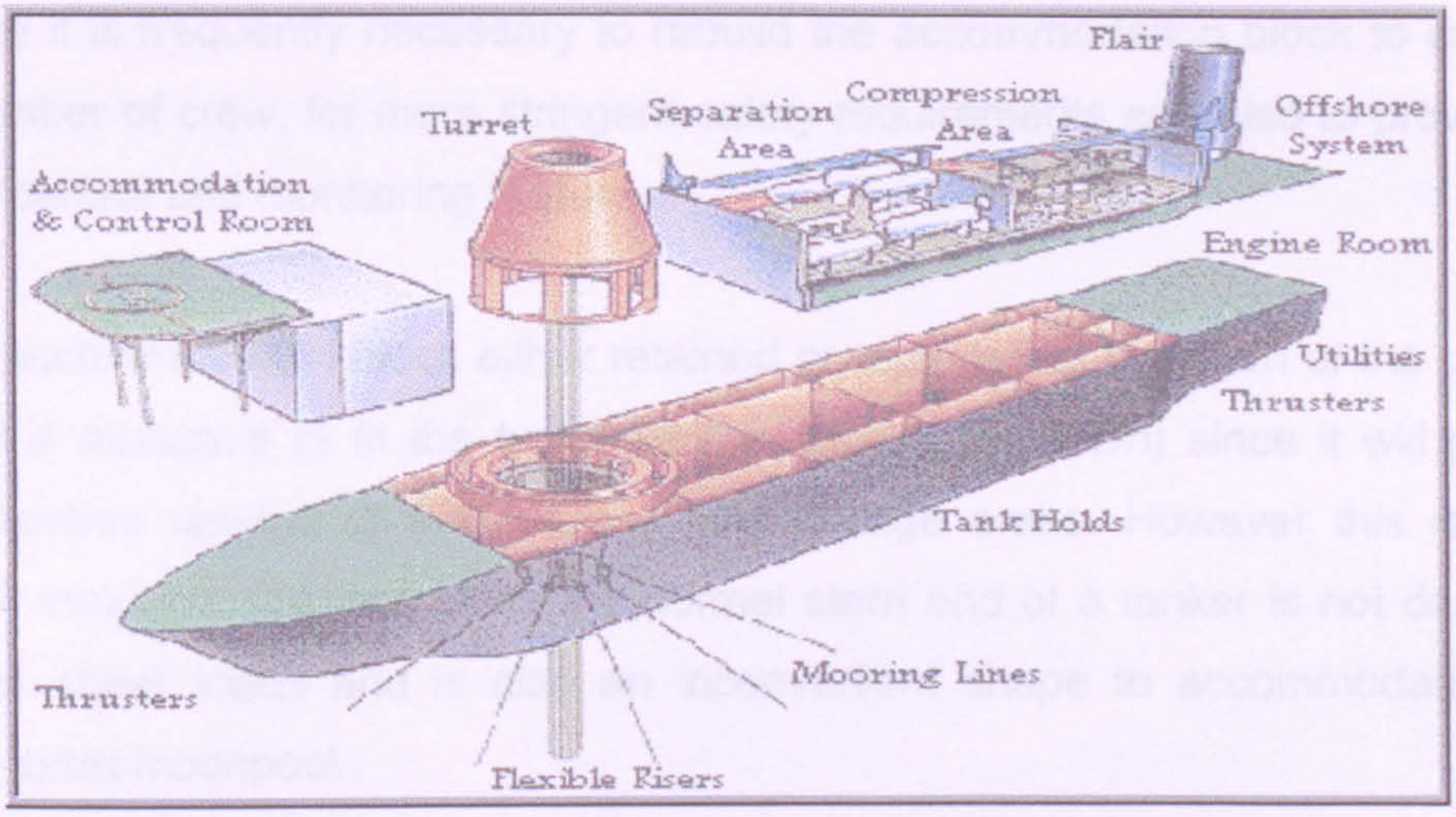

Figure 2-5 ***Petrojarl Foinaven FPSO*** *(Courtesy of Astano)*

2.4.1 FPSO Layout

2.4.1.1 General Arrangement Considerations

The primary factors governing the deck layout of an FPSO are:

- The process equipment must be located as close to midship as possible to minimise the effects of vessel motions.

- The accommodation block with the helicopter platform must be located clear of hazardous zones and ideally upwind of the flare stack.

- In the North Sea, export is always likely to be by tandem moored tanker and so the offloading facilities as well as the metering arrangements will be at the stern if the turret is near the bow (or at the bow if the turret is at the stern).

The application of these objectives makes a distinction between a converted tanker FPSO and a new-built FPSO.

2.4.1.2 Converted Tanker FPSO

In a conversion, it is desirable to make as much use as possible of the existing facilities (accommodation, pumping, power generation). Existing pumping and power generation facilities can often be integrated into the new production facilities. However, in practice it is frequently necessary to rebuild the accommodation block to cater for a larger number of crew, for more stringent safety requirements and also to provide large areas for control and monitoring features.

With the accommodation block either retained or replaced at the stern of the converted vessel, it is attractive to fit the turret aft (i.e. toward the stern) since it will place the accommodation upwind of the process and storage areas. However this is difficult, mostly for structural reasons since the normal stern end of a tanker is not designed to carry high shear loads and is also an inconvenient shape to accommodate a large diameter turret moonpool.

Generally the turret must be located at the forward end, where it can be fitted externally in a new specially constructed extension of the bow, or it can be fitted internally just aft of the collision bulkhead or in number one centre tank. For North Sea applications the second option "internal turret" is more suitable because of the severe motions experienced at the bow. In either case the accommodation block is located downwind of the turret and the process equipment as in ***Figure 2-6***.

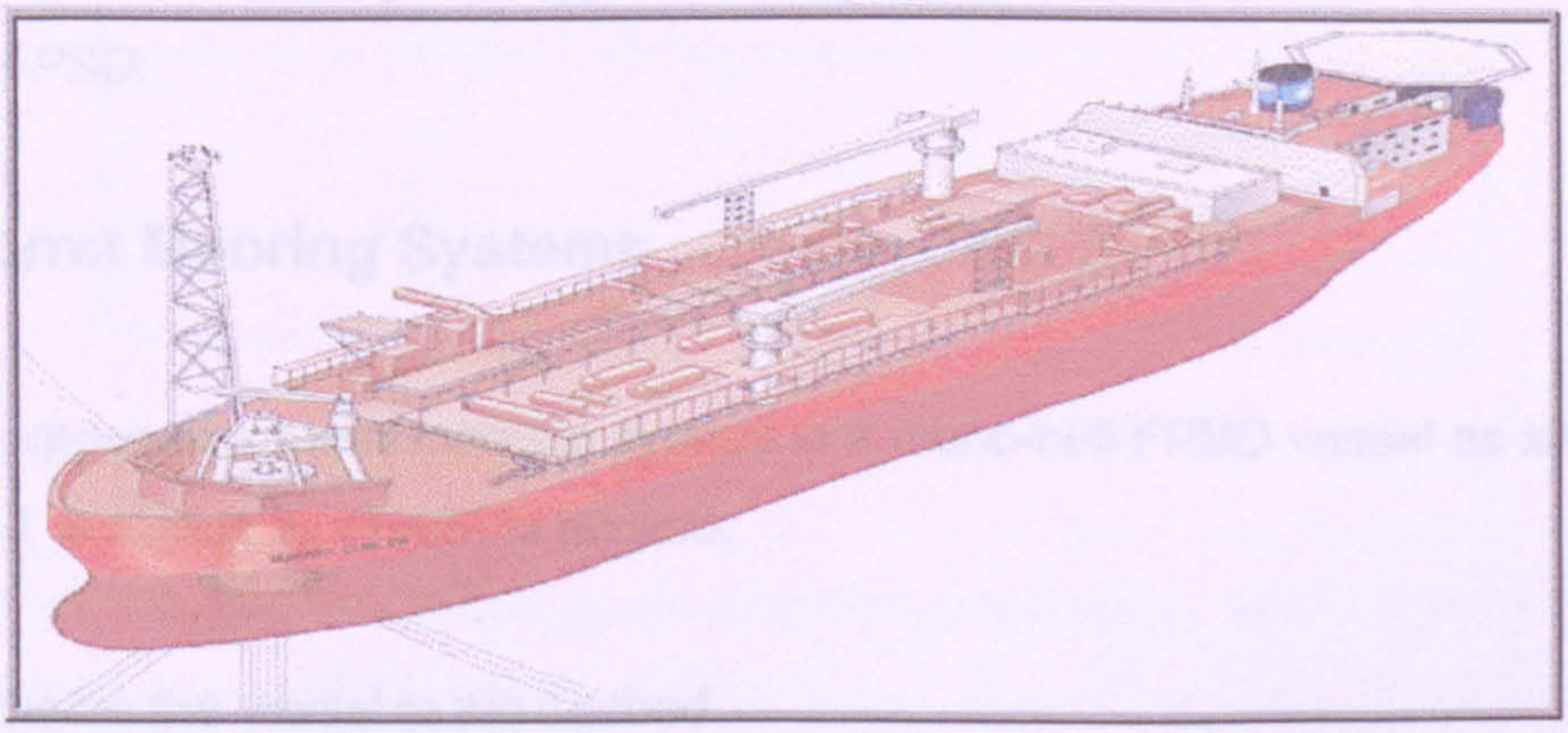

Figure 2-6 Curlew FPSO with AFT accommodation layout *(Courtesy of Maersk)*

2.4.1.3 New-Built FPSO

In a new-built FPSO placing the accommodation and helideck block at the extreme forward end with the turret aft, this position most easily satisfies the objectives above. This ensures that the accommodation and control areas are upwind of all hazardous functions: *turret, process equipment and flare*. This arrangement has generally been adopted on all early new-built FPSOs, for example: ***Figure 2-7*** *the Golar-Nor Petrojarl, BP Seillean, Kerr McGee Gryphon A.*

Figure 2-7 Petrojarl FPSO *(Courtesy of Golar Nor)*

However, more recently, the reverse arrangement with the accommodation at the stern end has also been considered and following a thorough assessment of the risks involved, has been accepted. Typical examples are: *BP Schiehallion FPSO, Shell Anasuria FPSO.*

2.4.2 Turret Mooring Systems

The purpose of a turret mooring system in a mono-hull FPSO vessel as identified by *Moksnes J. & Naess T.*, (1995) is twofold:

- It moors the vessel to the seabed
- It links the vessel to the subsea wells via the flexible risers.

Different types of turret mooring systems exist which satisfy these two requirements and it is convenient to split them into two groups:

- External turret mooring systems
- Internal turret mooring systems

2.4.2.1 External Turret Mooring Systems

The turret is mounted externally to the hull of the vessel either at the bow or at the stern. In its simpler version the turret is secured to a cantilever beam extending from the main deck of the vessel. Consequently the bearing arrangement is located above water and both the mooring lines and the risers are also attached above water. The advantages of this turret are its simplicity and minimum requirement for integration into the hull of the vessel; hence it's low cost.

Its main limitation is linked to the requirement to provide sufficient cantilever extension length and height in order to avoid interference between the mooring lines and the bow or stern of the vessel. This in turn limits its application to shallow water depths and relatively mild environments. A typical example is the turret of the *Mubaraka* FSU (stern mounted turret, installed offshore *Sharjah* in 1993), illustrated in ***Figure 2-8***.

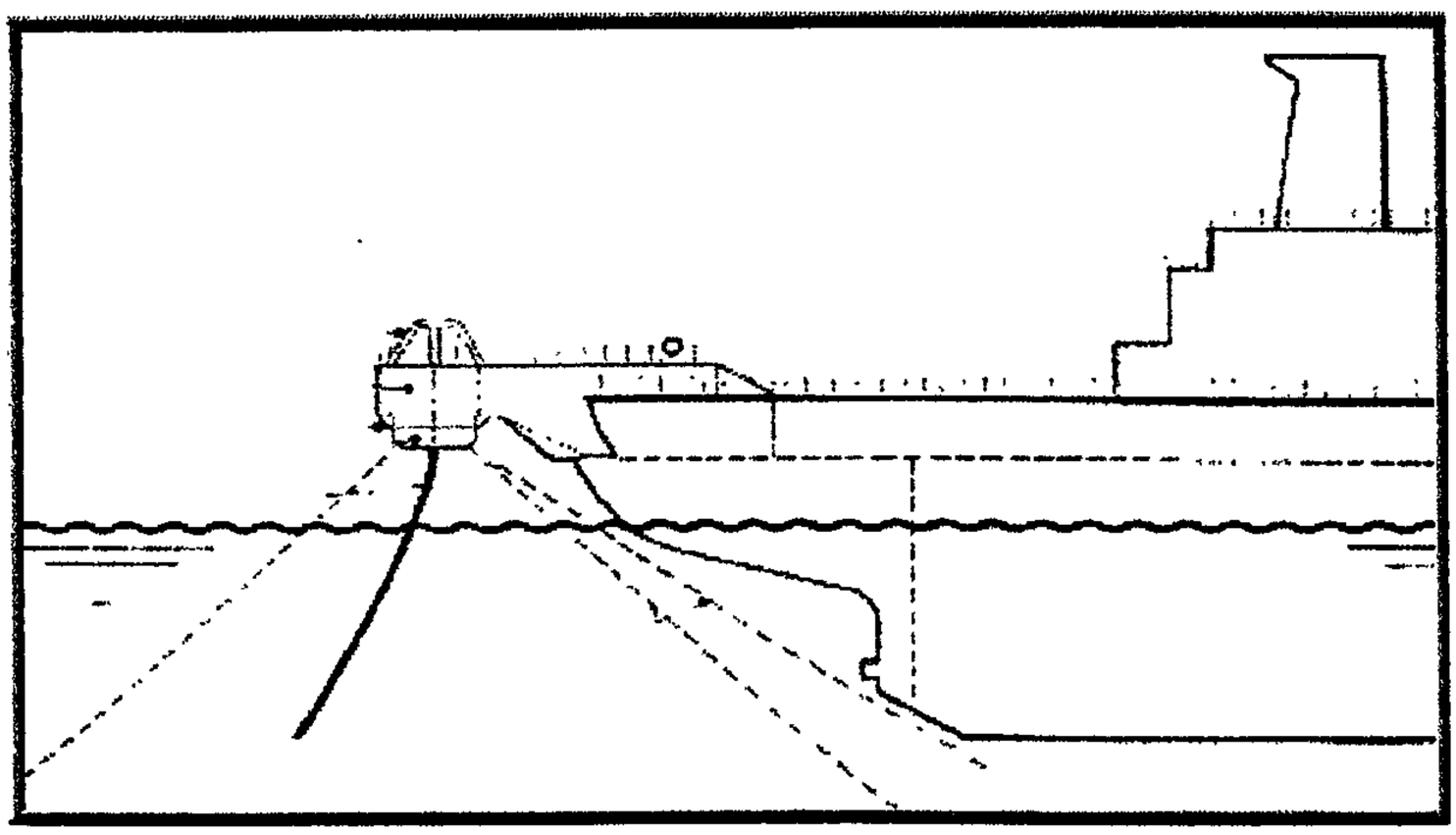

Figure 2-8 External Turret Design

A variation of this concept above is the bow-integrated turret, which can be secured to either one or two cantilever beams:

With one cantilever beam and one bearing arrangement this is integrated into the bulbous bow of the vessel, below water.

Typical example of this case is the turret of *Al Zafaraana* FPSO (installed in the Gulf of Suez in 1994) illustrated in ***Figure 2-9***.

Figure 2-9 External Bow Turret Design *(Courtesy of www.nortrans.com)*

With two cantilever beams and two bearing arrangements illustrated in ***Figure 2-10***; one beam extends from the vessel deck above water, the other extends from the vessel bulb below water and the turret extends over the full height of the vessel. Typical example of this case is the turret of the *Aquila* FPSO (installed in the Adriatic Sea, 850 m water depth).

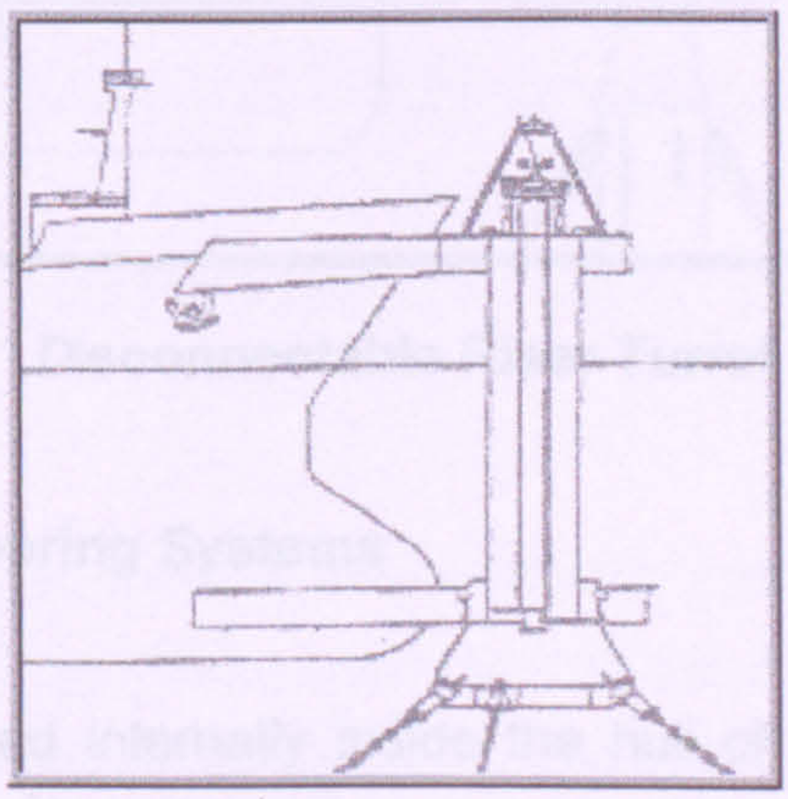

Figure 2-10 Two Cantilevers External Turret Design

In either case the mooring lines and the risers are attached below water and thus eliminate the risk of interference with the hull. This is achieved at the expense of a more complicated and costly vessel conversion and turret construction. The main limitations

of this concept are the diameter of the turret, which limits the space for fitting incoming product lines and its direct exposure to wave loads and slamming.
Hence it is again only applicable in mild environments, but it can be used in deep water.

Another variation of the first concept is the disconnectable riser turret mooring, which is specifically designed for environments prone to cyclones. The turret consists of a large buoyant riser column, which is suspended from a cantilever beam extending from the vessel deck. 'The mooring lines and risers are attached to this column and remain attached to it in all conditions. Disconnection takes place between the top of the column and the cantilever beam above a certain threshold in cyclone conditions.

A typical example is the turret of the *Wanea* and *Cossack* FPSO (installed offshore western Australia. 80m water depth, in 1995), illustrated in ***Figure 2-11***.

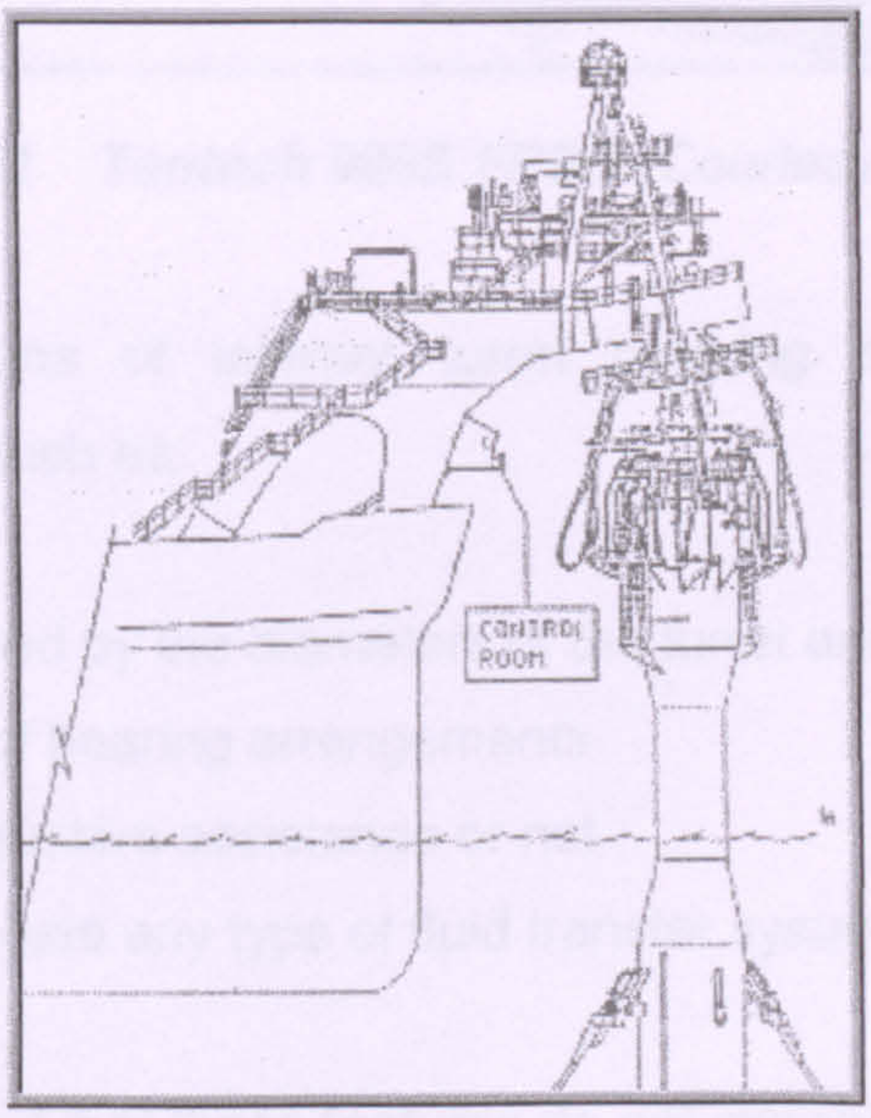

Figure 2-11 Disconnectable Riser Turret Mooring

2.4.2.2 Internal Turret Mooring Systems

The turret is mounted internally inside the hull of the vessel, normally in the forward half (i.e. between midship and bow). It consists of a large cylindrical structure rotating inside a cylindrical moonpool in the hull. The bearing arrangement can be mounted at vessel deck level above water, or inside the moonpool below water, or it can be a combination of both. The mooring lines and the risers are attached to the base of the turret, below water. The turret is integrated inside the hull of the vessel and is therefore protected from direct wave loads and the risk of collision. Other advantages

are its capacity for handling a large number of risers and its ability to withstand severe environments.

These advantages are gained at the expense of more complex turret structure and turret system integration inside the hull of the vessel, which can be seen clearly in ***Figure 2-12***, and consequently a higher cost.

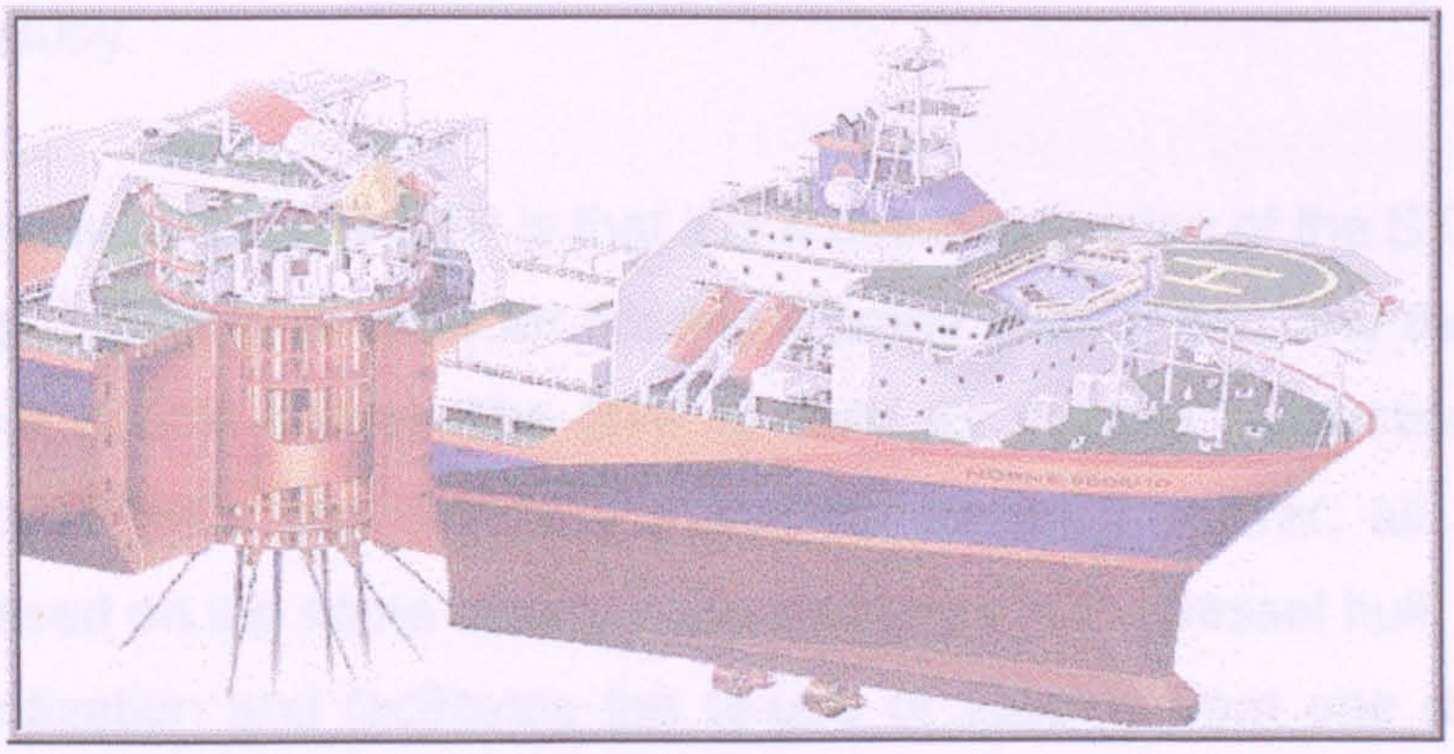

***Figure 2-12 Tentech 900S FPSO** (Courtesy of Statoil)*

There are several designs of internal turret mooring systems, which may be distinguished by features such as:

- Turret size as defined by the diameters of the turret and the moonpool
- Type and position of bearing arrangements
- Requirement for thrusters assistance or not
- Ability to accommodate any type of fluid transfer system

However, it should be noted that these features do not change the fundamental concept of the internal turret.

Disconnectable versions of the internal turret mooring system also exist. A large buoy located beneath the keel of the vessel characterizes the designs. When disconnected, the buoy submerges to a pre-determined depth approximately 35-40 meters below the surface where it stabilizes whilst still supporting the mooring lines and the risers. As before this design is for applications in cyclone prone areas.

Finally another variation of the disconnectable internal turret is the STP (Submerged Turret Production) illustrated in ***Figure 2-13***. This also consists of a buoy located beneath the keel of the vessel, but supporting only the flexible risers.

Increasing the capacity with respect to the number of risers that can be taken through the STP Buoy central turret is the focus at the moment. To achieve this, a larger buoy is being developed; which has a turret opening of 5000 mm compared to 2700 mm for the standard STP Buoy.

One of the key features of the STP is that it is a direct extension of the STL (Submerged Turret Loading). The STL is used for floating storage units (FSU) and therefore carries only a single or double swivel. The STP is used for floating production storage and offloading units (FPSO) and carries a multi-path swivel; however, all STL and STP systems are based on the same mating cone geometry in the vessel hull. This approach allows standardization and facilitates the re-use of vessels from one duty to another (e.g. FSU to FPSO).

Figure 2-13 Submerged Turret Production *(Courtesy of APL www.sol.no/apl/)*

The STP technology is simple, compact and flexible, making it suitable for a wide range of field developments and water depths, including for permanent weather independent operation, quick disconnect, deep water, shallow water.

Further details of mooring systems design and analysis can be fond in *Brown P. A. & Chandwani R.,* (1990) and in *Brown D. T. & Lyons J. G.,* (1995).

2.4.3 FPSO Processing Systems

With the increasing use of FPSOs as floating production facilities in the development of both marginal and now major oil fields West of Shetlands and Norway's *Asgard* field, the processing capability of these types of vessel has been rising steadily. The design throughput of the FPSO for the *Asgard* Field at 200,000 BOPD is now equivalent to some of the major fixed platforms such as *Scott / Nelson*.

BP's *Seillean* was probably the smallest FPSO in terms of production capability at around 15,000 BOPD through a single rigged riser. Since then the processing capability has steadily increased to around 50,000 BOPD for the likes of *Amerada Hess's AH001*. Now the latest generation of FPSOs for BP's West of Shetland fields like *Foinaven* and *Schiehallion* are over 150,000 BOPD. Floating production facilities are now a key piece of technology used to develop both marginal and major oil fields in deep waters.

Oxley M., (1997) emphasized that the main function of the processing systems illustrated in ***Figure 2-14*** and found on Floating Production Storage and Offloading units is to separate the reservoir fluids, oil, gas and water from each other, treat them where necessary and then either export or dispose of them efficiently and safely.

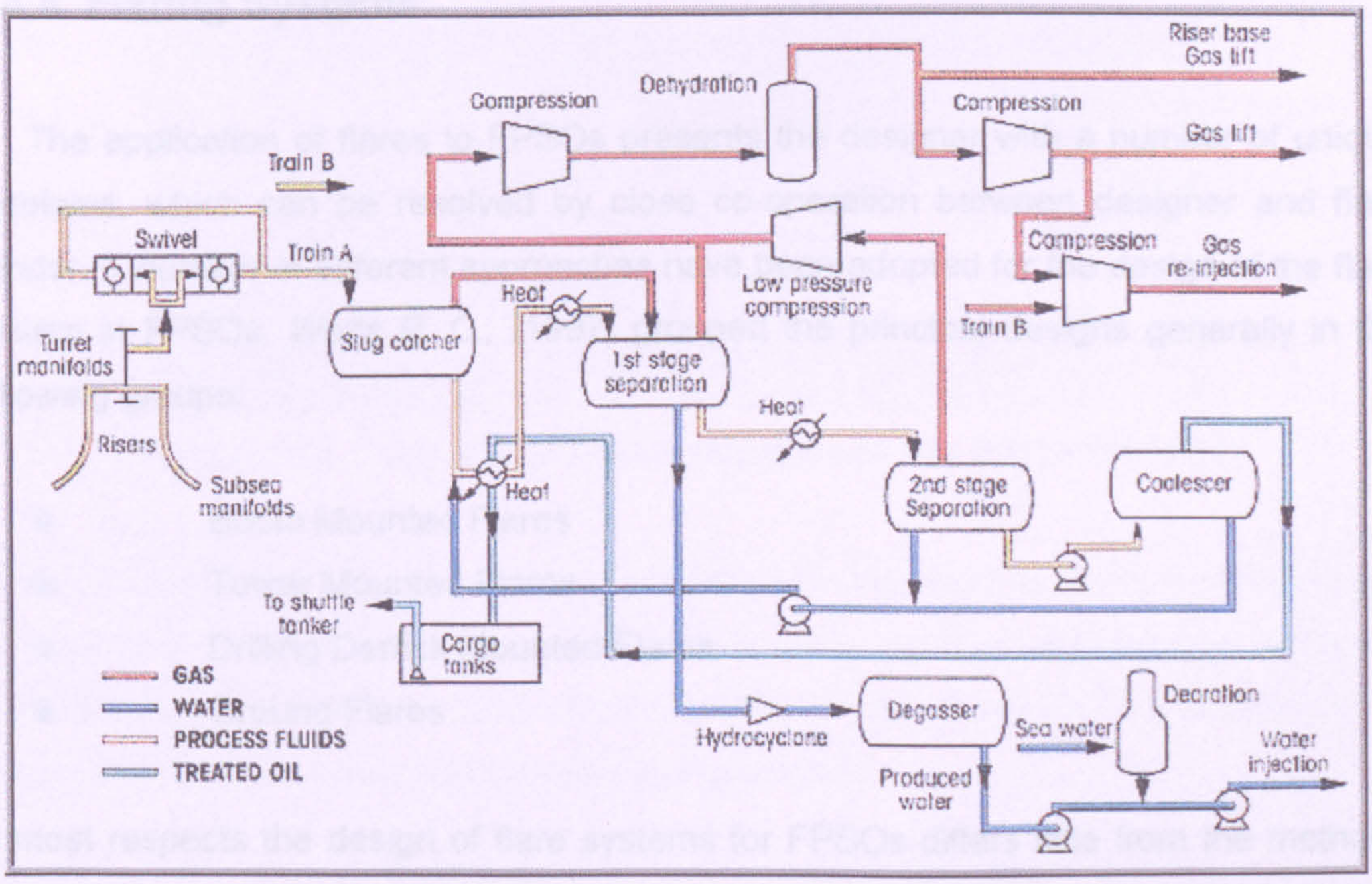

Figure 2-14 Processing Systems Block Diagram *(Courtesy of www.offshore-technology.com)*

Monohull FPSOs are capable of handling large topside loads. Topside processing equipment can either be constructed with the hull as illustrated in ***Figure 2-15*** or installed separately as *Pallets or Modules*, which can be commissioned prior to installation on board.

Figure 2-15 Processing Unit Constructed with the Hull *(Courtesy of www.offshore-technology.com)*

2.4.4 Flaring Systems

The application of flares to FPSOs presents the designer with a number of unique problems, which can be resolved by close co-operation between designer and flare vendor. A number of different approaches have been adopted for the design of the flare system in FPSOs. *Watts P. C.,* (1997) grouped the principal designs generally in the following groups:

- Boom Mounted Flares
- Tower Mounted Flares
- Drilling Derrick Mounted Flares
- Ground Flares

In most respects the design of flare systems for FPSOs differs little from the methods and criteria used for fixed platform flaring. However there are a number of special considerations, which must be taken into account.

2.4.4.1 Radiation Constraints

While semi-sub based FPSOs can effectively be treated as fixed platforms; for radiation design there are a number of unique features of ship-based systems (Monohulls) which have been cited by *McMurray R.,* (1982) and must be addressed.

2.4.4.2 Continuous Flaring

The tendency to flare all associated gas is much more common with FPSOs, as these installations are rarely tied into gas export lines. Thus if gas re-injection is not fitted, all gas must be flared. While this is not a problem itself, it does mean that the thermal effects from the flare will be felt on a continuous basis. The principal impact of this will be the high resultant temperatures on equipment and the deck plates around the flare stack.

2.4.4.3 Weathervaning

Monohull FPSOs always "weathervane" around a fixed point to keep bow wind.

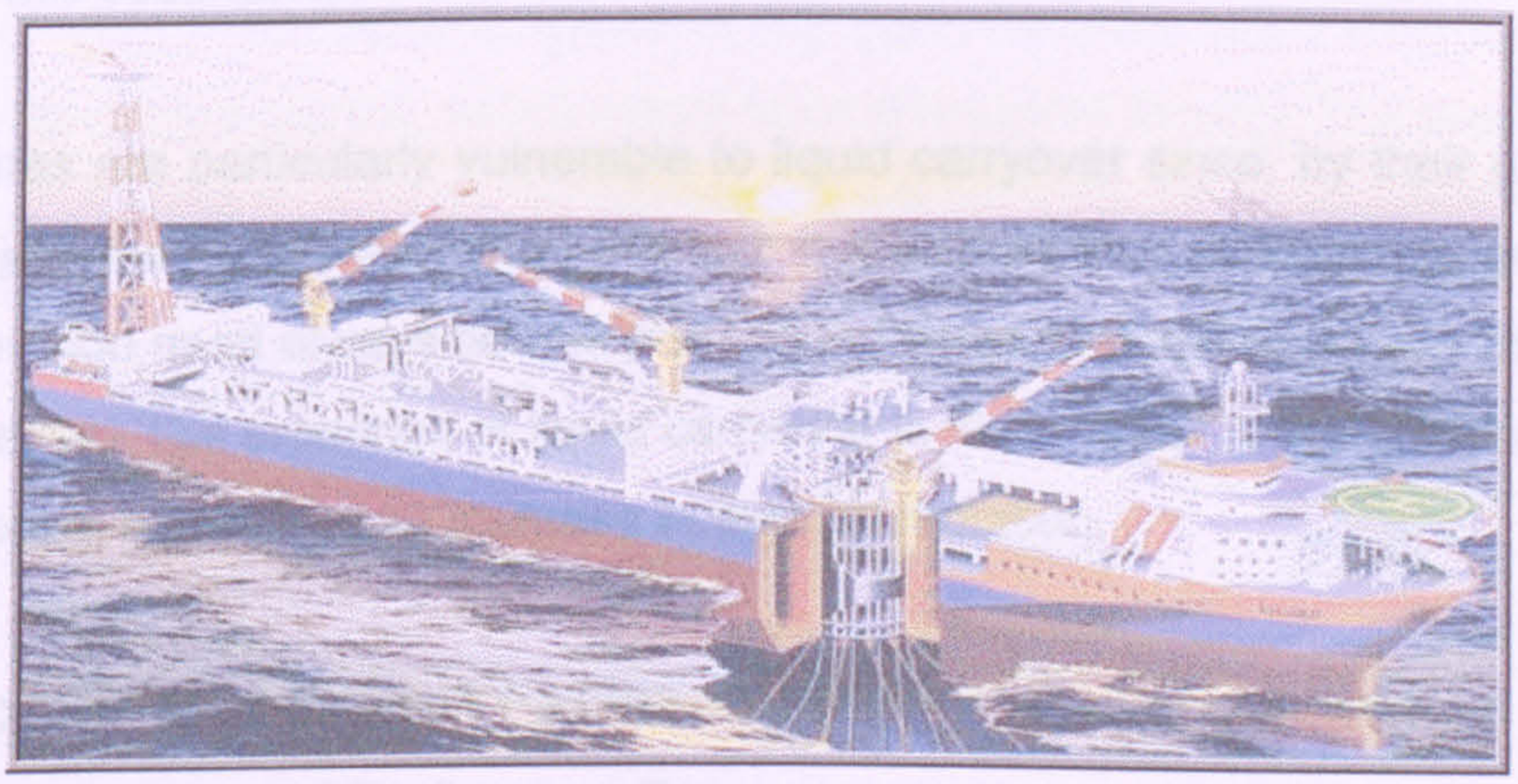

Figure 2-16 Downwind Flaring System on the ASGARD FPSO

This means that the flare is constantly subjected to wind from a very precise direction and the flare is either continuously blown away from the ship as illustrated in ***Figure 2-16***. Which is preferable or, more commonly, blown back along the ship resulting in an increase of radiation levels as illustrated in ***Figure 2-17***.

Figure 2-17 Upwind Flaring System on the Curlew FPSO (Courtesy of Maersk)

2.4.4.4 Liquid Carryover

Liquid carryover is a potential hazard for all oil producing installations, but the problem is more severe for Monohull FPSOs. The prospect of catastrophic liquid carryover causing burning liquid or flaming rain falling back onto the deck is unacceptable to operators and thus great care has to be taken in design and operation to prevent this occurrence.

Ground flares are particularly vulnerable to liquid carryover since, by their nature, they do not project the flame away from the ship but instead they confine it to an enclosed space. Provision must always be made in ground flares to catch liquid in a "drip tray" or a similar device. The presence of liquid carryover in flares leads to a significant increase in heat release, and hence an increase in thermal radiation.

2.4.5 Storage and Export Facilities

2.4.5.1 Oil Storage and Tanker Loading

Monohull FPSOs such as BP *SWOPS* often incorporate crude oil storage just below the top deck and thus very careful consideration needs to be given to limiting deck metal temperatures as far as possible in order to prevent undesirable heating of the stored crude oil.

The same consideration also applies to any shuttle tanker, which may be connected close to the flare and in fact even more care is required in such situations, since transfer hoses, and connections are directly exposed to heat radiation.

2.4.5.2 Export System Efficiency

Storage is readily available on a Monohull FPSO. Storage capacities of over 1.000.000 barrels are possible a company called ELF is considering (2,000,000 barrels storage for a vessel on the *Girassol* field, offshore Angola). Export can be either via shuttle tankers or pipeline. For the shuttle tanker option, offloading in a harsh environment could be either over the stern as illustrated in ***Figure 2-18*** or through a *Submerged Turret-Loading buoy* (STL) shown previously in (***Section 2.4.2***).

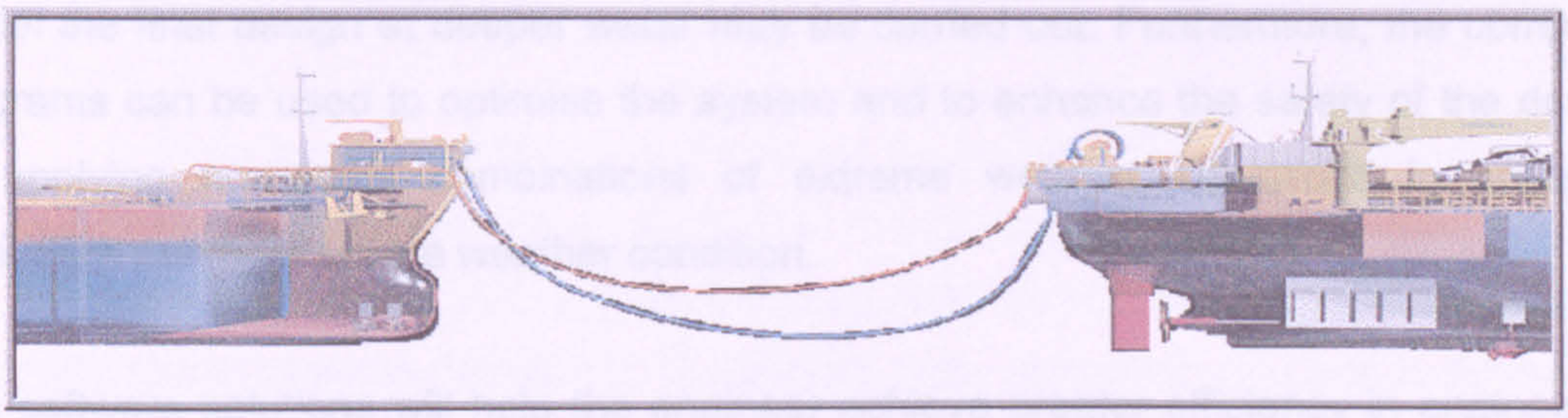

Figure 2-18 Offloading to a shuttle tanker

The ability to export the produced oil in a timely manner is critical to the overall efficiency of the FPSO, since a failure in the export system could lead to the FPSO storage being completely full, which would force production to stop. The selection of the system most suitable for a particular application will consider the following:

- Production rate
- Available storage
- Number and size of tankers and journey time
- Loading, connection, disconnection thresholds
- Equipment downtime
- Weather windows

The efficiency of the export system will be expressed in terms of "export uptime", which is a measure of the ability of the system to perform. "Export uptime" will be determined by a probabilistic study taking into account:

- Severe weather conditions
- Shuttle tanker breakdown
- FPSO off-take system breakdown

3. FPSO Structural Modelling & Design (*City FPSO 2000*)

3.1 State-of –the-Art Computational Design Tools

Computer programs on FPSO's structural design have been developed recently. By model testing of the systems at the available water depths the results of model tests can be tuned with the results of the computer program. By means of the tuned computer model the final design at deeper water may be carried out. Furthermore, the computer programs can be used to optimise the system and to enhance the safety of the design by applying numerous combinations of extreme weather conditions in order to determine the most severe weather condition.

The software solutions will help the engineer achieve greater efficiency in engineering and reduced costs in construction and operation of marine structures, which meet the requisite standards for quality, safety and reliability.

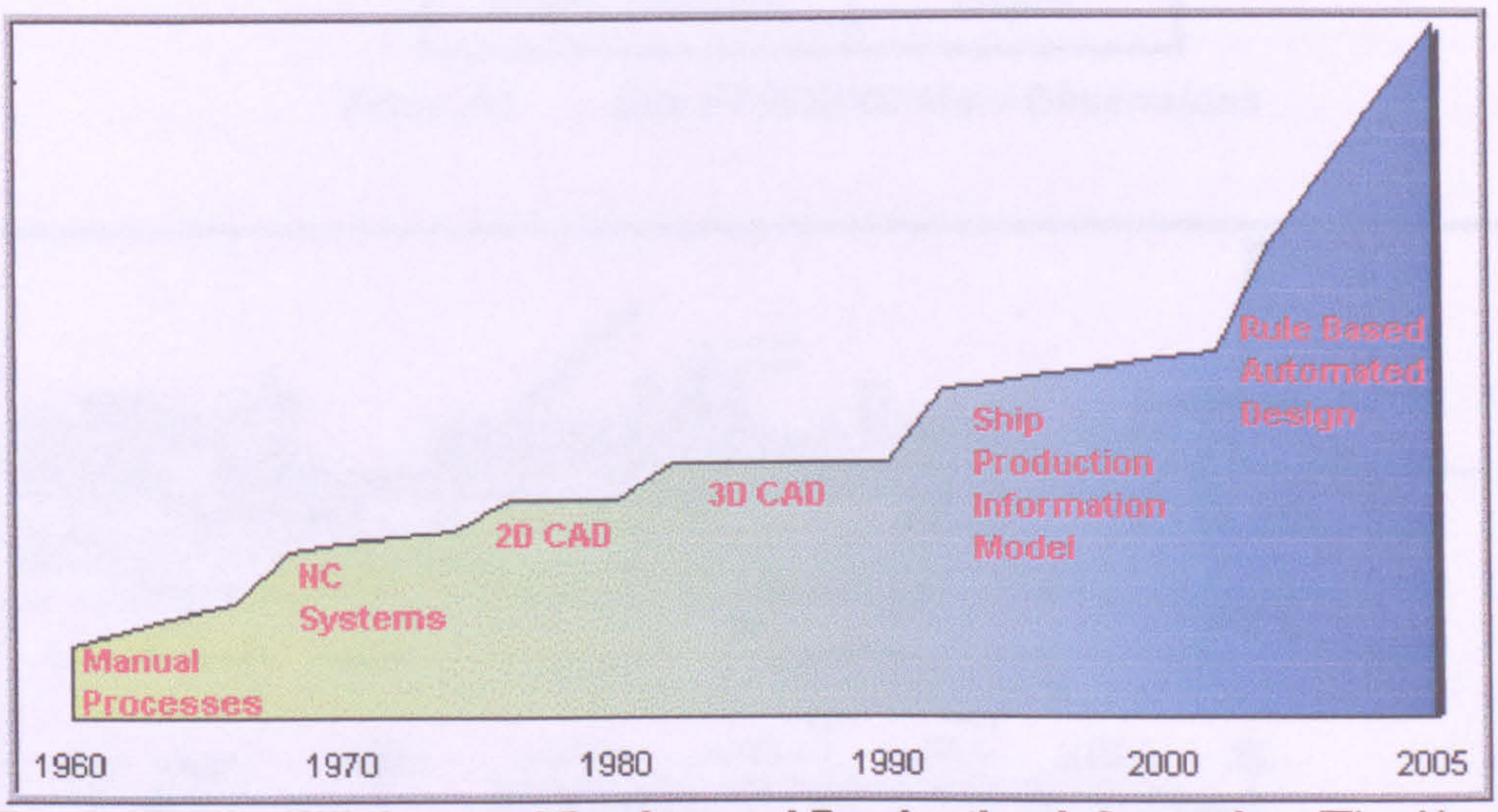

Figure 3-1 *Efficiency of Design and Production Information (The Naval Architect Oct. 97)*

Figure 3-1 gives an indication of the mounting use of information technology in shipbuilding field. IT development is a crucial part of the shipbuilding industry, where it has been criticised for failing to exploit the potential of information technology, but is determined to catch up specifically in the area of data exchange.

There are some noticeable joint initiatives from Classification Societies, particularly toward the development and implementation of electronic data exchange and management architecture, with a twofold function:

- To allow the exchange of key shipbuilding data during the initial design stage,
- To enable this data to be re-used and enhanced for survey, maintenance and repair purposes throughout a ship's lifecycle.

3.2 General FPSO Structural Design

In an initiative to design an FPSO for the purpose of this research, a complete design procedure conducted using the Classification Societies up-to-date rules; consequently all the scantling of the proposed structure has been completed for the City FPSO 2000 shown in ***Figure 3-2***. The vessel's main particulars' are given in ***Table 3-1***.

Length B.P.	265 (m)
Breadth, Moulded	45 (m)
Depth, Moulded	25 (m)

Table 3-1 City FPSO2000 Main Dimensions

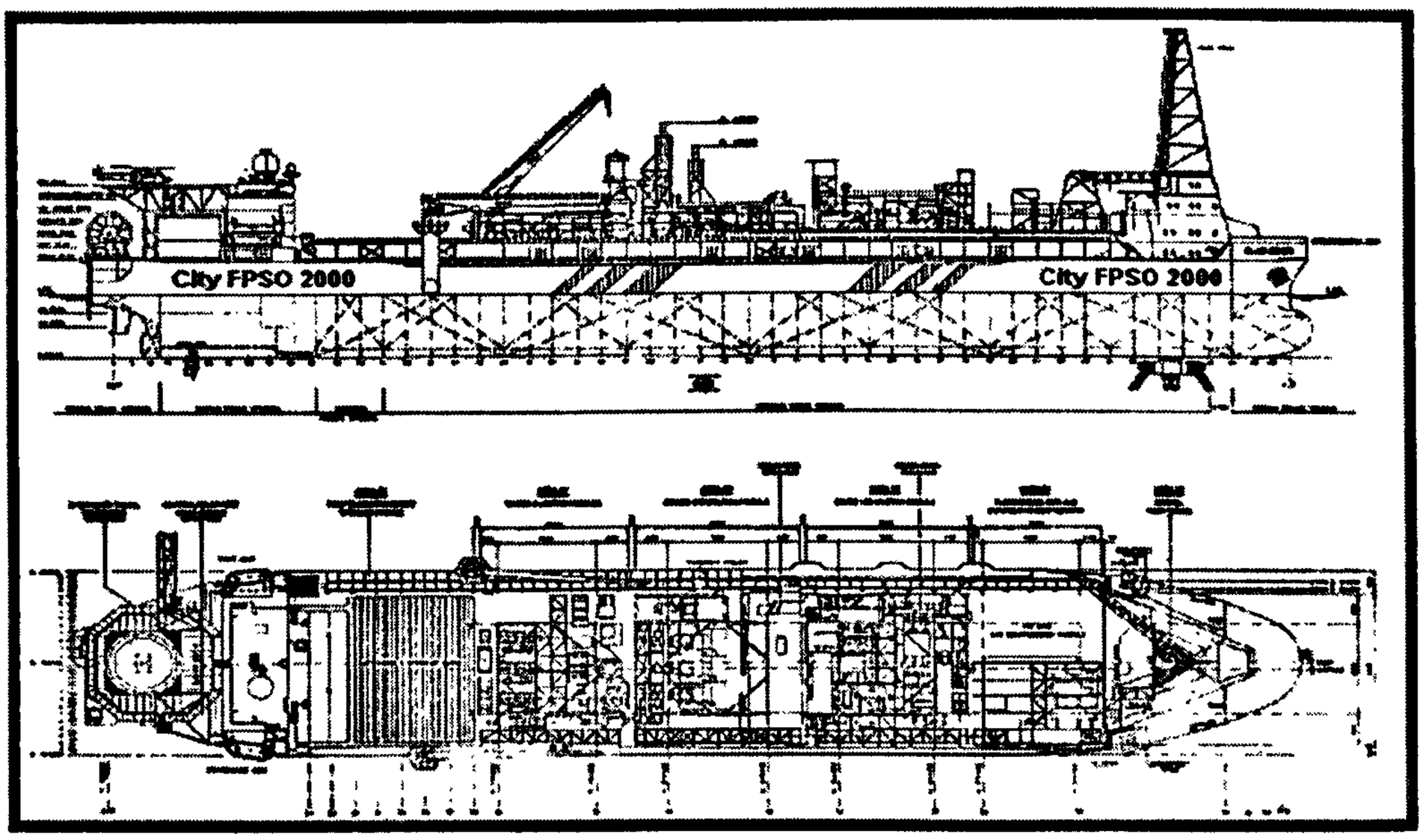

Figure 3-2 Schematic of City FPSO 2000

3.2.1 Modelling of Hull Form Geometry

This will in effect be the Lines plan which prepared at the time of the basic design, to give the required capacity, displacement, and propulsive characteristics. The lines plan is a drawing, to a suitable scale of the moulded lines of the vessel in plan, profile, and section.

Transverse sections of the vessel at equally spaced stations between the after and forward perpendiculars are drawn to form what is known as the body plan. Usually ten equally spaced sections are selected with half ordinates at the ends where a greater change of shape occurs.

A half transverse section only is drawn since the vessel symmetrical about the centre line, and forward half sections are drawn to the right (i.e. centre line) with aft half sections to the left.

Figure 3-3 and ***Figure 3-4*** illustrates typical FPSO's body plan, profile plan and half breadth plan views respectively.

Preliminary body plans are drawn initially to give the correct displacement, trim, capacity, etc., and must be laid off in plan and elevation to ensure fairness of the hull form. When the final faired body plan is available the full lines plan is completed showing also the profile or sheer plan of the vessel and the plan of the water-line shapes at different heights above the base.

The lines of the lateral sections in the sheer plan as indicated are referred to as "Bow lines" forward and "Stern lines" aft. Bilge diagonals may be drawn with "offsets" taken along the bilge diagonal to check fairness.

When the lines plan is complete a compiled "table of offsets" that is a list of the half breadths, heights of decks and stringer, etc, is prepared at each of the drawn stations. These "offsets" and the lines plan are then passed to a computer centre for full-scale fairing. It is to be ultimately used for ship stability, water resistance, manoeuvring, etc, which is out of the scope of this work.

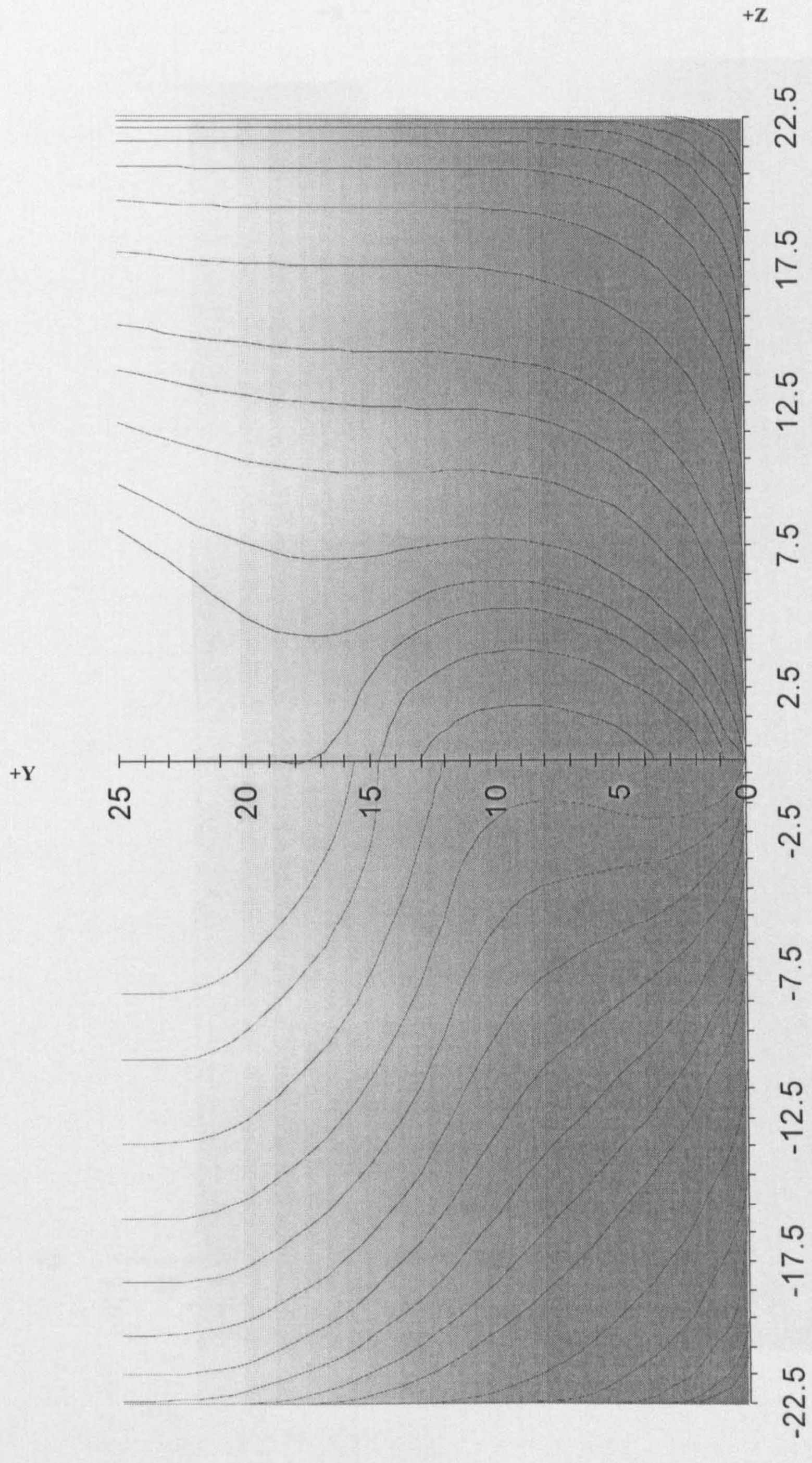

Figure 3-3 City FPSO 2000 Body Sectional Plan

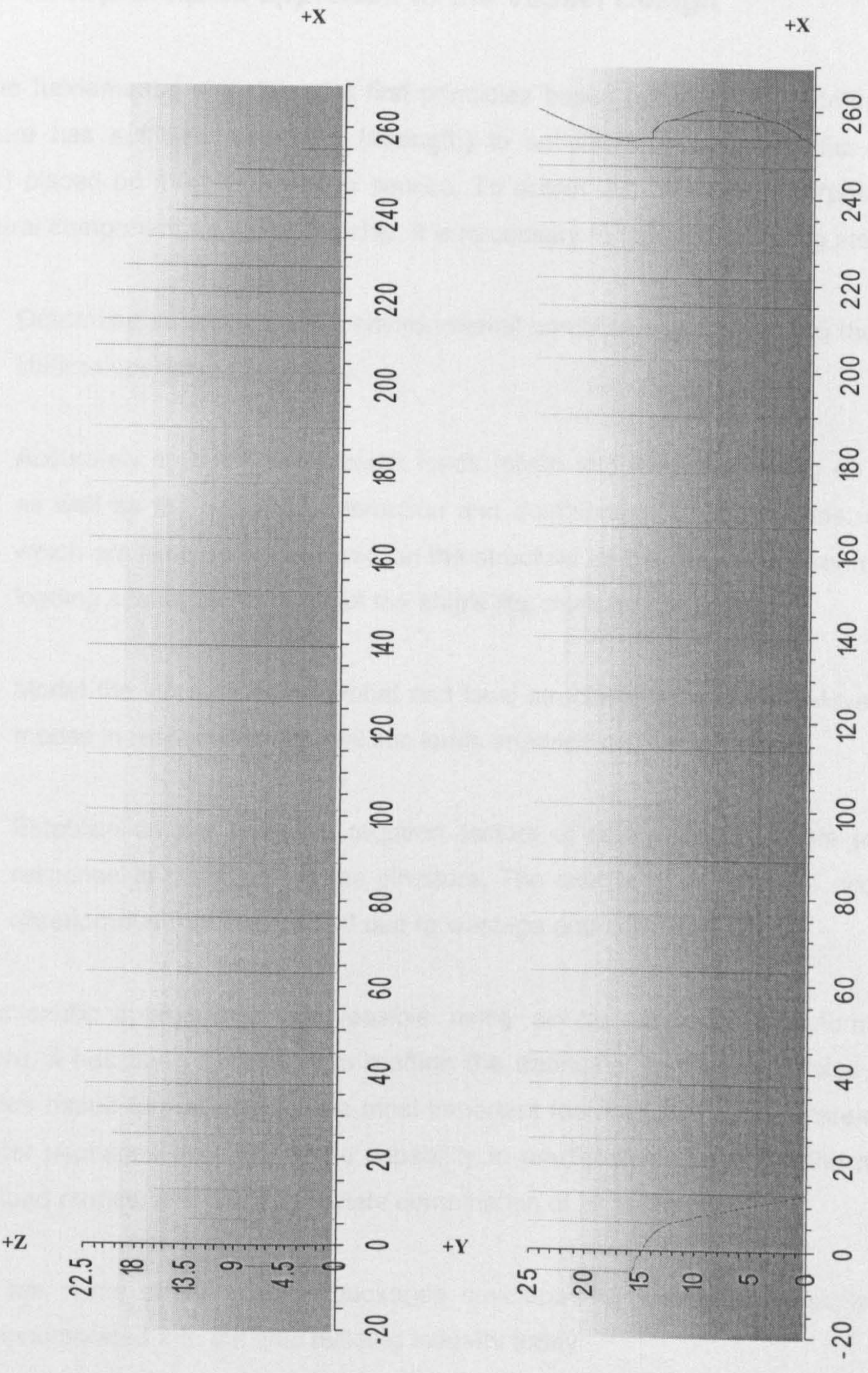

Figure 3-4 City FPSO 2000 Profile and Half Breadth Plan

3.2.2 First principles approach to the Vessel Design

The fundamental objective of a first principles based approach is to determine if a structure has sufficient capability (strength) to satisfactorily withstand the demands (loads) placed on it for its intended service. To obtain this "fitness for purpose" of any structural component, or the entire ship, it is necessary to take the following steps:

- Determine suitable realistic environmental conditions appropriate to the nominal lifetime operation of the ship.

- Accurately establish the realistic loads (static and dynamic) acting on the ship, as well as the expected interaction and combination of those loads. All loads, which are likely to be imposed on the structure by the natural environment in all loading scenarios, throughout the ship's life, must be considered,

- Model the strength of the global and local structures to resist all relevant failure modes in response to the realistic loads imposed on that structure.

- Establish criteria to obtain required factors of safety for the failure modes, in response to the loads on the structure. The criteria must take into account the deterioration that is expected due to wastage and corrosion.

This scientific approach is not feasible using simple empirical rule formulations; therefore, it has been necessary to reaffirm the traditional prescriptive Rules in a first principles based format. One of the most important features of the new state-of-the-art computer packages available is the capability to predict dynamic loads, the maximum loads, load ranges, and the appropriate combination of all these loads.

These are some of the popular packages developed by classification societies and widely incorporated into the ship building industry today:

- **NAUTICUSHULL** by DNV (Det Norske Veritas) of Norway
- **SHIPRIGHT** by LR (Lloyds Register) of U.K
- **SAFEHULL** by ABS (American Bureau of Shipping) of U.S.A
- **PRIMESHIP** by NK (ClassNK) of Japan
- **POSEIDON** by GL (Germanischer Lloyd) of Germany

The main initial design steps integrated in some of these packages are threefold:

- Generation of the midship section geometrical model, which contains principal dimensions, structural configurations, and relevant geometric parameters

- Calculation of section modulus information for the ship

- Determination of the required minimum value for the longitudinal scantlings according to the classification society's rules; this includes the structure of bottom, inner bottom, side shell, deck, and longitudinal bulkhead for both plating and longitudinals. Furthermore the design pressure is calculated based on the rules, as will as the minimum thickness values required (e.g. the illustrated ***Table 3-2*** based on the DNV rules, which are embedded in the *Nautics Hull* Package).

BOTTOM STRUCTURES		Ship Id	City FPSO 2000	
L = 265 m		NS	NV-32	NV-36
PLATES:				
Keel plate	**(Min. breadth = 2125 mm)**	20.3	18.7	18.2
Bottom and Bilge Plate		15.6	14.4	14.0
Inner Bottom Plate: in holds below hatch, no ceiling		15.0	14.0	13.7
Inner Bottom Plate: in holds without ceiling		14.0	13.0	12.7
Inner Bottom Plate: in holds if ceiling is fitted		13.0	12.0	11.7
Inner Bottom Plate: elsewhere		13.0	12.0	11.7
STIFFENERS:				
Stiffeners on dbl btm floors and girders		10.0	9.4	9.2
Stiffeners on single btm girders		8.7	8.3	8.2
Longitudinals: bottom/ inner bottom		10.0	9.4	9.2
Transverse frames		10.0	9.4	9.2
GIRDERS:				
Double bottom				
Centre Girder dblbtm: up to 2 m above Base Line		16.6	15.4	15.0
Centre Girder dblbtm: above 2 m above Base Line		11.3	10.7	10.5
Side Girders and Floors		11.3	10.7	10.5
Single bottom				
Centre Girder sglbtm: up to 2 m above Base Line		16.6	15.4	15.0
Centre Girder sglbtm: above 2 m above Base Line		11.3	10.7	10.5

Table 3-2 ***Minimum Thickness*** *(DNV Nauticus Hull)*

3.2.3 Definition of Tanks Geometry

Following the definition of the principle dimensions of the ship, (L, B and D) Length, Breadth and Depth respectively as illustrated in ***Figure 3-5***, the Lines Plan described in (***Section 3.2.1***) is used to define all of the ship hull's boundaries.

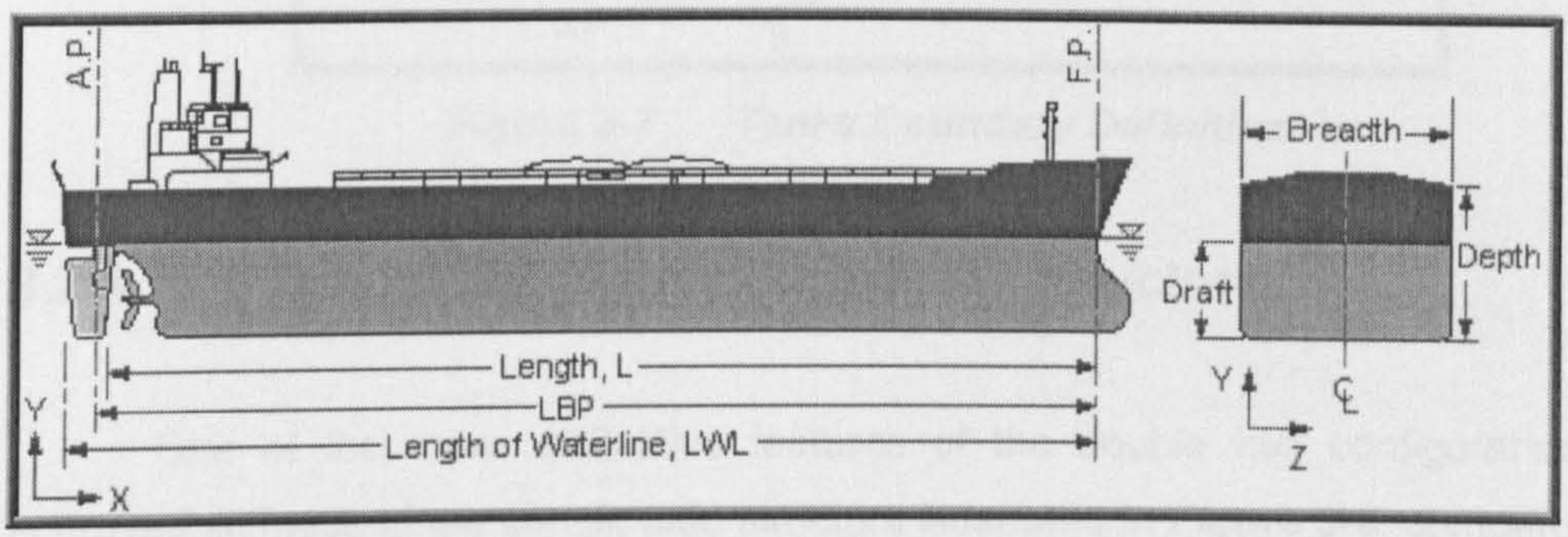

Figure 3-5 Ship Main Dimensions

The midship geometrical model (e.g. ***Figure 3-6***) is to be generated and the boundaries of the cargo tanks and ballast tanks are to be defined (e.g. ***Figure 3-7***) using a graphical user interface.

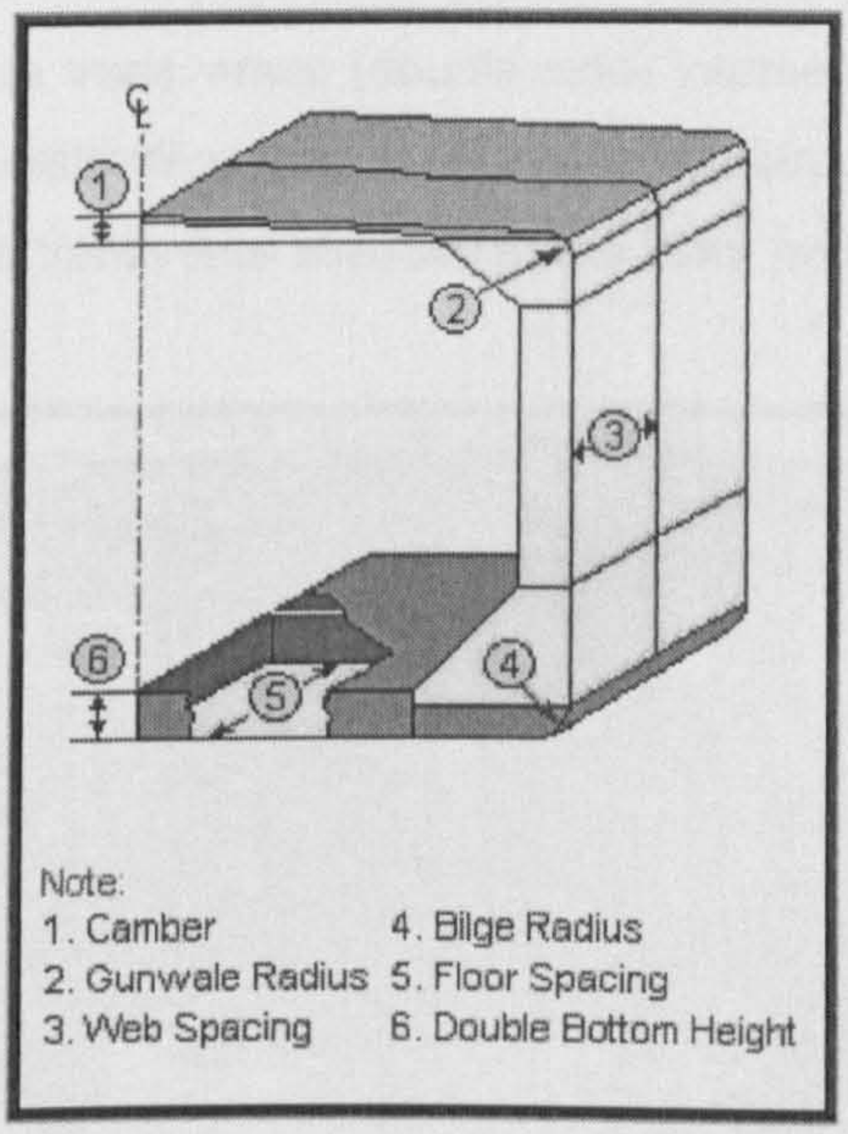

Figure 3-6 Midship Geometry

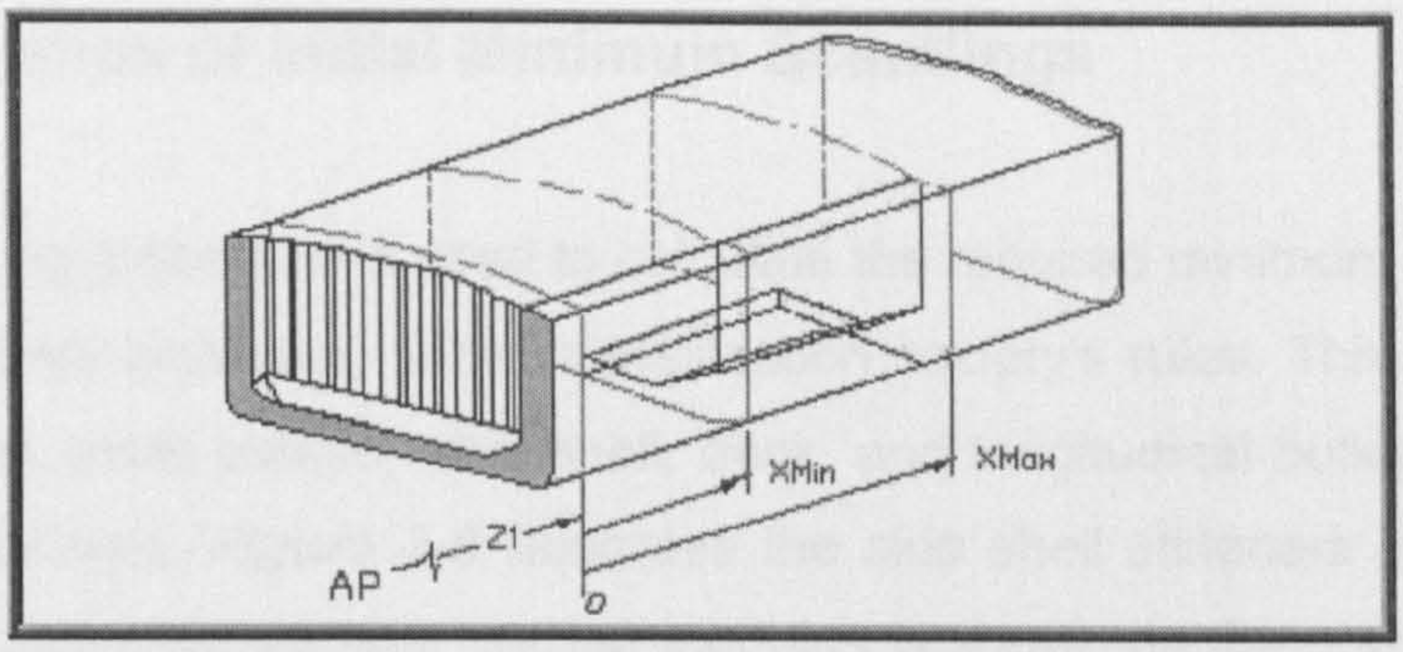

Figure 3-7 Tanks Boundary Definition

3.2.4 Stiffness of Transverse Supporting Structures

One of the more distinctive features of the double hull configuration is the improved stiffness of the double side structure illustrated in ***Figure 3-8***, compared to the side shell structure of single hull. In addition to the beneficial effects of increasing the horizontal hull girder section modulus and stiffness, it also provides relatively stiffer support to local longitudinal structures and transverse supporting members. Connections of supporting structures should be designed with caution; to prevent excessive stress concentrations noted by ABS in their rules guide *Steel Vessels*, (1997). This is especially important where deck transverses intersect with webs on longitudinal bulkheads, and where side transverses (double side) intersect with bottom transverses (double bottom). Another distinctive feature of double hull structure is the relatively large magnitude of compressive transverse stresses in the inner bottom.

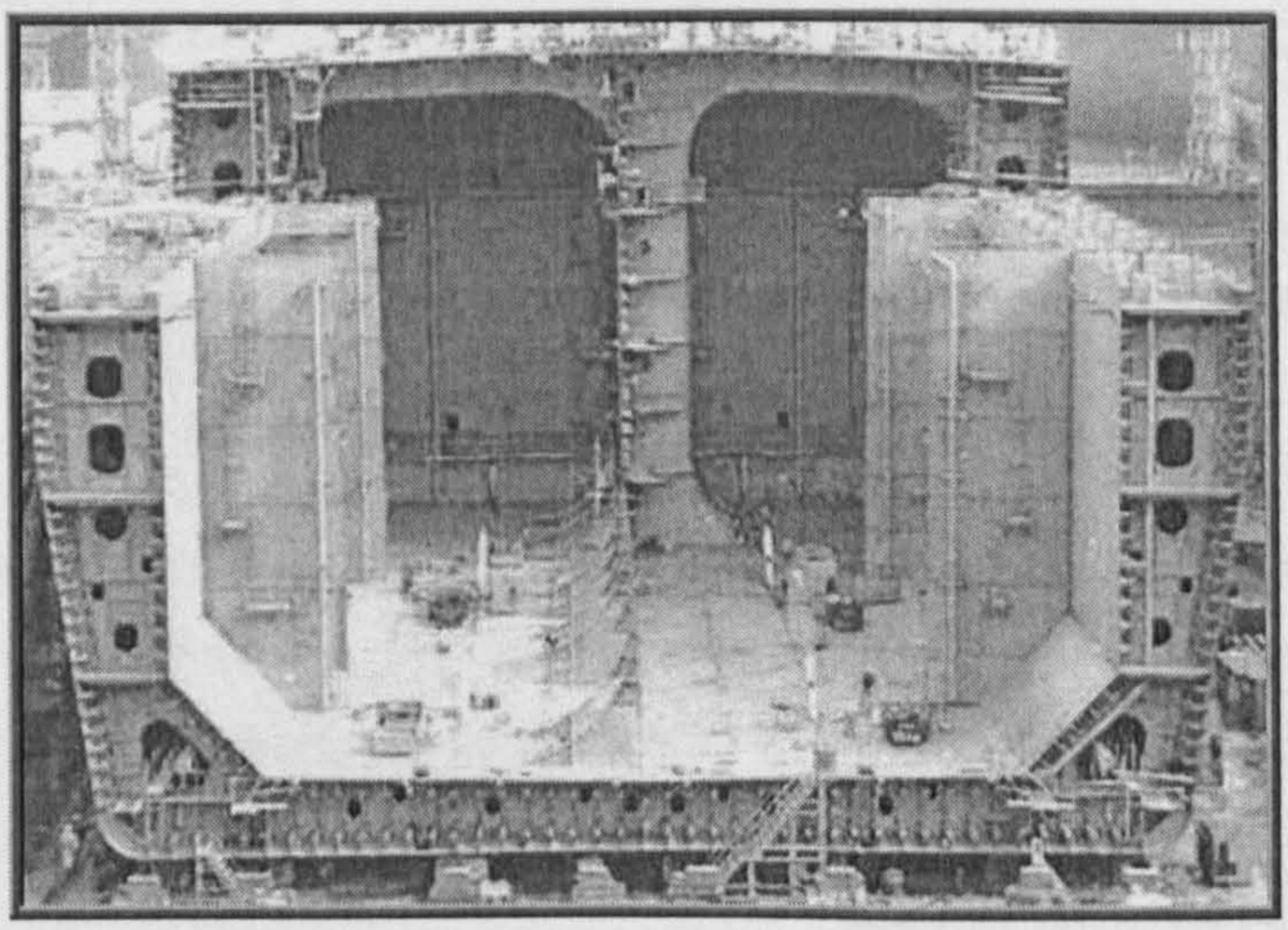

Figure 3-8 FPSO Midship Section Under construction *(Courtesy of www.offshore-technology.com)*

3.2.5 Determination of Initial Minimum Scantlings

This scantling procedure is used to calculate the required minimum value for the longitudinal scantlings according to the classification society's rules. This includes the structure of bottom, inner bottom, side shell, deck, and longitudinal bulkhead for both plating and longitudinals. ***Figure 3-9*** illustrates the side shell stiffeners scantling. For each section, the individual stiffener section modulus is shown on the graph along with the required section modulus at that location.

The selected section is highlighted on a midship section. On the graph, stiffeners that are at or below the minimum requirement are red while those that are above the net required section modulus are blue. The green line indicates the required section modulus.

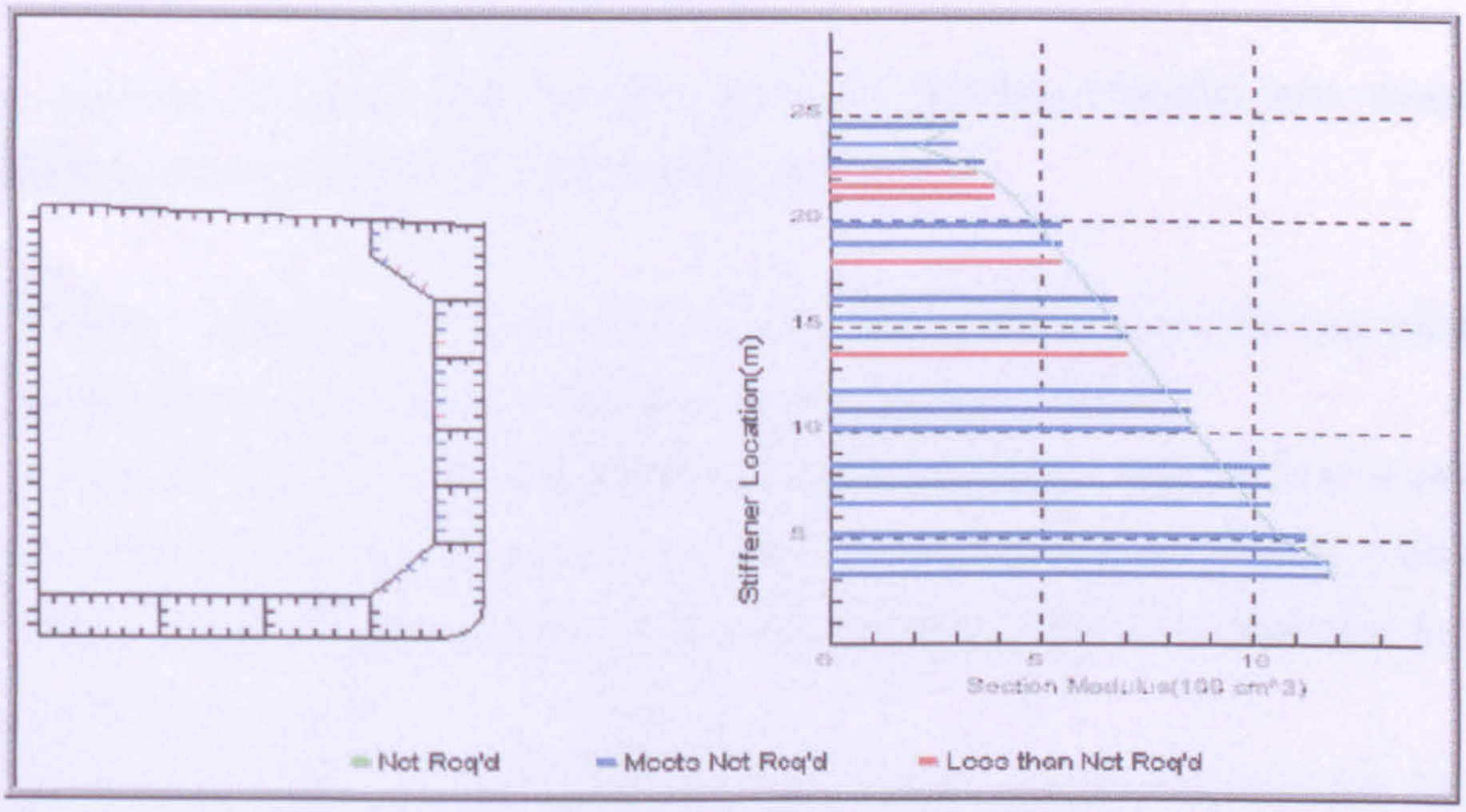

Figure 3-9 Net Required Section Modules vs. Net Offered Section Modules

(ABS Safehull)

The section modulus and overall properties of the structural members are to be calculated in the initial phase of the structural analysis. The classification societies assess the midship section modulus as illustrated in ***Figure 3-10***, for compliance with the hull girder strength criteria explained in the *ABS Steel Vessels*, (1997).

The individual longitudinal and transverse structural members are evaluated against the strength criteria, based on the nominal loads acting at each Location. This step of the process is repeated until the initial scantlings fully comply with the strength criteria for both local and hull girder strength.

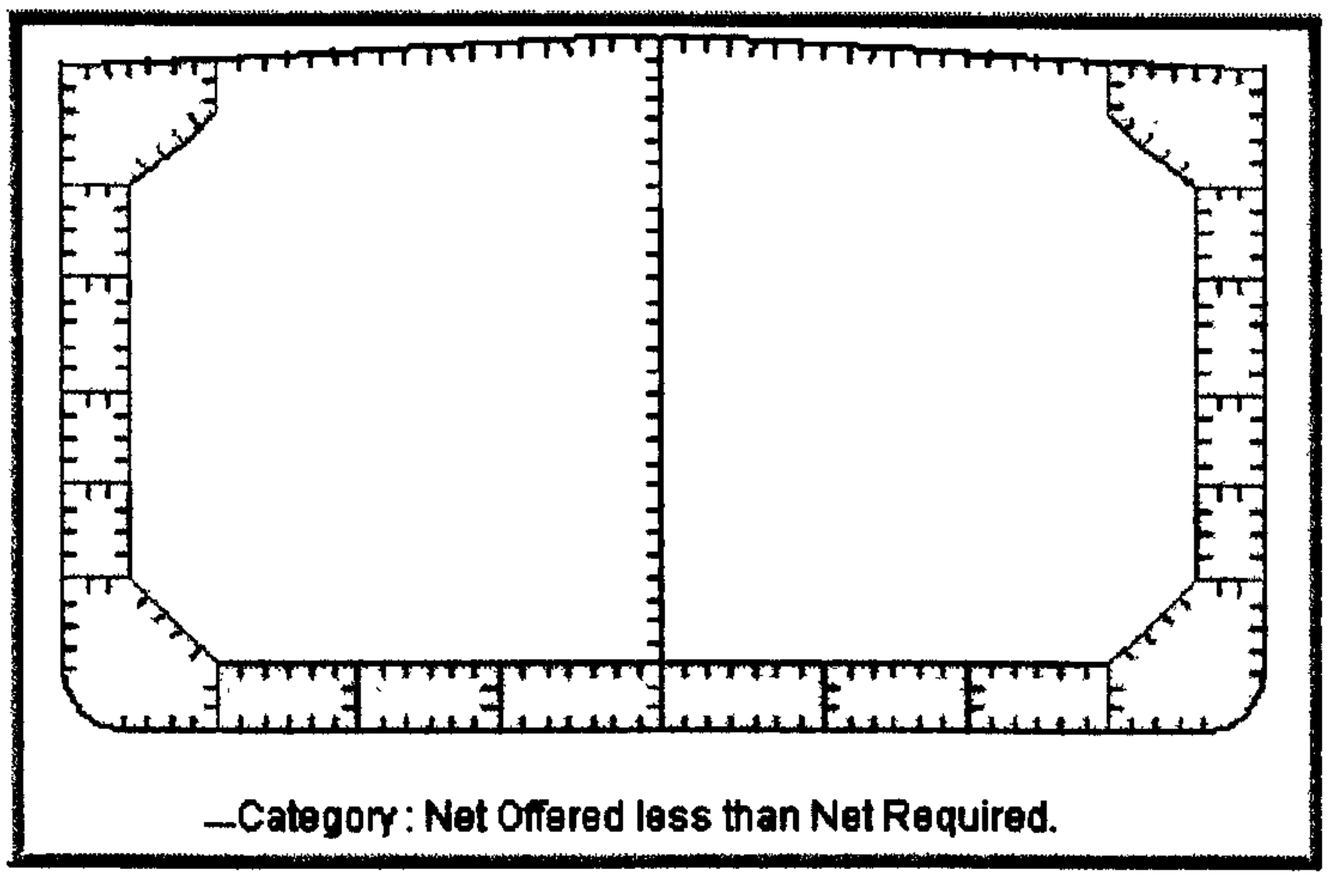

Figure 3-10 Global Profile View (ABS Safehull)

3.2.6 Materials for FPSOs Construction

It is common to divide the FPSO's structural building material into three zones hence these material zones can be identified as follows:

- ***Bottom Material*** of the hull girder's lower flange (taken from the keel plate to the higher of the upper turn of the bilge or inner bottom height).
- ***Side Material*** of the middle section of the hull girder. This section is measured from top of the bottom zone to the lower edge of the sheer strake. If there is no sheer strake, it is measured to the highest plate in the side shell (excluding the gunwale if it exists).
- ***Deck Material*** of the hull girder's upper flange. It extends from the top of the side zone to the upper deck.

Mild steel is used through out the structure of conventional tankers, but higher tensile steels been introduced in the more highly stressed regions of the modern vessels. High tensile introduced with Grades A & D steels for the heavier plating of the main hull strength members where the greatest stresses arise in FPSOs. Furthermore welded plating and immediate longitudinal framing of the top and bottom flanges of the hull girder, i.e. the deck and bottom shell, have a thickness exceeding 20 mm amidships, Grade D material is adopted. Higher tensile steels are now used extensively for the deck and bottom regions of new build and converted FPSOs. This leads to a reduction in the scantlings of these structural items with advantages both for the shipbuilder and owner.

The following lists some of the typical FPSOs building materials:

- **ABS:**

Material id	Yielding Stress N/mm^2	Ultimate Stress N/mm^2
MILD	235	400
HT32	315	470
HT36	355	490
HT40	390	510

Table 3-3 ABS Building Material

- **DNV:**

Material id	Yielding Stress N/mm^2	Ultimate Stress N/mm^2
NV-NS	235	400
NV-27	265	450
NV-32	315	470
NV-36	355	490
NV-40	390	510

Table 3-4 DNV Building Material

- **British Steel:** For FPSOs (Hulls, top-sides, turrets, moorings etc.)

Material id	Yielding Stress N/mm^2	Tensile Strength N/mm^2
355EM – 355EMZ	355	490

Table 3-5 British Steel Building Material

- **Dillinger Hütte GTS:**

Material id	Yielding Strength N/mm^2	Tensile Strength N/mm^2
Dimarine32	315	440-590
Dimarine36	355	460-620
Dimarine40	390	480-650

Table 3-6 Dillinger Hütte Gts Building Material

3.2.7 Process Plant

The process plant is usually placed on a frame structure elevated at a height of about 3.5 metres above the main deck on a number of supporting stools distributed on the deck as illustrated in ***Figure 3-11***. Equipment modules most sensitive to motions are likely to be placed towards midship. The modules are assembled in such a way to allow easy implementation and also fulfil the production requirements of the field.

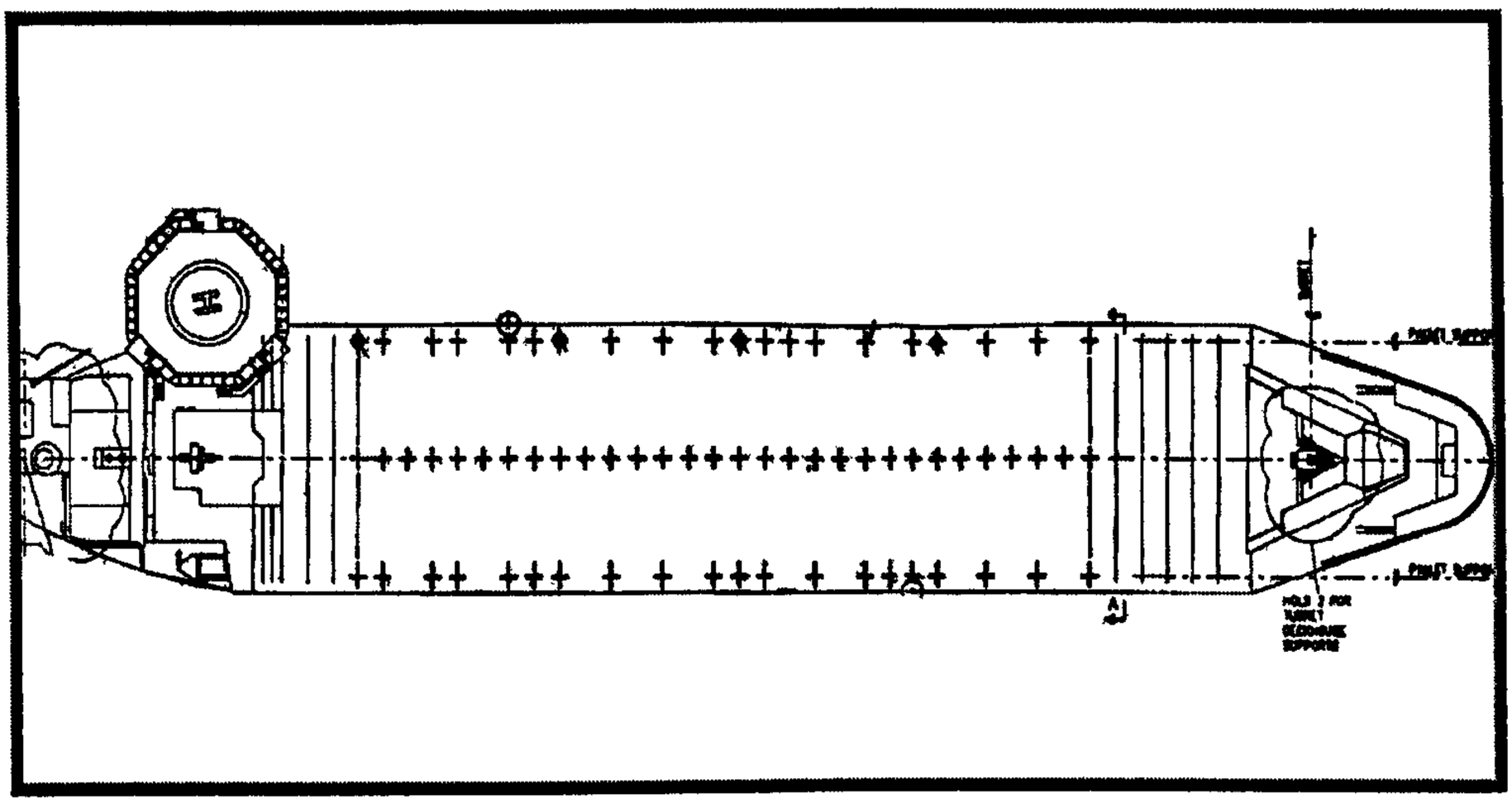

Figure 3-11 Supporting Stools *(indicated by the crosses on deck)*

3.3 FPSO's Structural Loads

Knowledge of all the loads acting on an FPSO is fundamental to achieving safety, where safety is defined as having an excess of capability (strength) compared with the demand (loads).

The loads that an FPSO experiences are dependent on the environmental conditions and are mainly dynamic in nature, where It is essential those relevant global and local loads are considered in an explicit manner and that their combination and phasing be representative of their time-dependent nature.

FPSO's Structure will be subjected to a great variety of static and dynamic loads during its lifetime. ***Table 3-7*** illustrates the loads on offshore and ship structures where FPSO's loads are possible combination of these loads.

Important loads applied to ships	Important loads on offshore structure
Stillwater bending moment	Dead (structural weight, and weight of permanently installed equipment)
Hydrostatic hull pressure	Live
Dynamic hull pressure	Hydrostatic
Wave bending and torsional moments	Environmental (wind, wave, currents, and earthquake)
Impact pressure due to slamming	Impact pressure due to slamming
Whipping	Whipping
Springing	Springing

Table 3-7 FPSOs Possible Loads

FPSO's loads may be categorized as follows:

- ***Permanent loads***, which are gravity loads that will not be removed, such as the weight of the structure, weight of permanent ballast and equipment and external hydrostatic pressure of permanent nature.

- ***Live loads***, which are loads associated with the operation and normal use of the structure, such as stored liquids, operation of cranes, helicopters and mooring of the vessel.

- ***Deformation loads***, which are associated with imposed deformation, such as prestressing and temperature.
- ***Environmental loads***, which are loads due to wind, waves, current, ice, snow and other environmental actions.

All loads that are varying in magnitude and/or direction will cause stress variations in the structure and may lead to fatigue damage.

3.3.1 Hydrostatic Loads

Hydrostatic loads are those loads induced by the FPSO's own weight, its cargo (or ballast) and buoyancy as illustrated in ***Figure 3-12***. A wide variety of possible conditions are considered to maximize local and global load effects. At an early design stage,

before a loading manual is available, approximate expressions based on parametric studies may be used to obtain estimates of the sagging and hogging still water bending moments amidships.

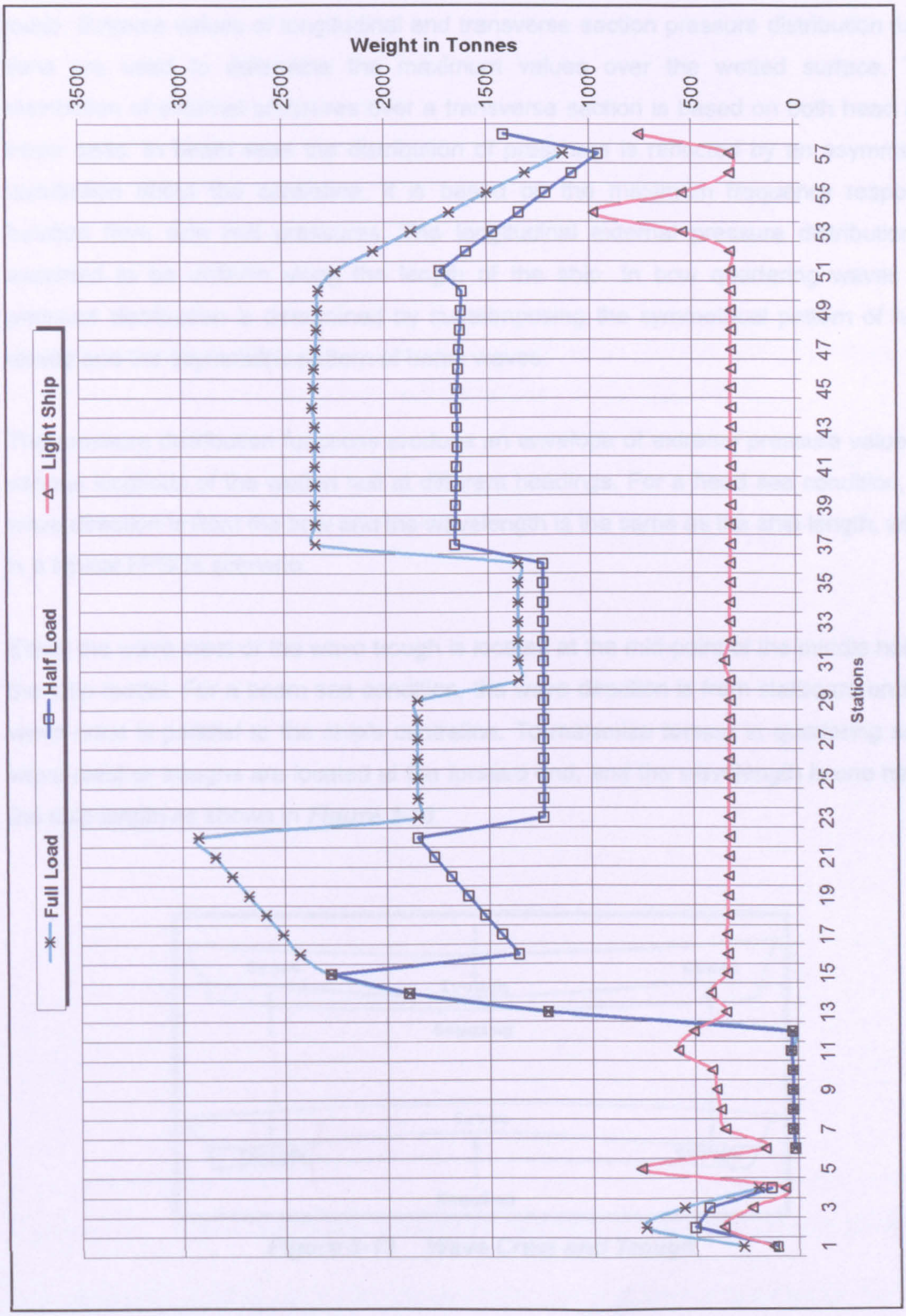

Figure 3-12 City FPSO 2000 Weight Distribution

3.3.2 Wave Induced Loads

The process for determining extreme values in the formulation of criteria for external pressures is more complicated than that required for deriving the hull girder loads. Extreme values of longitudinal and transverse section pressure distribution functions are used to determine the maximum values over the wetted surface. The distribution of external pressures over a transverse section is based on both head and beam seas. In beam seas the distribution of pressures is reflected by an asymmetric distribution about the centreline. It is based on the maximum frequency response function from side hull pressures. The longitudinal external pressure distribution is assumed to be uniform along the length of the ship. In bow quartering waves the pressure distribution is determined by superimposing the symmetrical pattern of head waves and the asymmetric pattern of beam waves.

The pressure distribution functions produce an envelope of extreme pressure values at various locations of the wetted hull at different headings. For a head sea condition, the wave direction is from the bow and the wavelength is the same as the ship length, which is a typical FPSOs scenario.

Either the wave crest or the wave trough is located at the mid-point of the middle hold of the ship model. For a beam sea condition, the wave direction is from starboard and the wave crest is parallel to the ship's centreline. To maximize torsion in quartering seas, wave crest or troughs are located at the forward end, and the wavelength is one half of the ship length as shown in ***Figure 3-13***.

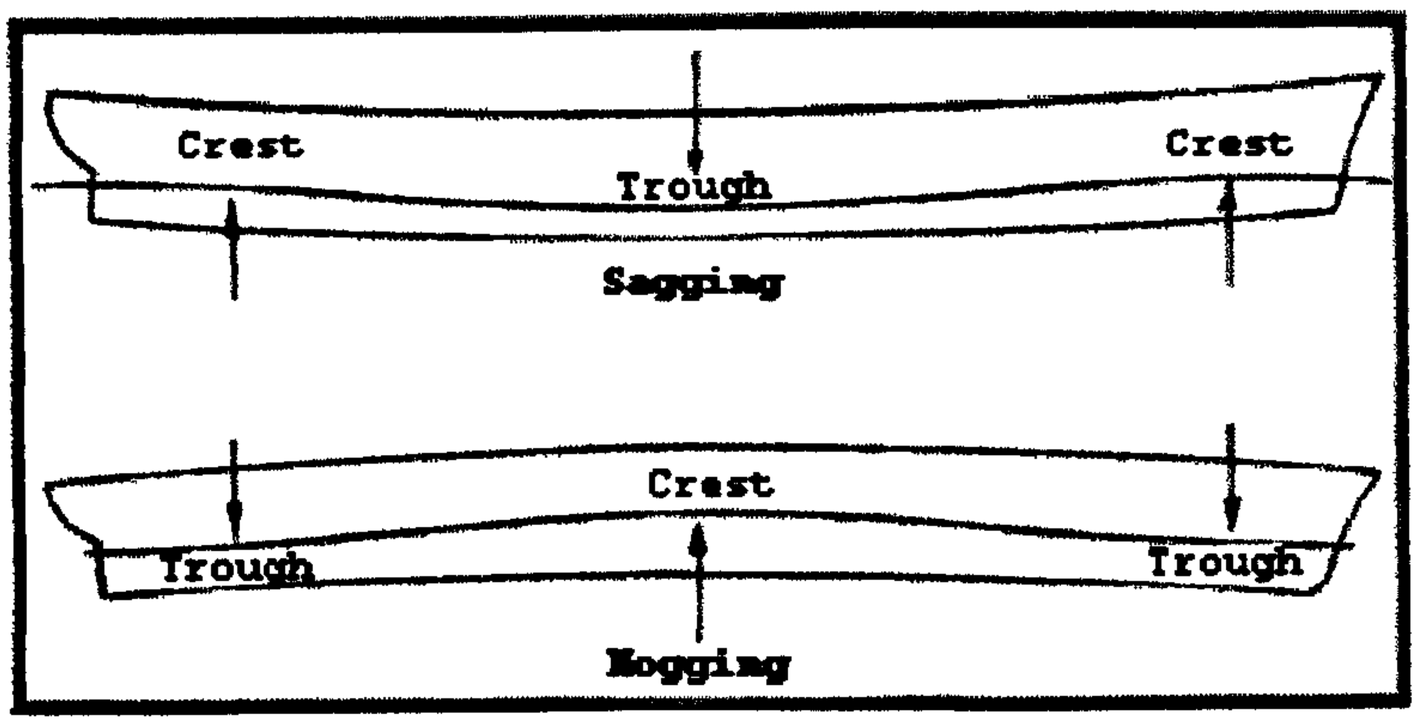

Figure 3-13 Wave Crest and Trough

Following extensive studies using state-of-the-art direct calculations of long-term values of ship motions and loads, parametric expressions are incorporated to closely represent wave induced loads as used in *ABS SHIPMOTION*, (1980) *and DNV WADAM*, (1993). Those taken into consideration include:

- Vertical wave bending moments, (VBM)
- Vertical wave shear forces,
- Horizontal wave bending moments, (HBM)
- Horizontal wave shear forces,
- Wave induced torsional bending moments, (TBM)
- External hydrodynamic pressures

Figure 3-14, ***Figure 3-15*** and ***Figure 3-16*** illustrate some of results the for the linear frequency response function of the load component for the City FPSO.

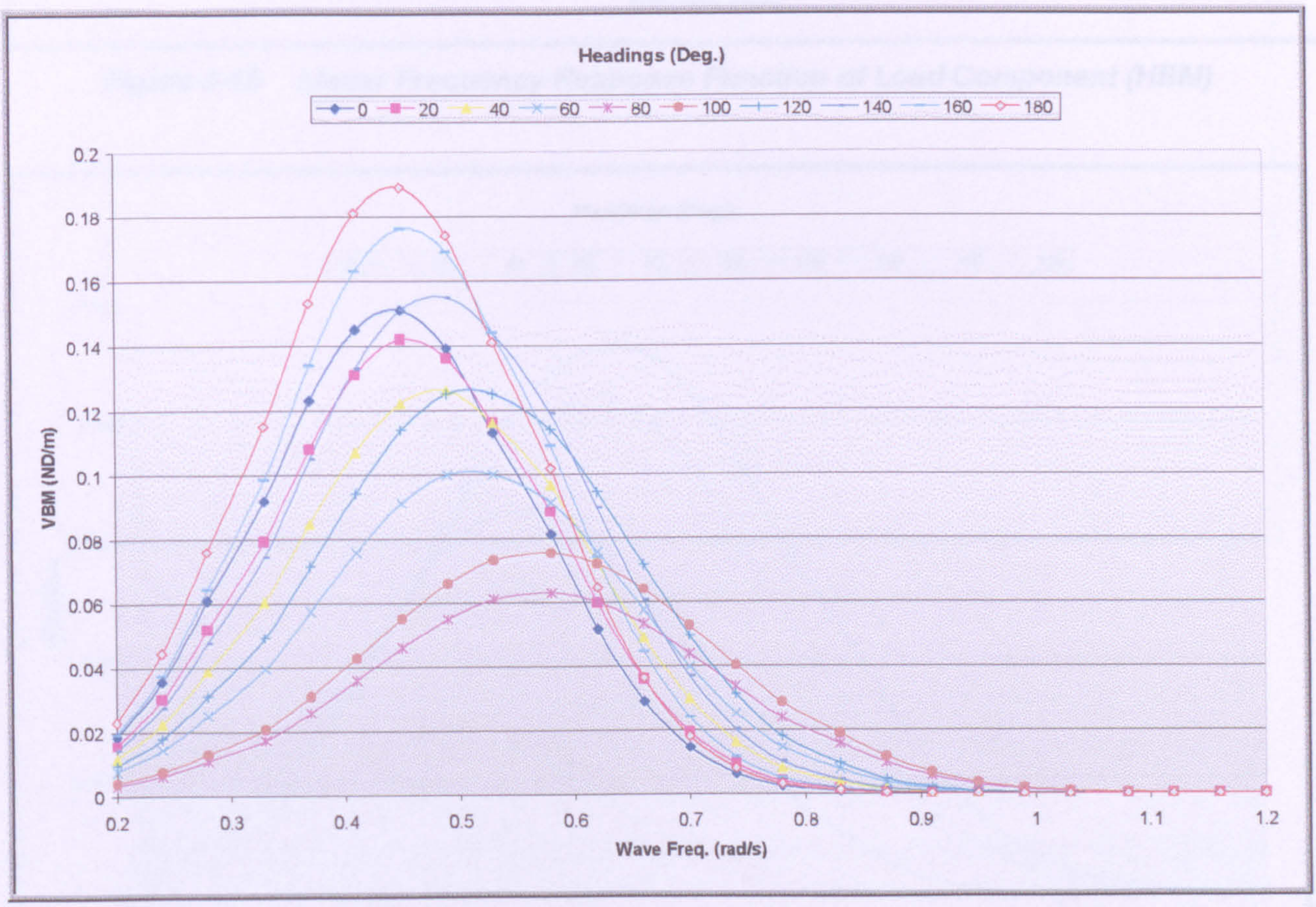

Figure 3-14 Linear Frequency Response Function of Load Component (VBM)

The results are given in a non dimensional format per unit wave amplitudes i.e. the amplitudes have been divided by ($\rho.g.L^2.B$).

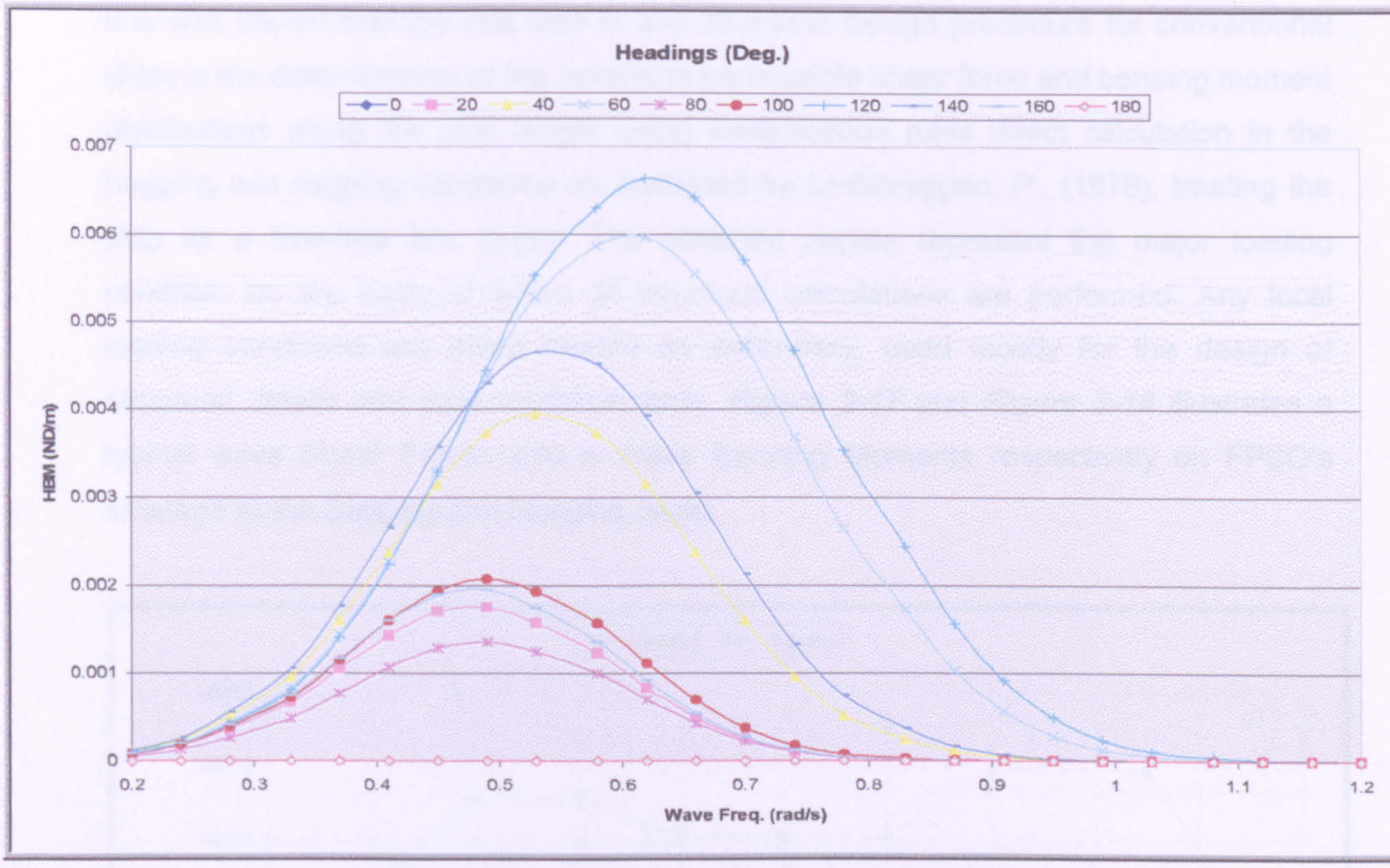

Figure 3-15 Linear Frequency Response Function of Load Component (HBM)

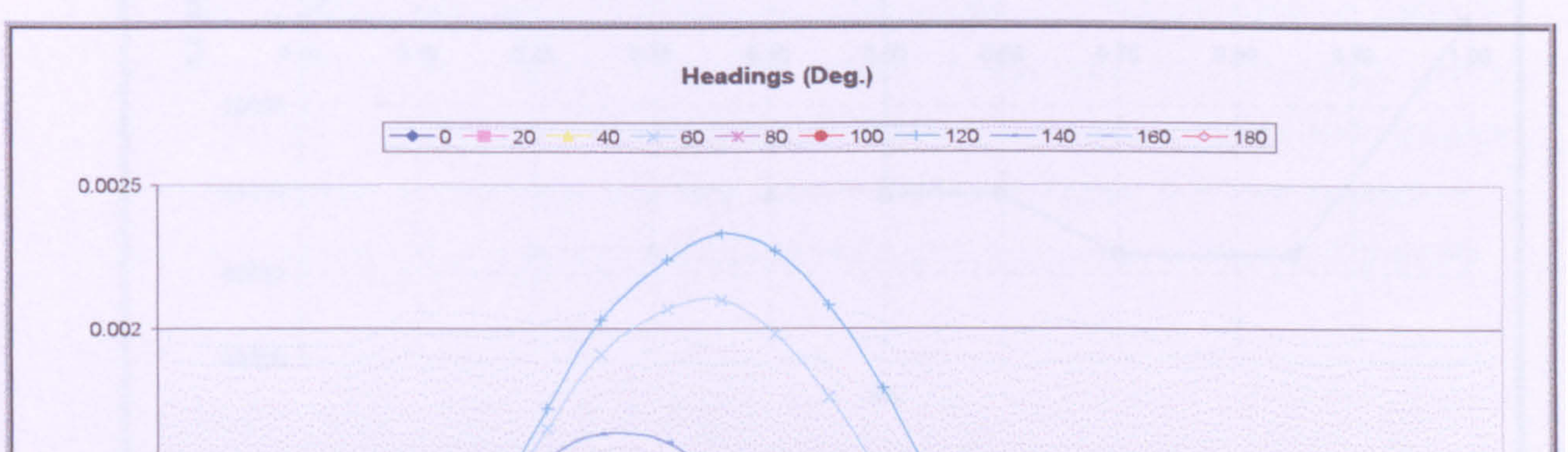

Figure 3-16 Linear Frequency Response Function of Load Component (TBM)

It is well known that the first step in any structural design procedure for conventional ships is the determination of the maximum permissible shear force and bending moment distributions along the ship length using classification rules direct calculation in the hogging and sagging conditions as illustrated by *Lertsbryggen, P.*, (1978), treating the ship as a free-free box girder. The obtained curves represent the major loading condition on the basis of which all structural calculations are performed. Any local loading conditions are being treated as secondary, used mostly for the design of structural details and local reinforcements. ***Figure 3-17*** and ***Figure 3-18*** illustrates a typical wave Shear Forces and a Wave Bending Moments respectively on FPSO's structure at the Sagging and Hogging cases.

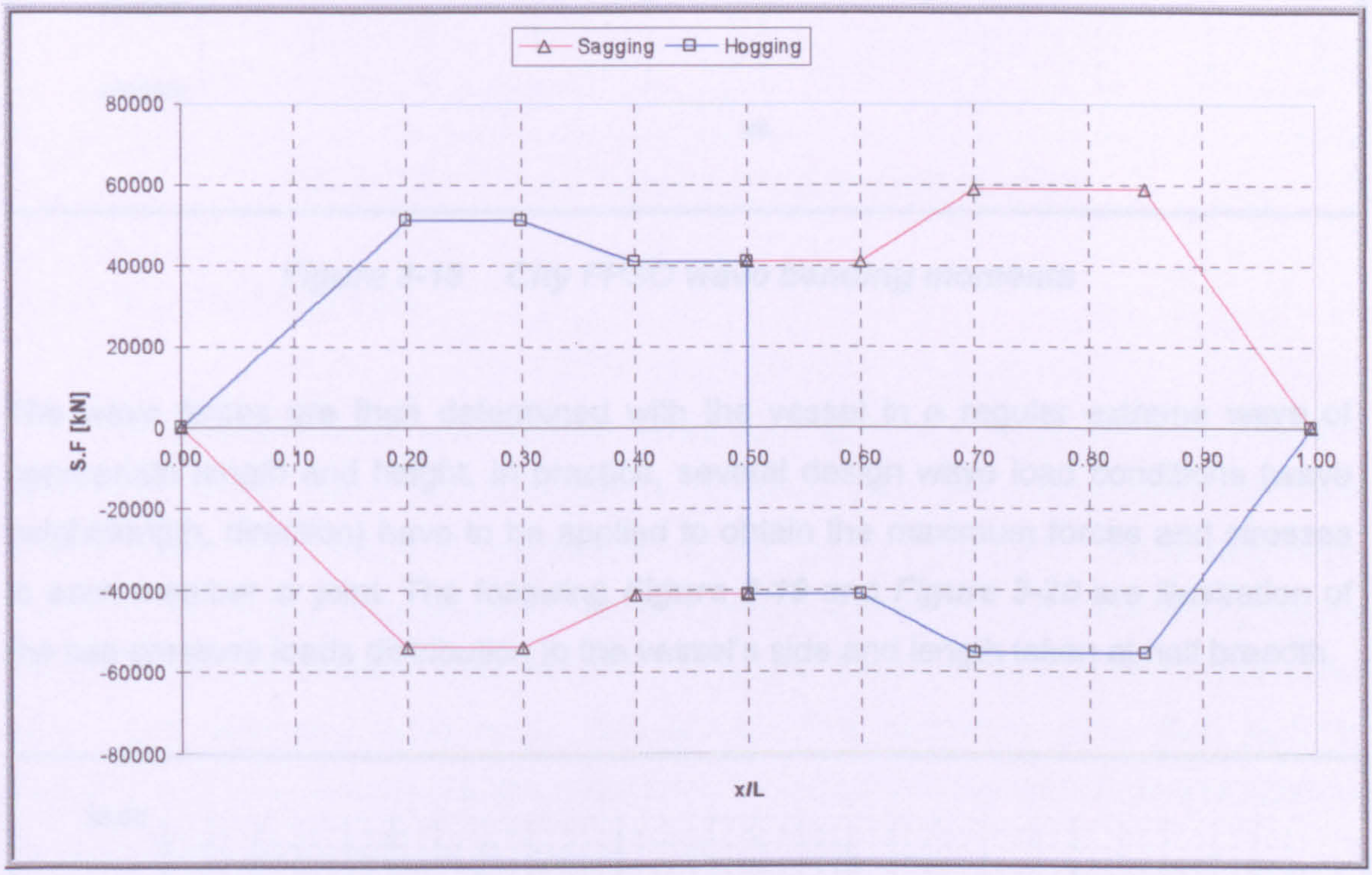

Figure 3-17 City FPSO wave shear forces

The forces and stresses due to external loads are commonly determined by separately calculating their local and global effects. In addition, the hydrostatic pressure yields a resultant load per unit length, i.e. the buoyancy, which will balance the own weight of the vessel. The global behaviour of most types of vessels, such as oil tankers and FPSOs is determined by using a frame model of the vessel. The functional loads are directly applied to the frame. The wave (and wind) loads fluctuate in a stochastic manner. However, experience has shown that the extreme effects (stresses, forces) due to waves can be determined accurately enough by the so-called design wave method.

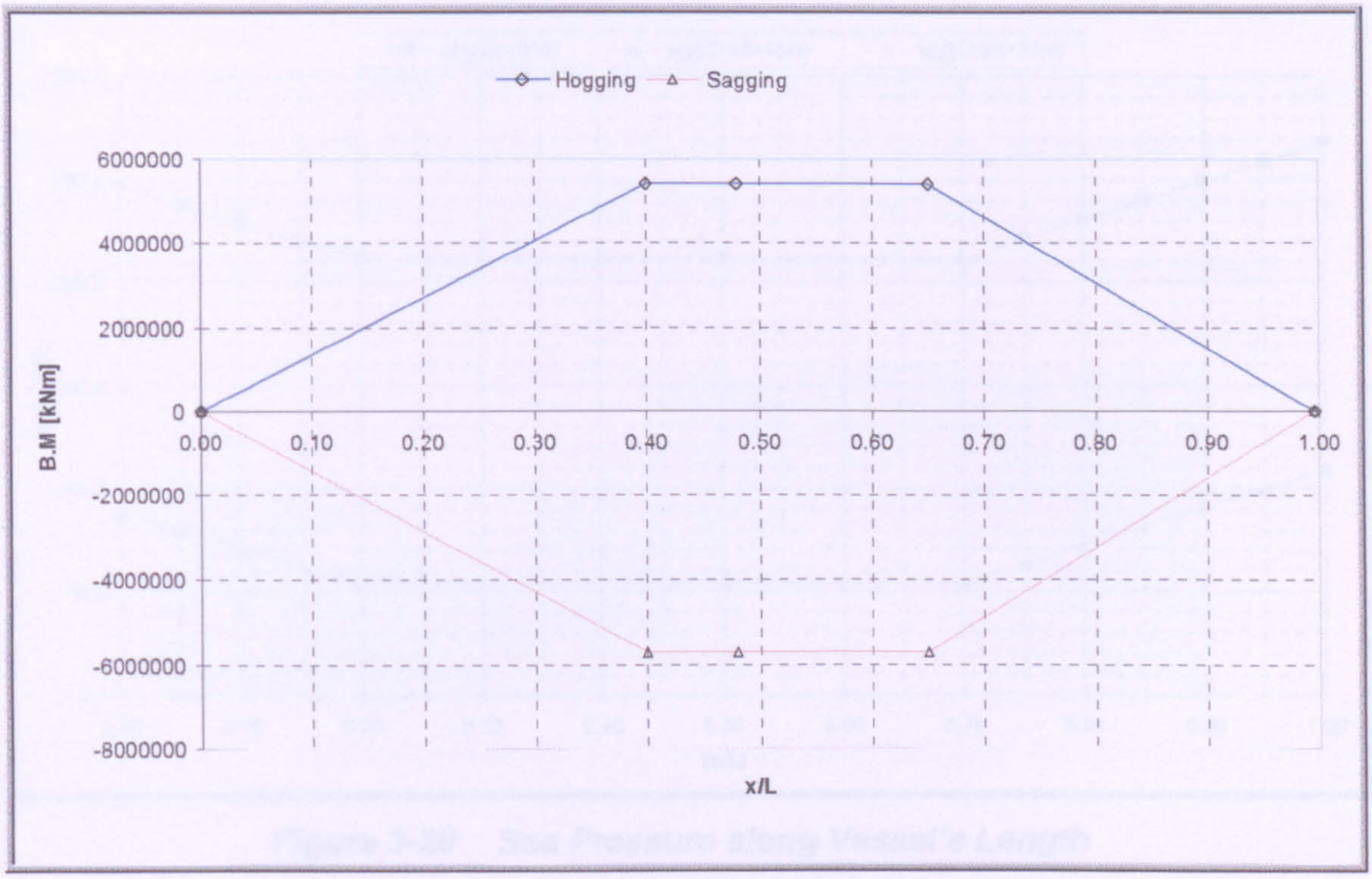

Figure 3-18 City FPSO wave bending moments

The wave forces are then determined with the vessel in a regular extreme wave of appropriate length and height. In practice, several design wave load conditions (wave height/length, direction) have to be applied to obtain the maximum forces and stresses in each member or joint. The following ***Figure 3-19*** and ***Figure 3-20*** are illustration of the sea pressure loads distribution to the vessel's side and length taken at half breadth.

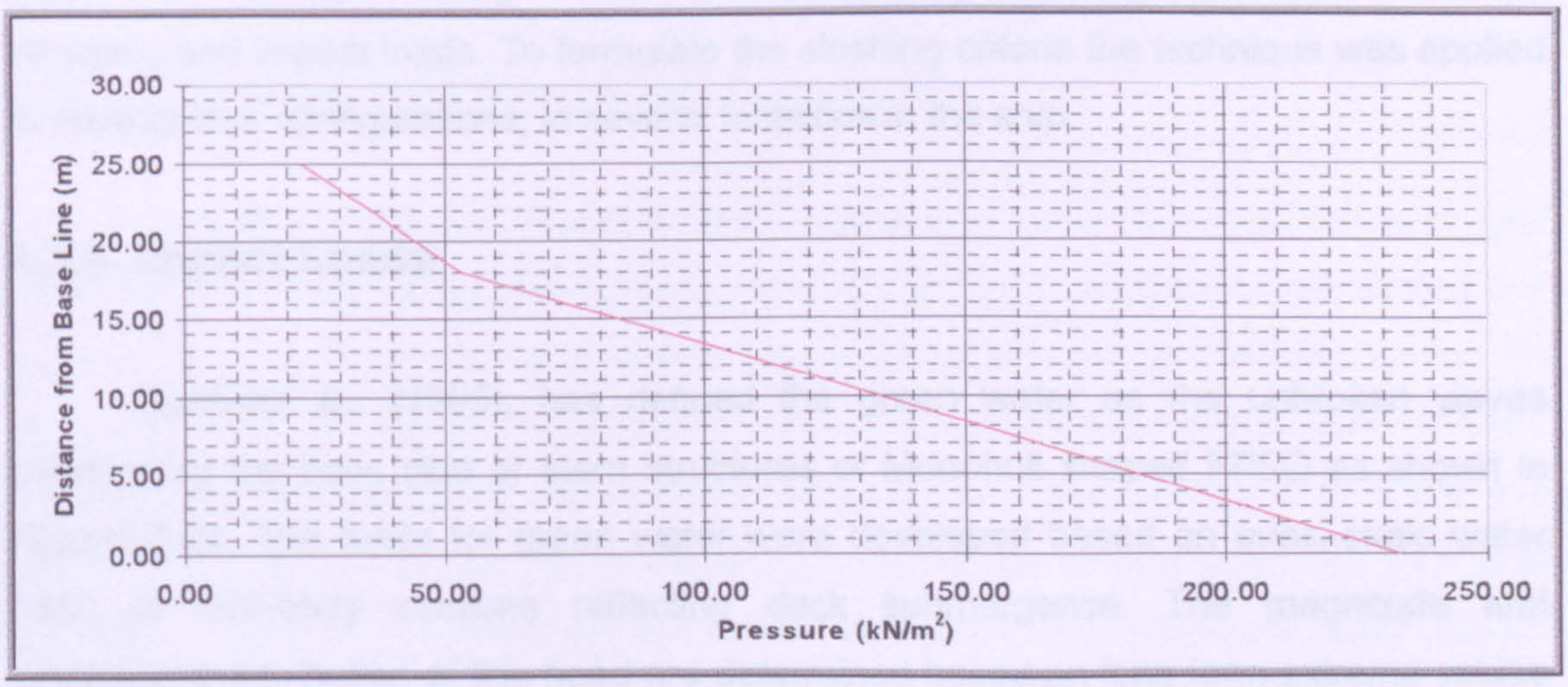

Figure 3-19 Sea Pressure Distribution on City FPSO's Side

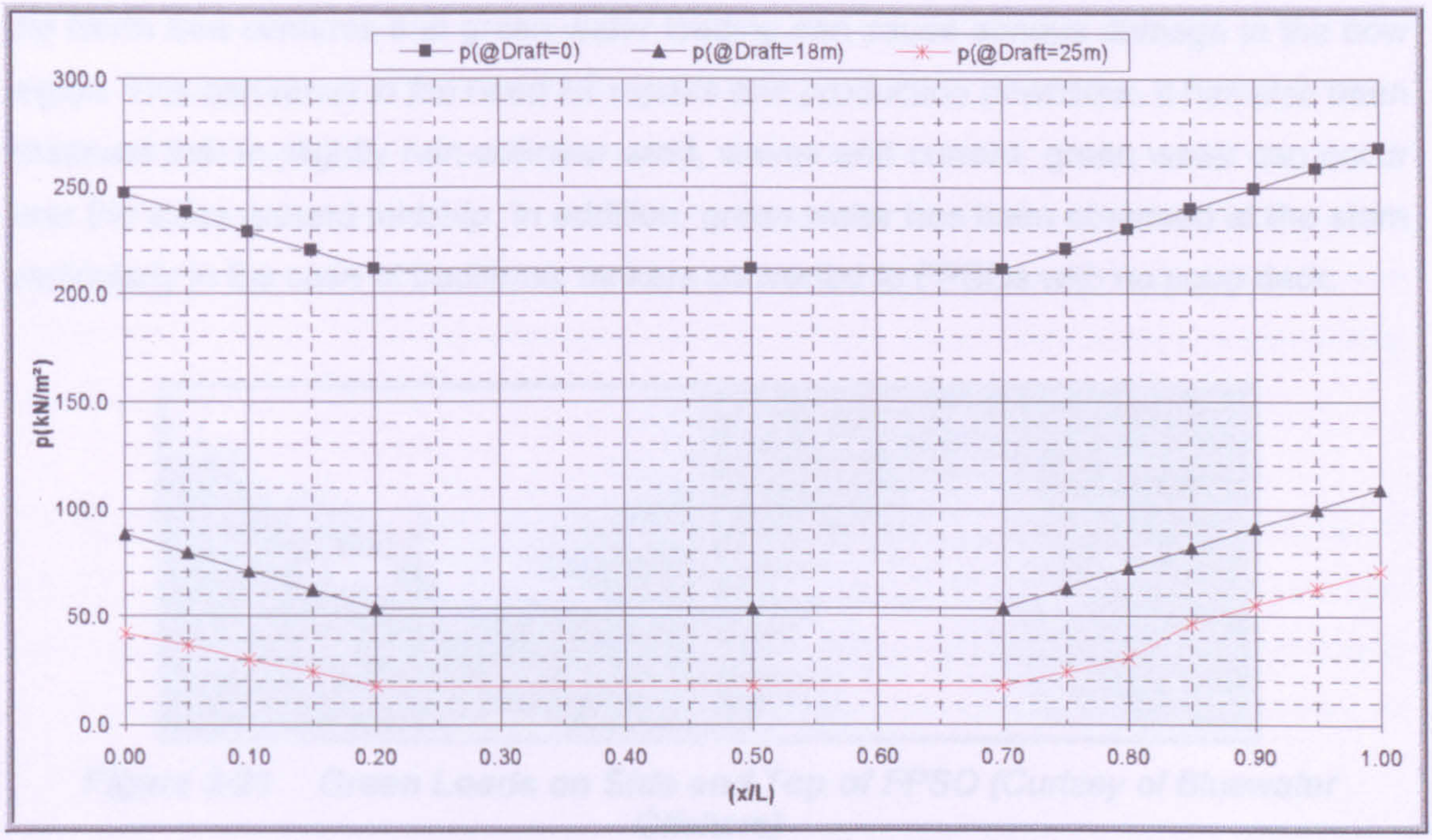

Figure 3-20 Sea Pressure along Vessel's Length

3.3.3 Sloshing Loads

For ships with large, partially filled tanks such as FPSOs, sloshing loads must be considered if the ship's natural period of motion is near the natural period of fluid motion. This may result in resonance of the fluid in the tank introducing high magnification of the fluid pressure loads. Existing approaches for determining these quasi static-sloshing loads, ware derived from a time domain finite difference technique, which was calibrated using model test results. This technique gives fluid surface elevation and impact loads. To formulate the sloshing criteria the technique was applied to several tank configurations, in several locations in the ship.

3.3.4 Impact Loads

Buchner, B., (1995), has defined the green water as the unbroken waves overtopping the bow, side or stern structures of Monohull shaped FPSO as shown in ***Figure 3-21***. The loads for green water were developed based on quasi-static water head at fore-body sections reflecting deck submergence. The magnitude and longitudinal distribution of this head are determined based on long term extreme values of relative motions and freeboards for forward sections of the ship. Bow impact loads are developed based on the vector sum of ship speed, which equals to zero in the FPSOs case, and wave speed, and bow geometry. Recent experience with FPSOs in

the North Sea confirms that green water loading can cause serious damage in the bow region. This can result in the need for repairs and production downtime. It has also been observed that in slightly non-collinear wind, waves and current, green water can occur over the sides around midship. In addition, green water has been observed at the stern particularly in the case of traditional tankers converted to FPSOs with no poop deck.

Figure 3-21 Green Loads on Side and Top of FPSO (*Curtsey of Bluewater Offshore)*

3.3.5 Liquid Cargo and Ballast Loads

The distribution of the total pressure on the tank boundary is determined using correlation functions and weighted functions. The dynamic pressure results from the change in pressure head due to roll or pitch motions. For ballast tanks, the static head is taken as the vertical distance from the highest point in the tank, to the point under consideration. The vertical distance between these two points after inclination defines the pressure head in the inclined condition.

3.4 FPSOs Critical Structural Locations

LR Right (1996) has applied direct calculation procedures in the structural appraisal and approval of new buildings and in various investigations on double hull vessels. Through these procedures and the wealth of information collected on the LR fleet database, a number of locations have been identified where good design, workmanship and alignment during construction are particularly important. These are usually locations where high stress variations can be experienced during the lifetime of the ship. These are referred to as critical locations. The structural detail design improvements that can be applied to increase the fatigue life of the structural components are provided. These detail improvements are intended to give the designer guidance for meeting the design criteria for structural detail components.

The application of 2 and 3-dimensional finite element analyses techniques to the hull structure enables the global and local capabilities of the hull structure to withstand static and dynamic loadings to be assessed. Such analyses will enable those high stress locations and joints within the cargo area of double hull oil tankers to be readily identified. Such locations will then, by their very nature, be at risk to fatigue damage unless appropriate measures are taken at the design stage and subsequently during construction.

Extensive experience in the application of finite element techniques to existing oil tankers and new double hull oil tankers, together with construction and `in service' experience of the performance of existing ship structures, already provide an awareness of those critical locations which merit particular attention either due to stress or alignment difficulties.

The actual combined loads resulting from the entire load cases can be transferred automatically to the finite element model using software packages such as listed in ***section 3.2.2*** above. The actual loads and resulting shear forces and bending moment results can be seen at (***section 4.4.3)*** below.

3.4.1 Critical areas

Stress concentrations occur in the primary structures of all FPSOs and are identified during the design process by such means as finite element calculations. The designer will modify the detail to alleviate the stress concentration either by redesign or increase in scantlings. However, even after modification that area will still, in general, be exposed throughout the life of the ship to stresses higher than in surrounding areas. The following ***Table 3-8*** Locations where correct alignment during construction is important and where high stress variations can be experienced during the lifetime of the ship.

Double hull vessel type	General location	Items susceptible to higher stress levels and misalignment
Smaller vessels below 20,000 tonnes dwt as illustrated in ***Figure 3-24***	Transverse section (Mid-hold)	Intersection of end brackets of transverse framing and primary webs with inner bottom plating and longitudinal bulkhead.

	Transverse bulkhead (Vertically corrugated)	Connections of corrugations to inner bottom. Connections of corrugations to deck. Connections of deck longitudinals to corrugations.
	Transverse bulkhead (Horizontally corrugated)	Connections of corrugations to longitudinal bulkhead and inner hull. Connection of inner bottom and bottom shell longitudinals to floors in way of lower stool.
Larger vessels up to Suez-max i.e. up to 150,000 tonnes dwt with No longitudinal bulkheads in cargo tanks as illustrated in ***Figure 3-22***	Transverse section (Mid-hold)	Intersection of inner bottom and lower hopper sloping plate. Intersection of longitudinal bulkhead (inner hull) with lower hopper sloping plate. Side web lower panels above lower hopper especially in way of openings. Connection of deck transverse end bracket to longitudinal bulkhead or topside tank sloping plating. Connection of topside tank sloping plating to longitudinal bulkhead. Side shell longitudinal connections to side web plating particularly in region between ballast and load waterlines. Where centreline longitudinal bulkhead fitted, toes of vertical web brackets to inner bottom, and toes of brackets from deck transverse to bulkheads.
	Transverse bulkhead (Vertically corrugated)	Connection of lower stool to inner bottom plating. Connection of lower stool to lower shelf plate. Connection of vertical corrugations to lower stool plate. Connection of vertical corrugations

		to upper stool plate. Connection of longitudinal deck girder system to upper stool. Connection of upper and lower shelf plates to side structure.
	Transverse bulkhead (Plane)	Connection of vertical stiffening to inner bottom. Connection of vertical stiffening to horizontal stringers. Connection of horizontal stringers to side girders. Connection of inner bottom and bottom shell longitudinals to floors in way of lower stool.
VLCC and ULCC vessels above 150,000 tonnes dwt with longitudinal bulkheads in cargo tanks as illustrated in ***Figure 3-23***	Transverse section (Mid-hold)	Intersection of inner bottom and lower hopper sloping plating. Double bottom floor panels at hopper and longitudinal bulkhead. Intersection of inner hull at side with lower hopper sloping plating. Side web lower panels above lower hopper especially in way of openings. Longitudinal bulkhead vertical transverse end bracket connection to inner bottom. Primary bottom bracket web toe connections to inner bottom and longitudinal bulkhead. Connections of wing cargo tank cross tie to inner hull at side. Connection of deck transverse end bracket to inner hull at side and longitudinal bulkhead. Bottom and inner bottom longitudinal connections to double bottom floor pillar stiffeners.

		Side longitudinal connections to side webs particularly in region between ballast and load waterlines.
	Transverse bulkhead (Plane)	Connection of horizontal stringers to longitudinal bulkhead and inner hull at side. Connection of vertical stiffening to horizontal girders and inner bottom. Connection of side shell and inner hull longitudinals to transverse bulkhead in double side. Connection of inner bottom and bottom shell longitudinals to floor in way of transverse bulkhead.

Table 3-8 Locations where correct alignment during construction is important and where high stress variations can be experienced during the lifetime of the ship

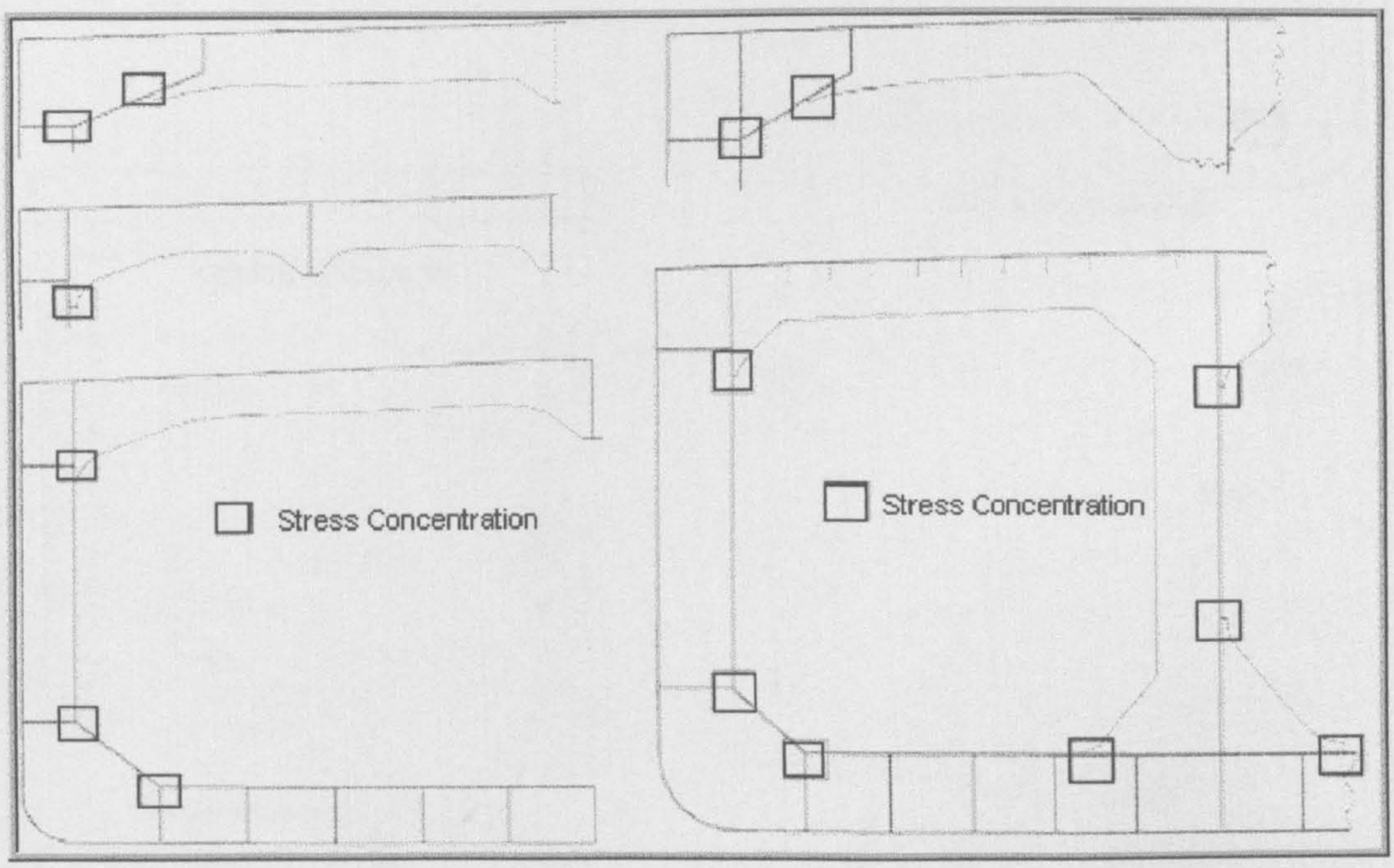

Figure 3-22 Critical Areas in Midship Section of a Vessel up to 150,000 tonnes dwt

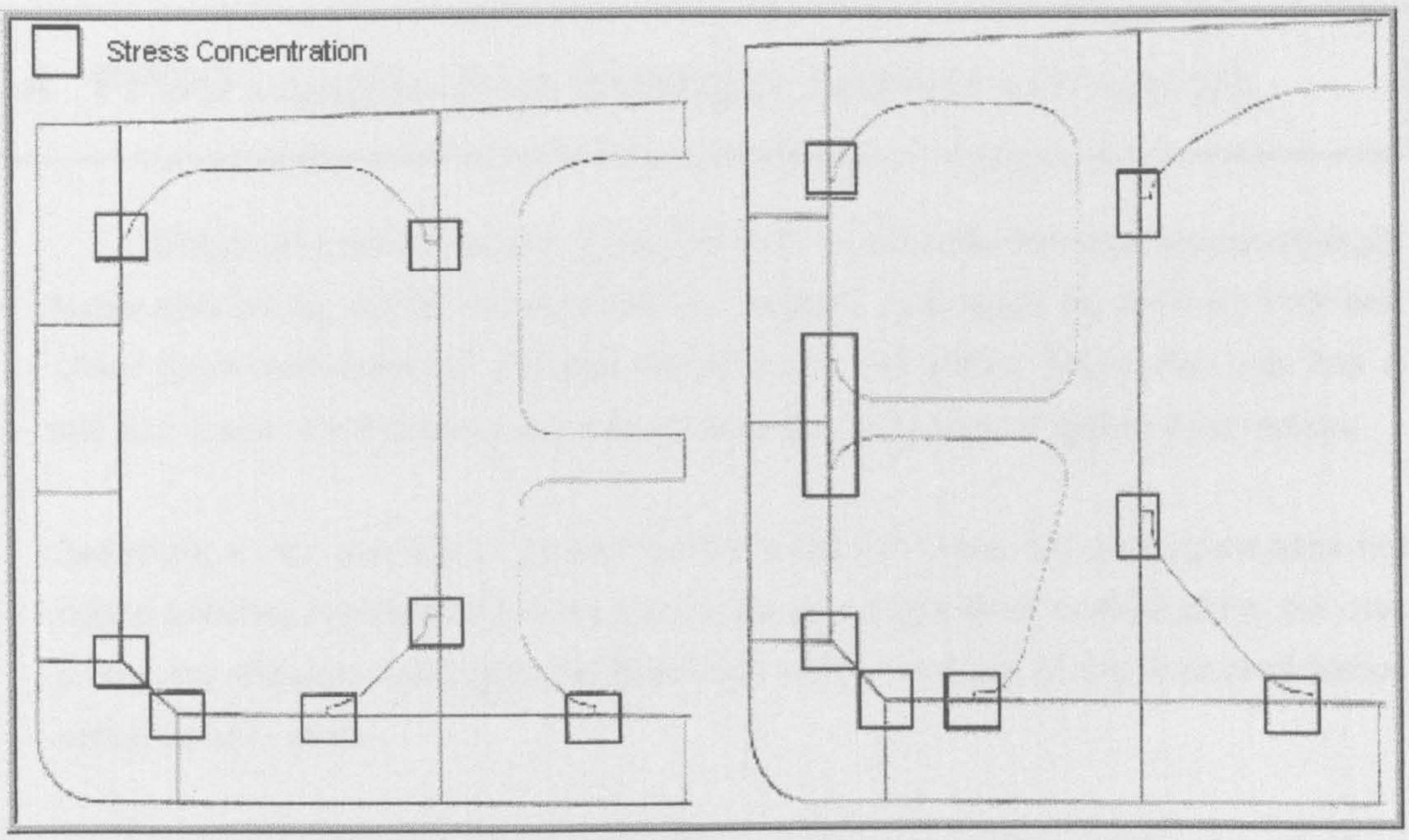

Figure 3-23 Critical Areas in Midship Section of a Vessel above 150,000 tonnes dwt

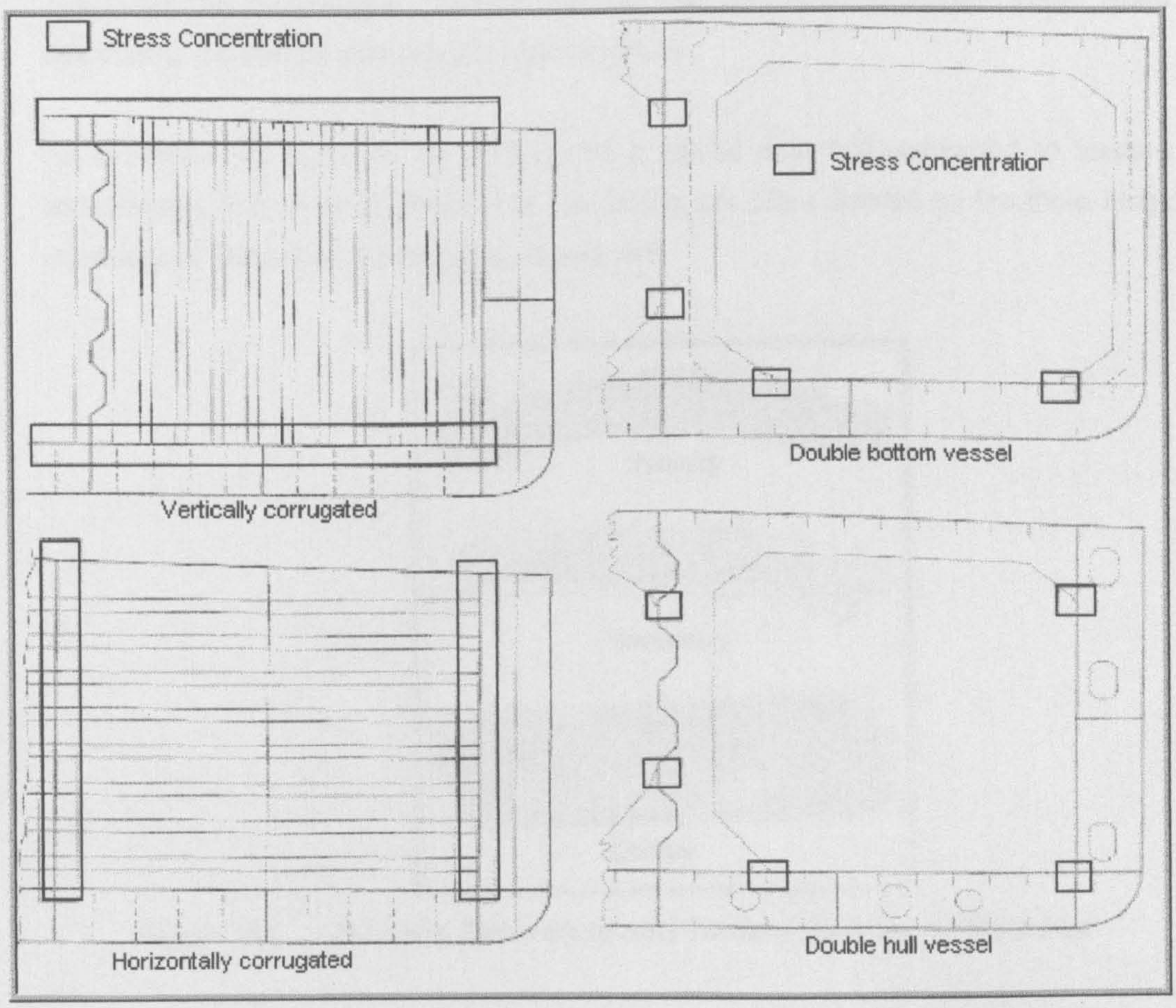

Figure 3-24 Critical Areas in Midship Section of a Vessel below 20,000 tonnes dwt

4. FPSO Longitudinal Strength Analysis (*Primary*)

Global structural analysis of an FPSO is to consider the longitudinal strength loads concerning overall strength of the vessel's hull, such as bending moment, shear force and torsional moment acting on a hull girder. Since the ship has a slender shape, it will behave like a beam from the point view of global deformation.

Assuming a ship moving diagonally across a regular wave; the wave generates not only a bending moment deforming the vessel in a longitudinal vertical plane but also a bending moment working in the horizontal plane, because of the horizontal forces acting on side shell.

In addition, the wave causes a torsional moment due to variation of the wave surface at different sections in the ship length. If the above longitudinal strength loads exceed the upper limit of longitudinal strength of a hull, the hull will be bent or twisted. Therefore the longitudinal strength load is one the most important loads when calculating the overall strength of a hull structure.

As explained by *Dow, R. S.*, (1981), for a typical ship hull subjected to loading experienced in a seaway, stresses in the plating are often defined by the three kinds of structural behaviour illustrated in ***Figure 4-1***.

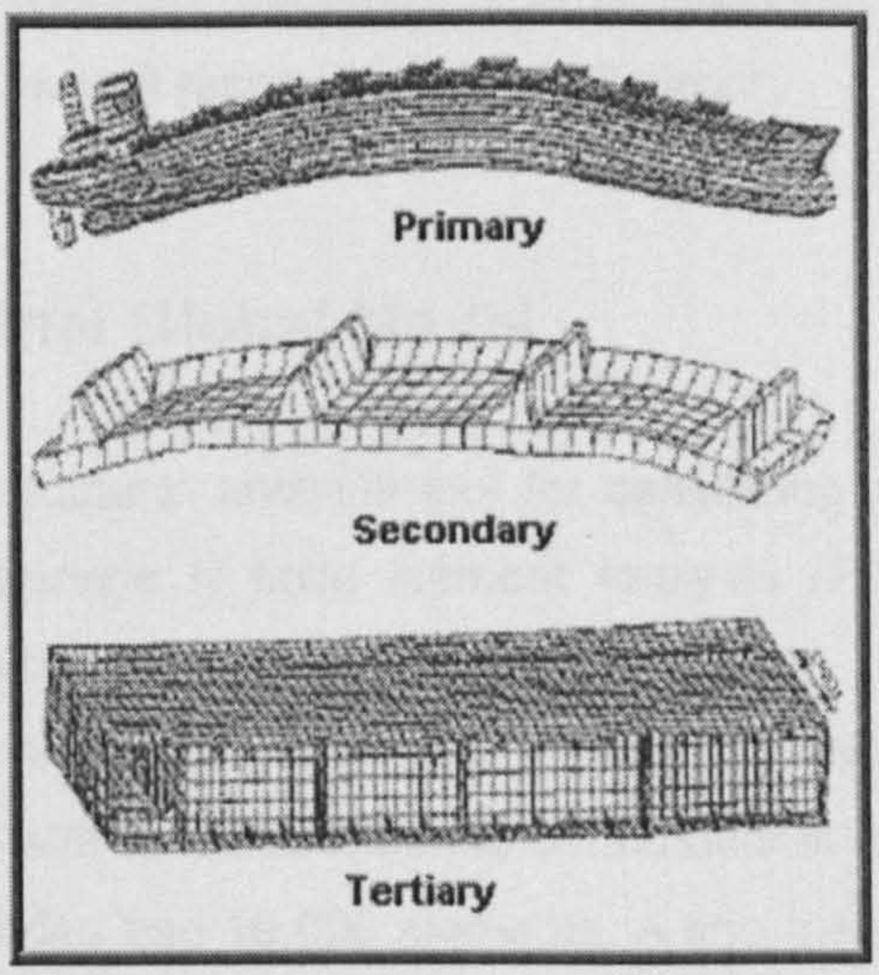

Figure 4-1 Primary, Secondary and Tertiary Bending of Ship Hull

- ***Primary bending***: This is a beam-like hull girder bending induced by hull girder loads (i.e., the bending moment and shear force). The plating acts like a membrane, and the resulting "primary stresses" are solely in plane.

- ***Secondary bending***: The stiffened panels, such as the side shell and double bottom, bend under lateral loading between transverse bulkheads, and in some cases between swash bulkheads and between deep web frames. The resulting "secondary stresses" are also in plane since the plating in this case acts as flanges of the longitudinal girders or longitudinal stiffeners.

- ***Tertiary bending***: The plating bends locally between stiffeners due to local pressure loads. The resulting "tertiary stresses" are out-of-plane bending stresses of the plate with different signs (compression and tension) on the two surfaces.

Among the three types of stresses in the longitudinal plating, only the "tertiary stresses" require the use of bending plates. However, a typical global model as described in (***Section 4.1.2***) is not fine enough to account for such stresses. To obtain local plate bending stresses, a minimum of four plate elements is needed between stiffeners. This is impractical and unnecessary for the objective of the intended analysis. Even the "secondary stresses" due to panel bending between transverse web frames are often unaccounted for because the grid lines of the model are generally in line with web frames, and there is no node between web frames to account for this type of "secondary bending". This is, however, acceptable for the purpose of determining the overall response of the hull girder.

4.1 Three-Dimensional Global Model

The most powerful structural analysis tool for calculating primary and indeed secondary and tertiary response is finite element analysis (FEA). This is now a standard tool in ship structural analysis and is particularly valuable where the structural configuration is complex or contains major discontinuities. A 3D-model would normally commence with a coarse mesh to obtain overall response. This could run to the order of 5,000 nodes and 10,000 elements. A fine mesh FEA to give more detail might then follow this. This could include up to 15,000 nodes and 30,000 elements.

The purpose of the 3-D global analysis is to determine the overall structural response of the hull girder, and also to obtain appropriate boundary conditions for use in the 2-D fine-mesh analysis of local structures. In general the hull structure considered in the 3-D global model is to include three cargo tanks of the parallel mid-body. All primary load-carrying members should be modelled. Secondary structural members, which may affect the overall load distribution, should also be accounted for.

4.1.1 Global Coordinate System of the Model

The global coordinate system of the finite element model is defined as follows:

- X-axis: Longitudinal (fore-and-aft), positive from aft to fore.
- Y-axis: Vertical, positive upwards.
- Z-axis: Transverse (athwart ships), positive toward outboard.
- Origin: Base line at centre at first transverse bulkhead of the aft end of model.

The six degrees of freedom for the nodes are defined as three translational degrees of freedom, and three rotational degrees of freedom with respect to the global x, y and z-axes of the finite element model. ***Figure 4-2*** illustrates the extent of the Midsection 3-D model.

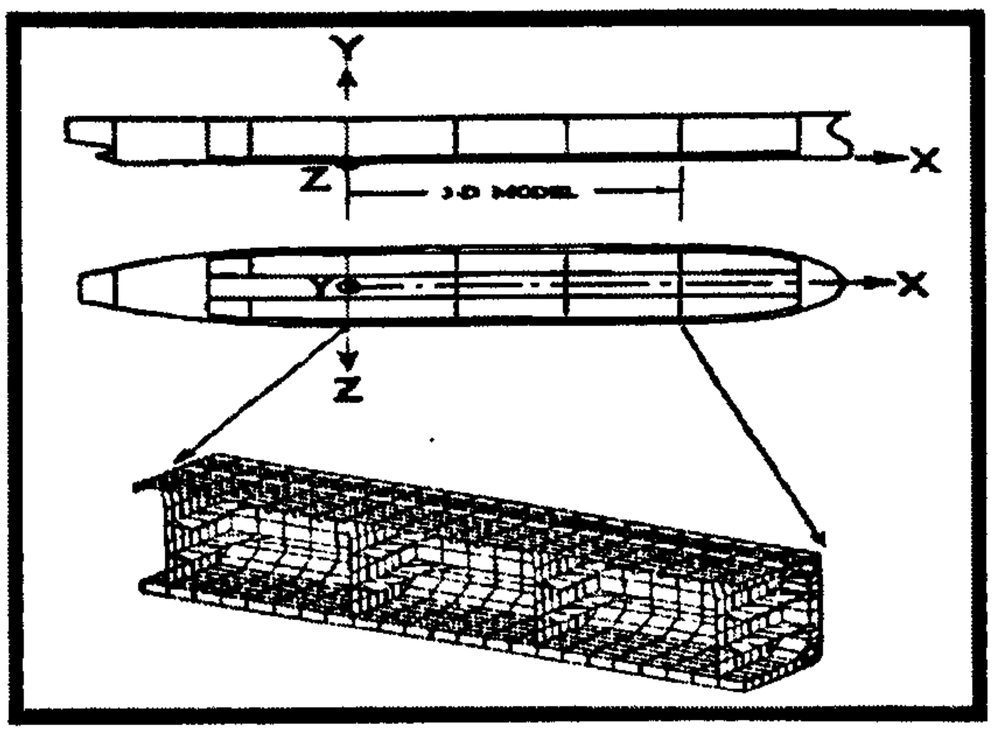

Figure 4-2 Extent of 3-D Global Model

4.1.2 Finite Element Modelling, General Practice

The approach of finite element modelling adopted is to use a 3-D coarse-mesh global model to obtain the overall response of the hull girder under the imposed sea loading. The stress results of the global model are used only to assess

the hull girder plating of the deck, side shell, bottom, inner bottom and longitudinal bulkheads. The assessment of the main supporting members of the hull girder is performed using 2-D and 3-D fine-mesh local models. The boundary conditions for the local models are the appropriate nodal displacements obtained from the 3-D global model analysis. Therefore, in developing the 3-D global finite element model, special attention should be paid to modelling as explained in *ABS*, (2000). The finite element model should include all primary load-carrying members, secondary structural members, which may affect the overall load distribution should also be appropriately accounted for. Structural idealization should be based on the stiffness and anticipated response of the structure, not wholly on the geometry of the structure itself.

It is desirable to have consistent modelling throughout the entire length of the three cargo tanks considered. However, the middle tank should always have the desired mesh, where more accurate results are expected (due to boundary effects) and are therefore used in the strength assessment. If approximations have to be made, do so only in the two end-tanks. It is also important to consider the relative stiffness between associated structural members and their anticipated response under the specified loading.

In general, the finer the mesh the more accurate is the result. (A coarse-mesh model tends to be stiffer.) A compromise should be made between the desired accuracy and the expected computer execution time and cost. It is reasonable to keep the size of the finite element model within a manageable limit, particularly, with regard to the processor speed and disk drive storage of the PC to be used.

The following is proper when creating the 3-D global model:

- The starboard side is the reference structure for the finite element model, i.e., the orientation of the Cartesian coordinate system defined in (***Section 4.1.1***) is on the starboard side.

- The frame spacing is uniform throughout the length of the three-hold model.

- The node numbering is a set procedure, with a maximum of 400 nodes per frame on the full ship model consisting of both sides.

- The nodes defining the deck, side shell, bottom, inner bottom, and longitudinal bulkheads are at the same athwart ship locations (y and z coordinates) throughout the length of the model.

- The scantlings of the hull plating and longitudinal stiffeners are uniform throughout the length of the model.

4.1.3 Generation of Elements

Based on the previous layout, the 3-D global model generated would have a relatively coarse distribution of elements. In general, the structural elements, whose geometry, configuration and stiffness approximate the actual vessel's hull structure, are mainly of the following three types:

- ***Truss elements*** (also called "rod" or "bar" elements), with axial stiffness only and constant cross-sectional area

- ***Beam elements***, with axial, torsional and bi-directional shear and bending stiffnesses and with constant properties along the length of member

- ***Plane-stress elements*** (commonly called "membrane" plate elements), with bi-axial and in plane shear stiffnesses and constant thickness, both triangular and quadrilateral

In most cases, the above three simple types of element will be sufficient for a good representation of the hull structure for the purpose of an overall response analysis. A model consisting of only membrane plate elements and rod elements would have only a maximum of three degrees of freedom per node.

4.1.3.1 Membrane Plate Elements

Modelling of a hull structure, the plating is typically represented by plane-stress (membrane) plate elements. In most cases, using bending plate elements is considered unnecessary. Using membrane plates instead of bending plates has the following two distinct advantages:

- In terms of degrees of freedom, the finite element model is about one half the sizes of those using bending plates. This is because a bending plate has 5 degrees of freedom per node while a membrane plate has only 2 degrees of freedom per node. As a result, the computation time for the analysis will be greatly reduced.
- The size of the output file is much smaller when membrane plates are used.

This is because, in addition to in-plane membrane stresses, a bending plate has bending stresses on the top and bottom surfaces. For a PC-based finite element analysis, this is very crucial to the often-limited capacity of disk drives available for storing the results. It is important to explain why using the supposedly more accurate bending plates is considered unnecessary. A typical FPSO hull consists of plating and stiffeners, longitudinal girders, horizontal girders and stringers, and transverse frames. Of necessity, all longitudinal plates (i.e., deck, bottom, inner bottom, side shell, and longitudinal bulkheads) are modelled by plate elements (i.e., membrane plates). In general, other internal primary load-carrying members are also more conveniently modelled by membrane plates whenever possible.

Stresses in these members are primarily in plane; any stresses caused by out-of-plane bending are considered to have insignificant effects on the overall response. For transverse web frames, the finite element mesh used in the 3-D global model is generally fairly coarse, and detailed modelling of the transverse structures is usually not possible. However, all transverse webs (i.e., bottom transverse, deck transverse, and vertical webs) should be properly accounted for and modelled by membrane plates. The faceplates "longitudinal plates" are modelled using rod elements. Major brackets should also be accounted for using a combination of membrane plates and rod elements.

Manholes on transverse and longitudinal structures, such as double bottom floors and longitudinal girders, are generally ignored in the global model. Leaving out plate elements or reducing plate thicknesses to account for such manholes in the 3-D model are not advisable, because this would sometimes result in unrealistic shearing stresses for the thinned plates or the adjacent elements. The actual behaviour of a round or elliptical manhole with or without a flange is quite different from the modelled thin plate or element opening, which is usually rectangular.

4.1.3.2 Beam Elements

Although some load-carrying structural members in an FPSO hull are beam-like (e.g., longitudinal girders, horizontal stringers, and transverse frames), beam elements are not commonly used in the finite element modelling of the hull structure, except the few cases indicated below. Instead of trying to determine the equivalent properties of the beams, it is easier to just follow the geometry of the hull structure in creating the model. More significantly, using beam elements often creates problems of connectivity between beams and membrane elements because of the incompatibility in the degrees of freedom. It is therefore recommended that the primary load-carrying members be modelled by membrane plate and rod elements combination.

4.1.3.3 Beams for Transverse Bulkhead Stiffeners

One exception is the stiffeners on transverse bulkheads. Typically, an FPSO's transverse bulkheads are either vertically stiffened and supported by two or three deep horizontal girders, or horizontally stiffened and supported by a few deep vertical webs. Bulkhead plating always modelled by membrane plates, and as recommended previously, the horizontal (or vertical) deep girders are also generally modelled by membrane plates, (for the webs), and rods (for the flanges).

On the other hand, the stiffeners are usually required to be modelled as beams, not rods, in order to take the applied loads. In this case, the bulkhead plating is expected to behave as a membrane, while the stiffeners are expected to undergo significant bending because of the spacing of the supporting deep girders. Because these beams would generally be connected to membrane plates on the deck and bottom, the degrees of freedom corresponding to twisting of the beams (i.e., θ y) for the nodes at these two locations should be concealed to eliminate possible "singularity" problems.

The nodes at the deck are also concealed in θ_z to represent the fixed end connection of the vertical stiffener to the deck longitudinal.

Based on the layout of the basic transverse grid, beam elements for these stiffeners can only be placed to coincide with the fewer grid lines, and lumping of stiffeners is therefore necessary. ***Figure 4-3*** illustrates a typical transverse bulkhead.

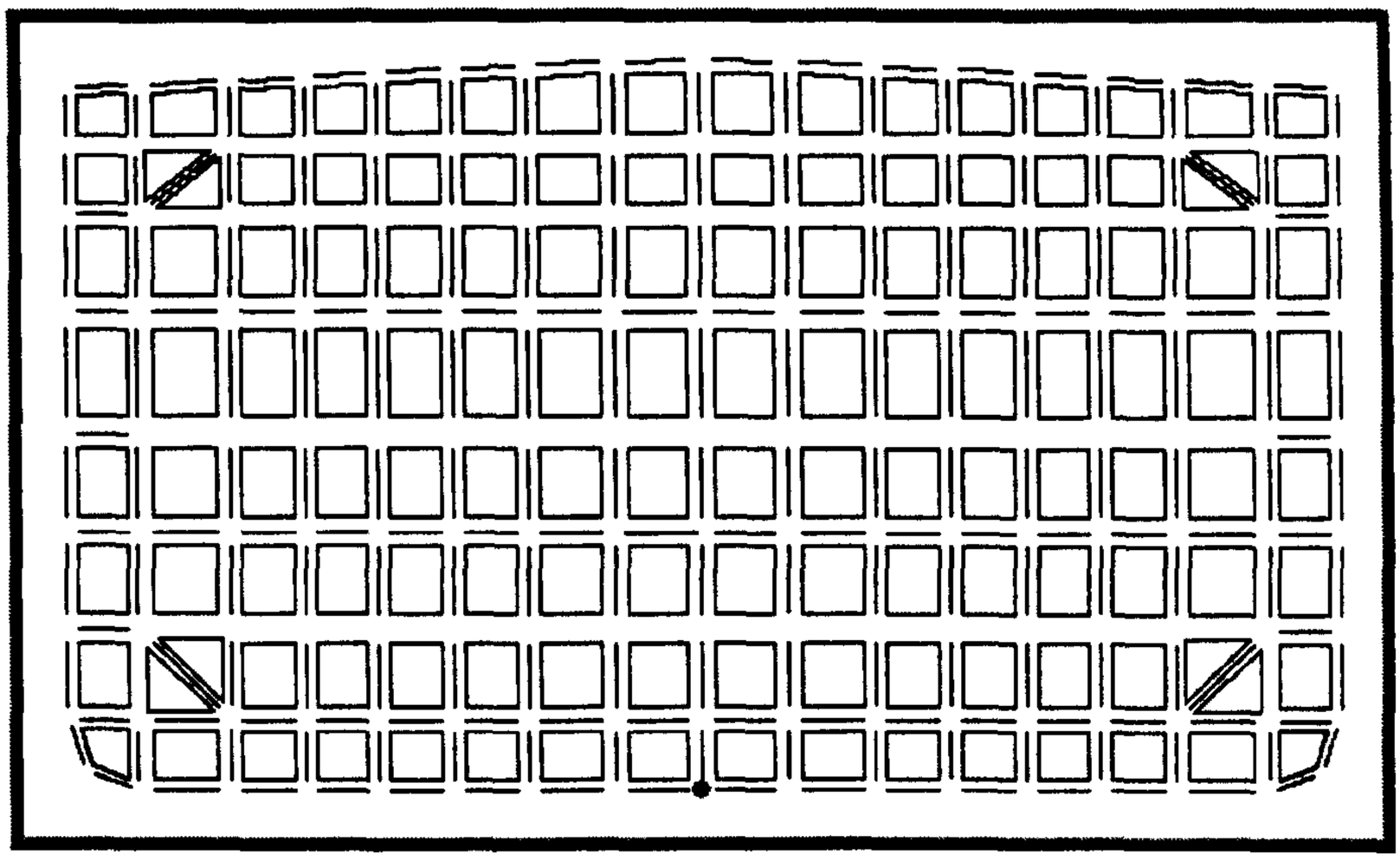

Figure 4-3 Lumping of Transverse Bulkhead Stiffeners

As can be seen in the figure, lumping of two to three stiffeners are made for each beam. To obtain an equivalent stiffness for the bulkhead stiffeners, lumping is made by adding together their respective sectional properties (i.e., the moments of inertia, axial areas and shear areas). If the stiffeners to be lumped have same scantlings; lumping simply then can be made by increasing the web thickness and flange area proportional to the number of stiffeners.

4.1.3.4 Beams for "Backing up" Membrane Elements

In some cases, beam elements are used to "back up" (i.e., to support) membrane plates. Because membrane plates and rods have only in-plane stiffness; any node connected only by membrane plates and rods in a plane will not have an out-of-plane degree of freedom. If the plane is in parallel or with a small angle to one of the three global planes, the out-of- plane degree of freedom will have zero or negligible stiffness. In this case, the out-of-plane degree of freedom will be fixed, unless such degree of freedom is "backed up" by a beam. As typically done for stiffened panels, with plating modelled by membrane plates and stiffeners by rods, the above situation is not uncommon. In most cases, "backing-up" by beams is unnecessary, and the zero-stiffness (or near zero stiffness) degrees of freedom can simply be fixed (automatically or manually). However, in the following two cases, using beams to back up such degrees of freedom are considered desirable or even necessary.

- To have better-looking deflection plots: There is nothing wrong with simply fixing the degrees of freedom with zero or negligible stiffness. The only problem is that the deflection plots look unreasonable, with some nodes hanging in space. Changing rod elements to beam elements to add stiffness to the degrees of freedom can solve this.

- Changing membrane plates to bending plates will have the same effect, but this is not advisable for reasons cited in (***Section 4.1.3.1***). "Slaving" the zero-stiffness degrees of freedom to the corresponding degrees of freedom of adjacent nodes having non-zero stiffness, if the employed finite element program has such a feature can best solve the problem?

- To take applied loads: In the solution process, any program will customarily ignore all loads applied to the zero-stiffness degrees of freedom. In certain cases, this will result in well-underestimated loads. For example, when an additional grid line is added between two transverse frames, some bottom or side shell nodes on this middle section may not have an out-of-plane degree of freedom, and as a result, all loads applied as distributed pressure loads to these nodes will not be accounted for. In this case, it becomes necessary to use beams to "back up" these nodes in order to properly carry and account for the loads.

In doing so, the beams should be extended to adjacent transverse frames to have proper supports. Sometimes, it may be more convenient to simply extend the beam elements over the entire length of the model, increasing somewhat the total number of degrees of freedom.

4.1.3.5 Truss (Rod) Elements Rod Elements for Longitudinals

Hull girder longitudinal stiffeners are typically modelled by truss (rod) elements, with axial stiffness only. The reasons for using rod elements instead of beam elements in modelling the longitudinals are the same for using membrane plates instead of bending plates in modelling the plating. As explained in (***Section 4.1.3.1***), the longitudinal plating is subjected to primarily in-plane loads under "primary" and "secondary" hull girder bending. This is also true for the longitudinal stiffeners, which in this case are subjected to mostly axial loads.

It is important that all longitudinal members (both plating and stiffeners) are included in the finite element model to ensure that the model's moment of inertia and section modulus resemble the actual ship's values. The hull girder's longitudinal stresses are direct results of these properties. The stresses obtained by the finite element model should be in close agreement with that determined by the beam theory as shown in (***Section 4.4.7***).

In general, there are not enough nodes to individually account for all longitudinals on the deck, bottom, inner bottom, side shell and longitudinal bulkheads. Lumping is therefore required. This can be done by lumping only the cross-sectional areas of the stiffeners, and placing the equivalent rod elements to appropriate nodes of the model (with due consideration not to affect the hull girder's moment of inertia). For longitudinal girders in the double bottom or other deep longitudinal girders, the associated stiffeners should also be lumped to the nodes of the plate elements representing the girders.

4.1.3.6 Rod Elements for Transverse Structures

For a typical 3-D global model, the finite element mesh used for transverse sections is generally fairly coarse, and detailed modelling of the transverse structures is usually not possible. However, when membrane plates model transverse webs, all faceplates should be accounted for and modelled by rod elements. If transverse brackets are modelled (by membrane plates); the faceplates for the brackets should also be included, as rod elements. For a typical FPSO hull structure, there are numerous secondary flat bars, stiffeners, tripping brackets and panel "breakers".

These structural members are mainly to provide local stiffness to plate panels against buckling or vibration. These secondary stiffening members generally need not be included in the global model as their influence on the overall response of the hull structure is negligible.

4.1.4 Boundary Conditions for the 3-D Global Model

As indicated earlier, the hull structure is generally symmetric with respect to the centreline plane, and advantages are usually taken to model just one side of the hull. If this is the case, the asymmetric loading needs to be decomposed into two

components, symmetric and anti-symmetric, and two sets of boundary conditions are required at the centreline plane of the finite element model to take the two components of load separately.

In other words, using a one-side model, two computer runs are required to account for asymmetric loading, symmetric loading with symmetric boundary conditions, and anti-symmetric loading with anti-symmetric boundary conditions.

To impose symmetric or anti-symmetric boundary conditions at the centreline plane, specific degrees of freedom for all nodes along the centreline plane (X-Y plane) should be suppressed, or as defined below:

Symmetric:	$Uz = 0$	$\theta x = 0$	$\theta y = 0$
Anti-symmetric:	$Ux = 0$	$Uy = 0$	$\theta z = 0$

Where *Ux*, *Uy*, and *Uz* are the three translational degrees of freedom, and θx, θy and θz are the three rotational degrees of freedom with respect to the global x, y and z axes of the finite element model. (Shown in ***Figure 4-4***)

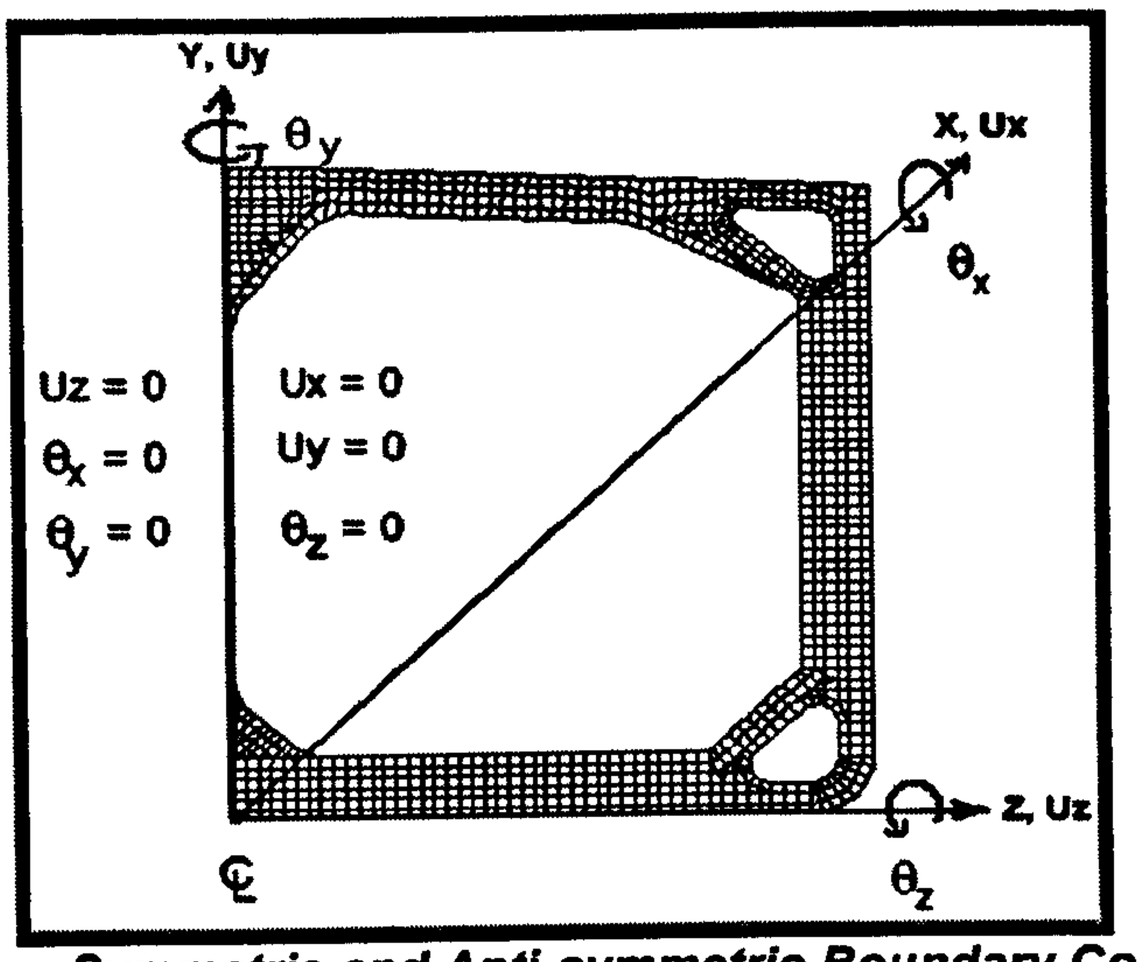

Figure 4-4 ***Symmetric and Anti-symmetric Boundary Conditions at Centreline***

4.1.5 Supports at Two Ends

In the state of static equilibrium, the three-cargo-hold free body of the hull girder is subjected to bending moments and shear forces at the two cut-off ends. The

bending moments will be expressed in terms of hull girder bending stresses, and imposed on the model as boundary nodal forces. However, for shear forces, it is generally more convenient to represent the shear forces by spring supports instead of shearing stresses. The finite element model needs to be in static stability, and these spring supports at the two ends can be used to support the model.

In practice, it has been found sufficient to consider only the vertical shear forces acting on the side shell and longitudinal bulkheads, and only the lateral shear forces acting on the deck, inner bottom and bottom shell. In other words, it is only necessary to place spring supports at these locations. The effects of shear forces on longitudinal girders or horizontal stringers are considered negligible in the global analysis.

The above addition of lateral shear forces is needed in the case of anti-symmetric loading, if a one-side model is used. When a full width model is used instead, the horizontal springs are also required to represent or to take the lateral shear forces induced by asymmetric loading. Furthermore, these shear forces on the deck, inner-bottom, bottom, side shell and longitudinal bulkheads can each be reasonably represented by two springs, as illustrated in ***Figure 4-5***.

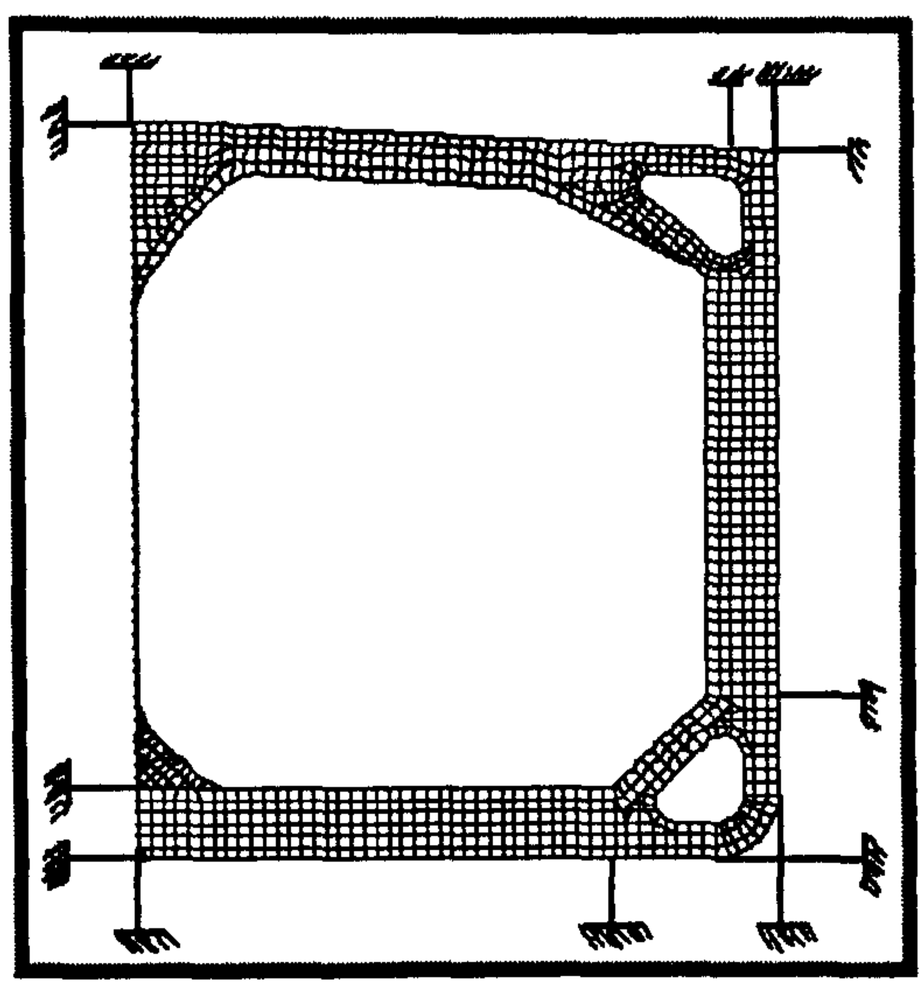

Figure 4-5 Spring Supports for 3-D Global Model

Using distributed springs along the plating would be more accurate, but are considered unnecessary. Any approximations involved in the previous boundary representation will be "dissipated" by the two end-tanks via the *St. Venant principle:*

"*The difference between the stresses caused by statically equivalent load systems is insignificant at distances greater than the largest dimension of the area over which the loads are acting*", resulting in reasonably accurate structural response in the middle tank, where results are used for strength assessment purposes. The springs are typically represented by truss (rod) elements, having only axial stiffness. The stiffness is equivalent to the support given to the considered end bulkhead by the cut-off longitudinal structural members. The resulting cross-sectional area can be determined by the following formula:

$$A = \left(\frac{1}{1+\nu}\right)\frac{A_s l}{L} = 0.77\ \frac{A_s l}{L}$$

Equation 4-1

Where A = Cross-sectional area of the bar

A_s = Shearing area of the beam (can be taken as the cross-sectional area of the considered side shell or longitudinal bulkhead)

E = Young's modulus of the material

V = Poisson's ratio of the material

L = Tank length (i.e., one half span of the beam)

l = Length of the bar

The bar area *A* is determined by a given bar length *l*, which can be any value. In practice, however, all values of *l* in the finite element model are conveniently chosen to be the same round figure, for example, equal to one meter.

The resulting cross-sectional area *A* is the total equivalent area for the structural member considered. When two springs are used for each structural member, connecting to the deck and bottom or port and starboard sides, the area for each spring should be divided by 2 or equal to A/2.

All nodal points for the spring supports should be totally fixed. That is, all six degrees of freedom for the support nodes should be set equal to zero. The above springs provide vertical and athwart ship supports to the finite element model. In order to have a statically stable structure, an additional support in the longitudinal (fore-and-aft) direction is required.

Fixing any node in the longitudinal direction can do this. However, in practice, a node on the side shell or longitudinal bulkheads near the hull girder neutral axis on the aft end section is usually chosen for this purpose. It is expected that the reactions resulting from any unbalanced loads in the longitudinal direction would be insignificant.

4.2 Application of Loads for 3-D Global Model

4.2.1 Combined Load Cases for Structural Analysis

For assessing the hull girder structure, realistic loads expected by the vessel were considered. These loads generally include static loads in still water, wave-induced hull girder bending and shear, external hydrodynamic pressure, and internal pressure. As illustrated in ***Table 4-1***, each of the eight load cases contains a "dominant load component" at its maximum value.

The remainder of the load components are the corresponding values derived from the parametric study developed by the classification society ABS to yield the combined effects for the portion of structure considered. These green loads are used in the finite element analysis as specified in *ABS*, (1997).

Hull-girder Loads	Load Case 1	Load Case 2	Load Case 3	Load Case 4	Load Case 5	Load Case 6	Load Case 7	Load Case 8
Vertical B.M.	Max. Sagging	Max. Hogging	*	*	*	*	*	*
Vertical S.F.	*	*	Max.	Max.	*	*	*	*
Horizontal B.M.	*	*	*	*	*	*	Max.	Max.
Horizontal S.F.	*	*	*	*	*	*	*	*
External Pressure	*	*	*	Max.	*	Max.	*	*
Internal Tank Pressure	*	*	Max.	*	Max.	*	*	*

Table 4-1 Combined Load Cases (* Corresponding Value)

The loading patterns of the eight cases for the considered three cargo holds are illustrated in ***Figure 4-6***. These load cases are designed for different tank configurations depending on vessel's size and tonnage.

The shaded area represents the loaded tanks, for the three common tank configurations, (single, double and triple tanks design); in the City FPSO 2000 design the second loading configuration (double tanks) is adopted.

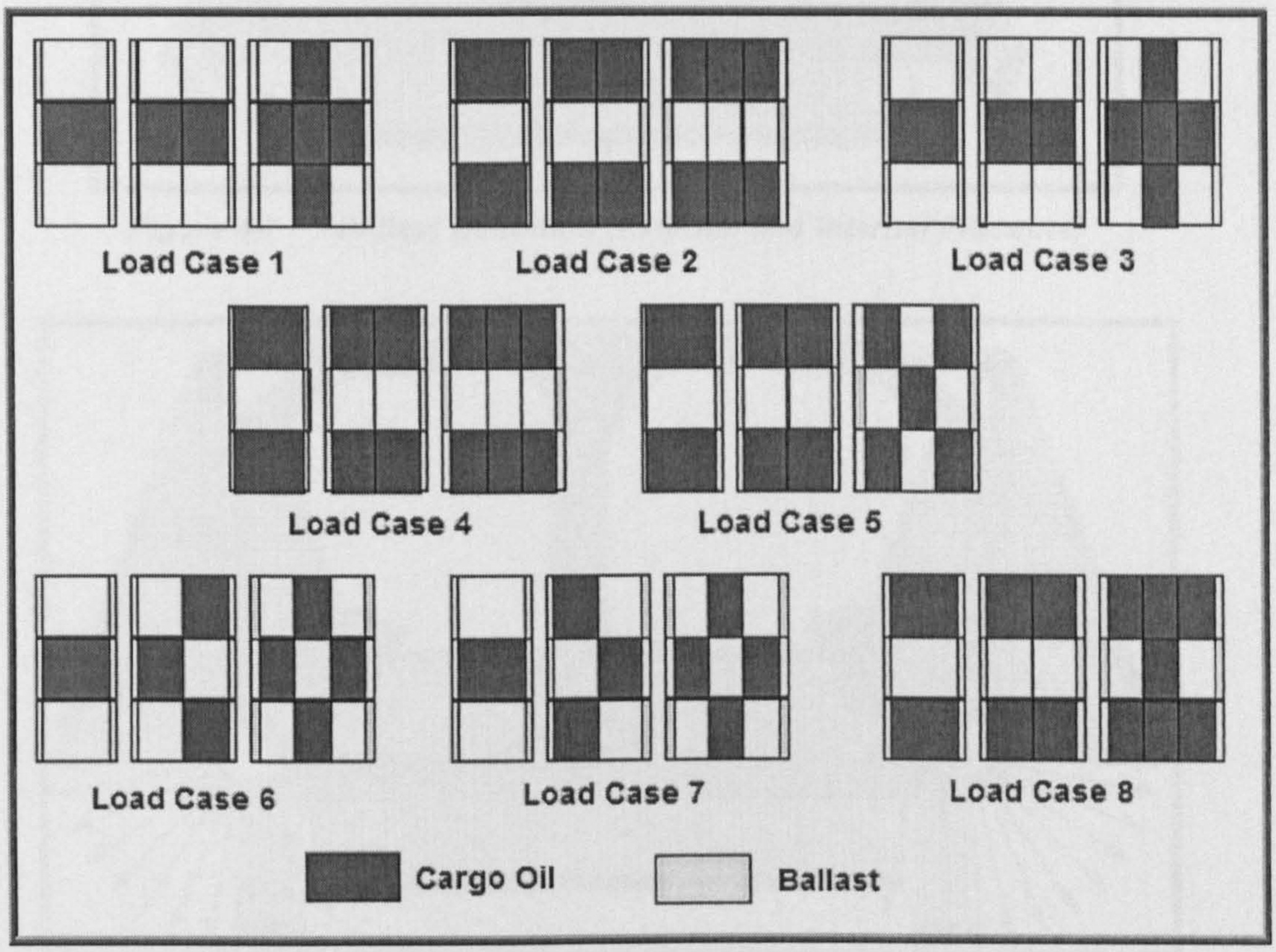

Figure 4-6 Loading Patterns for Standard Load Cases *(ABS Steel Vessels Rules 1997)*

Figure 4-7 and ***Figure 4-8*** show external, internal combined pressure loads. The transverse sections shown are the mid tank frame of the middle tank in the three hold model.

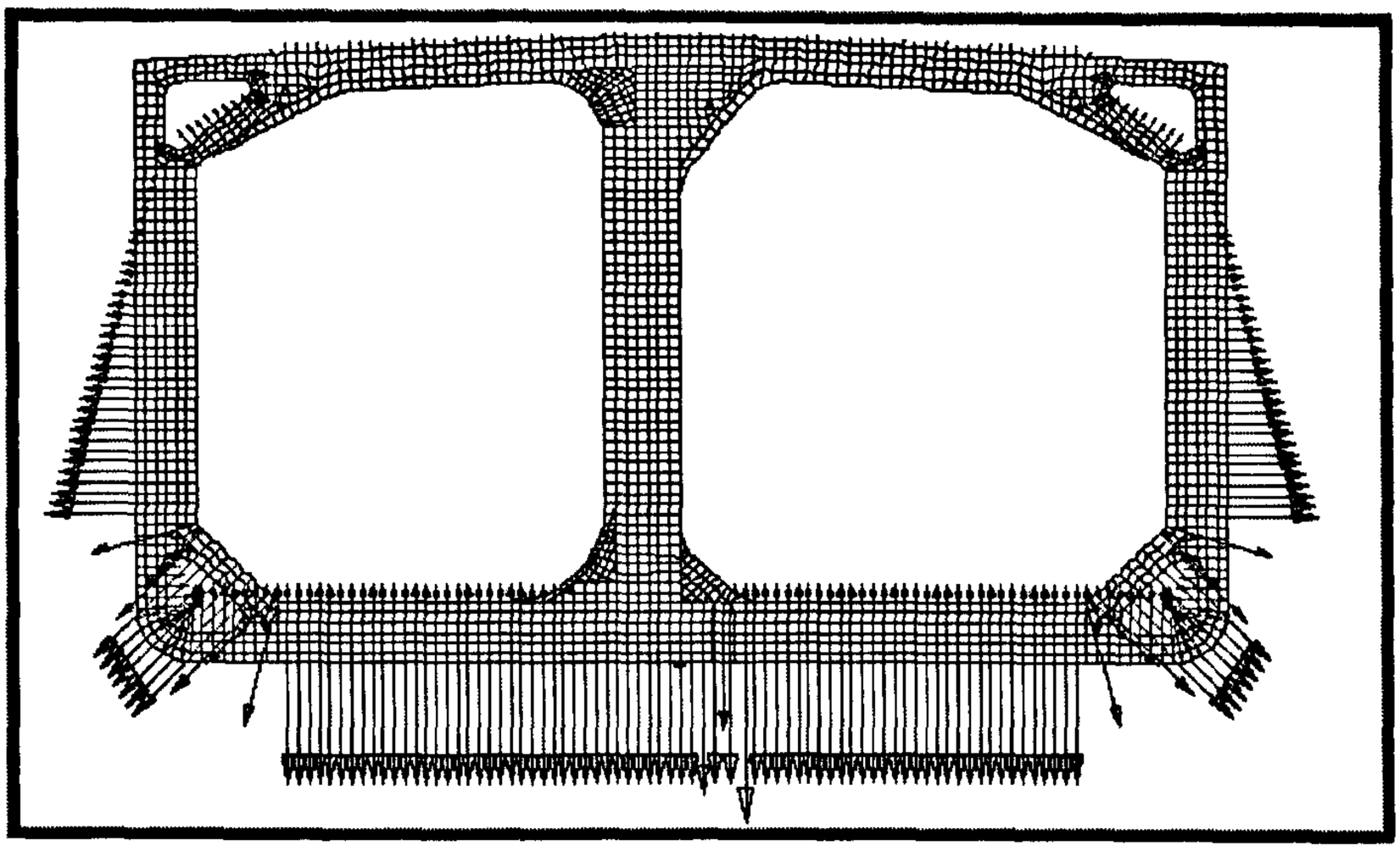

Figure 4-7 Ballast Condition (External and Internal Pressure)

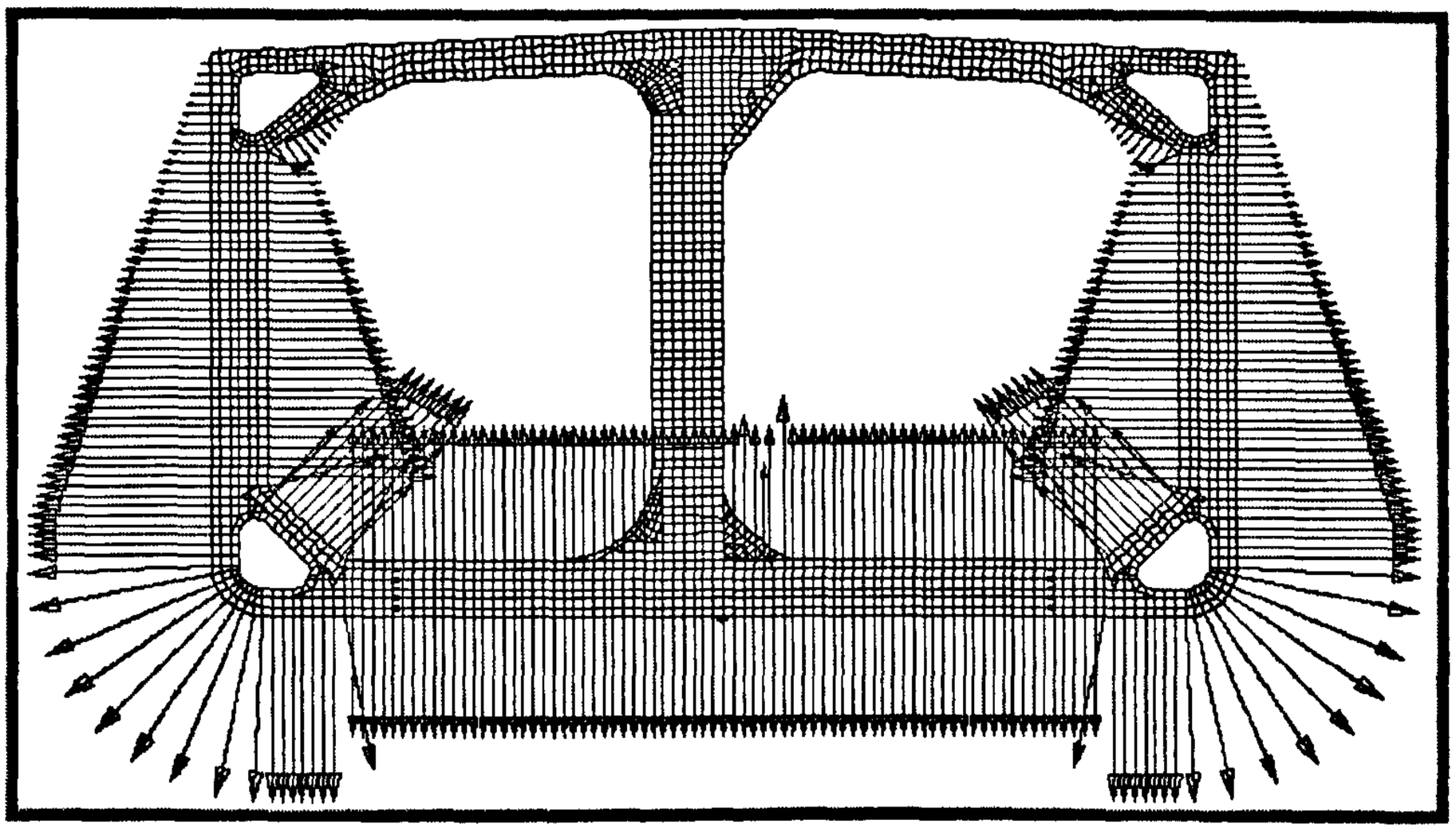

Figure 4-8 Full Load Condition (External and Internal Pressure)

4.3 Hull Girder Loads

To assess the strength of the hull girder and individual structural members, finite element structural analyses of the hull structure have been performed using the FEA approach to compare the strength of the vessel structure to the failure criteria for yielding, buckling and fatigue (strength assessment) which is often a time consuming process. To perform such an evaluation, one must create an accurate FEA model, apply loads, run the analysis and assess the results.

The common practice is to simplify the assessment procedure such as reducing the size of the finite element model, automating loads application and breaking the task into one global analysis followed by a series of local detailed analyses. Although the use of a higher mesh density and more structural detail will result in the most accurate stress predictions, such a model is much more time consuming to create, more prone to error during model creation and requires more computer resources to solve. However, if an insufficient number of elements are used, the structure will lack the correct flexibility leading to inaccurate results.

4.3.1 Failure Criteria for Ductile Materials

This is a significant yet large subject and can't be discussed in details within the scope of this research; however it can be summarized as follows:

- *Non Stress-Based Criteria*: The success of all machine parts and structural members are not necessarily determined by their strength. Whether a part succeeds or fails may depend on other factors, such as stiffness, vibrational characteristics, fatigue resistance, and/or creep resistance.

- *Stress-Based Criteria*: The purpose of failure criteria is to predict or estimate the failure/yield of parts or structural members.

The most common and well-tested theories applicable to isotropic materials are dependent on the nature of the material in question (i.e. brittle or ductile), and are listed in the following:

- *Brittle*: Maximum normal stress criterion and Mohr's theory.
- *Ductile*: Maximum shear stress criterion and von Mises criterion

The most common criterion used in the industry is von Mises (1913), also known as the maximum distortion energy criterion, octahedral shear stress theory, or Maxwell-Huber-Hencky-von Mises theory, is often used to estimate the yield of ductile materials. The von Mises criterion states that failure occurs when the energy of distortion reaches the same energy for yield/failure in uniaxial tension. Mathematically, this is expressed as:

$$\frac{1}{2}\left[(\sigma_1-\sigma_2)^2+(\sigma_2-\sigma_3)^2+(\sigma_3-\sigma_1)^2\right]\leq {\sigma_y}^2$$

Equation 4-2

This equation represents a principal stress ellipse as illustrated in the following ***Figure 4-9***. Also shown on the same figure is the maximum shear stress criterion (dashed line). This theory is more conservative than the von Mises criterion since it lies inside the von Mises ellipse. In addition to bounding the principal stresses to prevent ductile failure, the von Mises criterion also gives a reasonable estimation of fatigue failure, especially in cases of repeated tensile and tensile-shear loading.

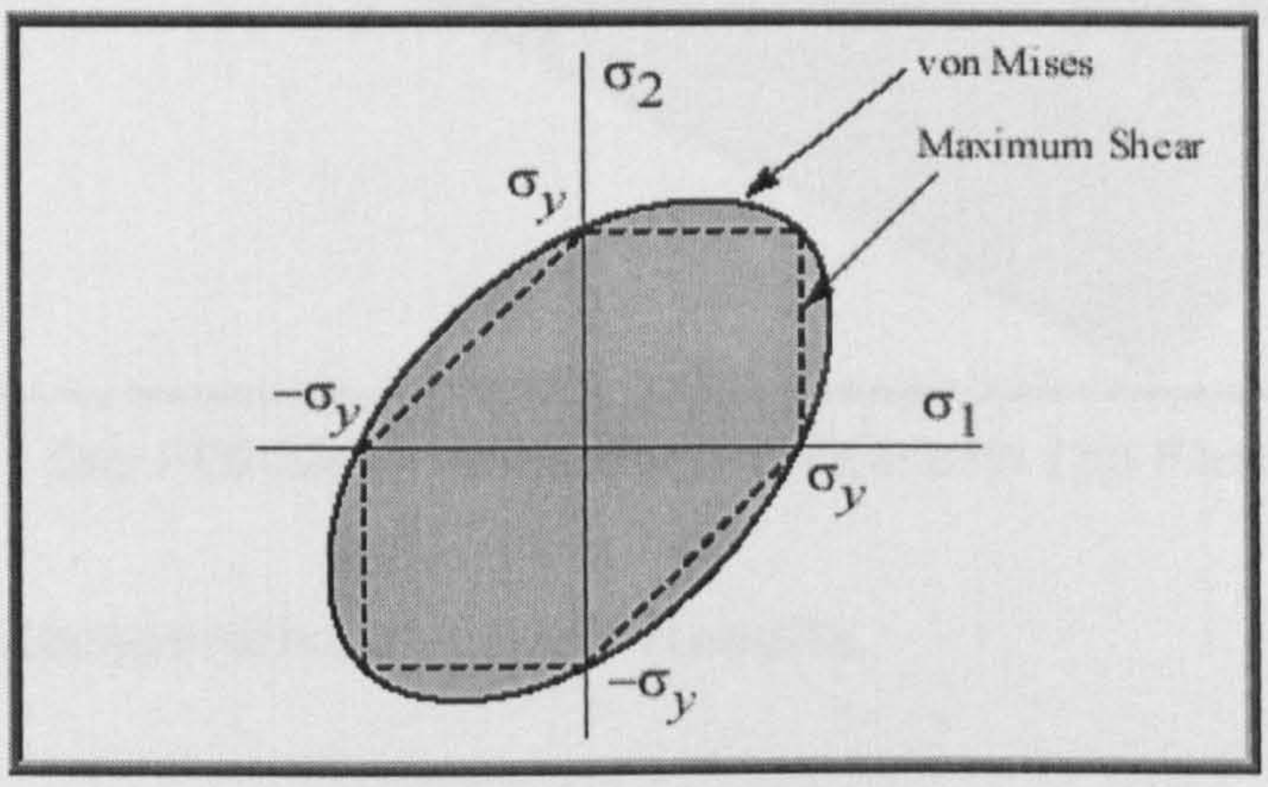

Figure 4-9 von Mises Criteria

4.4 The City FPSO2000 FEA

4.4.1 3D Hull Girder Mesh

A typical FEA model of a complex Monohull FPSO mid section used in the City FPSO 2000 is showed in ***Figure 4-10***.

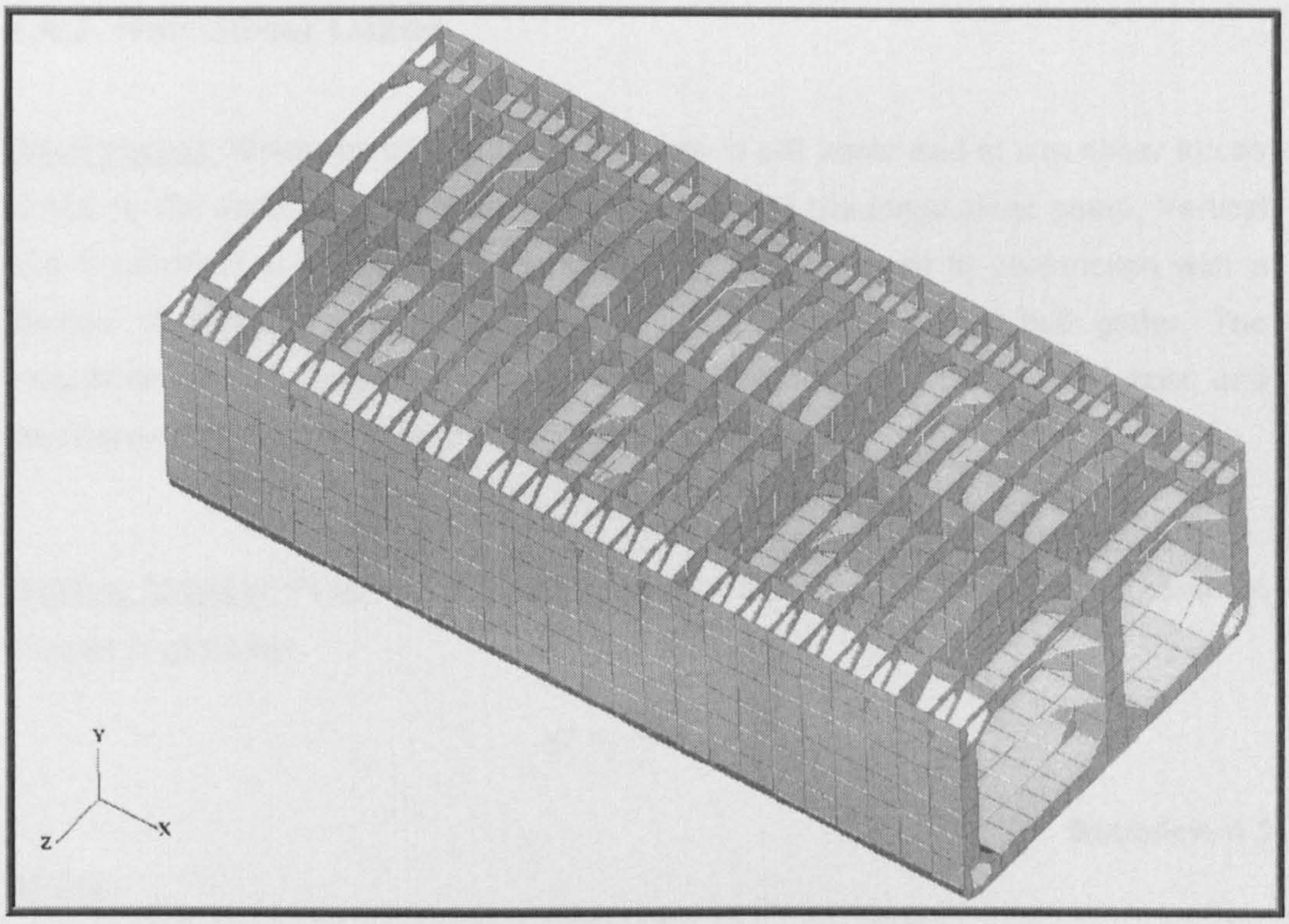

Figure 4-10 City FPSO2000 Midsection 3-D FEM with Top Plating Removed

4.4.2 (3-D) Comparative Analysis Results

The global analysis performed in a linear static mode using MSC-NASTRAN for Windows, where the pre and post processing have been handled using FEMAP.

The following ***Table 4-2*** gives a comparison of the load case number one results from City FPSO2000 to different 3D-Course mesh FEM from variant vessel sizes, to give a simple indication of early results.

Reference	***Vessel Dimensions (m) L x B x D***	***Max Von-MISES Elemental Results (MPa)***
City FPSO2000	265.0 x 45.0 x 25.0	230.5
Daewoo Ship Building (1993)	320.0 x 58.0 x 31.0	388.5
Sumitomo Heavy Industries (1993)	317.0 x 58.0 x 31.2	380.0
Tritron FPSO by Kvaerner oil & gas	313.0 x 48.2 x 25.2	284.6

Table 4-2 Comparison of Course Mesh Hull Girder Results

4.4.3 Hull Girder Loads

Shear Forces: When the vessel hogs and sags in still water and at sea shear forces similar to the vertical shear forces will be present in the longitudinal plane. Vertical and longitudinal shear stresses are complimentary and exist in conjunction with a change of bending moment between adjacent sections of the hull girder. The magnitude of the longitudinal shear force is greatest at the neutral axis and decreases towards the top and bottom of the girder.

Bending Stresses: From classic bending theory the bending stress (σ) at any point in a beam is given by:

$$\sigma = \frac{M}{I} \times y$$

Equation 4-3

Where:

M = applied bending moment.

y = distance of point considered from neutral axis.

I = second moment of area of cross-section of beam about the neutral axis.

Occasionally reference is made to the sectional modulus (Z) of a beam; this is simply the ratio between the second moment of area and the distance of the point considered from the neutral axis, i.e. I/y = Z. The bending stress (σ) is then given by:

$$\sigma = \frac{M}{Z}$$

Equation 4-4

The following graphs ***Figure 4-11***, ***Figure 4-12*** and ***Figure 4-13*** give a realistic practical account of the loads, shear forces and the resultant bending moment of the City FPSO hull girder structure, worse case scenario the sagging and hogging under hydrodynamic loads. Correlation with the beam theory can be seen at ***section 4.4.7***, below.

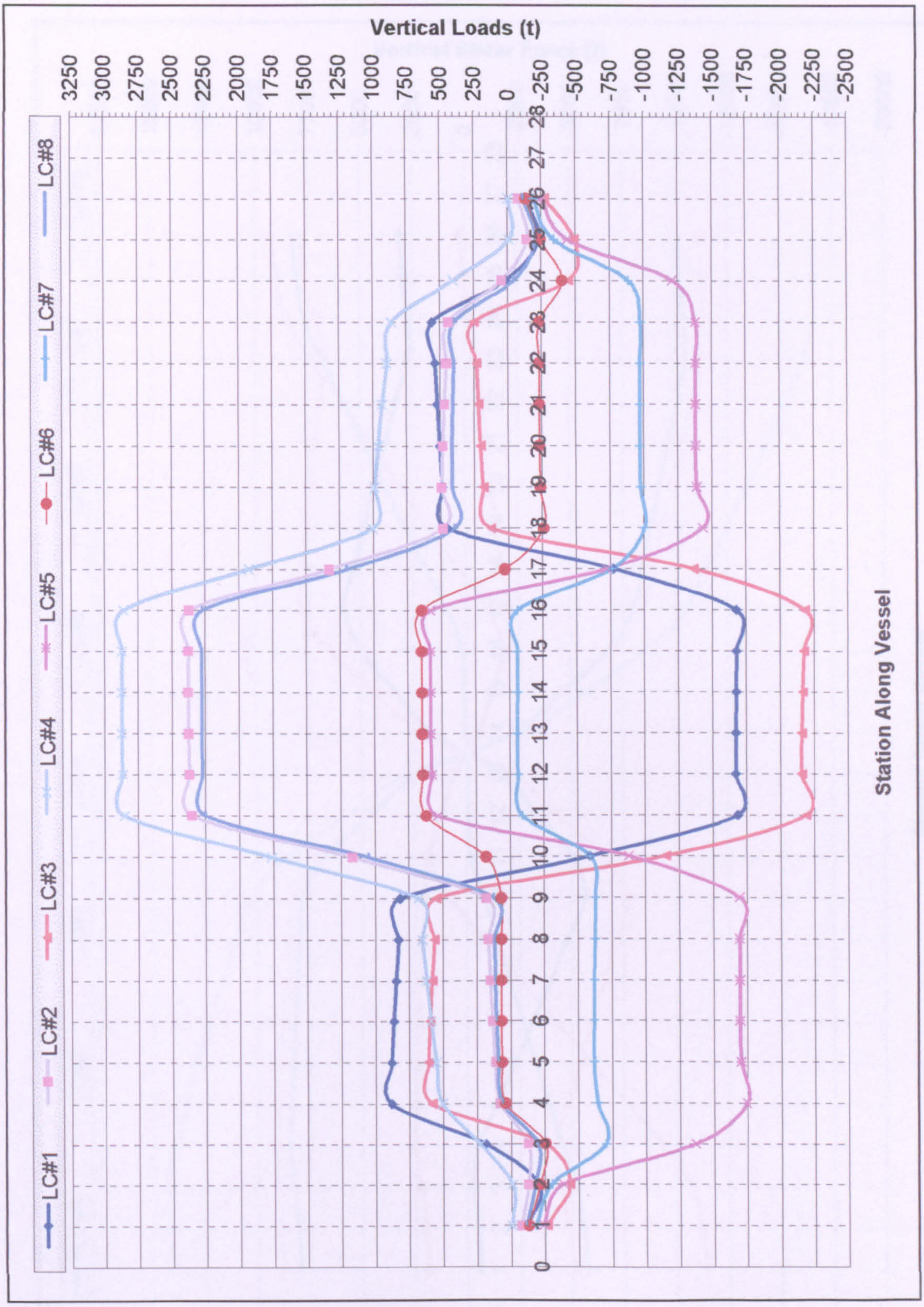

Figure 4-11 Vessels Vertical Load Case #1 to #8

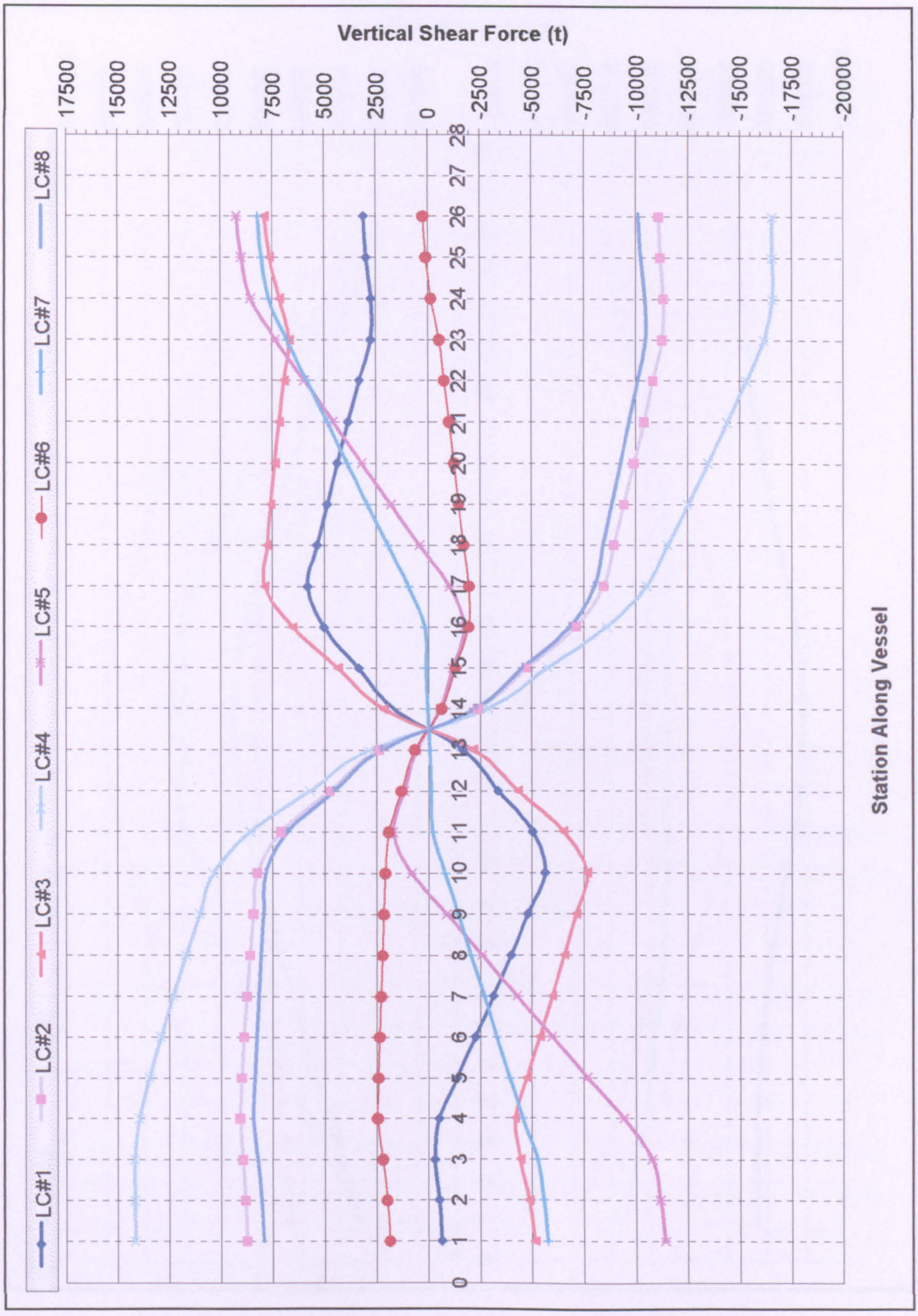

Figure 4-12 Vessels Vertical Shear Forces Case #1 to #8

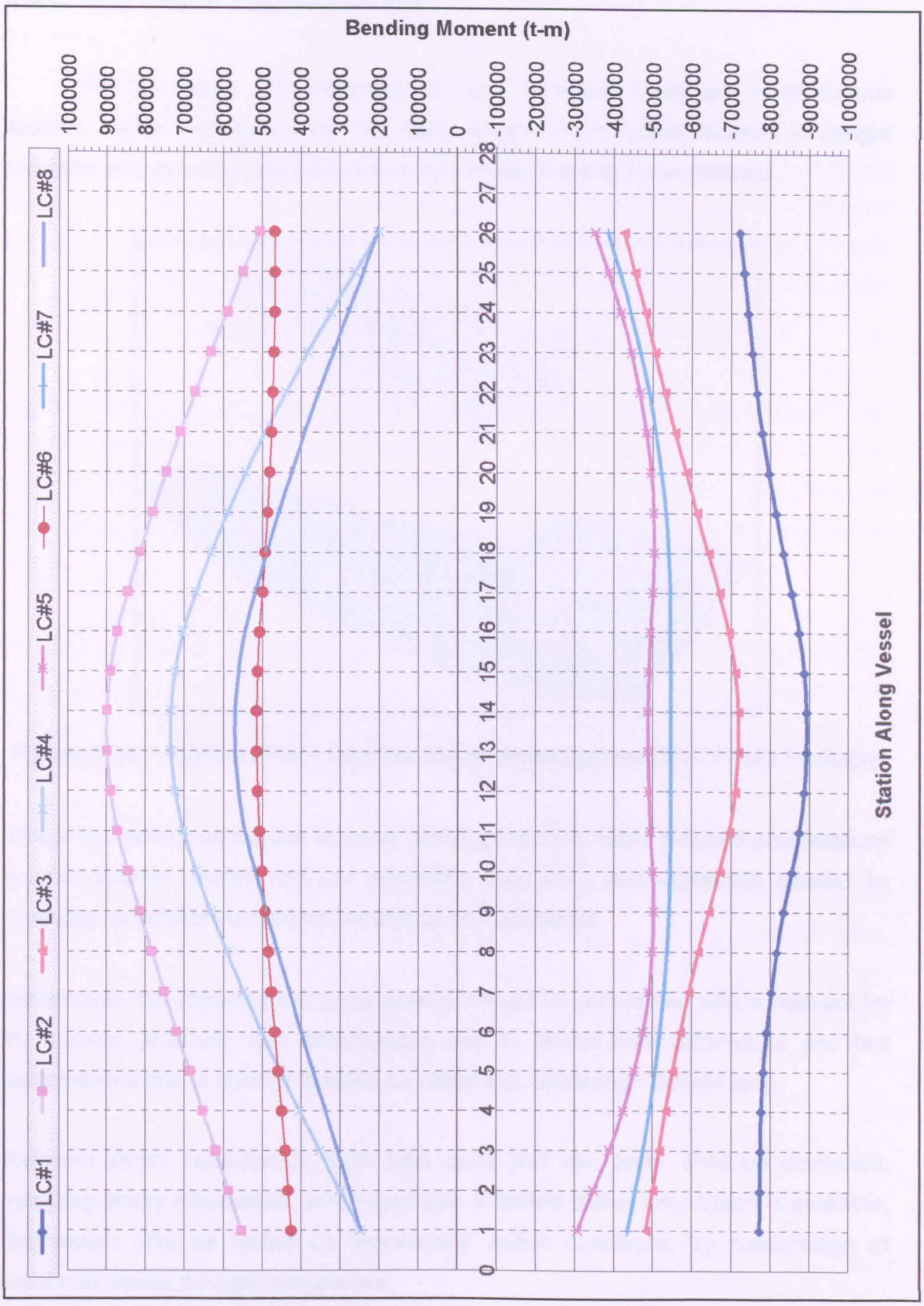

Figure 4-13 Vessels Bending Moments Case #1 to #8

4.4.4 Hull Girder Topside Loads

For the design and evaluation of deck structural loads due to production facilities shown in ***Figure 4-14***, the static weight of production facilities in upright condition and dynamic loads due to vessel's motions are to be considered.

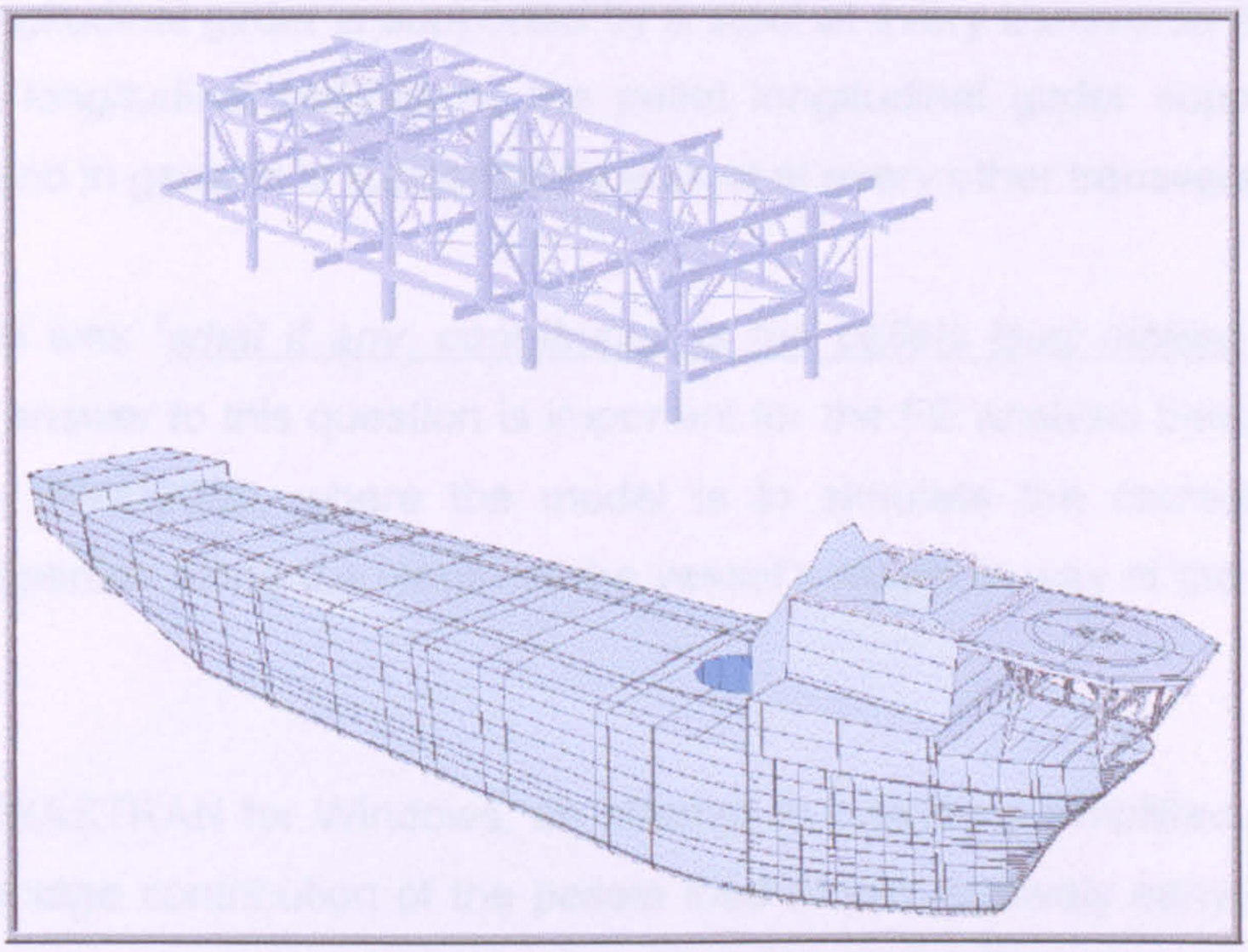

Figure 4-14 Typical FPSO Topside Frame Arrangement *(DNV FPSO Package)*

Where hull deformations due to wave bending moment, wave induced accelerations (inertia actions), vortex induced vibrations from wind and vibrations caused by operation of topside equipment are also to be considered.

Additionally, the following low cycle actions should be considered where relevant for the topside structure: hull deformations due to temperature differences and hull deformations due to change in filling condition e.g. ballasting / deballasting.

Relevant stress components, both high cycle and low cycle, shall be combined, including phase information, when available. If limited phase information is available, the design may be based on 'worst-case' action conditions, by combination of maximum stress for each component.

Due to the time limitations on this research it has been deemed appropriate to use a simplified approach, to estimate the contribution of topside loads to hull section properties, that the topside equipment is mounted on four pallets. Considering the

upper deck from aft to forward, each pallet is supported by "Cruciform" type stools at the vessel's centreline and wing longitudinal bulkheads.

Due to the installation requirement to provide a single lift for each pallet onto the vessel, the longitudinal girders in way of the stools are 1.2m deep and can be defined as: Vessel's centreline, Wing longitudinal bulkhead in way of the vessel's centreline the pallet longitudinal girder is supported by a stool at every transverse frame in way of the wing longitudinal bulkheads, the pallet longitudinal girder support is more intermittent and in general is supported by a stool at every other transverse.

The question was *"what if any, contribution is the pallets load making on the hull girder?* The answer to this question is important for the FE analysis being conducted on the City FPSO2000, where the model is to simulate the correct hull girder sectional properties along the length of the vessel's model in way of the cargo tanks region.

Using MSC/NASTRAN for Windows, an attempt to provide a simplified assessment of the percentage contribution of the pallets load at this relatively early stage of the analysis has been conducted. The process begins by modelling the hull girder with a series of node points at every transverse frame and distributed top loads of merely 7000 tonnes.

The combined stresses and deflection at the central transverse web-frame of the hull girder under the application of the normal and top loads are fond to be 230.5 MPa, 95.00 mm and 239.8 MPa, 96.81 mm respectively as shown in ***Figure 4-15*** and ***Figure 4-16***. This represents the response of the hull girder with and without the influence of the topsides support structure.

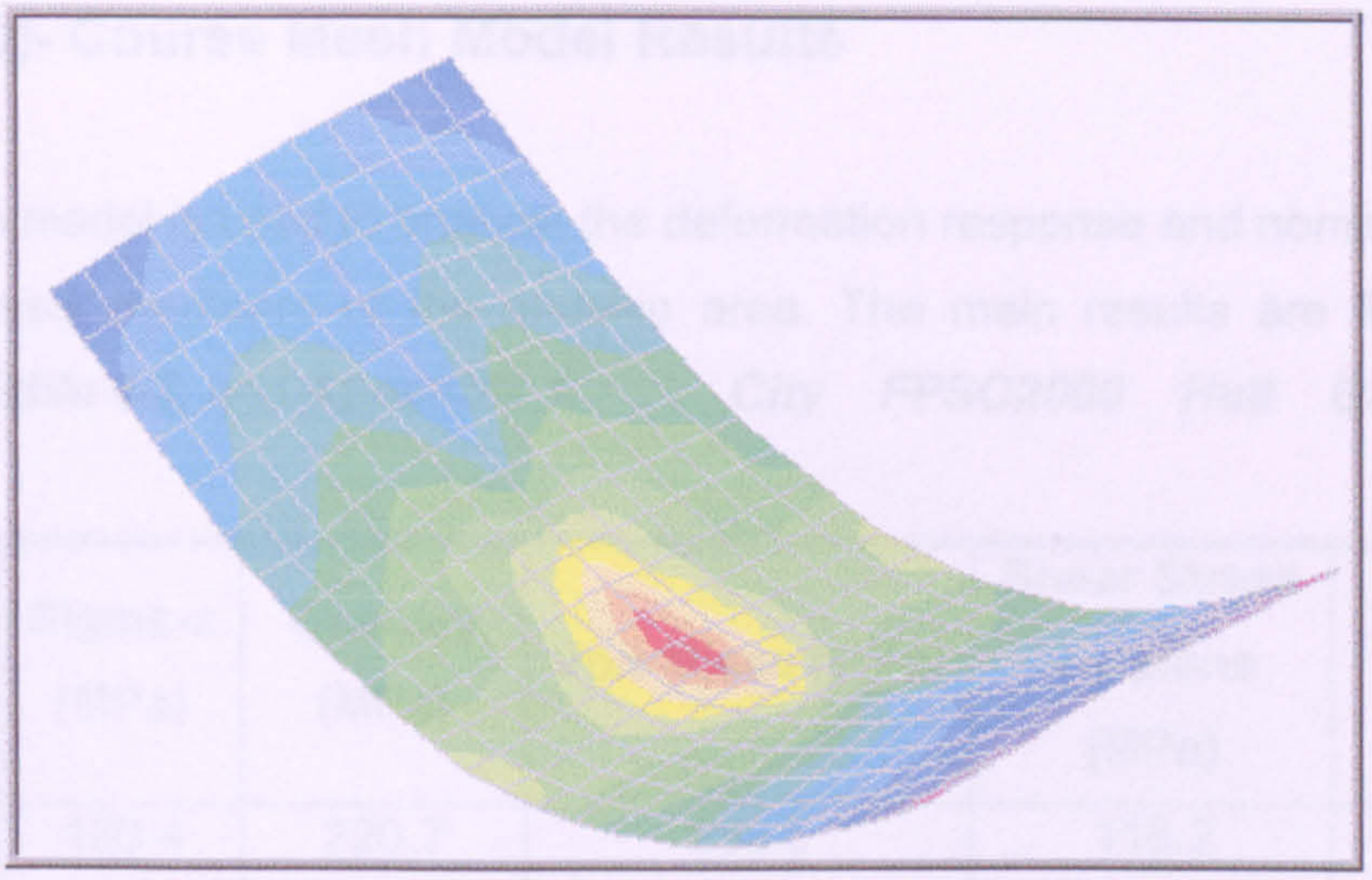

Figure 4-15 FPSO Deck Structure without Top Loads

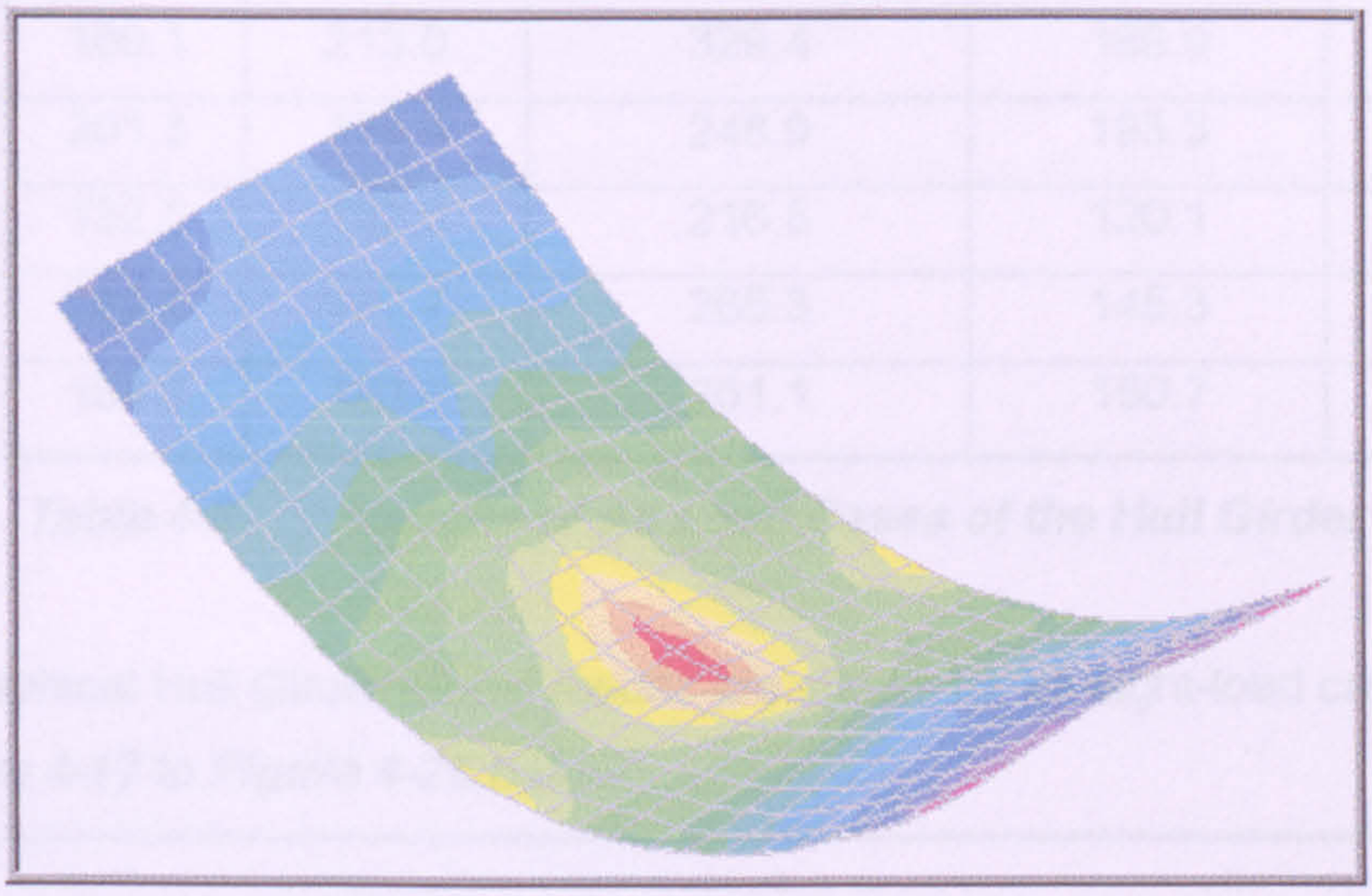

Figure 4-16 FPSO Deck Structure with Top Loads

It is assumed for the purposes of this analysis that the sectional properties of each pallet skid are the same. Under the same loading the modified model gave a combined stresses and deflection at amidships of 239.8 MPa and 96.81 mm respectively, which is 1.81 mm greater than the 95.0 mm deflection for the vessel model without topsides.

This increase represents a 1.87% change in hull girder response. On the above basis it is recommended that the section properties for the hull girder will not to be amended, as the influence of topsides loads on the hull girder is reasonably low.

4.4.5 (3D)- Course Mesh Model Results

The model is used to analyse the deformation response and nominal stresses of the primary members of the midship area. The main results are listed in the following ***Table 4-3***, and ***Appendix A City FPSO2000 Hull Girder FEA Results.***

oad Case#	Sigma-x (MPa)	Sigma-y (MPa)	Von-Mises (MPa)	Shear Stress x-y plane (MPa)	Deflection (mm)
1	186.4	220.7	230.5	118.2	95.0
2	165.9	260.8	265.3	142.1	117.2
3	197.5	186.0	259.7	144.8	90.3
4	169.1	213.0	329.4	189.9	113.9
5	201.3	159.4	248.9	193.3	70.6
6	132.5	152.0	216.5	120.1	67.0
7	232.8	187.7	265.3	145.3	71.2
8	186.8	193.6	261.1	150.7	92.0

Table 4-3 Results of All Load Cases of the Hull Girder

Typical graphical Hull Girder model results are shown for all eight-load cases starting from ***Figure 4-17*** to ***Figure 4-26 below***.

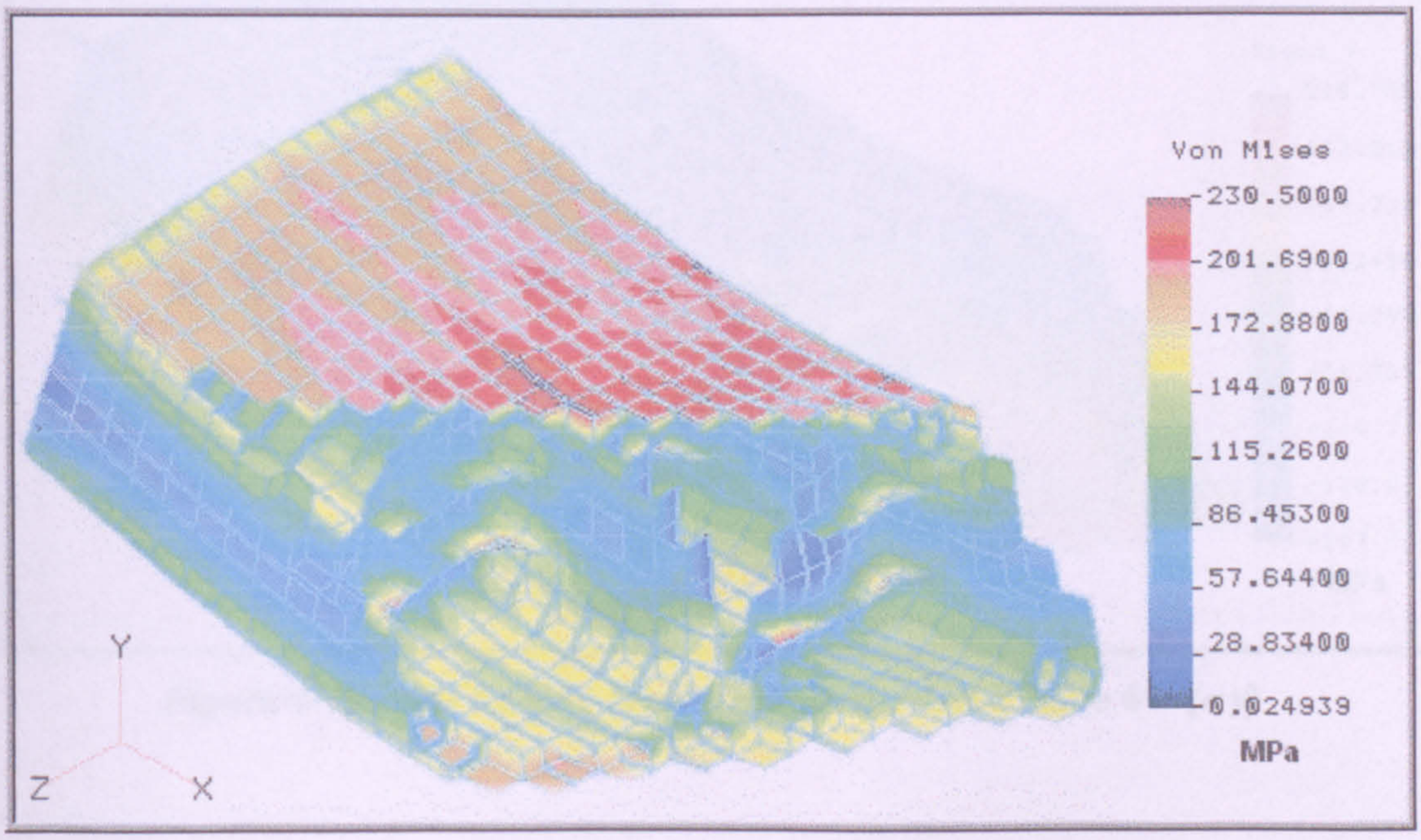

Figure 4-17 3D Course Mesh Hull Girder Load Case #1

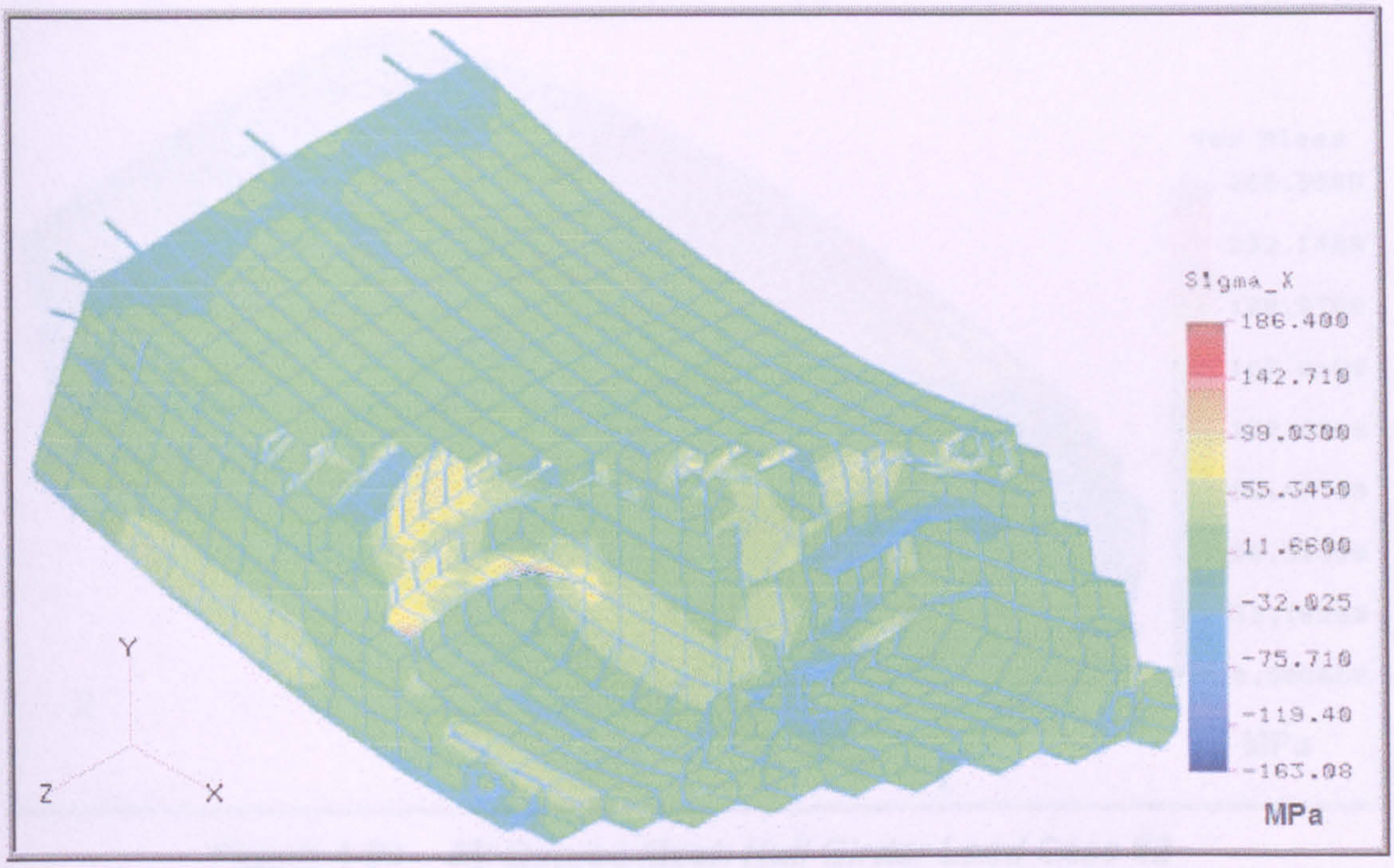

Figure 4-18 3D Course Mesh Hull Girder Load Case #1- (σx)

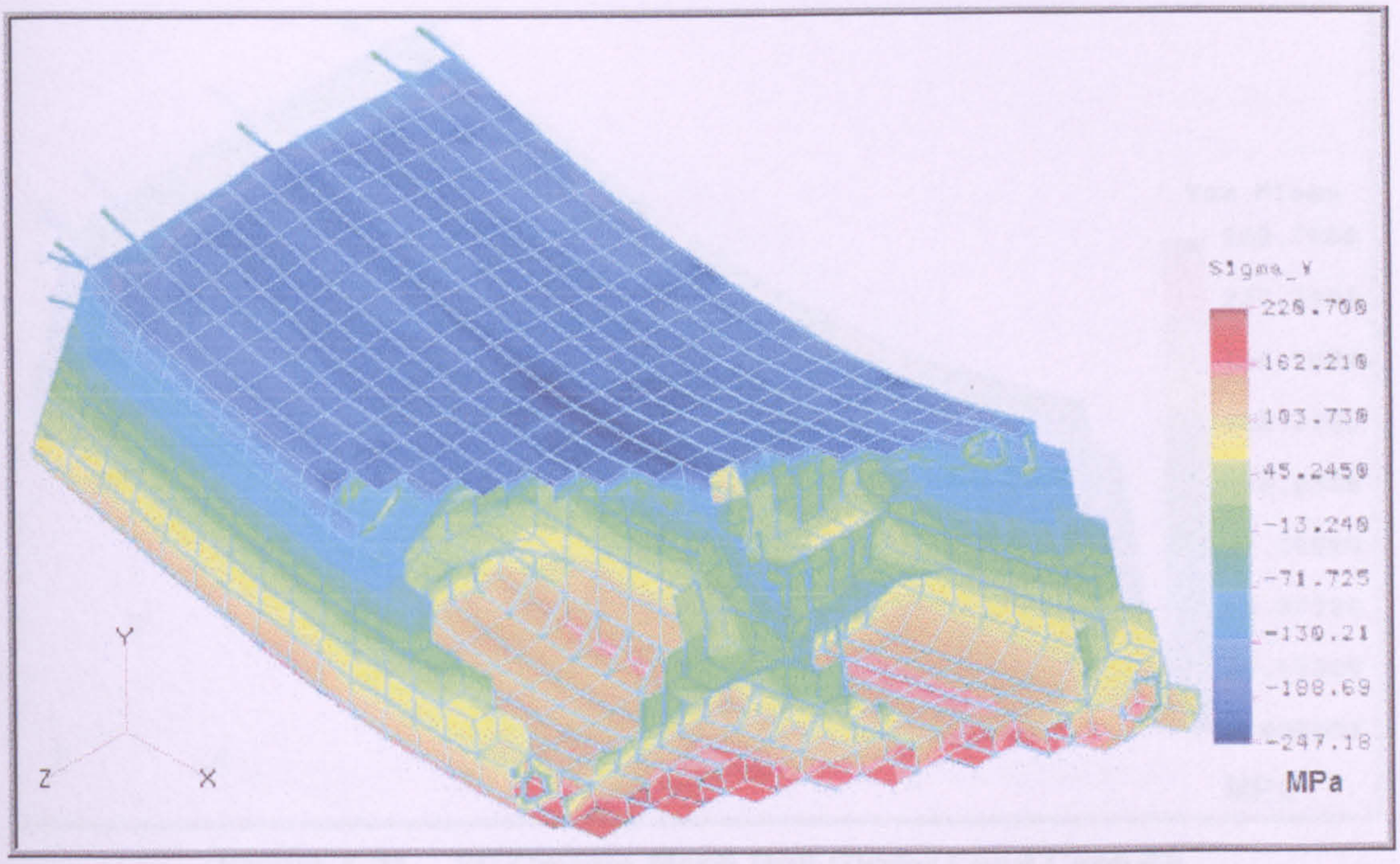

Figure 4-19 3D Course Mesh Hull Girder Load Case #1- (σy)

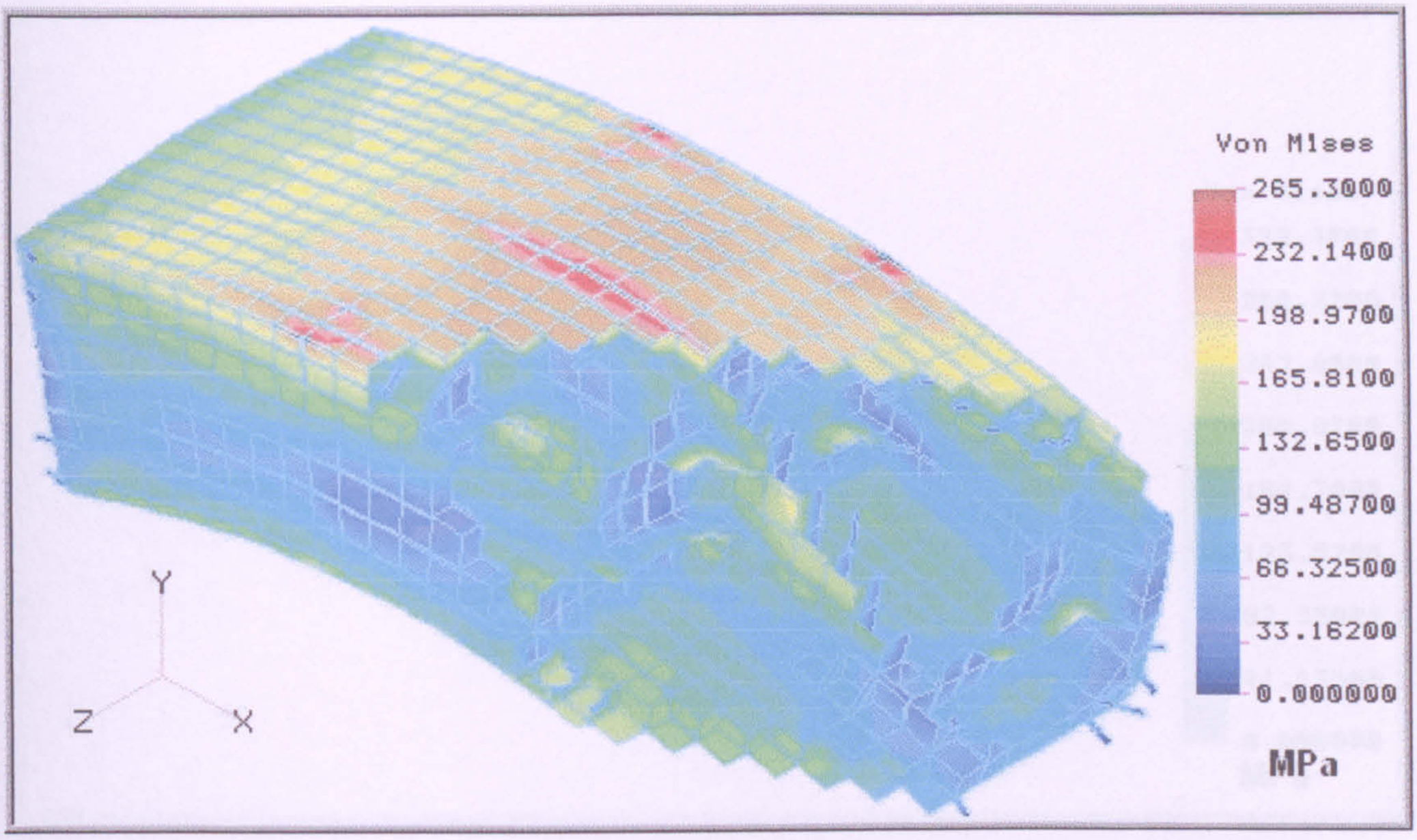

Figure 4-20 3D Course Mesh Hull Girder Load Case #2

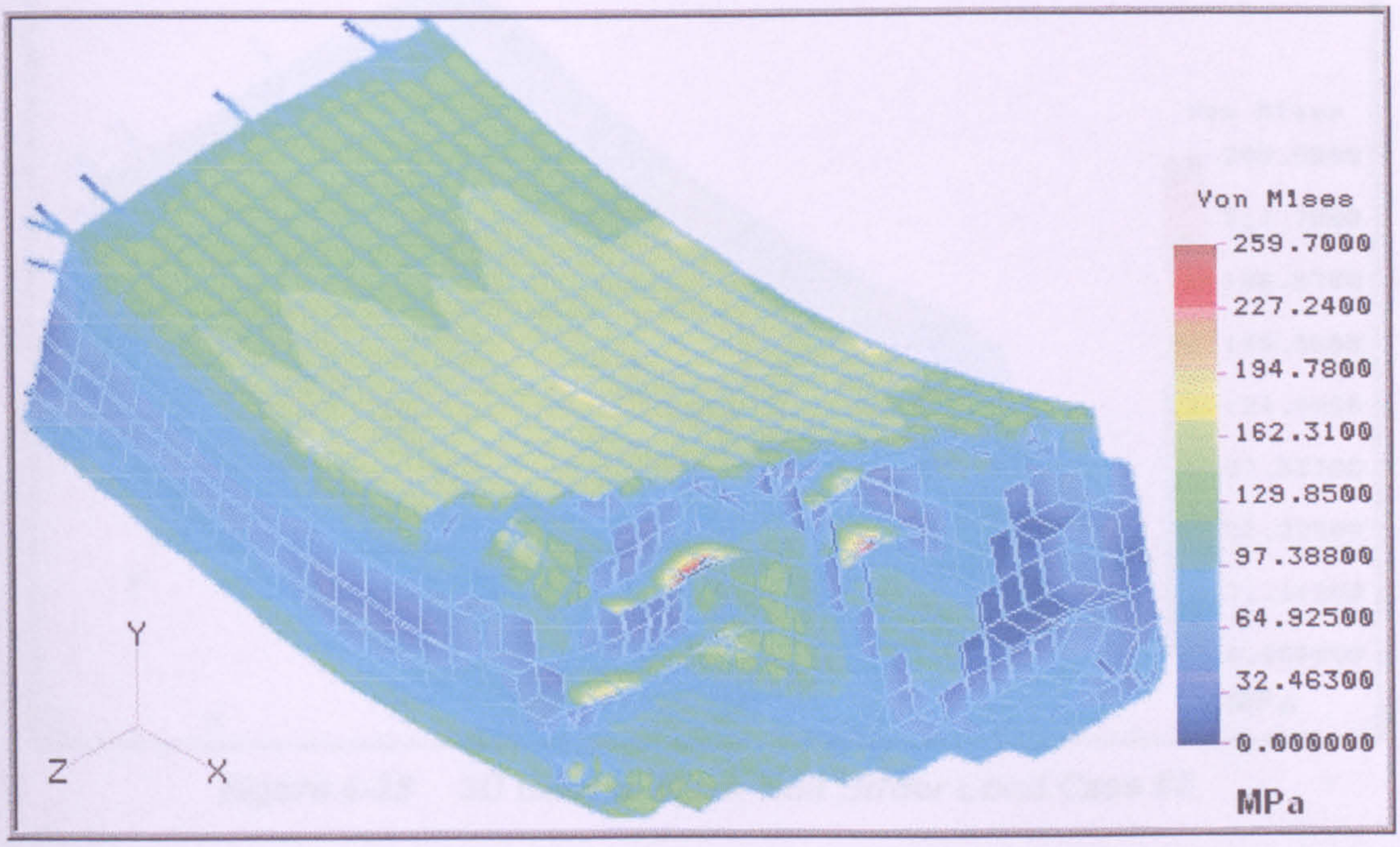

Figure 4-21 3D Course Mesh Hull Girder Load Case #3

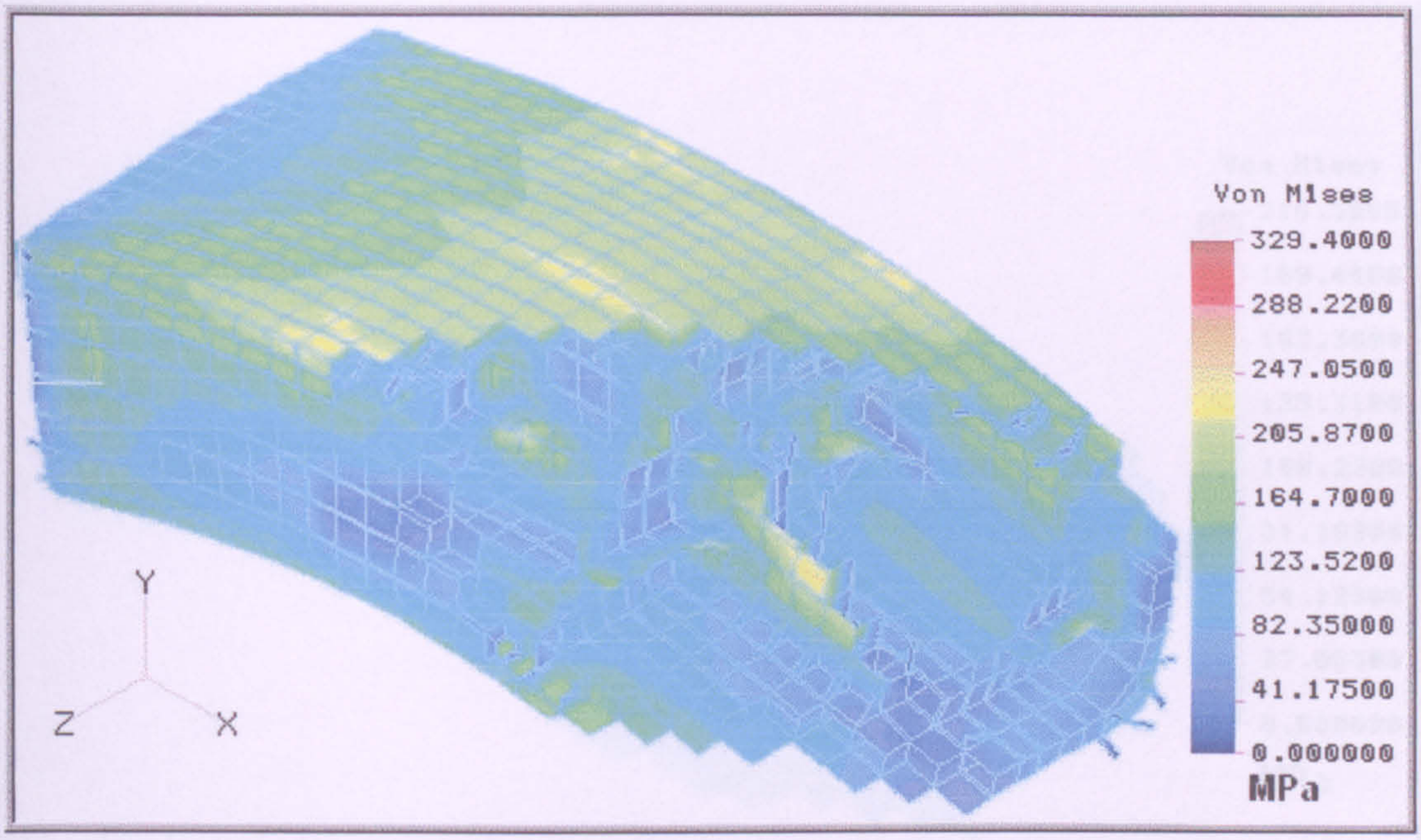

Figure 4-22 3D Course Mesh Hull Girder Load Case #4

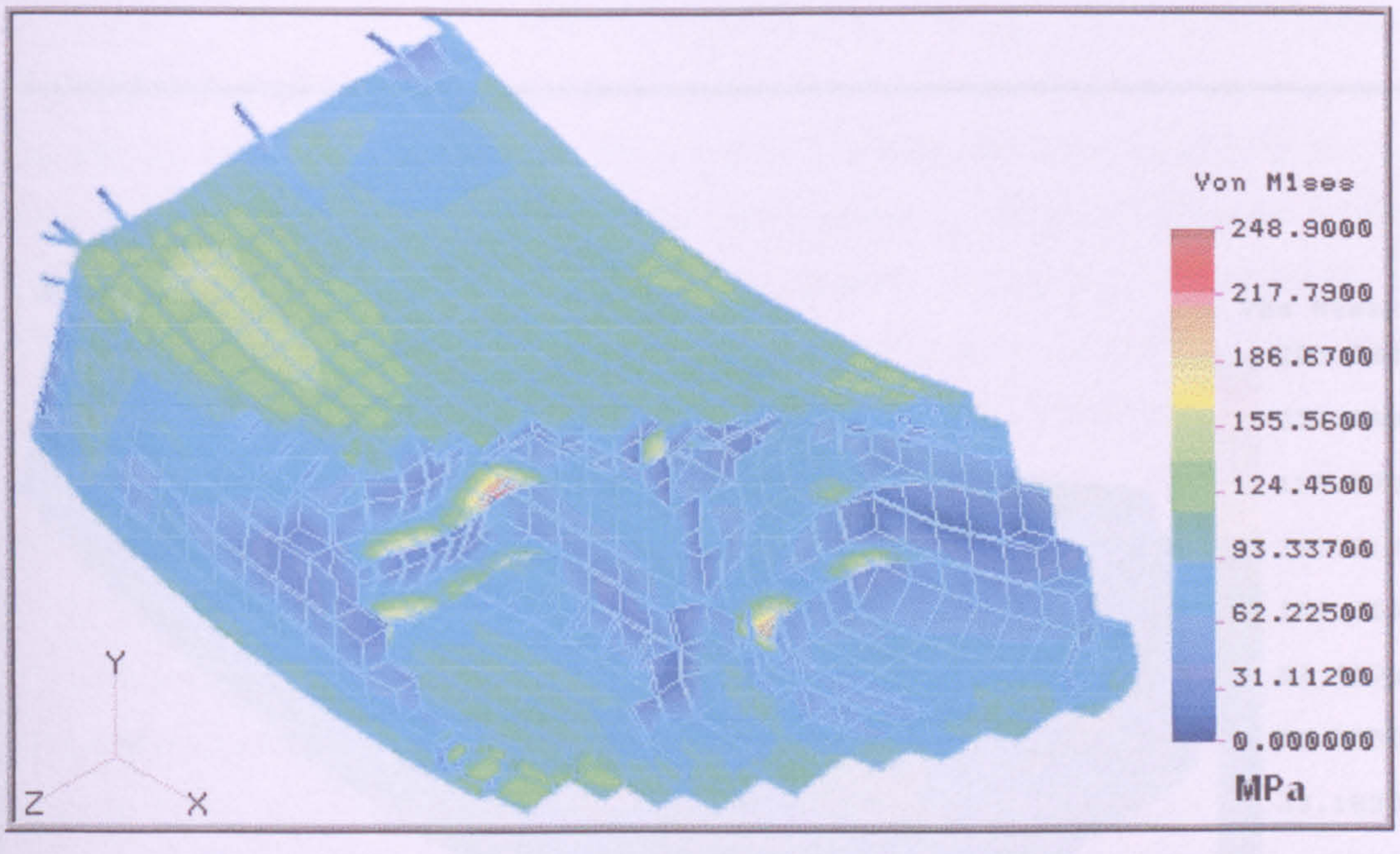

Figure 4-23 3D Course Mesh Hull Girder Load Case #5

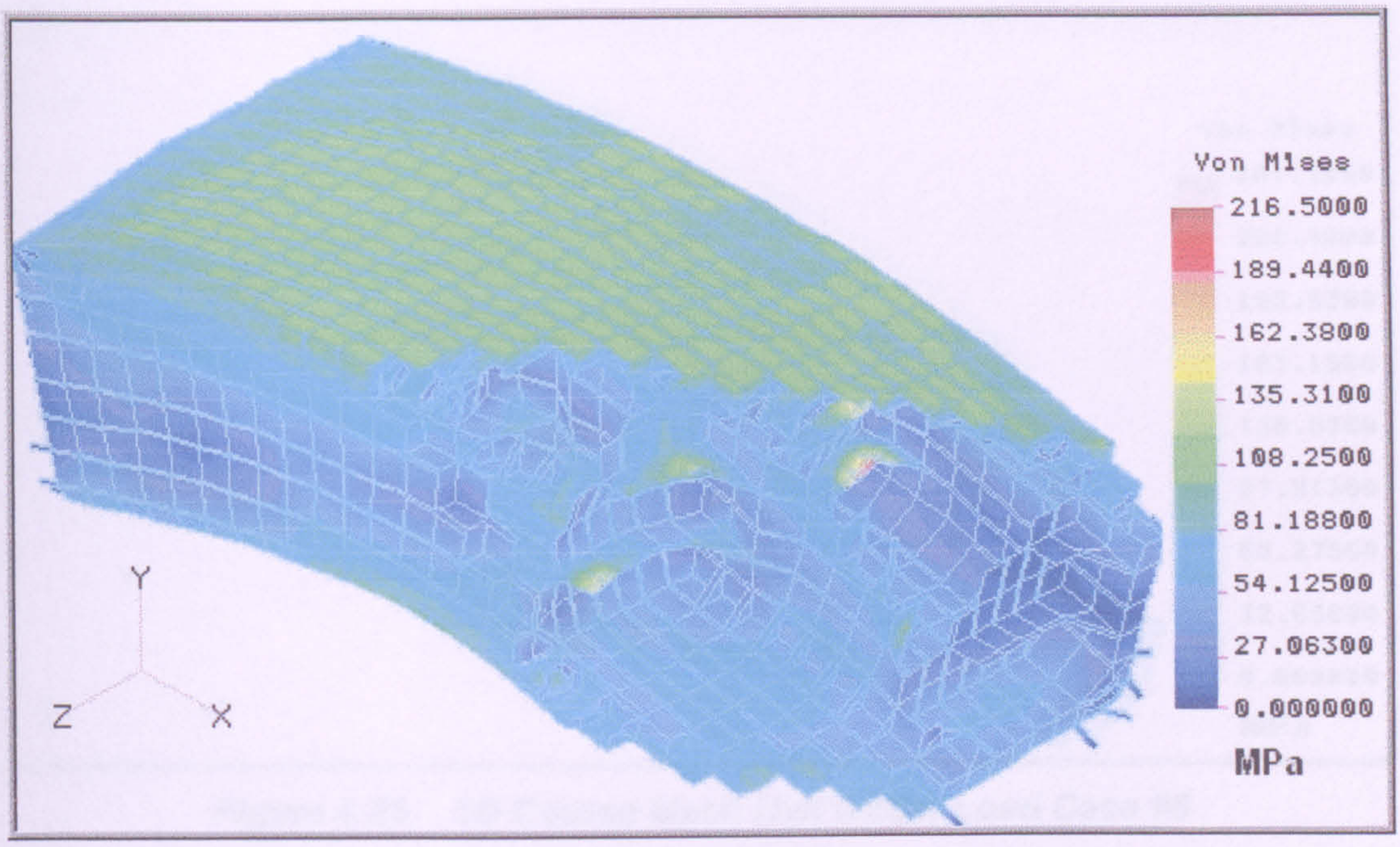

Figure 4-24 3D Course Mesh Hull Girder Load Case #6

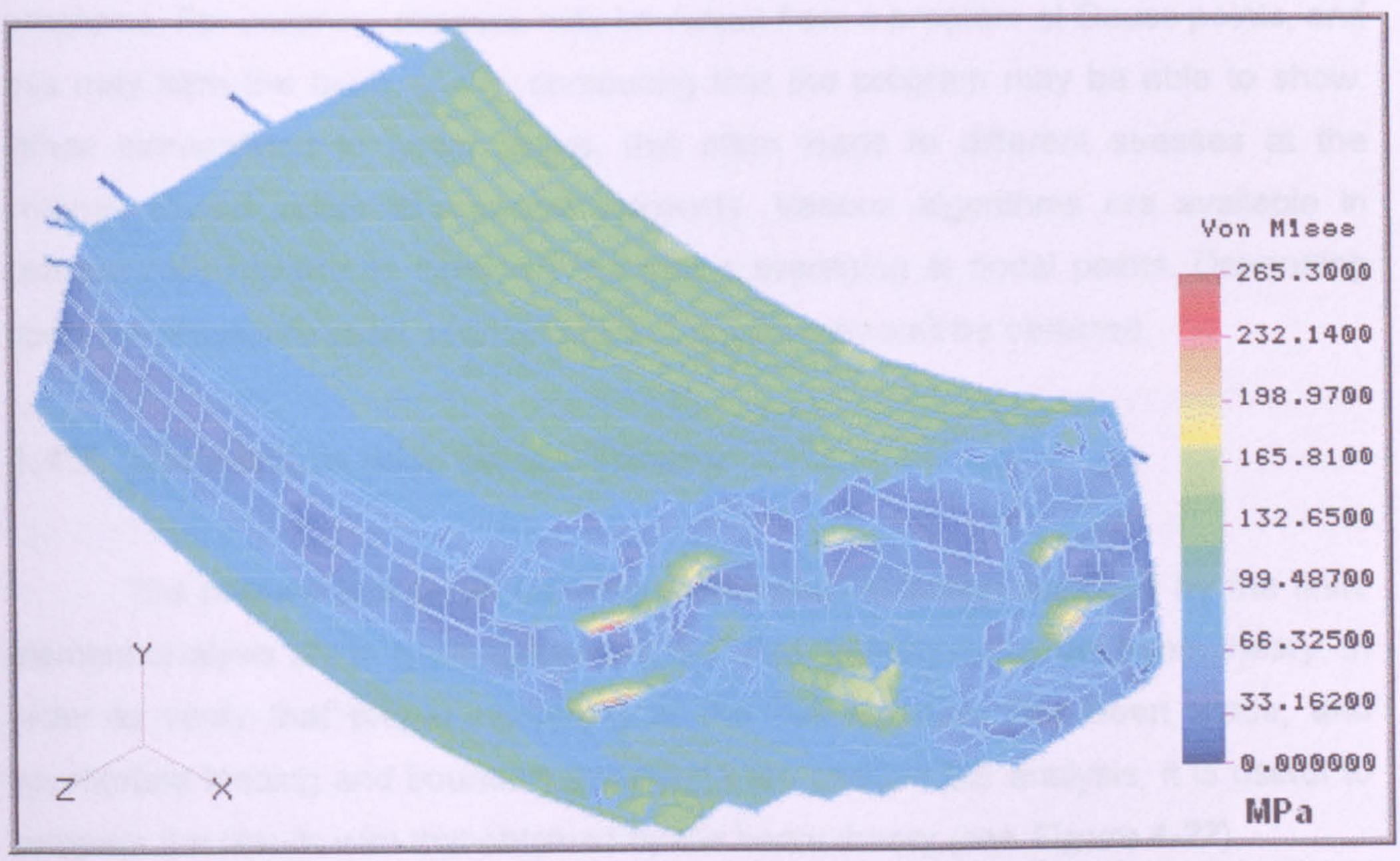

Figure 4-25 3D Course Mesh Hull Girder Load Case #7

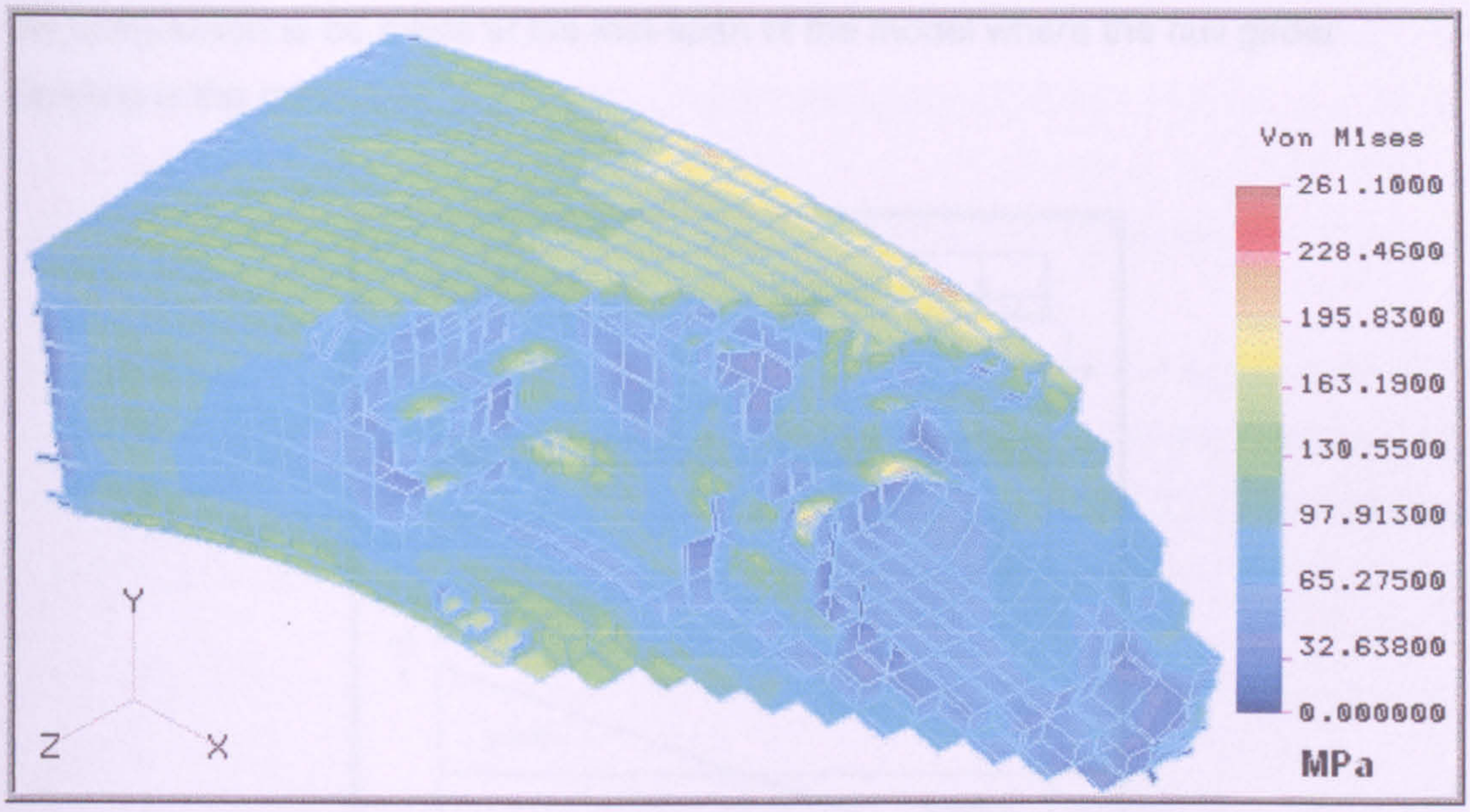

Figure 4-26 3D Course Mesh Hull Girder Load Case #8

4.4.6 Interpretation of Results from Finite Element Analysis

4.4.6.1 Stress Averaging

Care has to be exercised in interpreting the results from Finite Element programs. For instance, stresses may be output from a program at Gauss points, and this may form the basis of any contouring that the program may be able to show. When extrapolated to nodal points, this often leads to different stresses at the common nodal points of adjacent elements. Various algorithms are available in commercial programs to carry out the stress averaging at nodal points. Depending upon the procedure used, slightly different results may well be obtained.

4.4.7 Correlation with Beam Theory

The primary hull girder bending stress and deflection obtained by the finite element analysis are in good agreement with that determined by the beam theory. In order to verify that proper modelling of the hull structure has been made, and appropriate loading and boundary conditions are used in the analysis, it is useful to compare the results with that obtained by the beam theory (see ***Figure 4-27***).

The comparison was made in areas where effects of minimum local loads are. The best correlation can usually be obtained at the deck at side. It is also preferable for

the comparison to be made at the mid-span of the model where the hull girder bending is the maximum.

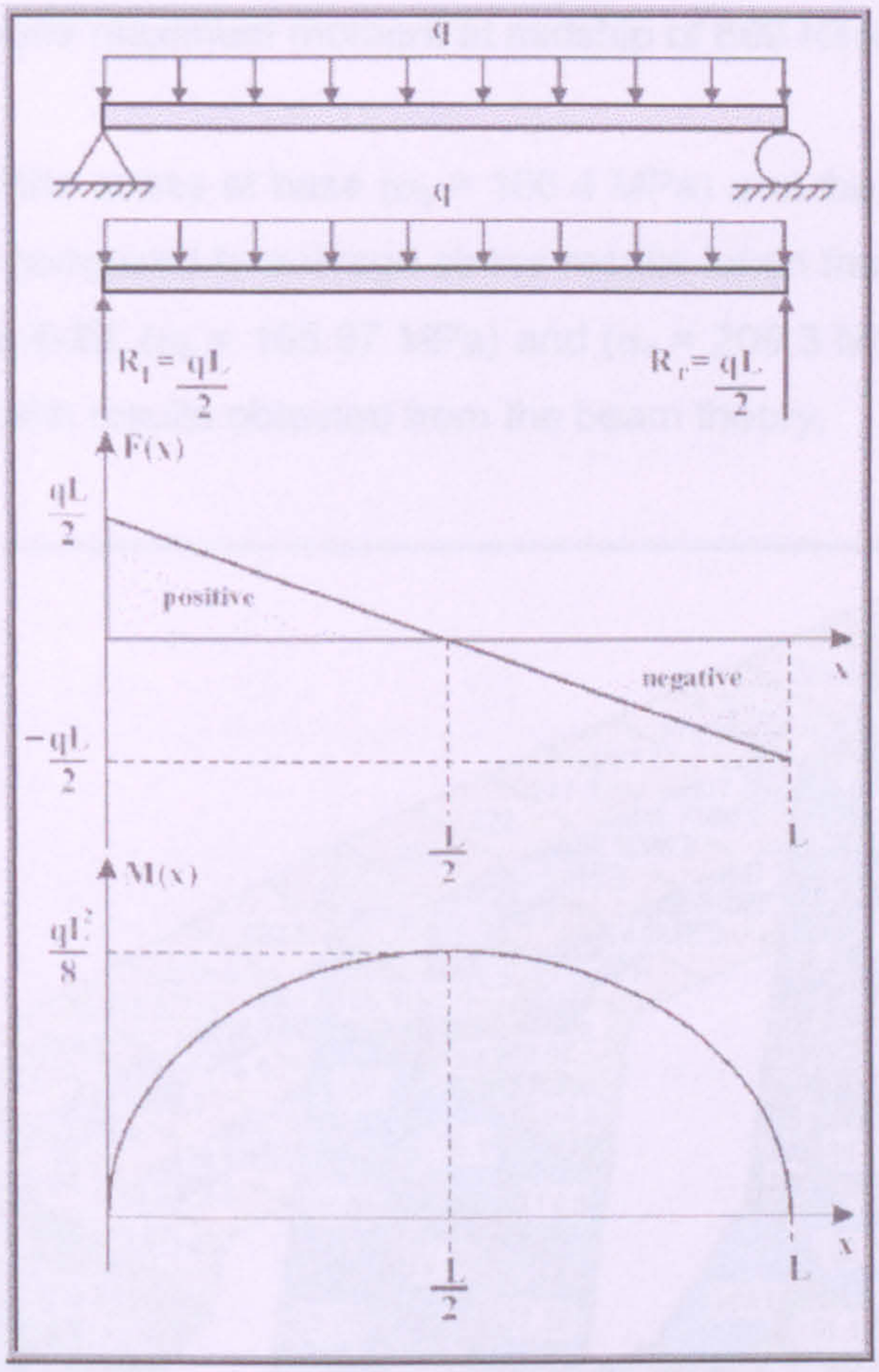

Figure 4-27 Shear Force and Bending Moment Diagrams for a Simply-Supported Beam under A Uniform Load

Because of secondary bending, shear lag, or stresses due to alternate hold loading, significant differences in hull girder bending stresses can be expected in areas near the vessel's centreline. Particularly, for simple form double-hull FPSOs with only two longitudinal bulkheads, the stress level can differ significantly.

The following calculations conducted at midship:

Three tank compartments (L = 77.7 m),

The FPSO's dead weight (w = 125,000 Tonne), with L = 265 m,

Hull Girder section inertia about neutral axis (I = 591.581 m^4),

Distance on neutral axis to deck at side (yd = 13.904 m),

Distance on neutral axis to moulded baseline {top of keel} (yb = 11.096 m),

Section modulus at deck at side (zd = 42.29 m^3),

Section modulus at moulded baseline {top of keel} (zb = 53.0 m^3).

q = 472 Tonne/m, gives maximum moment at midship of 899 KTonne-m.

From ***Equation 4-4*** the stress at base (σ_b = 166.4 MPa) and the stress at side (σ_d = 208.5 MPa). Which compared to average stress results taken from the FEM Analysis presented in ***Figure 4-28***, (σ_b = 165.97 MPa) and (σ_d = 209.3 MPa). The results are in good agreement with results obtained from the beam theory.

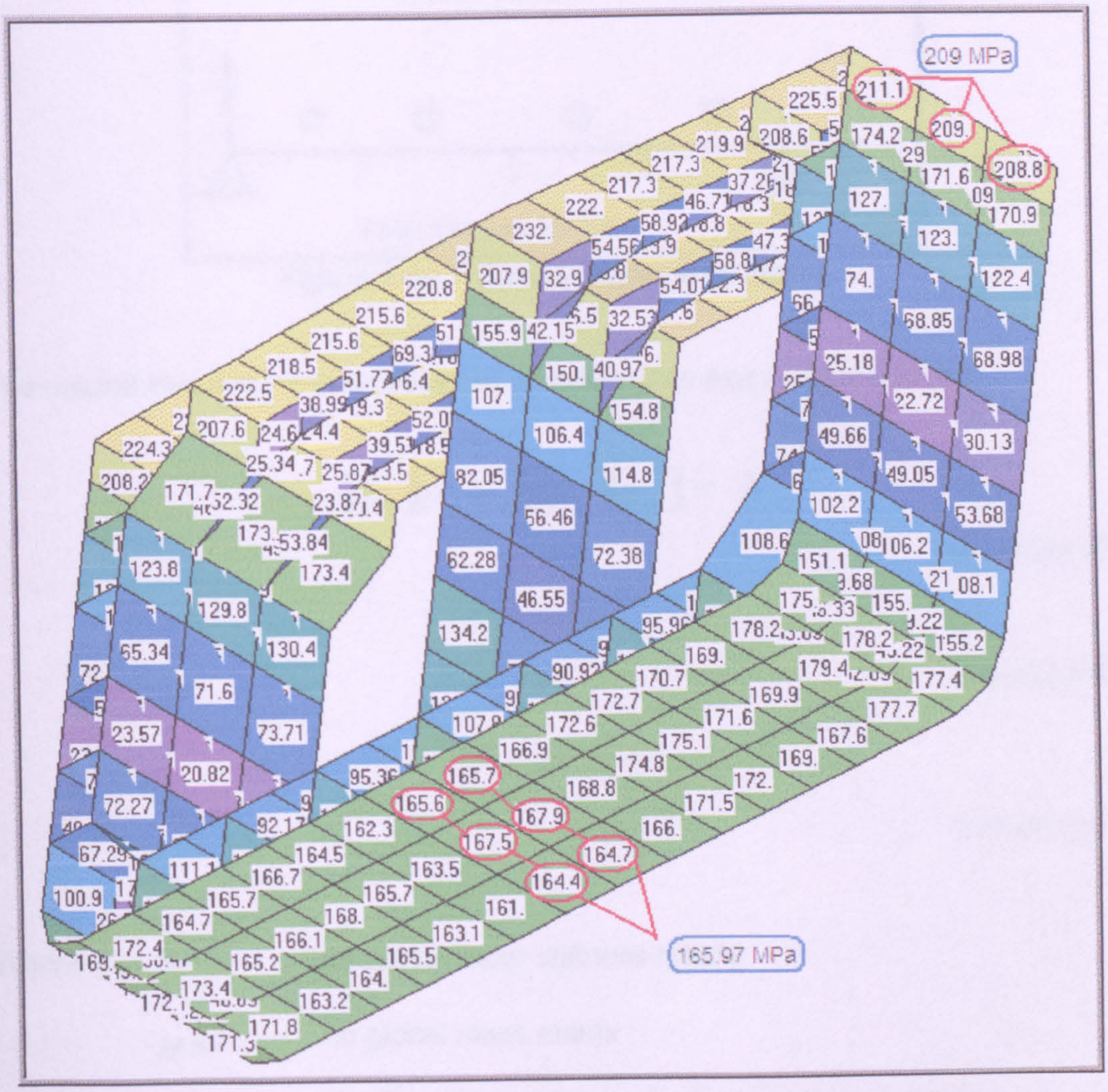

Figure 4-28 Bottom and Deck at Side FEA Results Verification

4.4.7.1 Comparison Using the Fundamental Natural Frequency

Avoiding errors in the modelling and input data is important to be checked, by simply comparing the numerical answers versus theoretical results obtained for the

fundamental frequency of the FPSO's Hull Girder Model. The resultant frequency has been compared to the corresponding theoretical value acquired from the theory presented at *Thomson, W. T.*, (1965), which correlate the result to the finite element analysis of a Simply Supported Beam of uniform cross section, as illustrated in *ANSYS*, (1994), and shown in ***Figure 4-29***.

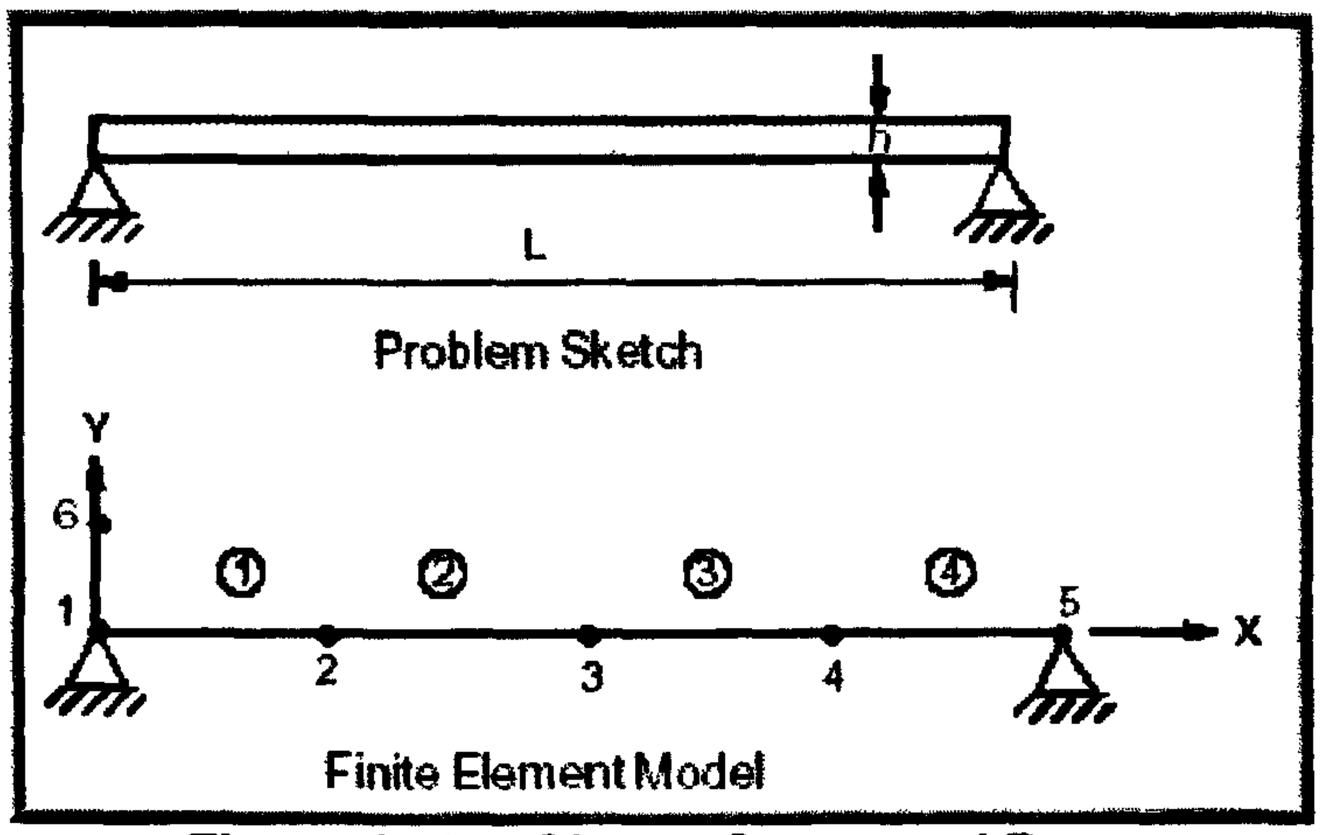

Figure 4-29 Simply Supported Beam

The natural frequency can be obtained by solving the eigen-value problem:

$$[K] + \lambda_i [M][\phi_i] = 0$$

Equation 4-5

$$\lambda_i = \omega_i^2$$

Equation 4-6

$$f_i = \frac{\omega_i}{2\pi}$$

Equation 4-7

Where K = The global linear stiffness matrix

M = The global mass matrix

i = The eigen-values that yield the natural frequencies

ϕ_i = The eigenvectors that represent the natural mode shapes

ω_i = The circular frequencies (radians per second)

f_i = The cyclic frequencies (hertz)

In solving the above eigen-value problem there are as many eigen-values and corresponding eigenvectors as there are unconstrained degrees of freedom. Often, however, only the lowest natural frequency is of practical interest. This frequency will always be the first mode extracted.

The *Lanczos* model solution was used with a coupled mass control for improved accuracy. The results of the analysis are in good agreement with that determined by the beam theory. The determined natural frequency of vibration and the corresponding mode shape is shown in ***Figure 4-30***, where the results comparison is presented in ***Table 4-4***.

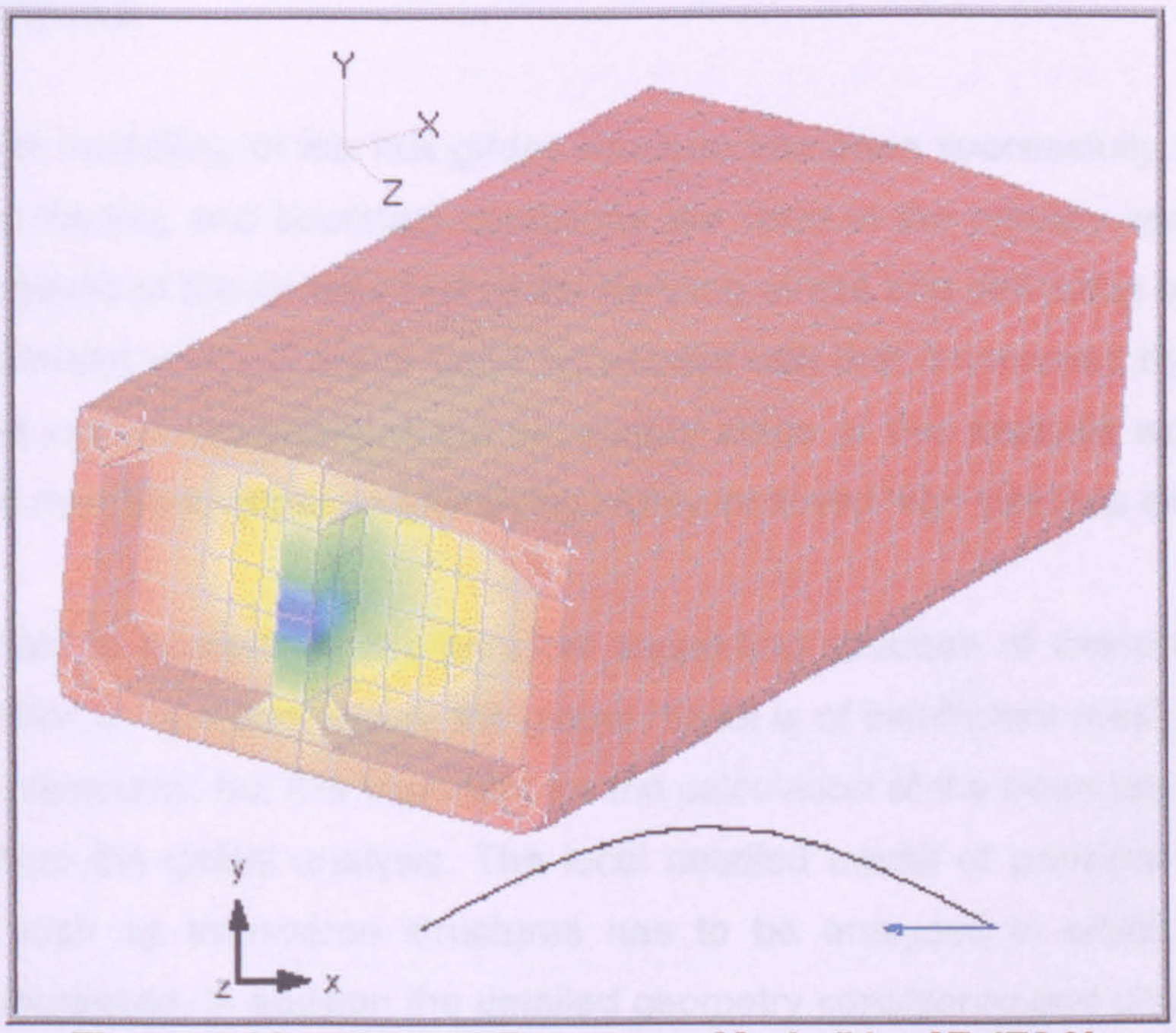

Figure 4-30 Natural Frequency Mode #1 = 27.470 Hz

Result	*Frequency (Hz)*	*Ratio*
Simply Supported Beam Theory	28.766	1.000
Simply Supported Beam FEM using ANSYS	28.767	1.000
City FPSO2000 Hull Girder	27.470	0.955

Table 4-4 Results Comparison of Natural Frequencies

As indicated previously, the purpose of the 3-D global analysis is to determine the overall response of the hull girder. The stress levels obtained by the 3-D global model should not be viewed as actual stresses expected in the hull structure, except for those in the hull girder plating. This is because the finite element mesh used in the 3-D global model is generally fairly coarse, and detailed modelling of internal structures is usually not possible. Although the 3-D global model offers a good representation of the primary and secondary bending of the hull girder, the model is considered inadequate to predict, with reasonable accuracy, the local behaviour of internal structures.

4.5 Remarks

Proper modelling of the hull girder structure has been successfully made, and appropriate loading and boundary conditions are used in the primary analysis. The analytical results of the primary hull girder bending stress and deflection obtained by the finite element analysis are in good agreement with that determined by the beam theory. The refined modelling of the secondary stage of this analysis would reveal much more needed information identifying highly localised high stresses areas.

It is important to account for the principal supporting structure of interest and local critical location in question, where the global model is of insufficient mesh density as explained previously, but it is important for the calculation of the boundary conditions obtained from the global analysis. The local detailed model of principal supporting members such as transverse structures has to be analyzed in which the mesh density is increased, in addition the detailed geometry considered and displacements calculated are applied as boundary conditions.

5. FPSO Transverse Strength Analysis (*Secondary*)

The transverse strength loads represents the loads which act on transverse members and cause structural distortion of a cross section, such as hydrostatic pressure on the outer shell, weight of cargo loads working on the bottom structure, ballast water pressure inducing the deformation of the ballast tank, etc.

For instance a transverse web-frame of the mid-section floating in sea water is subject to hydrostatic pressure due to surrounding water, and internal loading due to self weight and cargo weight. These loads are not equal to each other at every point; consequently loads working on the transverse member will produce transverse distortion as shown in the following ***Figure 5-1***.

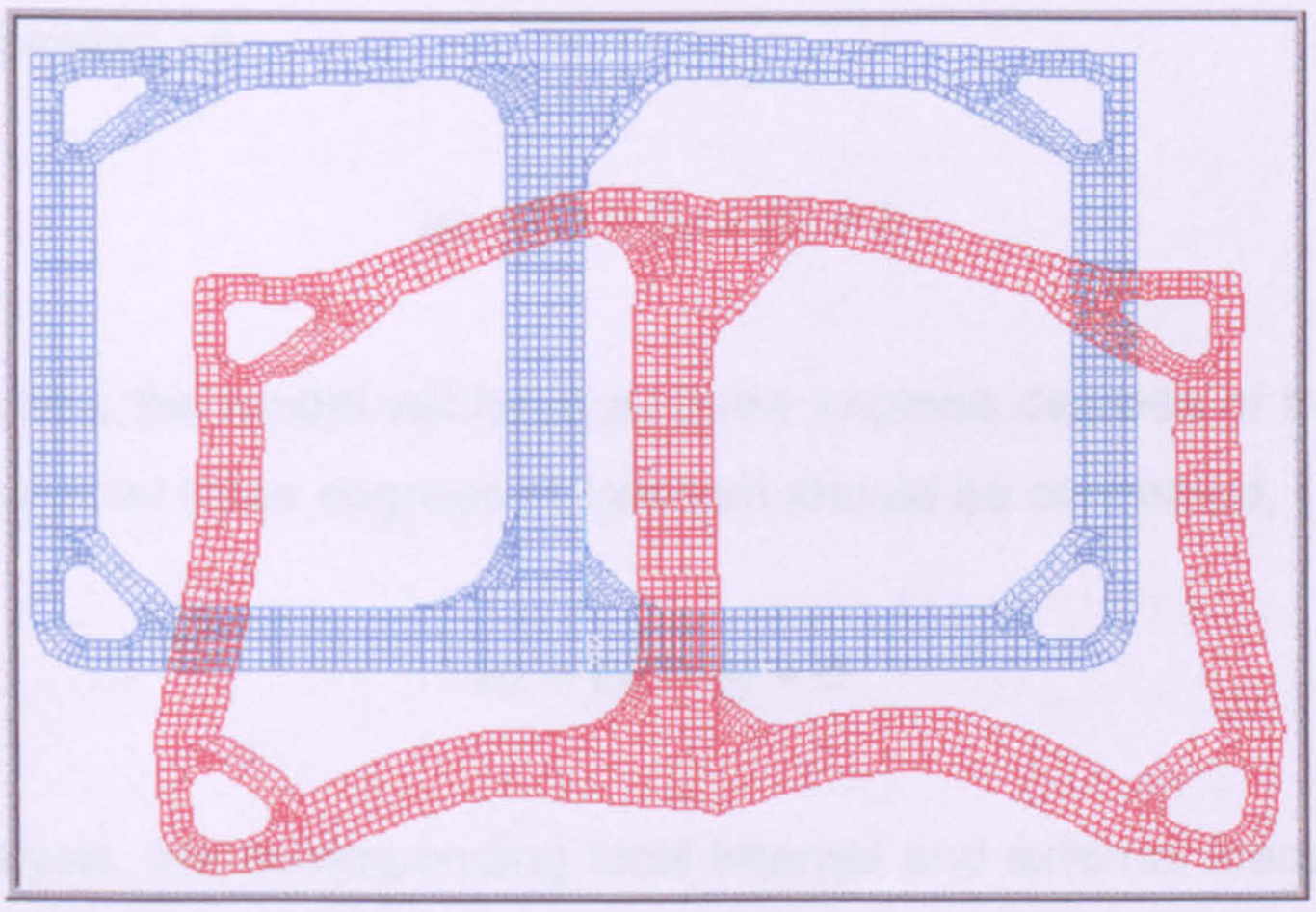

Figure 5-1 Distortion of Transverse Web Frame Structure

When considering transverse loads and longitudinal loads, the following characteristic is significant from the strength analysis point of view:

The distortion due to longitudinal loads does not affect the deformation of the transverse section; where the longitudinal bending moment or shear force can never have an influence on the distortion of the cross section. It is therefore necessary to recognise the transverse deformation of the ship's structure due to transverse loads, independently of the deformation induced by longitudinal load.

Transverse strength loads are commonly used in cases where we investigate the strength of primary members, such as transverse rings, transverse web frames, etc.

5.1 Two-Dimensional Fine-Mesh Analysis

In assessing the strength of internal main supporting structures, the behaviour of the structures can generally be determined by 2-D finite element models, with appropriate boundary conditions obtained from the 3-D global analysis. In using 2-D models, the analysis is a lot simpler, thus finer meshes can be employed to achieve more accurate representation of the structures.

The 2-D fine-mesh finite element models usually consist of only rod and membrane plate elements. A 2-D model in the X-Y coordinate-system will have only two in-plane degrees of freedom, namely, *ux* and *uy*, and the other four degrees of freedom should be concealed, i.e.,

$$uz = \theta x = \theta y = \theta z = 0$$

If beams are used, the model will have all three in-plane degrees of freedom, *ux, uy* and θz, and the other three degrees of freedom should be concealed, i.e.,

$$uz = \theta x = \theta y = 0$$

In the 2-D analysis, the corresponding local internal and external loads as applied to the 3-D global model should be applied to the individual 2-D models. In addition, boundary displacements obtained from the 3-D global analysis would be imposed on the models at locations where shear forces from the cut-off supporting members are expected to be significant.

5.1.1 FPSO's Transverse Frame Critical Locations

Some specific locations as marked in ***Figure 5-2*** were found to be subjected to high stresses (against yielding and buckling failures) under various loading conditions. These high stresses, except those in location 1 near the full load or ballast water line, are due primarily to high static loads. However, even in the cases with high static loads, significant portions of the stresses are motion-induced and

thus may also be susceptible to fatigue damage. The abovementioned critical locations, which require more careful evaluation in the 2-D fine-mesh analysis, are summarized as follow:

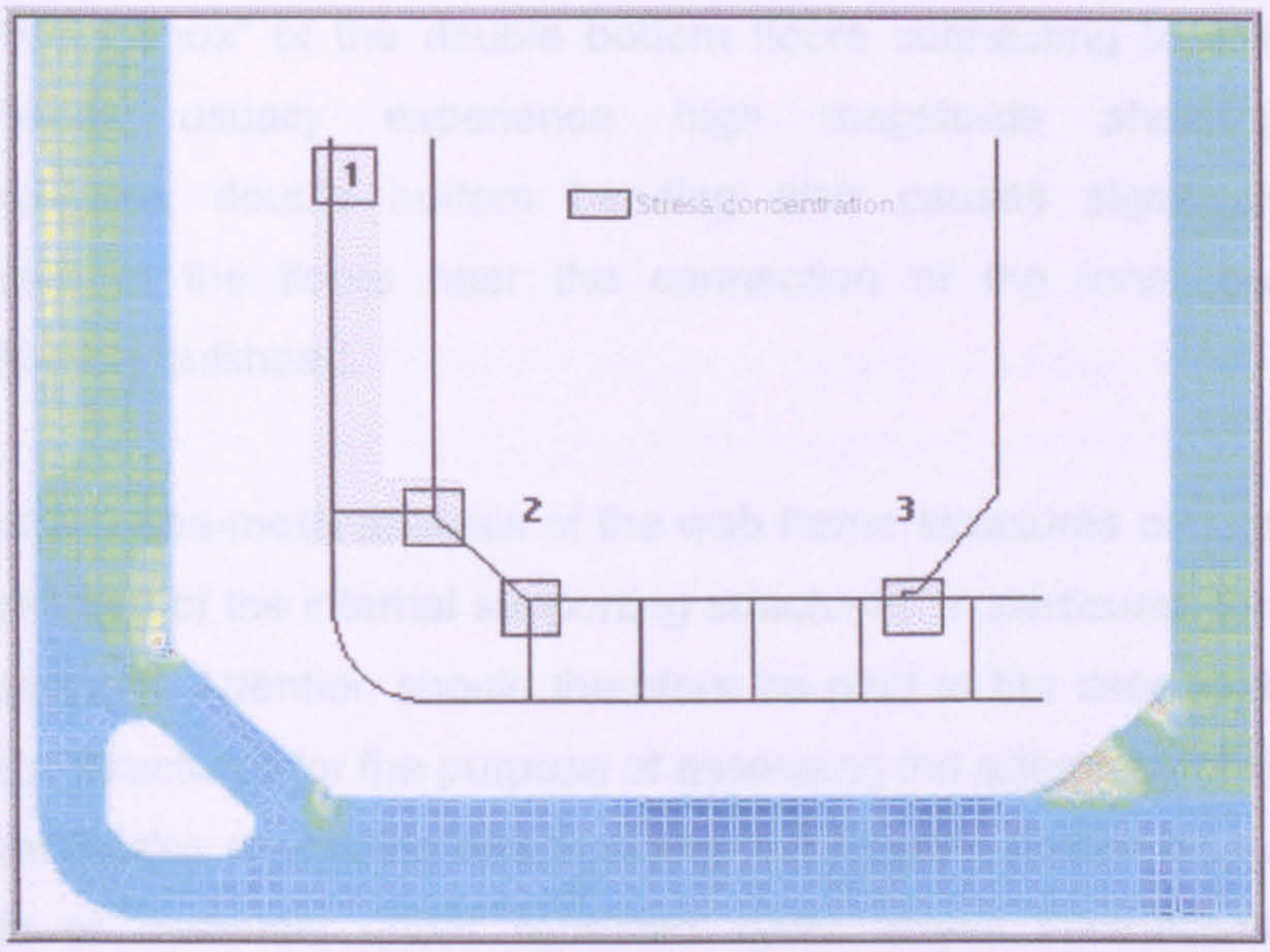

Figure 5-2 Critical Locations for Typical Double-Hull FPSO

- ***Locations 1:*** Location 1 is at the connections of the side longitudinals near the water line to transverse web frames. Location 1 also is at the similar connections at the transverse bulkheads. These connections are susceptible to fatigue damage, primarily due to cyclic external pressure acting on the vessel's shell by waves, and partly to internal pressure fluctuation induced by vessel motions. Similar problems also occur at the same locations on the longitudinal bulkheads.

- ***Location 2:*** Location 2 is at the lower part of the side transverse (or the double-side). Under large angles of roll, these areas are subjected to high magnitude shearing stresses resulting from significantly higher internal loads induced by the vessel's roll motions. Additional bending by the side transverse under the same loading further raises the stress level a significant amount on the inboard side of the side transverse near the bottom. Similar to location 2, the upper parts of the vertical webs at the side and longitudinal bulkhead also often experience high shearing stresses. This is because the upper portion of the transverses is usually designed with light scantlings, and under large angles of roll, considerable pressure head is added to the transverses resulting in high shear at the two ends. Additional bending by the

vertical webs and deck transverse also raises the stress level significantly in the area connecting to the deck transverse.

- ***Location 3:*** As in a fixed-end beam subjected to a uniformly distributed load, the "fixed ends" of the double bottom floors connecting to the longitudinal bulkheads usually experience high magnitude shearing stresses. Furthermore, double bottom bending also causes significant additional stresses in the floors near the connection of the inner bottom to the longitudinal bulkhead.

The intended 2-D fine-mesh analysis of the web frame structures considers primarily the overall strength of the internal supporting structures, in particular, the hull girder's transverse strength. Attention should therefore be paid to the determination of local stresses in the structures for the purpose of assessing the adequacy of the structures against failure modes of yielding and buckling, not fatigue. Where fatigue refers to a failure mode of materials under repeated cyclic stress fluctuations; the loads responsible for fatigue are generally not large enough to cause material yielding. Instead, failure occurs after a certain number of load or stress fluctuations.

5.1.2 (2-D) Fine Mesh Modelling, General Rules

It is useful to layout grids and key points directly on the structural drawings. Definition of elements as to their types, scantlings, and connectivity can also be best accomplished directly on the drawings. In doing so, the possible high stress areas where finer meshes are desired, and locations where boundary displacements need to be applied can also be more readily identified.

The general rules for developing the 3-D global model, indicated in (***Section 4.1.2***), are also applicable to the development of the 2-D fine-mesh models of the local structures. In addition, the following general rules concerning modelling techniques of the 2-D models should also be closely observed:

- In modelling a local structure, the web plating is generally modelled by membrane plates, both quadrilateral and triangular elements. Stiffeners on the web plating such as panel breakers, tripping brackets, flat bar stiffeners, etc., and the face plates of the webs are modelled by rod elements of

equivalent cross sectional areas. Where faceplates on brackets are tapered at the ends, the area of the rod elements should be reduced accordingly. The out-of-plane hull girder plating (i.e., bulkhead and shell) is also modelled by rod elements, using an appropriate effective width.

- It is often desirable to use finer meshes in the likely high stress areas (e.g., ***Figure 5-3*** below) in order to obtain better and more accurate stress distributions in these areas. In doing so, it is good practices to try to use a uniform mesh with smooth transition and avoid sudden changes in mesh sizes. Using a varying mesh size in 2-D models is usually more flexible and can be easily accomplished.

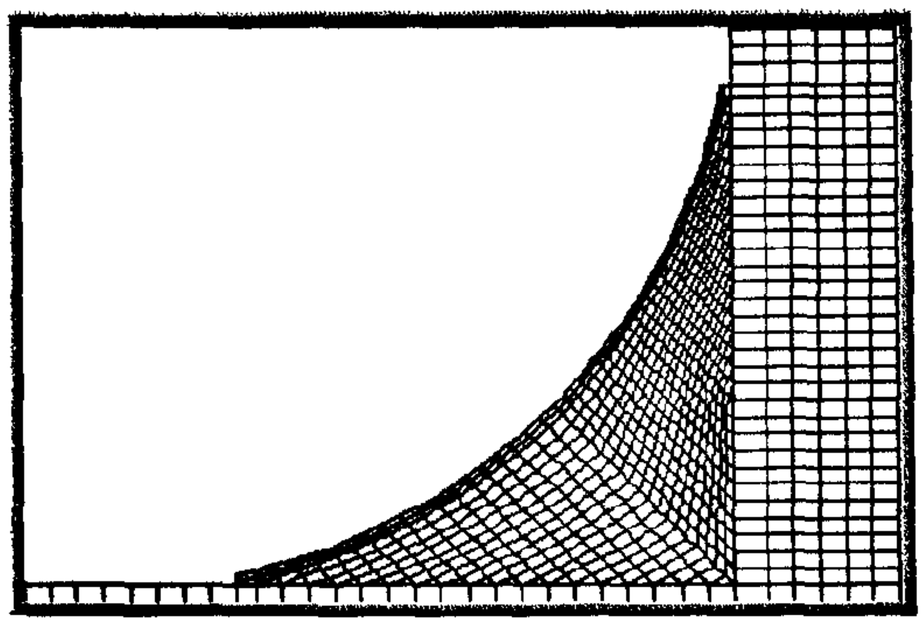

Figure 5-3 Finer Mesh at Critical Locations of the Web Frame

5.1.3 Boundary Conditions for 2-D Models

In the state of static equilibrium, the 2-D model of a given hull structure is actually supported by shearing stresses acting along the two cut-off planes. Taking the transverse web frame as an example, the said shearing stresses are present in the deck, bottom, inner bottom, side shell, longitudinal bulkheads, bottom girders, deck girders, and horizontal stringers at the fore and aft sections of the transverse web frame.

In a 3-D analysis, the shearing stresses on the two ends were applied directly to the two cut-off ends of the model using spring supports as discussed in (***Section 4.1.5***). However, in a 2-D analysis, the shear forces required to support the 2-D model are actually equal to the differences of the shear forces acting on the either side of the sections. These forces, as determined from the 3-D results, can be applied to the 2-D model either directly as boundary forces or their effect be represented by boundary displacements.

In practice, it is more convenient to use boundary displacements because nodal displacements can readily be obtained from the 3-D results and can also be systematically applied to the 2-D model. The locations and directions for which boundary displacements are to be applied may sometimes appear to be difficult to determine. These can probably best be determined from the point of view of the abovementioned shear forces acting on the model. Wherever the shear force (i.e., the out-of-plane stiffness) is expected to be significant, a boundary displacement should be imposed. ***Figure 5-4*** illustrates the locations and directions for the required boundary displacements for midship section configuration.

In specific, the following are noted with regard to the choice of locations and directions:

- Side shell, deck at side - Both horizontal and vertical displacements are applied.

- Bilge - For fairly large radius bilges, there would be corresponding 2-D and 3-D nodes for the nearest location of the flat of bottom and flat of side for appropriate displacement input (e.g., the midship configuration illustrated in ***Figure 5-4***).

- Bottom girders - At each bottom girder location, only one vertical displacement is applied, at bottom but not at the inner bottom (so as not to over restrain the double bottom).

- Deck girders - Vertical displacements are applied at deck.

- Side stringers - Horizontal displacements are applied at the side shell.

- Longitudinal bulkheads - When the bulkhead is vertical to deck, input only the vertical displacement. This is to avoid possible undue stress concentrations at the corner points where stresses are usually high.

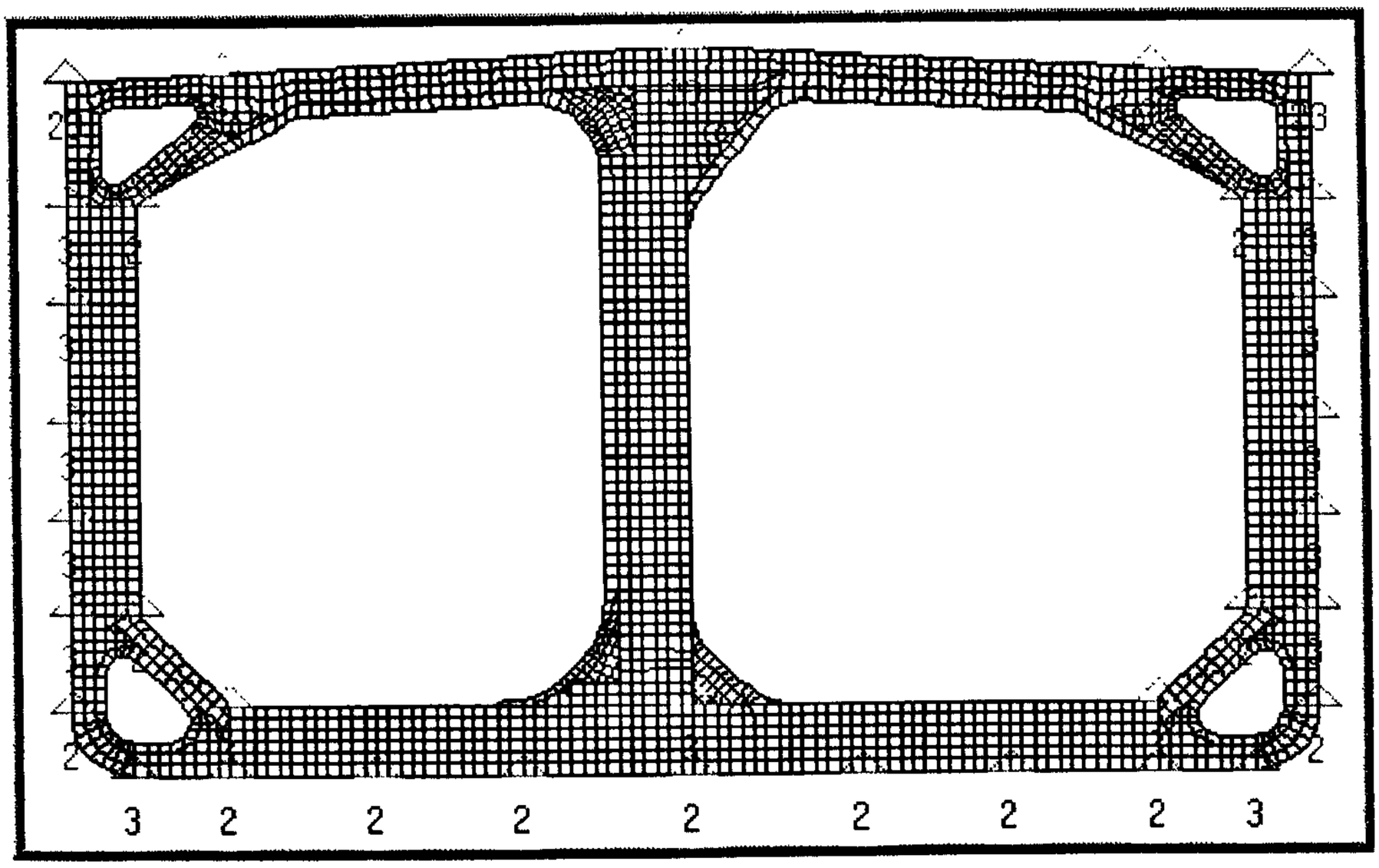

Figure 5-4 ***Boundary Conditions for 2-D Model of a Transverse Web Frame***
(numbers in red representing degree of freedom used)

The above scheme ensures that all shear forces (i.e., stiffness) in the hull girder plating are properly represented by two to four displacements. Note that the shear forces in girders and stringers are each represented by only one displacement (at bottom or side shell); so as not to excessively restrain the 2-D fine-mesh model, which is more flexible than the 3-D global model.

5.1.4 2-D Fine-Mesh Model of Transverse Web Frame

Recent computer programs can apply the external and internal pressure loads automatically to the model according to the specified frame location in relation to the 3-D global model. Similarly, boundary displacements are retrieved from the 3-D model and systematically input to the appropriate 2-D nodes. The automatic loading and retrieval of boundary displacements enables one to easily "step" the web frame through the 3-D global model. ***Figure 5-5*** illustrates a 2-D fine-mesh finite element model created, for the typical transverse web frame adjacent to a transverse bulkhead of a double-hull City FPSO2000.

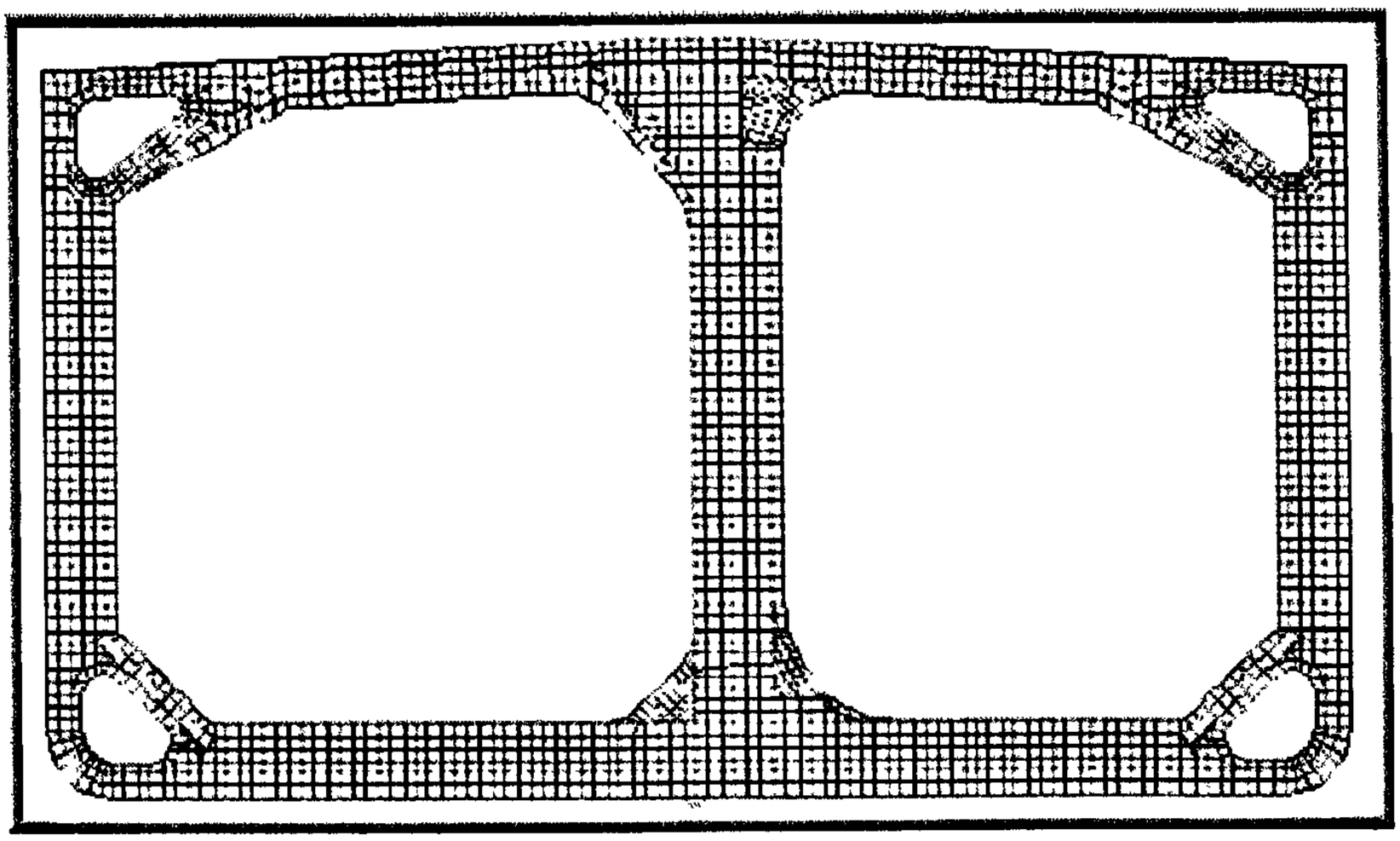

Figure 5-5 2-D Fine-Mesh Model of Transverse Web Frame

In the 2-D analysis, the same internal and external pressure loads applied to the 3-D global model should be used. Also, as indicated in the previous section, the pressure loads applied should be equivalent to that acting over the entire effective width of the transverse ring modelled in the 2-D model.

In most cases, the 2-D model of the typical transverse web frame can be used for analysing various transverses at different locations in the cargo hold, by changing loading and boundary conditions. The maximum stresses, however, usually occur at the mid-length of the tank, because the deformations of the web frame at this location are expected to be the maximum.

For FPSOs where the transverse bulkheads are supported by a number of deep horizontal girders, the web frame adjacent to the transverse bulkhead in way of the girders is to be included in the 2-D analysis, as presented in ***Figure 5-5***. This is because the extensions of the horizontal girders provide additional restraint to the adjacent web frames, and the response may be quite different from the typical web frame. In addition, most are designed excluding the strut, if the typical web frame is of a strut design. The model created for the typical web frame, in most instances can easily be modified to account for the scantling changes for the transverse web frame adjacent to a bulkhead.

Figure 5-6 illustrates the modelling of a bracket toe. In specific, the following are noted:

- All plate seams are taken to the nearest grid line (no averaging in most instances).
- All faceplates are idealized as rod elements of full cross-sectional area whether straight or contoured, and the taper of the face plate near a bracket toe is accounted for by taking the area of the taper at mid span of the associated plate element, it is known that these "soft toe" brackets reduce stress concentrations. In order not to induce unreasonable stress concentration in the 2-D model, the toe is modelled using a quadrilateral element as shown rather than a triangular element.

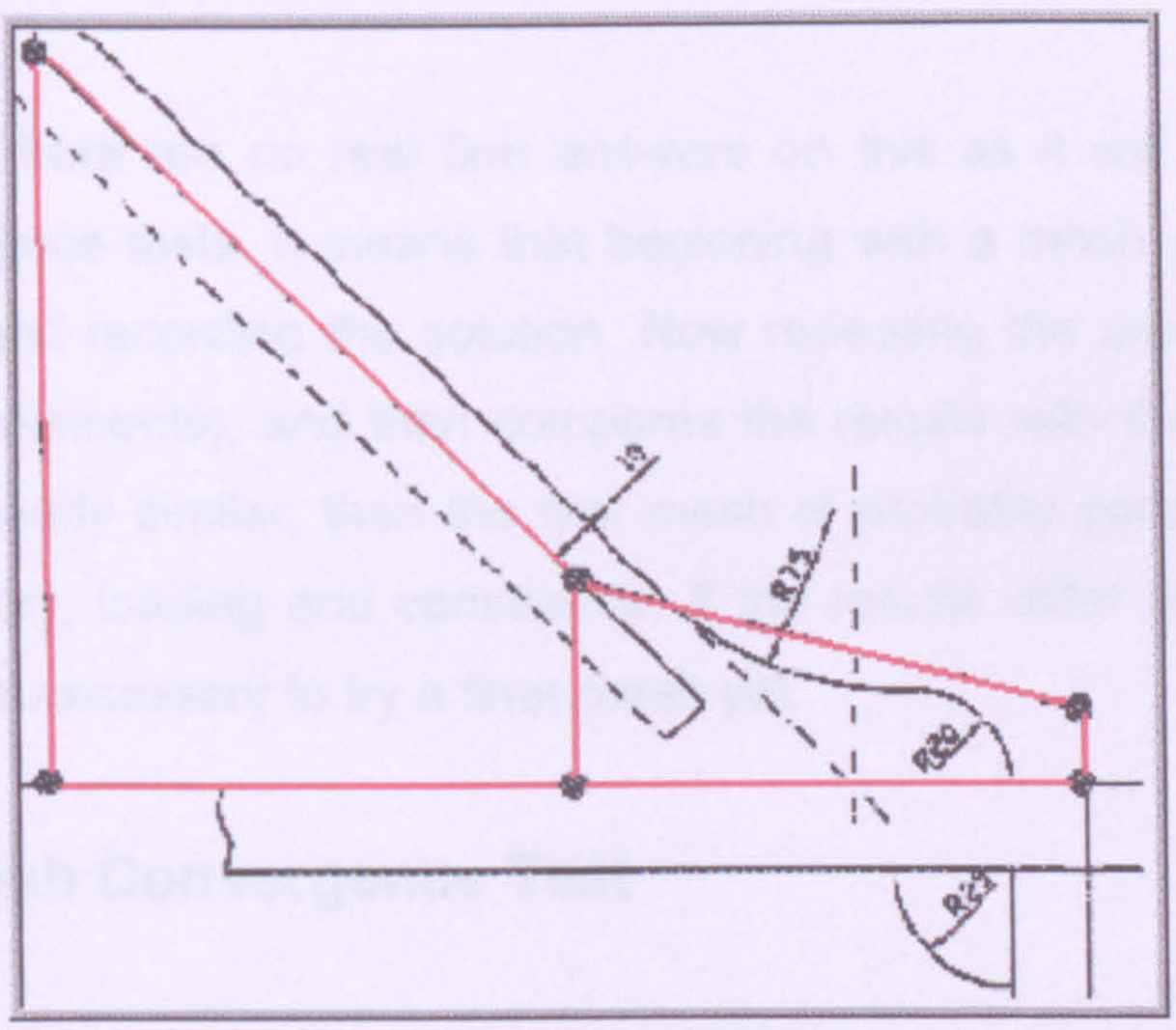

Figure 5-6 Modelling of Bracket Toe

- A sniped end of a panel breaker is idealized by taking one half area of the panel breaker for the bar element ending at the snipe.
- Tripping brackets are idealized using 2 to 3 averaged cross-sectional areas over the extent of the bracket.

5.2 FEM Convergence Testing

A fundamental principle of using the finite element procedure is that the body is sub-divided up into small discrete regions known as finite elements. These elements defined by nodes and interpolation functions. Governing equations are written for each element and these elements are assembled into a global matrix. Loads and constraints are applied and the solution is then determined.

5.2.1 The Problem

The question that always arises is: "*How small do we need to make the elements before we can trust the solution?*"

5.2.1.1 What to do about it?

In general there are no real firm answers on this as it will be necessary to conduct convergence tests. It means that beginning with a mesh discretization and then observing and recording the solution. Now repeating the problem with a finer mesh (i.e. more elements); and then compares the results with the previous test. If the results are nearly similar, then the first mesh is probably good enough for that particular geometry, loading and constraints. If the results differ by a large amount however, it will be necessary to try a finer mesh yet.

5.2.2 Fine Mesh Convergence Test

Finer meshes come with a cost however: more calculation time and large memory requirements both (Disk and RAM). It is desired to find the minimum number of elements that gives a converged solution. In general, it is necessary to conduct convergence tests on finite element model to confirm that a fine enough element discretization has been used. Creating several models with different meshes sizes and comparing the resulting deflections and stresses would do this. In general, the stresses will converge more slowly than the displacement, so it is not sufficient to examine the displacement convergence.

The finite element model used in the convergence testing has been extracted from the global course mesh model covering the width of two double bottom tanks as illustrated in the following ***Figure 5-7***.

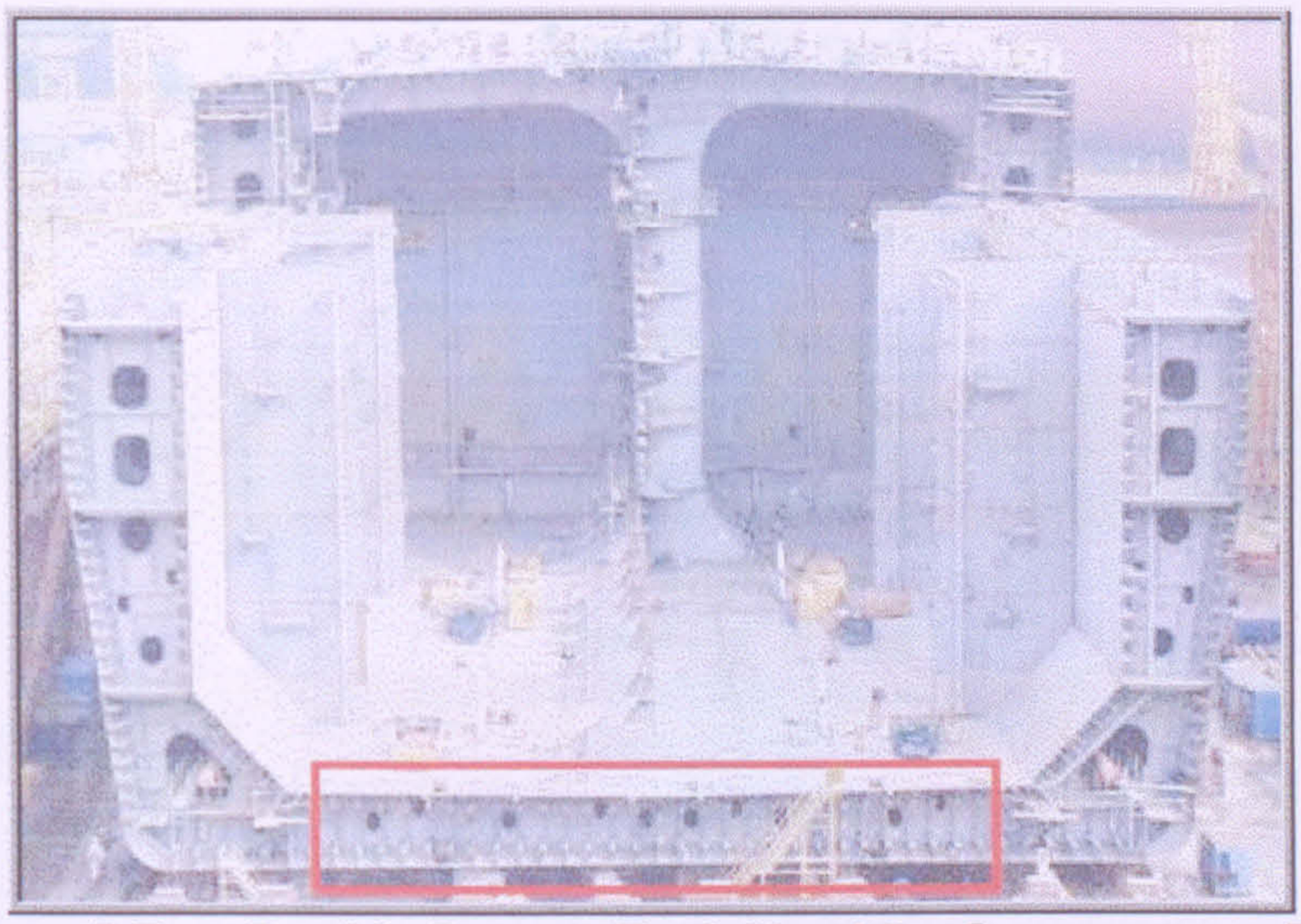

Figure 5-7 Double Bottom Tank Used for Convergence Test

Using the finite element model of the double bottom tank shown in ***Figure 5-8***, the converged results illustrated in ***Figure 5-9***, have been confirmed using linear analysis, where the shells von-Mises stress results, converged at mesh number five, using the normalized percentage maximum difference error estimation of the results. Consequently mesh number five has been adopted.

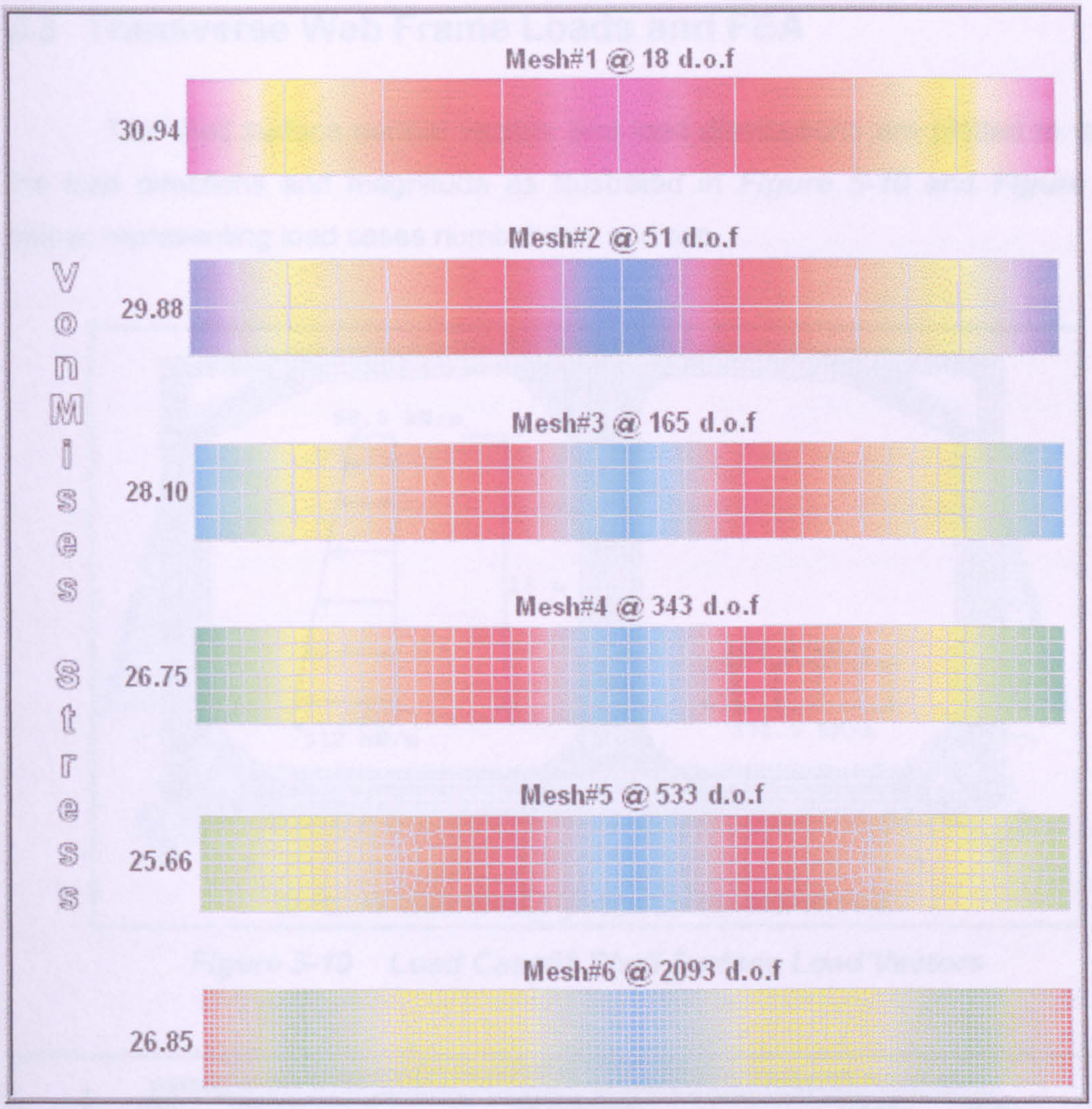

Figure 5-8 Convergence Solution Mesh

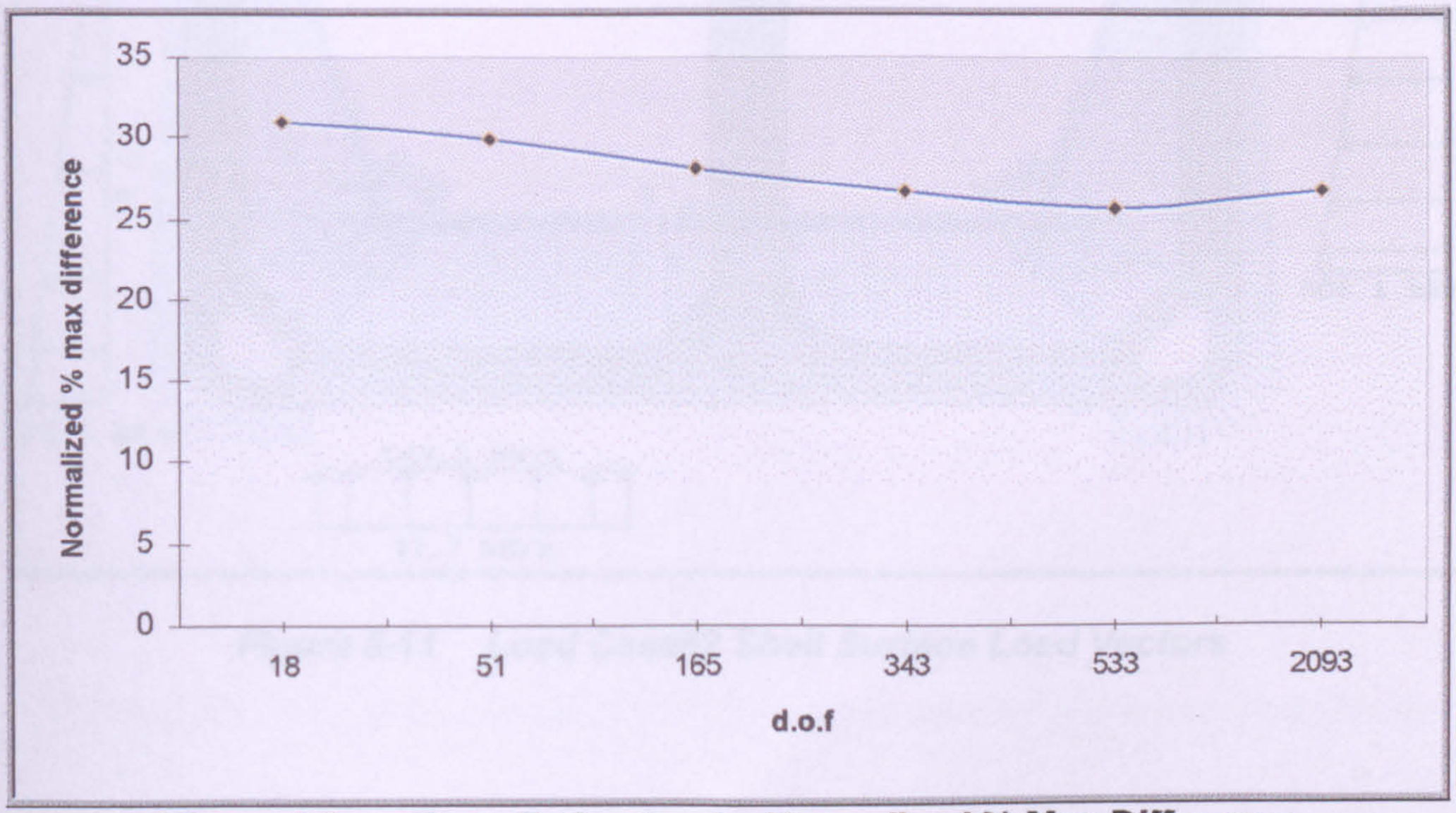

Figure 5-9 Error Estimate of a Normalized % Max Difference

5.3 Transverse Web Frame Loads and FEA

The shell surface normal vectors and load distributions are plotted to review the load directions and magnitude as illustrated in ***Figure 5-10*** and ***Figure 5-11*** below, representing load cases number one and two.

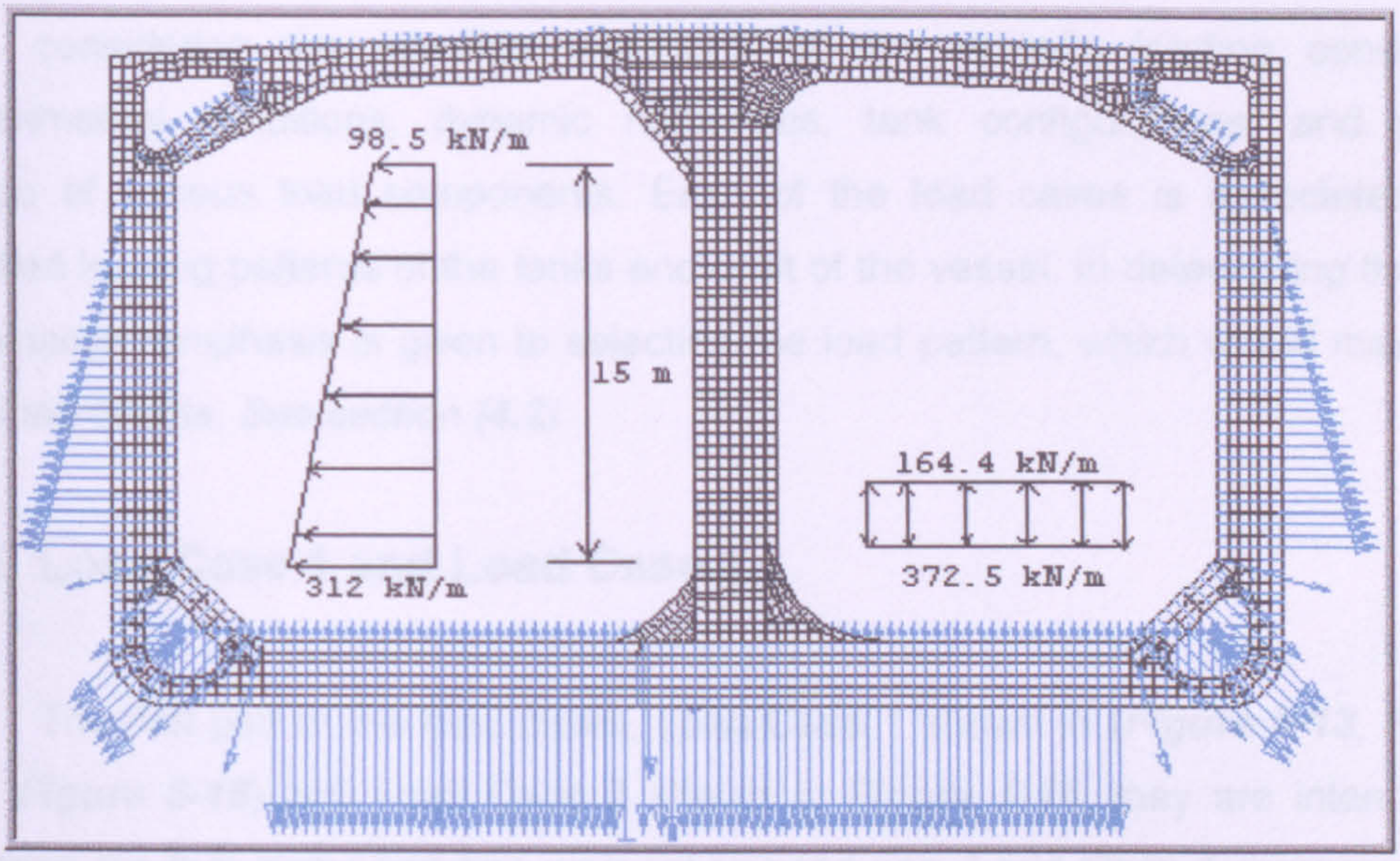

Figure 5-10 Load Case#1 Shell Surface Load Vectors

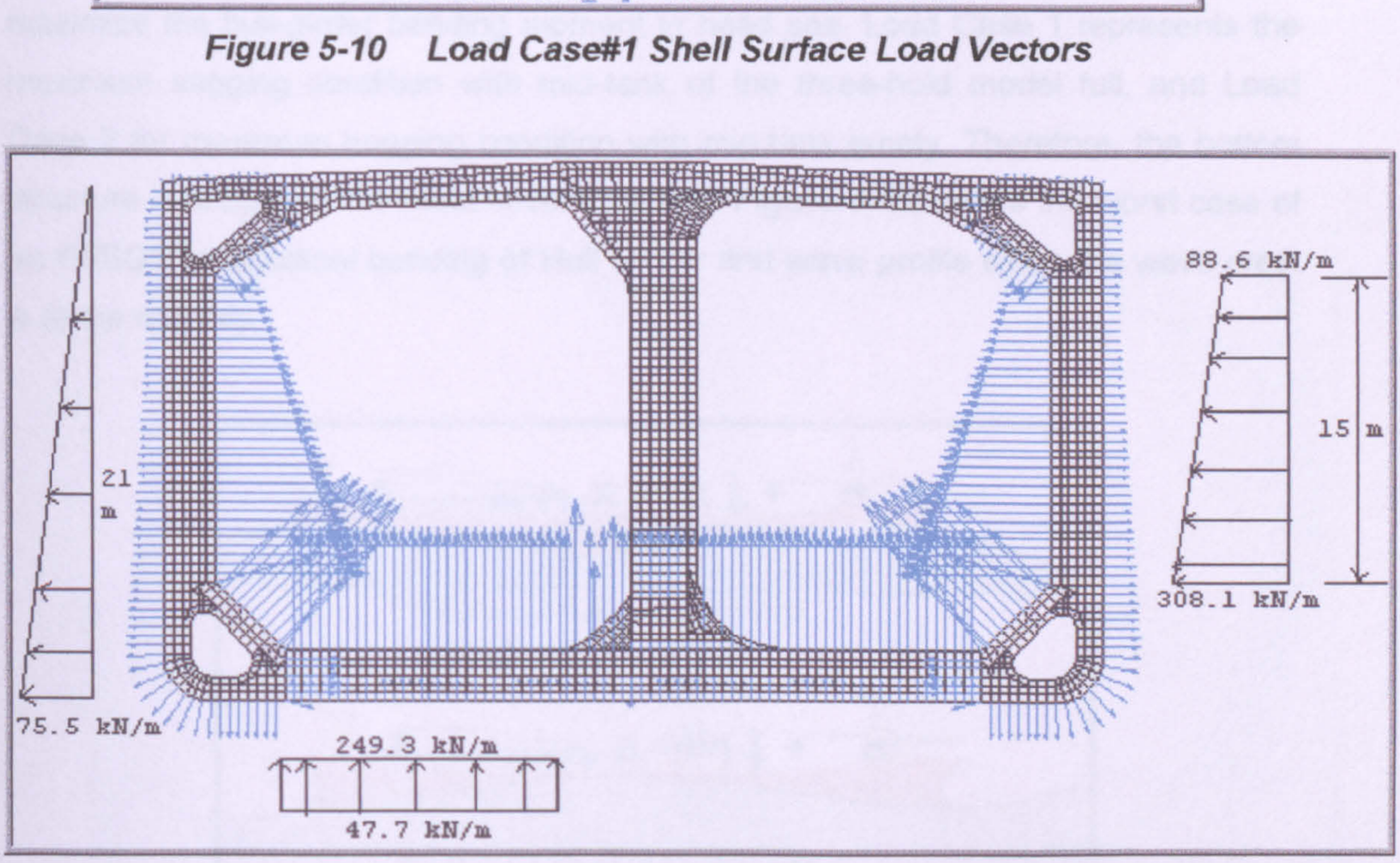

Figure 5-11 Load Case#2 Shell Surface Load Vectors

5.3.1 Combined Loads for Structural Analysis

To assess the strength of the hull girder and individual structural members, finite element structural analyses of the hull structure have been performed, such that resulting load effects satisfy the failure criteria. For this analysis eight load cases are selected, and the required load values for the analysis are defined for each load case, considering the possible variations of the vessel's loading conditions, environmental conditions, dynamic responses, tank configurations, and phase relation of various load components. Each of the load cases is associated with specified loading patterns of the tanks and draft of the vessel. In determining the load combination, emphasis is given to selecting the load pattern, which would maximize local load effects. *See section (**4.2**)*

5.3.2 Load Case 1 and Load Case 2

The first pair of the load cases, Load Case 1 shown in (***Figure 5-13***, ***Figure 5-14***, ***Figure 5-15***) and Load Case 2 shown in ***Figure 5-16***, they are intended to maximize the hull-girder bending moment in head sea. Load Case 1 represents the maximum sagging condition with mid-tank of the three-hold model full, and Load Case 2 for maximum hogging condition with mid-tank empty. Therefore, the bottom structure is subject to the most severe loading. ***Figure 5-12*** shows the worst case of an FPSO's longitudinal bending of Hull Girder and wave profile when the wave crest is at the midship.

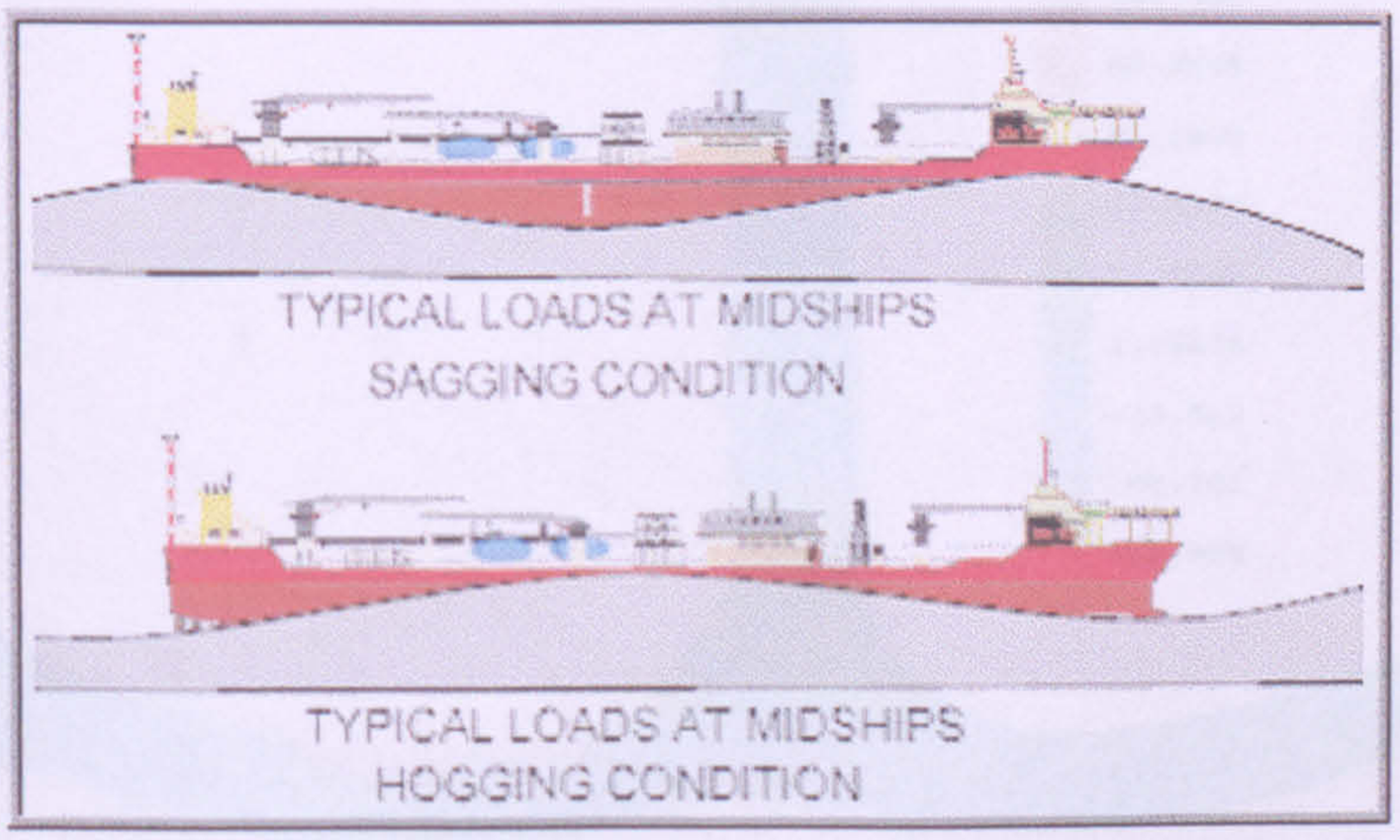

Figure 5-12 Worst Cases of an FPSO's Longitudinal Bending of Hull Girder

This condition is typically associated with the maximum hogging moment. Although these two load cases represent maximum sagging and hogging conditions, they do not represent the conditions at two time instances with the same loading.

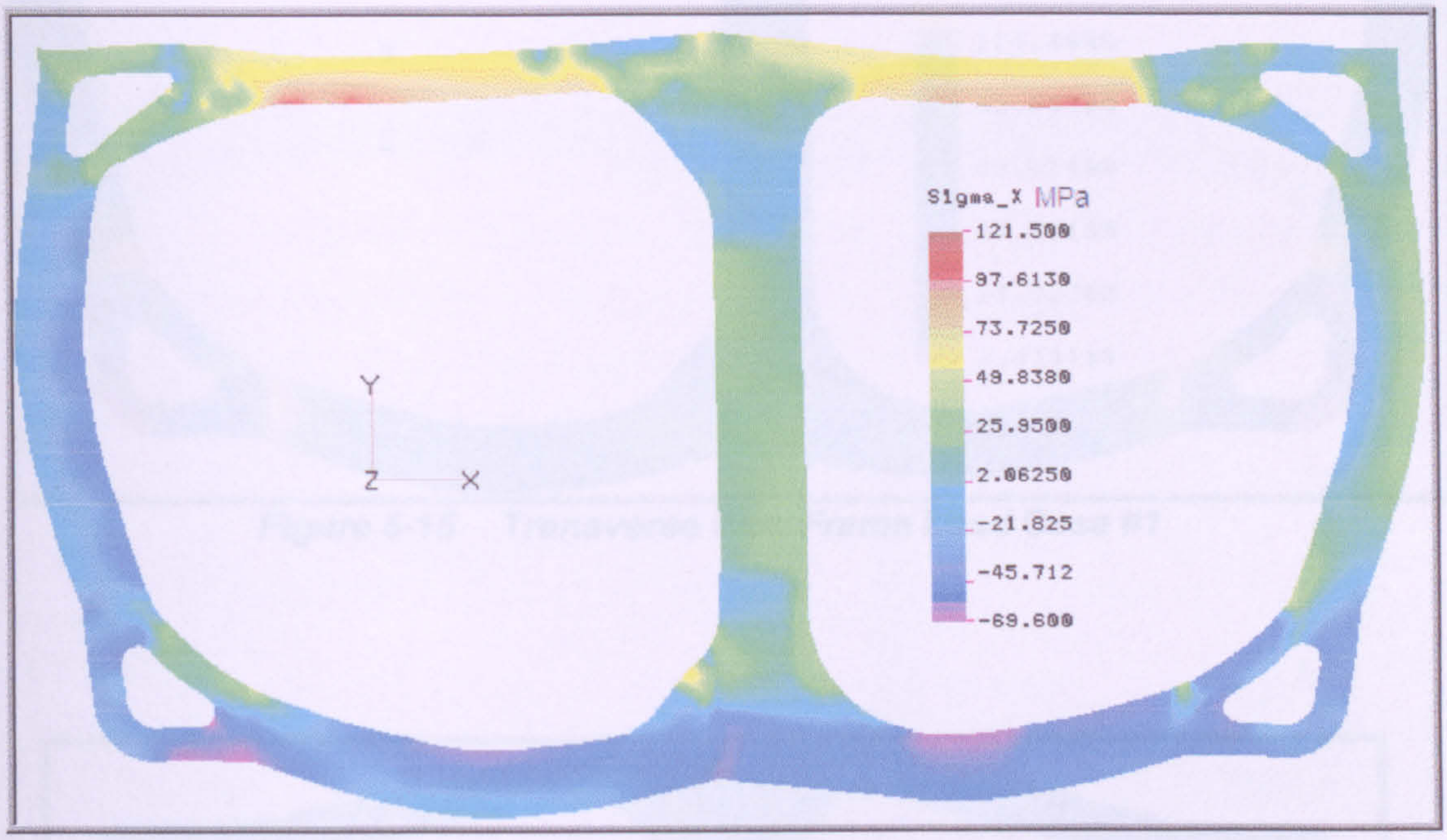

Figure 5-13 Transverse Web Frame Load Case #1

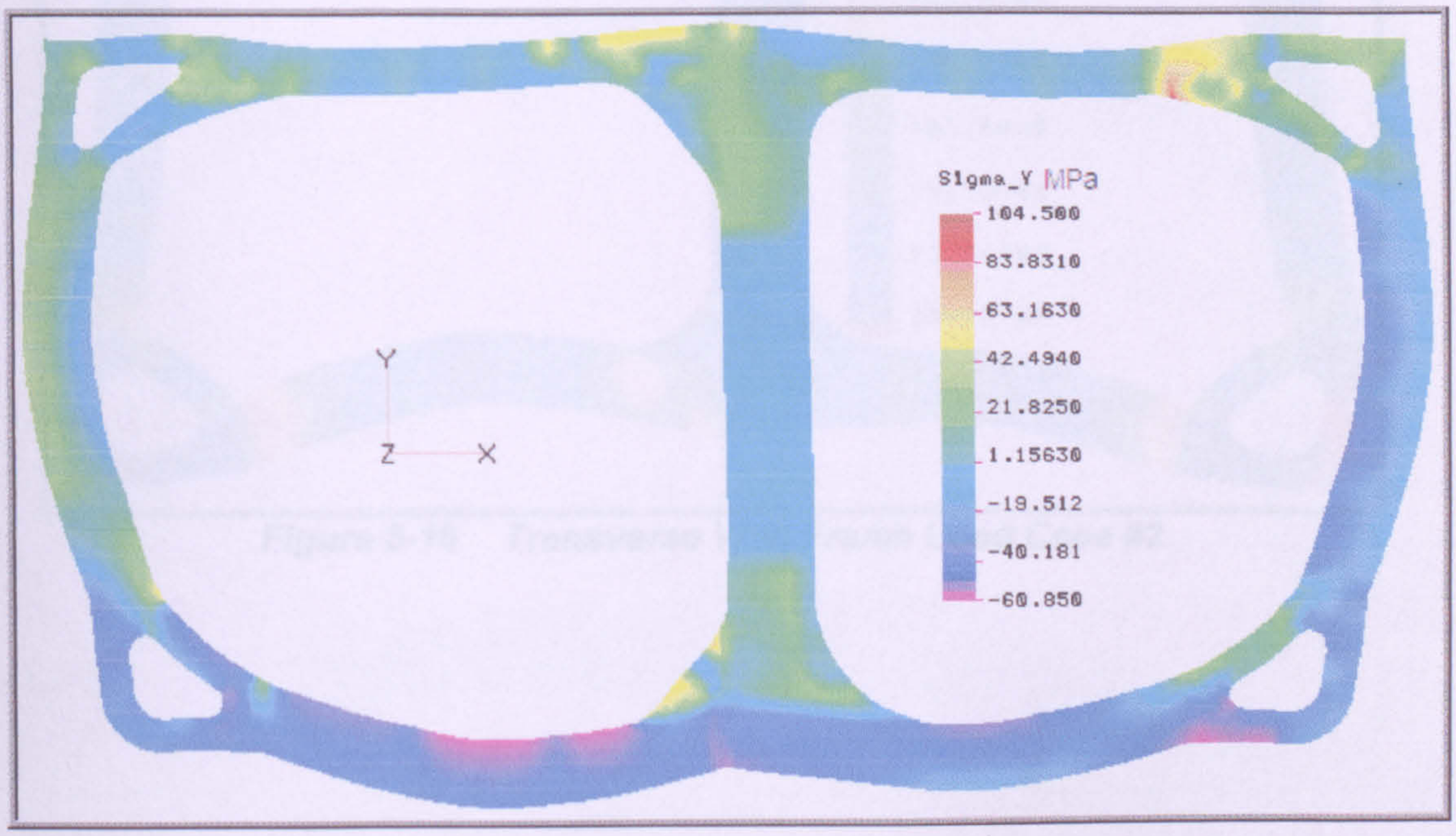

Figure 5-14 Transverse Web Frame Load Case #1

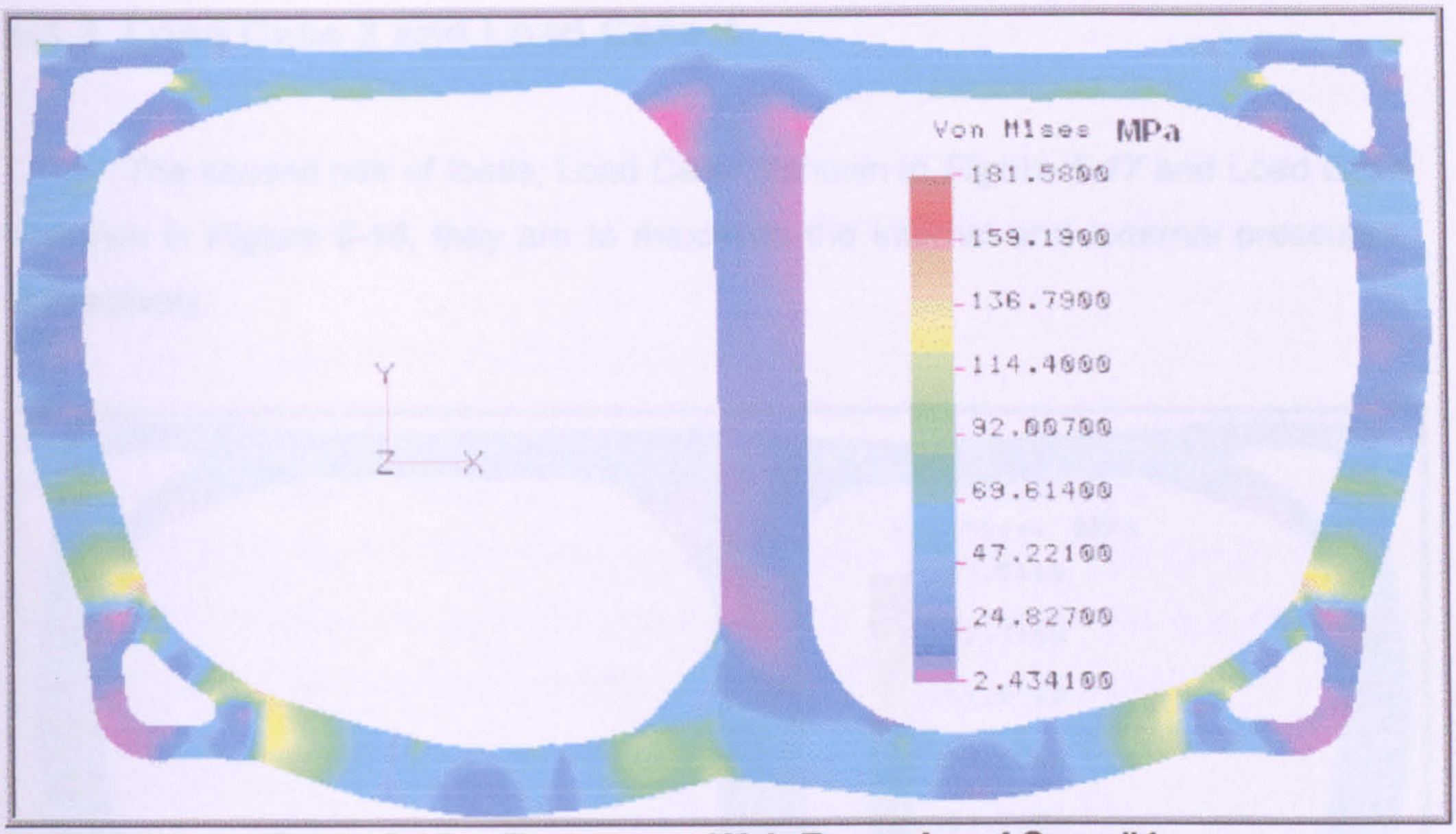

Figure 5-15 Transverse Web Frame Load Case #1

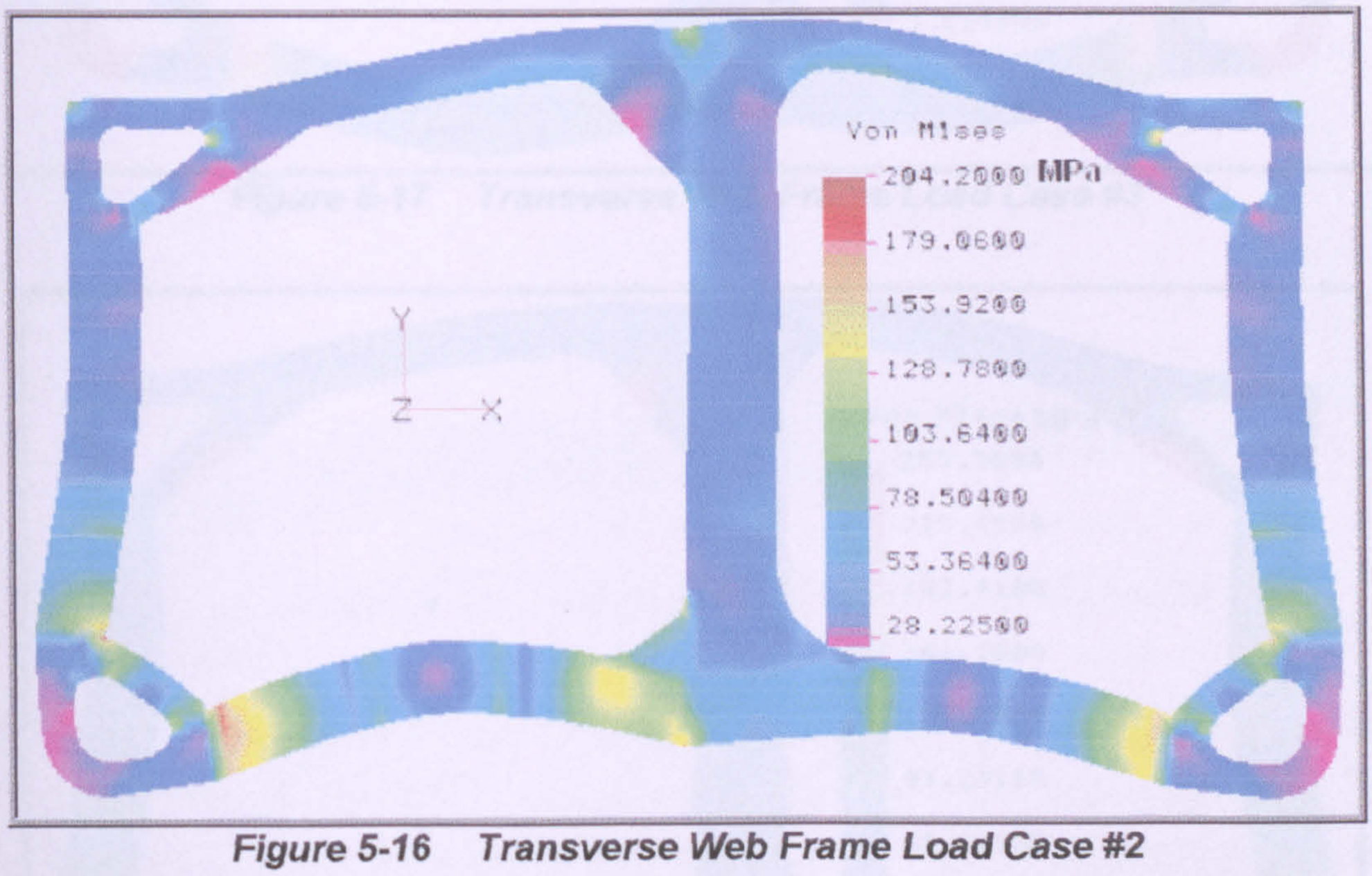

Figure 5-16 Transverse Web Frame Load Case #2

5.3.3 Load Case 3 and Load Case 4

The second pair of loads, Load Case 3 shown in ***Figure 5-17*** and Load Case 4 shown in ***Figure 5-18***, they are to maximize the internal and external pressures, respectively.

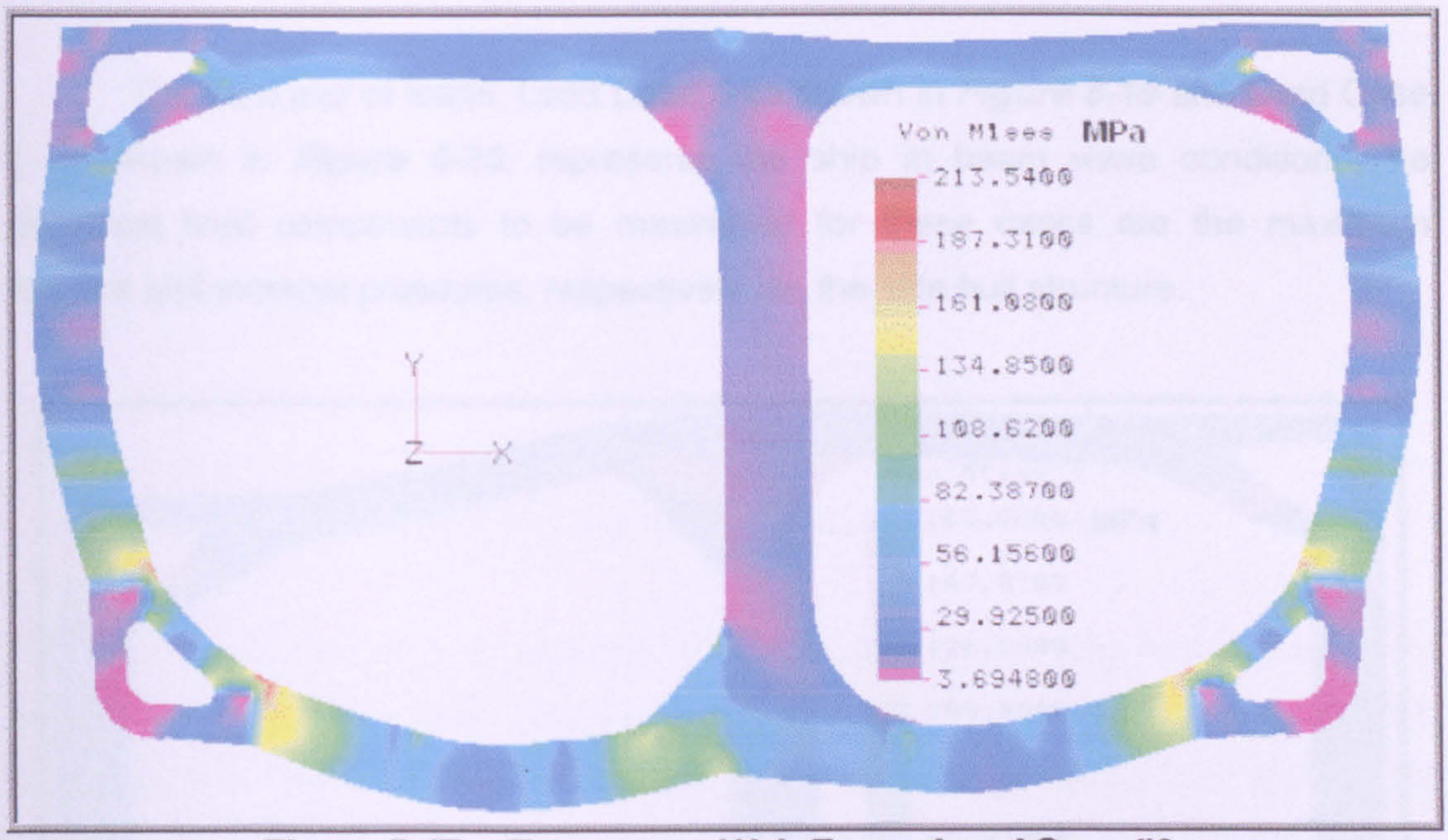

Figure 5-17 Transverse Web Frame Load Case #3

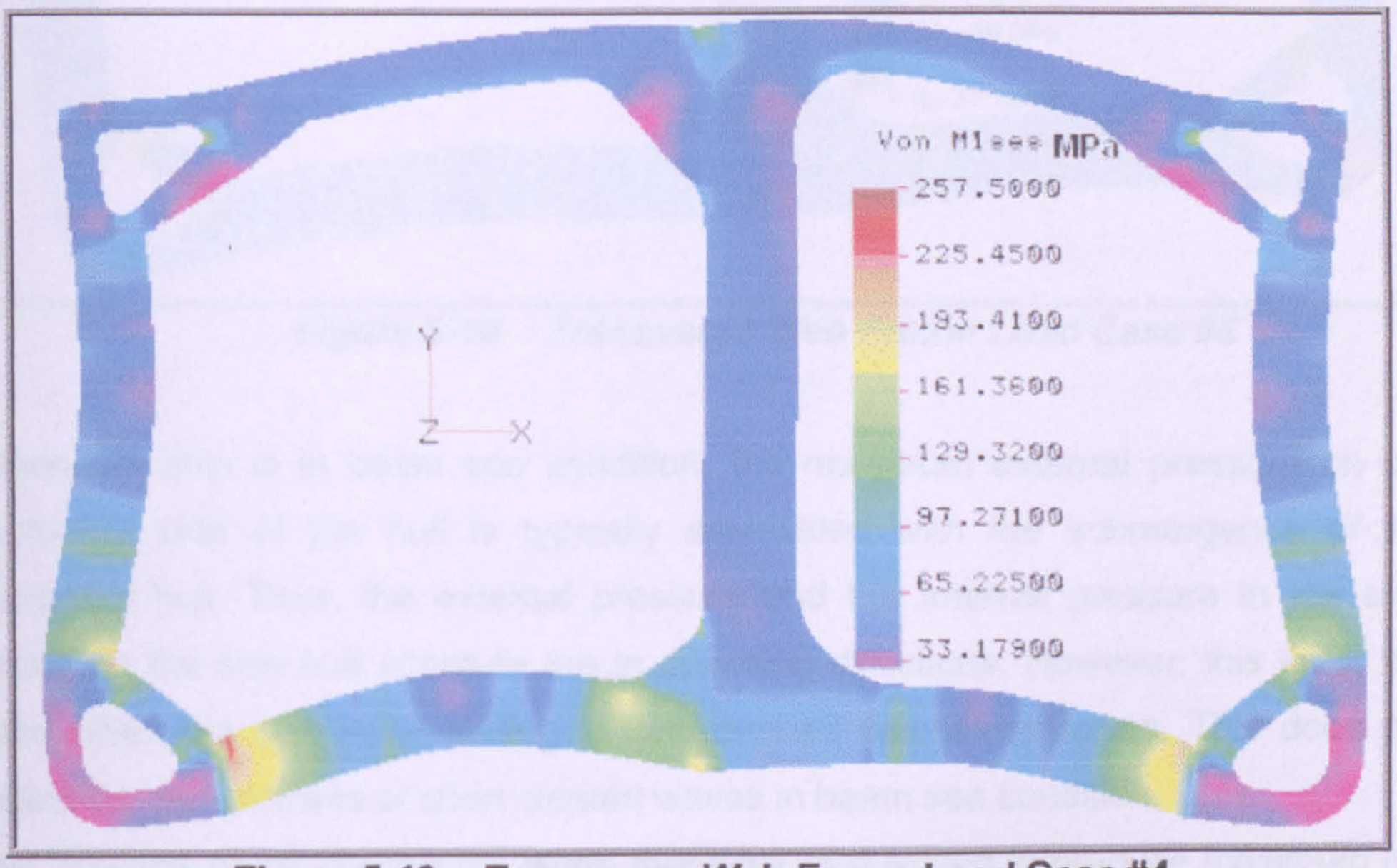

Figure 5-18 Transverse Web Frame Load Case #4

The corresponding draft and wave crest position are determined accordingly to maximize the net local load to the bottom, bulkhead, and side hull structure.

The distribution of the external pressure is similar to those of Load Cases 1 and 2, although the magnitude is different. The external pressure of Load Case 4 is the maximum value in head sea condition. The absolute maximum value occurs at beam sea condition. Internal tank pressures are distributed similarly to Load Cases 1 and 2.

5.3.4 Load Case 5 and Load Case 6

The third pair of loads, Load Case 5 as shown in ***Figure 5-19*** and Load Case 6 as shown in ***Figure 5-20***, represents the ship in beam wave condition. The dominant load components to be maximized for these cases are the maximum internal and external pressures, respectively, on the side hull structure.

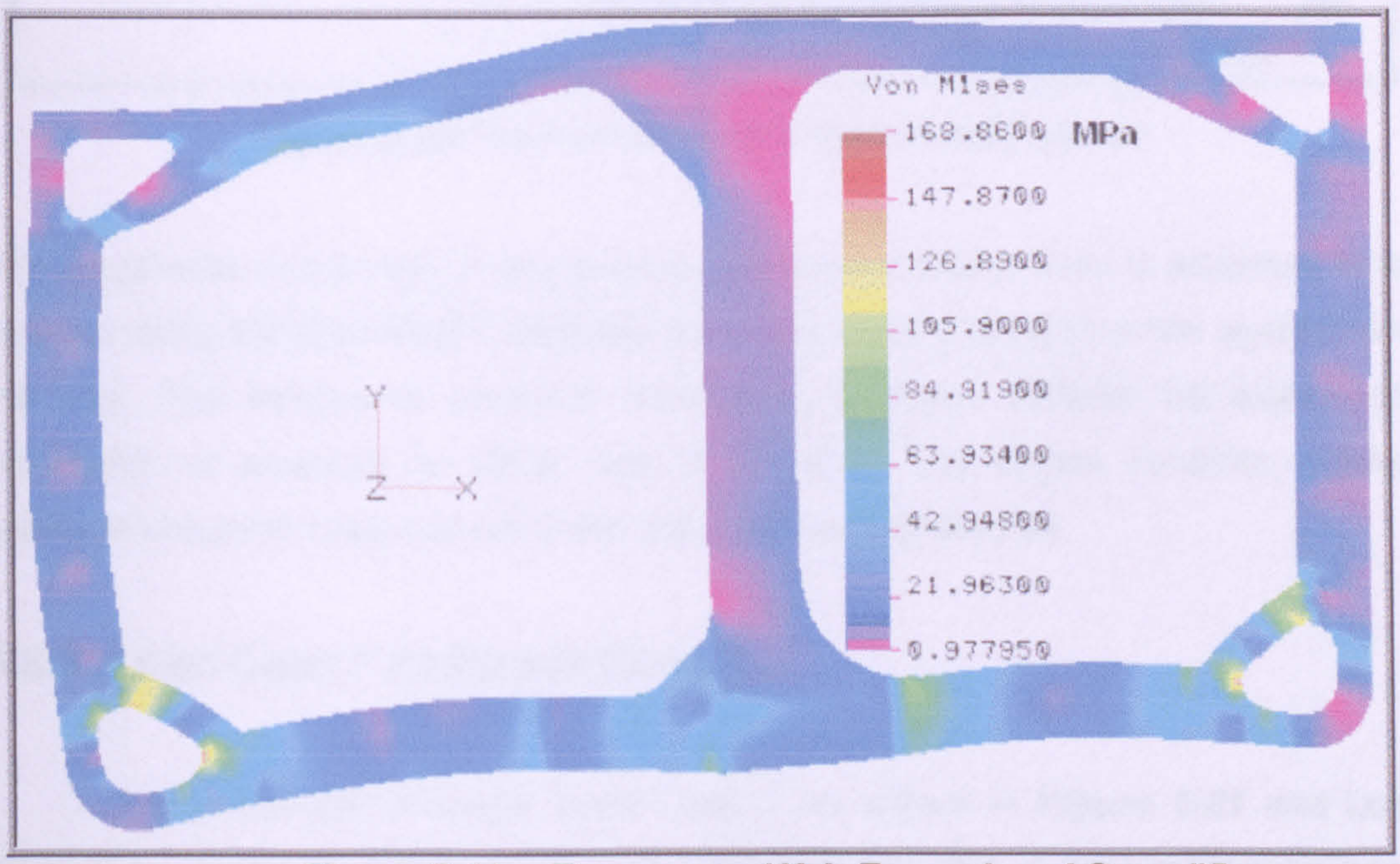

Figure 5-19 Transverse Web Frame Load Case #5

When the ship is in beam sea condition, the maximum external pressure on the starboard side of the hull is typically associated with the submergence of the starboard hull. Thus, the external pressure and the internal pressure in the tank acting on the side hull structure are in opposing directions. However, this is for the case when the ship is oscillating in long crested sinusoidal waves. This does not reflect the randomness of short crested waves in beam sea condition.

The direction of the internal pressure, therefore, is adjusted to produce maximum net load on the side hull structure.

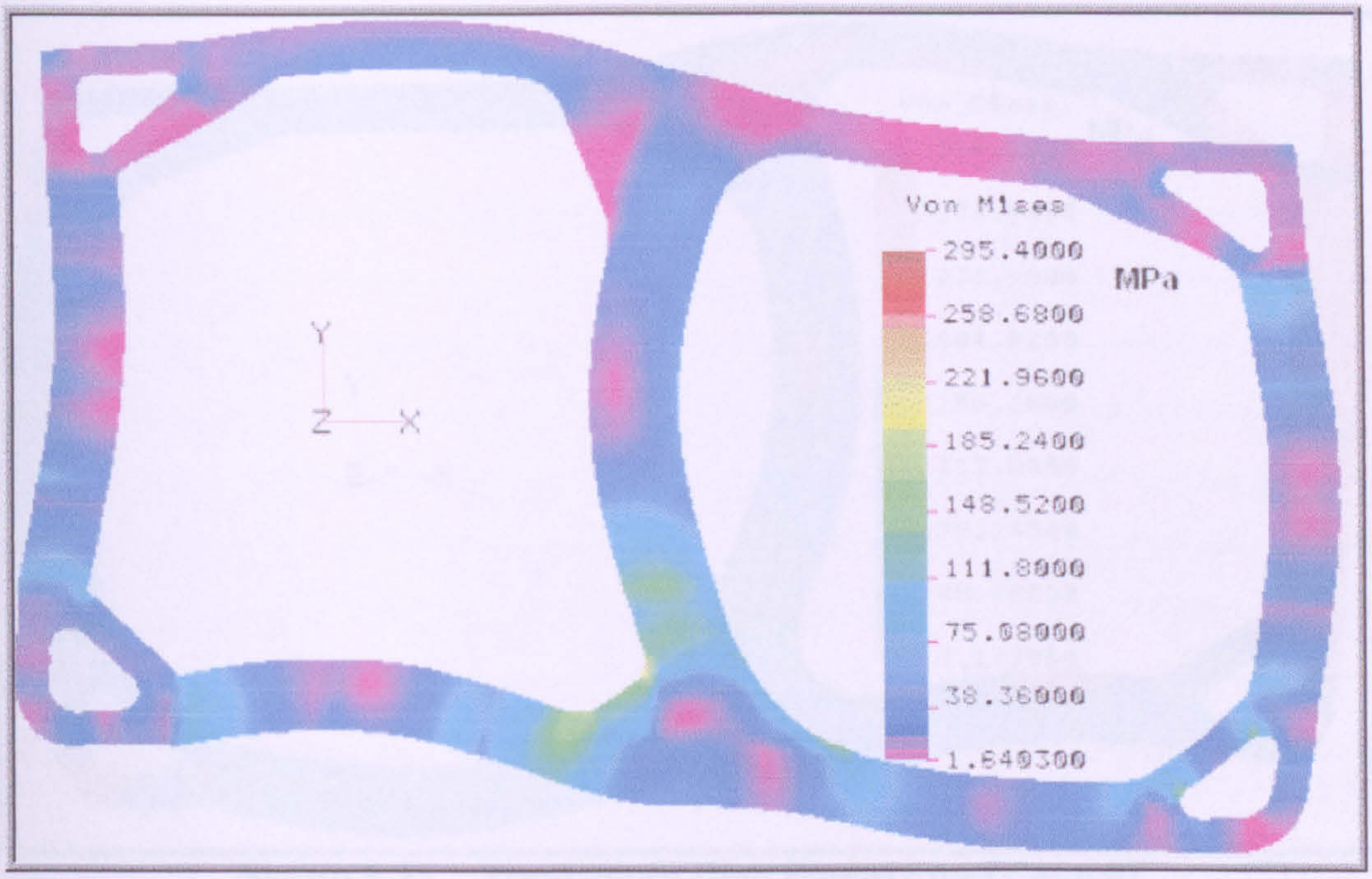

Figure 5-20 Transverse Web Frame Load Case #6

The lengthwise distribution of the external pressure in beam seas is assumed to be uniform along the ship length, because the wave crest is parallel to the centreline of the ship. The transverse sectional distribution, however, reflects the asymmetric distribution of pressure on either side of the ship. The largest dynamic external pressure occurs in Load Case 6 at the starboard side of the hull.

5.3.5 Load Case 7 and Load Case 8

The fourth pair of loads, Load Case 7 as shown in ***Figure 5-21*** and Load Case 8 as shown in ***Figure 5-22***, they represent the ship in bow quartering wave condition where the maximum horizontal bending moment and horizontal shear force are. Combining the head sea and beam sea conditions derives both the external and internal pressure distributions.

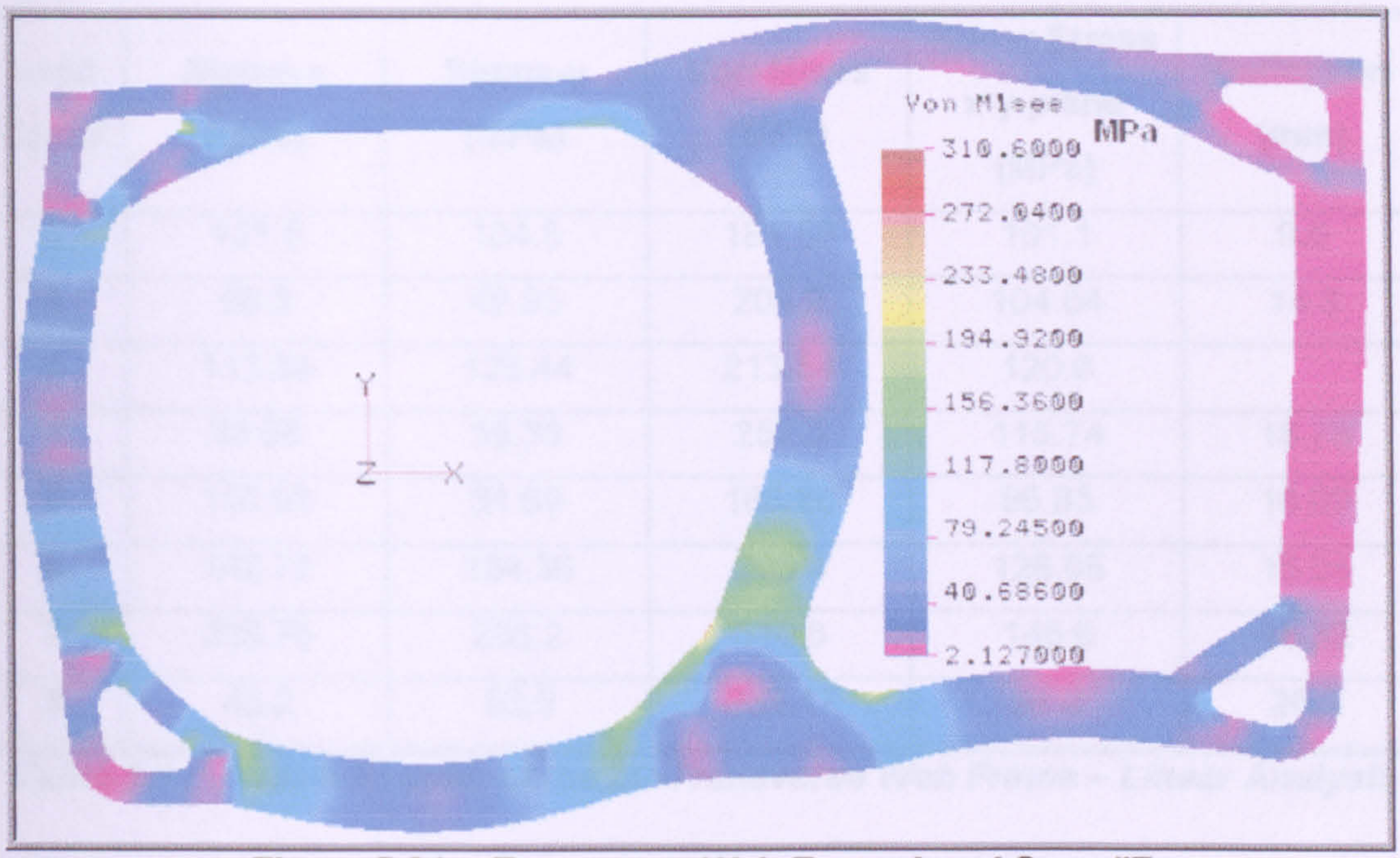

Figure 5-21 Transverse Web Frame Load Case #7

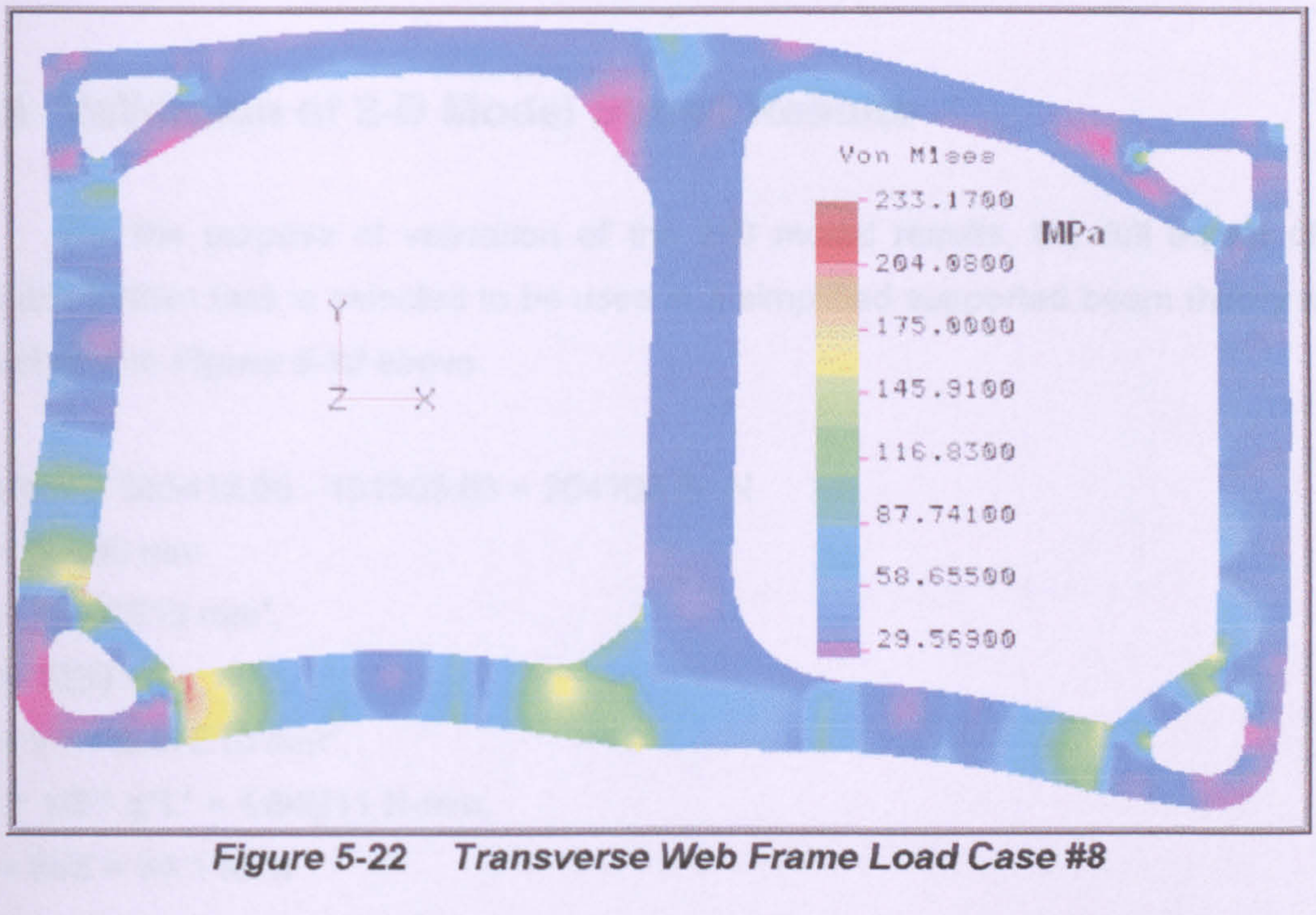

Figure 5-22 Transverse Web Frame Load Case #8

The mid-ship Web-Frame model has been used to analyse stresses in the main framing system. The basic model was generated and refined to match the convergence testing results. The main numerical results for the linear static analysis of the eight different load cases are listed on ***Table 5-1*** and ***Appendix B City FPSO2000 Web-Frame FEA Results.***

Load Case#	Sigma-x (MPa)	Sigma-y (MPa)	Von-Mises (MPa)	Shear Stress x-y plane (MPa)	Deflection (mm)
1	121.5	104.5	181.58	101.1	9.6
2	56.3	49.95	204.2	104.04	14.3
3	113.84	123.44	213.54	120.6	
4	38.68	38.33	257.5	115.74	18.73
5	110.93	81.69	168.86	96.83	16.09
6	142.75	134.36	295.4	128.65	15.04
7	238.75	236.2	310.6	145.6	15.32
8	45.2	53.5	233.17	97.3	26.5

Table 5-1 Main Results of the 2D-Transverse Web Frame – Linear Analysis

Stresses obtained by the 2-D fine-mesh analysis are to be used for assessing the adequacy of the structure for failure modes, especially, yielding and buckling.

5.4 Validation of 2-D Model Stress Results

For the purpose of validation of the 2-D model results, the full extent of a double bottom tank is selected to be used in a simplified supported beam theory test as shown in ***Figure 5-10*** above.

Forces = 365412.69 - 161305.83 = 204106.86 N

L = 13640 mm

I_{xx}= 1.776E13 mm^4,

Y = 1250 mm,

Z = I/Y = 8.07E10 mm^3,

M = 1/8 * q*L^2 = 4.84E11 N-mm,

σ = M/Z = 34.1 MPa

As it is revealed by the simple calculation above and compared to the FEM analysis average results of 32 MPa taken of the left double bottom tank as presented in ***Figure 5-23***, the results are in good agreement with the beam theory.

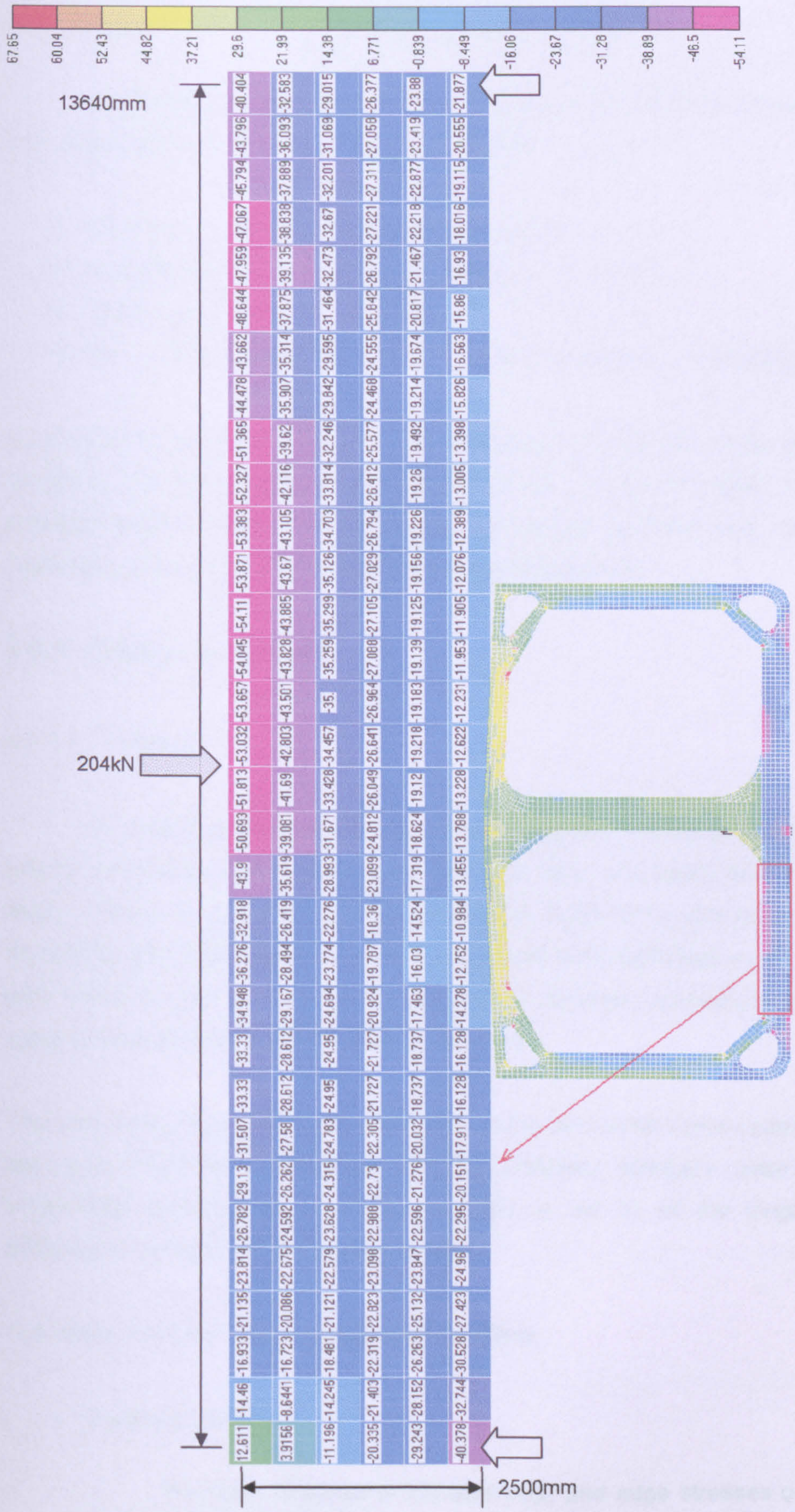

Figure 5-23 Results of mean stresses for analysis validation

5.5 Evaluation of 2-D Model Stress Analysis

In general, the FEM calculation produces several kinds of stresses. In case of 2-D model, the following stresses are calculated:

- Stresses at nodes or at centre of an element
- Stresses on upper surface, lower surface, or middle
- Normal stress or shearing stress
- Maximum principle stress, minimum principle stress, or combined stress

In general the principle stress is used as failure criterion for brittle materials, and combined (von-mises) stress for ductile materials such as mild steel. The Maximum principal stress is used for crack propagation analysis and the mean stress between upper and lower surface is used for plate buckling analysis.

5.5.1 Criteria of Failure

5.5.1.1 Yielding:

For reporting the stresses and displacements in the transverse web frame, a typical transverse web frame at the mid-ship area and away from the boundary region chosen to minimize boundary effects as seen in the previous analysis. The transverse frame analysis provides the stresses and deformations in a transverse web frame as part of the input to the fatigue damage calculations of any typical welding arrangements that would be carried out.

The web plate, deck plate, side shell plate, inner and outer bottom plates, centreline and side longitudinal bulkheads, tripping brackets, stringer's plate and central longitudinal bulkhead are modelled explicitly as will as all the longitudinals and stiffeners to simulate an accurate simulation.

The stress intensity can be categorized as follow:

- ***Uniaxial Loading:***

  For axial stresses in rod elements, and edge stresses or stresses in the extreme fibre of plate elements, the yielding criteria can be checked by

comparing the normal stresses directly to the yielding stress of the material. However, it is not advisable to use beam stresses for the same purpose. This is because in most cases beam elements are used to represent only the equivalent stiffness of the modelled hull structure, and the stresses determined are often not actual values expected in the structure.

- ***Biaxial Loading:***

For membrane plate elements, subjected to biaxial stresses, the theory of failure developed by H. Hencky and R. von Mises constitutes the limiting condition.

The yield stress is to be taken as:

- 235 N/mm^2 for normal mild steel
- 315 N/mm^2 for grade AH32 and DH32, or equivalent
- 355 N/mm^2 for grade AH36 and DI-136, or equivalent

The previous factors of safety are proposed by classification societies as a basis for assessment of the main FPSO's cargo tank length (main strength region of the hull structure).

The limit stress can be expressed as a factor of yield strength or ultimate strength of the material.

Hence: factor of safety $FOS = \frac{\sigma_{Limit}}{\sigma_{vonMises}}$

Various factors of safety exist as specified in the following codes and standards:

- Lloyd's Register of Shipping, Rules & Regulations for the Classification of Fixed Offshore Installations, (1997)

- Lloyd's Register of Shipping, Rules & Regulations for the Classification of Mobile Offshore Installations, (1997)

- Lloyd's Register of Shipping, Design Appraisal & Plan Approval of Ship Type FSU & FPSO Units at a Fixed Location, (1997)

- Det Norake Veritas, Factor of Safety and corrosion allowances, (1997)

- Health and Safety Executive, Offshore Installations Guidance on Design, Construction and Certification, (1990)

The FPSO safety factors for allowable stress ***Table 5-2*** in association with the previous codes and standards can be applied.

Operating conditions	Basic factors of safety
	2.5➔ for shear
	1.67➔ for axial tension and bending
	1.67➔for compression
	1.43➔ for the combined "comparative" stress
Extreme Storm Conditions	**Reduced factors of safety**
	1.88➔ for shear
	1.25➔for axial tension and bending
	1.25➔for compression
	1.11➔for the combined "comparative" stress
Damage Conditions	**Minimum factors of safety**
	1.72➔ for shear
	1.0➔for axial tension and bending
	1.0➔for compression
	1.0➔for the combined "comparative" stress

Table 5-2 Allowable Yielding Stress Factors of Safety

5.5.1.2 Buckling:

The FPSO's Finite Element Model is to be used in the assessment of the hull structure; a good example can be in accordance with the scope and methodology presented at *LR*, (1997).

Buckling stresses for unstiffened plate panels are to be used for evaluating the buckling strength of the structure. All unstiffened panels in the web plates having high magnitudes of compressive stresses should be checked against the specified buckling criteria. Another good practice for the stability of plating and stiffeners can be checked using the methodology described at *DNV*, (1995).

The required minimum factors of safety for lateral and torsional buckling of stiffeners are to be taken as listed in ***Table 5-3***:

Operating conditions	<u>Basic factors of safety</u>
	1.67➔ for shear buckling
	1.67➔for compression
Extreme Storm Conditions	<u>Reduced factors of safety</u>
	1.25➔for shear buckling
	1.25➔for compression
Damage Conditions	<u>Minimum factors of safety</u>
	1.0➔ for shear buckling
	1.0➔for compression

Table 5-3 Allowable Buckling Stress Factors of Safety

The factors of safety (λ) are defined as in the following ***Equation 5-1***:

$$\lambda = \frac{Calulated.Critical.Buckling.Stress}{Applied.Stress}$$

Equation 5-1

Thus, the factor of safety is the inverse of the "usage factor", defined by *DNV*, (1995). When buckling is the governing mode of failure, the geometric imperfections are to be assumed to be within the tolerances defined at *DNV*, (1995), where buckling strength formulations are given as a function of imperfection amplitude, the buckling

analysis is to be based on the maximum allowable imperfection amplitude unless measured data is available.

5.5.2 Discussion

The finite element analysis of the transverse frame has revealed high stresses in the vicinity of the cross-tie junction frames under certain loading conditions. This occurs also at the bulkhead slope to the double bottom intersection and side shell brackets on stiffeners. The majority of these critical locations have been reasonably addressed; an additional important location that shows high stress values is the web-toe and due to the importance of this critical location, insufficient analytical information available related to it and insufficient coverage by stress concentration factors given in recognised standards; it has been selected for the (zoom in) localised analysis. This particular localised model been used to assess the stress concentration at bracket toe end, as it will be demonstrated in the next section.

The global model is of insufficient mesh density as explained previously, but it is important for the calculation of the boundary conditions obtained from the global analysis. The local detailed model of principal supporting members such as transverse structures has to be analyzed in which the mesh density is increased, in addition the detailed geometry considered and displacements calculated are applied as boundary conditions.

6. FPSO Local Strength Analysis (*Tertiary*)

6.1 Transverse Web Frame Bracket Toe

In order to study the structural behaviour of an FPSO's Web-Toe, the 3-D global finite element model is to act as a parent model for the local structural detail model (web-toe). The following ***Figure 6-1*** shows the local model typical locations in an FPSO.

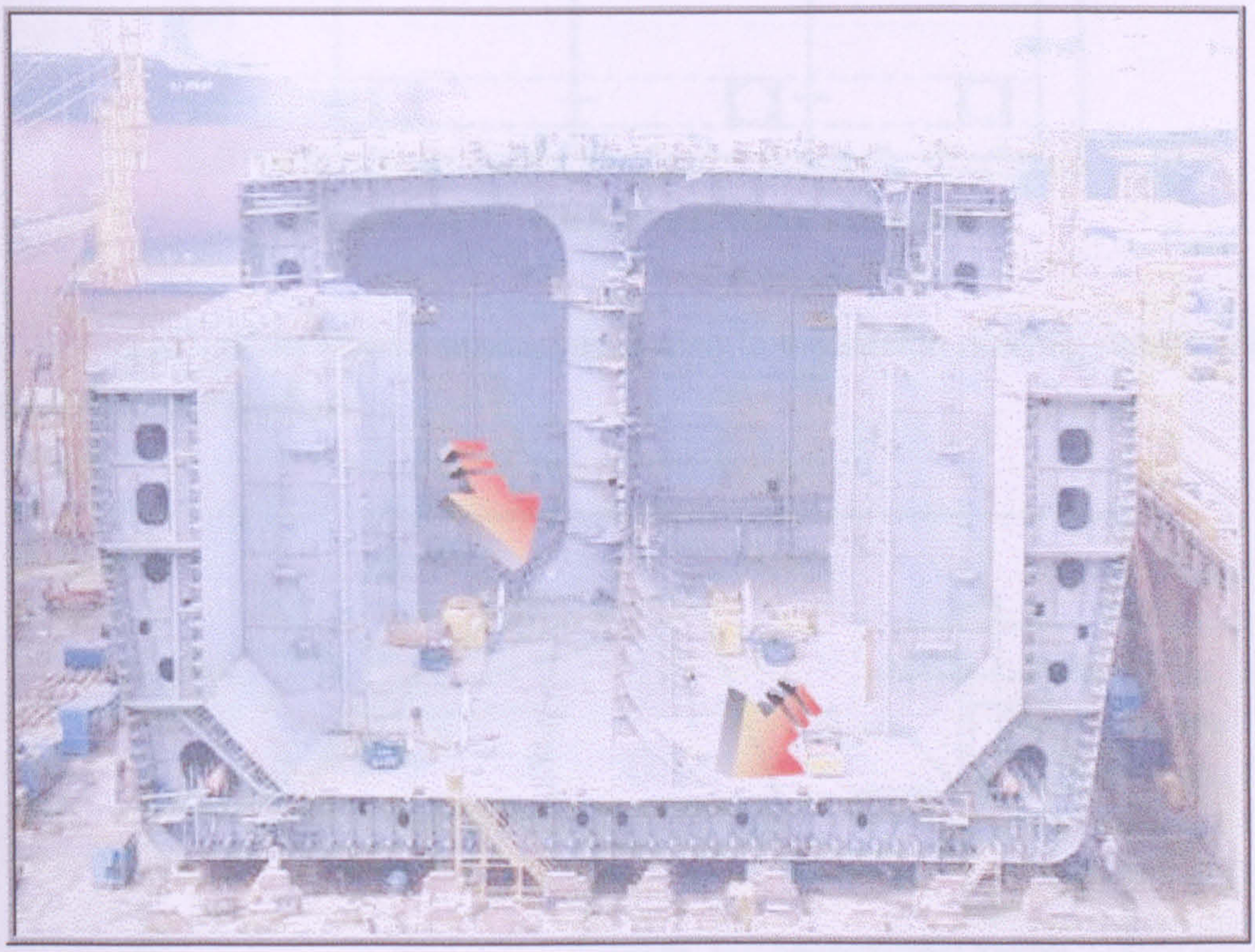

Figure 6-1 Typical Locations of a Transverse Web Frame Bracket Toe

6.1.1 Local Structural Detail Model

In generating the 3D local model, relatively fine mesh used closely to describe the geometry of the structure as well as the stiffness properties of the structure. Special attention paid to account for the effect of stress concentration due to change in geometry or in scantling in the high stress regions. This is important in the process of analyzing stresses in stiffeners subjected to large relative deformation. It is

important to account for the principal supporting structure of interest and local critical location in question, as illustrated in ***Figure 6-2***.

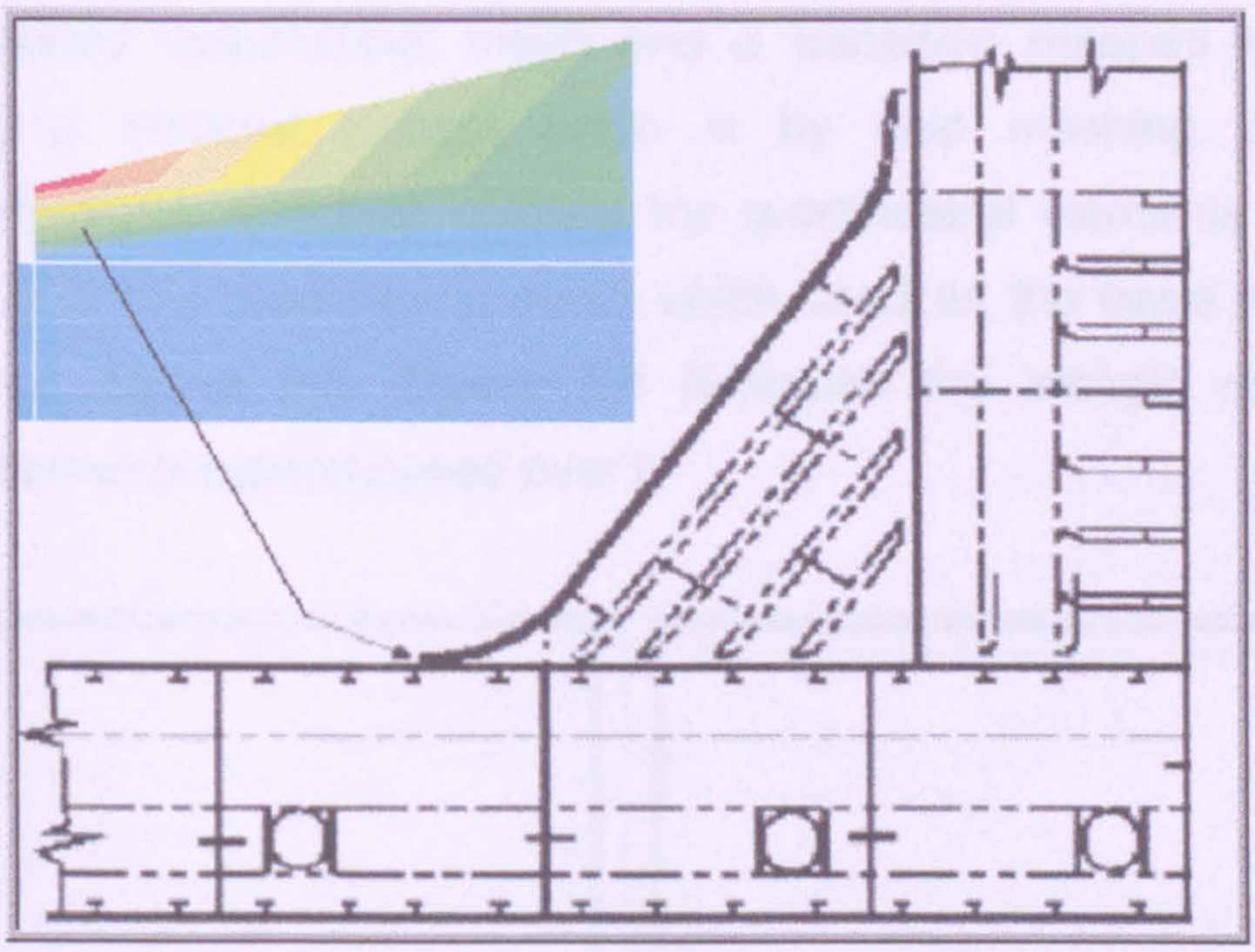

Figure 6-2 Web Toe Critical Location

The local detail model been modelled according to the design drawing details shown in the following ***Figure 6-3***.

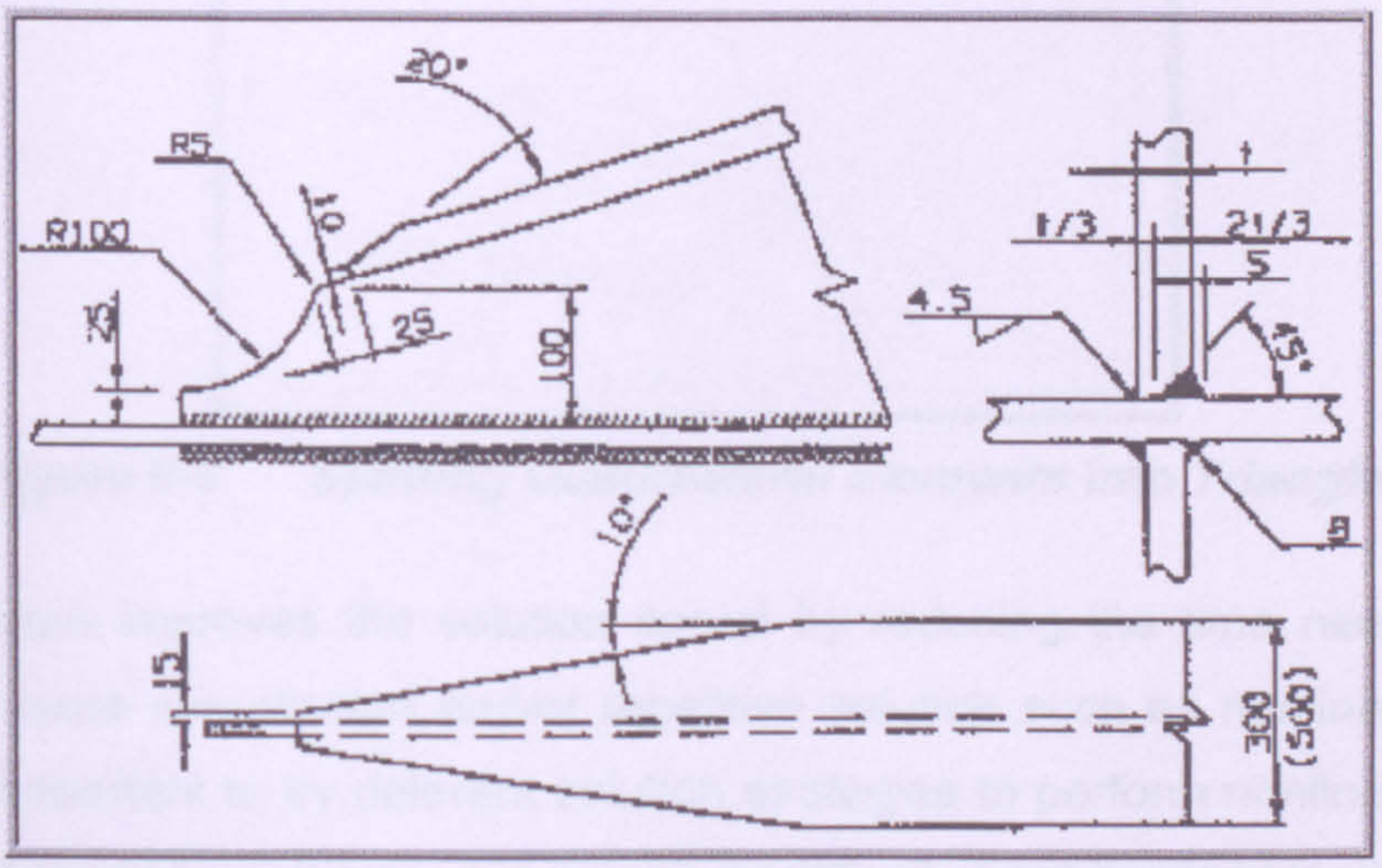

Figure 6-3 Web Bracket Structural Details

6.1.2 Triangle Elements

The fast tri mesh option in most of the recent pre-processors uses a method that creates triangles, which generally produces fewer triangles with better aspect ratios. This technique works particularly well for modelling transition regions between

fine and coarse meshes. Triangular shells can be mixed with quadrilateral shells within the same material property set based on work by *Belytschko, T., Liu, W. K. and Moran, B.* (2000). ***Figure 6-5*** demonstrates the relationship between a transitions mapped quadrilateral mesh and a transition mapped triangle mesh. Accomplishing a mapped triangle mesh is by map meshing the area with quadrilateral elements, and then splitting the quadrilateral elements into triangles. ***Figure 6-4*** shows the quadrilateral mesh which used as the basis for the triangle mesh shown in ***Figure 6-5***. ***Figure 6-6*** illustrates the triangle mesh, with the quadrilateral elements superimposed over it.

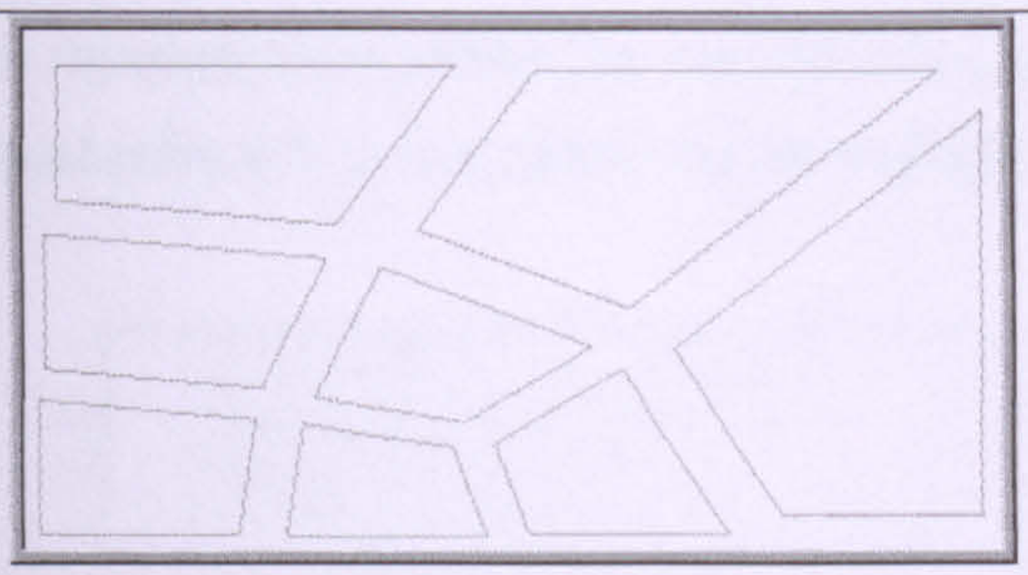

Figure 6-4 Quadrilateral elements

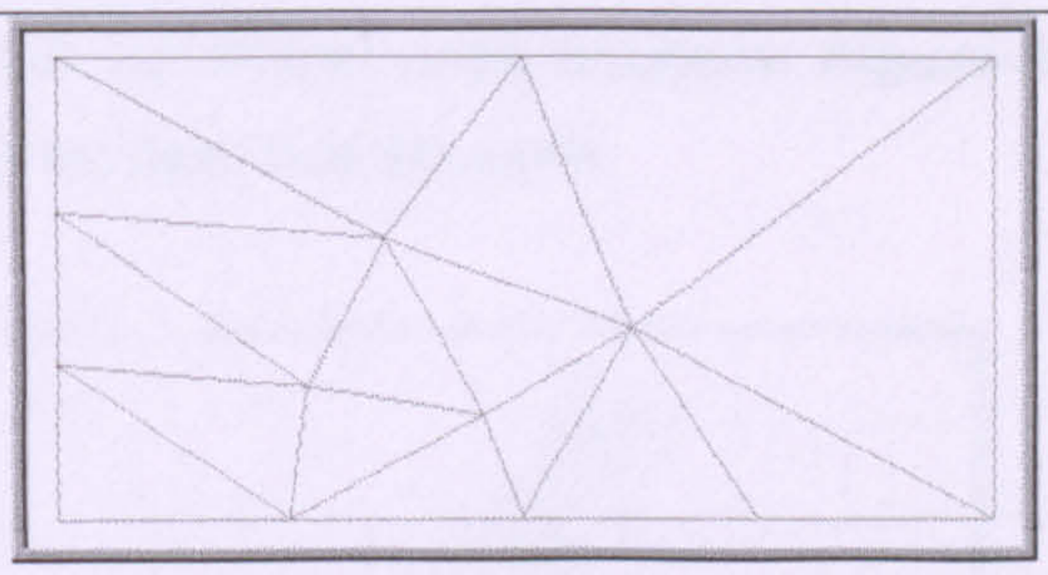

Figure 6-5 Triangular Elements

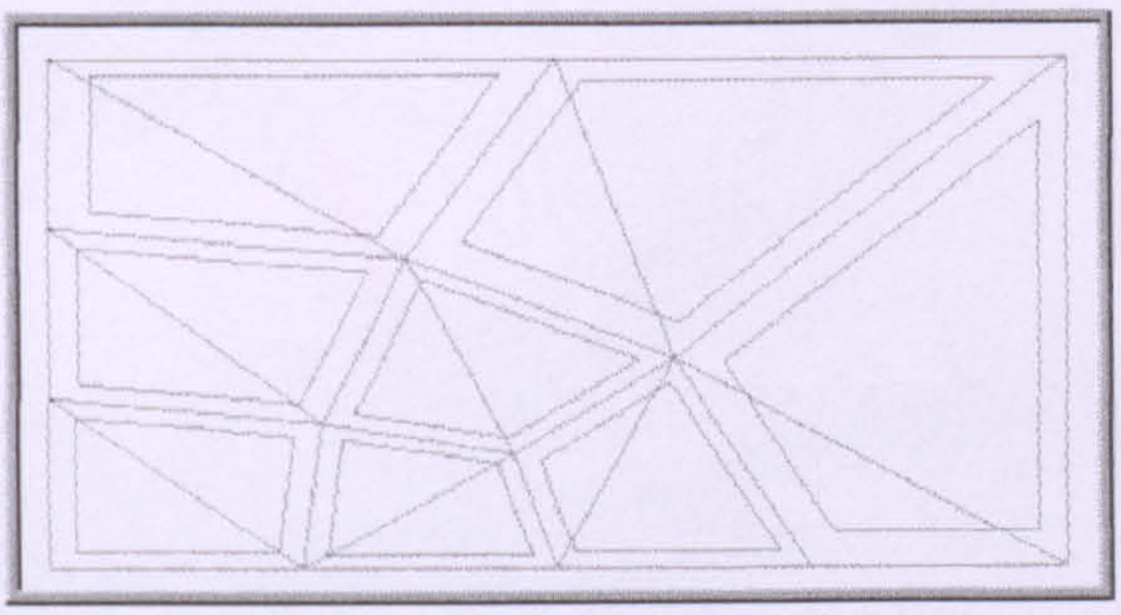

Figure 6-6 Splitting Quadrilateral Elements into Triangles

This procedure improves the solution speed by reducing the time needed for the analysis of more complicated and/or repetitive solution such as nonlinear analysis, where it is important to try deferent solution strategies to perform nonlinear analysis. As opposed to linear problems, it is extremely difficult, if not impossible, to implement one single strategy of general validity for all problems.

6.2 Transverse Web Frame Bracket Toe FEM

This section contains the detailed analyses, which demonstrate the structural adequacy of the Structural Assembly in question. These types of analyses used to demonstrate the overall structural characteristics and response can be:

- Linear static,
- Nonlinear static,
- Normal modes,
- Buckling
- Dynamic

6.2.1 Finite Element Model Description

An FE model of the enclosure assembly shown in ***Figure 6-8*** created using the FEMAP pre-processor. The model utilizes shell elements along with rod elements to represent the stiffeners. NASTRAN used to run all the modal solutions. ***Figure 6-7*** illustrates a 3-D fine mesh model idealising the Web-Toe structure.

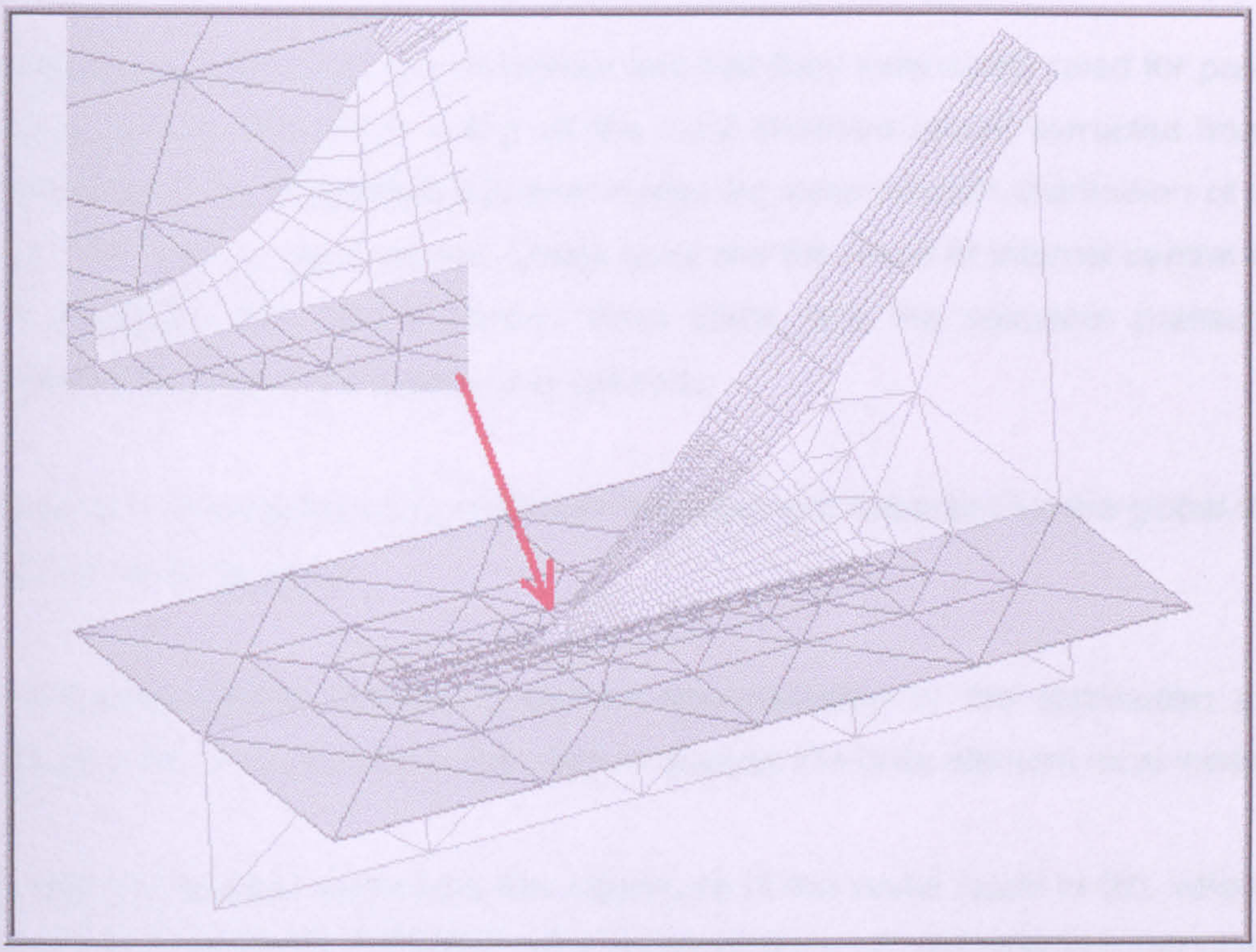

Figure 6-7 Finite Element Model of a Web-Toe

It is consisting of four main plates varying in thickness, plate (A) represents the double bottom tank transverse web, plate (B) represents the inner bottom, plate (C) represents the end bracket, and plate (D) represents the bracket stiffener.

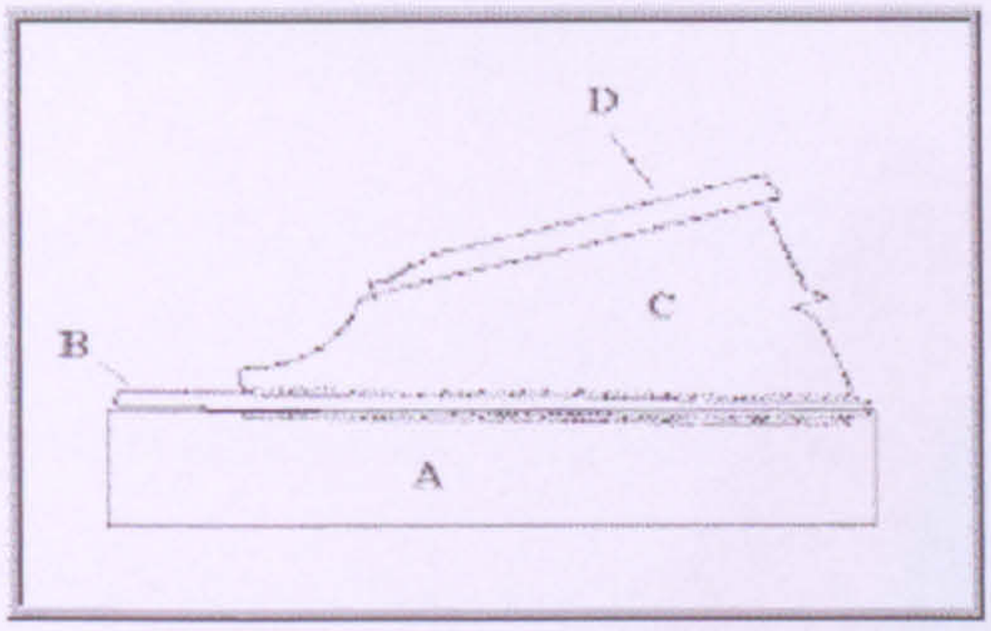

Figure 6-8 Web Toe Bracket Basic Plate Assembly

6.2.2 Model Loads

The local strength loads indicate the loads, which affect the local strength members, such as shell panels, stiffeners and connections between stiffeners.

The above load categories are so convenient that they extensively used for practical design purposes. The loads acting on the local structure model extracted from the global model and extrapolated between nodes for extra smooth distribution of loads where mesh size is much refined. Loads used are the result of internal central tanks cargo combined with double bottom tanks loads, and the seawater pressure as external load acting at the structure in question.

The model is constrained using enforced displacement extracted for the global model of the hull girder analysis.

The following ***Figure 6-9*** is a graphical representation of the distribution of the combined static and dynamic loads used to analyse the finite element local model.

The coloured contour represents the magnitude of the nodal loads in (N), where the arrows are to indicate the direction, as a representation of load case number one.

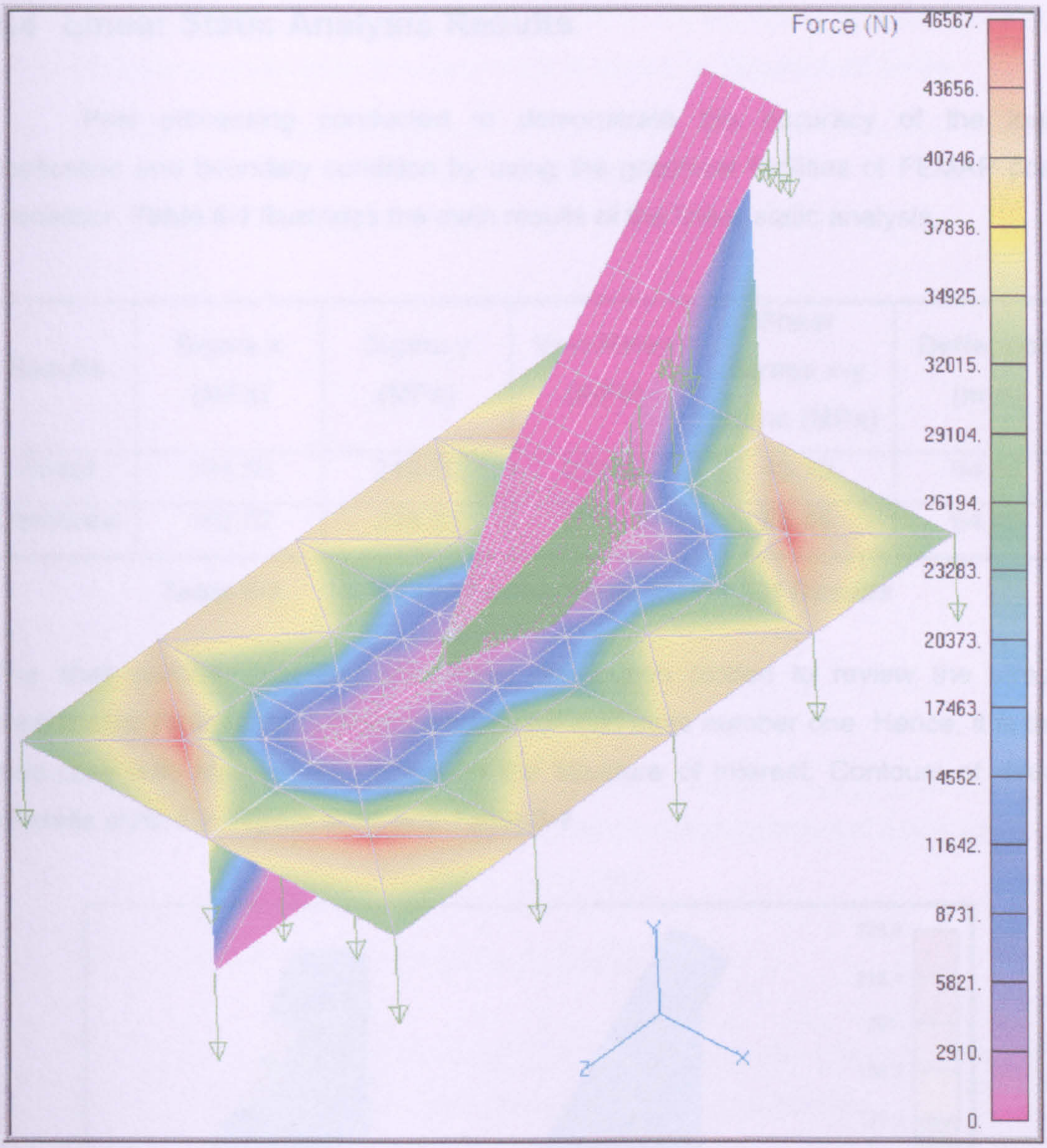

Figure 6-9 Load Case #1- Loads Distribution

6.3 Linear Static Analysis

Crisfield, M. A., (1986) explained that performing a linear static stress analysis is to apply static loads, such as forces or pressures, or known "imposed" displacements to a finite element model; Then adding elastic material data, boundary conditions, and other information such as the direction of gravity.

6.4 Linear Static Analysis Results

Post processing conducted to demonstrate the accuracy of the load application and boundary condition by using the graphical facilities of FEMAP post processor. ***Table 6-1*** Illustrates the main results of the linear static analysis,

Results	Sigma-x (MPa)	Sigma-y (MPa)	Von-Mises (MPa)	Shear Stress x-y plane (MPa)	Deflection (mm)
Nodal	134.90	218.00	229.80	43.20	94.66
Elemental	162.82	228.33	263.45	85.49	94.45

Table 6-1 Web Toe Linear Static Main FEM Results

The shell surface deflection and stress distribution plotted to review the stress magnitudes. Plots of the model generated for load case number one. Hence, it is the load case with Max bending effect on the structure of interest. Contours of direct stresses plotted in ***Figure 6-10***, and ***Table 6-1*** .

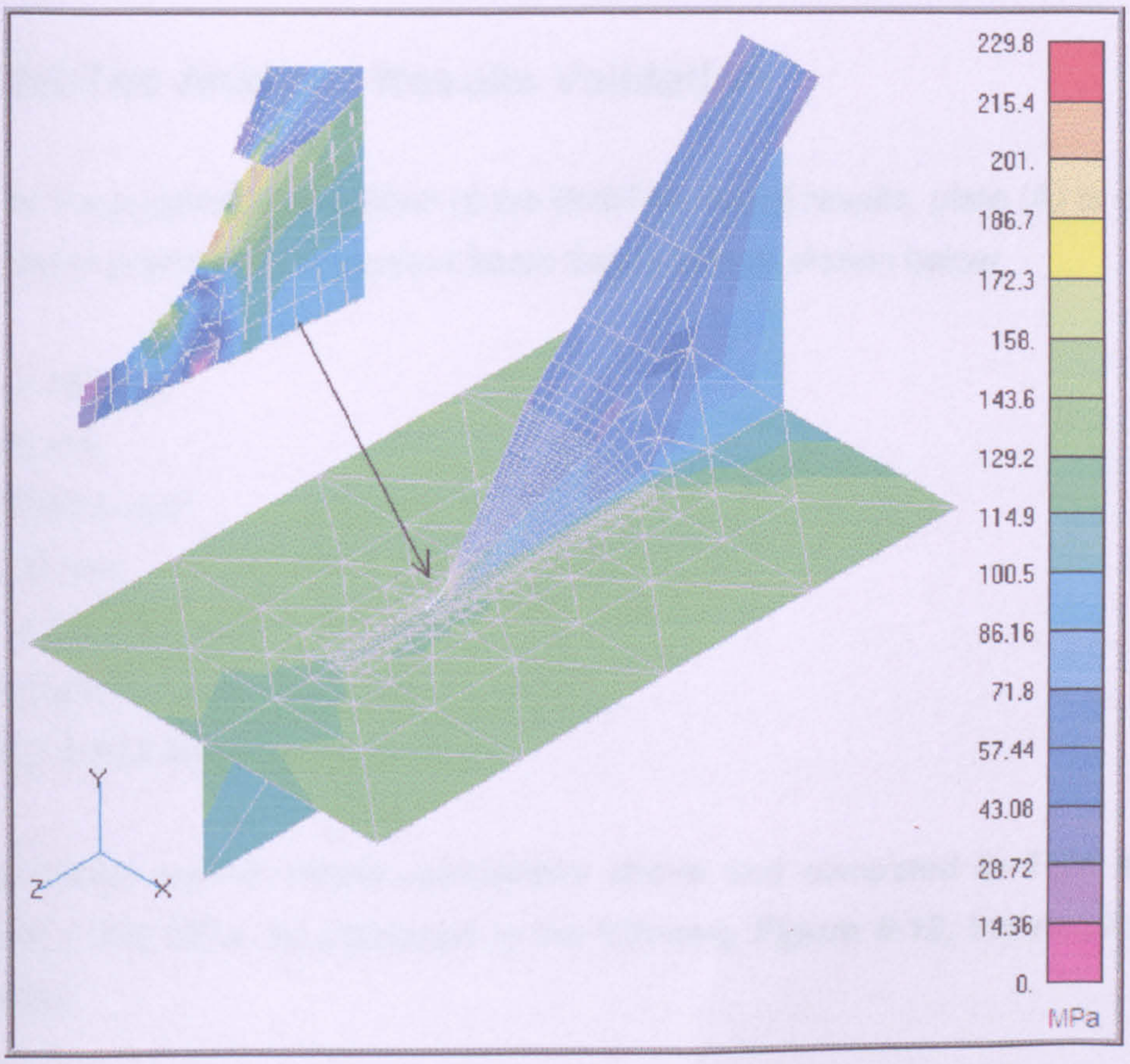

Figure 6-10 Web Toe Linear Static Von-Mises Nodal Stresses

The following line diagram represents an account for the combined stresses and total translation acting on the Web-Toe centre line as shown in ***Figure 6-11*** below.

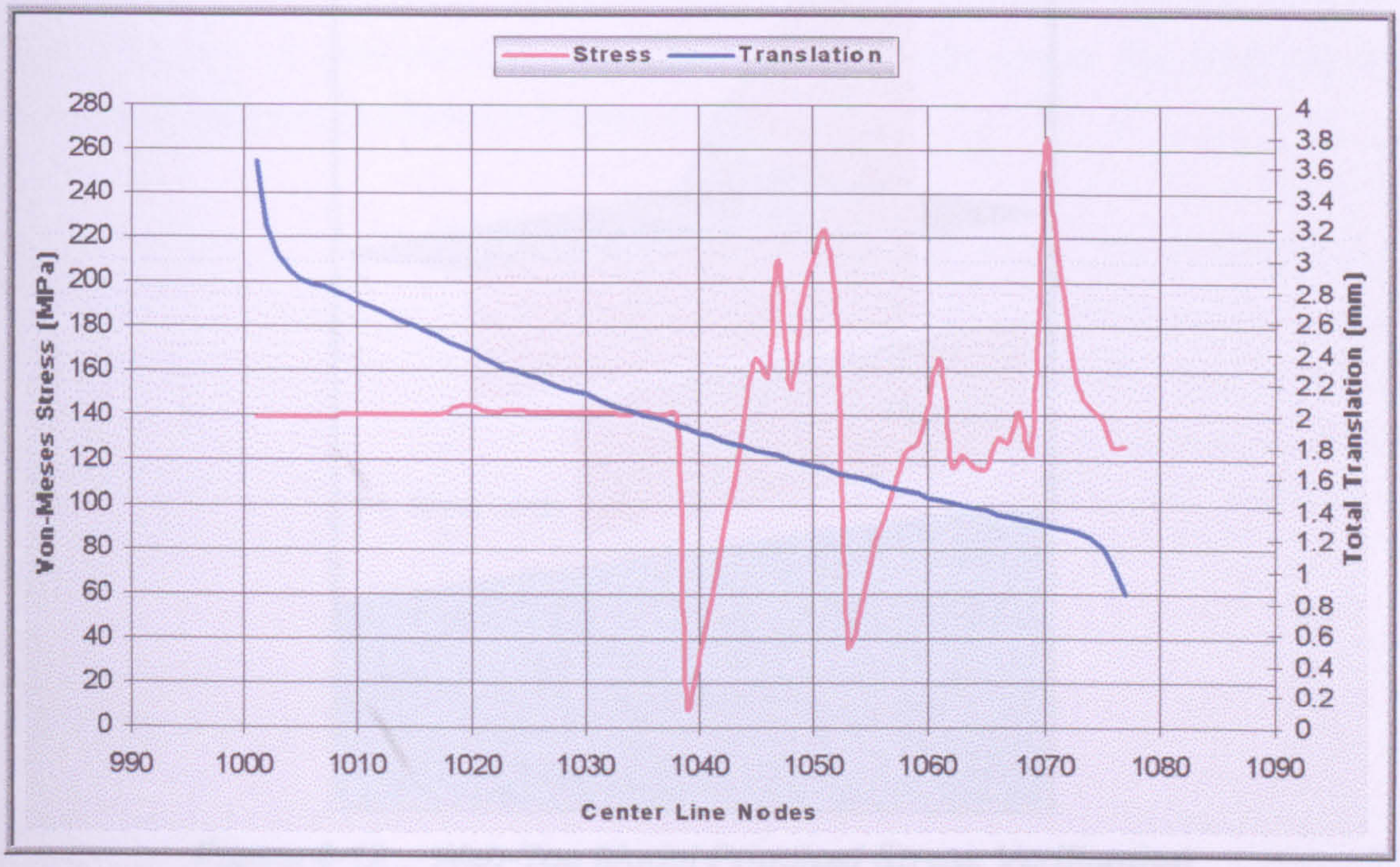

Figure 6-11 Line Graph of the Web-Toe Centre Line Combined Stresses and Total Translation

6.5 WebToe Analysis Results Validation

For the purpose of validation of the WebToe model results, plate (A) is selected to be used in a simplified supported beam theory test as shown below.

Forces = 155.9 N

L = 3080 mm

I_{xx}= 6.266E13 mm^4,

Y = 312.5 mm,

Z = I/Y = 2.005E8 mm^3,

M = 1/8 * q*L^2 = 1.8461E8 N-mm,

σ = M/Z = 0.923 MPa

As it is shown by the simple calculations above and compared to FEM analysis results of 0.932 MPa, as presented in the following ***Figure 6-12,*** the results are in agreement.

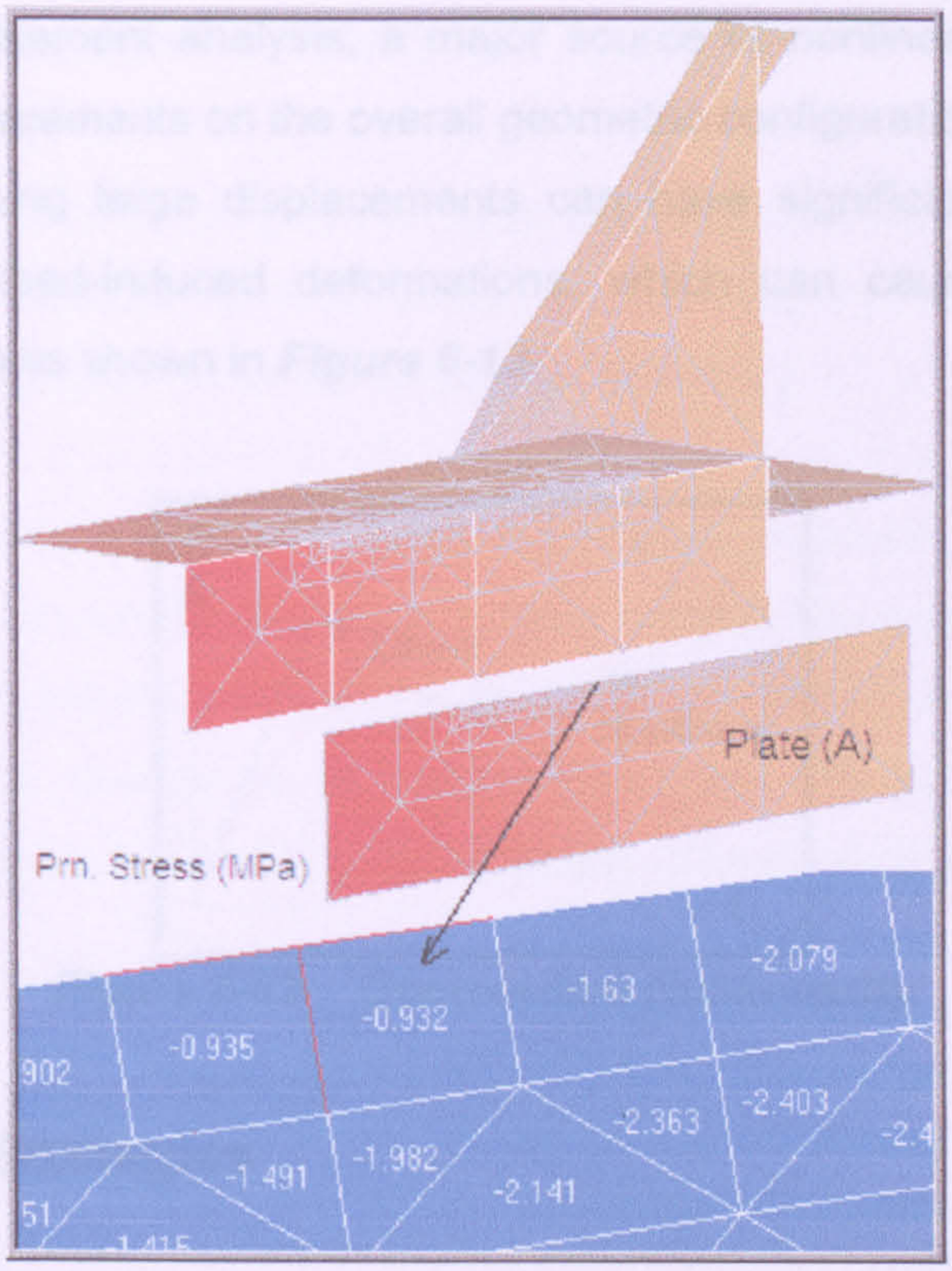

Figure 6-12 Web-Toe Model Principal Stress Verification

6.6 Nonlinear Static Analysis

Linear analysis is based on the linearity assumption and therefore valid as long as this assumption is valid. When the linearity assumption fails, linear analysis will produce wrong results and nonlinear analysis used. The linearity assumption is true if:

- All the materials in the model comply with Hooke's law, which is stress, is directly proportional to strain.

- The induced displacements are small enough so that you can ignore the change in the stiffness caused by loading. Nonlinear analysis offers a large displacement option when defining the material properties of a solid component or a shell.

- Boundary conditions do not vary during the application of loads. Loads must be constant in magnitude, direction, and distribution. They should not change while the model is deforming.

In nonlinear finite element analysis, a major source of nonlinearities is due to the effect of large displacements on the overall geometric configuration of structures. Structures undergoing large displacements can have significant changes in their geometry due to load-induced deformations, which can cause the structure to respond nonlinearly as shown in ***Figure 6-13***.

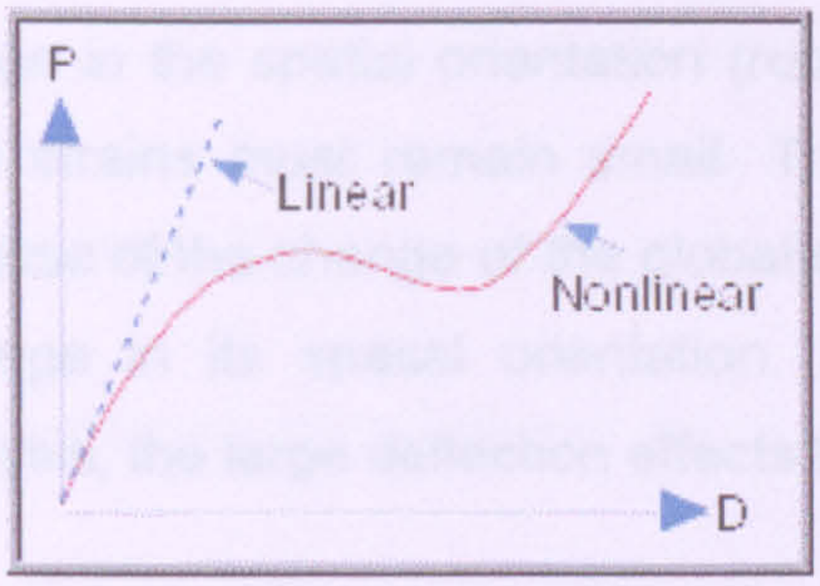

Figure 6-13 Geometrical Nonlinearity

6.6.1 Solution Strategies

For nonlinear problems, the stiffness of the structure, the applied loads, and/ or boundary conditions, all affected by the induced displacements as explained by *Allen, H. G.,* and *Al-Qarra, H. H,* (1987). The equilibrium of the structure established in the current configuration. At each equilibrium state along the equilibrium path, the resulting set of simultaneous equations will be nonlinear. Therefore, a direct solution will not be possible and an iterative method will be required.

Several strategies devised to perform nonlinear analysis. As opposed to linear problems, it is extremely difficult, if not impossible, to implement one single strategy of general validity for all problems. Very often, the particular problem at hand will force the analyst to try different solutions procedures or to select a certain procedure to succeed in obtaining the correct solution.

For these reasons, it is imperative that a computer program used for nonlinear analyses should possess several alternative algorithms for tackling wide spectrum of nonlinear applications. Such techniques would lead to increased flexibility and the analyst would have the ability to obtain improved reliability and efficiency for the solution of a particular problem.

6.6.2 Large Displacement Nonlinear Analyses

The use of the most general large displacement formulation will render "correct" solutions. However, in many cases, the use of a more restrictive formulation could be attractive because of its computational efficiency.

In this category, the change in the spatial orientation (rotation) of the elements can be finite but the induced strains must remain small. The overall stiffness of the structure will change because of the change of the global stiffness contribution of the element due to the change in its spatial orientation. By updating the element orientation during the analysis, the large deflection effects taken into consideration.

6.6.3 Numerical Procedures

There are different numerical procedures that incorporated in the solution of nonlinear problems using the finite element method. A successful procedure must include the following:

- A control technique capable of controlling the progress of the computations along the equilibrium path(s) of the system,
- An iterative method to solve a set of simultaneous nonlinear equations governing the equilibrium state along the path(s),
- Termination schemes to end the solution process.

Additional schemes such as line search, acceleration, and/or preconditioning improved to enhance the solution procedure.

Different control techniques devised to perform nonlinear analysis. These techniques classified as:

- Force Control
- Displacement Control
- Arc-Length Control

6.6.4 Iterative Solution Methods

6.6.4.1 Newton-Raphson (NR) Scheme

In this scheme, the tangential stiffness matrix formed and decomposed at iteration within a particular step as illustrated in ***Figure 6-14***. The NR method has a high convergence rate and its rate of convergence is quadratic. However, since the tangential stiffness formed and decomposed at iteration, which can be prohibitively expensive for large models, it may be advantageous to use another iterative method such as the modified Newton-Raphson or the Quasi-Newton.

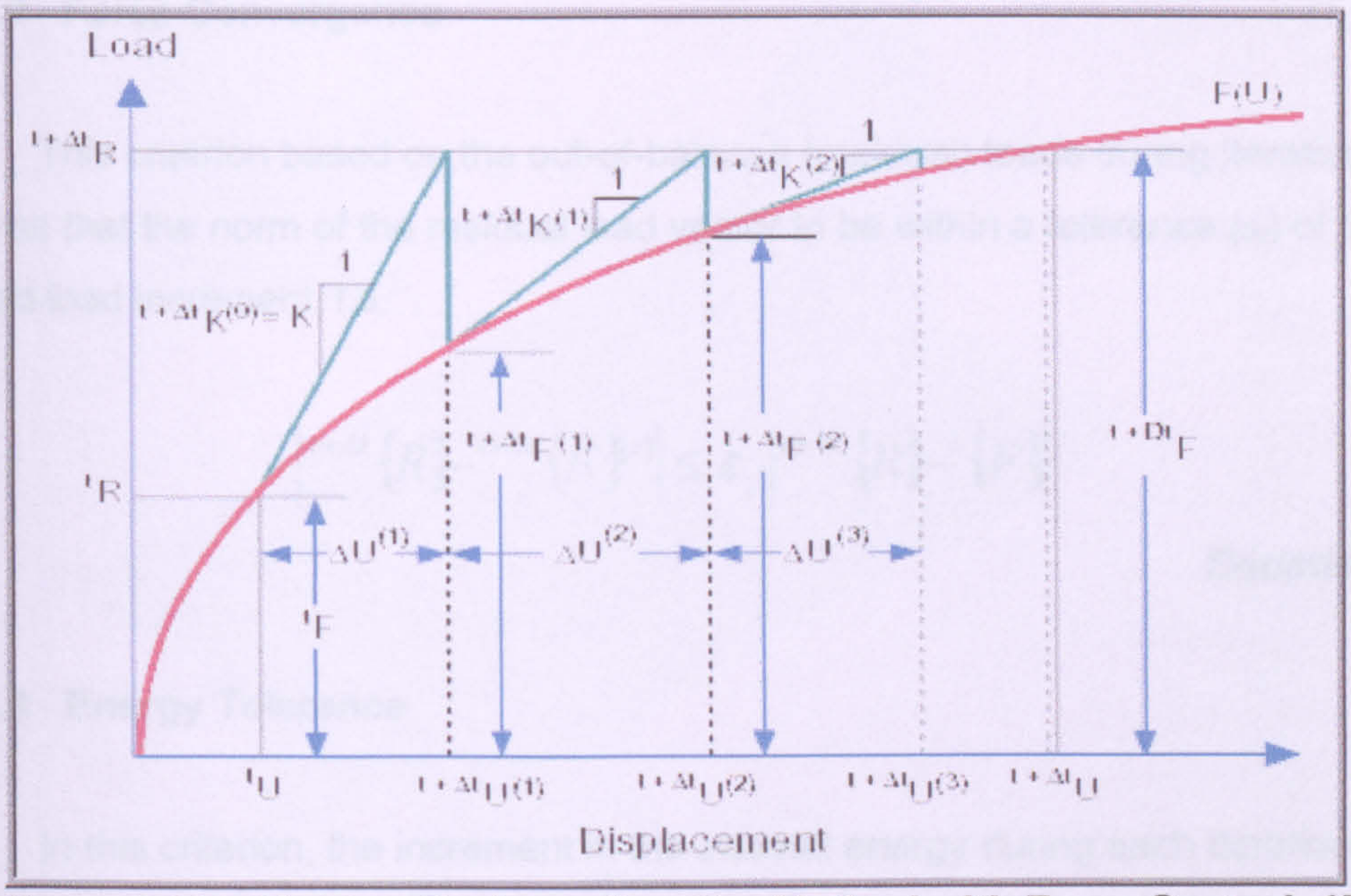

Figure 6-14 Newton-Raphson Iterative Method with Force Control, 1D

6.6.5 Termination Schemes

For an incremental procedure based on iterative methods to be effective, practical termination schemes provided. At the end of iteration, convergence evaluated within realistic tolerances. Very loose tolerances will lead to inaccurate results, while very strict tolerances can needlessly increase the computational cost. A bad convergence check can end the iterative process when the solution has not converged or allow the process to continue searching for unrealizable solution.

A number of procedures introduced as convergence criteria for terminating an iterative process.

6.6.5.1 Displacement Convergence

This criterion based on the displacement increments during iterations. Given by:

$$\left|\{\Delta U\}^{(i)}\right| \leq \varepsilon_d \left|{}^{t+\Delta t}\{U\}^{(i)}\right|$$

Equation 6-1

Where ε_d denotes the displacement tolerance

6.6.5.2 Force Convergence

This criterion based on the out-of-balance (residual) loads during iterations. It requires that the norm of the residual load vector to be within a tolerance (ε_f) of the applied load increment, i.e.

$$\left|{}^{t+\Delta t}\{R\} - {}^{t+\Delta t}\{F\}^{(i)}\right| \leq \varepsilon_f \left|{}^{t+\Delta t}\{R\} - {}^{t}\{F\}\right|$$

Equation 6-2

6.6.5.3 Energy Tolerance

In this criterion, the increment in the internal energy during each iteration, which is the work done by the residual forces through the incremental displacements, is compared with the initial energy increment. Convergence assumed realized when the following condition is satisfied:

$$\left(\{\Delta U\}^{(i)}\right)^T \left({}^{t+\Delta t}\{R\} - {}^{t+\Delta t}\{F\}^{(i-1)}\right) \leq \varepsilon_f \left(\{\Delta U\}^{(i)}\right)^T \left({}^{t+\Delta t}\{R\} - {}^{t}\{F\}\right)$$

Equation 6-3

Where (ε_f) is the energy tolerance; in addition to a number of schemes used as convergence criteria, one of these schemes based on the convergence of the residual loads, another based on the convergence of the incremental energy.

6.7 Nonlinear Static Analysis Results

Post processing conducted to demonstrate the results of the load application and boundary condition by using graphical facilities of FEMAP post processor. The shell surface deflection and stress distribution plotted to review the stress magnitudes. Plots for the model generated for load case number one. This analysis considered the geometric nonlinearity using large displacement formulation.

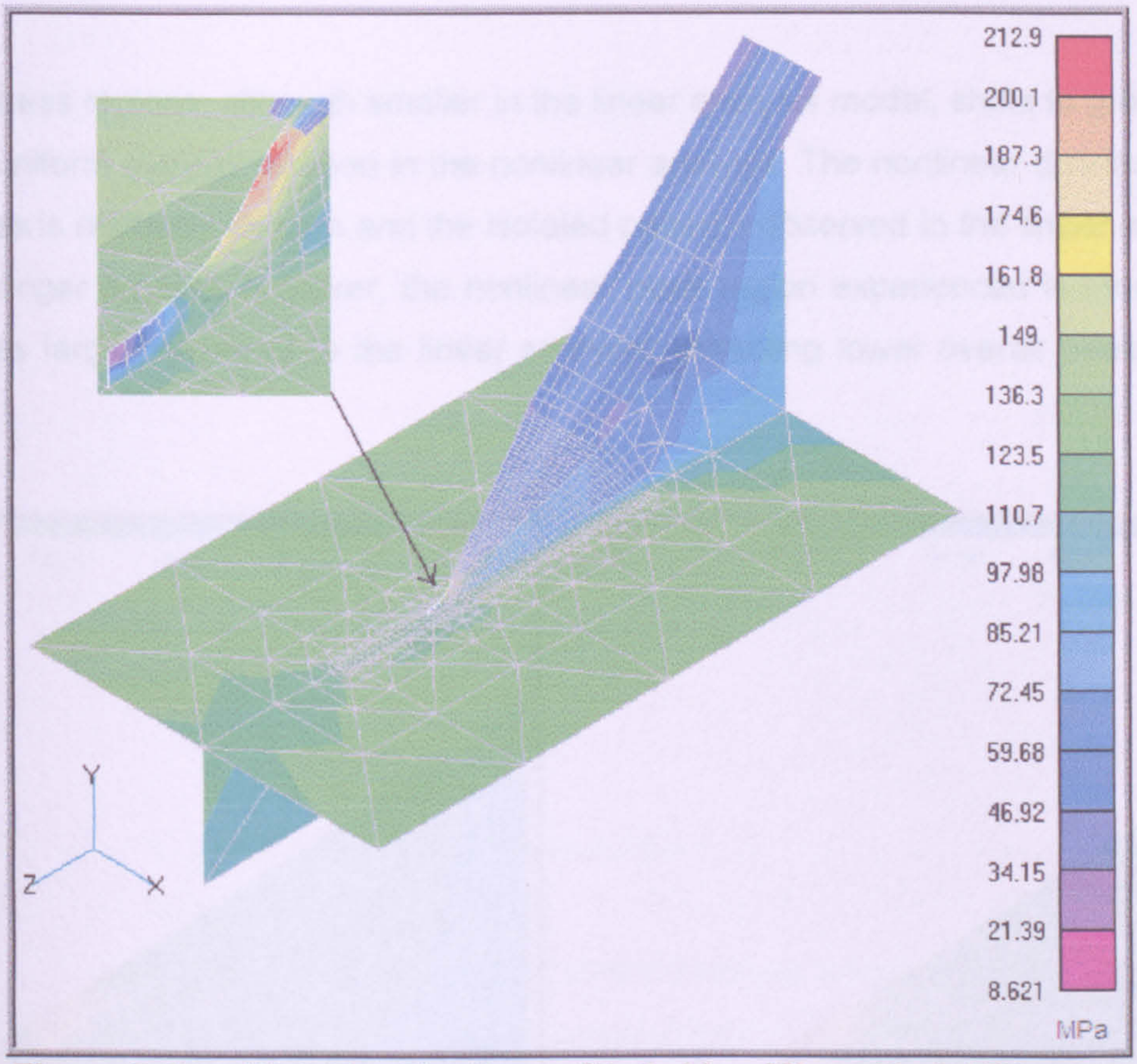

Figure 6-15 Web Toe Nonlinear Static Von-Mises Nodal Stresses

Table 6-2 illustrates the main results of the nonlinear static analysis,

Results	Sigma-x (MPa)	Sigma-y (MPa)	Von-Mises (MPa)	Shear Stress x-y plane (MPa)	Deflection (mm)
Nodal	144.60	176.35	212.90	71.80	94.66
Elemental	173.70	201.65	200.10	80.85	94.44

Table 6-2 Web Toe Nonlinear Static Main FEM Results

6.7.1 Linear & Nonlinear Static Analysis Results Comparison

While the linear static model is relatively easy to use and give reliable results, the present stage of the nonlinear modelling techniques requires a broad inside view in the numerical methods and are not applicable for everyday use. The nonlinear model appears to capture enhanced distribution of the maximum comparative stresses on the bracket-toe model when displayed in a discrete contour style as shown in ***Figure 6-16***.

High stress regions, although smaller in the linear analysis model, shifts to group in a much uniform manner as seen in the nonlinear analysis. The nonlinear distribution of stresses is relatively uniform and the isolated patterns observed in the linear analysis is no longer present; however, the nonlinear peak region experienced is more than twice as large compared to the linear analysis, attracting lower overall peak stress value.

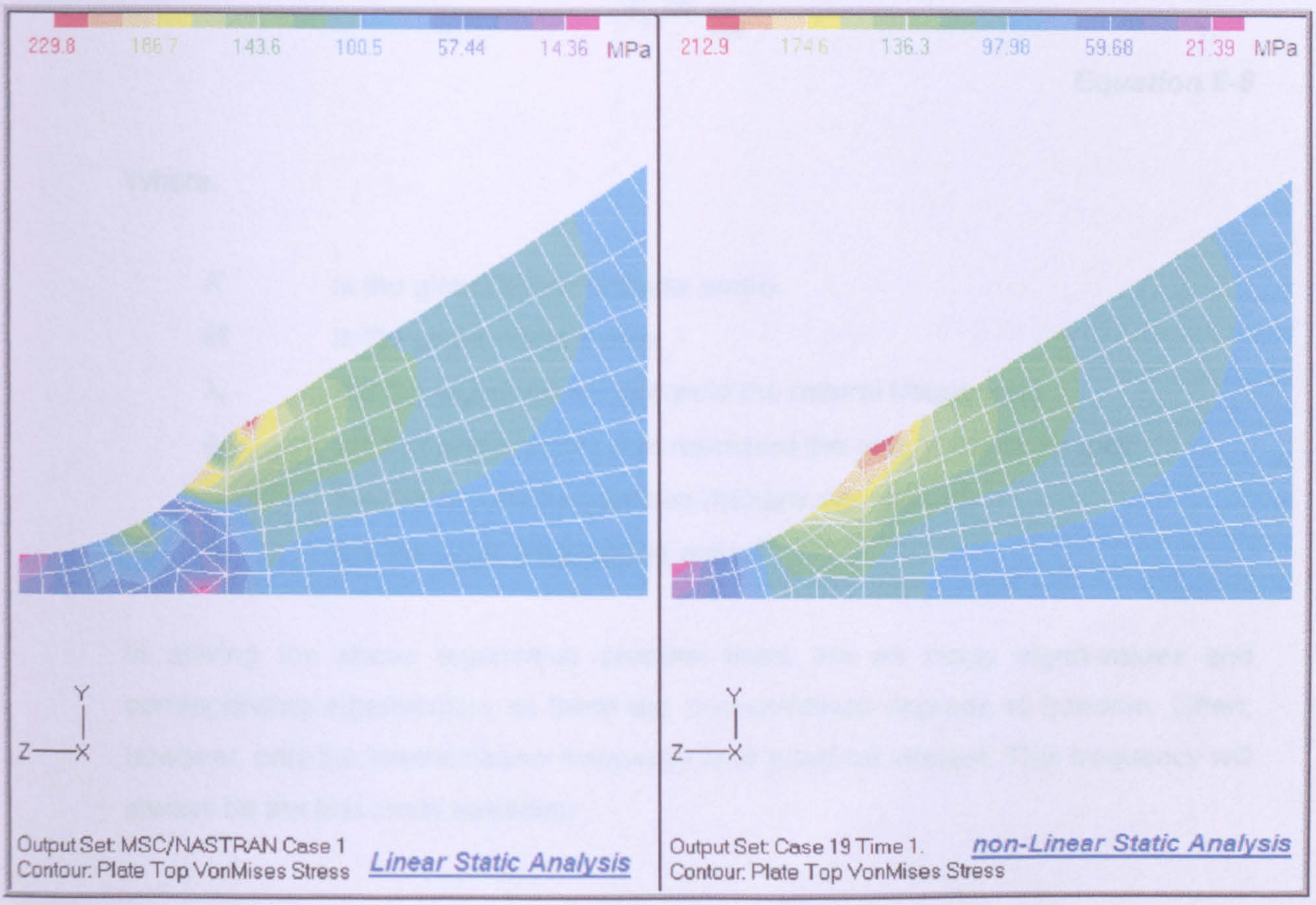

Figure 6-16 Comparison between Linear & Non-Linear Static Stresses

6.8 Normal Modes Analysis

Problems in structural dynamics divided into two broad areas as explained in *Flugge, W.,* (1962). In one, the objective is to determine natural frequencies of vibration and the corresponding mode shapes. In the other, the objective is to determine how the structure moves with time under an applied set of loads.

Determining natural frequency achieved by solving the Eigenvalue problem:

$$|[K]+\lambda_i[M]|[\phi_i]=0$$

Equation 6-4

$$\lambda_i=\omega_i^2$$

Equation 6-5

$$f_i=\frac{\omega_i}{2\pi}$$

Equation 6-6

Where,

K	is the global linear stiffness matrix
M	is the global mass matrix
λ_i	are the eigen-values that yield the natural frequencies
ϕ_i	are the eigenvectors that represent the natural mode shapes
ω_i	are the circular frequencies (radians per second)
f_i	are the cyclic frequencies (hertz)

In solving the above eigenvalue problem there are as many eigen-values and corresponding eigenvectors as there are unconstrained degrees of freedom. Often, however, only the lowest natural frequency is of practical interest. This frequency will always be the first mode extracted.

6.8.1 Normal Modes Analysis Results

The purpose of this is to demonstrate a finite element normal modes analysis by determining the normal modes of the Web Frame Bracket Toe using Nastran. The model natural modes calculated in Nastran and post-processed in FEMAP. The main objective of the analysis was to determine the fundamental frequencies and its corresponding mode shape for the assembly. The analysis shows that frequency to be 149.938 Hz is to be associated with the corresponding mode shape number one. Plots of additional mode shapes of the finite element model displayed on the following figures:

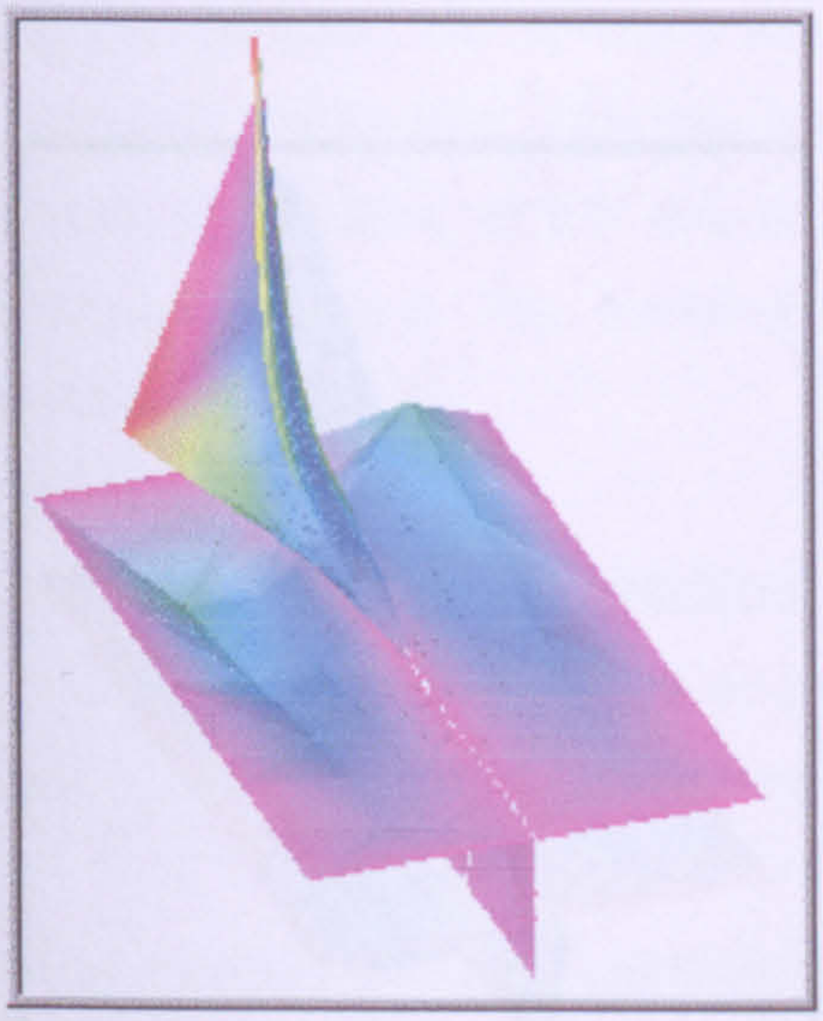

Figure 6-17 Mode#1 = 149.94 Hz

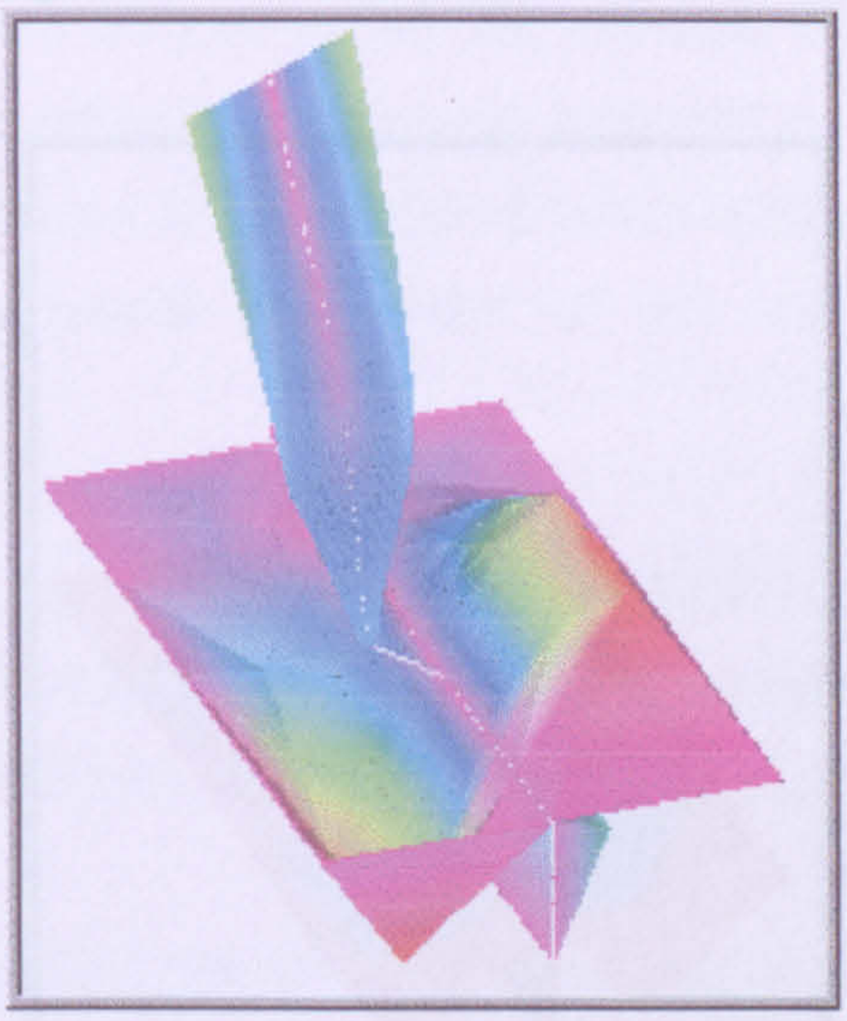

Figure 6-18 Mode#2 = 175.04 Hz

Figure 6-19 Mode#3 = 210.11 Hz

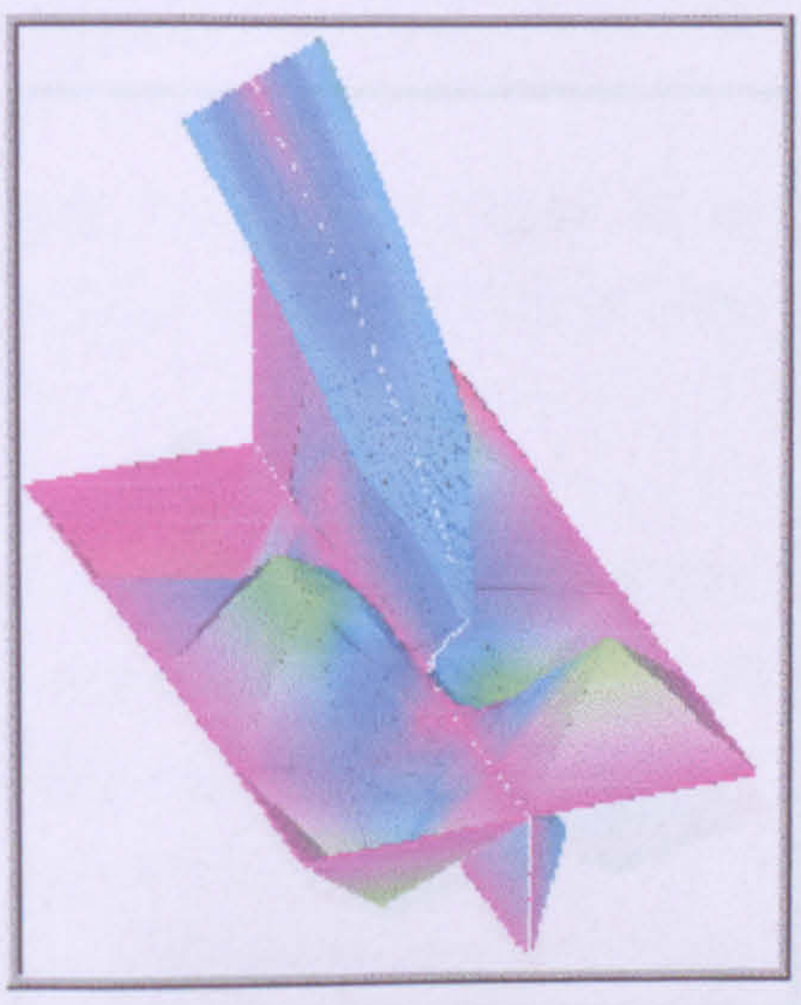

Figure 6-20 Mode#4 = 245.22 Hz

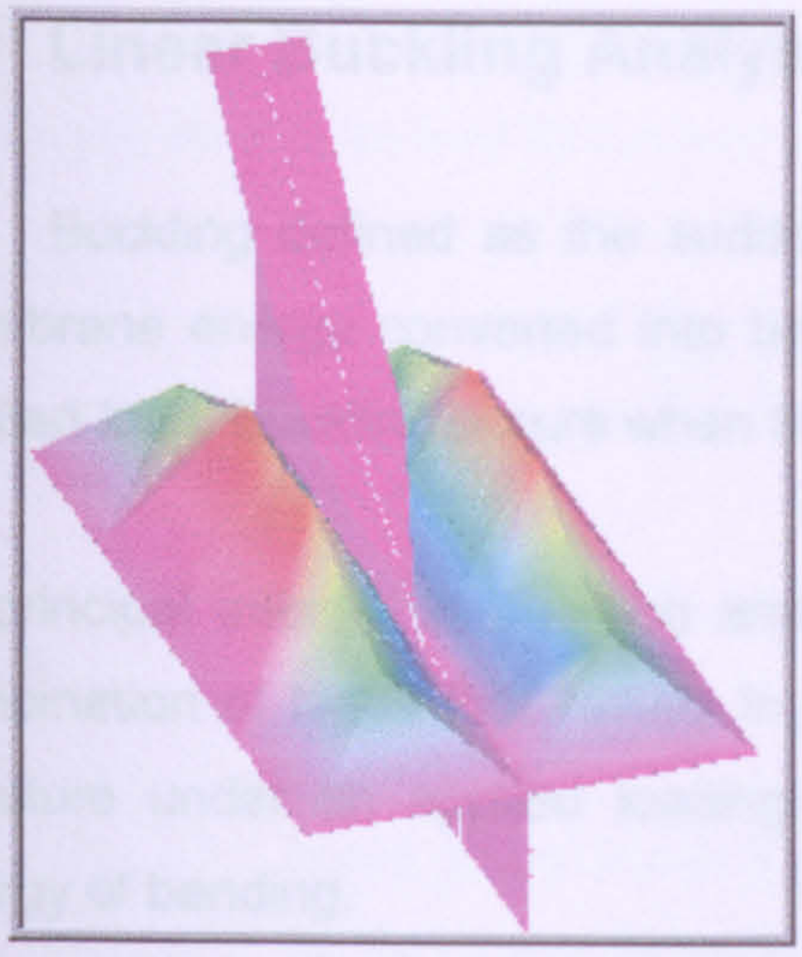

Figure 6-21 Mode#5 = 257.17 Hz

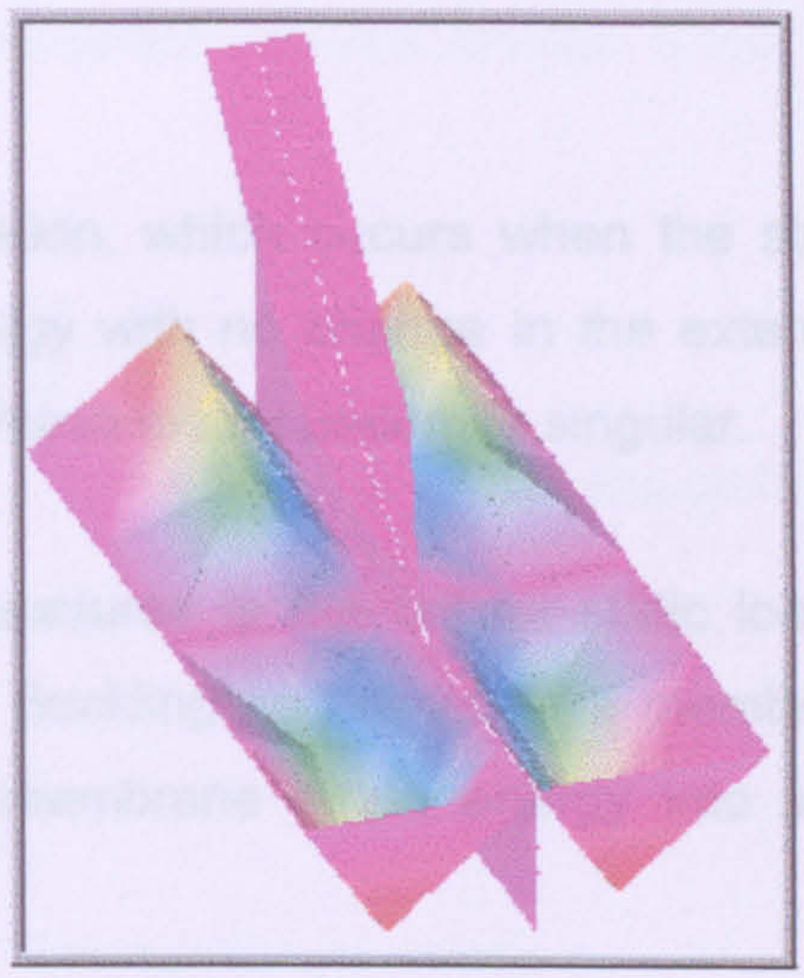

Figure 6-22 Mode#6 = 286.30 Hz

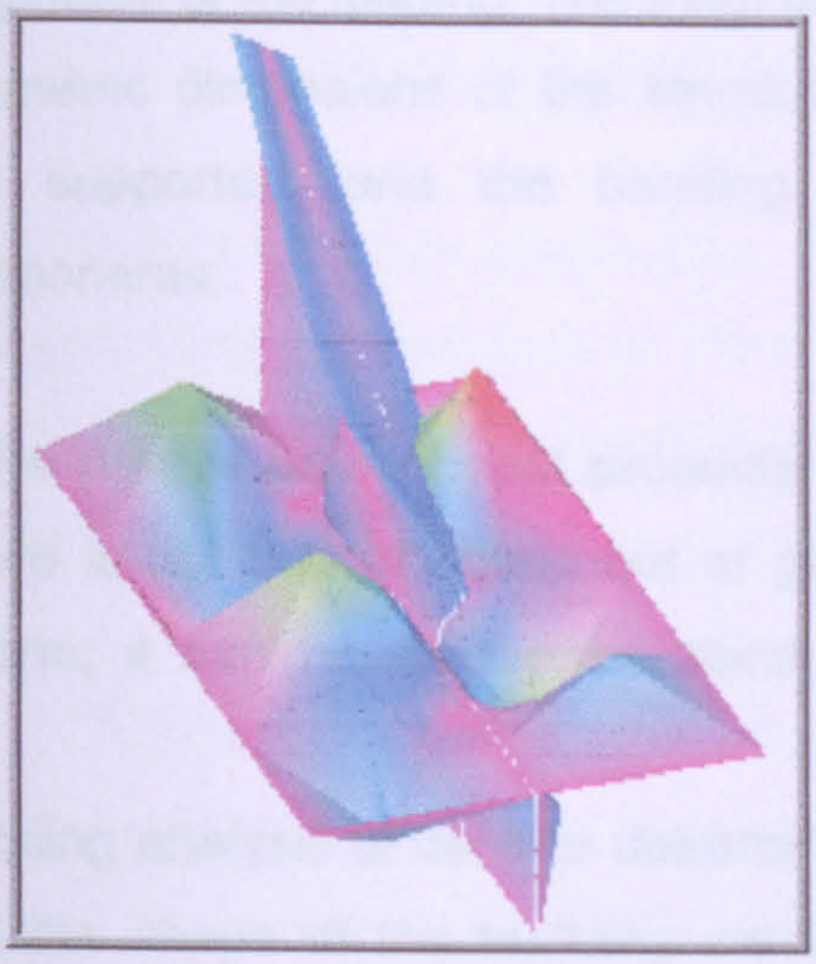

Figure 6-23 Mode#7 = 288.59 Hz

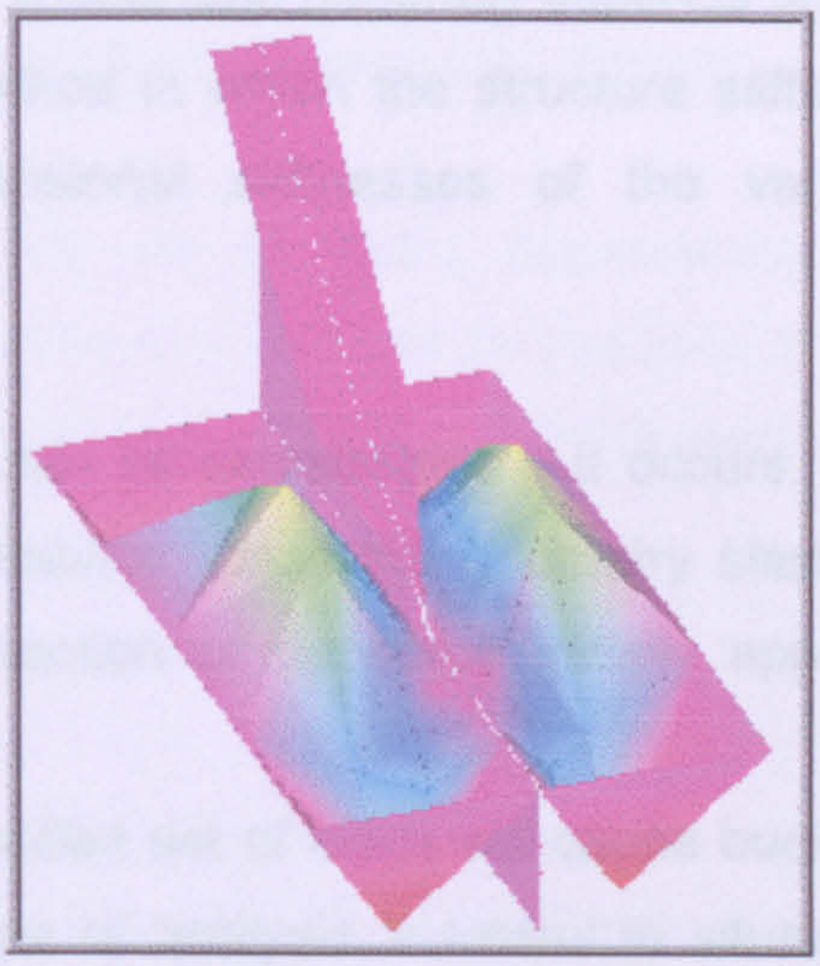

Figure 6-24 Mode#8 = 326.99 Hz

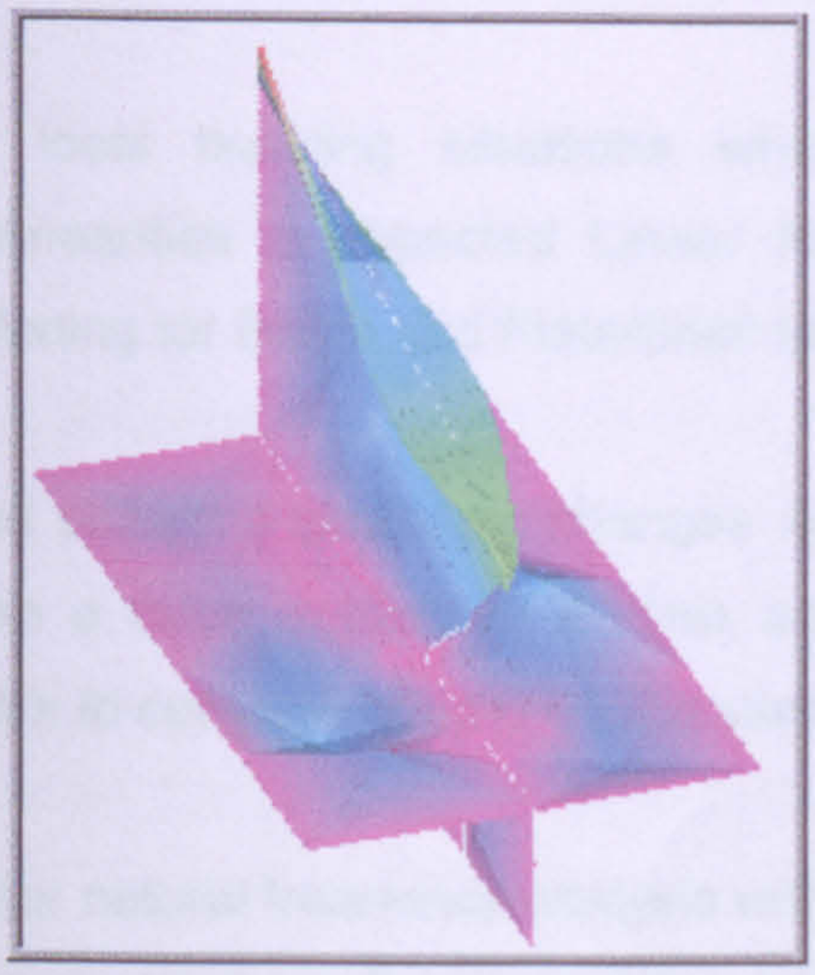

Figure 6-25 Mode#9 = 334.84 Hz

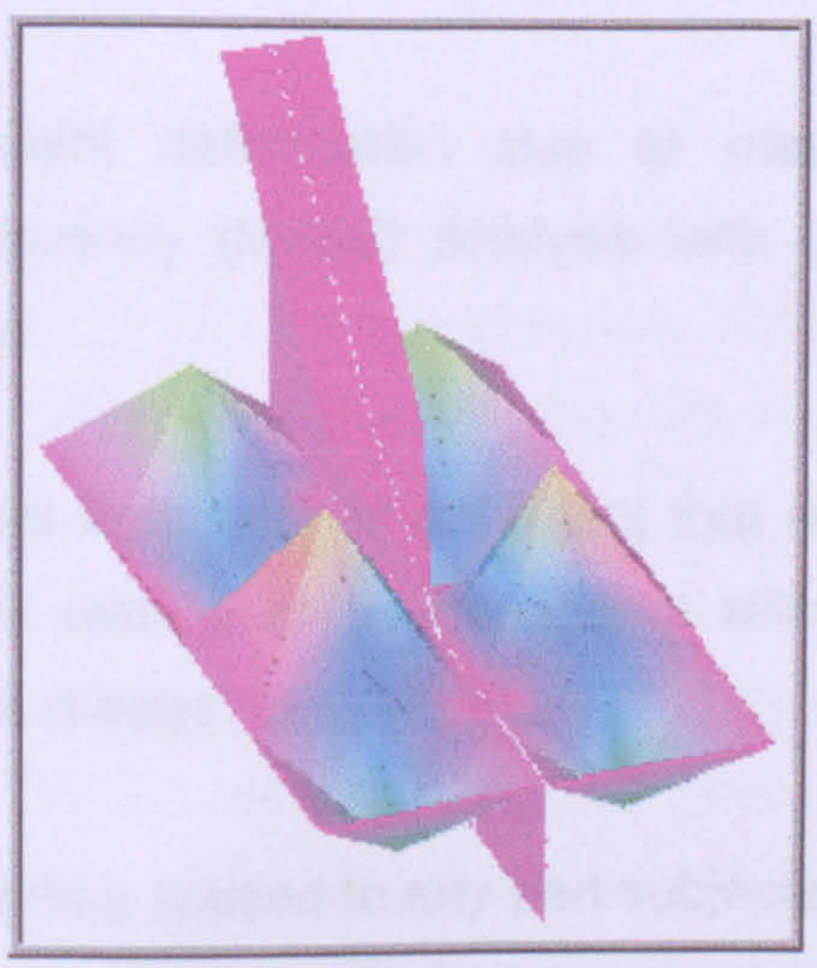

Figure 6-26 Mode#10 = 391.36 Hz

6.9 Linear Buckling Analysis

Buckling defined as the sudden deformation, which occurs when the stored membrane energy converted into bending energy with no change in the externally applied load. Buckling occurs when the total stiffness matrix becomes singular.

Of principal interest in buckling analysis of structures is the critical static load or combination of loads that results in instability. Buckling occurs when a member or structure under an applied loading converts membrane strain energy into strain energy of bending.

At this critical load, the structure will continue to deflect without an increase in the magnitude of the loading. The magnitude of the critical load generally depends on the geometric dimensions of the structure, the method in which the structure stiffened and supported, and the bending and extensional stiffnesses of the various components.

In the normal use of most products, buckling can be catastrophic if it occurs. The failure is not one of stress but of geometric stability. Once the geometry starts to deform, it can no longer withstand even a fraction of the force initially applied.

Buckling analysis is used to determine if a specified set of loads will cause buckling and the shape of the buckling mode. This type of analysis is useful in situations where an assembly subjected to an axial load or when a model undergoes edge compression. Then supports or stiffeners to prevent local buckling designed.

For local buckling situations where permanent deformation due to material nonlinearities is expected Linear Natural Frequency (Modal) Analysis with Load Stiffening for Beam and Plate/Shell Models used.

Load stiffening produces changes in the natural frequency of an object that result when a force applied to it. This analysis type uses a stress-dependent stiffness matrix to compute natural frequencies and mode shapes.

Linear natural frequency analysis with load stiffening applied to any part subjected to dynamic loading. Because natural frequencies change as applied forces change,

engineers must use load stiffening to receive accurate analysis results. It can also determine how force and frequency relate.

$$\left|[K_i]+\lambda_i[K_s][\phi_i]=0\right.$$

Equation 6-7

Where,

K_i	is the global linear stiffness matrix
K_s	Is the global differential or initial stress stiffness matrix
λ_i	are the eigenvalues that when multiplied by the applied loading gives the critical loading P_{cr}
ϕ_i	are the eigenvectors that represent the buckled mode shapes

In solving the above eigenvalue problem there are as many eigenvalues and corresponding eigenvectors as there are unconstrained degrees of freedom. Often, however, only the lowest buckling mode is of practical interest. This will *always* be the first mode extracted.

6.9.1 Buckling Analysis Module

FE package's buckling module evaluates natural frequencies and the corresponding mode shapes of a system (modal analysis). The module can also calculate the buckling loads and the associated mode shapes of eigen-value buckling problems.

Riks, E., (1986) shows that in a typical buckling analysis, the quantities computed include the critical loads at which the structure becomes unstable, and the corresponding buckling mode shapes. For eigenvalue buckling, the first few modes are of practical importance.

Modal analysis, which determines the natural frequencies and mode shapes, is an important phase in the design of many structural components. Similar to buckling, modal analysis involves the computation of eigen-values, and the solver provides many types of eigen-values extraction techniques. The following are some important features of the solver module:

- a variety of eigenvalue extraction procedures:
  - Subspace iteration,
  - Lanczos,
  - Jacobi,
  - Inverse power iteration (one pair only),
  - Guyan Reduction
- Frequency shift to calculate eigen-values in a specified range or to treat models with rigid body modes.
- Sturm sequence to check for missed modes,
- Lumped and consistent mass matrices for representing structural mass,
- In plane effects on stiffness,
- Soft-spring option to treat models with rigid body modes,
- Modal analysis of Piezoelectric Materials: calculates natural frequencies and mode shapes using Hexahedron SOLID elements to account for coupling between elastic and electric fields of piezoelectric materials.
- Non-axisymmetric mode extraction for axisymmetric models,
- Guyan Reduction:
  During design, when changes made, Guyan reduction would save significant time. The reduction enables exercising some degree of control over the extraction process, selectively ignoring those modes, which are of no or little value to a specific analysis of large complex models.
- Automatic Rigid or Hinge connection:
  Rigid or Hinge connections at the interface of incompatible solids and shell elements with mesh continuity at the interface.
- Large File management:

Partitioning of Large files (such as Stiffness Matrix file) into several drives/directories

- Spin Stiffening:
  Accounting for the large displacements effect for spinning structures

- Interface with the Nonlinear Module for Frequency and Buckling analyses (Refer to the Advanced Modules manual).

- Bonding of incompatible meshes, (similar to the one described for Static Analysis).

6.9.2 Assumptions and Limitations

The following assumptions and limitations apply to linear buckling analysis:

- The deflections must be small.

- The element stresses must be elastic.

- A minimum of five grid points per half sine wave (buckled mode shape) recommended.

- The distribution of the internal element forces due to the applied loads remains constant.

- The follower force effect is not included in the generation of differential stiffness (i.e., the directions and magnitudes of the applied forces are assumed to remain constant).

  Follower force effects included by using a NONLINEAR STATIC solution (see ***Section 6.3*** above, *Nonlinear Static Analysis*).

- The tangent stiffness term due to follower force effect is not included.

- Offsets should not be used in bar, beam, and shell elements.

6.9.3 FEM Linear Buckling Procedure

Solving a linear buckling problem follows the general procedure listed below:

- Define all desired loading: Apply static loads to the first sub-case. This sub-case treated as a static run. The applied loading will generate internal loads that used to formulate the differential stiffness or differential stiffness matrix.

- Run the buckling analysis: The second to n sub-cases must also reference an n Case Control command. Here, n is equal to the number of buckling analyses that is wanted to run. Each buckling sub-case may call out a unique eigenvalue solution.

- The differential stiffness matrix automatically generated for each element that supports differential stiffness. Elements that support differential stiffness are ROD, BAR, BEAM, QUAD, and TRIANGLE.

- Buckling loads calculation: by multiplying the eigen-values obtained in the second step by the appropriate applied loads to obtain the buckling loads for each buckling analysis.

- Each sub-case may have a different boundary condition; however, the global differential stiffness matrix based on the boundary conditions specified in the first sub-case.

6.9.4 Eigenvalue Buckling Analysis Results

The entry controls defined for the required the range and number of modes extracted. Here, the requested mode is one as shown in ***Figure 6-27***.

The eigenvalues always sorted in increasing order. Thus, the first mode is always the lowest. The eigenvalue for the first mode is equal to 1.66323, while the applied total force in load case one is equal to 71235 Newton. The lowest buckling load is then equal to:

$$P_{cr1} = \lambda_1 P_{xyz}$$

Equation 6-8

Sum of Forces P_{xyz} = 71235 N

P_{cr} = 1.66323 x 71235 N

P_{cr} = 118480.19 N

P_{cr} = 118.48 KN

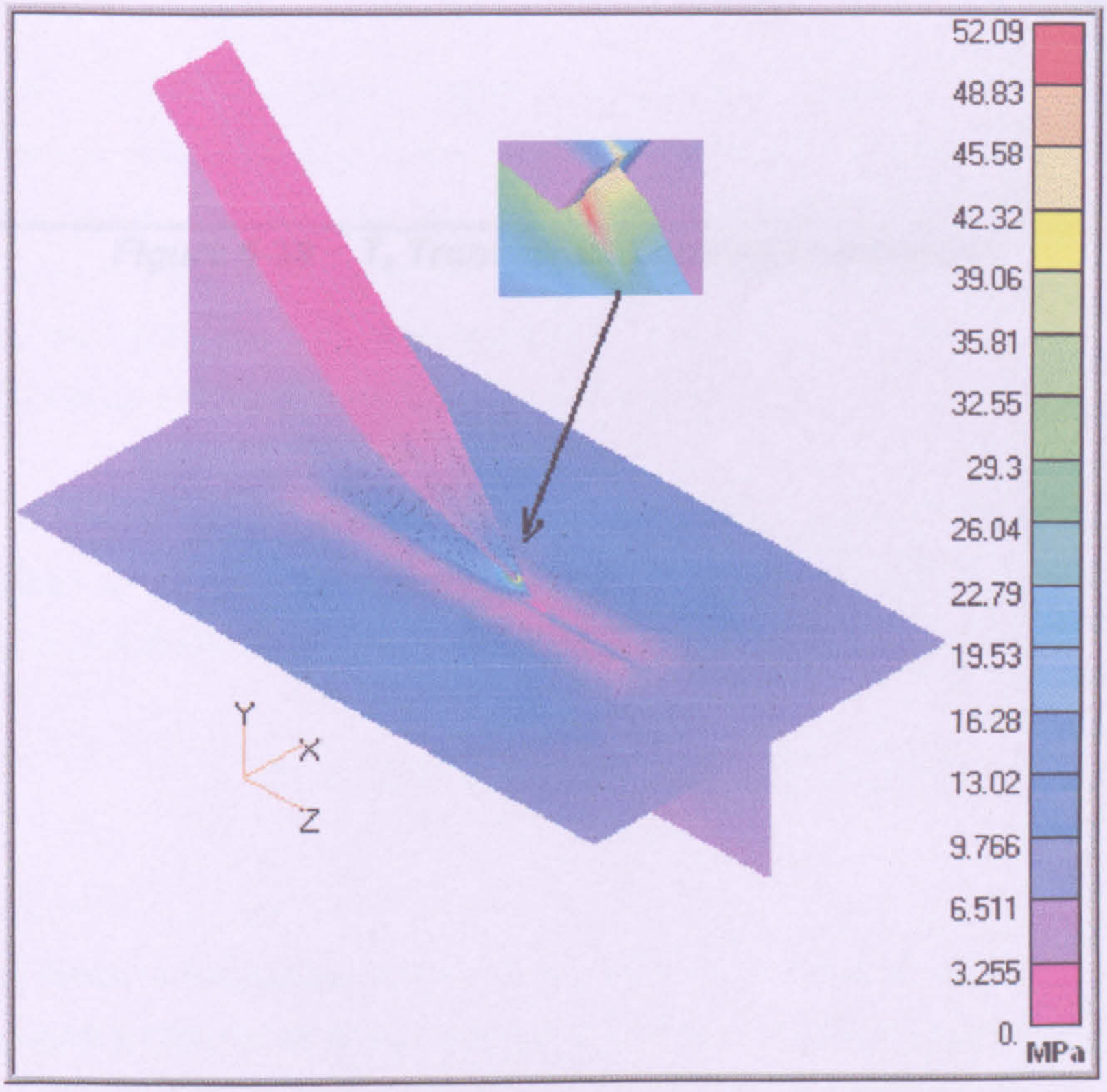

Figure 6-27 Web-Toe Buckling Analysis-Eigenvalue #1= 1.66323

As seen from T_z Translation values at ***Figure 6-28*** below, the model has a maximum deflection of 0.453mm. Since the load is less than the calculated critical load, the structure does not (snap-through) the maximum compression (deflection = 1).

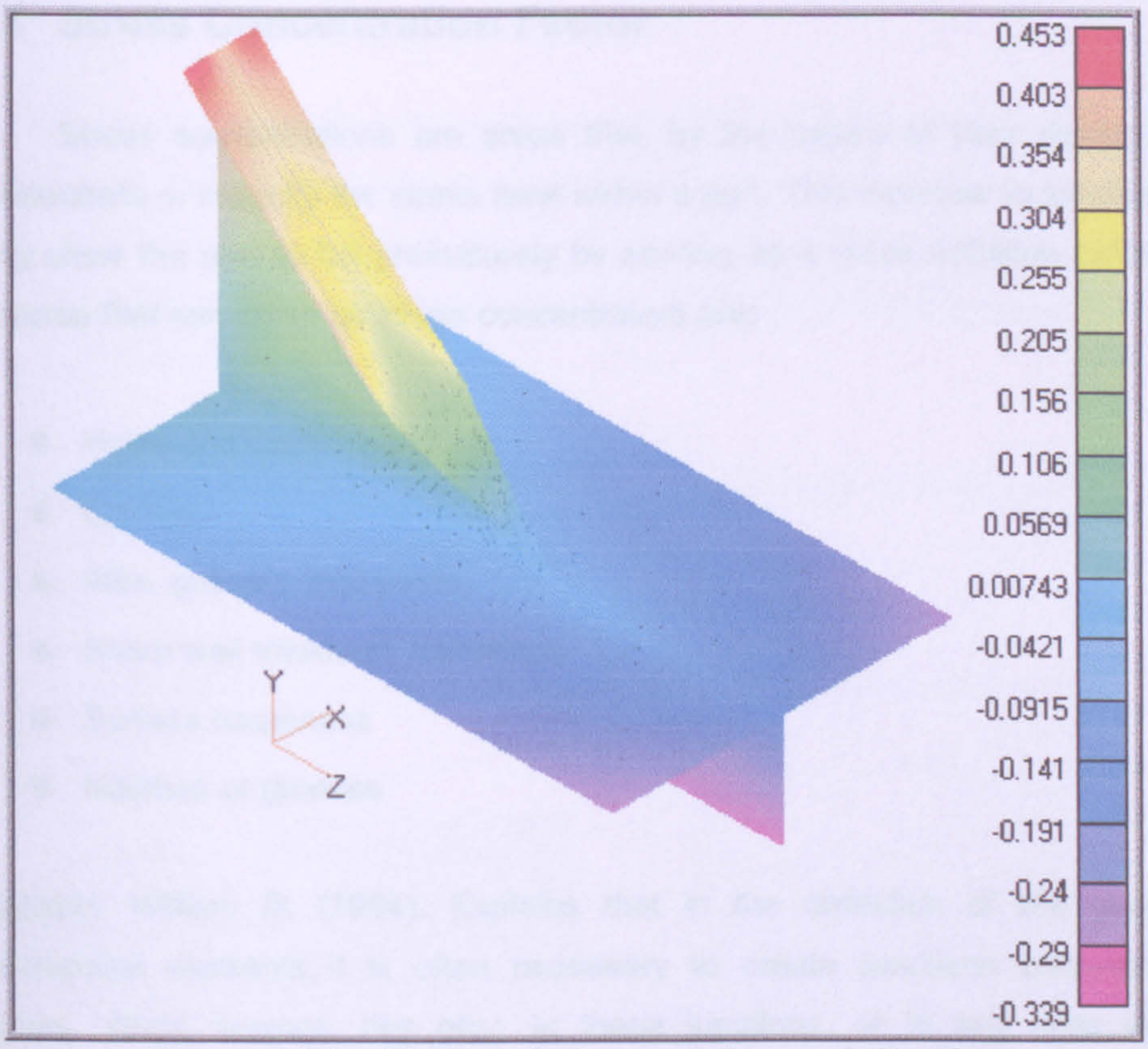

Figure 6-28 T_z Translation, maximum deflection

7. FPSO Stress Concentration Factor Evaluation

7.1 Stress Concentration Factor

Stress concentrations are areas that, by the nature of their design, tend to concentrate or magnify the stress level within a part. This increase in localized stress may allow the part to fail prematurely by serving as a crack initiation point. Design features that can serve as stress concentrators are:

- Holes and slots
- Corners
- Ribs, gussets, and posts
- Sharp wall thickness transitions
- Surface roughness
- Notches or grooves

Callister, William D, (1994). Explains that in the definition of the geometry of mechanical elements, it is often necessary to create junctions between sheets, planes, struts, trusses, ribs etc.; in these junctions, or in any area where the geometry of a part changes, there are shape transitions between regions of differing width, thickness etc. If these transitions are not sufficiently gradual, a stress concentration will arise in the area of the transition.

The extent of stress concentration in a particular junction or transition region described by the theoretical stress concentration factor K_t (also known as geometric stress concentration factor) defined as follows:

$$K_t = S_l(\text{local at transition}) / S_n(\text{nominal})$$

Equation 7-1

Those areas of the junction where the transition is not gradual will lead to a high local stress and a high value of K_t. Note here that K_t is a unit-less factor dependent only on the shape of the transition, not on any specific materials properties.

It is an excellent general practice trying to make areas of geometry transition as smooth as possible in order to avoid stress concentrations. This is particularly important when dealing with brittle materials in an application requiring dynamic fatigue loading. As such, fillets, radii and other geometry transition features made as large as feasibly possible.

The fracture of a material is dependent upon the forces that exist between the atoms. Because of the forces that exist between the atoms, a theoretical strength typically estimated to be one-tenth of the elastic modulus of the material. However, the experimentally measured fracture strengths of materials found to be 10 to 1000 times below this theoretical value.

Looking at ***Figure 7-1***, one can see a stress profile across a cross section containing an internal, elliptically shaped crack.

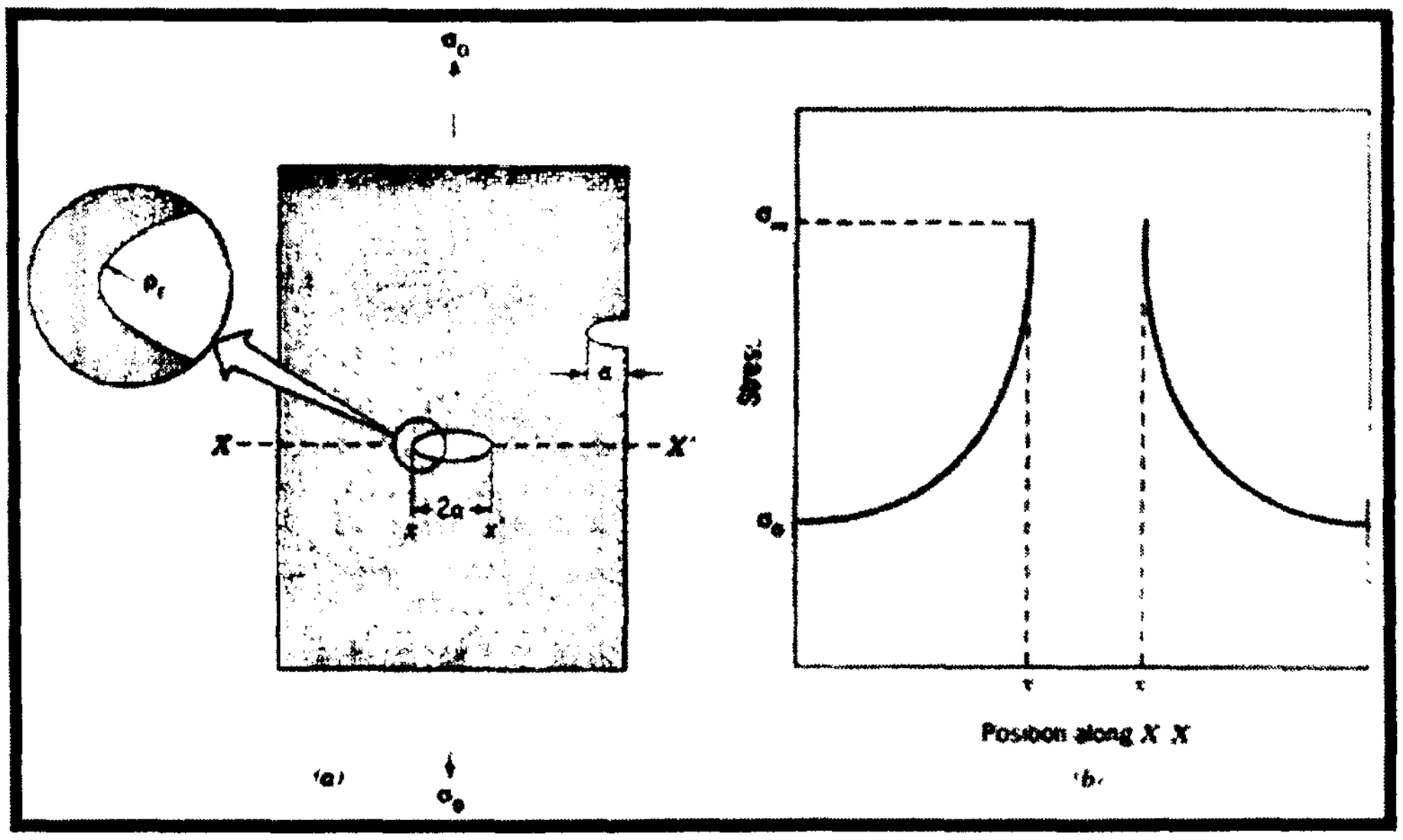

Figure 7-1 (a) The geometry of surface and internal cracks, (b) Schematic stress profile along the line X-X' in (a), demonstrating stress amplification at crack tip positions.

The discrepancy explained to exist because of the presence of small flaws or cracks found either on the surface or within the material. These flaws cause the stress surrounding the flaw amplified where the magnification is dependent upon the orientation and geometry of the flaw.

The stress is at a maximum at the crack tip and decreased to the nominal applied stress with increasing distance away from the crack. The stress is concentrated around the crack tip or flaw developing the concept of stress concentration. Stress raisers defined as the flaws having the ability to amplify an applied stress in the locale.

7.1.1 Determination of the Maximum Stress at the Crack Tip

If the crack assumed to have an elliptical shape and is oriented with its long axis perpendicular to the applied stress, the maximum stress, ***Equation 7-2*** can approximate σ_m at the crack tip, *Callister, William D*, (1994).

$$\sigma_m = 2\sigma_0\left(\frac{a}{\rho_t}\right)^{\frac{1}{2}}$$

Equation 7-2

Equation 7-2 Determines the maximum stress surrounding a crack tip. The magnitude of the nominal applied tensile stress is σ_o; the radius of the curvature of the crack tip is ρ_t and ***a*** represents the length of a surface crack, or half the length of an internal crack.

7.1.2 Determination of Stress Concentration Factor

The ratio of the maximum stress and the nominal applied tensile stress is denoted as the stress concentration factor, K_t, where K_t calculated by ***Equation 7-3***. The *stress concentration factor* is a simple measure of the degree to which an external stress amplified at the tip of a small crack; where σ_m is given by ***Equation 7-2*** above.

$$K_t = \frac{\sigma_m}{\sigma_0} = 2\left(\frac{a}{\rho_t}\right)^{\frac{1}{2}}$$

Equation 7-3

7.1.3 Stress Concentration Considerations

It is important to point out that stress amplification not only occurs on a microscopic level (e.g. small flaws or cracks,) but can also occur on the macroscopic level in the case of sharp corners, holes, fillets, and notches. Stress raisers are typically more destructive in brittle materials.

Ductile materials have the ability to deform plastically in the region surrounding the stress raisers, which in turn evenly distributes the stress load around the flaw.

The maximum SCF results in a value less than that found for the theoretical value. Since brittle materials cannot plastically deform, the stress raisers will create the theoretical stress concentration situation.

7.2 SCF Using Finite Element Analysis

Critical stress concentration areas for an FPSO structure shown in ***Figure 7-2*** are generally located at points of sudden geometric change and structural connection areas as shown, the stress distribution and some critical stress areas (shown by circles) for a transverse web frame.

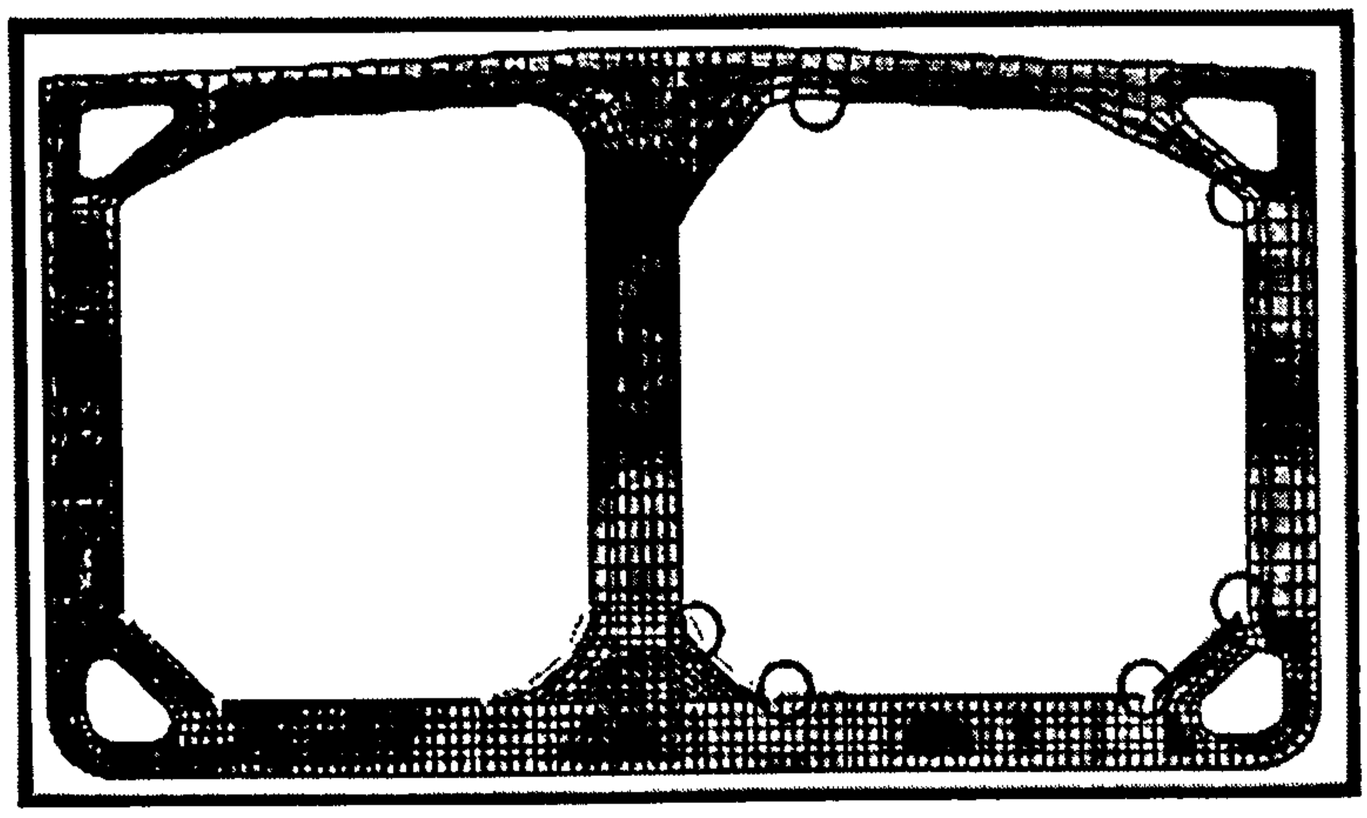

Figure 7-2 Critical Stress Areas for Transverse Web Frame

7.2.1 Finite Element Model Mesh Considerations

When FE-derived stresses used in a fatigue analysis; extra care taken to ensure they provide an accurate representation of the stress state at fatigue-sensitive locations. In practice, it is good to avoid geometric discontinuities; shape functions cannot reasonably approximate the displacement and stress fields in regions of discontinuity such as sharp corners. There can be no stress convergence at such features, and nothing gained by refining the mesh.

In defect-free components, cracks normally initiate from free surfaces, in particular corners and edges. In many cases, quadratic elements may be preferred to linear ones because the higher-order shape functions are better at extrapolating stresses to the nodes. A high level of accuracy is necessary only at the critical locations; the sole requirement of other parts of the model is that they transmit loads correctly to these parts i.e., they have the correct stiffness. The real criterion is accurate local stress in the critical regions.

Components modelled with shells may use element centroid or nodal results. If grid point stresses are used, care taken to ensure that the averaging process carried out with regard to coordinate systems and to whether results taken from top or bottom surfaces. Shells used only where stress fields can reasonably represented by shell elements; i.e., the scale of geometric features should be large compared to the thickness of the shells.

7.2.2 Finite Element Modelling and Hot Spot Stress

Due to the nature of the stress field at a hot spot region, there are questions on how to establish the hot spot stress, ***Figure 7-3***. For FPSO's structural joints, the notch effect due to the weld is included in the S-N curve and the hot spot stress derived by an extrapolation of the geometric stress to the weld toe as indicated in ***Figure 7-3***. The figure shows that the stress used as basis for such an extrapolation should be outside that affected by the weld notch, but close enough to pick up the geometric stress. As explained in all of the following references Yagi, J.; Machida, S.; Tomita, Y.; Matoba, M.; Kawasaki, T. (1991), Almar-Næss, A. (1985) , and Fricke, W. and Bogdan, R. (2001).

Definition of stresses used in the Classification Note is as follows:

- Nominal stresses are those derived from beam models or from coarse mesh FEM models. Stress concentrations resulting from the gross shape of the structure are included in the nominal stress.

- Geometric (hot spot) stresses include nominal stresses and stresses due to structural discontinuities and presence of attachments, but excluding stresses due to presence of welds. Stresses derived from fine mesh FEM models are geometric stresses. Effects caused by fabrication imperfections as e.g. misalignment of structural parts, are, however, normally not included in FEM analyses, and must be separately accounted for. The greatest value of the extrapolation to the weld toe of the geometric stress distribution immediately outside the region affected by the geometry of the weld, is commonly denoted hot spot stress.

- Notch stresses are the total stresses at the weld toe (hot spot location) and include the geometric stresses and the stresses due to the presence of the weld. The notch stress calculated by multiplying the hot spot stress by a stress concentration factor, or more precisely the theoretical notch factor, K_w. FEM may be used to determine the notch stress. However, because of the small notch radius and the steep stress gradient at a weld, a very fine mesh needed.

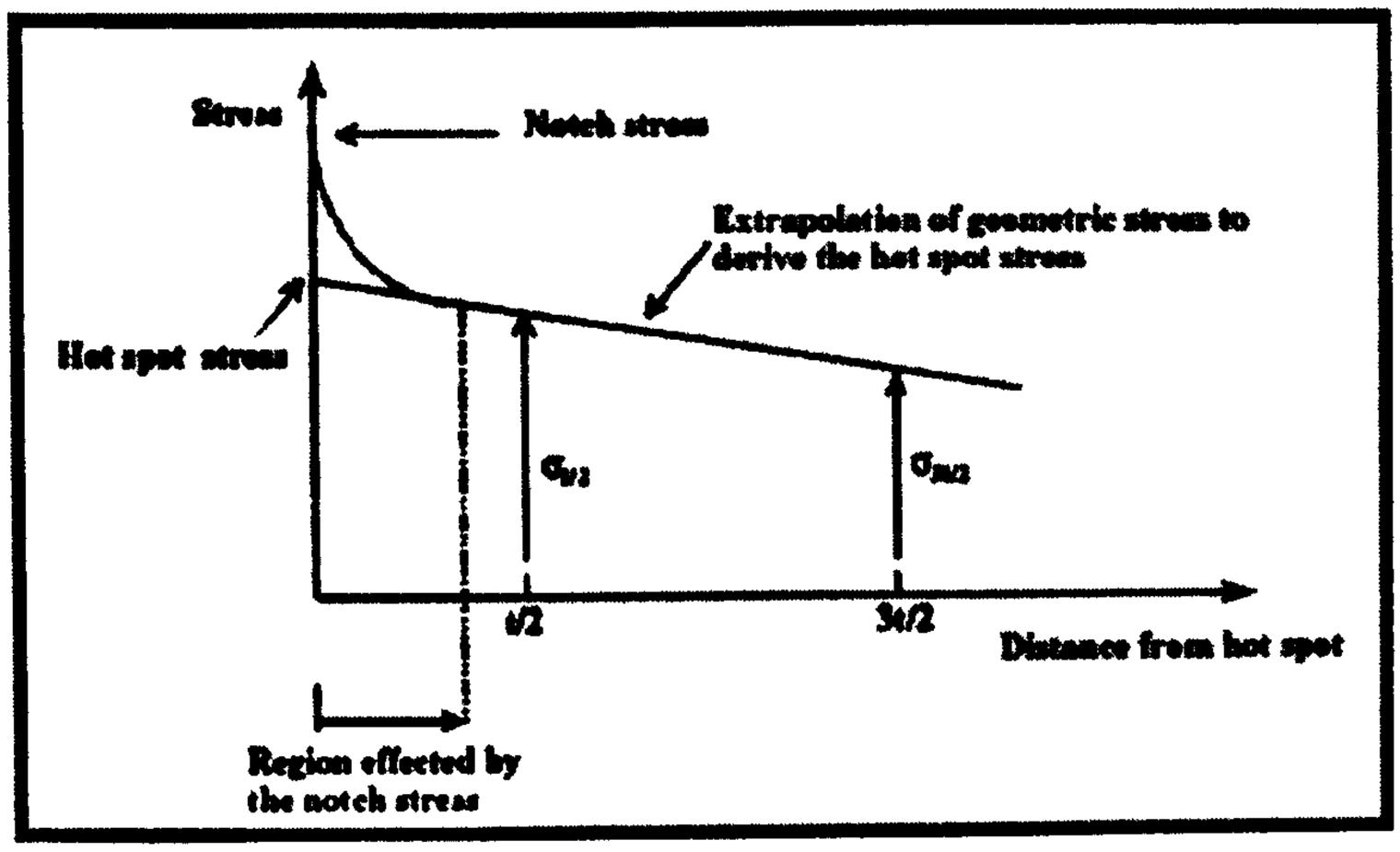

Figure 7-3 Stress distribution away from weld toe (Fricke 2001)

There are currently three different methods for derivation of hot spot stress (geometric stress) presented in the following:

- Linear extrapolation of stresses to the weld toe from stress at distances 0.4t and t from the toe (t = plate thickness); this method is recommended by the International Institute of Welding (IIW).

- Linear extrapolation of stresses to the weld toe from stress at distances 0.5t and 1.5t from the toe; favoured by some Classification Societies, in view of its greater simplicity, the use of the stress at a single point close to the weld toe, namely 0.5t, is of interest. Some of the Classification Societies, reference ***Figure 7-4*** below, use this method as discussed in more detail by Fricke (2001) due to its applicability to shell elements in FEMA.

- Stress at a distances 0.5t from the weld toe. (No extrapolation); for analysis by shell elements, the distance to the stress read out points is measured from the intersection lines, as the weld is not normally included in the model. For analysis by solid elements, the distance to the stress readout points measured from the weld toe.

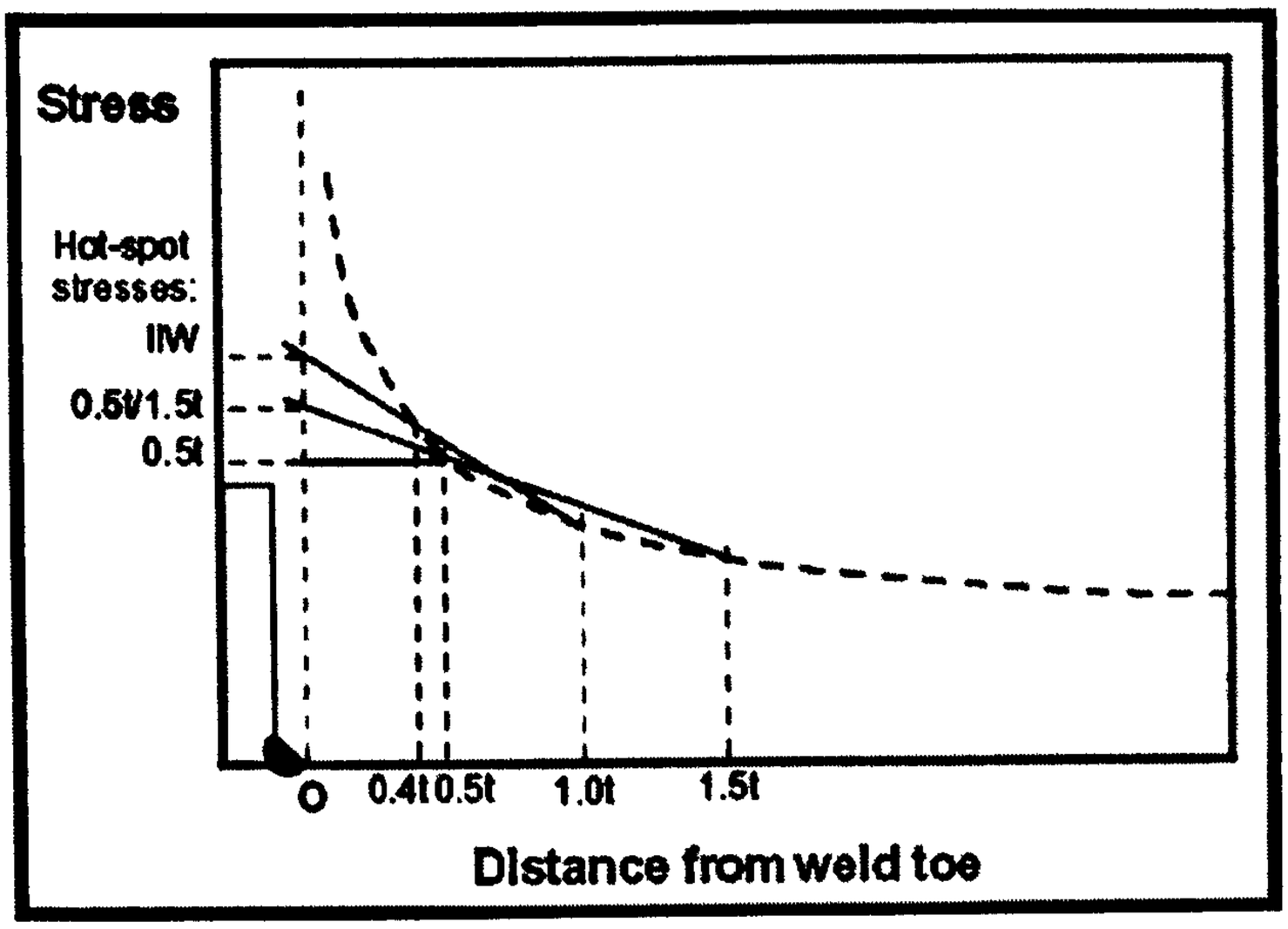

Figure 7-4 Three definitions of hot-spot stress considered in present evaluation

Note that the finite element modelling might influence the calculated stress at the hot spot region. Parameters affecting this are:

- Type of elements used,
- Size of elements at the hot spot region,
- How the stresses derived from the analysis (Gaussian stress, nodal stress etc.) These items also investigated in this project.

7.3 Stress Concentration Factors Determination Using FEA

It is required that SCFs be used to modify the nominal stress range, in the case of welded connections in complex structures. Selection of appropriate S-N data appears to be rather straightforward with respect to "standard details" or other similar reference.

The most obvious deficiency of the process is that one needs to have a definitive and consistent basis to obtain the SCF. There are reference books, which indicate that based on the theory of elasticity, the SCF to apply. However, when the SCF computed using the finite element analysis techniques, the SCF obtained can be quite variable depending on the mesh size.

This general description of the stress distribution is again inconclusive because one does not know in advance and with certainty the distances from the weld toe to where the indicated changes of slope for the stress gradient occur. For this reason, definite rules need to be established to determine the slopes and with this knowledge, criteria established to be used to find the stress at the weld toe which should be used in the fatigue assessment.

In this regard, approaches used to find the stress at the weld toe well established by the class societies, which reflect methods of structural idealization.

From detailed finite element analysis of structures, it may be difficult to evaluate what as "nominal stress". In most cases, it may therefore be more convenient to use an alternative approach for calculation of fatigue damage when local stresses obtained from finite element analysis.

It is realised that it is difficult to calculate the notch stress at a weld due to a significant scatter in local weld geometry and different types of imperfections. This scatter normally more efficiently accounted for by use of an appropriate S-N curve. In

this respect, should also mention that the weld toe region modelled with a radius in order to obtain reliable results for the notch stress.

If a corner detail with zero radiuses modelled, the calculated stress will approach infinity as the element size decreased to zero. The modelling of a relevant radius requires a very fine element, increasing the size of the computer model. In addition, a proper radius used for the analysis will likely be a matter for discussion. Hence, for design analysis a simplified numerical procedure used in order to reduce the demand for large fine mesh models for the calculation of SCF factors:

- The stress concentration or the notch factor due to the weld itself is included in the S-N curve used. The stress concentration due to the weld itself, K_w factor, may be based on standard values from Classification Societies rules or direct finite element calculations with very fine mesh of solid elements (weld radius has to be modelled)

- The stress concentration due to the geometry effect of the actual detail is calculated by means of a fine mesh model using shell elements (or solid elements), resulting in a geometric SCF factor K_g.

Iwahashi, Y. et al., (1998); emphasise that the aim of the finite element analysis is normally not to calculate directly the notch stress at a detail. Nevertheless, to calculate the geometric stress distribution in the region of the hot spot such that these stresses can be used either directly in the fatigue assessment of given details or as a basis for derivation of stress concentration factors.

This procedure denoted the hot spot method. It is important to have a continuous and not too steep, change in the density of the element mesh in the areas where the hot spot stresses are to be analysed. The geometry of the elements should be evaluated carefully in order to avoid errors due to deformed elements (*for example corner angles between 60 degrees and 120 degrees and length/breadth ratio less than 5*).

The size of the model should be so large that the calculated results not significantly affected by assumptions made for boundary conditions and application of loads. Thus, the main emphasis of the finite element analysis is to make a model that will give stresses with sufficient accuracy at a region outside that affected by the weld.

The model should have a fine mesh for extrapolation of stresses back to the weld toe in order to ensure a sufficiently accurate calculation of SCF.

FEM stress concentration models are generally very sensitive to element type and mesh size. By decreasing the element size, the FEM stresses at discontinuities will approach infinity. It is therefore necessary to set a lower bound for element size and use an extrapolation procedure to the hot spot to have a uniform basis for comparison of results from different computer programs and users.

On the other hand, in order to pick up the geometric stress increase properly, it is important that the stress reference points in 0.5t and 1.5t (see ***Figure 7-8*** below) be not inside the same element. This implies that element sizes of the order of the plate thickness used for the modelling.

If solid modelling used, the element size in way of the hot spot may reduced to half the plate thickness; in case the overall geometry of the weld is included in the model representation

Element stresses normally derived at the Gaussian integration points. Depending on element type, it may be necessary to perform several extrapolations in order to determine the stress at the location representing the weld toe. In order to preserve the information of the direction of principal stresses at the hot spot, component stresses used for the extrapolation.

When shell elements used for the modelling and the overall geometry of the weld is not included in the model, the extrapolation performed to the element intersection lines. If the (overall) weld geometry is included in the model, the extrapolation related to the weld toe. The stresses first extrapolated from the Gaussian integration points to the plate surface. A further extrapolation to the line A - B as shown in ***Figure 7-5*** then conducted.

The final extrapolation of component stresses carried out as a linear extrapolation of surface stresses along line A - B at a distance 0.5t and 1.5t from either the weld toe, or alternatively the element intersection line (where t denotes the plate thickness). Having determined the extrapolated stress components at the hot spot, the principal stresses calculated and used for the fatigue evaluation.

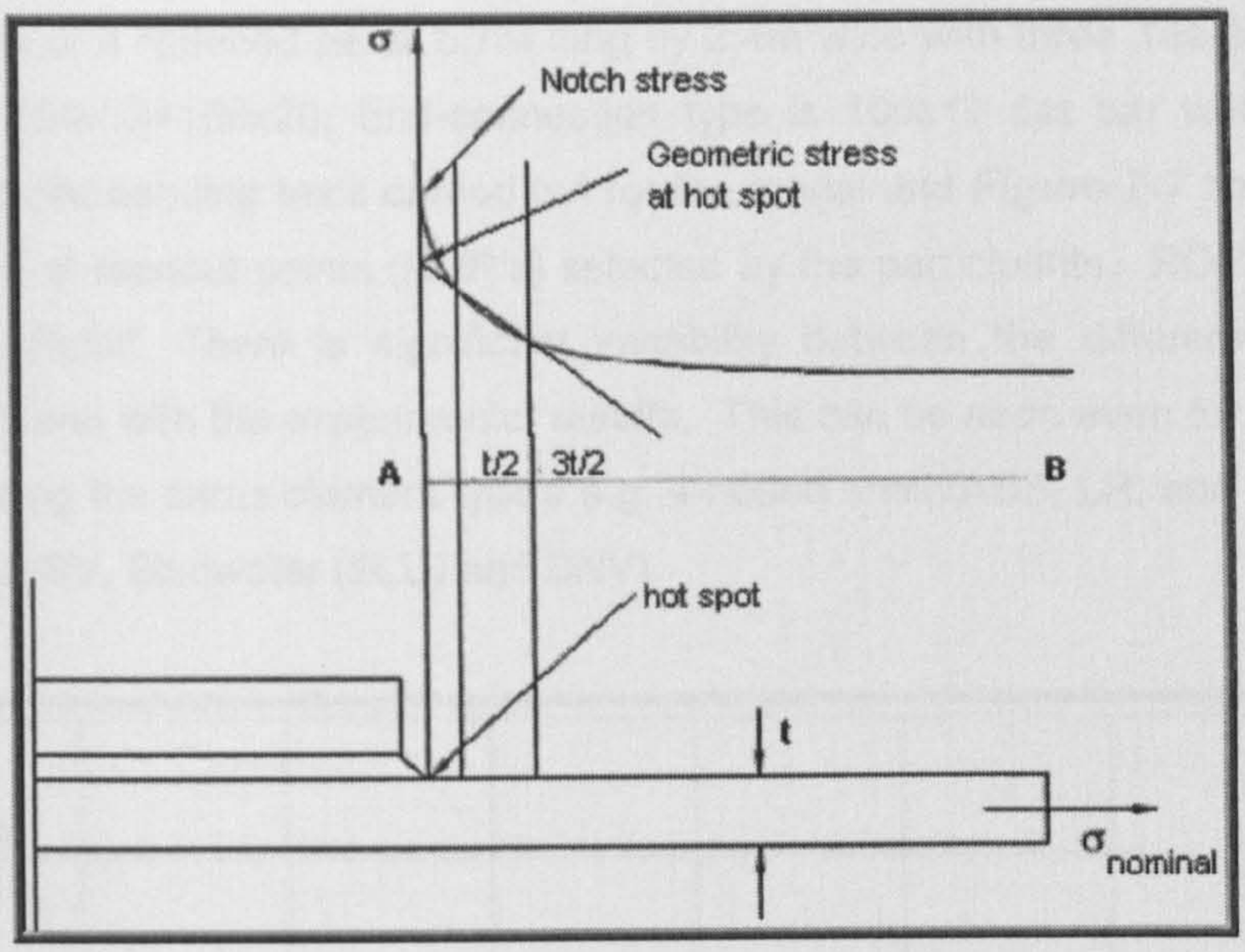

Figure 7-5 Stress Distribution and Extrapolation of Stresses

A great variability exists in selecting the type of stress and in evaluating; the stresses at the desired locations still exist in the industry today. It should be kept in mind that also the measured stresses contain some uncertainties, which was revealed in the tests by scattering strains obtained from different comparable locations and test models as given by I. Lotsberg, D. Ø. Askheim and T. Haavi, (2001). The joint industry project conducted with partners from most of classification societies, builders and designers to try to obtain a more definitive procedure for the hot spot stress approach. As part of that project, five different structural details where analyzed by the different classification societies using their respective approach. These analyses accompanied by laboratory fatigue testing as illustrated by ***Figure 7-6***.

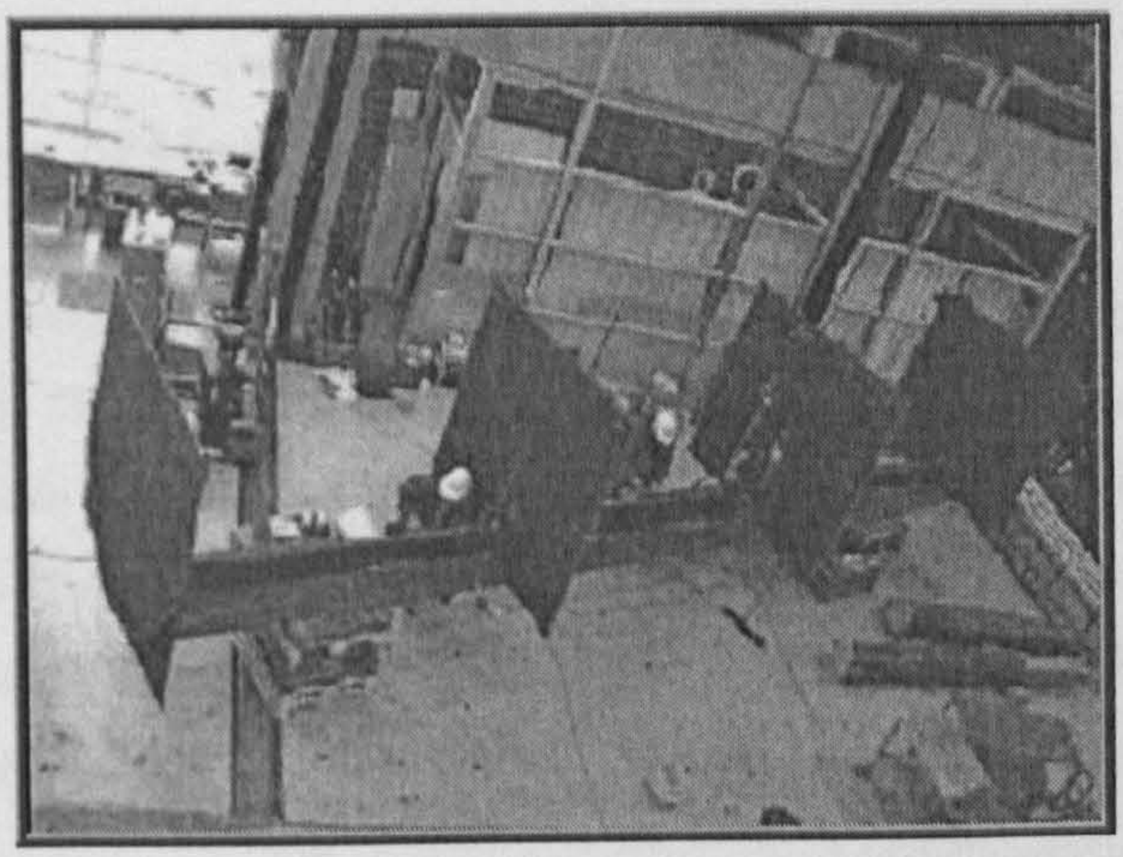

Figure 7-6 Full scale fatigue test specimen

A test model of a stiffened panel 5.7m long by 2.4m wide with three Tee stiffeners of dimension 350x12+150x20; End-connection type is 100x12 flat bar web stiffener, where a 3-point bending tests carried out for the model and ***Figure 7-7*** below shows the stresses at readout-points (ROP's) selected by the participants. ROP stands for "Read Out Point". There is significant variability between the different modelling approaches and with the experimental results. This can be seen even for the results obtained using the same element type's e.g. 4-noded shell (ABS, LR, and BV) and 8-noded shell (BV, Bluewater (BLU) and DNV).

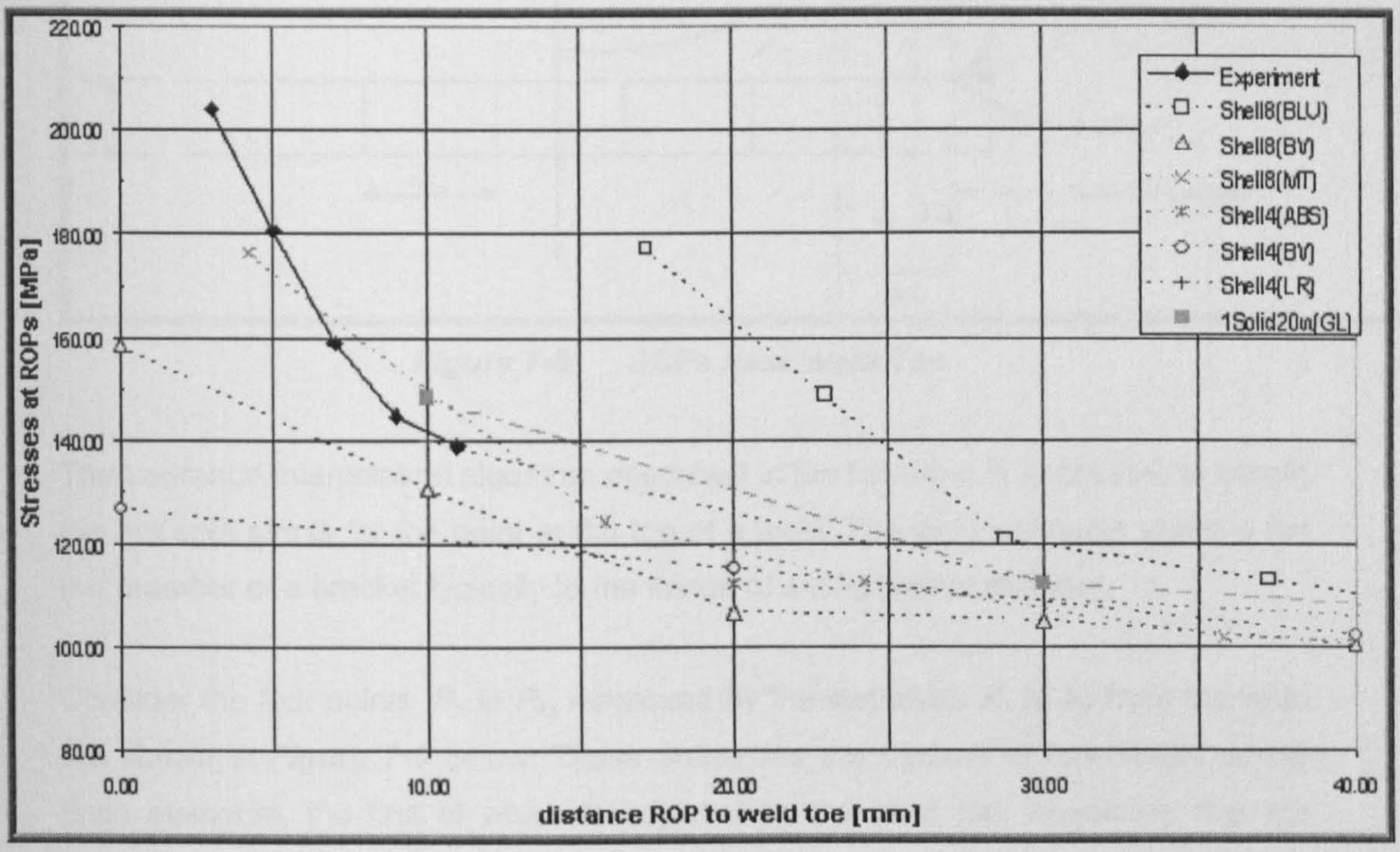

Figure 7-7 Different Comparable Locations and Test Models for SCF Evaluation

7.4 Evaluation of Hot Spot Stresses using FE Analysis

In the fine mesh finite element analysis approach, one needs to define the element size used. This is an area of uncertainty because both can improperly affect the calculated stress distribution the employed mesh size and the uniformity of the mesh adjacent to the weld toe. Therefore, it is necessary to use an established method as the one given below, with fine mesh model adjacent to the weld toe based on the actual plate thickness in size.

Weld hot spot stress can be determined from linear extrapolation to the weld toe, using calculated stresses at 0.5t and 1.5t from weld toe as shown in ***Figure 7-8***. Defining stresses are the principal centroidal stresses in the elements.

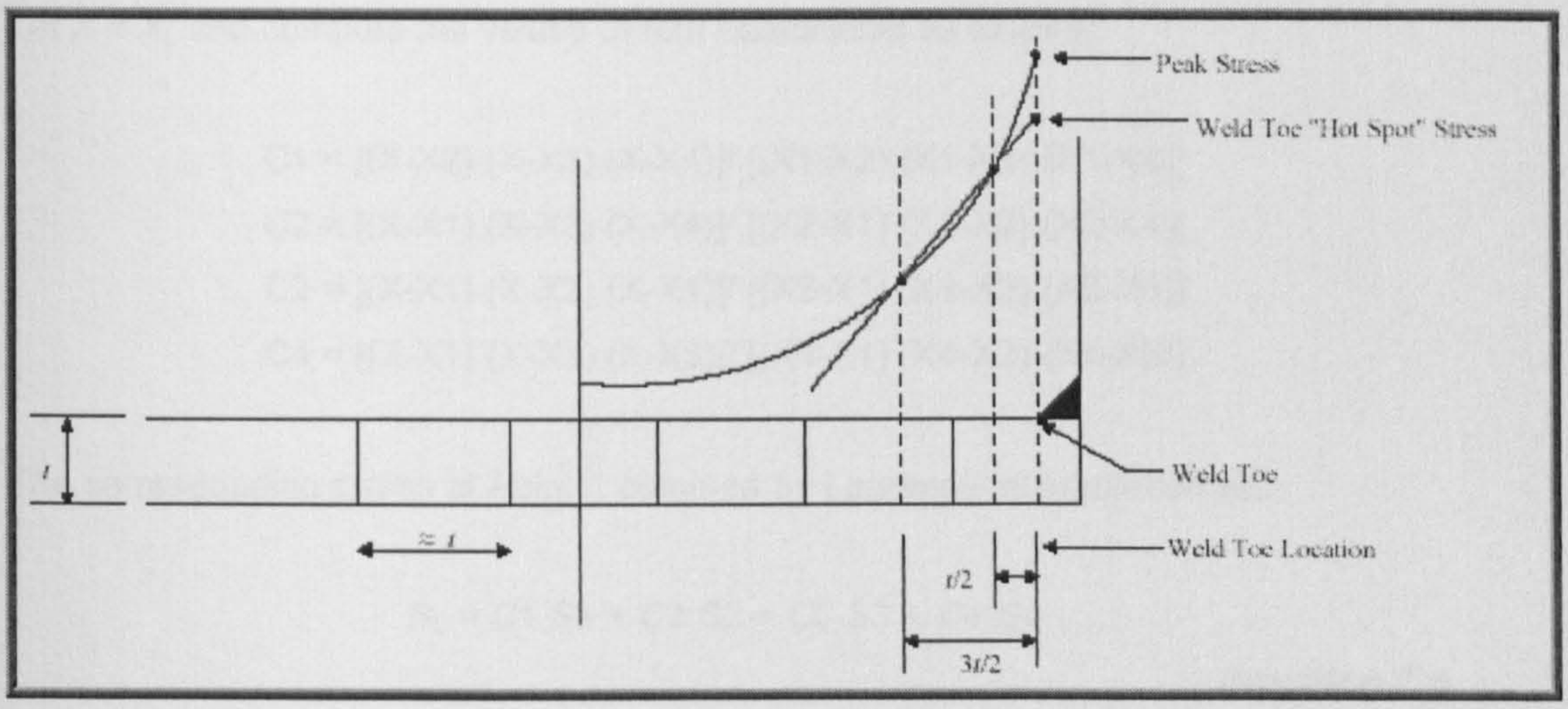

Figure 7-8 SCFs near Weld Toe

The Lagrange interpolation algorithm described in the following is applicable to obtain the hot spot stress for the point at the toe of a weld. The weld connects either a flat bar member or a bracket typically to the flange of a longitudinal stiffener.

Consider the four points, P_1 to P_4, measured by the distances X_1 to X_4 from the weld toe shown in ***Figure 7-9*** below. These points are the centres of four neighbouring finite elements, the first of which is adjacent to the weld toe. Assuming that the applicable components of the principal stresses S_i, at P_i have been determined from the FEM analysis, the "hot spot" stress, and the stress at the weld toe, determined by the following procedure:

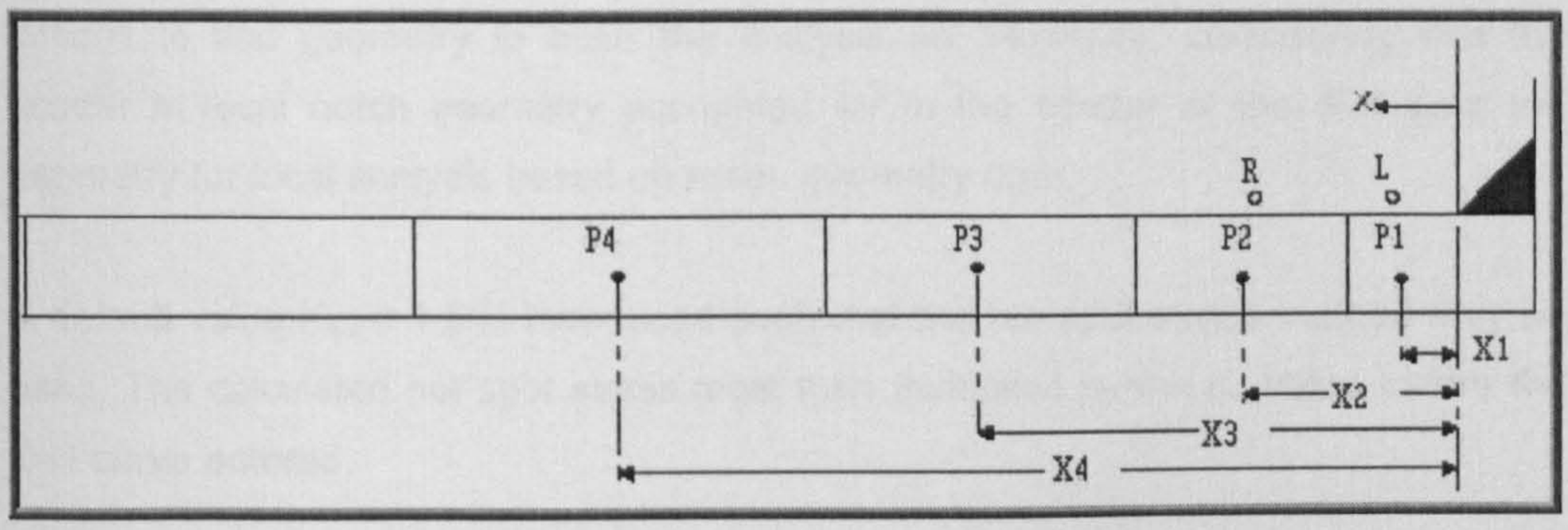

Figure 7-9 Nominal Stress Calculations

Select two points, L and R, such that points L and R are situated at distances 0.5t and 1.5t from the weld toe; i.e., X_L = 0.5t, X_R = 1.5t, as shown in ***Table 7-1***.

Where t denotes the thickness of the member to which elements 1 to 4 belong.
Let $X = X_L$ and compute the values of four coefficients as follows:

$$C1 = [(X-X2)\ (X-X3)\ (X-X4)]/\ [(X1-X2)\ (X1-X3)\ (X1-X4)]$$
$$C2 = [(X-X1)\ (X-X3)\ (X-X4)]/\ [(X2-X1)\ (X2-X3)\ (X2-X4)]$$
$$C3 = [(X-X1)\ (X-X2)\ (X-X4)]/\ [(X3-X1)\ (X3-X2)\ (X3-X4)]$$
$$C4 = [(X-X1)\ (X-X2)\ (X-X3)]/\ [(X4-X1)\ (X4-X2)\ (X4-X3)]$$

The corresponding stress at Point L obtained by Lagrange interpolation as:

$$S_L = C1\ S1 + C2\ S2 + C3\ S3 + C4\ S4$$

Equation 7-4

Let $X = X_R$ and repeat the steps to determine four new coefficients. The stress at point R can be interpolated likewise, i.e.

$$S_R = C1\ S1 + C2\ S2 + C3\ S3 + C4\ S4$$

Equation 7-5

The hot spot stress, S_0, given by:

$$S_0 = (3S_L - S_R)/2$$

Equation 7-6

The geometry of the local notch at a weld varies along the weld profile, and it may be difficult to find geometry to base the analysis on. However, considering that the scatter in local notch geometry accounted for in the scatter of the S-N data the geometry for local analysis based on mean geometry data.

A default value K_w, = 1.5 is introduced such that the hot spot stress method may be used. The calculated hot spot stress must then multiplied by the K_w value before the S-N curve entered.

Thickness=	**15**		S1 =	**56**	MPa
L=t/2	7.5		S2 =	**52**	MPa
R=3t/2	22.5		S3 =	**50**	MPa
			S4 =	**47**	MPa
X1=t	15		**Max. Stress in y Direction =**	**15**	MPa
X2=2*t	30		**Max. Stress in x Direction =**	**40**	MPa
X3=3*t	45				
X4=4*t	60				
CL1 =	2.1875		CR1 =	0.3125	
CL2 =	-2.1875		CR2 =	0.9375	
CL3 =	1.3125		CR3 =	-0.3125	
CL4 =	-0.3125		CR4 =	0.0625	
SL =	59.6875	MPa			
SR =	53.5625	MPa			
Hot Spot S =	**62.75**	MPa			
Structural Stresses Factor Kg-y =			4.183333		
Structural Stresses Factor Kg-x =			1.566875		
Bending SCF		(DNV) SCF (K) = Kg*Kw		**6.275**	
		Where Kw = 1.5			
Axial SCF				**2.353**	

Table 7-1 SCF Calculation

The following ***Figure 7-10*** illustrates the results of the Finite Element Analysis nominal stresses with respect to distance away from the weld toe.

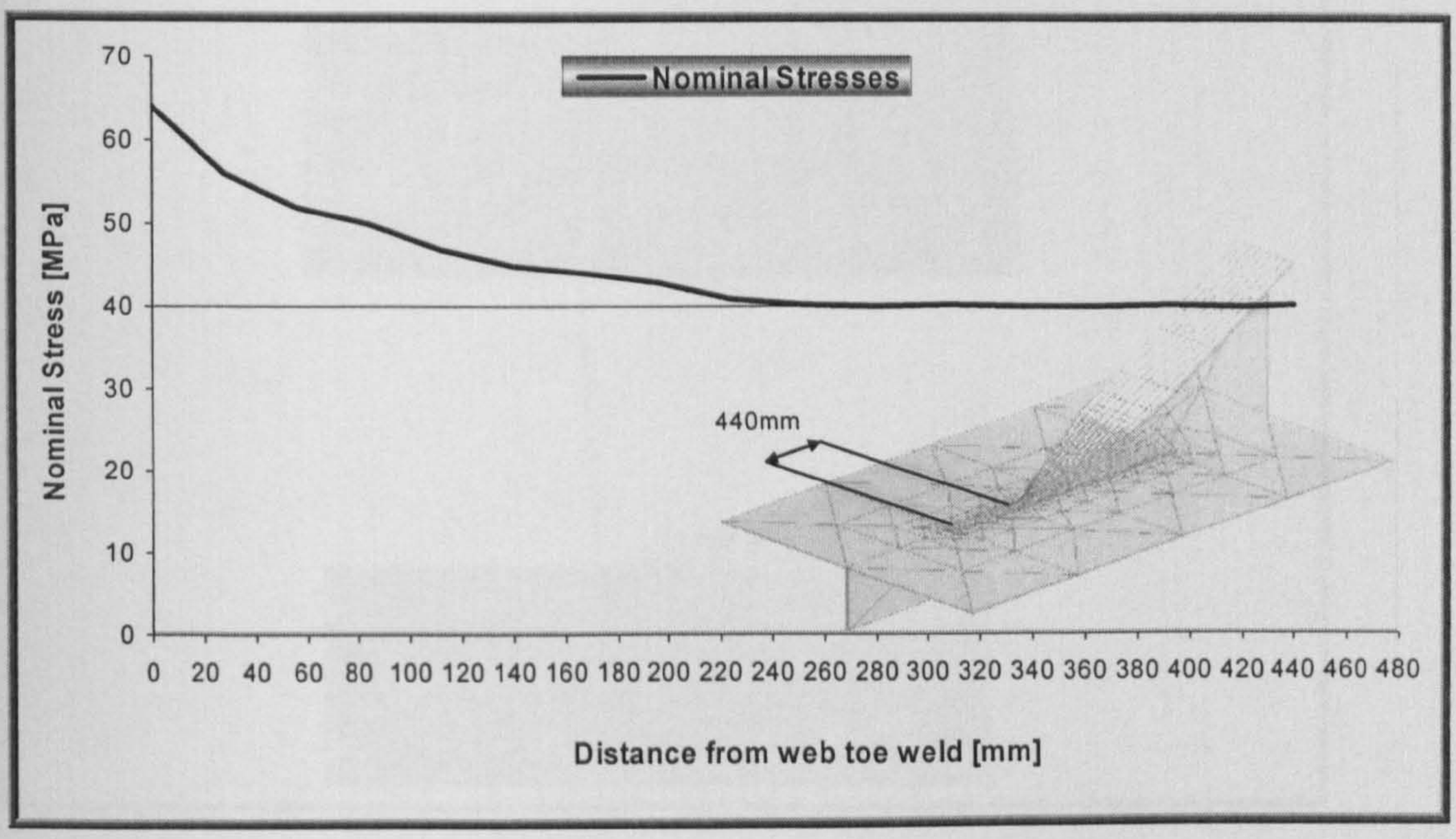

Figure 7-10 Stresses vs. Distance from Web Toe

It is also possible to obtain nominal stresses from the secondary 2D local finite element model of the Web-frame as shown in ***Figure 7-11 below.***

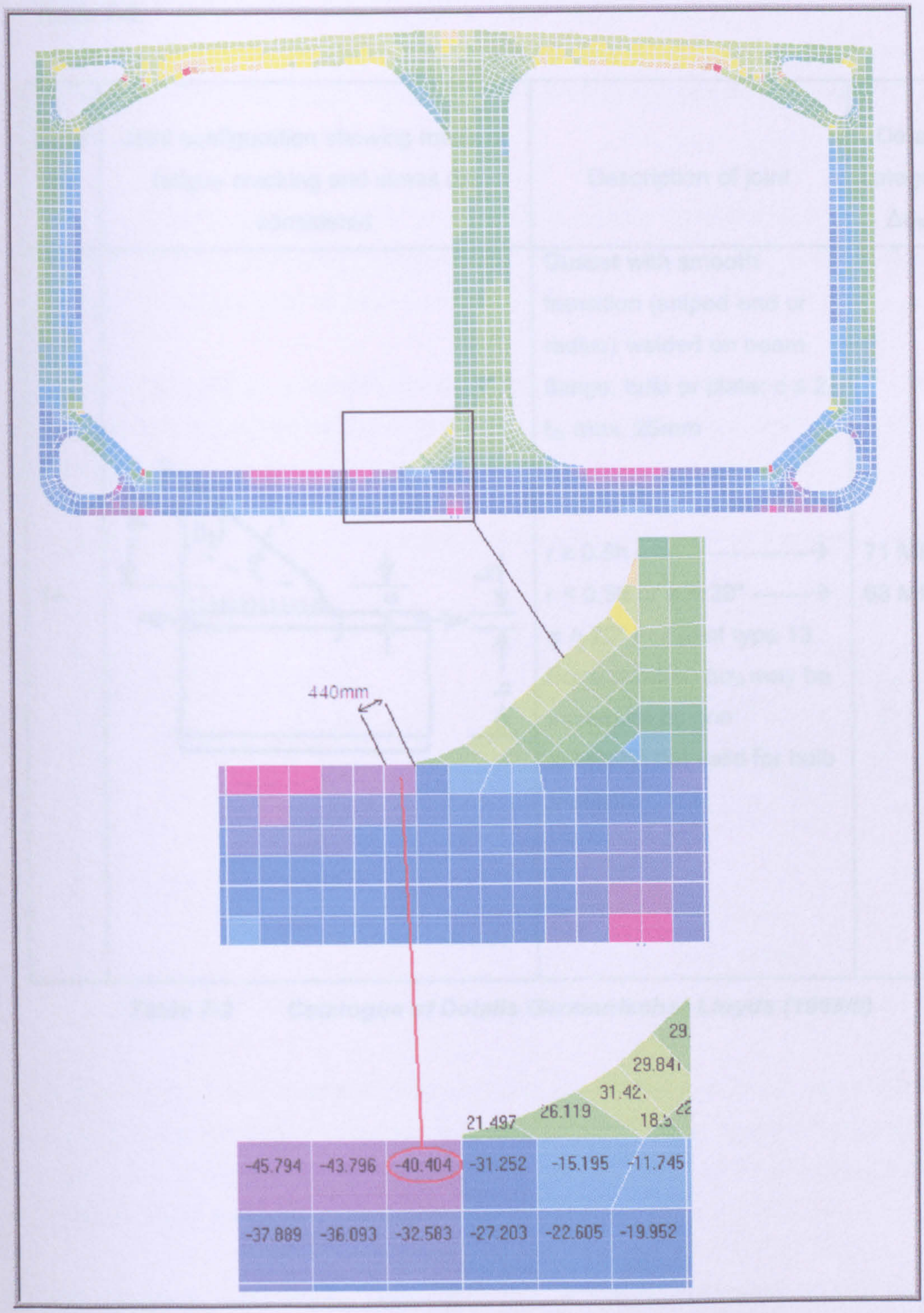

Figure 7-11 Evaluation of Nominal Stresses from 2D Web-Frame Model

Both approaches are valid in revealing the nominal stresses needed for the calculation of the stress concentration factor, where SCF= $(\sigma_{hot\text{-}Spot} / \sigma_{Nominal}) \times K_w$

The hot spot stress evaluated by finite element analysis is in good agreement with the available results for test specimen type number (14) published in the Catalogue of Details as per Construction Rules of Germanischer Lloyds (1998/II), shown in ***Table 7-2***.

Type No.	Joint configuration showing mode of fatigue cracking and stress (σ) considered	Description of joint	Detail category $\Delta\sigma_R$
14	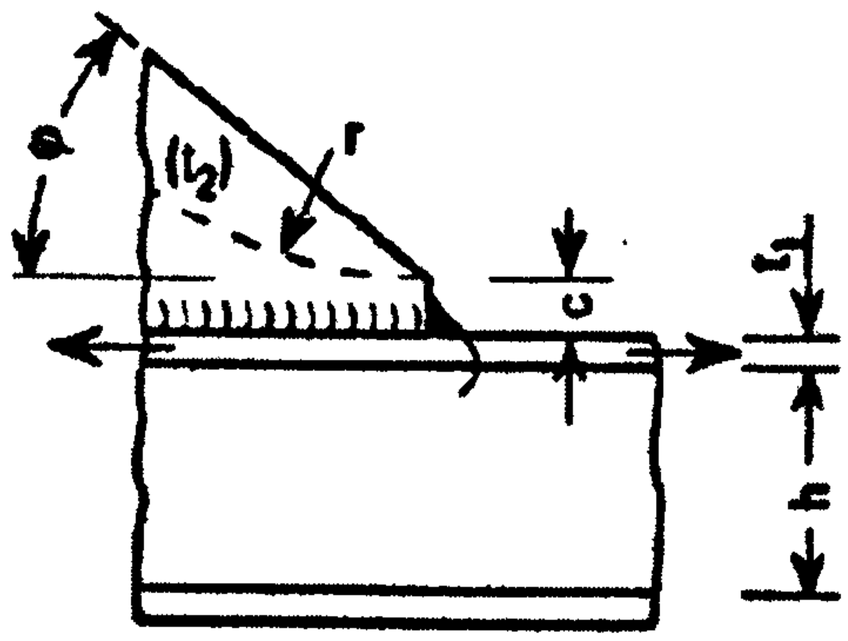	Gusset with smooth transition (sniped end or radius) welded on beam flange, bulb or plate; $c \leq 2\ t_2$, max. 25mm $r \geq 0.5h$ ——————→ $r < 0.5h$ or $\varphi \leq 20°$ ——→ $\varphi > 20°$ see joint type 13 For $t_2 \leq 0.5\ t_1$, $\Delta\sigma_R$ may be increased by one category; not valid for bulb profiles.	 71 MPa 63 MPa

Table 7-2 Catalogue of Details Germanischer Lloyds (1998/II)

7.5 SCFs Determined From Full Scale Models

Any arbitrary stress selected as the nominal stress for a loading mode, although convention often may favour a certain choice. A finite element analysis is normally used to compute each SCF, e.g., as the ratio of the local maximum principal stress to the nominal stress. However, it is an important practice to validate FEM results using full-scale models.

The procedure of SCF evaluation from full-scale models demonstrated for a bottom structure detail as illustrated in ***Figure 7-12***, which belong to a 136 m containership operating at a laden draft of 7.65 m with a speed of 14 knots.

The detail considered a bracket connection with a smooth bracket ending. The detail taken to be transversely adjacent to the hull centreline, implying that effects of hull girder horizontal bending and torsion neglected.

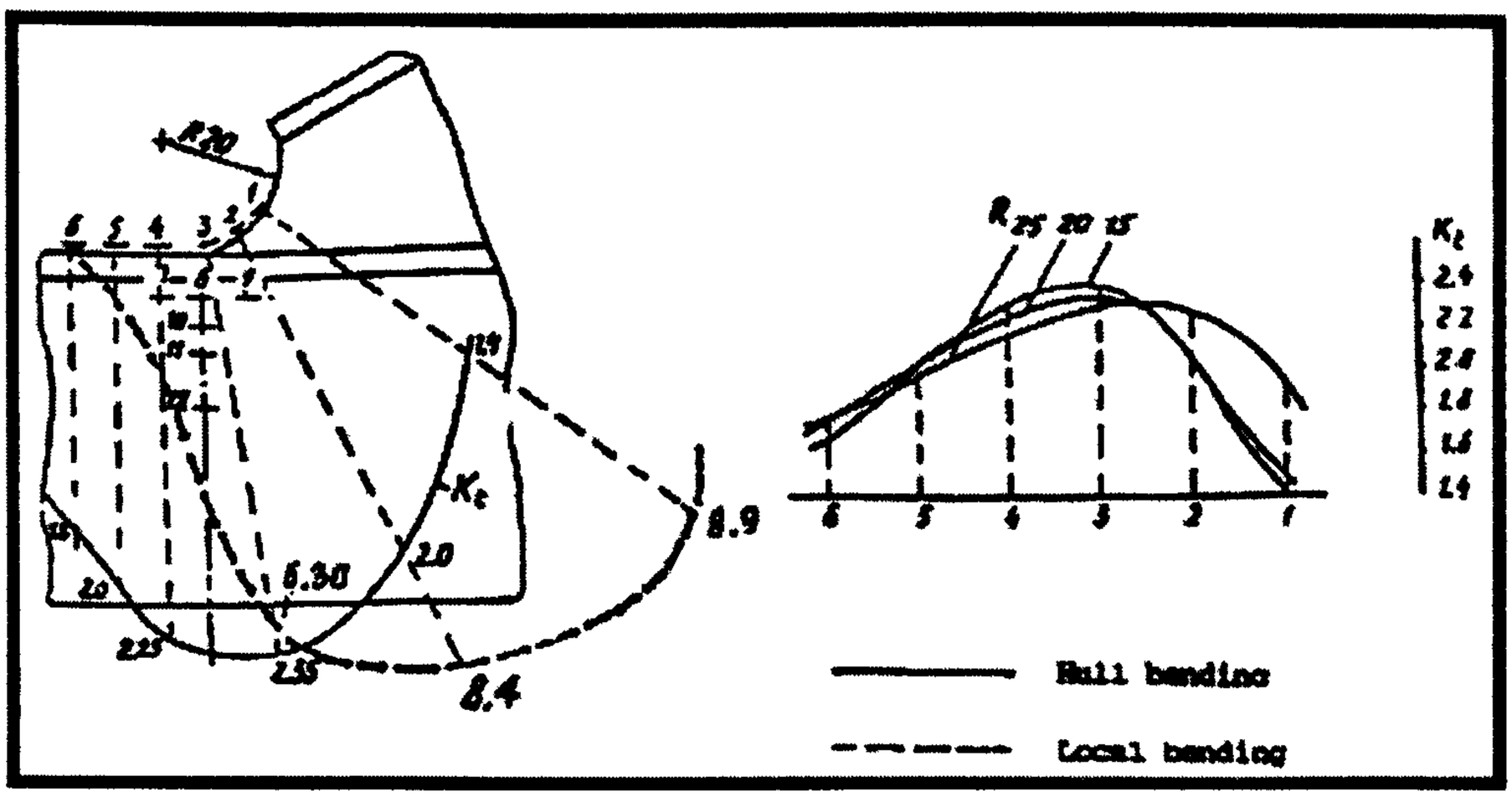

Figure 7-12 Experimentally Obtained SCFs (Pavlov & Petinov 1989)

At that location, the combined effects of stresses due to hull girder bending in the vertical plane and bottom structure bending due to applied pressure are considered. The stress in each loading mode is taken as the product of a nominal stress multiplied by a stress concentration factor.

The structural compatibility coefficients and stress concentration factors for the location under consideration obtained using a model test data, obtained from Pavlov & Petinov (1989). The values of theoretical stress concentration factors (SCF) thus

determined were K_x = 2.35 for axial loading from hull girder vertical bending, and K_y = 6.30 for bending of the double bottom structure. ***Table 7-3*** summarizes the structure applicable stress concentration factors and the corresponding SCFs from the City FPSO's web toe FEM analysis.

Results	Axial loading from hull girder vertical bending [SCF]	Bending of double bottom structure (external pressure) [SCF]
Experimental (Pavlov & Pentinov)	2.350	6.300
City FPSO's Web Toe FEM	2.353	6.275
% Error	- 0.13	+ 0.4

Table 7-3 Experimentally Obtained SCFs *(Pavlov & Petinov 1989)*

The comparison of hot spot stress results, provided from FE analysis and measurements from the full-scale experimental results, published by Pavlov & Petinov (1989). It shows that there is a good agreement between the calculated and the measured values for the hot spots located at the connection between the web frame and the double bottom plate, the difference in results being equal to - 0.13% and + 0.4% respectively. This deference in results is due to mesh fineness at the hot spot.

7.6 Bracket Toe Finite Element Parametric Study

A simplified parametric study conducted on the finite element model in question. The first step was to establish the effect of plate thickness on the hot-spot stresses. As it is observed from ***Figure 7-13*** below, the plate thickness parameter has an impact on the resultant hot spot stress of the model. This occurs when the change take place in one of the plates thickness separately, but not to ignore the fact that this effect is governed by the scantling rules for this structure i.e. any change should take place must keep the bracket toe overall geometrical dimensions in harmony with adjoining structure.

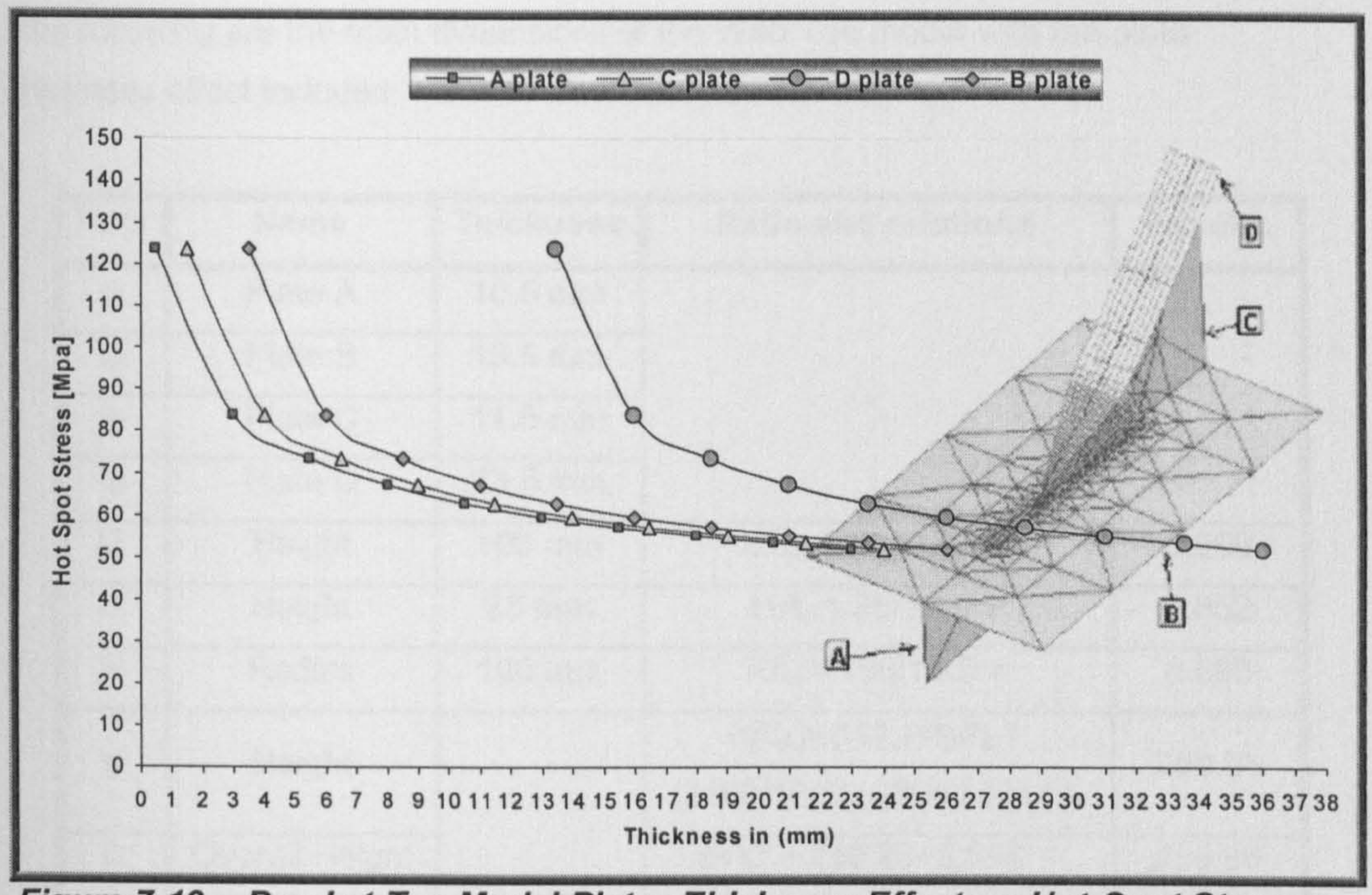

Figure 7-13 Bracket Toe Model Plates Thickness Effect on Hot-Spot Stresses

By dividing the web toe model to its basic structural components, four plates and the main feature of a curvature at the toe end illustrated in the following ***Figure 7-14***.

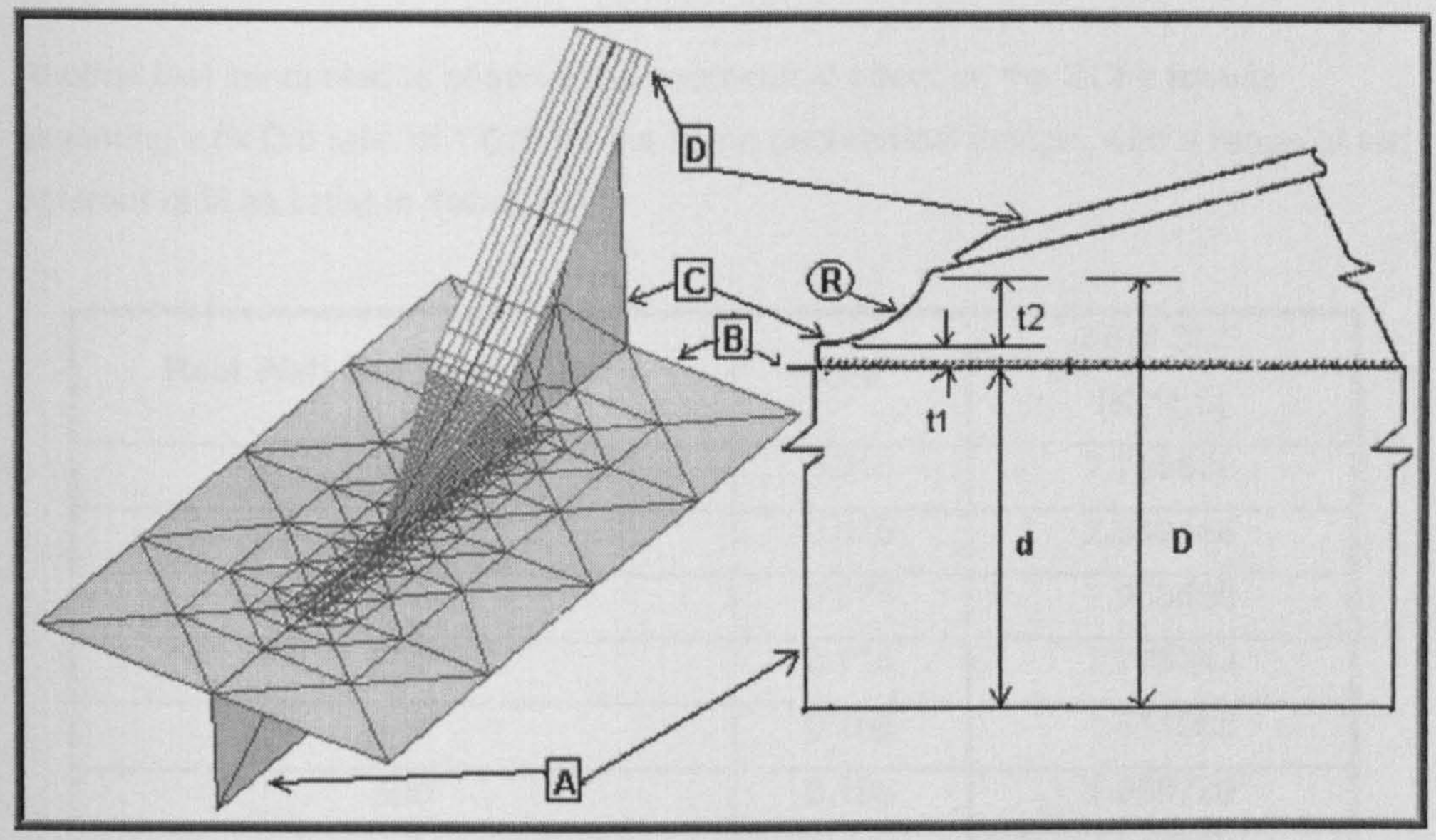

Figure 7-14 Bracket Toe Main Structural and Geometrical Features

The following are the main dimensions of the Web Toe model with the plate thickness effect included:

Item	Name	Thickness	Ratio and relations	Results
t_A	Plate A	10.5 mm		
t_B	Plate B	13.5 mm		
t_C	Plate C	11.5 mm		
t_D	Plate D	23.5 mm		
t2	Height	100 mm	$t2/t_c$ = 100/11.5 =	8.696
t1	Height	25 mm	$t1/t_c$ = 25/13.5 =	1.852
R	Radius	100 mm	R/t_c = 100/11.5 =	8.696
d	Height		$(d/t_A)+(t1/t_c)+t_B/t_B$ = (2460/10.5)+(25/11.5)+1 =	250.96
D	Overall Height		d+t2 = 250.96+8.696 =	259.66

Table 7-4 Web Toe Geometrical Ratios for SCF Analysis

The result of the aforementioned preparation conducted in an attempt to simplify the geometrical parameters into the following shape (D/d) = 0.0346 and (R/d) = 1.0346.

Another test conducted to observe the geometrical effect on the SCFs results; assuming a fix D/d ratio of 1.035 for the same geometrical design, with a range of ten deferent radii as listed in ***Table 7-5***.

Real Web Toe Radius [mm]	R/d	FEM SCF (K_g*1.5)
50	0.015	2.789636
100	0.035	2.342188
200	0.075	1.966509
300	0.115	1.775343
400	0.155	1.651088
500	0.195	1.560729
600	0.235	1.490584
700	0.275	1.433742
750	0.295	1.409009

Table 7-5 Parametric FEM SCF-(D/d=1.035)

The following ***Figure 7-15*** illustrates the results of the simplified parametric study graphically, for the D/d=1.035 ratio of the structure in question.

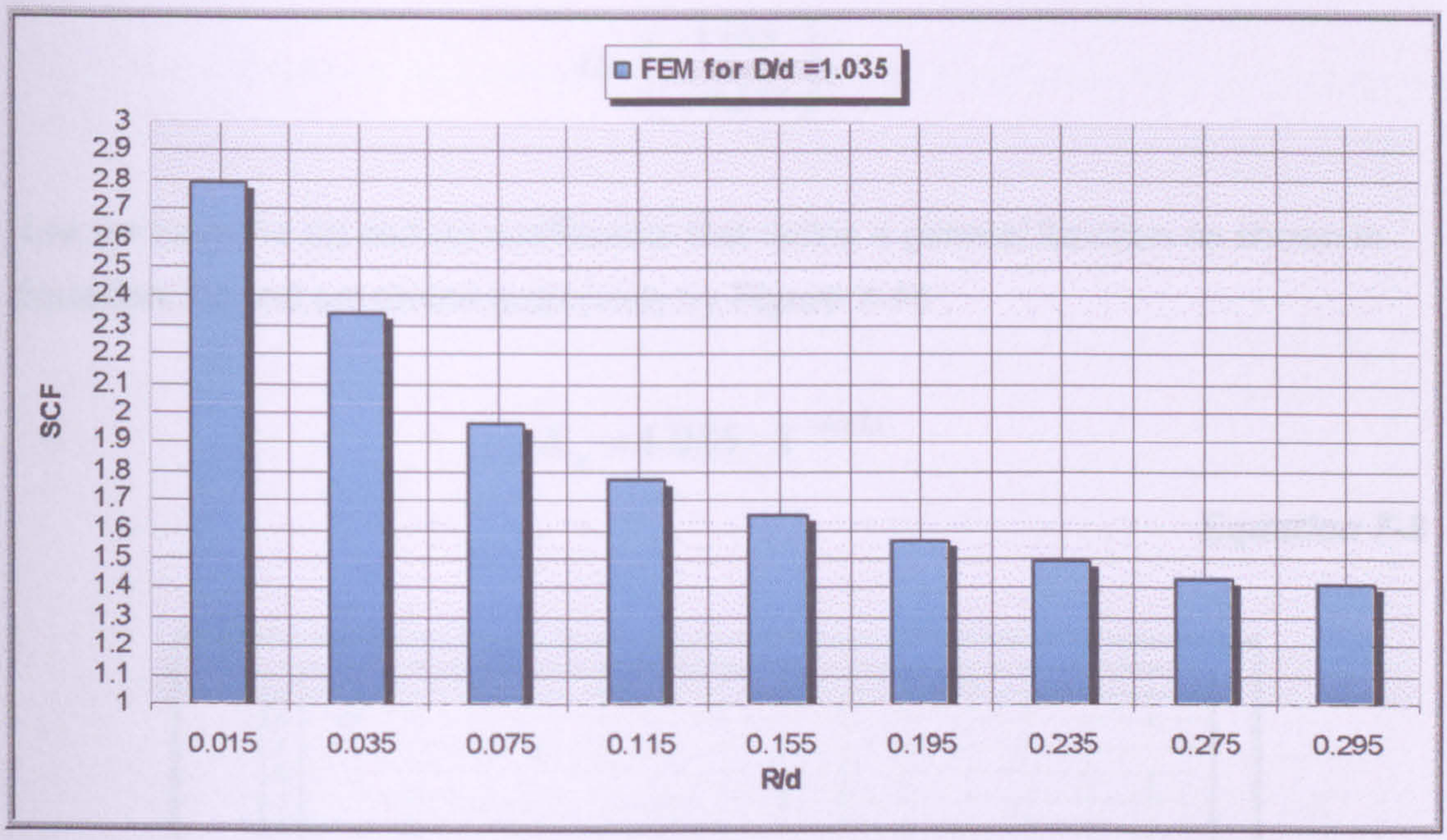

Figure 7-15 Web Toe SCF FEM and Analysis Parametric Study

It is clear that the above graph can be presented in a power fit form. Using MathCad, a mathematical model developed to present the power fit function of the results. With (*genfit)* function, taking the fitting function to be:

$$y = a \cdot x^{b}$$

Equation 7-7

Where (a) and (b) are unknown. From this model, defining a vector of guesses, and by trial and error it is possible to find representative values corresponding to (a = D/d) = 1.035.

$$\text{guess} := \begin{pmatrix} 0.9 \\ -0.3 \end{pmatrix}$$

Using (*genfit*) to find the parameters in the model function:

$$G := \text{genfit}(X, Y, \text{guess}, F)$$

Here are the values for the coefficients of the power function:

$$G = \begin{pmatrix} 1.035 \\ -0.244 \end{pmatrix},$$

Now we have the (a) and (b) coefficients that define a general function as shown in ***Equation 7-8*** and presented graphically by ***Figure 7-16***.

$$K_g = 1.035 \cdot X^{-0.244}$$

Equation 7-8

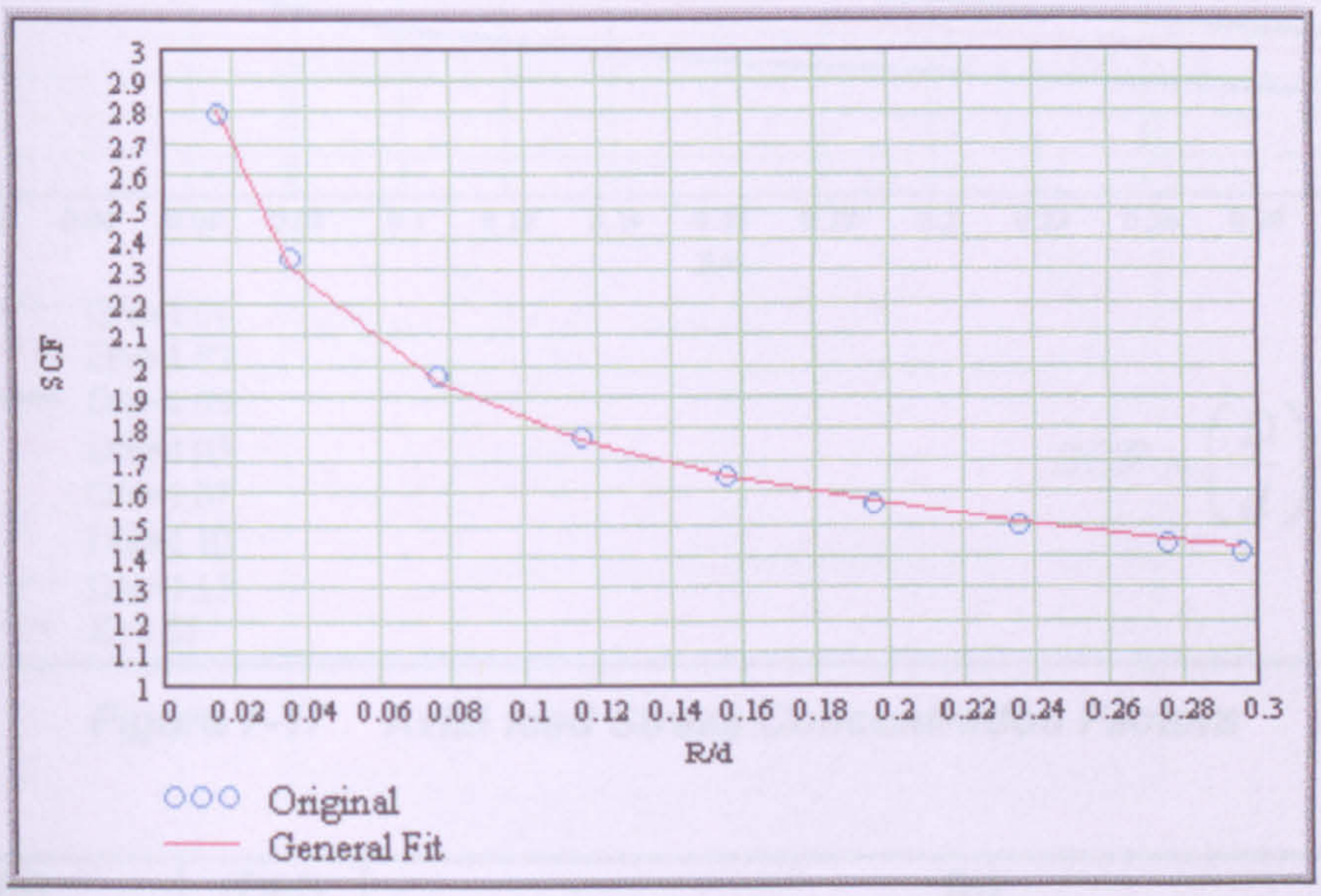

Figure 7-16 Curve Fitting of SCF Results

Equation 7-9 rewritten in more generalized terms as:

$$K_g = \left(\frac{D}{d}\right) \times \left(\frac{R}{d}\right)^{-b}$$

Equation 7-9

Where (b), for web toe models ranging from ($0.2 \leq b \leq 0.27$) for ($1.015 \leq D/d \leq 1.05$); furthermore, the calculated correlation coefficient found to be: (0.999).

A more generalized curves using ***Equation 7-9***, and base on Peterson's and Neuber theory for stress concentration factor of notched flat bar in tension (R.E. PETERSON, 1953). These curves presented in the following ***Figure 7-17*** and ***Table 7-6***.

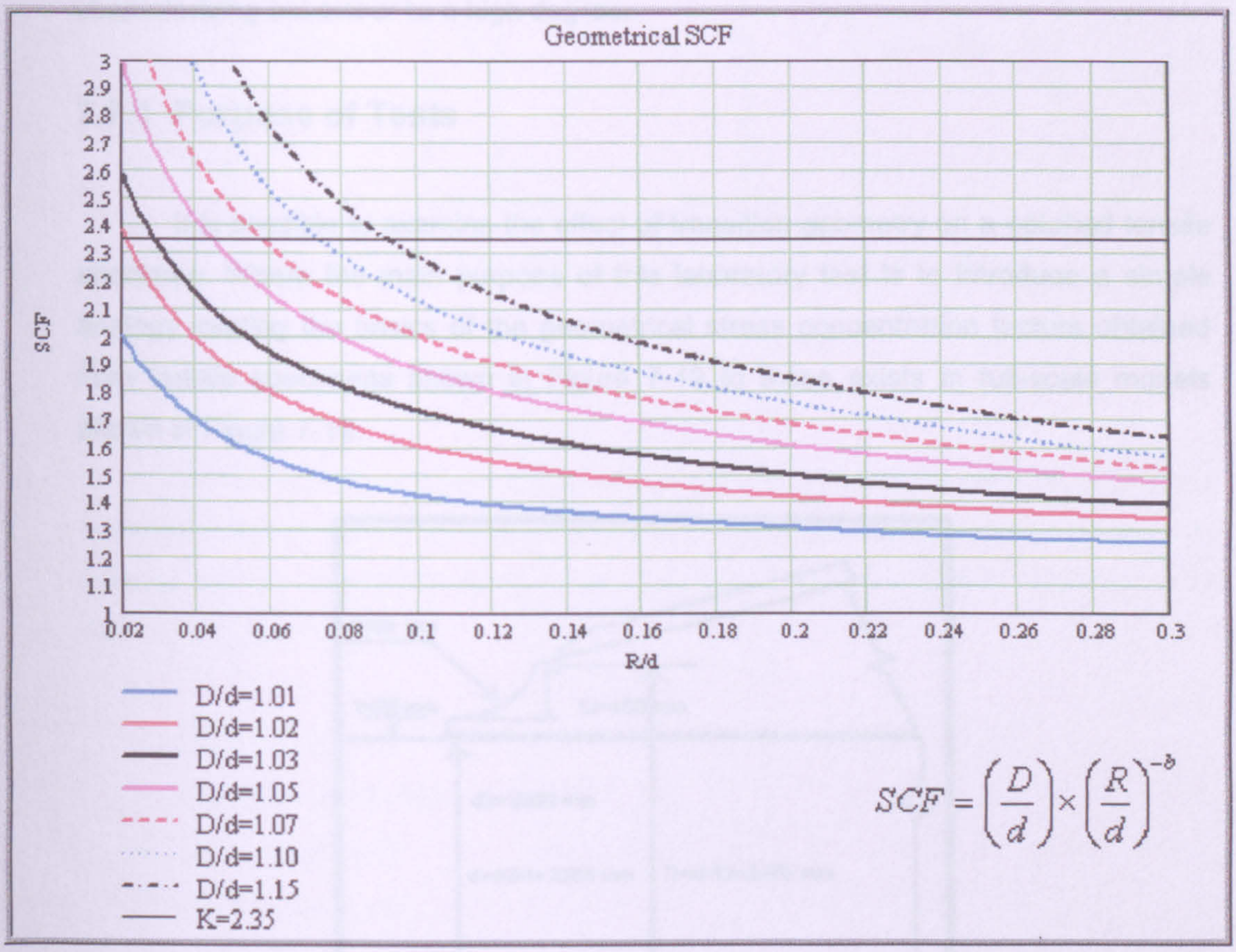

$$SCF = \left(\frac{D}{d}\right) \times \left(\frac{R}{d}\right)^{-b}$$

Figure 7-17 Axial load Stress Concentration Factors

(R/d)	(D/d)	(b)
x := 0.02, 0.021.. 0.3	1.01	$b101(x) := 48.757 \cdot x^4 - 37.806 \cdot x^3 + 10.825 \cdot x^2 - 1.2165 \cdot x + 0.1948$
	1.02	$b102(x) := 26.854 \cdot x^4 - 20.342 \cdot x^3 + 6.2369 \cdot x^2 - 0.7745 \cdot x + 0.2294$
	1.03	$b103(x) := 39.659 \cdot x^4 - 27.1 \cdot x^3 + 6.7761 \cdot x^2 - 0.6534 \cdot x + 0.2458$
	1.05	$b105(x) := 26.863 \cdot x^4 - 21.572 \cdot x^3 + 6.4837 \cdot x^2 - 0.7284 \cdot x + 0.2796$
	1.07	$b107(x) := 14.324 \cdot x^4 - 14.85 \cdot x^3 + 5.4041 \cdot x^2 - 0.7048 \cdot x + 0.301$
	1.10	$b110(x) := 56.121 \cdot x^4 - 46.912 \cdot x^3 + 13.876 \cdot x^2 - 1.6664 \cdot x + 0.3551$
	1.15	$b115(x) := 66.739 \cdot x^4 - 53.333 \cdot x^3 + 15.325 \cdot x^2 - 1.8993 \cdot x + 0.3808$

Table 7-6 Power equations (b) for SCF evaluation

7.7 SCFs Determined From Notched Tensile Specimens

Analytical models alone are often insufficient to obtain the desired confidence or accuracy. Analysis in conjunction with testing is often a cost effective path to characterizing behaviour to a high degree.

7.7.1 Purpose of Tests

It is possible to examine the effect of transition geometry on a notched tensile specimen. Where the main purpose of this laboratory test is to introduce a simple analogy relating the basics of the geometrical stress concentration factors obtained from tensile specimens shown in Figure 7-19 to those exists in full-scale models shown in Figure 7-18.

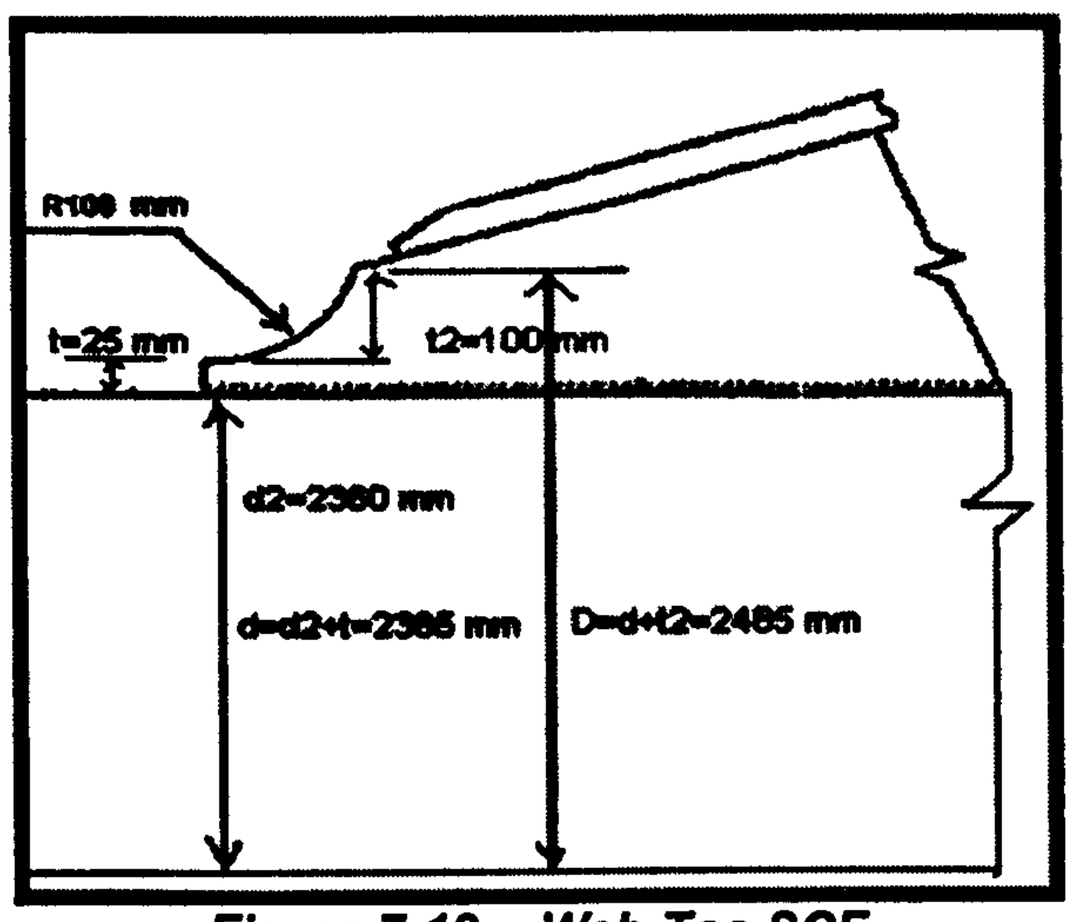

Figure 7-18 Web Toe SCF

From ***Figure 7-18*** the relation (R/d = 0.035) taken as the first geometrical parameter relating the web toe radius to the double bottom plate height, and the second parameter is (D/d = 1.035). In the tensile coupon, the same relations are valid also as shown in ***Figure 7-19*** below.

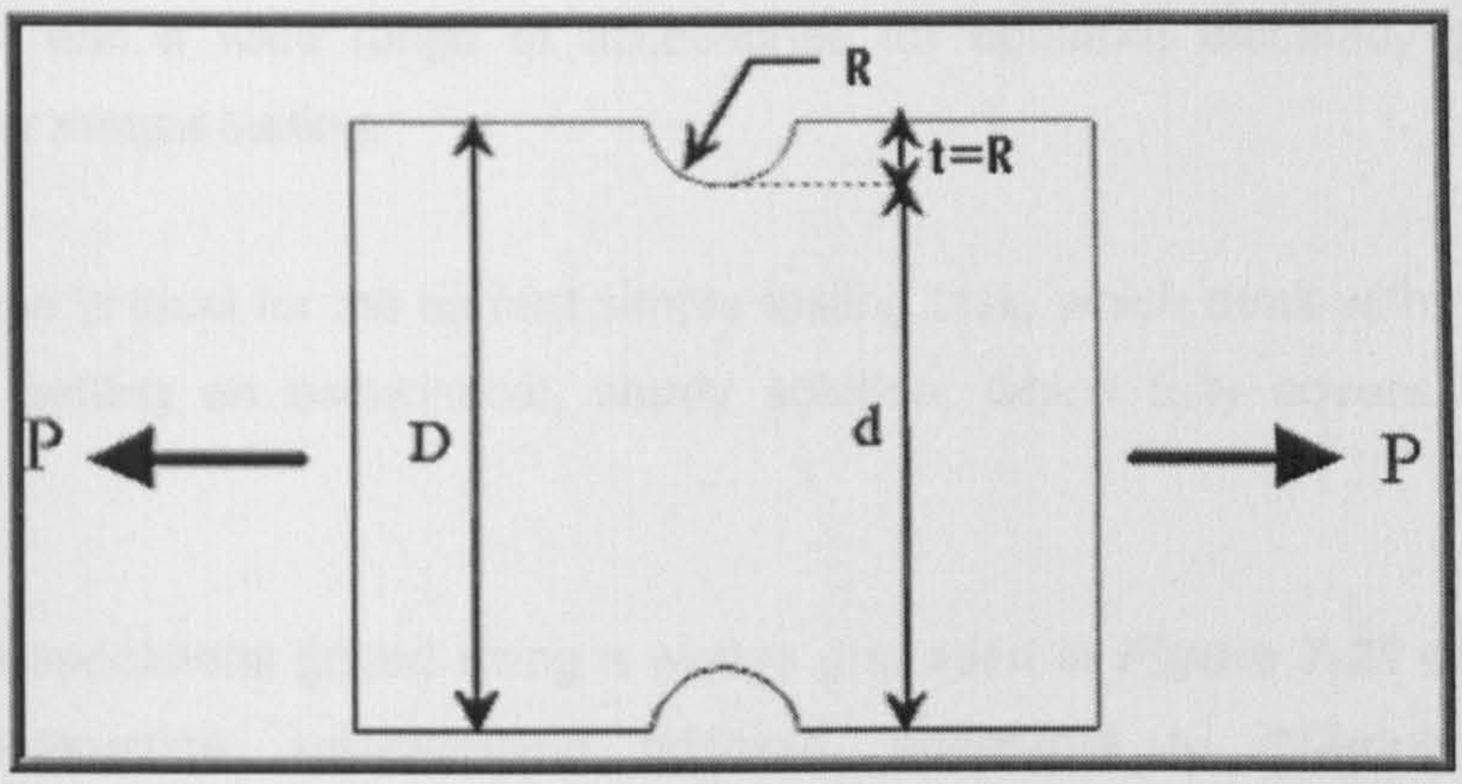

Figure 7-19 Tensile Coupon with Semicircular Notch

7.7.2 Equipment and Materials

Tensile testing equipment consists of several types of devices used to apply controlled tensile loads to test specimens. The main experimental components needed for the laboratory tests, using the City University 88440 DARTEC test System (***Figure 7-20***) are:

- Load cell unit
- Hydraulic pump unit
- Data Logger unit
- Control panel unit

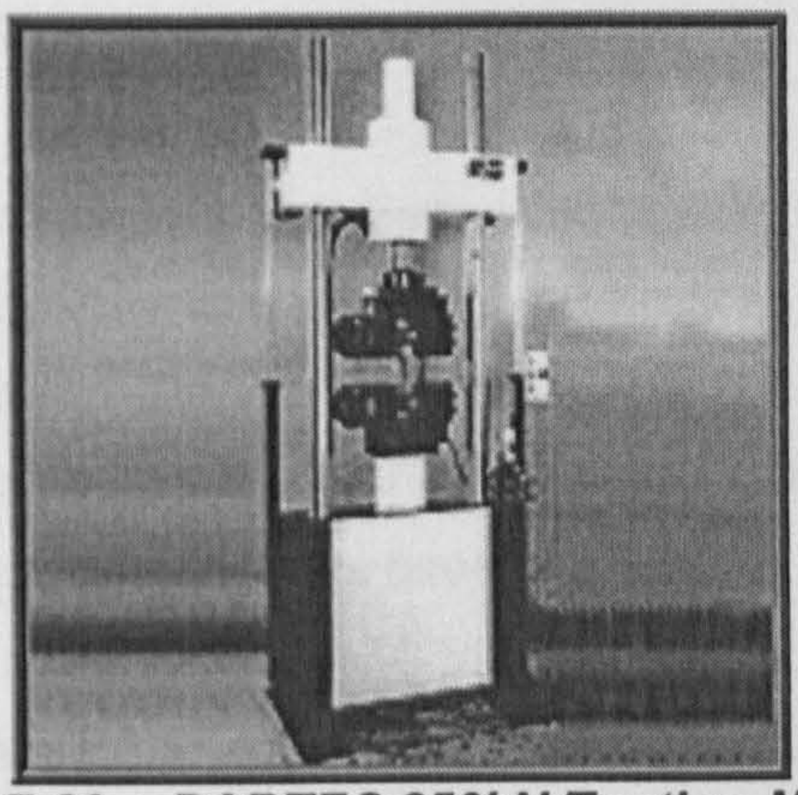

Figure 7-20 DARTEC 250kN Testing Machine

The above testing machine shown in ***Figure 7-20*** used for carrying out tensile tests with quasi- static stressing. The machine is of a floor standing design, with a versatile

control unit and a wide range of accessories for optimum efficiency giving total coverage for metals testing.

This machine is ideal for the current simple testing task, which dealt with reliably and accurately getting an economical, sturdy solution, which fully covers the testing needs.

The tensile specimens griped using a wedge grip seen in ***Figure 7-21*** consisting of simple construction, self-clamping principle, adaptable to differing specimen dimensions, through various jaw inserts.

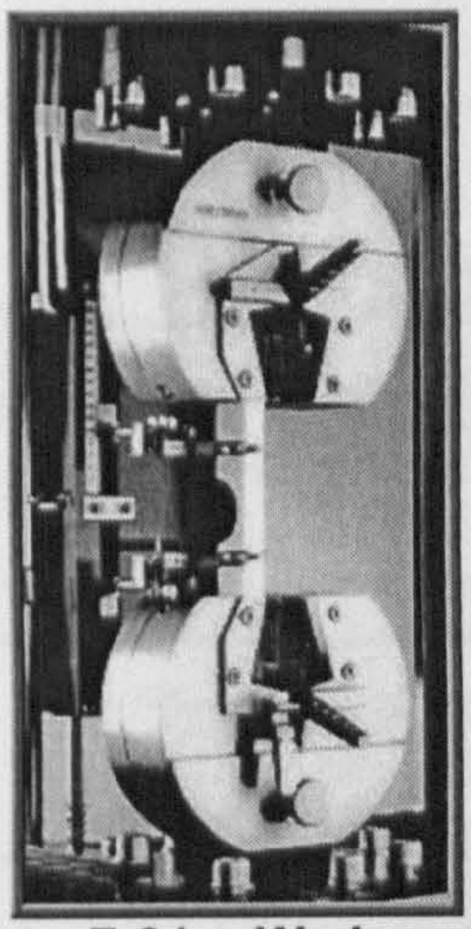

Figure 7-21 Wedge grips

7.7.3 Tensile Specimens

The test involves straining a test piece such as the one shown in ***Figure 7-22*** below by tensile force, generally to fracture, for determining the maximum force F_{max}, which defined as the greater force, which the test piece withstands during the test once the yield point passed. Eventually the evaluation of the corresponding tensile strength σ_{max} this corresponds to the max force F_{max}.

Stress in axially loaded structural member of a gradually changing or near constant cross section computed by the simple relationship:

$$\sigma_{\max} = \frac{F_{\max}}{a_{\max}}$$

Equation 7-10

Where F_{max} is the applied load and (a_{max}) denotes the cross sectional area of the tensile test specimen.

It is possible to choose the required dimensions needed for the tensile test specimen shown in ***Figure 7-22***, from the standards for flat specimens of tensile tests illustrated in ***Table 7-7***.

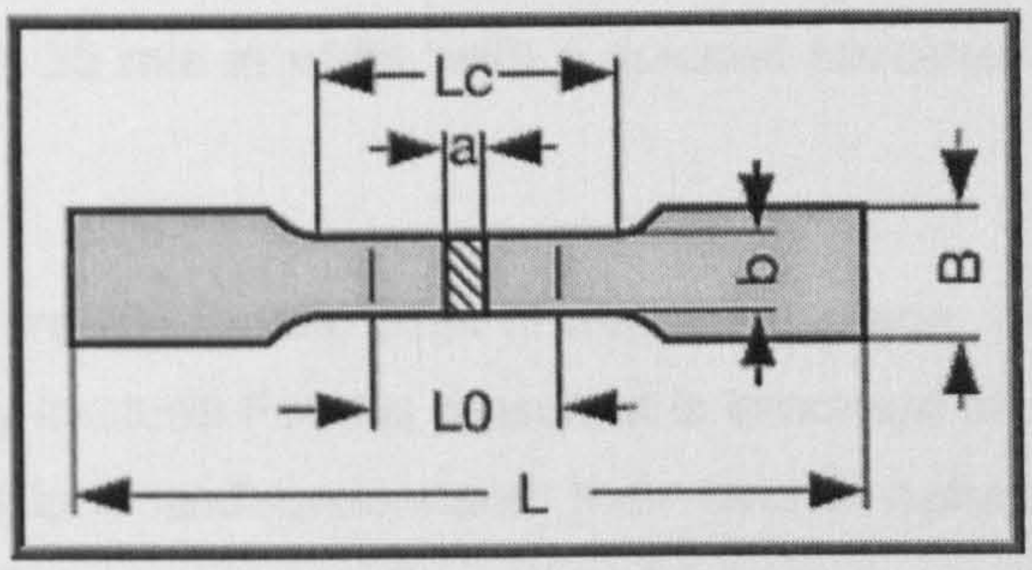

Figure 7-22 Test Piece Shape and Dimension

Norm/Standard	**a** in mm	**b** in mm	L_o in mm	**B** in mm	L_c in mm	**L** in mm
DIN EN 10.002 Typ 1	--	12.5 ± 1	50 ± 0.5	--	75	165
DIN EN 10.002 Typ 2	--	20 ± 1	80 ± 0.8	30	120	250
DIN EN 50 114	Up to 3	20 ± 1	80 ± 0.8	30	120	250
DIN EN 50 125	3	8	30	12	38	115
	5	16	50	22	65	175
	6	20	60	27	80	210
	8	25	80	33	105	260

Table 7-7 Typical Standard Flat Specimens Dimensions

Geometric discontinuities cause a large variation of stress locally, and often produce a significant increase in stress. This high stress local to the geometric discontinuity typically called (*stress concentration*) is the subject of investigation by means of tensile testing of a typical notched specimen shown in ***Figure 7-23***.

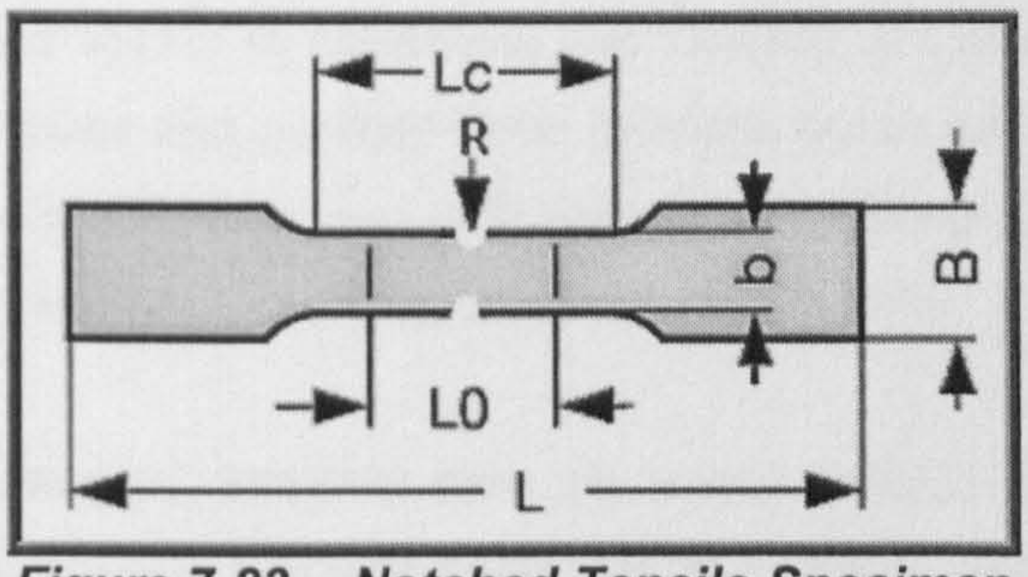

Figure 7-23 Notched Tensile Specimen

The radius (R) denotes the notch radius, where the (R/b) ratio should equal to 0.04 to simulate the same ratio from the full-scale web toe subject of this investigation.

The required specimen selected according to the (DIN EN 50 125) standard with a = 8 mm thickness, b = 25 mm in width, with a notched specimen of an R = 1 mm in radius.

Often, *stress risers* are the starting point of material damage, which ultimately leads to *material failure* by fracture! For this reason, it is important to realize the existence of stress concentrations and understand their overall behaviour for our typical geometric configuration in question. The ratio of the maximum stress to the average or nominal stress concentration factor (K):

$$K = \frac{\sigma_{\max}}{\sigma_{nom}}$$

Equation 7-11

The nominal stress usually defined as the net area of the *reduced* section similar to ***Equation 7-10***:

$$\sigma_{nom} = \frac{F_{nom}}{a_{reduced}}$$

Equation 7-12

This lab test will demonstrate *stress concentration* and *stress variation*s that occur for a plate with a semicircular hole under uniaxial tension experimentally and numerically (with the finite element method).

Six normal specimens tested to determine the Yielding & ultimate tensile stress or UTS for short three inline and another three of cross sectional orientation. All made from the same material BS Mild Steel with typical yield strength ranging from 295 to 310 MPa and a tensile strength ranging from 430 to 445 MPa.

Similarly, six other samples prepared from the same material and dimensions, with the introduction of semicircle notch at each side of 1 mm in radius. The notches cut right into the sides of the geometric centre of the gage length.

7.7.4 Stresses to be considered

When the potential fatigue crack is located in the parent material at the weld toe, the relevant hot spot stress is the range of maximum principal stress adjacent to the potential crack location with stress concentrations taken into account. Where this is, the local stress concentrations created by the joints themselves and by the weld-profile.

The design stress therefore regarded as the nominal stress, adjacent to the weld under consideration. However, if the joint situated in a region of stress concentration resulting from the gross shape of the structure, this must be taken into account in calculating the nominal stress.

As an example, for the weld shown in ***Figure 7-24 -a***, the relevant hot spot stress for fatigue design would be the *tensile stress*. For the weld shown in ***Figure 7-24 -b***, the stress concentration factor for the global geometry must in addition be accounted for, giving the relevant hot spot stress equal to SCF*σ, where SCF is the stress concentration factor due to the hole.

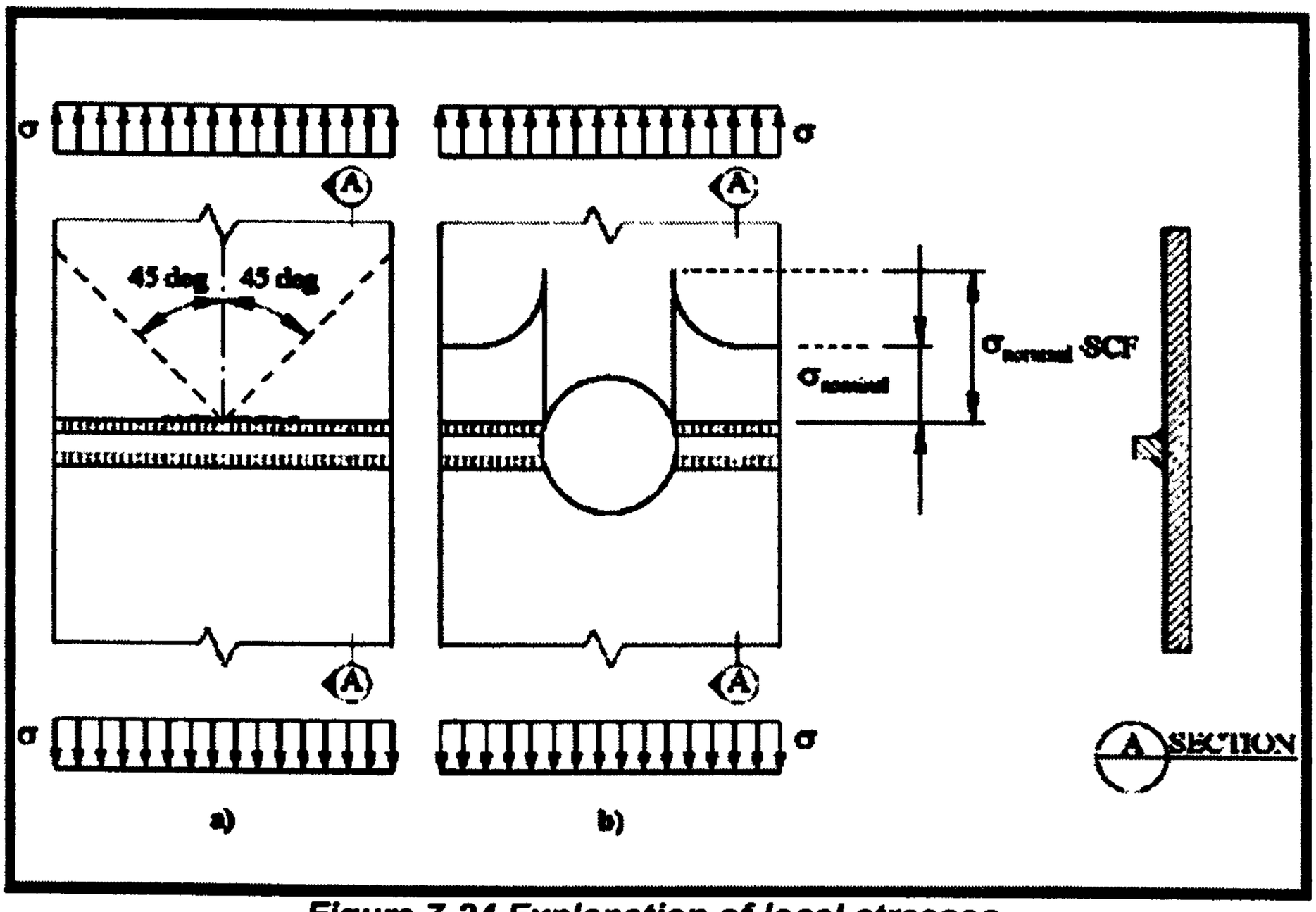

Figure 7-24 Explanation of local stresses

7.7.5 Test Procedure

Load applied by the use of hydraulic electrical pump and a complete computer controlled system designed by DARTEC. This final system comprises of a single 250kN double acting actuator capable of applying load in tension or compression. Oil supplied by an electrical powered hydraulic pump and controlled by a remote panel system.

Once a specimen positioned in the test equipment, all of the connections connected to the data logger and control panel. Small load applied and released which allows checks for any hydraulic leaks or loose electrical connections.

A set of zero readings taken and load applied in automatic increments up to tensile load. As the test progressed, it has closely monitored for signs of damage and ultimate failure. As failure becomes imminent, data recordings capture data at failure. The load then released with any recordings taken at the final zero point. The specimen then removed from the equipment.

7.7.6 Test Results

Sample	Normal Specimens			Notched Specimens			SCF
	Yielding Load (N)	Cross Sectional Area (mm^2)	Yielding Stress (MPa)	Yielding Load (N)	Cross Sectional Area (mm^2)	Yielding Stress (MPa)	
Inline-1	59784.30	200.201	298.621	23234.751	175.065	132.721	2.25
Inline-2	61832.88	200.0217	309.131	23307.450	174.920	133.246	2.32
Inline-3	62379.17	200.3401	311.370	22729.068	175.195	129.736	2.4
Cross-1	62618.17	199.8667	313.300	21902.753	174.775	125.320	2.5
Cross-2	61354.88	199.8347	307.028	23531.123	174.743	134.661	2.28
Cross-3	61593.88	200.2751	307.546	23316.665	175.133	133.137	2.31
Average	*61593.88*	*200.090*	*307.832*	*23003.635*	*174.972*	*131.470*	*2.343*
St. Dev.	1005.5	0.2	5.1	601.5	0.2	3.4	0.1
St. Dev. %	1.6324	0.107	1.654	2.615	0.108	2.6021	3.917363

Table 7-8 Tensile Specimens Experimental Results

The above ***Table 7-8*** lists the tensile tests results, along to the SCFs obtained; the following curves ***Figure 7-25*** and ***Figure 7-26*** represents normal and notch tensile tests respectively.

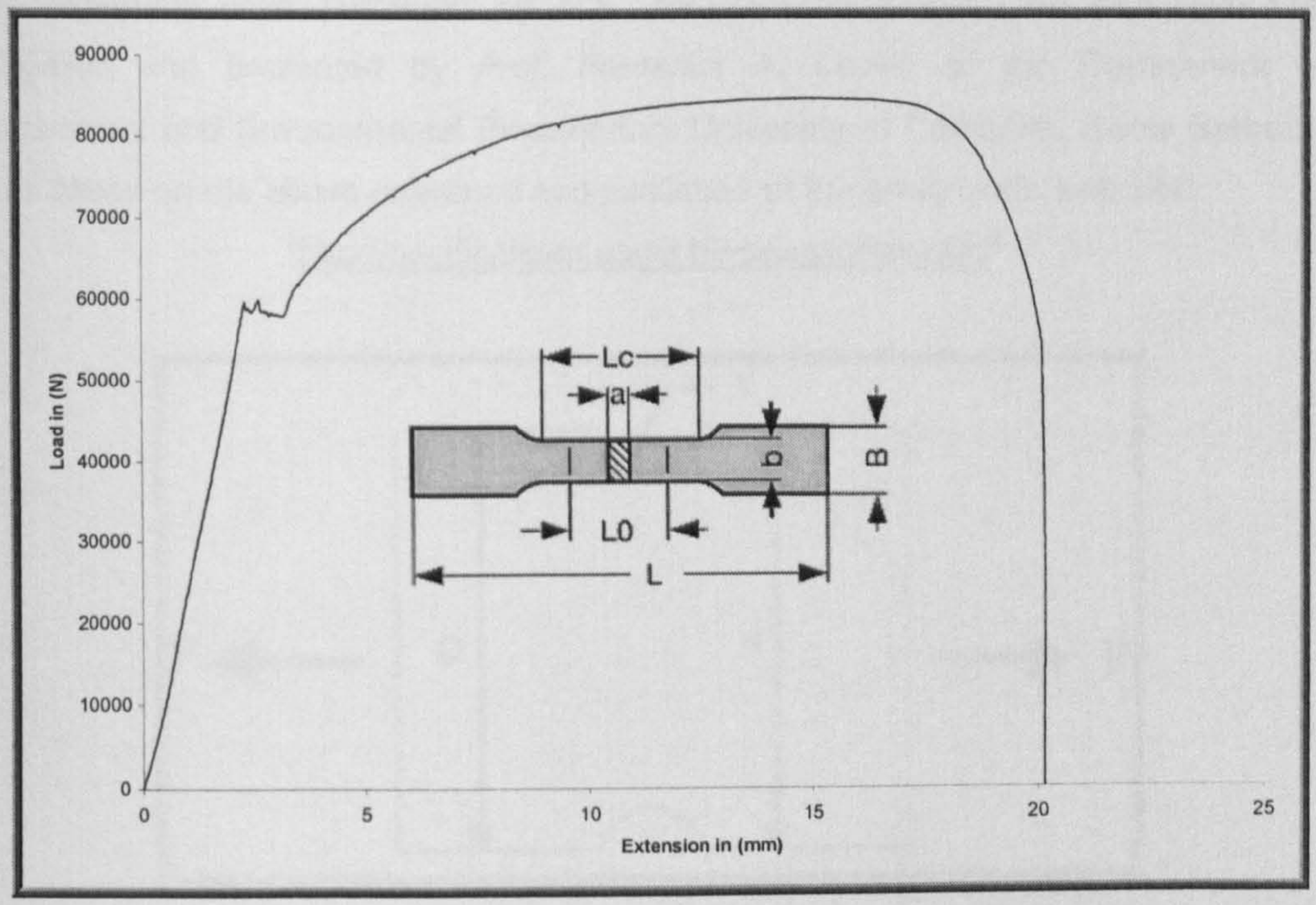

Figure 7-25 Normal Tensile Specimen

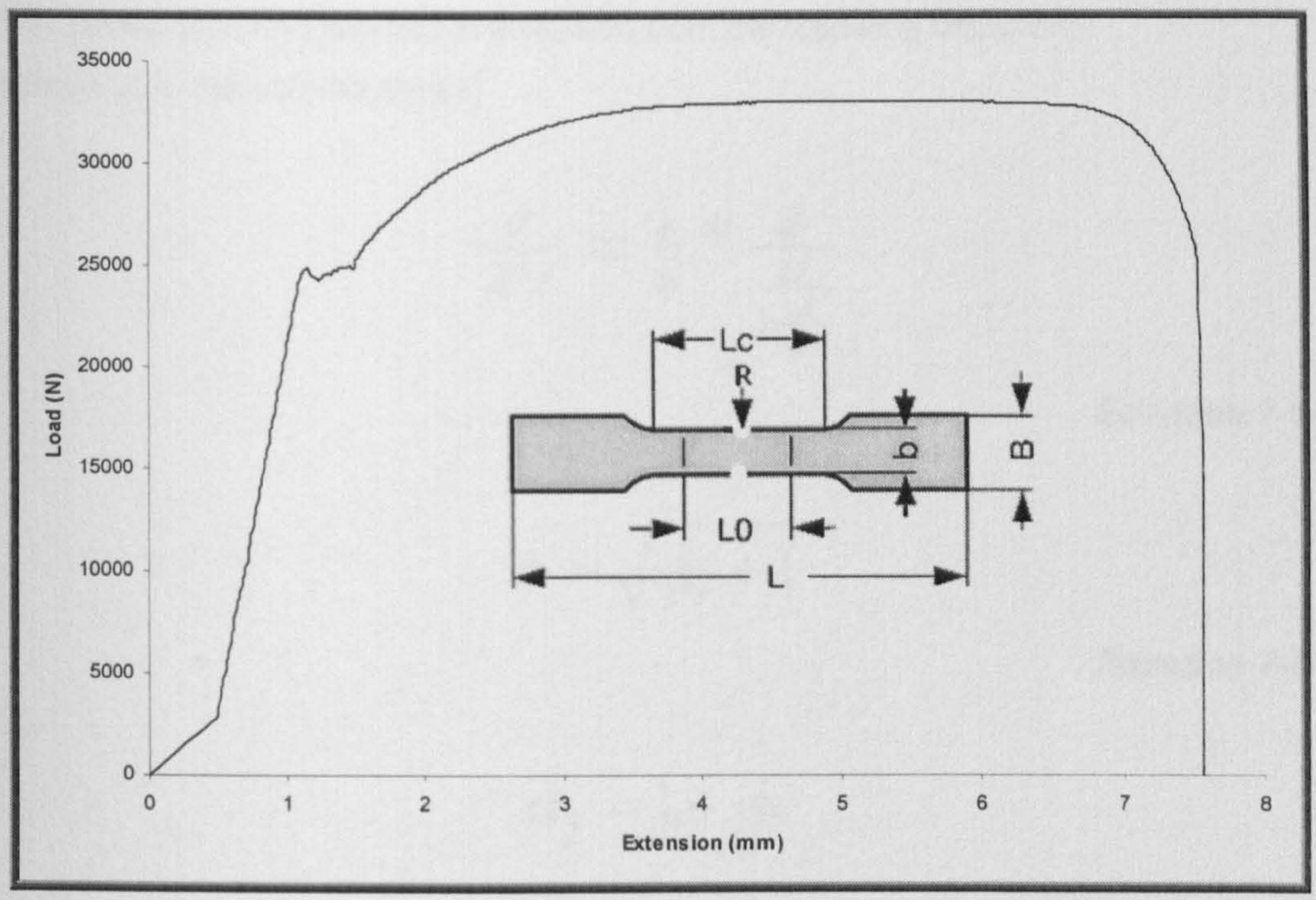

Figure 7-26 Notched Tensile Specimen

7.8 Theoretical SCFs Evaluation

It is possible to evaluate theoretically the SCF of a "Bar with Semi-Circular Edge Notches in Tension" as illustrated in ***Figure 7-27***, the SCFs evaluation is based on theoretical work published by R.E. PETERSON, (1974). An analytical tool prepared and presented by *Prof. Frederick A. Leckie* of the Department of Mechanical and Environmental Engineering, University of California, Santa Barbara. This based on the above reference and published at the professor's web site:

"http://pacific.pcsm.espci.fr/~sean/index.html"

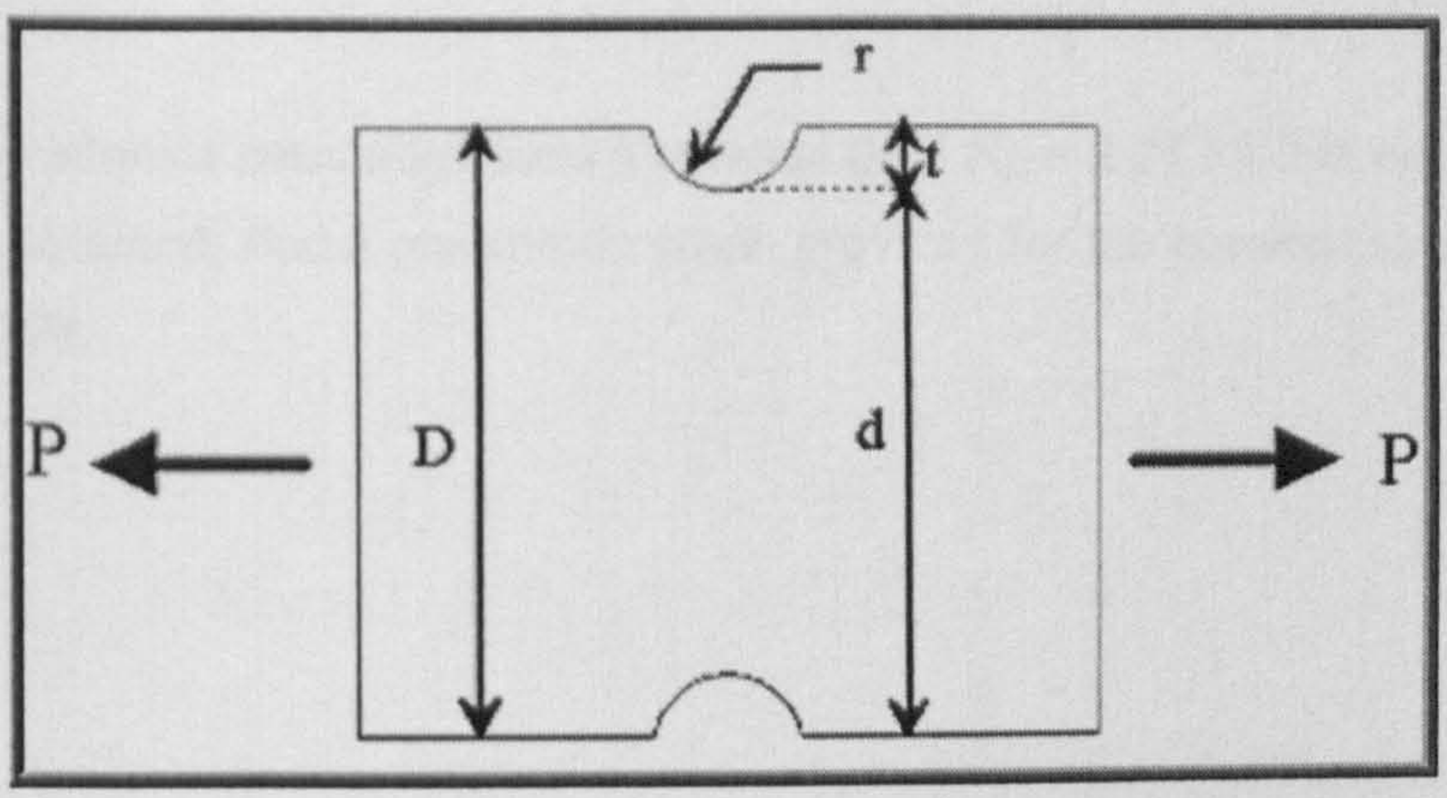

Figure 7-27 Bar with Semi-Circular Edge Notches in Tension

The stress concentration factor evaluated from the following equations:

Where (K is the nominal stress)

$$\frac{d}{2*r} = \frac{t}{r} * \frac{d}{\frac{D}{1-\frac{d}{D}}}$$

Equation 7-13

$$\Delta = \sqrt{\frac{d}{2*r} + 1}$$

Equation 7-14

$$\alpha_f = 1 + \frac{2}{\sqrt{\frac{r}{t}}}$$

Equation 7-15

$$\alpha_t = \frac{2*\Delta^2 * \sqrt{\frac{d}{2*r}}}{\Delta^2 * \tan^{-1}\left(\sqrt{\frac{d}{2*r}}\right) + \sqrt{\frac{d}{2*r}}}$$

Equation 7-16

$$K = \sqrt{\frac{(\alpha_f - 1)^2 * (\alpha_t - 1)^2}{(\alpha_f - 1)^2 + (\alpha_t - 1)^2}} + 1$$

Equation 7-17

By using the internet calculation form a nominal SCF K_n = ***2.31*** for this case of study in question obtained; And a parametric graph provided for the nominal stress shown in ***Figure 7-28.***

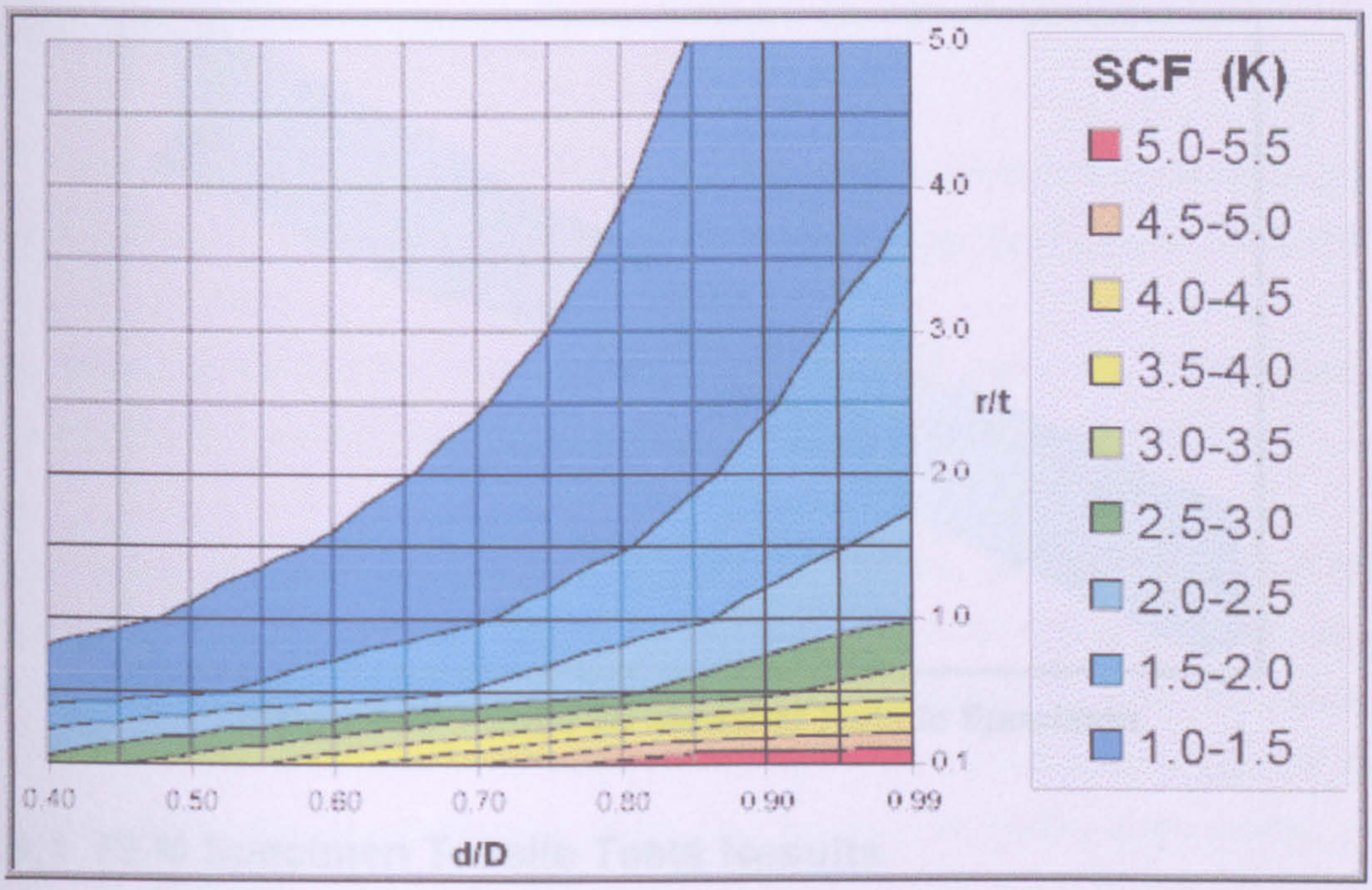

Figure 7-28 SCF Graph (http://pacific.pcsm.espci.fr/~sean/index.html)

7.9 Tensile Specimen SCF evaluation using FE analysis

Relatively few closed form elasticity solutions exist for problems concerning stress concentrations; rather it is customary to rely on experimental and/or numerical methods. Other experimental methods such as photo-elasticity technique are also classical experimental methods to compute stress variations in a member.

The value of SCFs depend on the shape and dimensions of the component being designed and can be calculated using finite element methods. Finite element analyses of the tensile specimens' geometries conducted using the ANSYS program, version (5.7). Three dimensions characterize the specimen geometry as shown in ***Figure 7-29*** below.

The tensile specimen models constructed using SOLID92 -- 3-D 10-Node Tetrahedral Structural Solid elements. These elements have quadratic displacement behaviour and are well suited to model irregular meshes.

Loading applied in the form of a constant pressure (tensile stress) at the end of the model. The dimensions simulated to be according to standard having no influence on the stress state near the notch root. The same loads imposed on both models in an attempt to investigate the stress intensity deference between the two models.

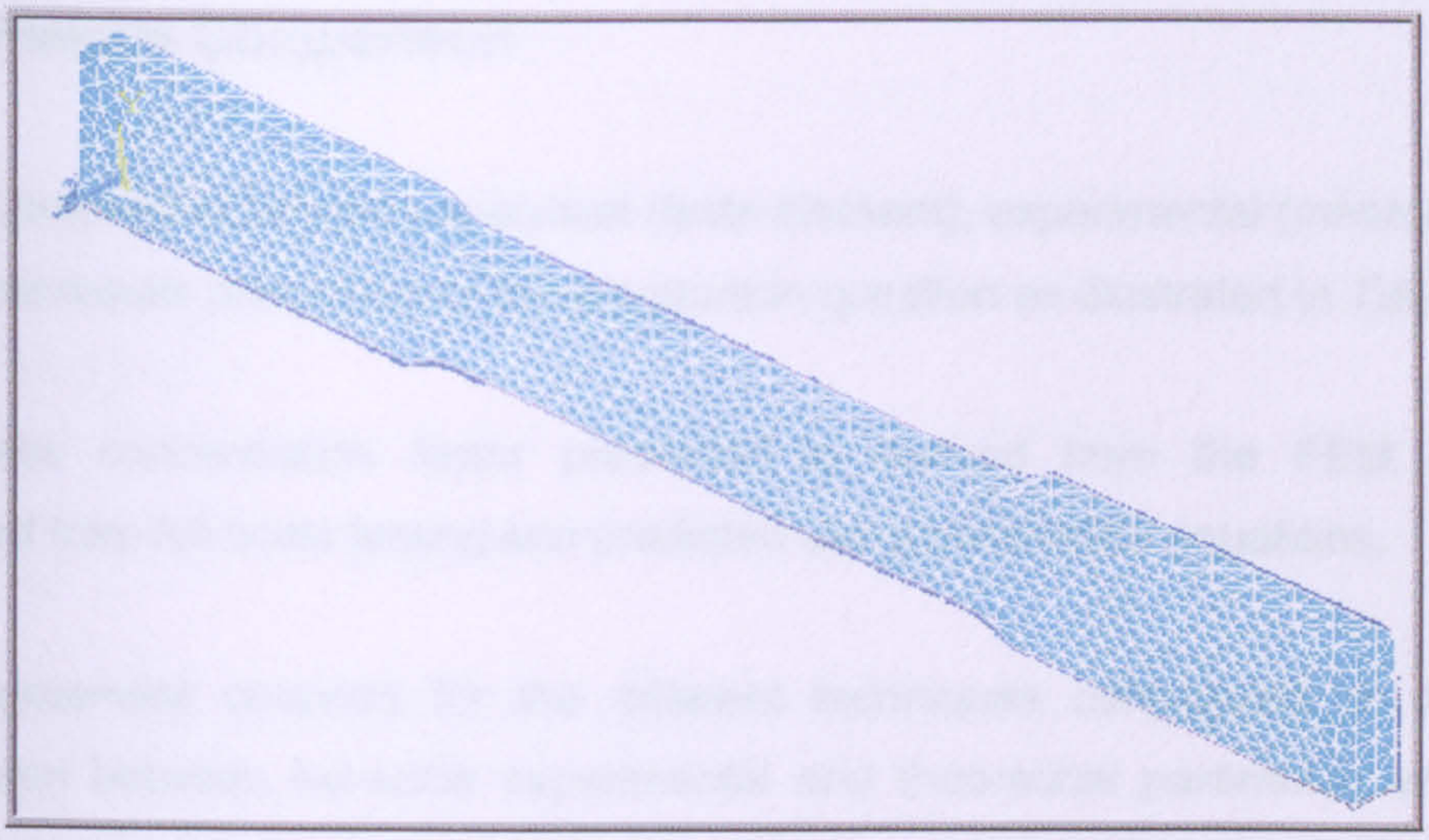

Figure 7-29 Solid 3D Model of Tensile Specimen

7.9.1 FEM Specimen Tensile Tests Results

The FEA results evaluated and plotted in terms of the elastic stresses. The stress concentration factor for the case in question *SCF = 2.30*, defined as max stress from normal tensile specimen model divided by notched model's max stress at notch shown in ***Figure 7-30***. Close-up investigation of the model, revels the variation of stress near the edge of the model, with a noticeable sharp increase in stress at the centre of the hole.

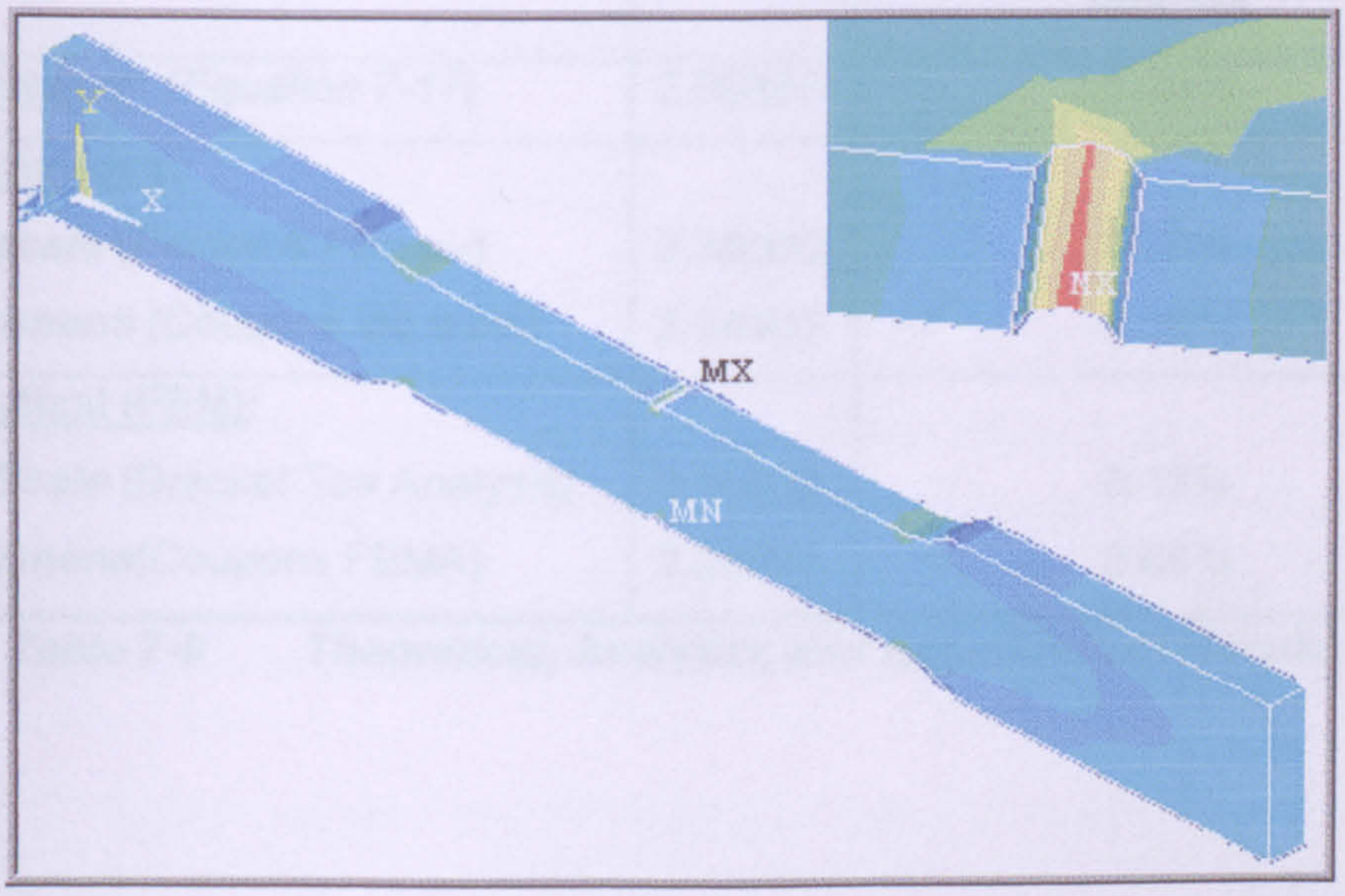

Figure 7-30 Notched 3D FEM Model

7.9.2 Results Comparison

Comparison between analytical (finite element), experimental (measured) and theoretical results presented for the structure in question as illustrated in ***Table 7-9***.

The stress concentration factor presented is derived from the FEM analysis, measured from full scale testing and predicted using parametric equations.

Good agreement obtained for the different techniques considered. In the SCF comparison between full-scale experimental and theoretical parametric equations, the closest agreement obtained with the equations published by *Prof. Frederick A. Leckie*. It can be seen that reasonable agreement is achieved from equations. The predicted SCFs are smaller than the measured values from the full-scale model.

SCF comparison of maximum measured values and those predicted from parametric equations, and analytical work; the equations are conservative, with the closest agreement obtained using the analytical and tensile experiments, particularly with the FE results. This relation of full-scale results demonstrated in ***Table 7-9*** to differ from the FEA values of SCF by less than 1% over the entire domain of validity.

Category	SCF	% Error from Full Scale Results
Theoretical: (*Equation 7-17*)	2.30865	1.76%
Experimental:		
Full scale (*Pavlov & Petinov*)	2.35000	0.00%
Specimens (Coupons lab tests)	2.34300	0.30%
Analytical (FEM):		
Full Scale (Bracket Toe Analysis)	2.35302	0.13%
Specimens(Coupons FEMA)	2.28690	2.69%

Table 7-9 Theoretical, Analytics and Experimental Results

7.9.3 Errors of Discretization

Why is it important to control discretization errors? It is very important for proper correlation of computed data with experimental results. Let us assume the following assumptions:

- ΦEXP is to be the experimental information of our model in question.

- ΦMOD the same information predicted theoretical by a mathematical model.

- ΦFEA the same information computed analytically from FEA.

The purpose of an experiment is to determine whether the mathematical model correctly describes the physical system being modelled, that is, whether ΦMOD is sufficiently close to ΦEXP.

Writing:

$$|\Phi MOD - \Phi EXP| = |\Phi MOD - \Phi FEA + \Phi FEA - \Phi EXP| < |\Phi MOD - \Phi FEA| + |\Phi FEA - \Phi EXP|$$

Equation 7-18

To assess the quality of the mathematical model it is necessary to ensure that:

$$|\Phi FEA - \Phi MOD| << |\Phi EXP - \Phi FEA|$$

Equation 7-19

In the absence of procedures for controlling the discretization errors, it is possible to correlate FEA results with experimental observations through near cancellation of two large errors: The sensitivity of the solution to the discretization parameters indicates large numerical errors.

$$\Phi EXP - \Phi FEA = (\Phi EXP - \Phi MOD) + (\Phi MOD - \Phi FEA) = \varepsilon$$

Equation 7-20

In this, case the error from Equation 7-20 ($\varepsilon = 1.0721$).

8. Development of a Design Method for FPSOs Fatigue

8.1 Overview

8.1.1 Causes and Recognition of Fatigue Failures

- Design deficiencies
- Manufacturing deficiencies
- Improper and insufficient maintenance
- Operational overstressing
- Environmental factors (i.e. heat, corrosion, etc.)
- Secondary stresses not considered in the normal operating conditions
- Fatigue failures

Most failures occur not because the applied load is too great, but because a small load is applied repeatedly, this kind of failure is a result of fatigue. Not surprisingly, a part's geometry has an impact on its structural performance. The geometry of a part can lead to stress concentrations. No matter how strong or tough the material that the part is made of, a poorly shaped design can have catastrophic consequences.

8.1.2 Physical Characteristics of Fatigue Cracking

Ed. A.F. Madayag, (1969), explains that improper and insufficient maintenance seems to be one of the most contributing factors influenced by some improper designs such as areas that are hard to inspect and maintain and the need for better maintenance procedures. In many circumstances the true load is difficult to predict resulting in a structure being stressed beyond its normal capabilities and structural limitations.

Metal fatigue is defined as a progressive failure of metal under cyclic loading, and two fatigue zones are evident when investigating a fracture surface due to fatigue, the fatigue zone and the rupture zone. The fatigue zone is the area of the crack propagation. The area of final failure is called the rupture or instantaneous zone. In investigation of a failed specimen, the rupture zone yields the ductility of the material, the type of loading, and the direction of loading. The relative size of the

rupture zone compared with the fatigue zone relates the degree of overstress applied to the structure. The amount of overstressing can be determined from the fatigue zone as highly overstressed if the area of the fatigue zone is very small compared with the area of the rupture zone, medium overstress if the size or areas of both zones are nearly equal, low overstress if the area of rupture zone is very small.

Fatigue cracks in steel vessels usually initiate at local notches in welded or flame-cut details, particularly details in high stressed primary and secondary structure, usually develop into through-thickness cracks several inches long before visibly detectable as seen in ***Figure 8-1***.

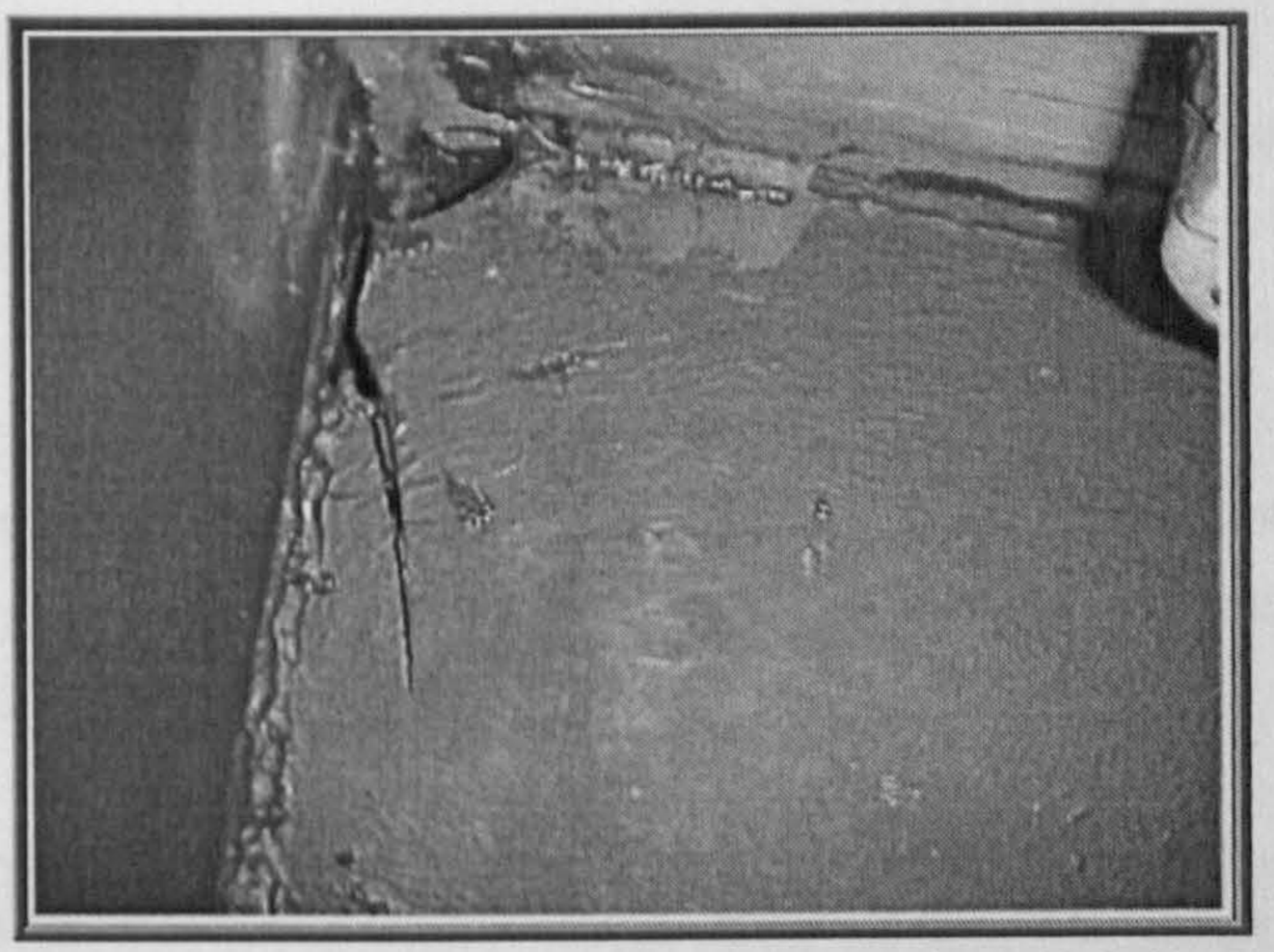

Figure 8-1 Typical Fatigue Crack *(Tanker Structure Co-operative Forum 1997)*

Some of these cracks initiate around prone areas of FPSO's hull structure, such as connections of side shell, longitudinals to transverse frames and bulkheads, particularly connections just below water line, connections of bottom longitudinals to transverse frames and bulkheads, connections of longitudinal bulkhead stiffeners to transverse frames and bulkheads, brackets toes of cross ties and bracket toes of transverses in wing and centre tanks.

The predominately cyclic fatigue loading are primarily wave-induced loads and motions, vertical bending of hull girder, lateral bending and torsion of hull girder, hydrodynamic pressure on side shell, bottom, and tank boundaries of the vessel. Other sources of cyclic fatigue are thermal stresses, machinery and propulsion vibration, hydrostatic pressure on side shell, bottom, and tank boundaries.

8.1.3 Design Considerations

Even if careful attention to good design practices is constantly the goal of designers, fatigue problems are sometimes introduced into the structure. Fatigue failures are often the result of geometrical or strain discontinuities, poor workmanship or improper manufacture techniques, material defects, and the introduction of residual stresses that may add to existing service stresses. Typical factors affecting fatigue include stress raisers, usually in the form of a notch or inclusion; most fatigue fractures may be attributed to notch effects. High strength materials are much more notch-sensitive than softer alloys.

Corrosion is another factor that affects fatigue. Corroded parts form pits that act like notches as shown in ***Figure 8-2***. Corrosion also reduces the amount of material which effectively reduces the strength and increases the actual stress. Decarburization, the loss of carbon from the surface of the material, is the next factor. Due to bending and torsion, stresses are highest at the surface; decarburization weakens the surface by making it softer. Finally, residual stresses which add to the design stress; the combined effect may easily exceed the limit stress as imposed in the initial design.

Figure 8-2 ***Combination of Fatigue Cracks and Localized Corrosion***
(Tanker Structure Co-operative Forum 1997)

8.1.4 Processing Factors

Stresses are normally highest at the surface of a structure, so it follows that fatigue usually initiates at the surface. Stress raisers are more likely to be present as a result of surface irregularities introduced by the design of the structure or produced in service or resulting from processing. Processing factors can introduce a detrimental or beneficial effect into a structure, usually in the form of effect on strength level or residual stress condition of the surface material. Therefore, the effect of processing on the mechanical properties of a material, especially the surface of the material, directly affects fatigue properties, where surface roughness increases with cyclic stress.

8.1.5 Fatigue Damage

Fatigue damages are known to occur more frequently for some ship types and categories of hull structure elements. The fatigue life is in particular related to the magnitude of the dynamic stress level, the corrosiveness of the environment and the magnitude of notch- and stress concentration factors of the structural details, which all vary depending on ship type and structure considered.

A major fraction of the total number of fatigue damages on FPSO's structure occurs in panel stiffeners on the FPSO's side and bottom and on the tank boundaries of ballast and cargo tanks. However, the calculated fatigue life depends on the type of stiffeners used, and the detail design of the connection to supporting girder webs and bulkheads. The *Schiehallion* FPSO is the world's largest new build vessel of its type, capable of storing 950,000 barrels of oil. The following images (***Figure 8-3*** & ***Figure 8-4***) are presented to give realistic insight on the scale of environmental damage sustained by FPSOs in the North Sea and the North Atlantic.

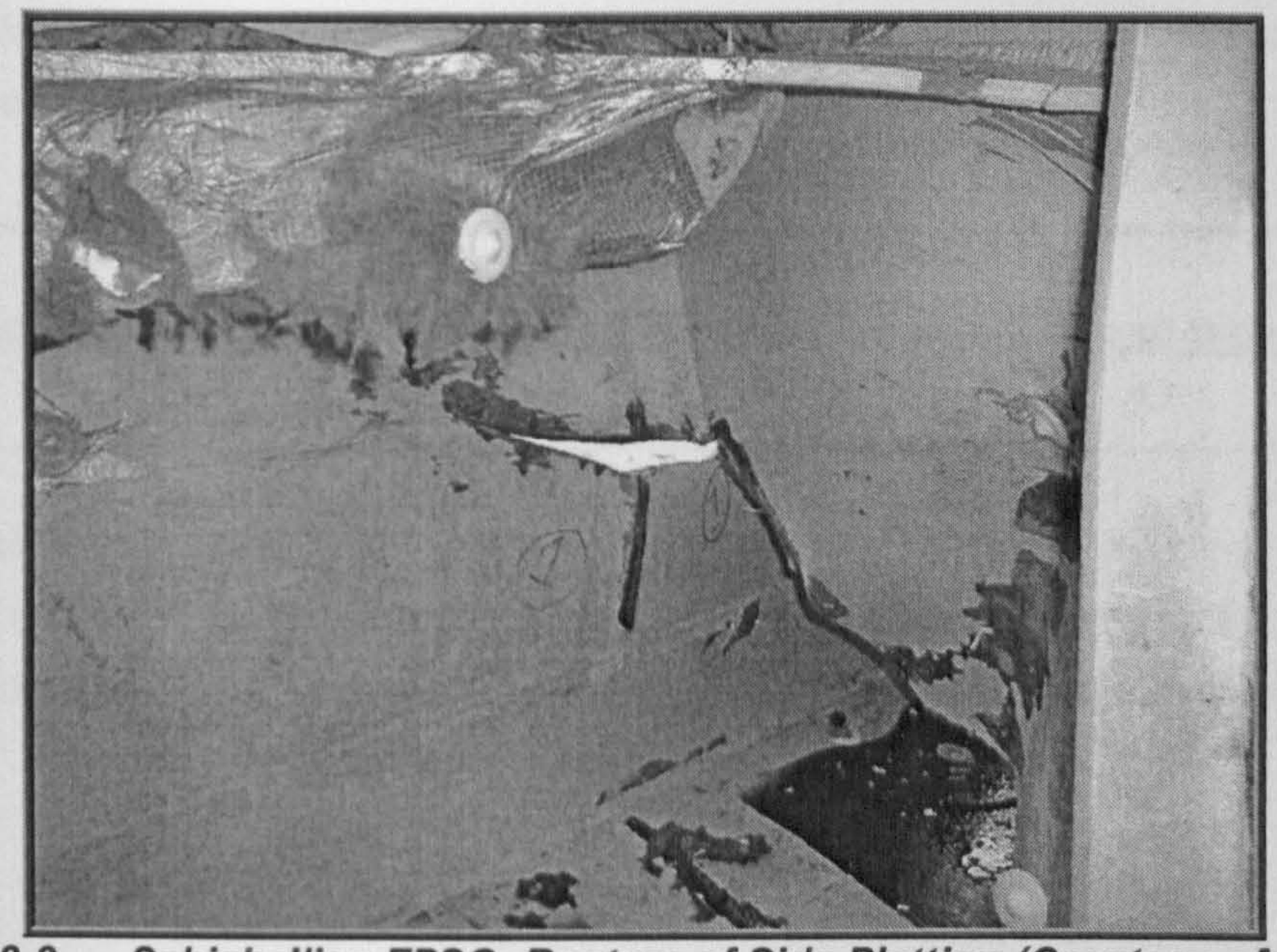

Figure 8-3 Schiehallion FPSO: Rupture of Side Platting (Courtesy of Harland and Wolff)

Figure 8-4 Schiehallion FPSO: Buckling of Stiffeners (Courtesy of Harland and Wolff)

In general unsymmetrical profiles will have a reduced fatigue life compared to symmetrical profiles unless the reduced effect of the unsymmetrical profile is compensated by an improved design for the attachment to transverse girder webs and bulkhead structures.

The main structural elements in the cargo area being of possible interest for fatigue evaluation are listed in ***Table 8-1***

Structure member	**Structural detail**	**Load type**
Side, bottom and deck plating and longitudinals	Butt joints, deck openings and attachment to transverse webs, transverse bulkheads, hopper knuckles and intermediate longitudinal girders	Hull girder bending, stiffener lateral pressure load and support deformation
Transverse girder and stringer structures	Bracket toes, girder flange butt joints, curved girder flanges, knuckle of inner bottom and sloped hopper side and other panel knuckles including intersection with transverse girder webs. Single lug slots for panel stiffeners, access and lightening holes	Sea pressure load combined with cargo or ballast pressure load
Longitudinal girders of deck and bottom structure	Bracket termination's of abutting transverse members (girders, stiffeners)	Hull girder bending, and bending / deformation of longitudinal girder and considered abutting member

Table 8-1 FPSO's Important Structural Elements for Fatigue Evaluation

The objective of the fatigue life evaluation is to ensure that critical structural details are fit for purpose in order to minimise the risk of fatigue cracking in service with

associated requirements involving expensive shutdown and repair. For new build FPSOs hulls the assessment will confirm the suitability of critical structural details for site specific design criteria. For conversions assessment will indicate critical areas of the structure requiring upgrading and confirm that the proposed scheme of modifications is acceptable.

Fatigue damage is a complex process and the development of fatigue cracks may be influenced by many variables not all of which are quantifiable. Fatigue cracking normally commences in welded connections at points of stress concentration resulting from an adverse combination of factors.

Fatigue life calculation of structural connections is a cumulative process largely based on the environment and loads experienced. Forces contributing to fatigue of the primary hull structure can generally be considered to have two components; i.e. hull girder bending and local pressure effects primarily due to waves. Where stress concentrations are present in association with significant magnitudes of stress variation then fatigue cracking may occur. Factors which influence performance, in that they affect the magnitude of stress ranges and stress concentrations, are as follows:

- The loading experienced.
- The quality of detail design.
- The standard of workmanship.
- Corrosion rates and magnitudes.

In addition similar structural details will differ in construction method, local material properties, member alignment, workmanship and levels of inspection which may be expected to lead to variations in the service performance of any particular detail.

Structural fatigue life evaluation together with experience gained from existing project survey records can also provide a valuable means to target inspections towards those areas demonstrated to be most at risk.

Fatigue damage starts prior to the initiation of a crack. With repeated loading, localised regions of slip (plastic deformation) develop. These deformations are accentuated by repeated loading, until a discernible crack finally appears.

The relative cycles for crack initiation and propagation depend on the applied stress. As the stress increases, the crack initiation phase decreases. At very low stresses (high cycle fatigue), therefore, most of the fatigue life is utilised to initiate a crack. At very high stresses (low cycle fatigue), cracks form very early.

The separation of high and low cycle fatigue is not clear-cut. Generally, the low cycle region is that which results from stresses that are often high enough to develop significant plastic strains. It is usually assumed that the separation zone for low and high cycles is of the order of 10^4 - 10^5 cycles to failure.

There are visual differences between high cycle (low stress) and low cycle (high stress) fatigue. In the latter, deformation resembles that seen with unidirectional loading. Strain hardening can occur and the slip bands are coarse. In high cycle fatigue, the slip bands are usually very fine.

Extensive laboratory modelling of fatigue behaviour was undertaken by the classification societies on a variety of structural configurations and yield strengths of steel to provide confidence in the fatigue design assessment. (See ***Figure 8-5***)

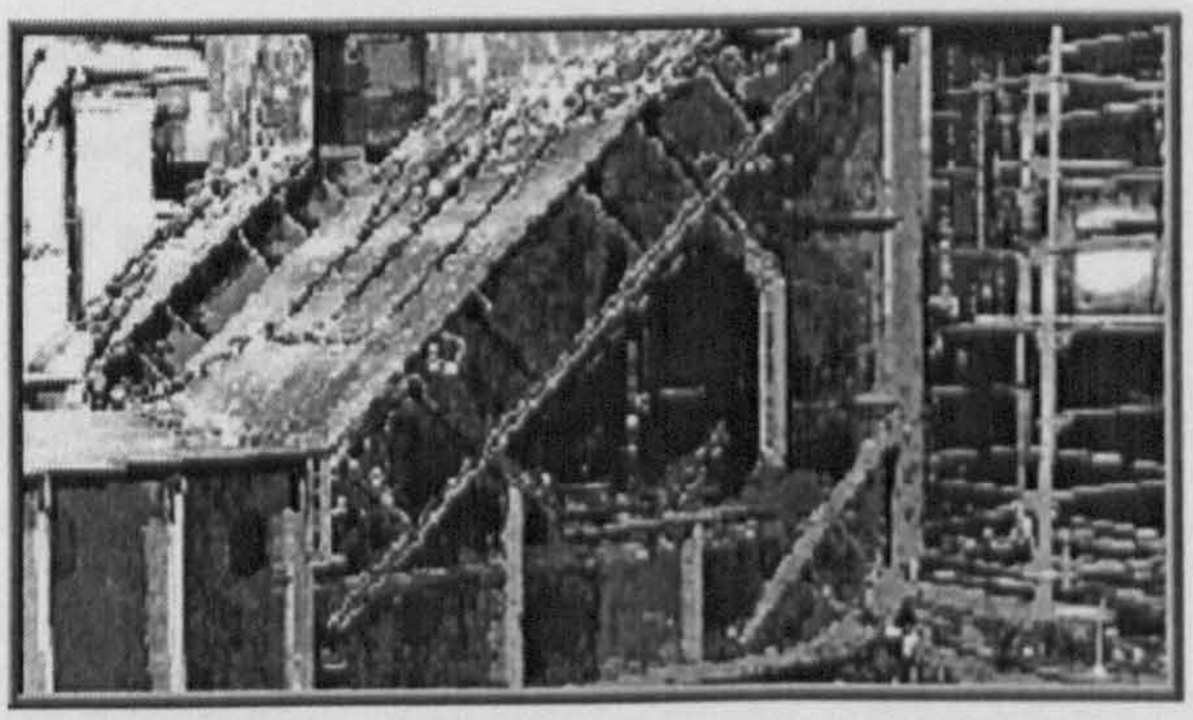

Figure 8-5 ***Laboratory Modelling of Fatigue Behaviour*** *(Courtesy of Lloyds Register of Shipping)*

8.2 Fatigue Analysis Basic Process

The following *Figure 8-6* below highlights the fatigue analysis basic process factors leading to fatigue life calculation.

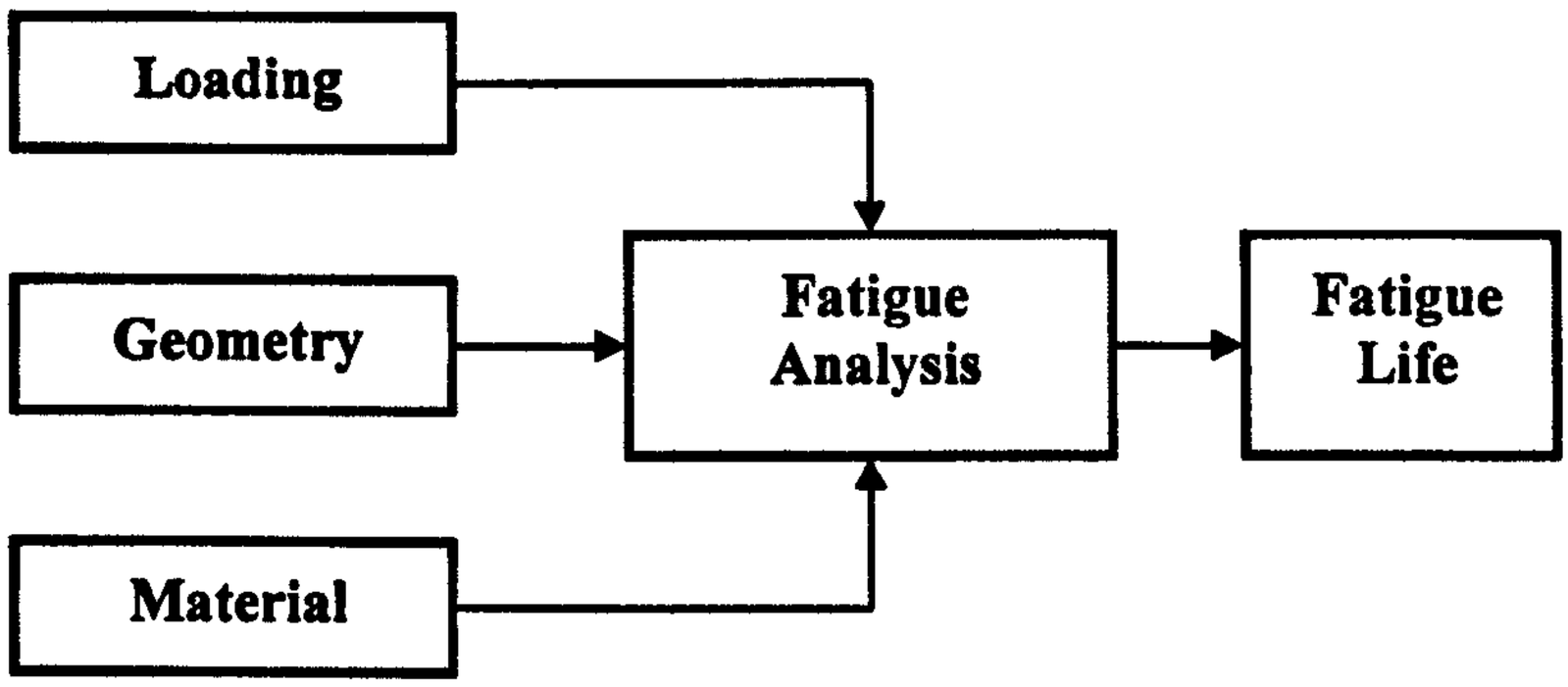

Figure 8-6 Fatigue analysis process

8.2.1 Loading

Loading information can be obtained using a number of different methods. Local or nominal strains can be measured by means of strain gages. Nominal loads can be measured through the use of load cells or, more recently, they can be derived externally by means of analysis.

Since early methodologies relied on measurement from physical components, the application of fatigue analysis methods has been confined to the analysis of service failures or, at best, to the latter stages of the design cycle where components and systems first become available.

The ability to predict component loads analytically means that physical components are no longer a prerequisite for durability analysis and so analysis can proceed much earlier in the design cycle.

It is important to note that, in this context, loading environment is defined as the set of phase-related loading sequences (time histories) that uniquely map the cyclic loads to each external input location on the component.

8.2.2 Geometry

In the context of fatigue analysis the term geometry is often used to describe how loads are transformed into stresses and strains at a particular point in a component. The effect of geometry may be determined in either one of two ways: Firstly, by means of an elastic stress concentration factor, K_t and secondly, by means of finite element analysis.

Stress concentration factors are used to calculate local stresses and strains at specific locations from their nominal equivalent or from the applied loading. Stress concentration factors for specific geometries are usually obtained theoretically from handbooks, experimental from stress analyses, or analytically from finite element methods.

Since the process needs to be repeated for every potential critical location within the component this approach becomes very bulky, particularly in situations where a large number of external loads are applied and multiple critical locations need to be considered. Finite element analysis can be used to calculate the stress distribution for an entire component or structure and so provides an ideal sign to durability analysis. By combining the linear elastic finite element methodology with fatigue analysis, the life at each node or element can be calculated.

8.2.3 Material

Another major input to fatigue analysis is a definition of how a material behaves under cyclic loading conditions. Cyclic material properties are used to calculate elastic-plastic stress-strain response and the rate at which fatigue damage accrues due to each fatigue cycle.

The material parameters required depend on the analysis methodology being used. Normally, these parameters are measured experimentally and may also be available in various handbooks and other publications. In situations where specific data are not readily available, approximate values may be deduced from static tensile properties such as ultimate tensile strength and ductility.

8.3 Fatigue Assessment of FPSOs Structure

The development of fatigue failure in stressed welded steel structure is influenced by a number of parameters including:

- The geometry of the connection and its welds.
- Steel material properties.
- The type, amplitude, mean, level and distribution of applied loading.
- The applied stress history.
- Fabrication and construction procedures.
- Post fabrication processes e.g. corrosion protection
- Localised environment

Fatigue life for a welded connection may be evaluated by reference to the long term distribution of stress ranges, determined by a suitable analytical technique, in combination with an appropriate S/N curve from which endurance can be found.

In general, any discontinuity in a stressed structure results in a local increase at the discontinuity. The ratio of the peak stress at the discontinuity to the nominal stress that would prevail in the absence of the discontinuity is referred to as the Stress - Concentration Factor (SCF). SCFs may be determined from published references, model tests and finite element analysis, etc.

The applied stress ranges should account for any stress concentration within the connection resulting from its shape but not the local stress concentration due to the presence of the weld, which is accounted for in the S/N curve.

The fatigue design curves are applicable to welded joints free from serious defects or discontinuities e.g. undercut, which can have a significant detrimental effect on fatigue strength. Fatigue damage/life may be estimated using the linear *Palmgren - Miner rule*.

The minimum design fatigue life for all structural components should not be less than the intended field life or 20 years whichever is greater. The cumulative damage ratio for individual components (normally taken as 1.0) should take account of the degree of redundancy and accessibility of the structure and also the consequence of failure.

For practical reasons it is also prudent to take into consideration the previous service history for conversions.

Cyclic loading due to waves, wind, current and mechanical vibration should be addressed in the fatigue evaluation, as relevant.

Service related factors which may influence the hull loads and should be considered include the following:

- Site specific environmental conditions. (For a conversion data relating to previous service may be based on a study of vessel records or where these are not readily available on an appropriate simplified representation of trading history).
- The effect of mooring forces.
- Extended service on location.
- Seas approaching predominantly from a narrow sector ahead, (180°).
- Zero ship speed.

Fatigue life assessment of all relevant and typical hull structural elements is required to demonstrate that structural connections have fatigue endurance consistent with the planned life of the vessel and compliance with minimum requirements.

Particular attention should be paid to connection details of the following:

- Main hull shell, bottom and decks.
- Main hull longitudinal stiffener connections to transverse frames and bulkheads (particularly those of the side shell in way of the wave zone).
- Openings in main hull.
- Integration of mooring system, with hull structure.
- mooring system structure
- Flare-tower.
- Major process equipment seat connections to hull.

For the main hull structure fatigue evaluation a minimum of three loading conditions should be included, typically: ballast (or light load) condition, 50% loaded and the fully loaded condition, with an appropriate amount of time allocated to each condition.

Two stress components should be considered the global and the local stress. The global stress component is caused by the hull wave bending moments. The local stress component is caused by the local effect of the wave pressure together with internal fluid action where significant.

Loadings are heavily influenced by the length of waves and their direction in relation to the ship length and draught. Wave directionality is narrow banded as the FPSO weather vanes.

In general, the global and the local stress components differ in amplitude, phase and location. The method of combining these stresses for the fatigue damage calculation will depend on the location in the structure.

- For deck components and adjacent side shell structure the local stress due to wave pressure can be considered as insignificant and the total stress in general to be the global stress, however local internal fluid loadings arising from ship responses may require consideration.

- For the bottom structure and adjacent side shell structure the intermittent wetting effect is insignificant. Local and global stress ranges can be calculated from the relative wave height and the wave bending moment, and combined using the phase information.

- For remaining side shell structure the situation close to the waterline is complicated by the non-linear effect of intermittent wetting. This can result in high frequency local bending stresses applied to the longitudinals and connection details at the transverse ring frames and bulkhead stiffeners. This may transfer moments resulting in further increased stresses in the side longitudinals. Similar considerations may apply in a lesser respect to longitudinal bulkhead stiffeners. In order to take this into account both the local and global stress ranges must be determined. For structure affected, the fatigue damage caused by the global and local stresses may be conservatively assessed by adding the stress ranges together. Alternatively the fatigue damage due to global and local stresses may be calculated separately and then combined using an appropriate relationship.

The major stress determining the fatigue loading spectrum of the Mooring System is the mooring system line loads. These loads are determined from model testing the FPSO and its mooring for a range of wave heights, using typical values for operating draft, and current. Site specific wave occurrence data is then used to derive a fatigue load spectrum. Fatigue appraisal needs to be carried out on the following items:

- turret structure
- main bearing
- main bearing attachment and support structure
- mooring lines
- mooring line chain stoppers and support structure

Castings are often used in the turret structure to simplify complicated weld detail joints. Special consideration needs to be given to these castings in fatigue. Fatigue loading of the support arrangements for process equipment, is governed solely by the inertia loads caused by motions of the FPSO. The process equipment vessels should be assumed to have a typical operating inventory. Allowance needs to be taken of the vertical, longitudinal and transverse centre of gravity positions, in determining the vessel global loads.

Consideration may also need to be given to the effect of hull displacements between process skid supports. Tall slender structures, such as flare towers, require special attention in respect of fatigue analysis. The summation of fatigue damage due to each of the following should be considered:

- vortex induced vibration of individual members,
- individual member loading due to roll, pitch and heave motions of the FF allowing for the member's vertical, longitudinal and transverse centre of gravity,
- Individual member loading due to wind load, allowing for wind variation with height and site specific wind data.

8.4 FPSO Structures

A key fundamental consideration related to fatigue performance in-service is the quality of detail design and construction. It is apparent that in many cases premature failure can be traced to inadequate detail design.

Fatigue strength is seriously reduced by the introduction of a stress raiser such as a notch or hole. Since actual structural elements invariably contain stress raisers like fillet welds, end brackets, cut-outs etc., it is not surprising to find that fatigue cracks in structural parts usually start at such geometrical irregularities. An effective way of minimising fatigue failure is by the reduction of avoidable stress raisers through careful design and the prevention of accidental stress raisers by careful fabrication together with attention to the relative stiffness of structural members to avoid secondary local restraint effects.

The most common types of imperfections are:

- Misalignment of structural member, poor fit up.
- Welding defects (such as undercut, lack of penetration, slag and porosity)
- Materials defects.
- Poor manufacture and fabrication procedures resulting in stress concentrations.
- Unfairness of plating.

Sudden changes in shape or section should always be avoided and for certain fatigue prone areas butt welds are preferred to double fillets. Where practical the use of symmetric stiffeners sections would also be advised.

Particular attention is required during design and construction when higher tensile steel material has been specified. Use of this material implies higher applied nominal and maximum stress levels with possible reduced fatigue performance.

In addition because the hull may then be relatively more flexible and have a lower natural frequency of vibration structural response to the more important short waves may be increased. Corrosion effects will be also magnified by the use of lighter scantlings.

The structural response is determined from first principles using a combination of simplified Finite Element beam model and analytical procedures. The structural response at the hot-spot locations is determined by using stress concentration factors associated with influence coefficients corresponding to each load component

applied to the structural member including interactive loading for primary supporting structure.

Short term stress response in irregular waves is achieved through combining the structural response influence coefficients and the regular wave load information. The resultant stress range is obtained by combining the structural response arising from each load component. A rigorous procedure is applied to account for the relative phase difference between each structural load component.

The fatigue damage rate and stress reversal frequency can be calculated from the short-term stress response and the fatigue strength characteristics of the structural detail.

The deterministic accumulated fatigue damage is converted into a probability of failure for a given number of service years using a probabilistic approach (***See Section 8.9***).

8.4.1 Structural Inspection

To ensure that the installation remains in a satisfactory condition it is a requirement for classification/certification that periodic surveys are carried out during service. These in-service inspections provide detection and monitoring capability regarding many aspects relating to the safety of the installation including structural damage and fatigue cracking and take the form of annual intermediate and special/major surveys.

To facilitate internal surveys it is essential that the compartment is properly cleaned and gas freed and that appropriate means of access and lighting are provided. This is clearly of particular importance for the in-situ survey of FPSO installations. The provision of access arrangements which enable the required surveys to be completed effectively and safely should be carefully considered during design.

The classification society's rules provide for *In-Water Surveys* (IWS) to allow inspections to be carried out on location in support of dry-docks. The IWS would require providing the information normally obtained from dry-docking. In this way the vessel can remain on station without dry-docking provided the IWS confirms that the vessel's condition remained satisfactory. It is not generally necessary to remove hull

coatings unless abnormalities have been discovered and further detailed examination required.

Continuous survey of hull, whereby all surveyable items are inspected in rotation over a 5 year period, is acceptable provided a detailed programme is developed.

A schedule for survey should be produced to guide and control all aspects of the inspection and replacement philosophy. The schedule should address:

- The overall design configuration
- Field life potential
- Minimum regulatory requirements
- Personnel qualifications
- Inspection schedules for all appropriate components/systems
- Replacement schedules
- Methods and procedures

Particular attention is to be paid to critical areas and also to areas of suspected damage or deterioration and to previously repaired areas. The survey should take into account locations highlighted by operational experience and design assessments.

The *Offshore Technology*, (1997) highlighted a strategy, which is currently receiving considerable attention; The probabilistic approach to inspection Schedules developed for fixed jacket structures and mobile offshore units, have demonstrated potential for significant cost savings without compromising safety criteria. The application of this approach to FPSO's is being studied.

8.4.2 Structural Repair

Whilst the necessity for repair may be effectively minimised by careful attention to detail design, fabrication and analytical calculations, experience indicates that structural problems may occur in service. Not all defects/cracks will have developed as a result of fatigue however; many will be due to inbuilt fabrication and welding defects.

Following discovery of a defect a detailed examination should be carried out in order to fully assess the structural implications. The following information should be obtained as appropriate:

- the location including structural boundaries when involved
- whether defect is internal/external
- extent of the defect
- risk of contamination
- prevailing conditions

Based on the information available a decision may be agreed by the operator and certifying authority regarding appropriate action. This may take the form of inspection monitoring and review, weld grinding or complete structural repair depending on the nature and severity of the problem. The intention is to ensure that the structural integrity of the unit is not compromised and remains fit for purpose.

Consideration should be paid to the following when developing proposed remedial repair and monitoring procedures:

- location and criticality of defect
- facilities required
- access arrangements
- materials/repair method/weld procedure
- protective coatings
- post repair inspection
- subsequent monitoring program

Typical repairs would range from carefully controlled grinding for small surface cracks to welded repairs of extensive damage and possibly local structural modification where repeated repairs have been made.

8.4.3 FPSO Strength and Stability

Floating production installations will be designed to endure long term deployment, perhaps in an extremely harsh environment. In order to minimise

production down time, vessels may be expected to operate without scheduled dry-dockings and be surveyed on station.

In order to fulfil these operational requirements it is necessary that the structure has adequate overall strength consistent with the long term site environment, and good local detail design to ensure satisfactory fatigue performance. In addition, high quality construction standards will be required of the building or conversion shipyards.

Ship classification rules can be used as an appropriate standard for the minimum structural requirements of an FPSO, however, additional factors will have to be considered at an early stage.

The maximum extreme wave bending moment and shear force is to be determined for the design environment, generally the fifty year storm. This will evaluate the long term extreme responses and will be based on the specific wave spectrum for the proposed location. The maximum wave bending moment and shear force may exceed the rule values, particularly in exposed locations.

In calculating the still water bending moments and shear forces, a range of conditions should be considered. These will include full load, ballast and intermediate conditions. In addition it will be necessary to include conditions where each tank is empty in turn. This will then allow the in location inspection of tanks to be carried out with minimum disturbance to production. Some recent designs have considered conditions with adjacent tanks empty to allow the possibility of "hot work" in tanks, should in location repairs ever be necessary.

It is unlikely that the additional weights of process equipment etc. added to a converted ship will significantly increase the still water bending moment; however, stability aspects will require careful examination when assessing the feasibility of a conversion. This is both because of the likely increase in the centre of gravity and the necessity to meet the requirements of damage stability criteria such as those specified in MARPOL the (International Convention for the Prevention of Pollution from Ships).

8.5 Fatigue Performance

It is essential that the fatigue performance of the vessel is carefully assessed. Although the design of trading tankers has a good degree of structural redundancy and can sustain fatigue cracking without catastrophic failure, they have the advantage of a regular dry-docking schedule which allows any necessary repairs to be carried out.

An FPSO unit will generally be expected to operate continuously throughout the field life without any scheduled dry-dockings.

FPSOs may experience a more difficult fatigue environment than a trading tanker because they are permanently exposed to fatigue loading, whereas a trading tanker may only spend approximately 70% of its life at sea.

FPSOs also experience a highly directional fatigue load spectrum from a narrow band from ahead. For conversions, the fatigue analysis should account for previous service. Reducing the risk of fatigue damage can be achieved by good detail design, for example, by following the requirements specified in the Classification Societies procedures.

Critical areas include the side shell longitudinals, particularly those between the deep draught waterline and a couple of metres below the light draught water line. The use of symmetrical sections is preferred for these longitudinals although this is not mandatory. It may also be necessary to increase scantlings above the rule minima in these areas.

For tanker conversions it is generally necessary to improve local detail design by the addition of lugs at bottom longitudinal to transverse connections, and the addition of soft brackets and backing brackets on side shell longitudinal to transverse connections, if these are not already fitted as illustrated in ***Figure 8-7.***

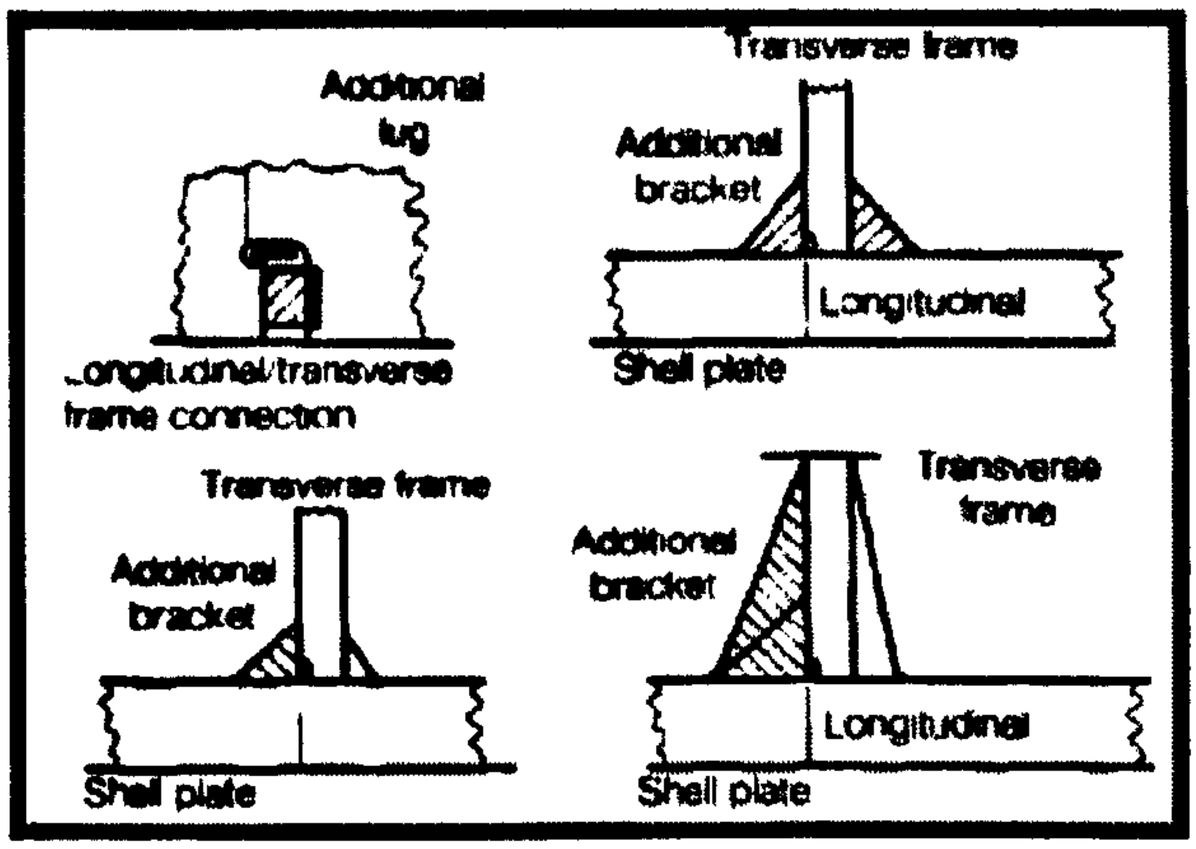

Figure 8-7 ***Modifications to FPSO Structural Details*** *(Tanker Structure Co-operative Forum)*

8.6 Major Factors Affecting Fatigue Behaviour

Several major factors have to be reviewed when comparing the anticipated fatigue performance of structures in navigating tankers and in FPSO's.

8.6.1 Types of Loads due to Waves

In calculation of sea responses one need to use some theoretical model to describe the wave energy in terms of heading and frequency content. Such descriptions have implications on the calculated stress ranges in terms of responses of the ship in terms of motions and sea pressures. This is today under evaluation based on full-scale measurement programs that will enable to correlate sea pressure calculations with simultaneous measurements of waves.

Several parties put quite some effort into full-scale measurements now that wave data become available through wave radars and Doppler sound devices. Preliminary findings indicate that common wave spectrum models may give too large stresses compared to the measured strains in moderate sea-states relevant for fatigue.

An FPSO has zero speed and the wave directions are reduced to head waves with a small spreading. This means increased wave loads on the fore-body, while the loading on the sides can be smaller due to the fact that rolling is far reduced. As seen in ***Figure 8-8*** FPSO heading 180°.

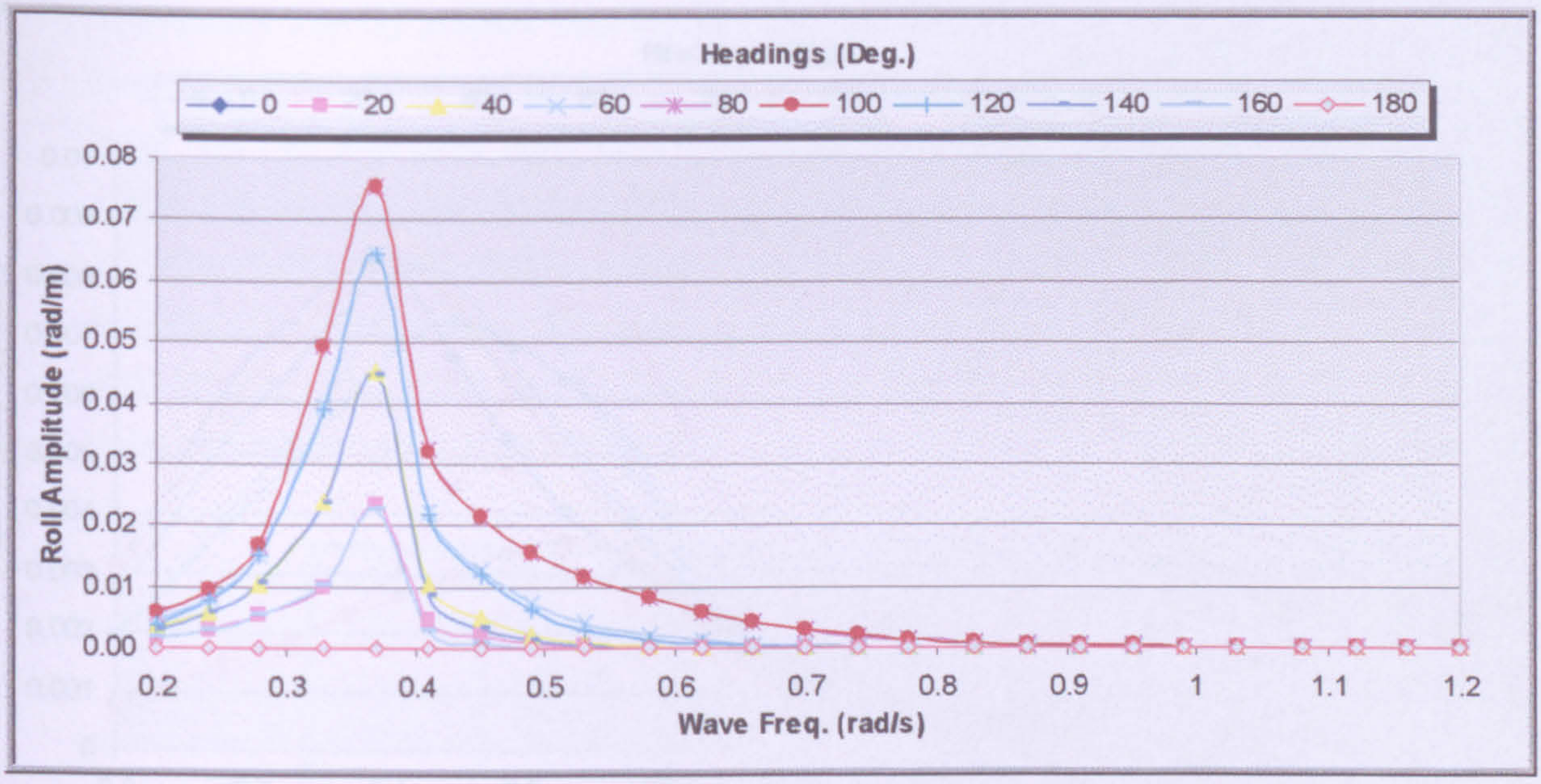

Figure 8-8 Roll Amplitude (rad/m), (Speed: = 0.00 %VS, Loading: = Full)

Due to dominant head waves, more attention has to be paid to pressure fluctuations magnified by heave and pitch motions especially at the vessel's ends as demonstrated in ***Figure 8-9*** and ***Figure 8-10***. Furthermore, vertical hull girder bending is more pronounced on an FPSO than on a navigating tanker.

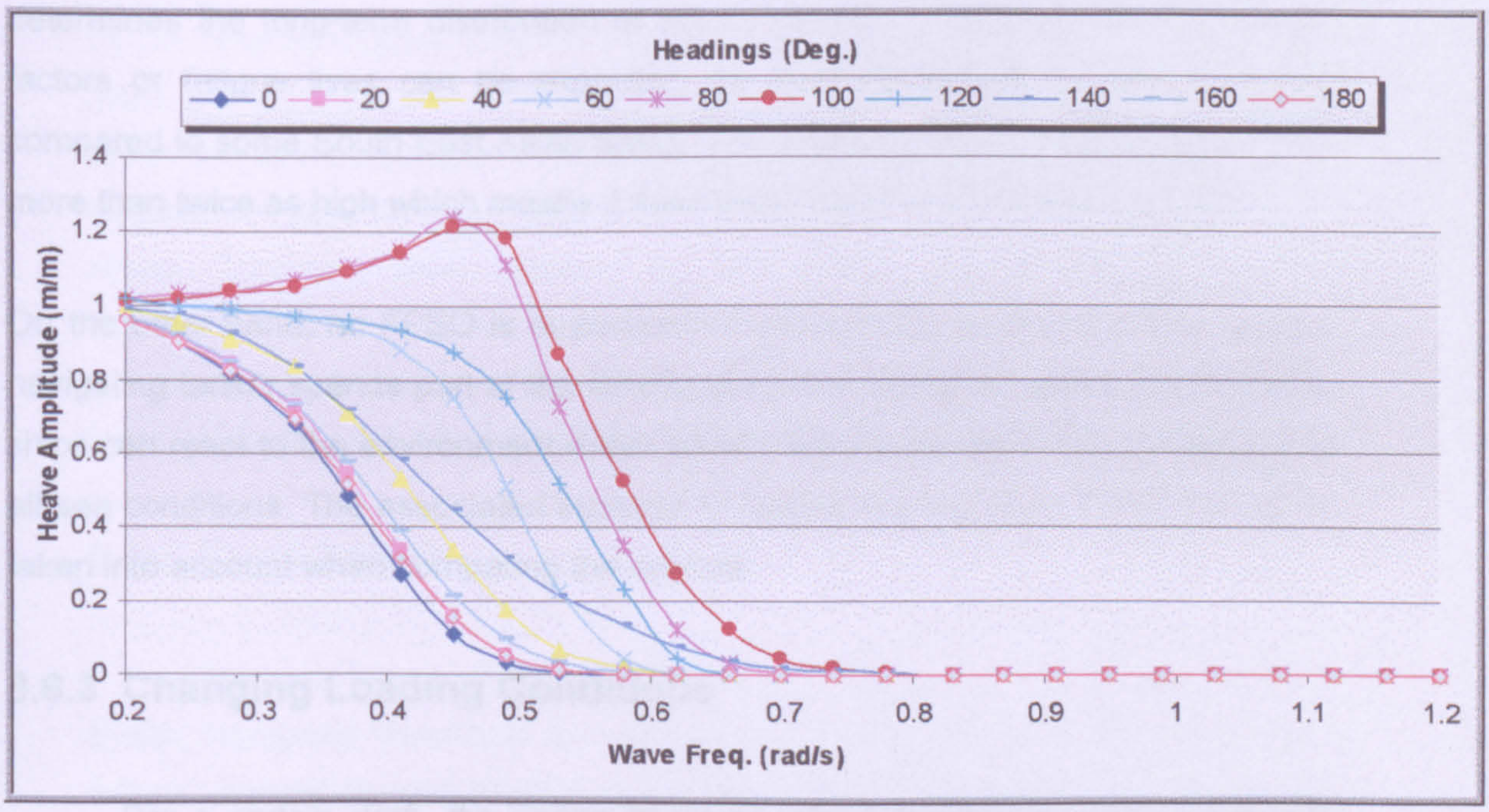

Figure 8-9 Heave Amplitude (m/m), (Speed: = 0.00 %VS, Loading: = Full)

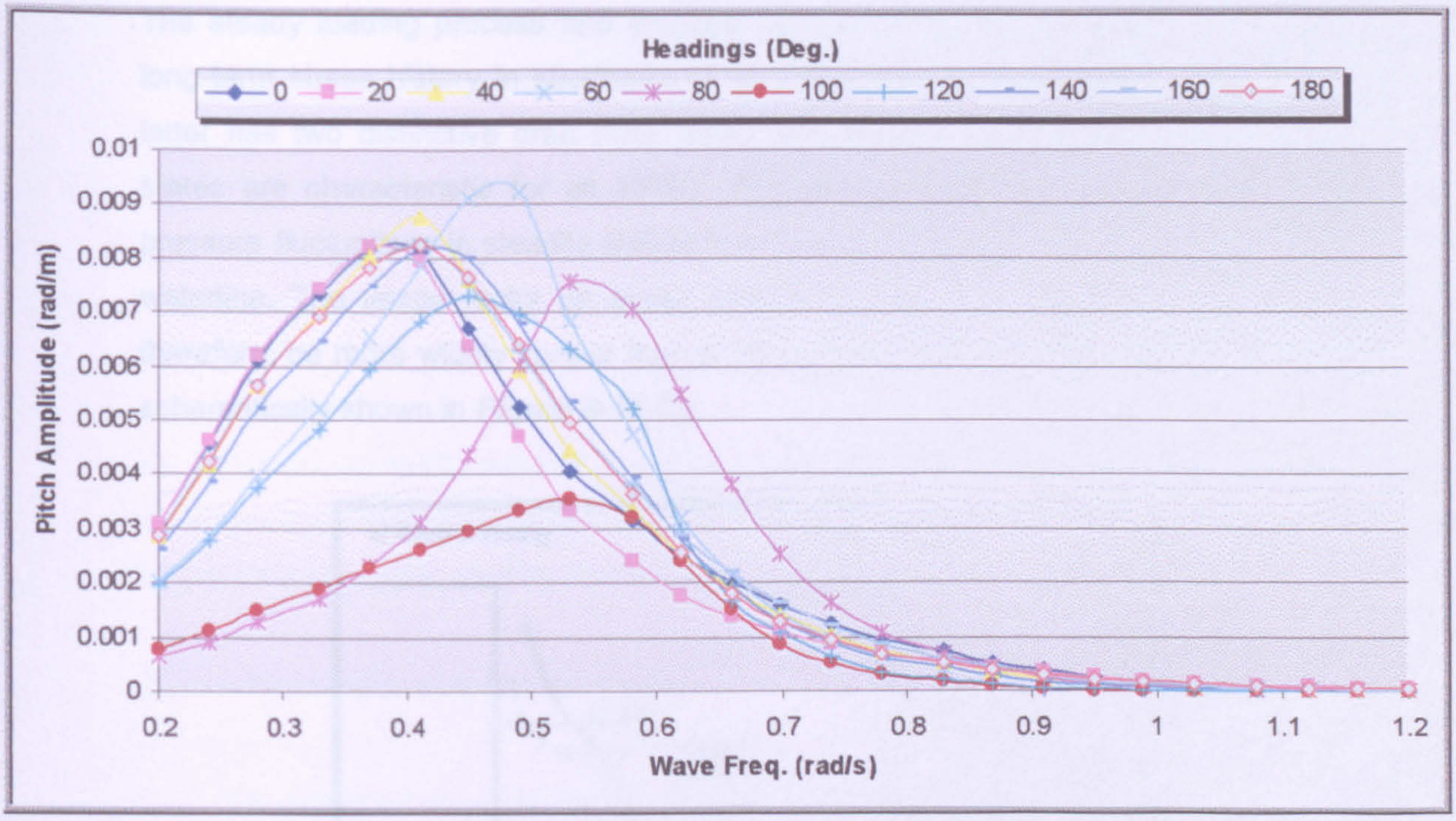

Figure 8-10 Pitch Amplitude (rad/m), (Speed: = 0.00 %VS, Loading: = Full)

8.6.2 Wave Climate

The wave climate of the operation area plays, of course, a dominant role and determines the long-term distribution of stress ranges. Completely different usage factors or fatigue lives can be expected, for example higher, in the North Sea compared to some South East Asian areas. The usage factor of stress range can be more than twice as high which means a theoretical factor of more than ten in life.

On the other hand, an FPSO is in permanent operation in its environment, while a navigating tanker spends part of the time in ports and sheltered areas. Furthermore, ships can react to the environment within certain limits while an FPSO is exposed to all sea conditions. The associated increase in fatigue loading of an FPSO has to be taken into account when comparing the vessels.

8.6.3 Changing Loading Conditions

For a certain draft, the usage factor of stress ranges caused by pressure fluctuations reaches high values in a smaller region if rolling is reduced as shown schematically in ***Figure 8-11*** (a).

The steady loading process and frequent offloading creates a completely different long-term stress history in structures of an FPSO than in a navigating tanker. The latter has two distinctive draft (fully laden and ballast), while several intermediate states are characteristic for an FPSO. This means that the area of largest side pressure fluctuations is steadily shifted from below the ballast waterline to the laden waterline. The usage factor on stress ranges caused by pressure fluctuation wills therefore, be more widely spread than in the case of one or two distinctive drafts as schematically shown in ***Figure 8-11*** (b).

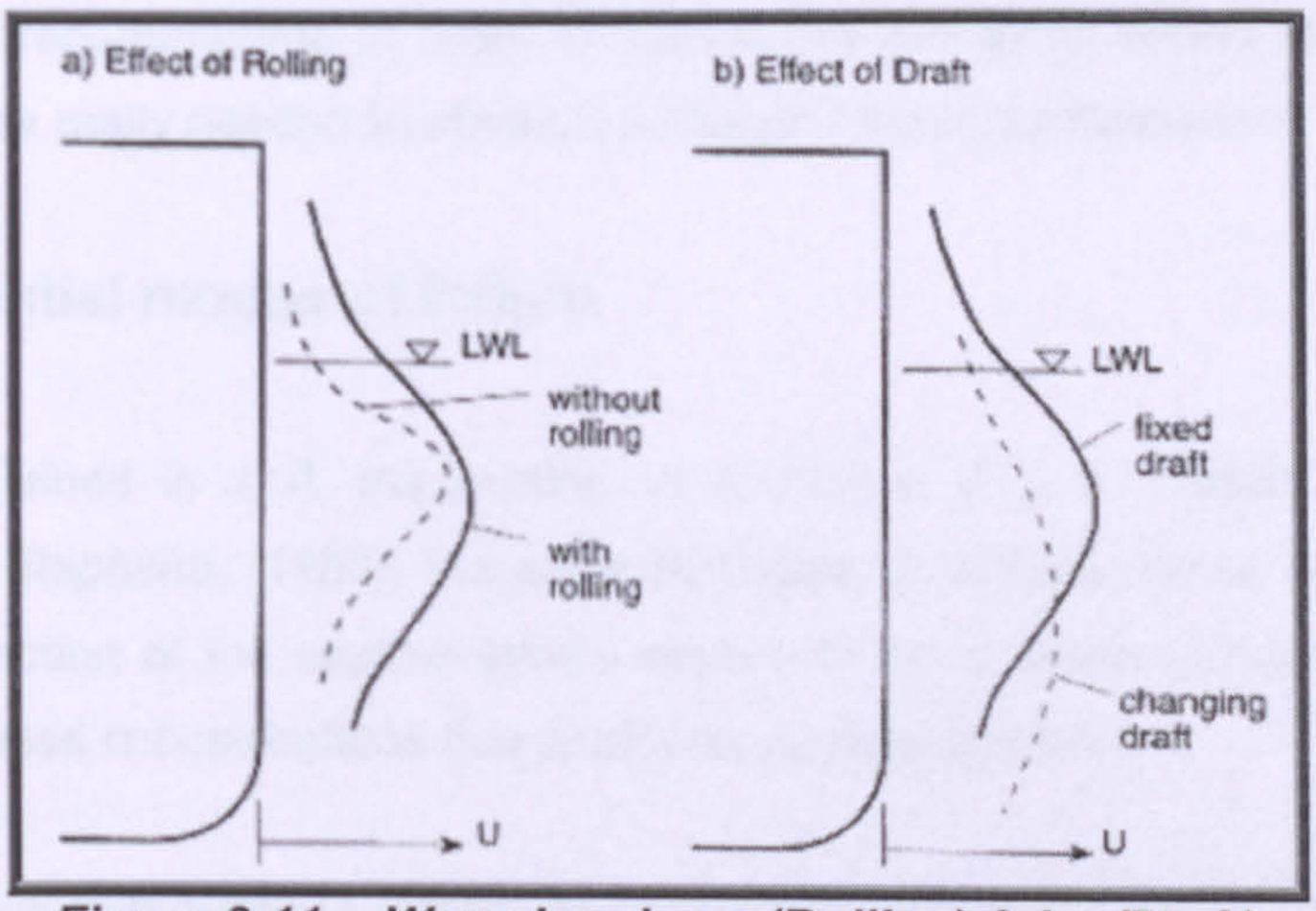

Figure 8-11 Wave Loads a= (Rolling) & b= (Draft)

On the other hand, more frequent changes between ballast and fully laden conditions might create problems in an FPSO with respect to low cycle fatigue. The number of cycles due to the loading and offloading can be between 500 and 1000 or even more within the service life that is quite high in case of local stresses exceeding the yield stress. Therefore, local stresses at intersections between longitudinals and transverses should be limited not only with respect to fluctuating wave loads, which is common practice at present for side longitudinals, but also with respect to hydrostatic loads which are largest in the bottom *W. Frick & H. Paetzold,* (1987).

8.6.4 Detail Design

The most important factor is detail design, coupled with adequate fabrication quality. Numerous theoretical and experimental investigations have shown that the fatigue strength depends highly on the geometry of the structural detail and the welded connections. Stress concentrations due to the structure and due to the

welded joints can often be reduced in order to achieve good fatigue behaviour even in case of increased nominal stresses.

Two effects are beneficial, firstly the reduced stress concentration due to the soft transition at the critical point, I. e. the bracket toe, and secondly the reduced nominal bending stress in the longitudinal due to the distance between bracket toe and theoretical supporting point.

As additional brackets, collar plates etc. result in additional building costs, extensive analyses are recommended in order to reduce the additional efforts to those areas where they are really needed to obtain a sufficient fatigue performance.

8.6.5 Potential modes of failure

As explained in *J. A. Bannantine, J. J. Comer, & J. L*, (1990) and in *H. O. Fuchs & R.I Stephens*, (1980), the potential modes of fatigue failure are dependent upon the direction of the applied stress relative to the position of the weld and the position of stress concentrations due to structural discontinuities.

For longitudinal butt welds in plates, dressed flush, and lying parallel to the direction of applied stress, the initiation of potential fatigue failures is expected at weld defect locations. In the 'as-welded' condition, fatigue cracks may be initiated at the weld start-stop positions or, weld surface ripples. For transverse butt welds in plates, essentially perpendicular to the direction of applied stress, the fatigue strength depends largely upon the shape of the weld profile. Fatigue cracks normally initiate at the weld toe.

Cruciform fillet weld joints may be separated into two distinct types depending on whether or not the fillet weld transmits direct load i.e. non-load carrying or load carrying cruciform joints. In the case of the non-load carrying cruciform joint, the fatigue crack will initiate at the weld toe and propagate through the thickness of the load bearing plate in a plane perpendicular to the direction of the applied stress.

In load carrying cruciform joints, in addition to the weld toe, acute stress concentration occurs at the root of the fillet weld and generally fatigue cracks are initiated at the root of the weld and propagate through the weld throat. The fatigue life

of such connections can be improved either by increasing the throat size of the fillet weld or by requiring improved weld penetration. In high stress regions however, such measures may not be adequate and there is then a need to specify a full penetration weld in order to achieve the necessary fatigue life for the joint.

Tee joints, since they represent a semi-cruciform joint, would be expected to demonstrate similar fatigue characteristics to the load bearing cruciform joint. However, if bending stresses are induced in the base plate material of the tee, which are of a similar or greater magnitude than the direct stress in the tee, then a fatigue crack may initiate in the base plate at the toe of the fillet weld, and propagate through the base plate.

Where tee or cruciform connections employ full penetration welds, and the plate material is subject to significant strains in a direction perpendicular to the rolled surfaces, it is recommended that consideration be given to the use of special plate material with specific through thickness properties.

For welded stiffeners and girders, fatigue cracks can be expected to be initiated at weld toes and may be associated with local stress concentrations at the weld ends of connecting end brackets or stiffeners.

8.6.6 Welds

Some commonly used weld details have low fatigue strength as explained in *Hobbacher A*, (1996). This applies not only to joints between members, but also to any attachment to a loaded member, whether or not the resulting connections are considered to be structural.

The heat-affected zone (HAZ) is of great importance to the fatigue strength of welds because this is usually the region where a fatigue crack will develop. Moreover, when the reinforcement of a butt weld is not removed, or when fillet welds are used, a resulting sudden change of section occurs, and stress concentrations occur at the weld toe.

8.7 Methodology of FPSOs Fatigue analysis Determination

8.7.1 Hotspot stress determination

It has been established from the previous chapter of this work, that the Hotspot Stress methodology is one of the potential methods leading to effective fatigue analysis evaluation.

A survey of the literature revealed only nine published papers containing hot spot stress S-N data relevant to structural details in FPSO structures *Yagi J and Tomita Y*, (1992) , *Kawono H and Inoue K*, (1993) , *Dexter R J, Tarquinio J E and Fisher J W*, (1994) , *Koskimaki M and Niemi E*, (1995) , *Marquis G B and Kahonen A*, (1995) , *Huther I, Lieurade H P, Sayki N and Buisson R*, (1996) , *Andrews, R. M*, (1996) , *Dahle T*, (1997) , and *Miki C and Tateishi K*, (1997). In addition, results from the recent JIP, *Kim, W. S*, (1999).

Although hotspot stresses determined by FEA in some cases, this was not generally the case and greater reliance placed on measured stresses. Therefore, in the present JIP assessment the fatigue test results were evaluated in terms of hot-spot stresses estimated from measured strains, FEA results only being used in one case, *Dahle T*, (1997), when measured stresses were not quoted.

An advantage of using measured stresses is that allowance is included for any secondary stresses in the test specimens, for example due to misalignment, which would not be included in FEA of an idealised geometry. Consequently, scatter in the fatigue data reduced. However, against this it needs to be concluded that the resulting hot-spot stress S-N curve will be less conservative as a design curve than one based on lower-bound FEA estimates of the hot-spot stresses, as used in the evaluation of fatigue data from the present JIP by *Fricke W*, (2001)

In most cases it proved possible to determine the extrapolated hot spot stress and the stress 0.5t from the weld toe. There was not usually sufficient information to determine the third hotspot stress, by extrapolation from stresses 0.5t and 1.5t from the weld toe, but where possible this was also estimated.

Nowadays sophisticated analysis methods are available for reliable fatigue life predictions of FPSO as highlighted in *Maddox S. J.*, (1997), Obviously different approaches need to be applied for newly built FPSO's or hulls converted from existing tankers as explained in *DNV*, (2000).

It is to be mentioned that most of the FPSO's in service world-wide still have to prove that they meet the expectations regarding their fatigue life performance, as the majority of them have been in use for less than 10 years.

It is necessary to point out that the hot-spot stress SN curves must be matched to the specific modelling approach and/or extrapolation method adopted. Classification Societies have been participating in a joint industry project with partners from ship builders and designers to try to obtain a more definitive procedure for the hot-spot stress approach.

The adopted methodology procedure illustrated in
Figure 8-12 is used in regard of the Fatigue Calculation by the participants in the joint industry project (JIP).

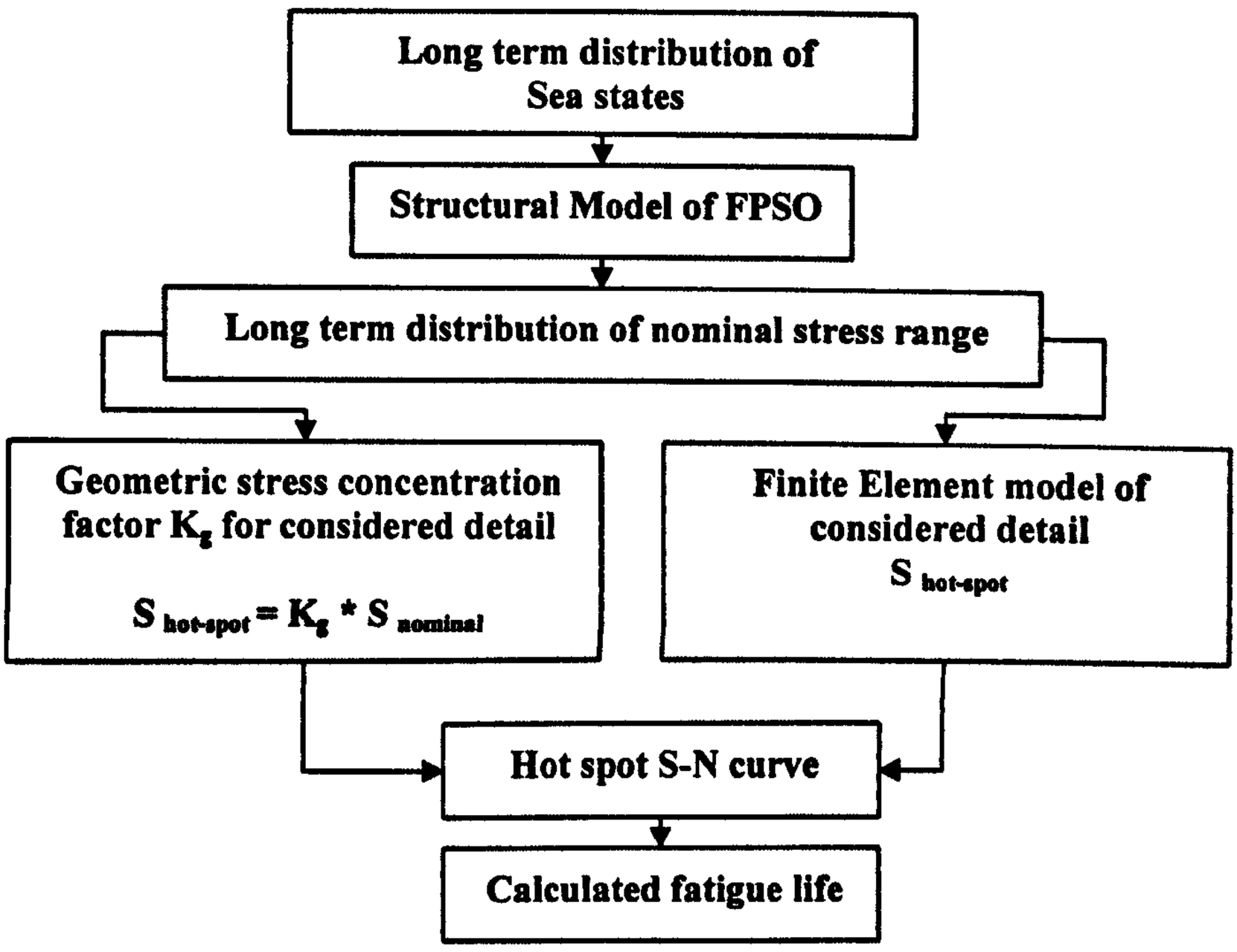

Figure 8-12 Schematic Fatigue Life Calculation "Fatigue Capacity" JIP

8.7.2 S-N Curves

HSE, (1995) emphasise that the S-N data and stress concentration factors (SCFs) related to each other and therefore should be considered together so that there is a consistent basis for the fatigue assessment. A material's fatigue characteristics are fatigue strength and fatigue limit. The fatigue strength is the stress range beyond which the material will fail at a specified number of stress cycles.

The fatigue limit is the fatigue strength corresponding to an infinite number of stress cycles. The S-N curve, shown in ***Figure 8-13*** below represents the dependence of the life of the 'specimen' in a number of cycles, *N*, to the maximum applied stress range, *S*. *N* is usually taken (unless specified otherwise) as the number of stress cycles to cause a complete fracture in the "specimen". Usually no distinction is made between the number of cycles to initiate a crack and the number of cycles to propagate the crack completely through the specimen, although it can be appreciated that the number of cycles for crack propagation will vary with the dimensions of the specimen.

Fatigue tests for high cycle fatigue are usually carried out for 10^5 to 10^7 cycles and sometimes to 5×10^8 cycles for non-ferrous metals. For a few important engineering materials such as steel and titanium, the S-N curve becomes horizontal at a certain limiting stress. Below this limiting stress, which is called the fatigue limit, or endurance limit, the material can presumably endure an infinite number of cycles without failure.

The basic design curves consist of linear relationships between $\log(S_B)$ and $\log(N)$. They are based upon a statistical analysis of appropriate experimental data and may be taken to represent two standard deviations below the mean line.
Thus the basic S-N curves are of the form *Steel Vessels*, (1997)):

$$\log(N) = \log(C_2) - m \log(S_B)$$

where

$$\log(C_2) = \log(C_1) - 2\sigma$$

N is the predicted number of cycles to failure under stress range S_B;

C_1 is a constant relating to the mean S-N curve;

σ is the standard deviation of log N;

m is the inverse slope of the S-N curve.

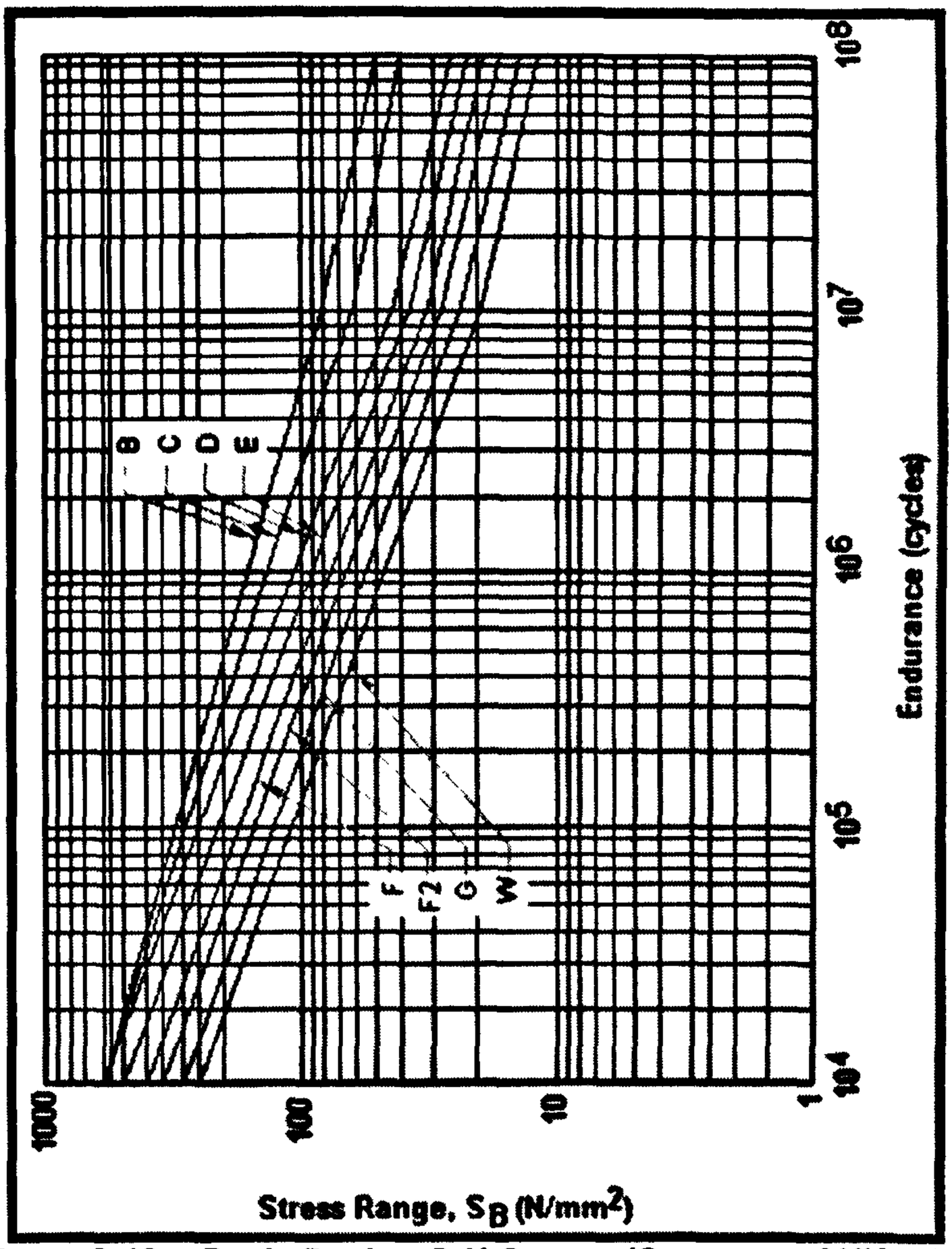

Figure 8-13 Basic Design S-N Curves (Courtesy of UK HSE)

The relevant values of these terms are shown in the table below.

Class	C_1	C_4		m	Standard deviation		C_2
		Log10	loge		Log10	loge	
B	2.343×10^{15}	15.3697	35.3900	4.0	0.1821	0.4194	1.01×10^{15}
C	1.082×10^{14}	14.0342	32.3153	3.5	0.2041	0.4700	4.23×10^{13}
D	3.988×10^{12}	12.6007	29.0144	3.0	0.2095	0.4824	1.04×10^{12}
E	3.289×10^{12}	12.5169	28.8216	3.0	0.2509	0.5777	1.04×10^{12}
F	1.726×10^{12}	12.2370	28.1770	3.0	0.2183	0.5027	0.63×10^{12}
F2	1.231×10^{12}	12.0900	27.8387	3.0	0.2279	0.5248	0.43×10^{12}
G	0.566×10^{12}	11.7525	27.0614	3.0	0.1793	0.4129	0.25×10^{12}
W	0.368×10^{12}	11.5662	26.6324	3.0	0.1846	0.4251	0.16×10^{12}

Table 8-2 Basic S-N Curves Data (Courtesy of UK HSE)

Since the fatigue properties of higher tensile steels are generally similar to those of mild steel, the higher allowable general stress magnitudes could entail a shorter fatigue life in standard details. Assuming that the fatigue life is a function of the stress range to the third power, it is clear that detail design requires special consideration to reduce the effects of stress concentrations. If higher tensile steels are incorporated and hence higher stress levels are accepted, then structural details, which would have been acceptable in mild steel structure, might not be adequate.

The occurrence of cracking in ships is of prime concern from both a safety and maintenance point of view. Experience has shown that fatigue cracks in ships' structures are normally of a self-limiting nature. However, the existence of fatigue cracking may, if not repaired, render the structure susceptible to subsequent brittle or fast fracture. Thus both types of cracks are significant from a maintenance point of view. Fatigue cracks, if not repaired, may also initiate catastrophic failure as a consequence of the more extensive use of structural optimisation leading to a decrease in the level of structural redundancy.

8.7.3 S-N curves for welded connections

Several of the traditional fatigue design codes divide structural details into classes, each with a corresponding design S-N curve. A large number of ship structural details are different from the details the traditional S-N curves have been derived for. It may therefore be difficult to separate the calculated stress into the stress level that is embedded in the S-N curves and the stress level that must be applied together with the S-N curves.

Due to this, it was considered more convenient to develop a basic S-N curve that could be used for fatigue analysis of all welded structural details. This could be achieved by developing appropriate stress concentration factors to be used to obtain the local notch stress used together with the basic S-N curve. Inherent in the S-N curves for classified details are both the notch stress and also the stress field over the crack growth area giving the actual crack growth development.

This may be considered to give more accurate fatigue lives than the use of a single S-N curve and stress concentration factors. However, the difference between these two concepts is evaluated to be of minor importance for practical fatigue design of

ship structural details, as the main portion of the fatigue life is within the initial stage of the crack size development.

8.7.4 Stresses to be Associated with S-N curves

It is important that there is consistency between the way the S-N curves are derived and defined and the way the stress in the structure is calculated. It is necessary to know what stress is inherent in the considered S-N curve, how this stress is determined and how the corresponding stress from numerical analysis should be evaluated. Definition of stresses used in the Classification Societies Notes is as follows:

- Nominal stresses are those derived from beam models or from coarse mesh FEM models. Stress concentrations resulting from the gross shape of the structure are included in the nominal stress.

- Geometric (hot spot) stresses include nominal stresses and stresses due to structural discontinuities and presence of attachments, but excluding stresses due to presence of welds. Stresses derived from fine mesh FEM models are geometric stresses. Effects caused by fabrication imperfections as e.g. misalignment of structural parts, are, however, normally not included in FEM analyses, and must be separately accounted for. The greatest value of the extrapolation to the weld toe of the geometric stress distribution immediately outside the region affected by the geometry of the weld, is commonly denoted hot spot stress.

- Notch stresses are the total stresses at the weld toe (hot spot location) and include the geometric stresses and the stresses due to the presence of the weld. The notch stress may be calculated by multiplying the hot spot stress by a stress concentration factor, or more precisely the theoretical notch factor, K FEM may be used to determine the notch stress. However, because of the small notch radius and the steep stress gradient at a weld, a very fine mesh is needed.

Traditionally fatigue calculations are based on the nominal stresses and the use of geometry dependent S-N curves. S-N curves may also be developed based on the

concept of hot spot stresses saying that the effect of the notch stress due to the local weld detail is imbedded in the curve, or alternatively, based on the notch stress where the influence of the weld is included.

All concepts have their advantages and disadvantages:

8.7.5 Nominal Stress Approach

Advantages: Inherent in the S-N curves for classified details accounts for both the notch stress and the stress field over the crack growth area.

Disadvantages: It is difficult in practical design of ship structural details to define the nominal stress level to be applied together with the geometry specific S-N curves. Further, the use of a limited number of established S-N curves in the fatigue design complicates the utilisation of improved local design and workmanship in the fatigue life assessment.

8.7.6 Geometric Stress (Hot Spot Stress) Approach

Advantages: Using the hot spot stress method the local notch effect is embedded in the S-N data, and one may say that the large variation in local notch geometry is accounted for in the scatter of the S-N data.

Disadvantages: The hot spot stress has to be determined by extrapolation of stresses outside the notch region. The finite element mesh has to be fine enough to represent the geometric stress in this region. Extrapolation should be performed from points at least 0.3t outside the notch. Practise for extrapolation has varied as its basis is founded on experience from test measurements and numerical analysis of stress distributions at the hot spot region.

8.7.7 Notch Stress Approach

Advantages: The notch stress need not be separated from the geometric stress, and the notch stress is derived as the finite element size approaches a small value provided the notch root radius is modelled.

Disadvantages: The geometry of the local notch at a weld varies along the weld profile, and it may be difficult to find geometry to base the analysis on. However, considering that the scatter in local notch geometry is accounted for in the scatter of the S-N data the geometry for local analysis may be based on mean geometry data.

During evaluation of these concepts, a basic S-N curve was selected by classification societies for welded connections that was also applicable for smooth machined specimens having a stress concentration factor K = 1.0 by definition. This corresponds then to the notch stress concept. However, a default value K = 1.5 is introduced such that the hot spot stress method may be used. The calculated hot spot stress must then be multiplied by the K value before the S-N curve is entered.

A procedure that allows the effects of fabrication methods and workmanship to be explicitly accounted for in the fatigue analyses is believed to contribute to improved local geometry and workmanship in shipbuilding. In this way one may say that the advantages of both the concepts described above have been utilised.

8.8 Calibration of S-N Curves

8.8.1 Introduction

In order to perform fatigue life analyses it is necessary to have precise knowledge about the stress level for a given loading in a critical structural detail. Traditionally the nominal stress has been used to describe the fatigue loading. The increase in the stress level at the hot-spot due to the geometry of the detail is taken into consideration through the choice of the S-N curve.

The finite element method makes it possible to directly obtain the hot-spot stress. Unfortunately, for certain geometries the accuracy of the finite element results depends directly on the element size for a given type of element. A finer mesh will in general improve the accuracy of the results; but will also increase the amount of time necessary for the analysis. The calculated hot-spot stress converges to the actual stress in the structure with decreasing element size.

The procedure for the evaluation of fatigue damage for engineering applications is typically based on the use of S-N curves in combination with the Palmgren-Miner summation rule.

The use of S-N curves for fatigue life evaluations requires that the stresses used in the analysis are compatible with the stresses used for the derivation of the S-N curves. In the case of the S-N curves derived from tests of tubular joints the curves are based on the measured hot-spot stress. This requires that for the fatigue life analysis of a tubular joint the hot-spot stress has to be determined either through analysis or based on parametric formulae. S-N data for most of the small-scale welded test specimen is represented based on the nominal stress, F/A for axial loading and M/W for bending (F = axial force, A cross section, M bending moment, Z = section modulus). In order to use these curves for the fatigue life evaluation of complex details the nominal stress in the detail has to be determined.

If the nominal stress is used for fatigue life analysis, the influence of the local geometry on the hot-spot stress has to be accounted for through the choice of the S-N curve. For complex ship details the nominal stress can not be easily evaluated whereas the hot-spot stress can be obtained from finite element analysis in a straightforward manner as explained in the previous chapter. It is therefore desirable to develop calibrated S-N curves that are suitable for the use with hot-.spot stresses obtained from finite element analyses.

In the following the calibration method is described. The calibration method is applied to a published S-N test resulting in S-N curve that is suitable for the use with hot-spot stresses obtained from finite element analyses. The hot-spot stresses are obtained following the procedure developed in the previous chapter.

8.8.2 Development of Calibration Model

Two methods are available to obtain S-N curves that are suitable for the use with hot-spot stresses obtained from finite element analyses.

- Perform S-N tests for welded specimens that are similar to the structural details that are to be analysed and measure the principal stress at a defined distance from the hot-spot. From the finite element analysis of the structural

detail the principal stress at the same distance from the hot-spot can be calculated. This procedure ensures that the stress used for the definition of the S-N curve and the stresses obtained from the calculation are compatible. This procedure is very expensive since extensive S-N tests have to he performed of specimen that are comparable to the structural details to be analyzed. Nevertheless this procedure provides the largest degree of compatibility between S-N curve and analysis results.

- Calibrate existing S-N curves for the use with hot-spot stresses. This calibration requires that the calculated fatigue damage based on the original curve and the nominal stress is equal to the fatigue damage based on the calibrated curve in combination with the hot-spot stress.

8.8.3 Theoretical Calibration Model

The calibration model is developed based on the assumption that the S-N curve resulting from a series of S-N tests are represented in terms of the nominal stress σ_{nom}. The nominal stress is defined as:

$\sigma_{nom} = F/A$ Uniaxial tensile loading

$\sigma_{nom} = M/Z$ bending moment

Where:

F = axial force

A = area of cross-section

M = bending moment

Z = section modulus

The general form of this type of S-N curve is thus given by:

$$N = C(\Delta\sigma_{nom})^{-m}$$

Equation 8-1

Where:

$\Delta\sigma_{nom}$ = Stress range based on nominal stress

m = Negative inverse slope of S-N curve

log C = Intercept with log N axis

The parameters (C) and (m) are based on the curve fitting procedure that has been used to define the S-N curve. (m) Represents the negative inverse slope of the S-N curve in a log-log scale. For configurations where the contribution of the crack initiation period is insignificant e.g. welded structures this parameter can be obtained from fracture mechanics. Most design S-N curves for welded geometries therefore have a slope parameter m = 3.0.

In order to calibrate existing S-N curves the parameter (m) is held constant. The nominal stress is based on (F/A) or (M/Z). Due to the presence of the welded attachment this stress is increased with a maximum value of (K_t*σ_{nom}) at the beginning of the attachment. Where K_t represents the stress concentration factor and is defined as:

$$K_t = \frac{\sigma_{max}}{\sigma_{nom}}$$

Equation 8-2

In order to use the hot-spot stress (K_t*σ_{nom}) for the calculation of the fatigue damage the S-N curve has to be modified. The number of cycles to failure at a given stress range for a particular test specimen is based on constant amplitude tests. The modified S-N curve therefore has to result in the same number of cycles to failure for a given hot-spot stress (K_t*σ_{nom}). ***Figure 8-14*** shows the relation between the modified and the original S-N curve.

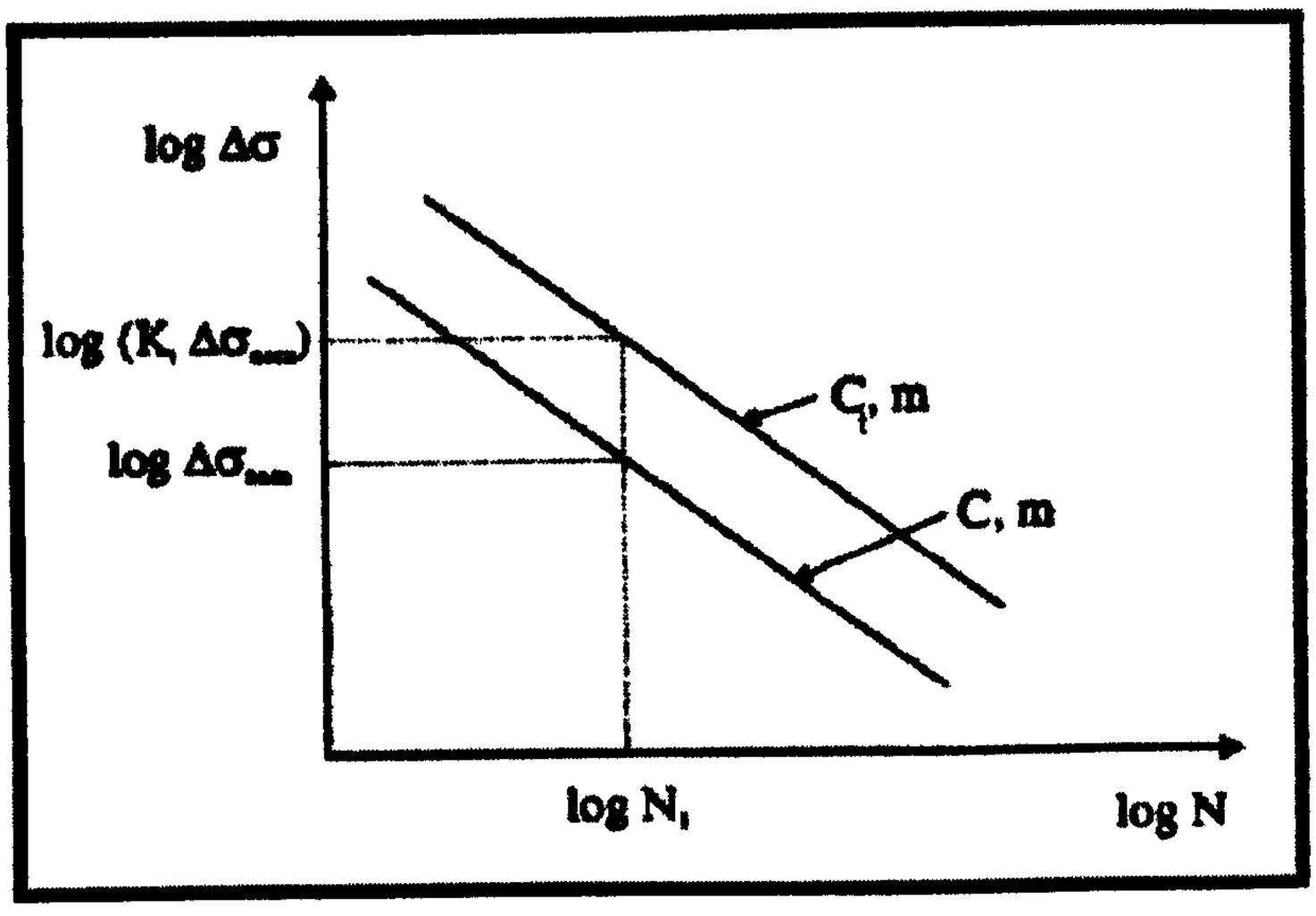

Figure 8-14 Relation between the Modified and the Original S-N Curve

The two curves have the same slope but the parameter C has been replaced by C_t the following equation has been used to derive C_t:

$$N = C(\Delta\sigma_{nom})^{-m} = C_t(K_t\Delta\sigma_{nom})^{-m}$$

Equation 8-3

The curve parameter C_t of the modified S-N curve can therefore be expressed as

$$C_t = C * K_t^m$$

Equation 8-4

The modified S-N curve is depends on the method for obtaining the hot-spot stress. The curve has to be used in combination with hot-spot stresses that are obtained in the same way as the hot-spot stress used for the determination of C_t.

If the hot-spot stresses are compatible the calibration method used ensures that the use of the modified S-N curve in combination with the hot-spot stress ($K_t*\sigma_{nom}$) will result in the same fatigue life as would be obtained with the original S-N curve in combination with the nominal stress (σ_{nom}).

8.8.4 Calibration Results and Conclusions

Based on the calibration procedure developed in section ***8.8.3*** the S-N curves modified for the use with hot-spot stresses are developed for published S-N curves. The hot-spot stress is obtained through a finite element analysis as illustrated in the Web-Toe case study in the previous chapters. Using ***Equation 8-4*** the modified curve parameter C is found. The choice of the calibration examples should be governed by the availability of test data. The documentation of S-N test results has to include both the geometry of the test specimen and the curve parameters of the resulting S-N curve. In many cases no geometry information is available. This information is available for our structure in question (Web-Toe) from the use of the SCF results evaluated Theoretically, Analytically and Experimentally. S-N data and stress concentration factors (SCFs) are related to each other and therefore should be considered together so that there is a consistent basis for the fatigue assessment. See ***Figure 8-15***.

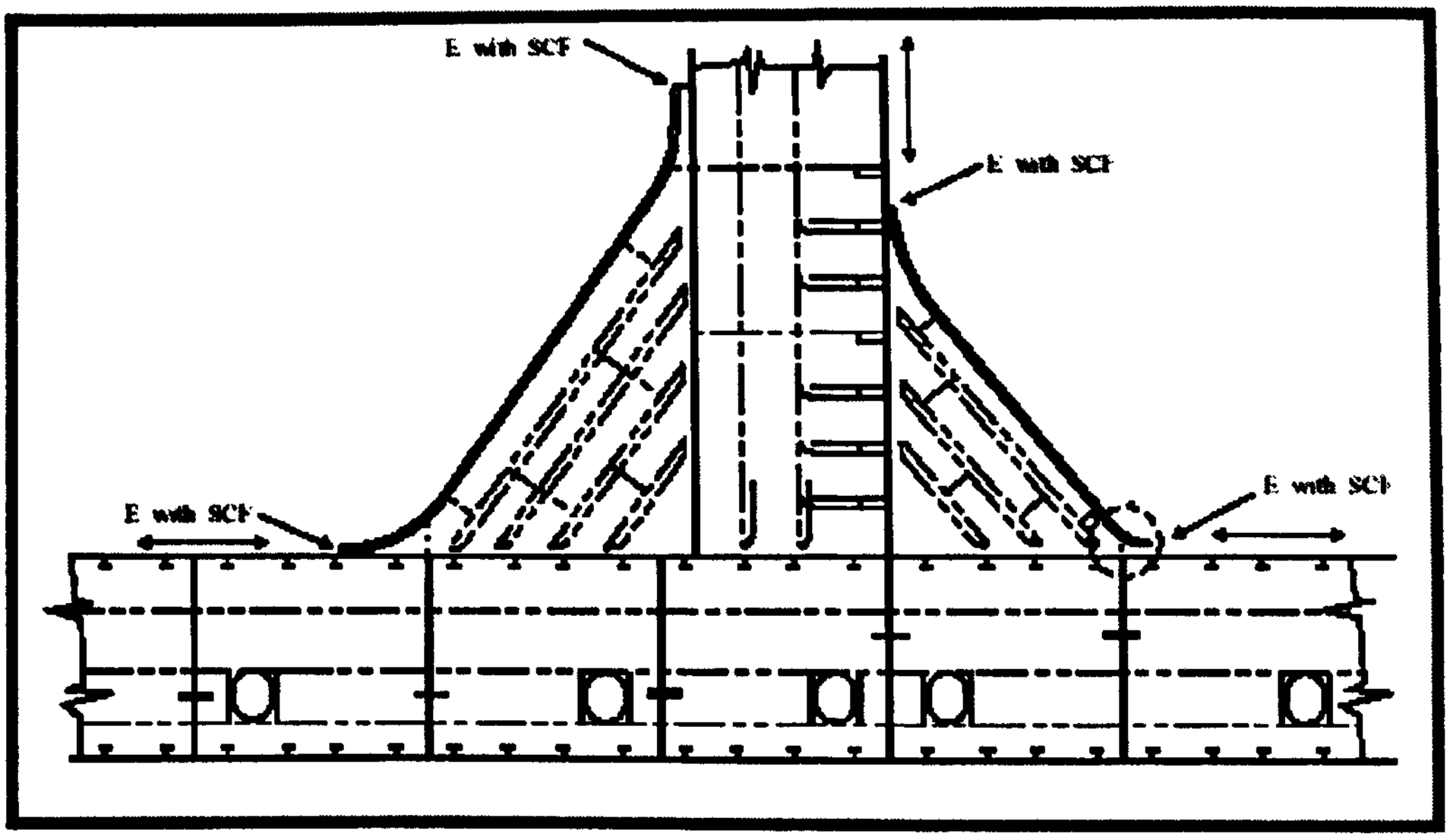

Figure 8-15 Fatigue Class Designation and SCFs Determined for the Connection between Transverse Bulkhead Vertical Web and Double Bottom Girder

The Hotspot method is an acceptable method which can be used to extract and interpret the "near weld toe" element stresses and to obtain a (linearly) extrapolated stress at the weld toe. When stresses are obtained in this manner, the use of the E Class S-N data is considered to be acceptable.

The UK HSE S-N curve of the E class shown in ***Figure 8-13*** above and related data presented in ***Table 8-2*** above, used in the implementation of the calibration procedure on the Web-Toe. The structure geometry and test results are documented in the previous chapter. The UK HSE S-N curve of the E class has the following parameters:

$$C = 3.289 \times 10^{12}$$

$$m = 3.0$$

The stress concentration factor K_t has been obtained from the hot-spot by linear extrapolation to the hot-spot and also from full scale model testing. The following stress concentration factor K_t has been obtained from full scale testing:

$$K_t = 2.35$$

Based on the calibration procedure described in the previous section ***8.8.3*** using the S-N curve parameters listed above the calibrated S-N curve with the following curve parameters obtained using ***Equation 8-4***:

$$m = 3.0$$

$$C_t = 4.268 \times 10^{13}$$

$$\text{Log } C_t = 13.630$$

Based on the approach developed in section ***8.8.3***, the E class S-N curve has been calibrated and presented in ***Figure 8-16*** below for use with hot-spot stresses obtained through finite element analyses or other methods. The calibrated curve for this structure is therefore especially useful for application purposes since it can be used in place of the standard curves.

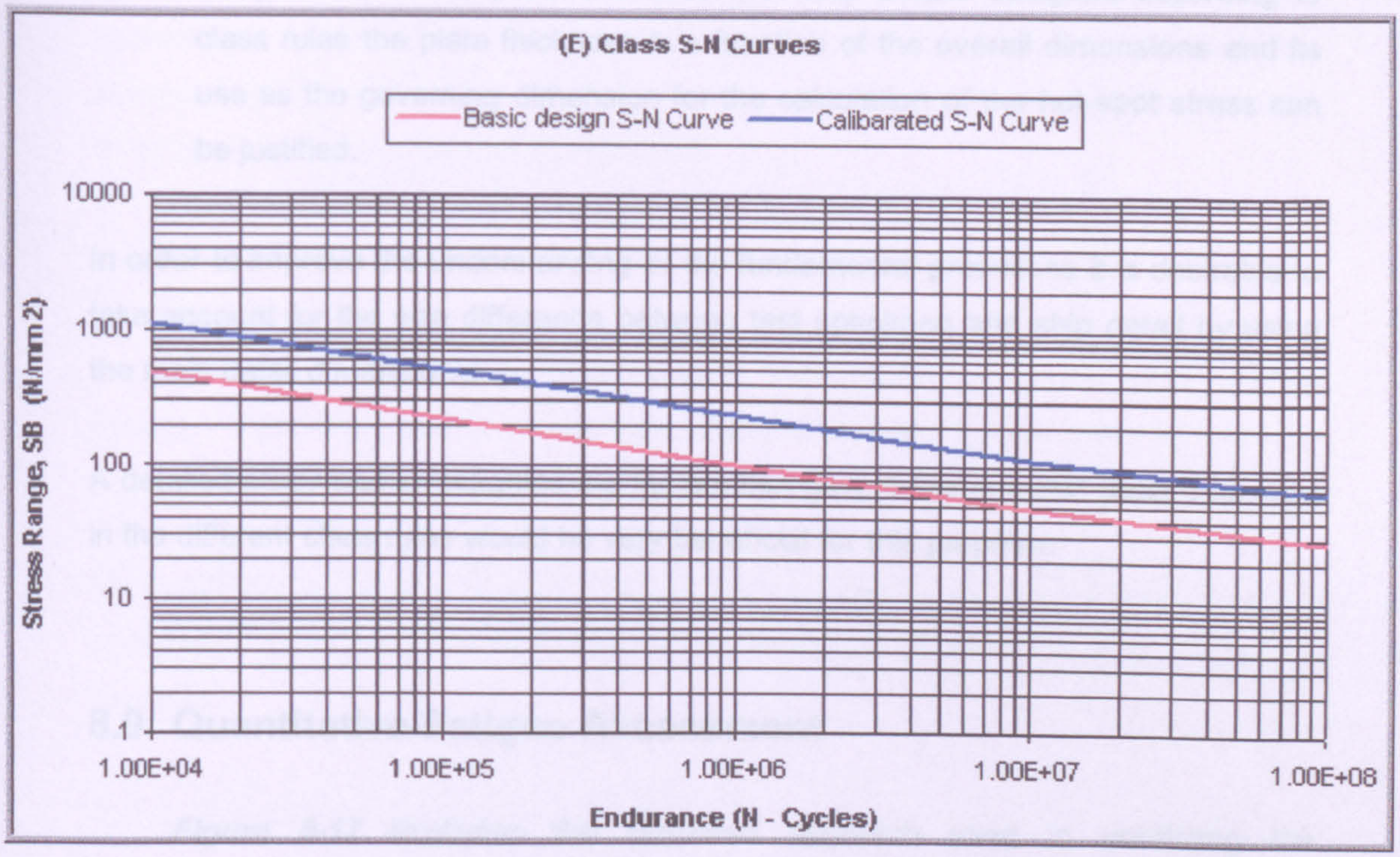

Figure 8-16 Original and Calibrated S-N Curves (E-Class)

In order to use the developed calibrated S-N curves for engineering applications pre-cautions have to be taken to ensure that the stress distribution near the hot-spot is calculated with sufficient accuracy.

The problem of calculating the fatigue damage for ship details using hot-spot stresses obtained through finite element analyses can be viewed as a two-part process. A suitable S-N curve defined and the scale difference between the small scale specimen and the ship detail accounted for. The two parts can be clearly separated which makes the solution more clear:

- The developed calibration process ensures that for the actual test specimen the calibrated S-N curve used to analyse the fatigue life for constant amplitude loading in combination with hot-spot stresses obtained from finite element analyses will result in the actually observed mean fatigue life.

- The second problem, the dimension problem is only approximately resolved. The definition of stress recovery procedures and minimum mesh sizes has the purpose to relate the small scale fatigue test specimen to the actual ship details. The use of the plate thickness as the governing dimension is somewhat misleading since in many cases the stress distribution is independent of the plate thickness. For ship details designed according to class rules the plate thickness is a function of the overall dimensions and its use as the governing dimension for the calculation of the hot-spot stress can be justified.

In order to improve the understanding of the fundamental processes it is desirable to take account for the size difference between test specimen and ship detail by using the main detail dimensions.

A detailed study that investigates the factors that govern the required plate thickness in the different class rules would be very beneficial for this purpose.

8.9 Quantitative Fatigue Assessment

Figure 8-17 illustrates the simplified approach used in predicting the cumulative fatigue damage due to wave-induced loads. The simplified Weibull approach for design of standard hull structure, using the operating design envelope (standard loading conditions, usage, trading route), with parametric equations for loads and motions at reference probability level been used, where the global and local structural response based finite element analysis or beam, plate, and grillage theory using Long-term Weibull distribution of stress range characterized by shape factor and stress range at reference probability level is used.

To evaluate the fatigue life of the hull structure, two basic sets of information are customarily required, namely, the material characteristics cast in the form of S-N curves and the long-term stress distribution (or stress histogram) of the structure. Both sets of information should be determined in a satisfactory manner. For stress histograms, it is necessary to account for all stress variations during the life of the vessel, with due consideration given to its loading conditions, speed, wave environments, motion response, and resulting loads and structural response.

The fatigue damage induced in the connections of the longitudinal stiffeners to the transverse web frames is calculated by a long term spectral analysis approach which includes the global vertical and horizontal bending moments, and the dynamic pressure effects around the waterline. The dynamic pressure effects take into account the relative wave elevation due to ship motions and use a probabilistic assessment of the relative wave heights within each seastate to calculate the non-linear pressure effects around the waterline.

From this dynamic pressure *Response Amplitude Operators* (RAOs) are established for each analysis position which can be combined with details of the local structure of the model to produce stress RAOs at each connection due to the local bending between transverse frames. A spectral analysis method is then used to combine global and local stresses to calculate the RMS (*Root Mean Square Value*) fatiguing stress at each connection.
The total fatigue damage of each connection is calculated using the Palmgren-Miner summation procedure for every combination of loading condition, heading angle, and seastate.

8.9.1 Spectral Fatigue Analysis

Depending on how the long-term stress distribution is determined, the analysis procedure for fatigue assessment of hull structures can be defined as the so-called "*simplified fatigue analysis*" shown in ***Figure 8-17*** or as the so-called "*spectral fatigue analysis*" shown in ***Figure 8-18***, described with the assumption that the long-term stress histogram of the hull structure follows the Weibull probability distribution as explained in *Wallodi Weibull*, (1945).

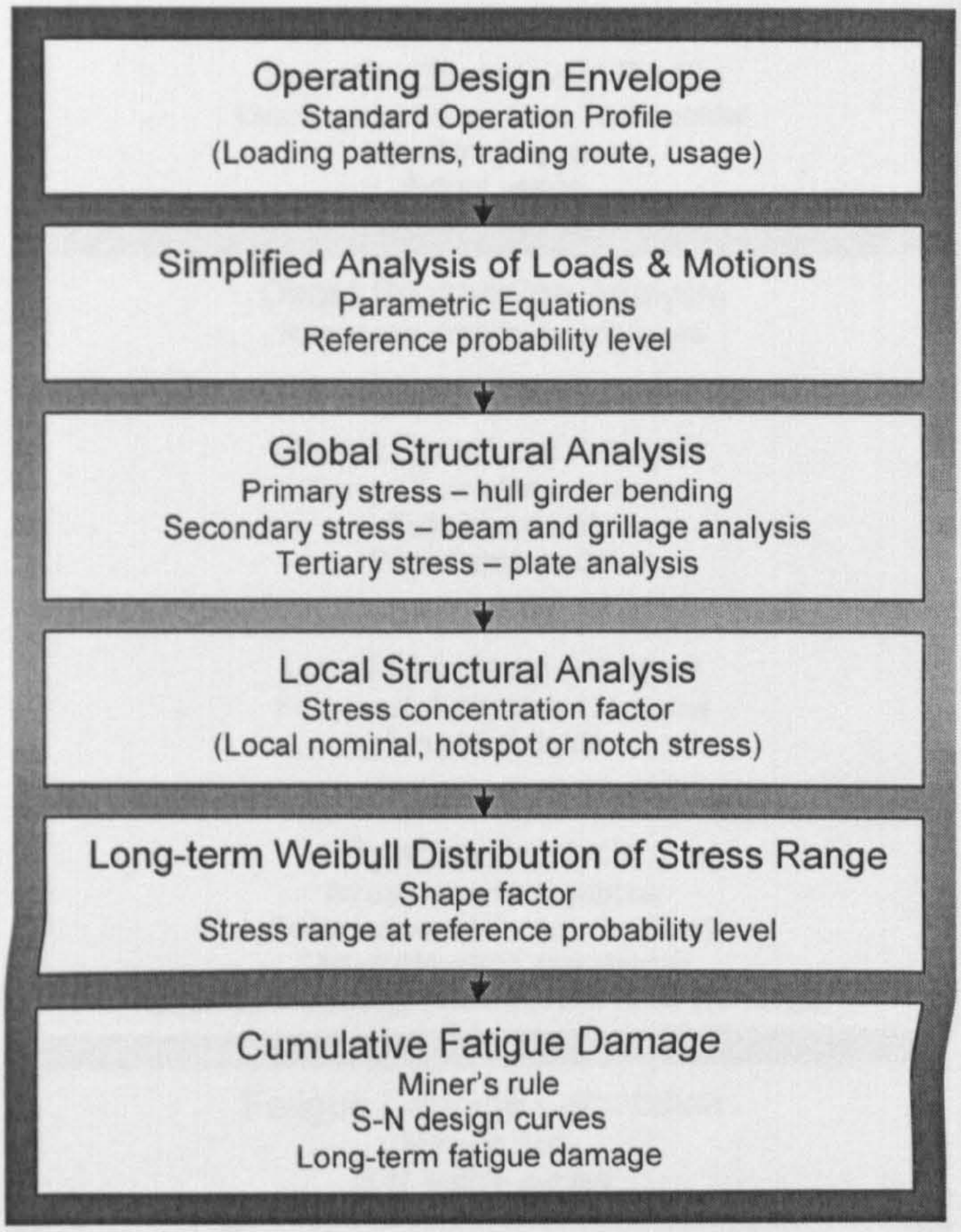

Figure 8-17 Simplified Weibull Approach

Spectral fatigue analysis usually used for novel designs or extra level of assurance, where specific operational profile (actual loading conditions, usage, and trading route) and direct seakeeping analysis using finite element analysis of global and local structural response, deriving short-term distributions of stress range from stress power spectral density functions for different sea states and operating conditions and the weighted sum of short-term cumulative fatigue damages computed.

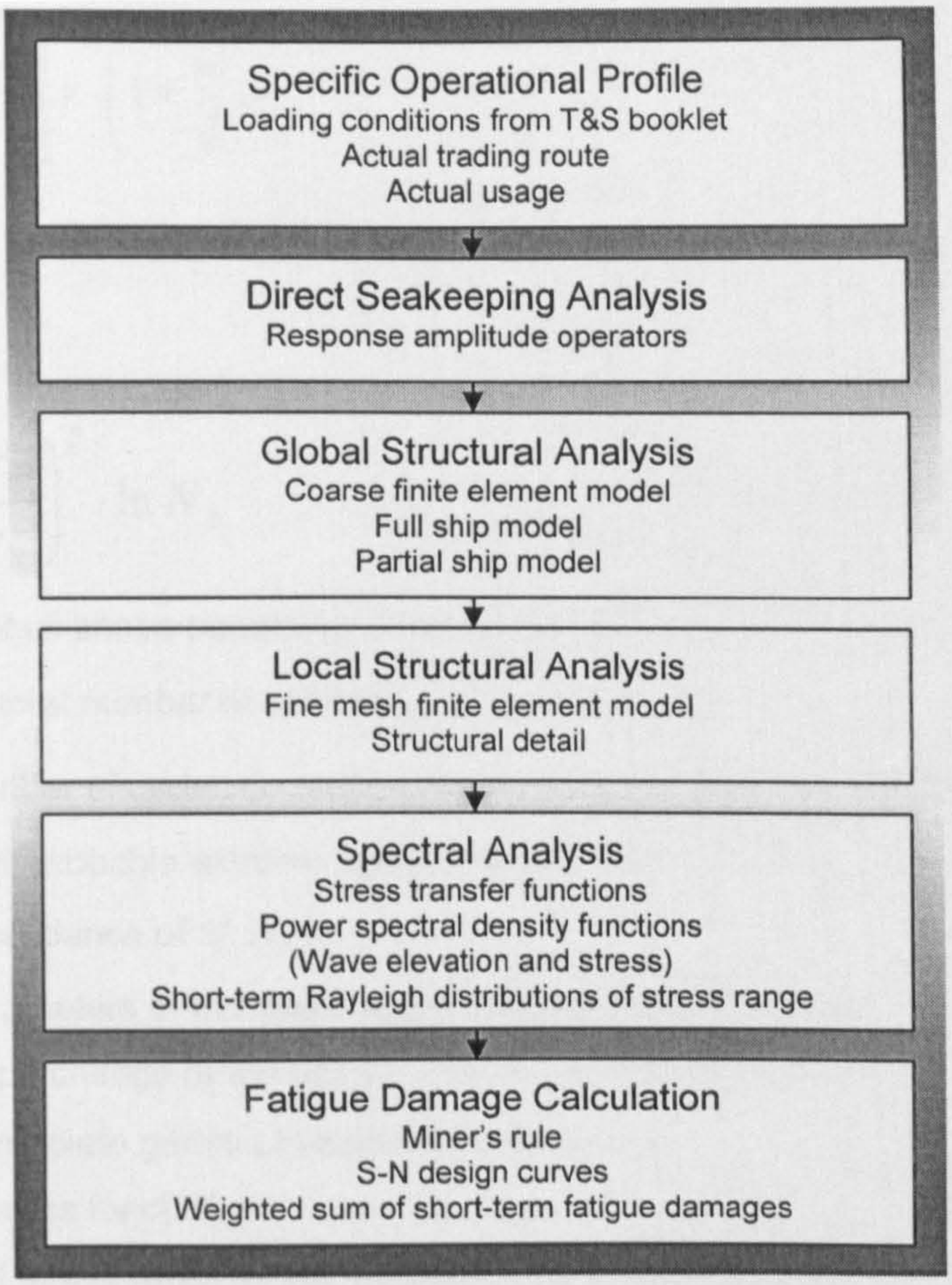

Figure 8-18 Spectral Approach

It has been known that a vessel's long-term stress distribution resulting from random sea loading can be fit closely into the two- parameter Weibull probability distribution. Based on the assumption, fatigue damage (D) or fatigue life over a required service life can be obtained by linear sum of partial fatigue damages (Palmgreen-Miner's law), or in a closed form as expressed in the following ***Equation 8-5.***

$$D = \frac{N_L}{C} \cdot \frac{{\sigma_R}^m}{(\ln N_R)^{\frac{m}{\xi}}} \mu \cdot \Gamma\left(1 + \frac{m}{\xi}\right)$$

Equation 8-5

Where: ***(Predicted Fatigue Life = Design Service Life / Fatigue Damage)***

$$\mu = 1 - \left\{ \gamma \cdot \left(1 + \frac{m}{\xi}, \nu \right) - \nu^{\frac{-\Delta m}{\xi}} \cdot \gamma \cdot \left(1 + \frac{m + \Delta m}{\xi}, \nu \right) \right\} \div \Gamma \left(1 + \frac{m}{\xi} \right)$$

Equation 8-6

Where:

ν $\left(\frac{\sigma_q}{\sigma_R} \right)^{\xi} \cdot \ln N_R$

ξ Weibull shape parameter of stress range

N_L f*T total number of cycles in life time

N_R Number of cycles corresponding to the probability of exceedance $1/N_R$

σ_R Most probable extreme stress range in *NR* cycles (i.e., at the probability of exceedance of $1/N_R$)

C, m Parameters of the upper segment of the S-N curve

Δm Slope change of the upper to lower segment of the S-N curve

γ Incomplete gamma function, Legendre form

Γ Gamma function

σ_q S-N stress range at the intersection of two segments

T Base time period, taken as the design life of the structure (seconds)

f Life time average of the response zero-crossing frequency (Hz)

D Cumulative fatigue damage ratio

The uncertainty of the long-term distribution of the wave-induced wave bending moments in ships has been assessed, relating it to ocean areas, ship routes, ship speeds and ship types as mentioned in *IACS*, (1997). Weibull distributions have been fitted to the calculated values of long-term distributions and their shape factor has been related to the ship length.

The number of load cycles in a ship lifetime has been evaluated by the classification societies, and characteristic values were derived for different levels of probability. A two-parameter Weilbull distribution defined by a characteristic value and a shape factor has been proposed as a load model to be adopted in design rules for the assessment of fatigue damage in ship structures.

The model uncertainty of the two parameters *defining the distribution is assessed as* a function of the method of fitting the long-term distribution, of ship speed and of the climatological data.

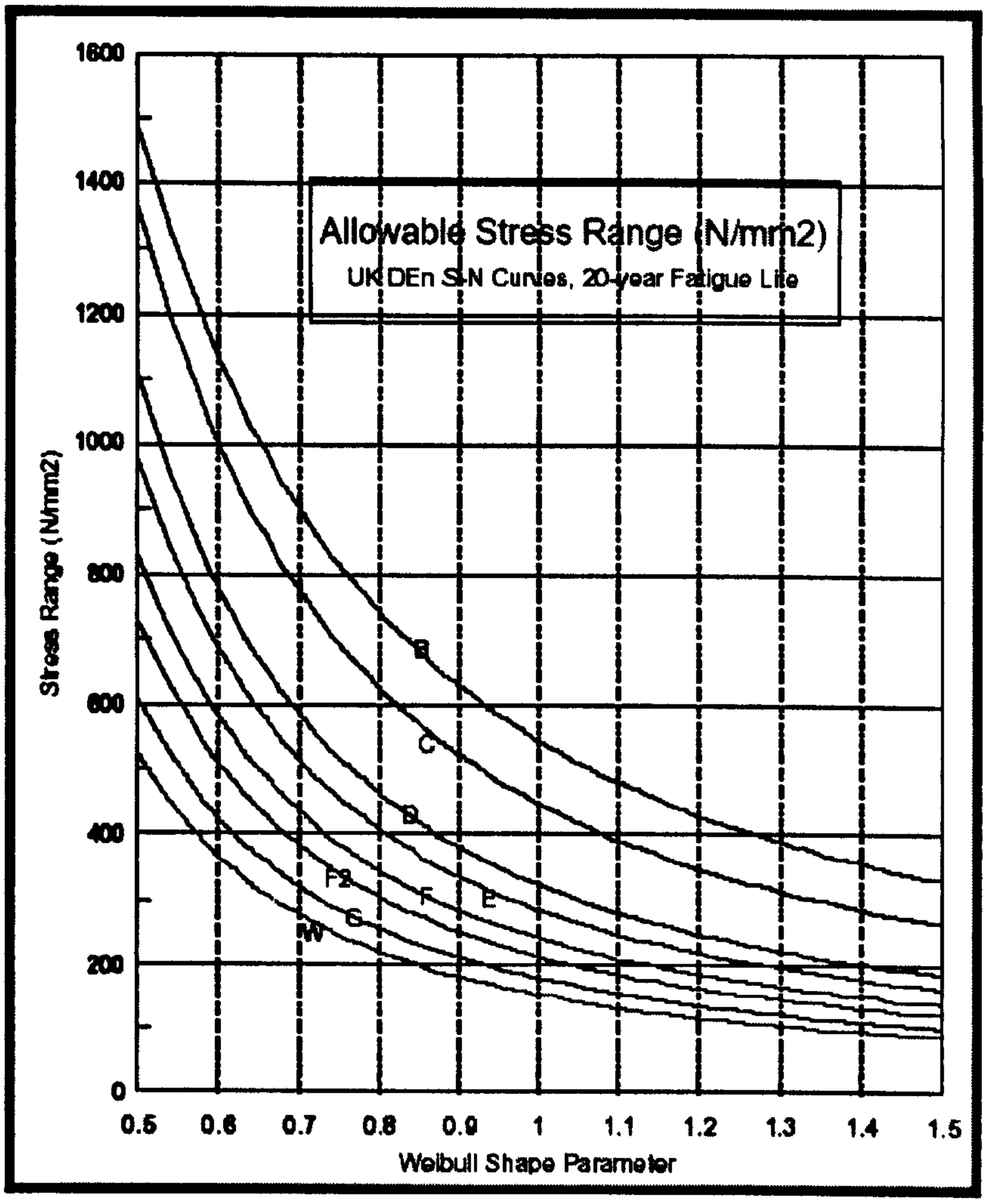

Figure 8-19 Weibull Shape Parameter

As can be seen in *Equation 8-5*, the two parameters of the Weibull distribution used are the stress range σ_R at the probability of exceedance of $1/N_R$, and the *Weibull shape parameter* ξ *Figure 8-19* above. For a given set of σ_R, ξ and *S-N* curve, the fatigue damage (or fatigue life) can be readily obtained using the equation. Similarly, for a given set of ξ, *S-N* curve and a specified fatigue damage (or fatigue life), the stress range σ_R can be determined.

The assessment procedures developed from various sources including the Palmgren-Miner linear damage model, U. K. HSE S-N curves, environment data of the FPSO mooring location, etc. In assessing the adequacy of the structural configuration and the initially selected scantlings, the fatigue strength of the hull girder and individual structural members or details is to be in compliance with the failure criteria.

The fatigue criteria established by classification societies allow consideration of a broad variation of structural details and arrangements so that most of the important structural details in the vessel can be assessed for their adequacy in fatigue strength. To this end, the structural response should be calculated by a finite element structural analysis as defined previously. Due consideration should be given to structural members or details expected to have high stresses. While this is a simplified analysis, some judgments are still required in applying the approach to the actual design.

To apply the simplified fatigue analysis, one of the two parameters of the Weibull distribution required is the long term stress distribution parameter or the Weibull shape parameter (ξ in ***Equation 8-5***). The fatigue damage is directly represented by the numerical value of this parameter; a higher value indicates higher fatigue damage. The Weibull shape parameter typically varies between 0.8 and 1.1, depending on the dominant period of the hull structural response and the considered wave environments.

The probability density function $f(\sigma)$ and cumulative distribution function, $F(\sigma)$ of the Weibull distribution of stress ranges σ are expressed by:

$$f(\sigma) = \frac{\xi}{C}\left(\frac{\sigma}{C}\right)^{\xi-1} \cdot e^{-\left(\frac{\sigma}{C}\right)^{\xi}}$$

Equation 8-7

$$F(\sigma) = 1 - e^{-\left(\frac{\sigma}{C}\right)^{\xi}}$$

Equation 8-8

The probability of exceedance $p(\sigma)$ can then be expressed by:

$$p(\sigma) = 1 - F(\sigma) = e^{-\left(\frac{\sigma}{C}\right)^{\xi}}$$

Equation 8-9

$$N = \frac{1}{p(\sigma)} = e^{\left(\frac{\sigma}{C}\right)^{\xi}}$$

Equation 8-10

$$\ln N = \left(\frac{\sigma}{C}\right)^{\xi}$$

Equation 8-11

Based on the above expression, it can be shown that the stress range σ_R determined at N_R cycles or $p=1/N_R$ is related to the life-time stress range σ_L determined at the life-time cycles N_L or $p = 1/N_L$, by the following equation:

$$\sigma_R = \sigma_L \left(\frac{\ln N_R}{\ln N_L}\right)^{\frac{1}{\xi}}$$

Equation 8-12

Using the formula of the *simplified fatigue analysis* presented in the preceding section, the allowable stress range σ_L for the design life can then be found as follows:

$$\sigma_L = \frac{\sigma_R}{D^{1/m}} \left(\frac{\ln N_L}{\ln N_R}\right)^{\frac{1}{\xi}}$$

Equation 8-13

The allowable stress ranges for a design life of 20 years for the eight U.K. HSE *Basic Design S-N Curves* were determined for a range of the Weibull shape parameter from 0.5 to 1.5, and the results are presented in *Figure 8-19* above.

Results of the fatigue evaluation given in a numerical example using Lloyds Register ShipRight FDA and presented in all of the following fatigue results representation

formats, the most probable extreme stress ranges, the allowable stress ranges, fatigue lives, damage ratios, and failed structural element list, etc. are presented in ***Figure 8-20***, ***Figure 8-21*** and ***Figure 8-22*** for the same Mid frame side shell structure of the City FPSO2000.

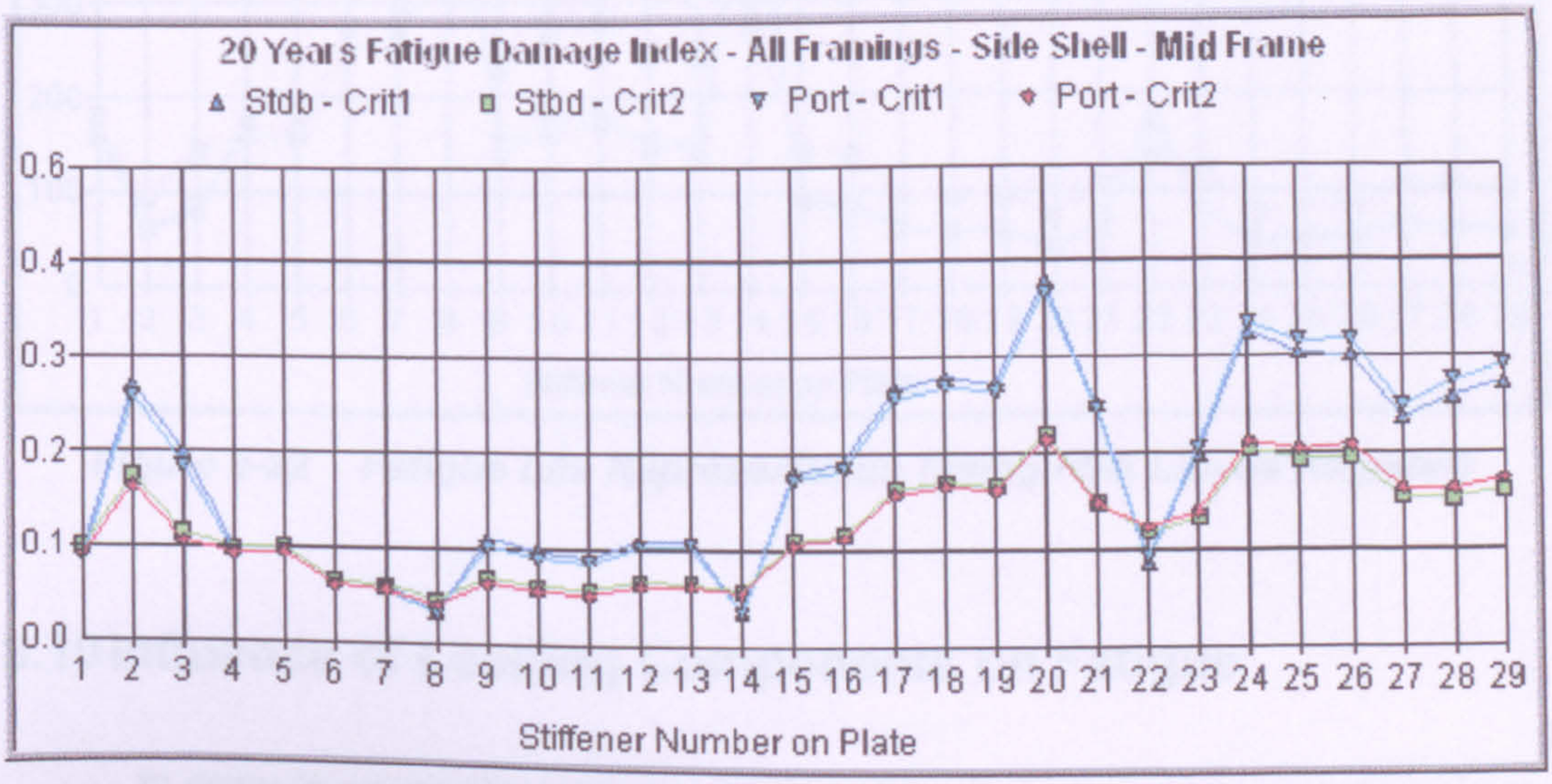

Figure 8-20 Fatigue Damage Index Representation (using FDA Lloyds Register)

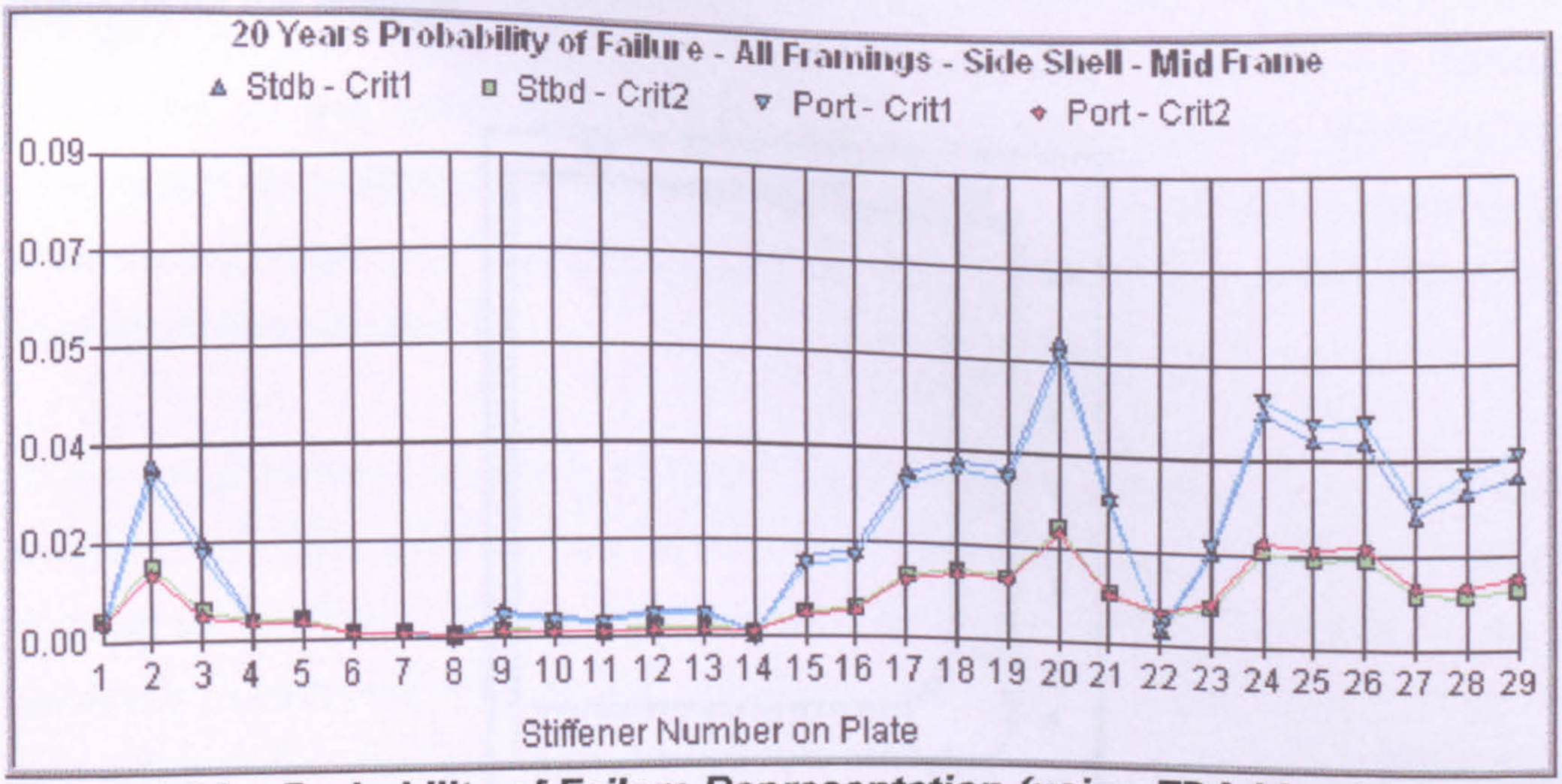

Figure 8-21 Probability of Failure Representation (using FDA Lloyds Register)

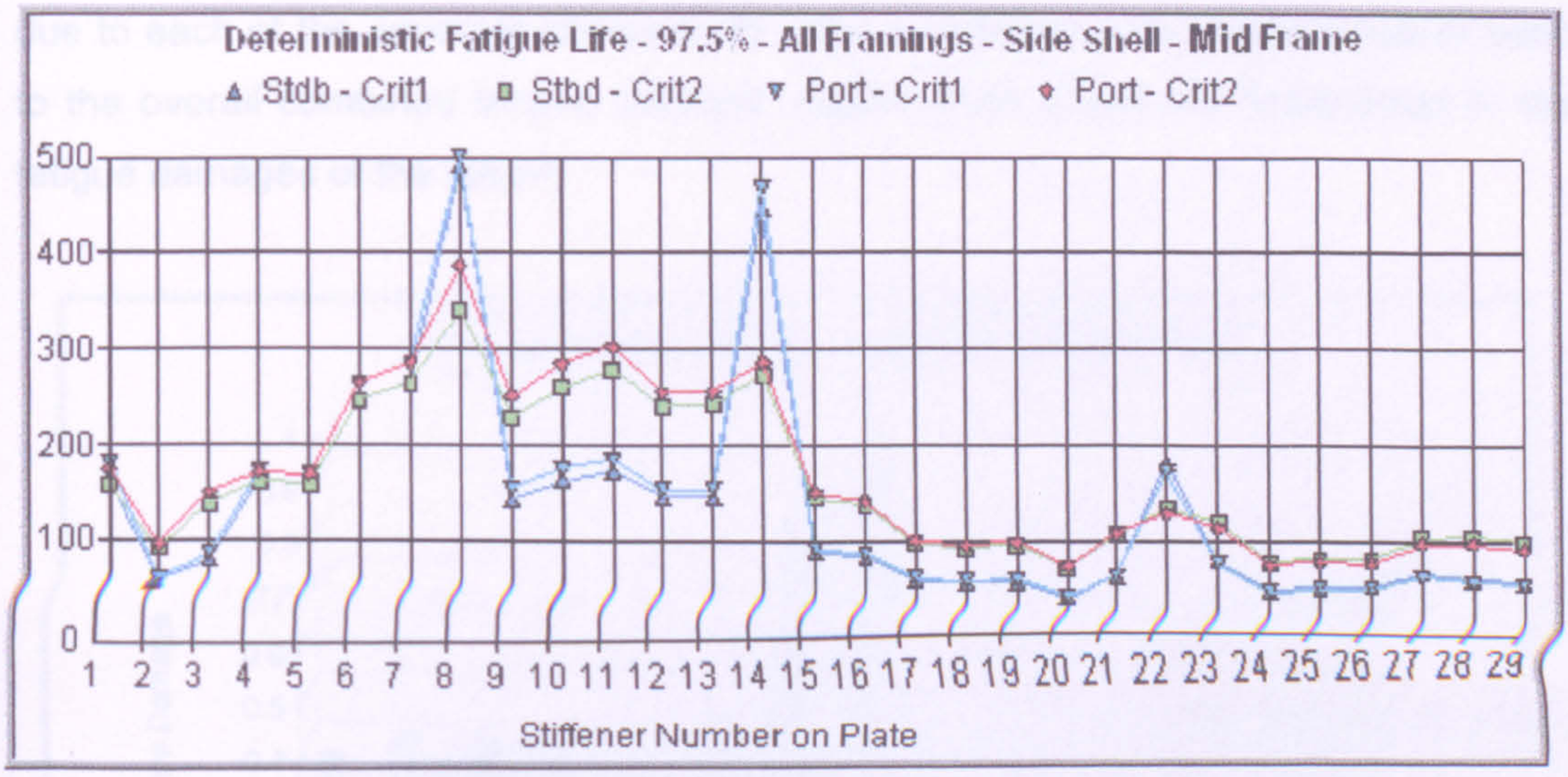

Figure 8-22 Fatigue Life Representation (using FDA Lloyds Register)

8.10 Influence of Loading Components on Fatigue

In order to asses the influence of the three primaries fatigue loadings on the overall fatigue life, a fatigue assessment was performed on a typical double bottom vessel. ***Figure 8-23*** shows a sketch of the hull configuration and details the 14 positions for the analysis.

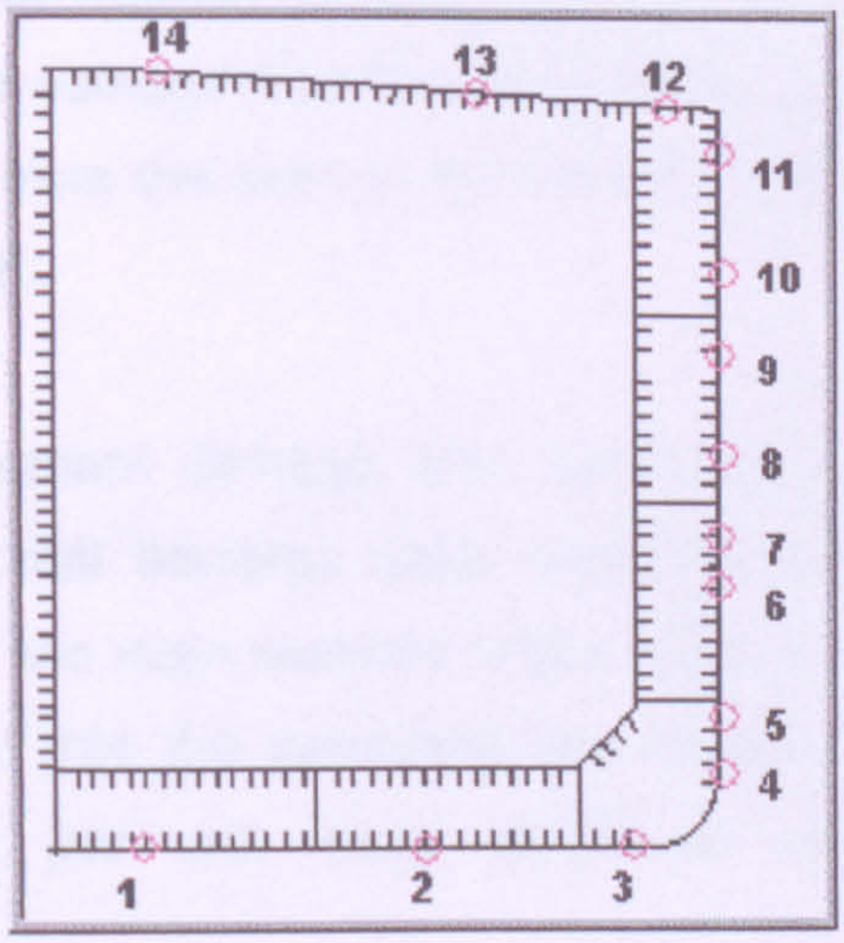

Figure 8-23 Analysis Locations (Keel 1-3, Side-shell 4-11, Deck 12-14)

Analysis locations 1 to 11 included both global and local loading effects, and locations 12 to 14 included only the global bending effects. The fatigue damages for each position were calculated to each loading component separately and for the combined loading including the phasing. The relative magnitudes of fatigue damages

due to each of the separate components used to determine the significance of each to the overall combined fatigue damage. ***Figure 8-24*** shows the breakdown of the *fatigue damages of the vessel.*

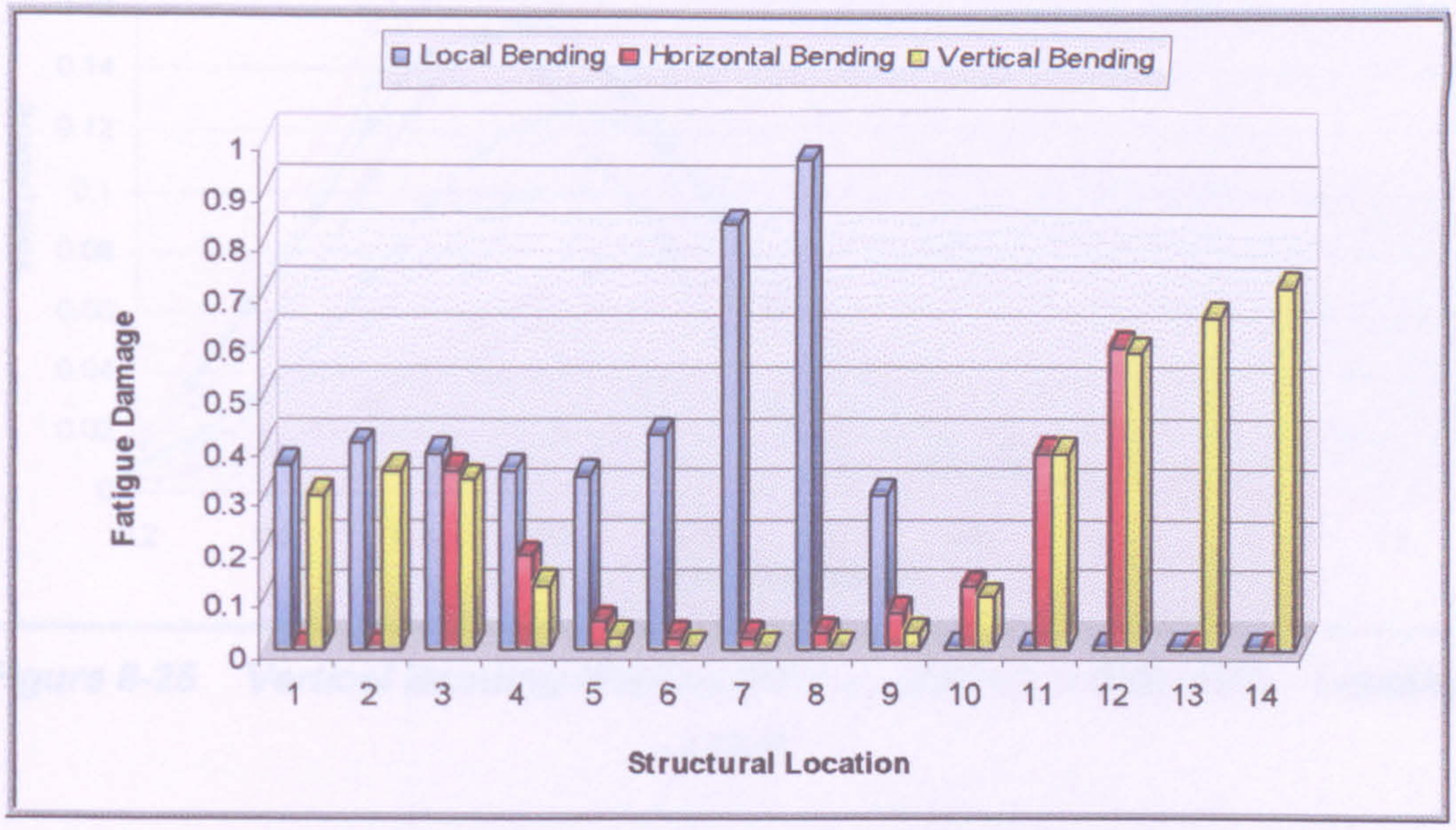

Figure 8-24 Breakdown of the Fatigue Damage Due to Different Loading Components

Looking at the results, the fatigue damage around the waterline area is dominated by the local bending effect whereas in the deck and keel locations, the damage dominated by the global vertical bending loads. As would be expected, the contribution to the fatigue damage from the vertical bending moment reduces as the analysis positions move from the keel to the vertical neutral axis position (between analysis positions 6 and 7.

The vertical bending moment damage then increases to maximum in the deck longitudinals. The horizontal bending loads contribute little to the over a fatigue damage for an FPSO for two main reasons; firstly, since the FPSO is turret moored it generally "weathervanes" into the prevailing sea direction. (See ***Figure 8-25*** ND: non-dimensional format per unit wave amplitude i.e. Amplitude divided by $(\rho \cdot g \cdot L^2 \cdot B)$.

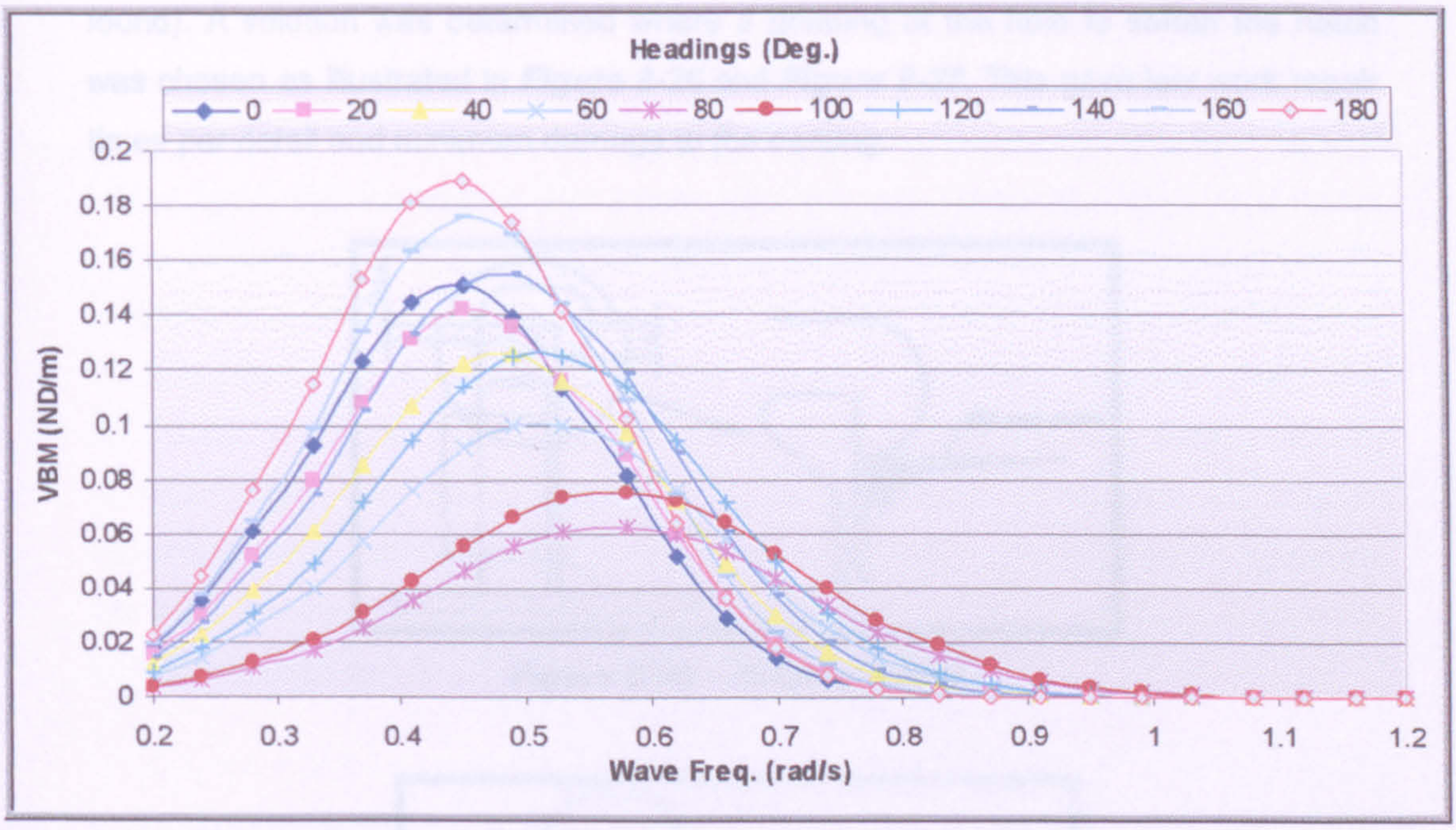

Figure 8-25 Vertical Bending Moment (ND/m), (Speed: = 0.00 %VS, Loading: = Full)

This means that most of the time spent around the head seas condition for which the horizontal bending loads are significantly reduced. The second is that for the FPSO section analysed the horizontal section modulus is much higher (up to 3 times) than the vertical modulus, which results in much lower resultant stresses. The fatigue damage in the side shell longitudinals around the waterline is dominated by the local bending due to the dynamic pressure effects. From previous experience these have been the highest fatigue damage areas within a tanker and have required structural repairs and modifications.

8.11 Experience related to FPSOs

Several projects have been hampered by cost overruns lately due to oil companies and governmental requirements being stricter than anticipated during construction. Most of these requirements have been related to non-structural items, but also fatigue requirements have made quite dramatic impacts on some designs due to the large number of details. However there have also been some repairs made that has not been as expensive as indicated due to choice of simple solutions.

An example of this is the Figure below, where one became aware that the notch on the connection to the frame was too hard after a thorough investigation (no cracks

found). A solution was determined where a grinding of the hole to soften the notch was chosen as illustrated in ***Figure 8-26*** and ***Figure 8-27***. This gave low work repair times per detail and minimum damage to the coating.

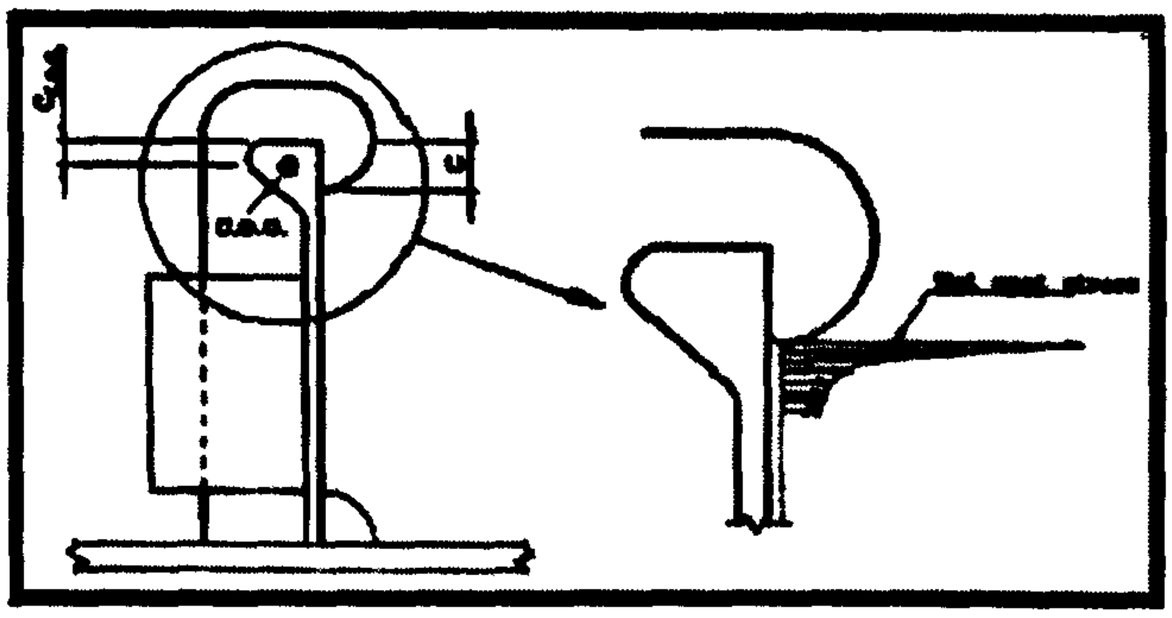

Figure 8-26 Original detail

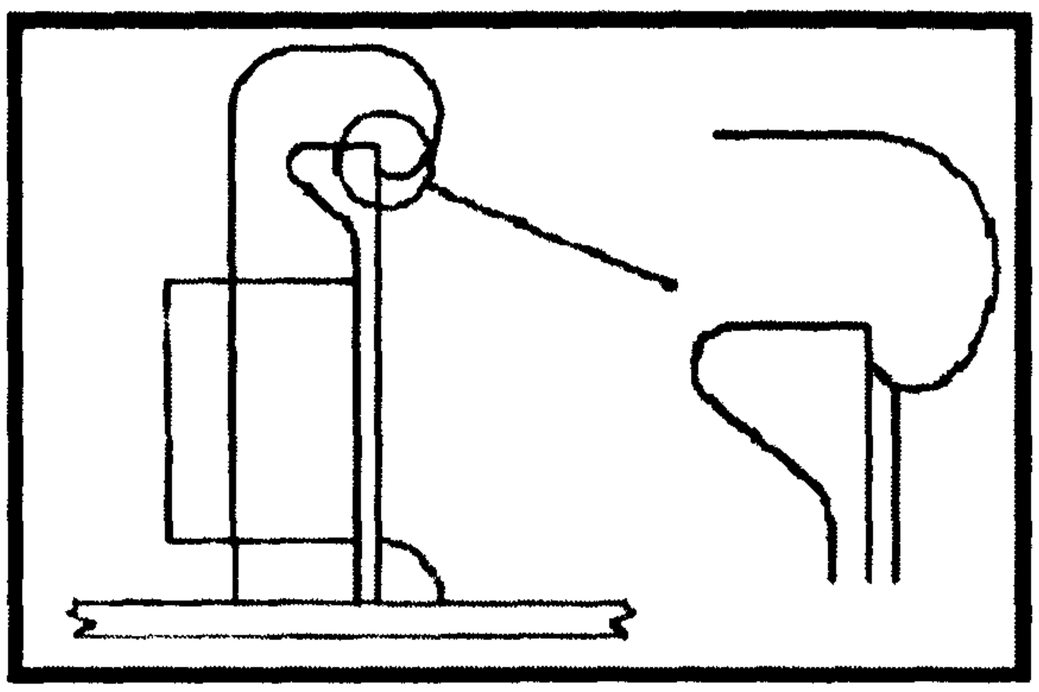

Figure 8-27 **after grinding (soft toe)**

In the JIP on "FPSO – Fatigue Capacity, Improved Fatigue and Fracture Performance of FPSO units", where most oil companies and significant classification societies are participants, there has been a considerable progress on detail design guidelines and it is expected that this will result in common standards acceptable to all parties with respect to fatigue. Damages have also been seen on ship bows, and it is believed that wave loads on bows and green seas effects will be given more attention in the future.

Due to these vessels inability to position them based on the weather forecasted, they may have to stand up against the most severe part of any storm. When the wind blows at its hardest the waves are not at their highest but are at their steepest. These steep waves will generate the largest bow loads and most severe green seas. There have also been reports of green sea damages to deck mounted equipment on FPSOs.

Looking at the available methods for calculation as described earlier, it is advised that such effects be considered by direct calculations that are calibrated against model tests and experience. For green seas the bulk carrier accidents have given focus on green seas and there have been comparative studies been made to enable predictions of green seas, for example as presented at IMO (International Maritime Organisation) meeting in December 1998 where the sea loads on hatch covers was discussed. The green seas result in a water height on deck but also a large velocity of water racing over the deck will have to be considered. Model tests still play an important role in calibrating theory, but since model tests can normally not generate the most severe steepness in waves, one still has to rely on a certain extrapolation into the most severe conditions by calculations.

8.12 Summary

Fatigue damage is mainly created by the small to medium sea states by virtue of the number of stress cycles they create. It is therefore essential that due attention is given to this part of the life time stress spectrum if reliable fatigue life estimations are desired. This is only be achieved by using a spectral method of analysis which reconstructs the entire stress spectrum giving due attention to the combination of the various load components, as well as the number of stress cycles created by the incident waves in each seastate.

9. Conclusions

Procedures for assessing both the strength and fatigue characteristics of an existing hull structure have been presented. An attempt has been made to offer a useful methodology for applying existing structural criteria developed for offshore and ship construction, to the assessment of FPSO structures. In which it has been concluded that the conversion does not alter considerably the design of the vessel from that of the original tanker ship.

The analysis and subsequent calculations given in this research work demonstrate with conservatism that the hull girder structure has sufficient capacity to withstand the anticipated loads for an FPSO design. The maximum combined comparative stress (Von-Mises) found to be between 217 MPa and 329 MPa for the global model. Also the transverse strength investigation of the refined midship web-frame revealed a maximum combined stress (Von-Mises) in the vicinity of 169 MPa to 311 MPa. Furthermore a localised stress analysis revealed a maximum comparative combined linear static analysis stress of 230 MPa to 213 MPa non-linear static analysis of the transverse web-toe detail.

The cyclic stresses in the hull girder caused by wave effects are the primary cause for fatigue damage, where wave effects cause hull bending, local pressure variation on the vessel hull and internal pressure variation. It is however important that a reasonable usage of height tensile steel can lead to efficiently light and sufficiently strong hull structures if appropriate measures are taken against the increase of local stress range accompanied with the usage of height tensile steel.

The strength assessment procedure considers both overall hull girder strength and structural member strength and uses actual member thickness gauging in lieu of as built scantlings. The fatigue assessment procedure provides a methodology for assessing the accumulated fatigue damage using the criteria's base environment service.

The general implications of fatigue in FPSOs have been outlined. In order to effectively control fatigue damage, it is necessary to develop an improved methods to determine the Long-Term Loading and Analysis Procedures for the analytical

evaluation of fatigue damage. This study has been focused on developing a general system to analyse fatigue damage in Critical Structural Details in FPSOs.

This system has largely been based on fatigue damage evaluation procedures originally developed for offshore oil platforms. Due to the complexity of ship critical structural details it was necessary to alter these procedures and, in particular, develop calibrated design S-N curves that can be used with hot-spot stresses obtained from finite element analyses.

The development has been based on practical considerations and the experience gained from the finite element analysis of actual structural details. A research projects to develop a more complete data structure for a future FPSO structural database is of great importance. This project could be used as a starting point.

It is of significant importance that a detail design work should be extended to incorporate further detail design arrangements of FPSOs, to reflect in service experience of their fatigue performance, design and construction practice, as well as any significant data made available from research studies.

The fatigue strength criteria specified in this study is based on the assumptions that all structural joints and welded details are properly designed and fabricated and is compatible with the anticipated working stress levels at the locations considered. It is important to closely examine the loading patterns, stress concentrations and potential failure modes of the structural joints and details in highly stressed regions. The structural performance of the details in question determined using fine-mesh models of the structural details with appropriate boundary conditions determined from the global model.

A calibration procedure has been developed to obtain S-N curves that can be used in conjunction with hot-spot stresses obtained from finite element analyses. The procedure uses original (UK-HSE) S-N data and calibrates the curves using the results from the SCFs analysis.

Calibration analyses can be used to replace the (UK-HSE) curves, where these curves are essential for the development of an integrated system for the fatigue life evaluation of FPSOs critical structural details.

In order to be compatible with the developed calibrated curves the hot-spot stresses have to be determined using the recommended procedure. It has to be verified that the finite element mesh is fine enough to calculate the hot-spot stress with sufficient accuracy. Additional research has to be performed to verify and validate the developed calibrated S-N curve. In addition, it is important to investigate the influence of the size difference between the original S-N test specimen and the actual FPSO details.

Improved recommendations for the mesh size and stress recovery procedures in FPSOs details have to be developed, where the effects of multi- axial stress distributions have to be studied further.

The simplified load estimation procedure does not take into account the effects of internal cargo and external pressure non-linear contributions. In addition, the contribution of corrosion fatigue in ballast tanks has to be investigated further.
The influence of construction methods and manufacturing quality on the fatigue life estimation of critical structural details has to be further studied. A calibration of the fatigue life evaluation process based on large-scale model tests has to be performed to increase the accuracy of the analysis procedure.

In spite of the difficulties to assess the fatigue strength of FPSO's structure due to the complexity of the structure itself and to the randomness of the sea loads, it has been possible to develop methods to determine the risk or not of failure of vessel welded joints during its design life time. The methods are based on direct calculations or conventional Classification Society rules approaches, but in both cases require the application of large FE idealizations.

For the structural stress and failure criteria determination, statistics represent a fundamental tool. Statistics and probabilities are extensively used to characterise the occurrence of the sea states and FPSO site conditions such as loading cases, wave frequency, wave directions, current, temperature, the stress short and long term distributions, fatigue details capability (S-N curves), failure criteria: Miner sum or safety index.

The progresses to come will therefore concern the improvement in uncertainties descriptions and S-N curve notch stress definition, the development of easiest probabilistic approaches to use for design offices, the calibration of the probabilistic

safety index. Although the presented methods are based on the linear cumulative Miner sum, a new step will be the development of a non linear cumulative damage based on crack propagation approach.

Nonlinear static stress analyses can produce more accurate stress results than linear static stress analyses for models that undergo loading in a concentrated area, have small features such as a small fillet radius or have constraints that act over small regions. This is because linear static stress analyses only produce stresses based on the initial shape of the object, whereas nonlinear static stress analyses determine stresses based on the object's deformed shape or material properties under loading. Hence any future studies in this field would reveal excellent technical information.

Attention of future research activities should be given to the new development in structural monitoring using fiber-optics as a reliable tool providing real-time accurate data required for a more reliable fatigue structural analysis of FPSOs. The reason for fitting hull stress monitoring systems is to acquire, display and record information on hull condition to use the information as a basis for making decisions that will improve operational efficiency and safety; reduce probability of structural failure in heavy weather conditions by early warning and provide operators with a basis for optimal inspection and maintenance.

Bow design and green loads effect, turret design, mooring lines and risers; the current analysis of the hull fatigue does not include cyclical loadings imposed by the mooring and riser systems; hence the fatigue analysis of the turret integration structure, reinforcement of the bow section and its interface with the hull structure is out of the scope of this research and need to be addressed in any future work.

APPENDICES

Appendix A City FPSO2000 Hull Girder FEA Results

Model : C:\CityFPSO2000\Webframe.MOD Report: Element
Format : NASTRAN CQUAD4 Stresses
Sort By : 7033..VonMises Stress in Ascending Order

Output Set 1 - Load Case 1

Set MAX/MIN Summary	Table	Set	ID	Value
Loc. X NormStress	Minimum	1	7336	-165.771
	Maximum	1	4673	186.432
Loc. Y NormStress	Minimum	1	3456	-236.277
	Maximum	1	3736	220.725
Loc. XY ShearStress	Minimum	1	4346	-112.207
	Maximum	1	6803	119.944
PrnStress Angle	Minimum	1	4237	-8.99956
	Maximum	1	6953	8.99986
MajorPrn Stress	Minimum	1	1038	-53.9393
	Maximum	1	3736	220.984
MinorPrn Stress	Minimum	1	3456	-236.277
	Maximum	1	4114	88.8392
VonMises Stress	Minimum	1	7677	1.10625
	Maximum	1	4020	230.489

Output Set 2 - Load Case 2

Set MAX/MIN Summary	Table	Set	ID	Value
Loc. X NormStress	Minimum	2	4673	-157.684
	Maximum	2	7336	165.908
Loc. Y NormStress	Minimum	2	3750	-205.984
	Maximum	2	3456	260.833
Loc. XY ShearStress	Minimum	2	8651	-139.808
	Maximum	2	8535	140.177
PrnStress Angle	Minimum	2	5374	-8.9915
	Maximum	2	6446	8.99922
MajorPrn Stress	Minimum	2	3750	-113.432
	Maximum	2	3456	257.034
MinorPrn Stress	Minimum	2	1542	-253.112
	Maximum	2	6152	53.4954
VonMises Stress	Minimum	2	2906	1.19417
	Maximum	2	1542	265.302

Output Set 3 - Load Case 3

Set MAX/MIN Summary	Table	Set	ID	Value
Loc. X NormStress	Minimum	3	7336	-197.799
	Maximum	3	4673	197.525
Loc. Y NormStress	Minimum	3	3456	-181.604
	Maximum	3	3736	186.005
Loc. XY ShearStress	Minimum	3	4346	-133.148
	Maximum	3	6803	142.487
PrnStress Angle	Minimum	3	6179	-8.99834
	Maximum	3	723	8.99988

MajorPm Stress	Minimum		3	7745	-36.4438
	Maximum		3	4352	227.909
MinorPm Stress	Minimum		3	7336	-201.191
	Maximum		3	4114	103.161
VonMises Stress	Minimum		3	7678	2.49237
	Maximum		3	6803	259.745
Output Set 4 - Load Case 4					
Set MAX/MIN Summary	Table	Set		ID	Value
Loc. X NormStress	Minimum		4	4673	-156.534
	Maximum		4	1918	169.124
Loc. Y NormStress	Minimum		4	1542	-214.122
	Maximum		4	3456	213.073
Loc. XY ShearStress	Minimum		4	8651	-187.801
	Maximum		4	8535	187.916
PrnStress Angle	Minimum		4	3444	-8.99819
	Maximum		4	3456	8.99945
MajorPrn Stress	Minimum		4	3736	-133.494
	Maximum		4	6752	234.348
MinorPrn Stress	Minimum		4	1542	-323.46
	Maximum		4	6152	53.463
VonMises Stress	Minimum		4	4567	1.81499
	Maximum		4	1542	329.421
Output Set 5 - Load Case 5					
Set MAX/MIN Summary	Table	Set		ID	Value
Loc. X NormStress	Minimum		5	4673	-179.888
	Maximum		5	2679	201.345
Loc. Y NormStress	Minimum		5	3352	-139.517
	Maximum		5	825	159.435
Loc. XY ShearStress	Minimum		5	1589	-137.979
	Maximum		5	1933	127.821
PrnStress Angle	Minimum		5	6830	-8.99618
	Maximum		5	1275	8.99969
MajorPrn Stress	Minimum		5	6057	-80.1186
	Maximum		5	6809	224.552
MinorPrn Stress	Minimum		5	4673	-184.022
	Maximum		5	1293	112.879
VonMises Stress	Minimum		5	4559	0.266441
	Maximum		5	2678	248.926
Output Set 6 - Load Case 6					
Set MAX/MIN Summary	Table	Set		ID	Value
Loc. X NormStress	Minimum		6	4554	-153.145
	Maximum		6	1918	132.539
Loc. Y NormStress	Minimum		6	3803	-152.419
	Maximum		6	3939	152.017
Loc. XY ShearStress	Minimum		6	4679	-105.799
	Maximum		6	4516	116.657
PrnStress Angle	Minimum		6	651	-8.99665
	Maximum		6	3322	8.99882
MajorPrn Stress	Minimum		6	3750	-93.9909
	Maximum		6	4382	189.06
MinorPrn Stress	Minimum		6	4241	-179.758
	Maximum		6	6878	53.3442
VonMises Stress	Minimum		6	8532	2.1132
	Maximum		6	4516	216.54

Output Set 7 - Load Case 7

Set MAX/MIN Summary	Table	Set	ID	Value
Loc. X NormStress	Minimum	7	7216	-193.017
	Maximum	7	4554	232.812
Loc. Y NormStress	Minimum	7	5647	-179.263
	Maximum	7	3803	187.737
Loc. XY ShearStress	Minimum	7	7350	-139.258
	Maximum	7	4679	143.784
PrnStress Angle	Minimum	7	3764	-8.99905
	Maximum	7	4084	8.99861
MajorPrn Stress	Minimum	7	3097	-44.4876
	Maximum	7	4554	238.827
MinorPrn Stress	Minimum	7	7216	-194.794
	Maximum	7	4116	109.549
VonMises Stress	Minimum	7	2578	0.846292
	Maximum	7	4679	265.331

Output Set 8 - Load Case 8

Set MAX/MIN Summary	Table	Set	ID	Value
Loc. X NormStress	Minimum	8	4673	-161.691
	Maximum	8	1918	186.823
Loc. Y NormStress	Minimum	8	3803	-173.105
	Maximum	8	3364	193.63
Loc. XY ShearStress	Minimum	8	8651	-133.373
	Maximum	8	8535	149.381
PrnStress Angle	Minimum	8	4020	-8.99774
	Maximum	8	4009	8.99972
MajorPrn Stress	Minimum	8	4114	-118.817
	Maximum	8	6752	202.481
MinorPrn Stress	Minimum	8	1542	-212.308
	Maximum	8	282	69.835
VonMises Stress	Minimum	8	4394	1.45523
	Maximum	8	8535	261.104

Set MAX/MIN Summary	Table	Set	ID	Value
Loc. X NormStress	Minimum	3	7336	-197.799
	Maximum	7	4554	232.812
Loc. Y NormStress	Minimum	1	3456	-236.277
	Maximum	2	3456	260.833
Loc. XY ShearStress	Minimum	4	8651	-187.801
	Maximum	4	8535	187.916
PrnStress Angle	Minimum	1	4237	-8.99956
	Maximum	3	723	8.99988
MajorPrn Stress	Minimum	4	3736	-133.494
	Maximum	2	3456	257.034
MinorPrn Stress	Minimum	4	1542	-323.46
	Maximum	5	1293	112.879
VonMises Stress	Minimum	5	4559	0.266441
	Maximum	4	1542	329.421

Appendix B City FPSO2000 Web-Frame FEA Results

Model : C:\CityFPSO2000\Webframe.MOD Report: Element
Format : NASTRAN CQUAD4 Stresses
Sort By : 7033..VonMises Stress in Ascending Order

Output Set 1 - Load Case 1

Set MAX/MIN Summary	Table	Set	ID	Value
Loc. X NormStress	Minimum	1	657	-6.96372
	Maximum	1	2139	121.497
Loc. Y NormStress	Minimum	1	1829	-60.8461
	Maximum	1	1979	104.47
Loc. XY ShearStress	Minimum	1	617	-96.248
	Maximum	1	225	101.093
PrnStress Angle	Minimum	1	3051	-8.99217
	Maximum	1	3538	8.9951
MajorPrn Stress	Minimum	1	147	-51.4714
	Maximum	1	2017	148.913
MinorPrn Stress	Minimum	1	1	-116.05
	Maximum	1	767	42.999
VonMises Stress	Minimum	1	3021	3.20996
	Maximum	1	225	181.583

Output Set 2 - Load Case 2

Set MAX/MIN Summary	Table	Set	ID	Value
Loc. X NormStress	Minimum	2	4356	-108.511
	Maximum	2	678	56.2994
Loc. Y NormStress	Minimum	2	4367	-153.747
	Maximum	2	657	49.9479
Loc. XY ShearStress	Minimum	2	224	-114.988
	Maximum	2	1	104.04
PrnStress Angle	Minimum	2	3114	-8.99512
	Maximum	2	3523	8.96398
MajorPrn Stress	Minimum	2	767	-38.8971
	Maximum	2	1	130.72
MinorPrn Stress	Minimum	2	4367	-193.516
	Maximum	2	147	37.5459
VonMises Stress	Minimum	2	1871	1.98072
	Maximum	2	224	204.208

Output Set 3 - Load Case 3

Set MAX/MIN Summary	Table	Set	ID	Value
Loc. X NormStress	Minimum	3	657	-67.7591
	Maximum	3	2139	113.842
Loc. Y NormStress	Minimum	3	146	-64.5794
	Maximum	3	4367	123.439
Loc. XY ShearStress	Minimum	3	2017	-101.047
	Maximum	3	224	120.633
PrnStress Angle	Minimum	3	3026	-8.97508
	Maximum	3	2119	8.99184
MajorPrn Stress	Minimum	3	147	-46.6709
	Maximum	3	4361	169.533
MinorPrn Stress	Minimum	3	1	-126.288
	Maximum	3	767	32.2015
VonMises Stress	Minimum	3	2081	4.55274
	Maximum	3	224	213.54

Output Set 4 - Load Case 4

Set MAX/MIN Summary	Table	Set	ID	Value
Loc. X NormStress	Minimum	4	4356	-140.273
	Maximum	4	1423	38.6846
Loc. Y NormStress	Minimum	4	4367	-191.353
	Maximum	4	485	38.3332
Loc. XY ShearStress	Minimum	4	224	-142.828
	Maximum	4	1	115.741
PrnStress Angle	Minimum	4	3096	-8.99086
	Maximum	4	3069	8.9846
MajorPrn Stress	Minimum	4	4367	-46.7252
	Maximum	4	1	130.862
MinorPrn Stress	Minimum	4	4367	-236.166
	Maximum	4	146	28.9241
VonMises Stress	Minimum	4	1872	1.09406
	Maximum	4	224	257.479

Output Set 5 - Load Case 5

Set MAX/MIN Summary	Table	Set	ID	Value
Loc. X NormStress	Minimum	5	3420	-69.5065
	Maximum	5	684	110.927
Loc. Y NormStress	Minimum	5	4367	-93.5252
	Maximum	5	657	81.6862
Loc. XY ShearStress	Minimum	5	2067	-87.4602
	Maximum	5	650	96.8282
PrnStress Angle	Minimum	5	2018	-8.9983
	Maximum	5	4297	8.99724
MajorPrn Stress	Minimum	5	3446	-20.3588
	Maximum	5	678	126.646
MinorPrn Stress	Minimum	5	4367	-132.673
	Maximum	5	657	66.7383
VonMises Stress	Minimum	5	3152	0.984124
	Maximum	5	650	168.857

Output Set 6 - Load Case 6

Set MAX/MIN Summary	Table	Set	ID	Value
Loc. X NormStress	Minimum	6	3536	-227.586
	Maximum	6	3456	142.755
Loc. Y NormStress	Minimum	6	3538	-220.956
	Maximum	6	3446	134.361
Loc. XY ShearStress	Minimum	6	3537	-136.957
	Maximum	6	3421	128.653
PrnStress Angle	Minimum	6	621	-8.99965
	Maximum	6	572	8.99172
MajorPrn Stress	Minimum	6	2084	-46.2202
	Maximum	6	3421	174.082
MinorPrn Stress	Minimum	6	3536	-308.641
	Maximum	6	3457	68.6432
VonMises Stress	Minimum	6	2809	2.31224
	Maximum	6	3536	295.371

Output Set 7 - Load Case 7

Set MAX/MIN Summary	Table	Set	ID	Value
Loc. X NormStress	Minimum	7	3456	-174.975
	Maximum	7	3536	238.757
Loc. Y NormStress	Minimum	7	3446	-163.738
	Maximum	7	3538	236.222

Loc. XY ShearStress	Minimum		7	617	-139.793
	Maximum		7	3537	145.557
PrnStress Angle	Minimum		7	1827	-8.97658
	Maximum		7	2056	8.98045
MajorPrn Stress	Minimum		7	3457	-83.5261
	Maximum		7	3536	324.77
MinorPrn Stress	Minimum		7	3458	-198.46
	Maximum		7	3554	41.7205
VonMises Stress	Minimum		7	1750	0.777988
	Maximum		7	3536	310.6

Output Set 8 - Load Case 8

Set MAX/MIN Summary	Table	Set	ID	Value
Loc. X NormStress	Minimum	8	4371	-121.813
	Maximum	8	2057	45.1597
Loc. Y NormStress	Minimum	8	4367	-174.804
	Maximum	8	2057	53.487
Loc. XY ShearStress	Minimum	8	224	-130.166
	Maximum	8	133	97.276
PrnStress Angle	Minimum	8	3523	-8.99496
	Maximum	8	2898	8.99738
MajorPrn Stress	Minimum	8	4367	-38.4574
	Maximum	8	164	126.094
MinorPrn Stress	Minimum	8	4367	-217.655
	Maximum	8	2057	39.7602
VonMises Stress	Minimum	8	470	1.25933
	Maximum	8	224	233.169

Set MAX/MIN Summary	Table	Set	ID	Value
Loc. X NormStress	Minimum	6	3536	-227.586
	Maximum	7	3536	238.757
Loc. Y NormStress	Minimum	6	3538	-220.956
	Maximum	7	3538	236.222
Loc. XY ShearStress	Minimum	4	224	-142.828
	Maximum	7	3537	145.557
PrnStress Angle	Minimum	6	621	-8.99965
	Maximum	8	2898	8.99738
MajorPrn Stress	Minimum	7	3457	-83.5261
	Maximum	7	3536	324.77
MinorPrn Stress	Minimum	6	3536	-308.641
	Maximum	6	3457	68.6432
VonMises Stress	Minimum	7	1750	0.777988
	Maximum	7	3536	310.6

REFERENCES

(ABS) American Bureau of Shipping - 1992, 'The Silent Partner of Progress' - SSC Ship Structural Committee Surveyor 15

(ABS) American Bureau of Shipping - 1995, 'Guide for Fatigue Strength Assessment of Tankers', ABS 23

(ABS) American Bureau of Shipping - 1996, 'Guide for building and classing floating production, storage and offloading systems' – ABS Rules 19

(ABS) American Bureau of Shipping - 2000, 'SAFEHULL, Dynamic Ship Design and Structural Assessment' – Version 7.01-Online Manuals 75

(BP) British Petroleum - 1992, 'Fatigue Evaluation of Tanker Structures' - TSCF Tanker Structure Co-operative Forum – Shipbuilders Meeting 17

(DNV) Det Norske Veritas - 1998, 'Fatigue Assessment of Ship Structures', DNV 24

(DNV), Det Norske Veritas. - 1963, 'Finite Element Analysis of Ship Structures' – Res. Dept., Report No. 63-14-S. 18

(GL) Germanischer Lloyd - 1998, 'Catalogue of Details /II' – GL-Technology 25

(GL) Germanischer Lloyd - 1998, 'Rules and Regulations, I – Ship Technology, Part 1 – Sea going Ships, Chapter 1 – Hull Structures' - Hamburg 24

(LR) Lloyd's Register of Shipping - 1996, 'Ship-Right Structural Detail Design Guide, Procedures Manual', LR 22

Almar-Næss, A. - 1985, 'Fatigue Handbook – Offshore Structures' - Tapir Publishers, Trondheim 165

Andrews, R. M - 1996, 'The effect of misalignment on the fatigue strength of welded cruciform joints' - Fatigue Fract. Engng.Mater. Struct. Vol.19. No.6, pp755-768 225

Beghin, D. - 1991, 'Comparative Fatigue Behaviour of Structural Details of VLCC's', SSC and SNAME 25

Belytschko, T., Liu, W. K. and Moran, B. – 2000, 'Nonlinear Finite Elements for Continua and Structures'- J. Wiley & Sons, New York, 2000, 600 pp. ISBN 0-471-98773-5 and 0-471-98774-3 (Pbk) 138

Brown D. T., Lyons J. G., - 1995, 'Advances in Mooring Lines'- Under Water Technology journal 39

Brown P. A., Chandwani R. - 1990, 'Interaction between Flexible Risers and Mooring Lines within a FPSO System'- LAPEC Rio de Jeneiro 39

Callister, William D - 1994, 'Materials Science and Engineering: An Introduction - 3rd Edition' - John Wiley & Sons, Inc.: New York 161, 163

Crisfield, M. A., – 1986, 'Finite Elements and Solution Procedures for Structural Analysis, Vol. I: Linear Analysis - Pineridge Press Limited, U.K.- ISBN 0-906674-53-0 141

Dahle T - 1997, 'Fatigue behaviour of a railway component - application of new design criteria and TIG re-melting techniques' - in Welded High-Strength Steel Structures, Proc. 1st North European Engineering and Science Conference (NESCO I), EMAS Publishing, Cradley Heath, West Midlands, p.519-526 225

Dexter R J, Tarquinio J E and Fisher J W - 1994, "Application of hot spot stress fatigue analysis to attachments on flexible plate' - Proc. 13 Intl. Conf. 'Offshore Mechanics and Arctic Engineering', ASME, New York, p85-92 225

DNV - 1995, 'Buckling Strength Analysis, Classification Notes 30.1' - DNV 134

DNV - 1997, 'Classification Notes 30.1 with Factor Of Safety and corrosion allowances' - DNV 133

DNV - 2000, 'Recommended Practise RP203. *Fatigue Assessment of Offshore Structures*' - Det Norske Veritas, Oslo 226

ed. A.F. Madayag – 1969, 'Metal Fatigue: Theory and Design' – John Wiley & Sons, Inc.,.. 199

Francois, M., Healy B., Fricke W. – OTC- 12144 - 2000, 'FPSO Integrity; Comparative study on fatigue load calculation methods' – OTC-12144 17

Fricke W - 2001, 'Recommended hot-spot analysis procedure for structural details of FPSOs and ships based on round-robin FE analysis' - ISOPE, Stavanger , June 225

Fricke, W. and Bogdan, R. - 2001, 'Determination of Hot Spot Stress in Structural Members with In-Plane Notches Using a Coarse Mesh' - Doc. XIII-1870-01, International Institute of Welding 165
Geometrically Nonlinear Analysis of Structural Membranes. - *Comput. Struct.* Vol. 25, No. 6, pp. 871-876 145
H. O. Fuchs & R.I Stephens - 1980, 'Metal Fatigue in Engineering' - John Wiley & Sons, Inc.: New York, ISBN 0-471-05264-7 223
Handbook of Engineering Mechanics - McGraw-Hill Book, New York, 1962, pp. 61-6, 61-9 151
Hobbacher A - 1996, '*Fatigue Design of Welded Joints and Components*' - IIW Abington Publishing, Abington, Cambridge 224
HSE - 1990, 'Offshore Installations: Guidance on Design, Construction and Certification' - (Fourth Edition, 1990)-HSE 133
HSE - 1995, 'Offshore Installations: Guidance on Design, Construction and Certification'. HSE. London' - John Wiley & Sons, Inc.: New York 227
Huther I, Lieurade H P, Sayki N and Buisson R - 1996, 'Fatigue strength of longitudinal non-load carrying welded joints. Use of the hot spot stress approach' - in Fatigue of Welded Components and Structures, Proc. 3rd Intl. Spring Meeting, Les Editions de Physique, Les Ulis Cedex A, France, p.57-64 225
I. Lotsberg, D. Ø. Askheim and T. Haavi - 2001, 'Full Scale Fatigue Testing of Side Longitudinals in FPSOs' - Det Norske Veritas, Oslo, Norway 171
IACS – 1997, 'Report on the development of a unified procedure for Fatigue Design of Ship Structures'- Ad HOC Group 243
Iwahashi, Y. et al., - 1998, 'Finite Element Comparative Study of Ship Structural Detail.' - *Marine Structures* 11, pp. 127 – 139 169
J. A. Bannantine, J. J. Comer, & J. L - 1990, 'Fundamentals of Metal Fatigue Analysis' - Handrock, Prentice-Hall Inc. ISBN 0-13-340191-X 223
John Ferguson. – Lloyds Register of Shipping - 1990, 'Crude oil Carriers in the 1990's' – Lloyds Register of Shipping. 18
Kawono H and Inoue K - 1993, 'A load approach for the fatigue strength evaluation of ship structure in Fatigue Design' - Proc. Intl Symposium, Mechanical Engineering Publications Limited, Bury St Edmunds,p.95-108 225
Kim, W. S - 1999, 'Fatigue Tests of Typical Welded Joints' - Hyundai Heavy Industries Co., Ltd. Ulsan (unpublished) 225
Koskimaki M and Niemi E - 1995, 'Fatigue strength of welded joints in three types of stainless steel' - IIW Doc. XIII-1603-95 225
Lotsberg, I. - Det Norske Veritas - 2000, 'Background and Status of the FPSO Fatigue Capacity JIP' – OTC-Houston, Texas 17
Lotsberg, I., Nygard, M. and Thomsen, T. - 1998, 'Fatigue of Ship Shaped Production and Storage Units', OTC - 8775 26
Lotsberg,I., Askheim,D., Haavie,T., D. - 2001, 'Full Scale Fatigue Testing of Side Longitudinals in FPSOs', OMAE RIO 4 – 8 JUNE 2001 26
LR - 1997, 'Design Appraisal & Plan Approval of Ship Type FSU & FPSO Units at a Fixed Location' - Guidance Notes Allowable stresses in accordance with Appendix 2, paragraph 4 - 1997-LR 133
LR - 1997, 'Design Appraisal and Plan Approval of Ship Type FSU and FPSO Units at Fixed Location' – Structural 134
LR - 1997, 'Rules & Regulations for the Classification of Fixed Offshore Installations' - Part 9-LR 131, 132
LR - 1997, 'Rules & Regulations for the Classification of Mobile Offshore Installations' - LR 132
LR Right - 1996, 'Fatigue Design Assessment Procedure' – Lloyds Register of Shipping 66
Maddox S J - 1997, 'Developments in fatigue design codes and fitness-for-service assessment methods' - IIW International Conference on *Performance of Dynamically loaded Welded Structures,* WRC, New York, pp22-42 226
Marquis G B and Kahonen A - 1995, 'Fatigue testing and analysis using the hot spot method' - VTT Publication No. 240 'High Cycle Spectrum Fatigue of Welded Components', P O Box 2000, Fin-02044 VTT, Finland 225
McMurray R. (Kaldair Inc.) - 1982, 'Flare Radiation Estimated' - Hydrocarbon Processing 42
Miki C and Tateishi K - 1997, "Fatigue design of cope hole details in steel bridges' - Int.J. Fatigue, Vol.19, No.6, p.445-455 225

Millar, J. L., and White,R. J., – OTC-12145 - 2000, 'The Structural Integrity of FPSO's/FSU's – A Regulator's View' – OTC-12145 20
Moksnes J. , Naess T. , Eriksen K. & Fjeld S. - 1995, 'Floating Production Systems'- OTC 7911 34
Offshore Technology - 1997, 'Review of Structural Monitoring' - Health and Safety Executive OTO 97040 215
Owen Hughes and Paul Franklin, – SNAME- T&R Report No. R-41, 'Definition and Validation of a Practical Rationally-Based Method for the Fatigue Analysis and Design of Ship Hulls' – SNAME- T&R Report No. R-41 21
Oxley M. (Altra Consultants Ltd.) - 1997, 'FPSO Processing Systems' - OCS Technology Group 40
Paulling, J. R. – J. Ship Res. - 1964, 'The Analysis of Complex Ship Structures by the Finite Element Technique' – J. Ship Res 18
Pavlov & Petinov - 1989, 'Fatigue life calculation of ship structural assemblies' – 4th international symposium on practical design of ships and mobil units (PRADS-89),Varna Bulgaria 178, 179
Petershagen, H., Fricke, W., Massel, T - 1991, 'Application of Local Approach to the Fatigue Strength Assessment of Welded Structure in Ships' – (International Institute of Welding) Technical Report – Doc. XIII-1409-91 25
R.E. PETERSON, - 1953, 'Stress Concentration Factors ' – John Wiley, & Sons 184
R.E. PETERSON, - 1974, 'Stress Concentration Factors ' – John Wiley, & Sons 193
Riks, E., – 1979, 'An Incremental Approach to the Solution of Snapping and Buckling Problems - *Int. J. Numer. Meth. Eng.*, 15:529-551 155
Rucho,P., Maherault,T., Chen,W., Berstad,A., Samnøy,G. - 2001, 'Comparison of Measurements and Finite Element Analysis of Side Longitudinals', OMAE RIO 4 – 8 JUNE 2001 26
Steel Vessels – 1997, 'Specialised Vessels and Services PART 5'- ABS 53, 227
Stokes A. (MAI) & Llewelyn D. (BP) - 1996, 'Floating Production Systems The Real Costs' - OCS Technology Group 29
U.K. Department of Energy London - 1990, 'Offshore Installations: Guidance on Design, Construction and Certification' - Section 21:Steel, fourth edition January 23, 24, 25
W. Frick & H. Paetzold – 1987, 'Application of Cyclic Strain Approach to the Fatigue Failure of Ship Structural Details' – Journal of Ship Research, Vol.31,pp.177-185 222
Wallodi Weibull – 1945, 'A statistical representation of fatigue failure in solids' – Transactions of the royal institute of technology, Stockholm, Sweden., ... 240
Watts P. C. (Kaldair Inc.) - 1997, 'Flaring - an FPSO Designer's Nightmare?' - Floating Production Systems Conference 41
Wennesland J. M. (Maritime Group AS) - 1995, 'Development Of Floating Production Sys. For The New Era' - OTC 7944 30
Yagi J and Tomita Y - 1992, 'Definition of hot spot stress in welded plate type structure for fatigue assessment (Report 1),' - J. Society of Naval Architects of Japan, Vol.169, June, p311-318 (IIW Doc XIII-1414-91) 225
Yagi, J.; Machida, S.; Tomita, Y.; Matoba, M.; Kawasaki, T. - 1991, 'Definition of Hot Spot Stresses in Welded Plate Type Structure for Fatigue Assessment.' - IIW-Document IIW-XIII-1414-91, International Institute of Welding 165
Yoneya, T., Kumano, A., Yamamoto, A., and Shigemi, T. - 1993, 'Hull Cracking of very Large Ship Structures' – Technical Report, Integrity of Offshore Structures. NK Japan 16, 17